รายงานวิจัยฉบับสมบูรณ์

โครงการ "การสังเคราะห์ สมบัติสเปกโทรสโกปี สมบัติทางแม่เหล็ก และโครงสร้างผลึกของสารประกอบเชิงซ้อนพอลินิวเคลียร์คอปเปอร์(II) ที่มีออกโซแอนไอออนเป็นลิแกนด์สะพาน"

โดย รศ.ดร. สุจิตรา ยังมี และคณะ

กุมภาพันธ์ 2549

รายงานวิจัยฉบับสมบูรณ์

โครงการ "การสังเคราะห์ สมบัติสเปกโทรสโกปี สมบัติทางแม่เหล็ก และโครงสร้างผลึกของสารประกอบเชิงซ้อนพอลินิวเคลียร์คอปเปอร์(II) ที่มีออกโซแอนไอออนเป็นลิแกนด์สะพาน"

โดย รศ.ดร. สุจิตรา ยังมี และคณะ

กุมภาพันธ์ 2549

สัญญาเลขที่ BRG4680012

รายงานวิจัยฉบับสมบูรณ์

โครงการ "การสังเคราะห์ สมบัติสเปกโทรสโกปี สมบัติทางแม่เหล็ก และโครงสร้างผลึกของสารประกอบเชิงซ้อนพอลินิวเคลียร์ คอปเปอร์(II) ที่มีออกโซแอนไอออนเป็นลิแกนด์สะพาน"

คณะผู้วิจัย

1. รศ.ดร. สุจิตรา ยังมี	มหาวิทยาลัยขอนแก่น
2. ผศ.ดร. เชวง ภควัตชัย	มหาวิทยาลัยสงขลานครินทร์
3. รศ.ดร. ณรงค์ศักดิ์ ชัยชิต	มหาวิทยาลัยธรรมศาสตร์
4. Prof. Jan Reedijk	Leiden University, The Netherlands.

สนับสนุนโดยสำนักงานกองทุนสนับสนุนการวิจัย

สัญญาเลขที่ BRG4680012

โครงการ "การสังเคราะห์ สมบัติสเปกโทรสโกปี สมบัติทางแม่เหล็ก และโครงสร้างผลึกของสารประกอบเชิงซ้อนพอลินิวเคลียร์คอปเปอร์(II) ที่มีออกโซแอนไอออนเป็นลิแกนด์สะพาน"

รายงานวิจัยฉบับสมบูรณ์

บทคัดย่อ

งานวิจัยนี้เป็นการศึกษาเพื่อหาสภาวะการเตรียมและวิเคราะห์สารเชิงซ้อนหลายนิวเคลียสของคอปเปอร์ (II) ที่มีหมู่ออกซาเลต ไฮโดรเจนฟอสเฟต และ ฟอร์เมตเป็นลิแกนด์สะพาน เชื่อมระหว่างไอออนคอปเปอร์(II) และมีได-2-พิริดิลามีนเป็นคีเลติงลิแกนด์ โดยศึกษาสมบัติทางสเปกโทรสโกปี สมบัติทางแม่เหล็ก (5-300 K) และโครงสร้างผลึกจากวิธีทางเอกซเรย์ รวมทั้งศึกษาความสัมพันธ์ระหว่างโครงสร้างกับสมบัติทางแม่เหล็กและ superexchange pathway ของสารเชิงซ้อนแต่ละระบบ

ผลิตภัณฑ์ที่สังเคราะห์ได้สำหรับระบบที่มีหมู่ออกซาเลตเป็นลิแกนด์สะพาน ได้แก่ $[Cu_2(dpyam)_4(\mu\text{-}C_2O_4)](BF_4)_2.3H_2O$ **(I)**, $[Cu_2(dpyam)_4(\mu\text{-}C_2O_4)](ClO_4)_2.3H_2O$ **(II)**, $[Cu_2(dpyam)_4(\mu\text{-}C_2O_4)](PF_6)_2.2H_2O$ **(III)**, $[Cu_2(dpyam)_2(\mu\text{-}C_2O_4)(NO_3)_2((CH_3)_2SO)_2]$ **(IV)**, $[Cu_2(dpyam)_2(\mu\text{-}C_2O_4)(NO_3)_2((CH_3)_2NCOH)_2]$ **(V)**, $[Cu_2(dpyam)_2(\mu\text{-}C_2O_4)Cl_2]$ **(VI)** และ $[Cu_2(dpyam)_2(\mu\text{-}C_2O_4)Br_2]$ **(VII)** ผลิตภัณฑ์ทั้งหมดเป็นสารเชิงซ้อนแบบสองนิวเคลียส โดยสาร **I-III** มีโครงสร้างแบบ compressed rhombic octahedral ส่วนสาร **IV** และ **V** มีโครงสร้างแบบ elongated tetragonal octahedral จากการศึกษาสมบัติทางแม่เหล็ก พบว่า สาร **I-III** มีสมบัติแบบเฟอร์โรแมกเนติกอย่างอ่อน ขณะที่สาร **IV** และ **V** เกิดอันตรกิริยาระหว่างไอออนคอปเปอร์(II) ทั้งสองแบบแอนติเฟอร์โรแมกเนติกอย่างแรง ซึ่งสอดคล้องกับข้อมูลทางโครงสร้างของสารเชิงซ้อนเหล่านี้ นอกจากนี้ยังได้อธิบายในรายละเอียดถึงความสัมพันธ์ระหว่างโครงสร้างกับสมบัติทางแม่เหล็ก และ superexchange pathway ของสารในระบบนี้

กรณีสารเชิงซ้อนที่มีหมู่ไฮโดรเจนฟอสเฟตเป็นลิแกนด์สะพานนั้น ผลิตภัณฑ์ที่สังเคราะห์ได้ ได้แก่ $\{[Cu_3(dpyam)_3(\mu_3,\eta^3\text{-}HPO_4)(\mu_3,\eta^4\text{-}PO_4)(H_2O)](PF_6).3H_2O\}_n$ **(I)**, $[Cu(dpyam)(\mu_2,\eta^3\text{-}HPO_4)]_n$ **(II)**, $[Cu(dpyam)(\mu_2,\eta^2\text{-}H_2PO_4)(H_2PO_4)]_2$ **(III)**, $[Cu_4(dpyam)_4(\mu_4,\eta^3\text{-}HPO_4)_2(\mu\text{-}Cl)_2](X)_2$, X = Cl .$6H_2O$ **(IV)** และ Br .$6H_2O$ **(V)** และ $[Cu_4(dpyam)_4(\mu_3,\eta^3\text{-}HPO_4)_2(NO_3)_2(H_2O)_2](NO_3)_2$.$2H_2O$ **(VI)** สาร **I** และ **II** มีโครงสร้างต่อกันเป็นโซ่ยาวผ่านสะพานไฮโดรเจนฟอสเฟต สำหรับสาร **III** เป็นโมเลกุลแบบสองนิวเคลียส

ที่มีหมู่ไฮโดรเจนฟอสเฟตเชื่อมระหว่างไอออนคอปเปอร์(II) ทั้งสอง ส่วนสาร **IV V** และ **VI** เป็นสารเชิงซ้อนแบบสี่นิวเคลียสโดยมีหมู่ไฮโดรเจนฟอสเฟต เชื่อมไอออนคอปเปอร์(II) ทั้งสี่ในรูปแบบการโคออร์ดิเนตที่แตกต่างกัน ผลิตภัณฑ์ทั้งหมดในระบบนี้มีสิ่งแวดล้อมรอบไอออนคอปเปอร์(II) แบบ distorted square pyramidal ซึ่งบ่งบอกด้วยค่า τ ที่มีค่าอยู่ในช่วง 0.001-0.57 จากการศึกษาสมบัติทางแม่เหล็ก พบว่า ผลิตภัณฑ์ทั้งหมดมีสมบัติทางแม่เหล็กแบบแอนติเฟอร์โรแมกเนติกอย่างอ่อน ซึ่งสอดคล้องกับข้อมูลทางโครงสร้างของสารในระบบนี้

ผลิตภัณฑ์ที่สังเคราะห์ได้สำหรับระบบที่มีหมู่ฟอร์เมตเป็นลิแกนด์สะพาน ได้แก่ $[Cu_2(dpyam)_2(\mu\text{-}O_2CH)(\mu\text{-}OH)(\mu\text{-}OCH_3)](ClO_4)$ **(I)**, $[Cu_2(dpyam)_2(\mu\text{-}O_2CH)(\mu\text{-}OH)_2](ClO_4)\cdot H_2O$ **(II)**, $[Cu_2(dpyam)_2(\mu\text{-}O_2CH)(\mu\text{-}OOCH)(\mu\text{-}OH)](PF_6)$ **(III)**, $[Cu_2(dpyam)_2(\mu\text{-}O_2CH)(\mu\text{-}OH)(\mu\text{-}Cl)](X)$, $X = ClO_4 \cdot 0.5H_2O$ **(IV)**, PF_6 **(V)** และ BF_4 **(VI)** ผลิตภัณฑ์ทั้งหมดเป็นสารเชิงซ้อนคอปเปอร์(II) แบบสองนิวเคลียสและเป็นสารเชิงซ้อนที่มีสะพานเชื่อมระหว่างไอออนคอปเปอร์(II) แบบสามสะพาน โดยสาร **I III IV** และ **V** มีโครงสร้างแบบ distorted trigonal bipyramidal มีสะพานไฮดรอกโซเชื่อมไอออนคอปเปอร์(II) ทั้งสองในตำแหน่งแอกเซียล ส่วนสาร **II** มีโครงสร้างแบบ distorted square pyramidal โดยมีหมู่ไฮดรอกโซทั้งสองเชื่อมอยู่ระหว่างไอออนคอปเปอร์(II) ในตำแหน่งอิเควทอเรียล และจากการศึกษาสมบัติทางแม่เหล็กพบว่าสารเชิงซ้อน **I III IV** และ **V** มีการคู่ควบระหว่างไอออนคอปเปอร์(II) แบบเฟอร์โรเมกเนติก ส่วนสาร **II** มีอันตรกิริยาดังกล่าวเป็นแบบแอนติเฟอร์โรเมกเนติก โดยมีค่า singlet-triplet energy gap J เท่ากับ -122.54 ซม$^{-1}$ ซึ่งเป็นค่าที่ได้จากการคาดคะเนโดยใช้ความสัมพันธ์ ระหว่างค่า J กับมุมสะพาน θ ของระบบสารเชิงซ้อนสองนิวเคลียสแบบพลานาร์ที่มีสะพานไดไฮดรอกโซ นอกจากนี้ได้อธิบายถึงความสัมพันธ์ระหว่างโครงสร้างกับสมบัติทางแม่เหล็ก รวมทั้ง superexchange pathway ของสารเชิงซ้อนในระบบนี้

สัญญาเลขที่ BRG4680012

โครงการ "การสังเคราะห์ สมบัติสเปกโทรสโกปี สมบัติทางแม่เหล็ก และโครงสร้างผลึกของสารประกอบเชิงซ้อนพอลินิวเคลียร์คอปเปอร์(II) ที่มีออกโซแอนไอออนเป็นลิแกนด์สะพาน"

รายงานวิจัยฉบับสมบูรณ์

Abstract

The polynuclear copper(II) complexes with the di-2-pyridylamine ligand and the bridging oxoanions, namely oxalate, hydrogenphosphate and formate have been synthesized and characterized spectroscopically (IR, VIS and EPR) and their molecular structures determined by X-ray diffraction analysis. The temperature variable magnetic susceptibilities (5-300° K) are measured and the magneto-structural correlation investigated and discussed as well as the superexchange pathways.

The synthesis and characterization of the dinuclear oxalato-bridged copper(II) complexes $[Cu_2(dpyam)_4(\mu\text{-}C_2O_4)](BF_4)_2.3H_2O$ **(I)**, $[Cu_2(dpyam)_4(\mu\text{-}C_2O_4)](ClO_4)_2.3H_2O$ **(II)**, $[Cu_2(dpyam)_4(\mu\text{-}C_2O_4)](PF_6)_2.2H_2O$ **(III)**, $[Cu_2(dpyam)_2(\mu\text{-}C_2O_4)(NO_3)_2((CH_3)_2SO)_2]$ **(IV)**, $[Cu_2(dpyam)_2(\mu\text{-}C_2O_4)(NO_3)_2((CH_3)_2NCOH)_2]$ **(V)**, $[Cu_2(dpyam)_2(\mu\text{-}C_2O_4)Cl_2]$ **(VI)** and $[Cu_2(dpyam)_2(\mu\text{-}C_2O_4)Br_2]$ **(VII)** are described. X-ray analysis of compounds **I-V** are reported with geometry of **I-III** being compressed rhombic octahedral and that of **IV** and **V** being elongated tetragonal octahedral. Compound **I** and **II** exhibit a very weak ferromagnetic interaction between the Cu(II) ions while a strong antiferromagnetic coupling is found for **IV** and expected for **V**. This is in agreement with their structural features found.

In case of the polynuclear hydrogenphosphato-bridged copper(II) complexes, X-ray analysis of complexes $\{[Cu_3(dpyam)_3(\mu_3,\eta^3\text{-}HPO_4)(\mu_3,\eta^4\text{-}PO_4)(H_2O)](PF_6)\cdot 3H_2O\}_n$ **(I)**, $[Cu(dpyam)(\mu_2,\eta^3\text{-}HPO_4)]_n$ **(II)**, $[Cu(dpyam)(\mu_2,\eta^2\text{-}H_2PO_4)(H_2PO_4)]_2$ **(III)**, $[Cu_4(dpyam)_4(\mu_4,\eta^3\text{-}HPO_4)_2(\mu\text{-}Cl)_2](Cl)_2\cdot 6H_2O$ **(IV)**, $[Cu_4(dpyam)_4(\mu_4,\eta^3\text{-}HPO_4)_2(\mu\text{-}Br)_2](Br)_2\cdot 6H_2O$ **(V)** and $[Cu_4(dpyam)_4(\mu_3,\eta^3\text{-}HPO_4)_2(NO_3)_2(H_2O)_2](NO_3)_2\cdot 2H_2O$ **(VI)** are reported. Compounds **I** and **II** involve the polymeric chain structure while compound **III** exhibits a dinuclear unit. Compounds **IV-VI** display the tetranuclear unit, all of which involve the five-coordinate geometry, but different in a small structural distortion indicated by τ values ranging from 0.001 to 0.57. All compounds in this series present a singlet ground state. The overall magnetic behaviour for each

compounds indicates a week antiferromagnetic interaction between Cu(II) ions, in agreement with their structural features found.

In case of the formato-bridged copper(II) compounds, the triply-bridged dinuclear copper (II) complexes $[Cu_2(dpyam)_2(\mu\text{-}O_2CH)(\mu\text{-}OH)(\mu\text{-}OCH_3)](ClO_4)$ **(I),** $[Cu_2(dpyam)_2(\mu\text{-}O_2CH)(\mu\text{-}OH)_2](ClO_4)\cdot H_2O$ **(II),** $[Cu_2(dpyam)_2(\mu\text{-}O_2CH)(\mu\text{-}OOCH)(\mu\text{-}OH)](PF_6)$ **(III),** $[Cu_2(dpyam)_2(\mu\text{-}O_2CH)(\mu\text{-}OH)(\mu\text{-}Cl)](ClO_4)\cdot 0.5H_2O$ **(IV),** $[Cu_2(dpyam)_2(\mu\text{-}O_2CH)(\mu\text{-}OH)(\mu\text{-}Cl)](PF_6)$ **(V)** and $[Cu_2(dpyam)_2(\mu\text{-}O_2CH)(\mu\text{-}OH)(\mu\text{-}Cl)](BF_4)$ **(VI)** have been synthesized and characterized. X-ray analysis of compounds **I-V** are reported with geometry of **I, III, IV** and **V** being distorted trigonal bipyramidal and that of **II** being distorted square pyramidal. Compounds **I** and **IV** show a very similar magnetic behaviour (J = +62.5 and 79.1 cm^{-1}) and also in case of **III** and **V** (J = +30.8 and +36.7 cm^{-1}) which are in agreement with their structural data. That of **II** is expected to involve a moderate antiferromagnetic coupling (J = -122.54 cm^{-1}) between Cu(II) ions, based on the bridging angle following Hodson and Hatfield's linear relationship which is usually applied successfully for the planar dihydroxo-bridged complexes.

สัญญาเลขที่ BRG4680012

โครงการ "การสังเคราะห์สมบัติสเปกโทรสโกปีสมบัติทางแม่เหล็กและโครงสร้างผลึกของสารประกอบเชิงซ้อนพอลินิวเคลียร์คอปเปอร์ (II) ที่มีออกโซนอนไอออนเป็นลิแกนด์สะพาน"

รายงานสรุปความก้าวหน้าของโครงการประจำปี

Executive Summary

The more insight in the structural aspects of polynuclear transition metal compounds that influence their magnetic properties has been the primary objective of this research. Because of the varieties of geometries and coordination numbers displayed by the copper(II) ion and in order to extend a search to polynuclear copper(II) complexes with different coordination modes of bridging ligands, the polynuclear copper(II) complexes with the terminal di-2-pyridylamine ligand and three different oxoanion bridging ligands, namely oxalate, hydrogenphosphate and formate are prepared in order to relate the structural parameters to their magnetic properties, besides the coordination chemistry of these kinds of complexes. The aim of the research is twofold, **First** to synthesize new polynuclear copper(II) complexes containing the oxalate, hydrogenphosphate and formate as bridging ligands with variety of coordination and bridging modes resulting different environments around the copper(II) ion. The structural modification for each series is based on the preparative conditions and type of anion and solvent molecule. Measuring the temperature variable magnetic susceptibilities of these new compounds brings up the **second** aim of the research; to investigate structural factors that influence the type and magnitude of magnetic interaction between copper(II) ions and the superexchange pathway investigated and discussed.

This research is divided into three parts. Part I describes the synthesis, characterization (elemental analysis, IR, EPR, and X-ray analysis) and magneto-structural correlation of the polynuclear oxalato-bridged copper(II) complexes Those of the polynuclear hydrogenphosphato-bridged and formato-bridged copper(II) complexes are described in Part II and Part III of the research, respectively.

Part I addresses the synthesis, characterization and magneto-structural correlation of seven dinuclear oxalato-bridged copper(II) complexes $[Cu_2(dpyam)_4(\mu\text{-}C_2O_4)]X_2$, X = $(BF_4)_2.3H_2O$ **(I)**, $(ClO_4)_2.3H_2O$ **(II)** and $(PF_6)_2.2H_2O$ **(III)**, $[Cu_2(dpyam)_2(\mu\text{-}C_2O_4)(NO_3)_2((CH_3)_2SO)_2]$ **(IV)**, $[Cu_2(dpyam)_2(\mu\text{-}C_2O_4)(NO_3)_2((CH_3)_2NCOH)_2]$ **(V)** and $[Cu_2(dpyam)_2(\mu\text{-}C_2O_4)X_2]$,

X= Cl (**VI**) and Br (**VII**). Compounds **I-III** display the identical environment, a compressed rhombic octahedral coordination geometry of the rather unique $CuN_2O_2N_2'$ (4+2) chromophore with a slightly different distortion in the bond lengths and bond angles. The oxalato bridge links both copper(II) ions in the equatorial positions. This axially-compressed octahedral (4+2) geometry is uncommon as most of other dinuclear μ-oxalatodicopper(II) complexes found in literature have five-coordinate geometries, a square-pyramidal structure with the counter anion or solvent molecule occupying the axial position. Some compounds present an additional bond, giving rise to an axially-elongated octahedral geometry. In addition, **I-III** are three rare examples of 4+2 compressed rhombic coordination resulting from a pseudo Jahn-Teller effect, the apparent compression is due to dynamic interconversion between two of the possible axial elongations. Complexes **IV** and **V** exhibit an elongated tetragonal octahedral environment of both CuN_2O_2O' O'' chromophores. Both copper atoms are linked through an oxalato bridge in the equatorial positions and both axial positions are occupied by the nitrate anion and the DMF or DMSO solvent molecule for **IV** and **V**, respectively. Unfortunately, the crystals of the Cl and Br compounds (**VI** and **VII**) are not good enough for X-ray analysis. Hence, the proposed structures have been made, based on their spectroscopic properties to be a square pyramidal geometry with the halide occupying in the axial position.

Compounds **I** and **II** have the singlet-triplet energy gaps J = +3.38 and +2.42 cm^{-1}, respectively, which confirms a very weak ferromagnetic interaction between two Cu(II) ions within these complexes. Both compounds involve the compressed rhombic octahedral geometry, which the unpaired electrons of the Cu centres are not in d_{x2-y2} orbital but rather in d_{z2} orbitals. Therefore, magnetic orbitals are perpendicular to the oxalate plane, hence overlap very poorly with the oxalato σ orbitals, resulting in a weakness of the ferromagnetic interaction. In contrast, **IV** has the J value of –305.1 cm^{-1} which is distinct both in the sign and magnitude of the J value. This indicates the strong antiferromagnetic interaction between two Cu(II) centres within the complex. As **IV** exhibits an elongated octahedral geometry, the unpaired electrons of the Cu centres are in d_{x2-y2} orbitals. Hence, there are well oriented to interact with the oxalate σ orbitals and the maximized antiferromagnetic interaction is expected. However, the magnetic exchange interaction may be slightly weakened by the structural distortion such as the displacement of the copper atom out of the basal plane (-0.077 and 0.077 Å), the tetrahedral distortion of the basal plane (7.2°), the copper atom deviation from the oxalate plane (-0.098 and +0.098 Å), and the dihedral angle of 7.0° between the basal plane and the oxalate plane. It is noted that the structure

and structural distortion of **III** is very comparable to those of **I** and **II**, and that of **V** is very similar to that of **IV**. Thus **III** and **V** are predicted to have a very weak ferromagnetic and strong antiferromagnetic interaction, respectively.

Part II of this research describes the synthesis, characterization (elemental analysis, thermogravimetric analysis, IR, EPR, and X-ray analysis) and magnetic properties of six polynuclear hydrogenphosphato-bridged copper(II) complexes $\{[Cu_3(dpyam)_3(\mu_3,\eta^3\text{-}HPO_4)(\mu_3,\eta^4\text{-}PO_4)(H_2O)](PF_6)\cdot 3H_2O\}_n$ **(I)**, $[Cu(dpyam)(\mu_2,\eta^3\text{-}HPO_4)]_n$ **(II)**, $[Cu(dpyam)(\mu_2,\eta^2\text{-}H_2PO_4)(H_2PO_4)]_2$ **(III)**, $[Cu_4(dpyam)_4(\mu_4,\eta^3\text{-}HPO_4)_2(\mu\text{-}Cl)_2]X_2$, X = Cl $\cdot 6H_2O$ **(IV)** and Br $\cdot 6H_2O$ **(V)** and $[Cu_4(dpyam)_4(\mu_3,\eta^3\text{-}HPO_4)_2(NO_3)_2(H_2O)_2](NO_3)_2\cdot 2H_2O$ **(VI)**. Compounds **I** and **II** exhibit polymeric chains of the $[Cu_3(dpyam)_3(\mu_3,\eta^3\text{-}HPO_4)(\mu_3,\eta^4\text{-}PO_4)(H_2O)]^+$ cation and $[Cu(dpyam)(\mu_2,\eta^3\text{-}HPO_4)]$ unit, respectively with the novel bridging coordination modes $\mu_3,\eta^3\text{-}HPO_4$ and $\mu_3,\eta^4\text{-}PO_4$ for **I** and $\mu_2,\eta^3\text{-}HPO_4$ for **II**. The trimeric unit in **I** involves two CuN_2O_2O' chromophores with a tetrahedrally distorted square-based pyramidal geometry (τ = 0.17 and 0.13) and a CuN_2O_3 chromophore with an intermediate five-coordinate geometry (τ = 0.57). Compound **II** displays a distorted square-based pyramidal geometry of the CuN_2O_2O' chromophore with τ = 0.12. Compound **III** is a dinuclear compound consisting of the $\mu_2,\eta^2\text{-}H_2PO_4$ bridge and the monodentate H_2PO_4 group with a distorted square pyramidal CuN_2O_2O' chromophore (τ = 0.12). **IV**, **V** and **VI** are tetranuclear compounds consisting of the tetrameric units $[Cu_4(dpyam)_4(\mu_4,\eta^3\text{-}HPO_4)_2(\mu\text{-}Cl)_2]^{2+}$, $[Cu_4(dpyam)_4(\mu_4,\eta^3\text{-}HPO_4)_2(\mu\text{-}Br)_2]^{2+}$ and $[Cu_4(dpyam)_4(\mu_3,\eta^3\text{-}HPO_4)_2(NO_3)_2(H_2O)_2]^{2+}$, respectively. Complexes **IV** and **V** are isostructural, both having the $\mu_4,\eta^3\text{-}HPO_4$ bridging coordination mode with the halide bridges. Each copper(II) environment are in a range of the distorted square pyramidal geometry of CuN_2O_2X chromophores with τ = 0.02-0.05 for **IV** and τ = 0.001-0.07 for **V**. Complex **VI** exhibits two different geometries, a tetrahedrally distorted square-based pyramid (τ = 0.32) of two CuN_2O_2O' chromophores and an intermediate five-coordinate geometry (τ = 0.52) of the other two CuN_2O_3 chromophores with an unprecedented $\mu_4,\eta^3\text{-}HPO_4$ bridging coordination mode.

The magnetic interaction in **I** calculated from Curie-Weiss law out of the χ^{-1} versus T plot, results in a Curie-Weiss constant Θ = -4 K, indicating a weak antiferromagnetic interaction. This weak interaction can be understood by the fact that the three Cu ions are not equal to each other, the Cu(1) distances to Cu(2) and Cu(3) are large (5.218, 5.942 Å), while the Cu(2)-Cu(3)

distance is shorter (4.407 Å), so magnetically it can be also understood as a dinuclear identity which form a polymeric chain via a single Cu ion. Compounds **II** and **III** have the singlet-triplet energy gaps J = -26.20(2) and -2.85(1) cm^{-1}, respectively, which confirm the medium and weak antiferromagnetic interactions, respectively between neighboring Cu(II) ions. Because of the square pyramidal geometry in **II** and **III** the spin density is mostly in the d_{x2-y2} orbitals of the copper(II) ions. Although the $H_nPO_4^{(3-n)-}$ bridges, join the copper atoms in an equatorial-equatorial configuration, both square bases are not parallel in the same plane with an anti-anti or syn-anti configuration of the $H_nPO_4^{(3-n)-}$ bridges. Consequently, the superexchange coupling through the phosphate anion (Cu-O-P-O-Cu) can be expected to be non negligible. The antiferromagnetic couplings found in **II** and **III** are thus in agreement with this structural feature and the large Cu-Cu distances. Compound **IV** has the singlet-triplet energy gaps $2J_1 = 2J_2 = 22(1)$ cm^{-1}, $2J_3 = -79.4(7)$ cm^{-1}, $2J_4 = 46(3)$ cm^{-1} for different pathways. Those of **V** are $2J_1 = 2J_2 = 33.3(7)$ cm^{-1}, $2J_3 = -83.1(5)$ cm^{-1}, $2J_4 = 12(2)$ cm^{-1}. This concludes that both compounds present a singlet ground state. Compound **VI** has the singlet-triplet energy gaps $J_1 = -20.4(1)$ cm^{-1} and $J_2 = -10.1(2)$ cm^{-1}. In light of the longer distance of the inner Cu-Cu ions (Cu(1)-Cu(2)), the found J values seem to be reasonable. The phosphate bridges in **VI** join copper atoms in an equatorial-equatorial modes between two distorted square pyramidal chromophores which have a marked tetrahedral twist of the square bases and the large Cu-Cu distance and link the copper atoms in the equatorial-axial and axial-axial configuration modes between two different geometries (τ = 0.32 and 0.52). The antiferromagnetic interaction found in **VI** is thus in agreement with this structural feature.

Part III describes the synthesis, characterization and magneto-structural correlation of six dinuclear formato-bridged copper(II) complexes $[Cu_2(dpyam)_2(\mu\text{-}O_2CH)(\mu\text{-}OH)(\mu\text{-}OCH_3)](ClO_4)$ **(I)**, $[Cu_2(dpyam)_2(\mu\text{-}O_2CH)(\mu\text{-}OH)_2](ClO_4)\cdot H_2O$ **(II)**, $[Cu_2(dpyam)_2(\mu\text{-}O_2CH)(\mu\text{-}OOCH)(\mu\text{-}OH)](PF_6)$ **(III)** and $[Cu_2(dpyam)_2(\mu\text{-}O_2CH)(\mu\text{-}OH)(\mu\text{-}Cl)](X)$, X = $ClO_4 \cdot 0.5H_2O$ **(IV)**, PF_6 **(V)** and BF_4 **(VI)**. Complexes **I-V** are the triply-bridged dinuclear copper(II) complexes involving the distorted trigonal bipyramidal geometry of CuN_2O_3 chromophores with the τ values of 0.61, 0.59, 0.60 and 0.72 for **I**, **III**, **IV** and **V**, respectively and the distorted square pyramidal CuN_2O_2O' chromophore with τ = 0.27 for **II**. The formate anion in all compounds bridges two copper atoms in a syn-syn arrangement in the trigonal plane. Compound **III** involves an additional monoatomic formato bridge, coordinated also in the trigonal plane. The hydroxo bridge

within **I**, **III**, **IV** and **V** occupies one of the axial positions with the bridging Cu-O-Cu angles of 104.0, 107.2, 104.8 and 105.9° for **I**, **III-V**, respectively. The Cu environment in **II** is found to be distinct as compared to others in this series and involves some tetrahedral twist of the square bases, 23.8°. Additionally, the dimeric unit is not exactly planar with a dihedral angle between both basal planes of 14.4°. Both hydroxo groups bridge two Cu(II) ions in an equatorial-equatorial configuration with the bridging Cu-O-Cu angles of 95.8 and 96.0° while the triatomic formato group links both Cu(II) ions in the axial positions. The crystals of **VI** is not suitable for X-ray analysis, therefore its structure is characterized by elemental analysis and the spectroscopic properties, and the distorted trigonal bipyramidal geometry similar to those of I, III, IV and V has been proposed with the molecular formula of $[Cu_2(dpyam)_2(\mu\text{-}O_2CH)(\mu\text{-}OH)(\mu\text{-}Cl)](BF_4)$ **(VI)**.

The magnetic properties of compounds **I** and **IV** mutually show a very similar behaviour with the singlet-triplet energy gaps (J) of +62.5 and +79.1 cm^{-1}, respectively and the very similar structure is also found **III** and **V** with J values of +30.8 and +36.7 cm^{-1}. The ferromagnetic interaction in the latter two compounds is smaller than that of the former two compounds, resulting in the conclusion that the bigger the bridging Cu-O(H)-Cu angle and the longer the Cu-Cu distance, the smaller the ferromagnetic interaction is found. It is noted that the τ values in the studied ranges do not affect the magnitude of exchange interaction. The coordination geometry around each copper(II) ion of **I**, **III**, **IV** and **V** is distorted trigonal bipyramidal, which the unpaired electron resides primarily in d_{z^2} orbital with orientation along the apical hydroxo bridging ligand. In this case a major σ pathway via (Cu-OH-Cu) is possible for the electron delocalization via the d_{z^2} magnetic orbitals, corresponding to the weak or strong ferromagnetic interaction. The unpair electron of first copper ion couples with an electron in p-orbital of oxygen atom and the unpair electron of second copper ion couples with an electron in the other p-orbital of oxygen atom resulting in the existence of two parallel unpair electrons, each from different p-orbitals. A strong magnetic interaction requires both good σ orientation of the magnetic orbitals and good superexchange properties of the bridging atom(s). Therefore, these complexes contribute a moderate ferromagnetic exchange. It should be noted that when the copper(II) geometry is close to regular square pyramidal, an often strong antiferromagnetic interaction will be predominant, but a reduction of an antiferromagnetic contribution will be observed when the geometry becomes closer to trigonal bipyramidal. Compound **II** exhibits the distinct copper(II) environment, a distorted square pyramidal geometry, as compared to other complexes which the unpaired electron is located in a $d_{x^2-y^2}$ type orbital. The $d_{x^2-y^2}$ magnetic orbital in **II** is directed

toward both hydroxo bridges, the Cu-O-Cu angles of 95.8 and 96.0°. For these bridging angles, a moderate antiferromagnetic coupling ($J = -122.54\ cm^{-1}$) should be expected following Hodgson and Hatfield's linear relationship which is usually applied successfully for the planar dihydroxo-bridged complexes.

The results of this research would be used as basis for suggestion for further research in the field of magnetochemistry research and would benefit as a basic knowledge for structural modification in order to design the potential magnetic materials. Parts of this research have been published for publication as attached in the back of the research report.

TABLE OF CONTENTS

LIST OF ABBREVIATIONS

dpyam	Di-2-pyridylamine or 2,2'-bipyridylamine
bipy	2,2'-bipyridyl or di-2-pyridyl
phen	1,10-phenanthroline
DMF	Dimethylformamide
DMSO	Dimethylsulfoxide
μ_B	Bohr magneton
μ_{eff}	Magnetic moment
EPR	Electron paramagnetic resonance
mT	miliTesla
kK	KiloKeyser (1000 cm^{-1})

Part I

Synthesis, Crystal Structure, Spectroscopic and Magnetic Properties of Dinuclear Oxalato-Bridged Copper(II) Compounds

Synthesis, Crystal Structure, Spectroscopic and Magnetic Properties of Dinuclear Oxalato-Bridged Copper(II) Compounds

1.1 Introduction

The oxalate anion is a versatile ligand, having the wide variety of topologies for coordination geometries with transition metal ions. The oxalate ion has been proven to be a bridging ligand to design magnetic materials and many oxalato-bridged complexes have been prepared and characterized[1-19]. The magnetic properties of oxalato-bridged copper(II) complexes is strongly dependent on the geometry around the copper ions and the bridging mode of oxalate ligand[9]. Eight different coordination modes of oxalate ligand have been reported for the oxalato copper(II) complexes (Figure 1)[1, 4]. The coordination **modes b** and **e** (Figures 1b and 1e) are commonly observed.

A number of dinuclear copper complexes with an oxalato bridge, generally formulated as $[(NN)Cu(m\text{-}C_2O_4)Cu(NN)]X_n$, where NN is a chelating ligand, and X is a counter anion or a solvent molecule, have been structurally characterized[2-15]. Analysis of the structural factors that influence the magnitude of the magnetic interactions allowed to tune the value of the singlet-triplet energy gap (J values) in oxalato-bridged dinuclear Cu(II) complexes from approximately 0 to approximate -400 cm^{-1} by playing on the nature of the terminal ligand (tridentate and/or didentate nitrogen donors) or of the counter ions, taking advantage of the plasticity effect of the Cu(II) coordination sphere[2]. It is extremely difficult to control the value of structural parameters during the synthetic process and great difficulties are faced to establish the magneto-structural correlation. In order to extend the investigation by modifying the terminal ligand to the more flexible, nitrogen donor didentate dpyam ligand, we now describe the synthesis, the crystal structure, and the magnetic properties of seven new μ-oxalato Cu(II) complexes, $[Cu_2(dpyam)_4(\mu\text{-}C_2O_4)]X_2$, X = $(BF_4)_2.3H_2O$ **(I)**, $(ClO_4)_2.3H_2O$ **(II)** and $(PF_6)_2.2H_2O$ **(III)**, $[Cu_2(dpyam)_2(\mu\text{-}C_2O_4)(NO_3)_2((CH_3)_2SO)_2]$ **(IV)**, $[Cu_2(dpyam)_2(\mu\text{-}C_2O_4)(NO_3)_2((CH_3)_2NCOH)_2]$ **(V)** and $[Cu_2(dpyam)_2(\mu\text{-}C_2O_4)X_2]$, X= Cl **(VI)** and Br **(VII)**. The ligand dpyam has been selected primarily because of the fact that it also has a N- H H-bond donor function that might interfere with the oxalate bridging ligand.

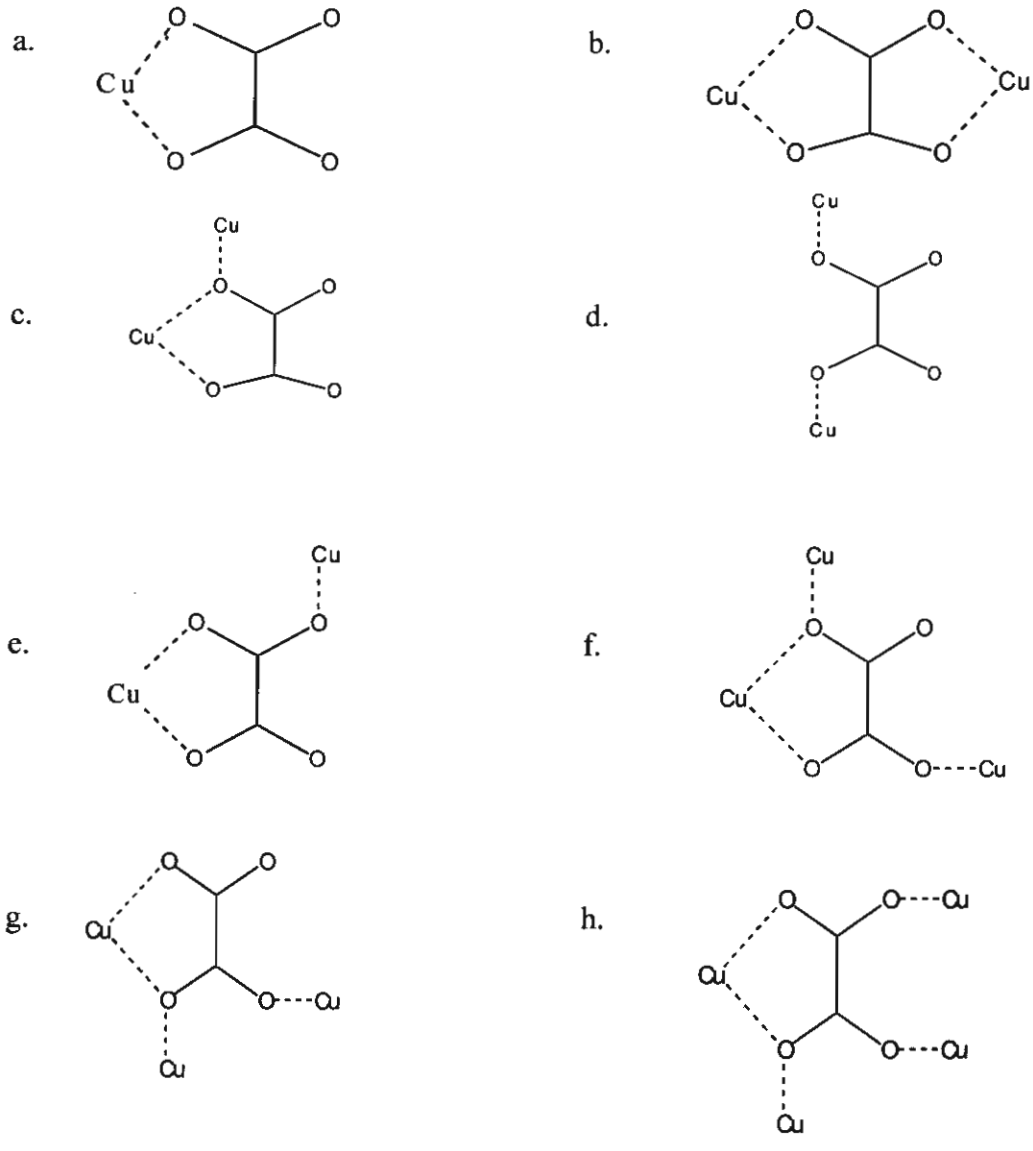

Figure 1 Different coordination modes of oxalate ligand for the oxalato copper(II) complexes

1.2 Aims and Scopes

The objective of the first part of this research is to examine and develop the preparation work of the polynuclear copper(II) complexes containing the oxalate oxoanion as a bridging ligand and the di-2-pyridylamine as a chelate didentate terminal ligand. The products are characterized by the elemental microanalyses and their spectroscopic properties (IR, solid state VIS, EPR (room

temperature and liquid nitrogen temperature)). The crystal and molecular structures were determined by X-ray crystallography. The room temperature magnetic moment and the temperature variable susceptibilities (5-280 K) are measured and the magneto-structural correlation together with the superexchange pathways are investigated and discussed in comparison with other relevant complexes.

1.3 Experimental

1.3.1 Reagents and physical measurements

All reagents are commercial grade materials and were used without further purification. Elemental analyses(C, H, N) were performed by the Microanalytical Service of Science and Technological Research Equipment Center, Chulalongkorn University on Perkin-Elmer PE2400 CHNS/O Analyzer. Copper content was determined on atomic absorption spectrophotometer. IR spectra were recorded with a Biorad FTS-7/PC FTIR spectrophotometer as KBr pellets/and or as nujol mulls in the 4000 – 450 cm^{-1} spectral range. Solid-state (diffuse reflectance) electronic spectra were recorded as polycrystalline samples on a Perkin-Elmer Lambda2S spectrophotometer over the range 8000–18000 cm^{-1}. X-band powder EPR spectra were obtained on a Jeol RE2x electron spin resonance spectrometer using DPPH (g = 2.0036) as a standard. Magnetic susceptibility measurements (5-280 K) were carried out using a Quantum Design MPMS-5 5T SQUID magnetometer (measurements carried out at 1000 Gauss). Data were corrected for magnetization of the sample holder and for diamagnetic contributions, which were estimated from the Pascal constants.

1.3.2 Syntheses

$[Cu_2(dpyam)_4(\mu\text{-}C_2O_4)](BF_4)_2 .3H_2O$ (I)

A solution containing di-2-pyridylamine (0.342 g, 2.0 mmol) in ethanol (20 ml) and sodium oxalate (0.068 g, 0.5 mmol) in water (10 ml) was added to a solution of copper(II) tetrafluoroborate hydrate (0.237 g, 1.0 mmol) in water (10 ml). The resulting green solution was allowed to evaporate at room temperature. After two weeks, green crystals of **I** were obtained, which were filtered off, washed with mother liquor and were dried in air. Calc. For $[Cu_2(dpyam)_4$

(μ-C_2O_4)](BF_4)$_2$.3H_2O : C, 44.74; H, 3.76; N, 14.90; Cu, 11.27 %. Found: C, 44.82; H, 3.68; N, 14.85; Cu, 11:33 %.

[Cu_2(dpyam)$_4$(μ-C_2O_4)](ClO_4)$_2$ .3H_2O (II)

This compound was prepared by adding a hot methanol (40 ml) of di-2-pyridylamine (0.342 g, 2.0 mmol) to hot aqueous solution (60 ml) of copper(II) perchlorate hydrate (0.371 g, 1.0 mmol). The mixture was heated at *ca.* 70 c° with continuous stirring for 10 minutes, then the solid sodium oxalate (0.134 g, 1.0 mmol) was added. The resulting hot solution was filtered to remove impurities. After standing at room temperature for a week, green crystals of **II** were obtained. They were filtered off, washed with mother liquor and air-dried. Calc. For [Cu_2(dpyam)$_4$(μ-C_2O_4)](ClO_4)$_2$.3H_2O: C, 43.76; H, 3.67; N, 14.58; Cu, 11.03 %. Found: C, 43.69; H, 3.60; N, 14.61; Cu, 10.87 %.

[Cu_2(dpyam)$_4$(μ-C_2O_4)](PF_6)$_2$ .2H_2O (III)

This compound was prepared by adding a solution (10 ml) of oxalic acid (0.063 g, 0.5 mmol) to a suspension of copper(II) hydroxidcarbonate hydrate (0.221 g, 1.0 mmol) in 10 ml water. The mixture was added by a solution of di-2-pyridylamine (0.342 g, 2.0 mmol) in 20 ml ethanol and potassium hexafluorophosphate (0.184 g, 1.0 mmol) in 10 ml water. The resulting blue solution was filtered to remove impurities. After two weeks, green crystals of **III** were obtained. They were filtered off, washed with mother liquor and were dried in air. Calc. For [Cu_2(dpyam)$_4$(μ-C_2O_4)](PF_6)$_2$.2H_2O: C, 41.15; H, 3.29; N, 13.71; Cu, 10.37 %. Found: C, 41.38; H, 3.36; N, 13.71; Cu, 10.08 %.

[Cu_2(dpyam)$_2$(μ-C_2O_4)(NO_3)$_2$((CH_3)$_2$SO)$_2$] (IV)

A hot dimethylsulfoxide (10 ml) of di-2-pyridylamine (0.342 g, 2.0 mmol) was added to a hot aqueous solution containing copper(II) nitrate trihydrate (0.482 g, 2.0 mmol) and oxalic acid (0.126 g, 1 mmol) in dimethylsulfoxide (23 ml). The green solution was allowed to evaporate at room temperature. After a week, green crystals of **IV** formed. They were filtered off, washed with mother liquor and were dried in air. Calc. For [Cu_2(dpyam)$_2$(μ-C_2O_4)(NO_3)$_2$((CH_3)$_2$SO)$_2$]: C, 37.27; H, 3.61; N, 13.37; Cu, 15.17 %. Found: C, 37.34; H, 3.55; N, 13.44; Cu, 14.37 %.

[Cu_2(dpyam)$_2$(μ-C_2O_4)(NO_3)$_2$(CH_3)$_2$NCOH)$_2$] (V)

A solution containing di-2-pyridylamine (0.342 g, 2.0 mmol) in 10 ml dimethylformamide was added to a solution containing copper(II) nitrate trihydrate (0.482 g, 2.0 mmol) in 20 ml dimethylformamide and sodium oxalate (0.068 g, 0.5 mmol) in 10 ml water. Then 30 ml of dimethylformamide was added and the resulting green solution was filtered to remove impurities.

After four months, green crystals of **V** were obtained which were filtered off, washed with mother liquor and air-dried. Calc. For $[Cu_2(dpyam)_2(\mu\text{-}C_2O_4)(NO_3)_2]$: C, 38.77; H, 2.66; N, 16.44; Cu, 18.65 %. Found: C, 39.17; H, 2.35; N, 15.22; Cu, 17.60 %.

$[Cu_2(dpyam)_2(\mu\text{-}C_2O_4)Cl_2]$ (VI)

A solution of oxalic acid (0.063 g, 0.5 mmol) in 10 ml water was added slowly to a solution containing copper(II) chloride dihydrate (0.170 g, 1.0 mmol) in 40 ml water and di-2-pyridylamine (0.342 g, 2.0 mmol) in 40 ml dimethylformamide. The green solution was allowed to evaporate at room temperature. After a week, green crystals of **VI** were obtained. They were filtered off, washed with mother liquor and air-dried. Calc. For $[Cu_2(dpyam)_2(\mu\text{-}C_2O_4)Cl_2]$: C, 42.05; H, 2.88; N, 13.38; Cu, 20.22 %. Found: C, 41.38; H, 2.86; N, 13.35; Cu, 19.76 %.

$[Cu_2(dpyam)_2(\mu\text{-}C_2O_4)Br_2]$ (VII)

A solution of sodium oxalate in 10 ml water (0.067 g, 0.5 mmol) was added to a solution containing copper(II) bromide (0.223 g, 1.0 mmol) and di-2-pyridylamine (0.342 g, 2 mmol) in 60 ml of 2:1 water/dimethylformamide mixture, yielding a green solution. Slow evaporation of this solution at room temperature, green powder of **VII** formed, was filtered off, washed with mother liquor and dried in air. Calc. For $[Cu_2(dpyam)_2(\mu\text{-}C_2O_4)Br_2]$: C, 36.84; H, 3.53; N, 11.71; Cu, 17.72 %. Found: C, 36.53; H, 3.49; N, 11.68; Cu, 17.32 %.

1.3.3 Crystallography

Reflection data for **I** and **III** were collected at 298 K on a 1K Bruker SMART CCD area–detector diffractometer using graphite monochromated MoK_α radiation (λ = 0.71073 Å) at a detector distance of 4.5 cm and swing angle of –35°. A hemisphere of the reciprocal space was covered by combination of three sets of exposures; each set had a different ϕ angle (0, 88, 180°) and each exposure of 10 s for **I** and 30s for **III** covered 0.3° in ω. Data reduction and cell refinements were performed using the program SAINT[20]. An empirical absorption correction by using the SADABS[21] program was applied, which resulted in transmission coefficients ranging from 0.659 to 1.000 for **I** and 0.5454 to 1.0000 for **III**. The structure was solved by direct methods and refined by full–matrix least–squares method on $(F_{obs})^2$ with anisotropic thermal parameters for all non–hydrogen atoms using the SHELXTL-PC V 6.12[22] software package. All hydrogen atoms were geometrically fixed and allowed to ride on the attached atoms. Two BF_4^- groups and three water molecules are disordered with site occupancies of 0.5 for both conformers.

The hydrogen atoms of the lattice water molecules could not be located at all. For **III**, one of the hydrogen atoms of each lattice water molecule could not be located and the hexafluorophosphate groups are well ordered.

Reflection data for **II** were collected using an Enraf-Nonius MACH3 diffractometer with Mo Ka radiation (λ = 0.70183 Å) at 298 K. An absorption correction was performed by using the Psi-scan program, which resulted in transmission coefficients ranging from 0.917 to 1.000. The structure was solved by direct methods using SHELXS-97[23] and refined by the least-squares method F^2_{obs} using SHELXL-97[24]. The non-hydrogen atoms were located on the E map or successive Fourier difference syntheses and anisotropically refined. All other hydrogen atoms were geometrically fixed and allowed to ride on the attached atoms except the water hydrogen atoms, which could not be located at all. One of the perchlorate groups showed disorder which was resolved in two sets with occupancies of 0.5 for both conformers.

A crystal of compound **IV** was selected and mounted to a glass fiber using the oil-drop method. Data were collected on a Rigaku AFC-7S diffractometer (graphite-monochromated MoKα radiation, ω-2θ scans). The intensity data were corrected for Lorentz and polarization effects, for absorption (psi-scan absorption correction) and extinction. The structures were solved by direct methods. The programs TEXSAN[25], SHELXS-97, SHELXL-97 were used for data reduction, structure solution and structure refinement, respectively. Refinement of F^2 was done against all reflections. The weighted R factor, *wR*, and goodness of fit *S* are based on F^2. Conven tional R factors, R, are based on *F*, with *F* set to zero for negative F^2. All non-H atoms were refined anisotropically. The H atoms were introduced in calculated positions and refined with fixed geometry with respect to their carrier atoms.

Reflection data of **V** were collected on a 4K Bruker SMART APEX CCD area-detector diffractometer with graphite monochromated Mo Kα radiation (λ= 0.71073 Å) (at a detector distance of 6.0 cm and swing angle of -28°) using SMART program. Raw data frame integration was performed with SAINT, which also applied correction for Lorentz and polarization effects. Absorption corrections were applied using SADABS, provided an empirical absorption correction and put the standard deviations of measured intensities onto absolute scale. The structures were solved by direct methods. The software package SHELXTL V 6.12 was used for structure solution and structure refinement. All non-H atoms were refined anisotropically except the nitrate-O atoms and the methyl-C atoms of DMF. The H atoms were introduced in calculated positions and refined with fixed geometry with respect to their carrier atoms. The nitrate groups

are disordered with site occupancies of 0.48 and 0.52 for both conformers. Both methyl groups of the dimethylformamide ligands are also disordered with site occupancies of 0.44 and 0.56 for both conformers and some of the methyl hydrogen atoms could not be located. The crystal and refinement details for complexes **I-V** are listed in Table 1, Appendix IA.

1.4 Results and Discussion

1.4.1 Description of the crystal structures

1.4.1.1 Description of $[Cu_2(dpyam)_4(\mu\text{-}C_2O_4)](BF_4)_2 .3H_2O$ (I) and $[Cu_2(dpyam)_4(\mu\text{-}C_2O_4)](ClO_4)_2 .3H_2O$ (II)

The structures of **I** and **II** are made up of oxalate bridged non-centrosymmetric dinuclear cations $[(dpyam)_2Cu(C_2O_4)Cu(dpyam)_2]_2^+$, non-coordinating BF_4^- and ClO_4^- anions and water molecules of crystallization. The structures are depicted in Figs. 2 and 3 together with the numbering scheme. Selected bond distances and angles are listed in Table 1, Appendix IB.

Compounds **I** and **II** are found to be isomorphous and isostructural, the copper coordination spheres in both complexes display an identical environment. Each copper atom in **I** and **II** has a compressed rhombic octahedral coordination geometry with the equatorial plane formed by two nitrogen atoms from a dpyam ligand and two oxalate-oxygen atoms (Cu-N distances vary from 2.094(6) to 2.145(7)Å and from 2.095(8) to 2.141(9) Å, for **I** and **II** respectively, while Cu-O distances vary from 2.189(8) to 2.252(8) Å and from 2.141(10) to 2.305 (9) Å, for **I** and **II**, respectively). The axial positions are occupied by the other nitrogen atoms of the dpyam ligand (Cu-N distances vary from 2.006(7) to 2.024(6) Å and from 2.000(8) to 2.025 (8) Å , for **I** and **II**, respectively), resulting in the rather unique $CuN_2O_2N_2'$ (4+2) chromophore[5-10]. This axially-compressed octahedral (2+4) geometry[11] is uncommon as most of other dinuclear μ-oxalatodicopper(II) complexes found in literature have five-coordinate geometries. This geometry has only been previously observed in the dinuclear oxalato-bridged Cu^{II} complexes with a tetradentate terminal ligand. This geometry arise due to the flexible nature of the dpyam ligand compared to the bpy, phen or other didentate chelate ligands which are found to have a

square-pyramidal structure with the counter anion or solvent molecule occupying the axial position and the general formula of $[(NN)Cu(\mu\text{-}C_2O_4)Cu(NN)]X_n$, (in which X = counter anion or solvent molecule). Some compounds of this formula present an additional bond to X, giving rise to an axially-elongated octahedral geometry. In addition, the compounds **I** and **II** are two rare examples of 2+4 compressed rhombic coordination resulting from a pseudo Jahn-Teller effect. As in almost all the cases of observed Jahn-Teller compression examined in detail to date, the apparent compression is due to dynamic interconversion between two of the possible axial elongations.

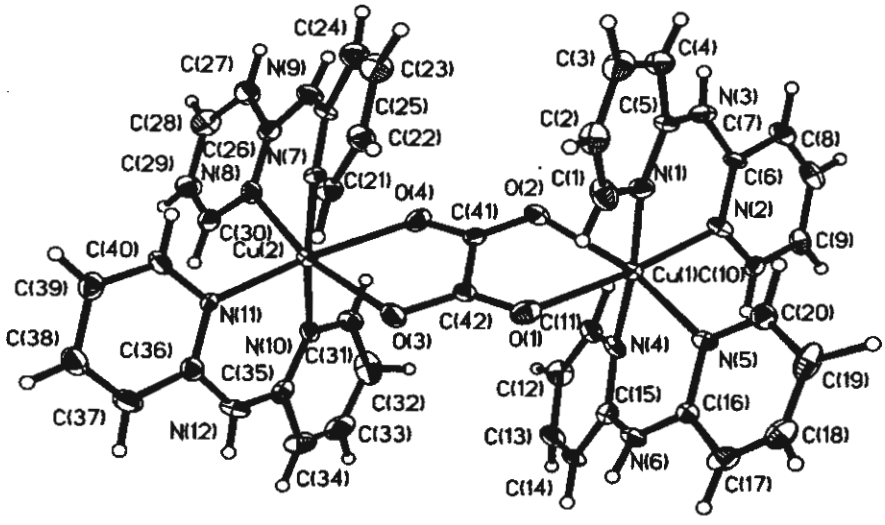

Figure 2 The molecular structure of **I**

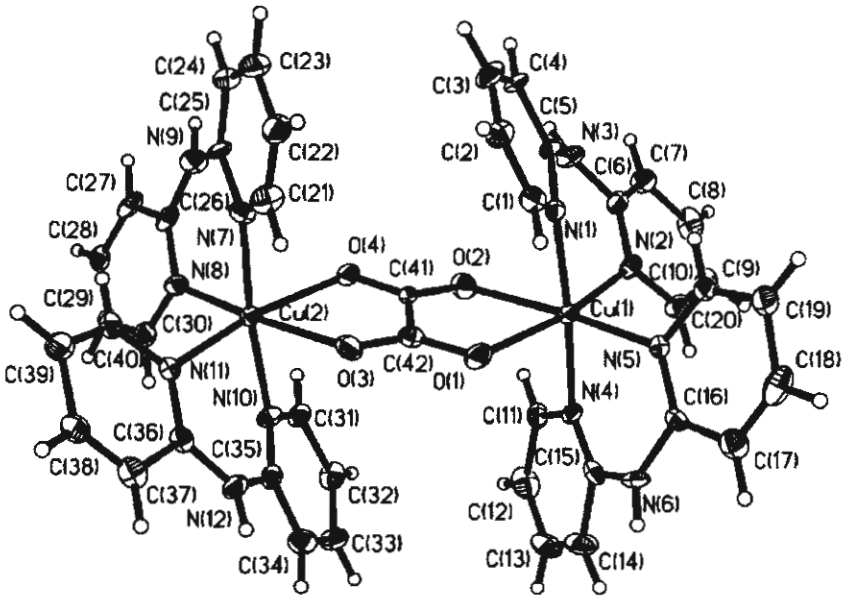

Figure 3 The molecular structure of **II**

For compound **I**, the lattice is stabilized by hydrogen bonding between the amine-N and F_{BF4} (N---F distances 2.974-3.189 Å) and O_{water} (N---O distances 2.750-2.923 Å).

For compound **II**, the lattice is similarity further stabilized by hydrogen bonding between the amine-N and O_{ClO4} (N---O distances 3.059-3.334 Å) and O_{water} (N---O distances 2.828-2.843 Å) and between the O_{water} and O_{ClO4} (O---O distance 3.094 Å) and $O_{oxalate}$ (O---O distance 3.002 Å).

1.4.1.2 Description of $[Cu_2(dpyam)_4(\mu\text{-}C_2O_4)](PF_6)_2 .2H_2O$ (III)

The structure of **III** consists of a noncentrosymmetric dinuclear $[(dpyam)_2Cu(C_2O_4)Cu(dpyam)_2]^{2+}$ cation, two non-coordinated PF_6^- anions and two crystallization water molecules. An ORTEP plot, together with the numbering scheme of the compound is shown in Fig. 4, with relevant distances and angles in Table 2, Appendix IB.

The chromophore of **III** is very similar to the recently published compounds $[Cu_2(dpyam)_4(C_2O_4)](ClO_4)_2(H_2O)_3$ and $[Cu_2(dpyam)_4(C_2O_4)](BF_4)_2(H_2O)_3$. The two copper(II) ions of the complex cation are linked through an oxalato bridge, leading to a Cu…Cu distance of

5.737(2) Å. The copper atoms are involved in the rather unique $CuN_2O_2N'_2$ (4+2) chromophore, and lie in the uncommon compressed rhombic octahedral environment. The equatorial coordination positions are occupied by two oxalate oxygen atoms and two nitrogen atoms of the dpyam ligand (Cu-O and Cu-N distances range from 1.992 to 2.448 Å) and the other two nitrogen atoms from each dpyam ligand in axial positions (Cu-N bond lengths in the range 1.979-2.098 Å). There is a very slight tetrahedral distortion of the equatorial planes [dihedral angles between CuN_2 and CuO_2 planes = 3.2 and 1.2° for Cu(1) and Cu(2) centers, respectively], therefore both four- donor atoms basal planes are planar [r.m.s.d's = 0.0263 and 0.0028 Å] and the copper atom are displaced by 0.0350 and 0.0168 Å from the basal planes toward N(5) and N(11) atoms for the Cu(1) and Cu(2) centers, respectively. The two basal planes are parallel to each other with dihedral angle of 1.4°. The oxalate divalent anion is planar (r.m.s.d = 0.0132) and it bridges the two copper atoms in the nearly symmetric mode of coordination. The copper atoms deviate by 0.2339, -0.1947 Å for the Cu(1) and Cu(2), respectively, from the oxalate plane. The dimeric entity is slightly folded in a chair form, the basal planes make the angles of 7.2 and 5.7° and with the oxalate mean plane.

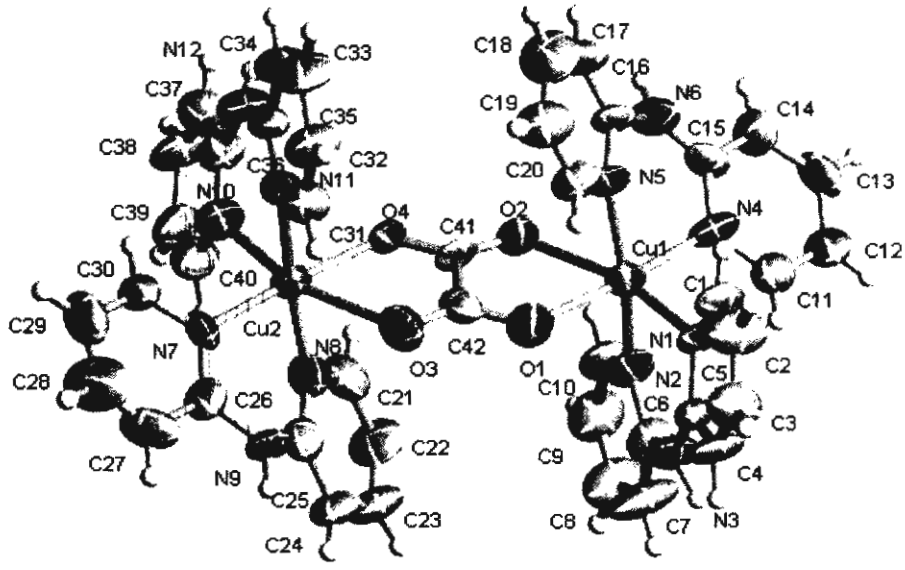

Figure 4 The molecular structure of **III**

The lattice is similarly further stabilized by hydrogen bonding between amine-N and F_{PF6} (N---O distances 3.075 - 3.391 Å) and O_{water} (N---O distances 2.952 - 2.965 Å) and between the O_{water} and F_{PF6} (O---F distance 3.088 Å) and $O_{oxalate}$ (O---O distances 2.956 – 3.348 Å).

1.4.1.3 Description of $[Cu_2(dpyam)_2(\mu\text{-}C_2O_4)(NO_3)_2((CH_3)_2SO)_2]$ (IV)

The structure of **IV** consists of centrosymmetric $[Cu_2(dpyam)_2(\mu\text{-}C_2O_4)(NO_3)_2((CH_3)_2SO)_2]$ molecules. The structures are depicted in Fig. 5 together with the numbering scheme. Selected bond distances and angles are listed in Table 3, Appendix IB. The geometry around the copper atom can be considered as an elongated tetragonal octahedral environment with the equatorial plane CuN_2O_2 formed by two nitrogen atoms of dpyam ligand and two oxygen atoms of oxalate bridge [Cu-N bond lengths = 1.986(2) and 2.002(2) Å; and Cu-O bond lengths = 1.994(2) and 1.998(2) Å], with the axial sites occupied by an oxygen atom of the nitrato groups [Cu-O 2.502 (2) Å] and the oxygen atom of the dimethylsulfoxide group [Cu-O 2.331(2) Å)], giving an approximately $CuN_2O_2O'O''$ chromophore. Both copper atoms are linked through an oxalato bridge, leading to a copper-copper distance of 5.220(2) Å.

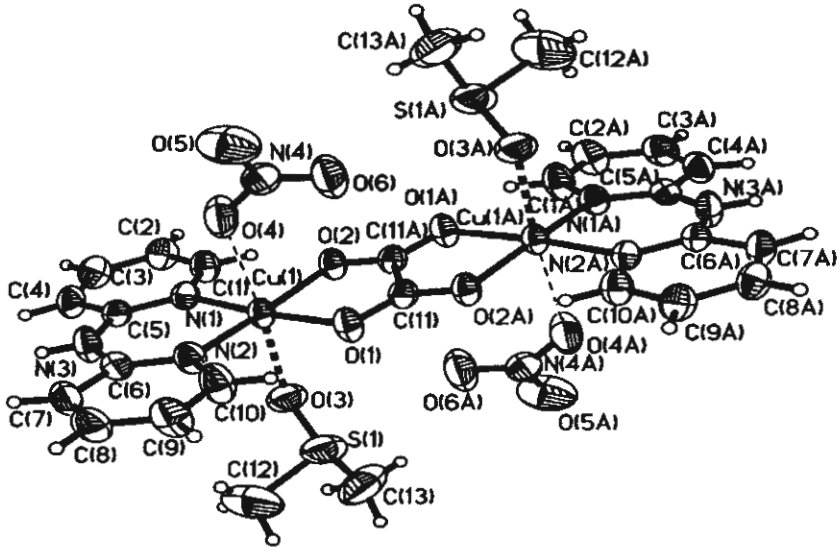

Figure 5 The molecular structure of **IV**

The axial O_2NO-Cu-$OS(CH_3)_2$ angle is 174.8(7)°. The 'bite' angles of dpyam and oxalate ligands are 93.3(1) and 82.3(1)°, respectively. The four donor atoms on the equatorial plane are not perfectly planar, showing a tetrahedral distortion, with dihedral angle of 7.2° formed between the O-Cu-O and N-Cu-N planes. The copper atoms are displaced by 0.0770 and -0.0770 Å from the basal planes toward O(4) and O(4A) atoms for the Cu(1) and Cu(1A) centers, respectively in the opposite side. Two basal planes are exactly parallel to each other.

The oxalate divalent anion is exactly planar due to the inversion center halfway along the bond C(11)-C(11A) and it bridges the two copper atoms in the nearly symmetric mode of coordination. The copper atom deviates by –0.0981 and 0.0981 Å for the Cu(1) and Cu(1A) from the oxalate plane. The equatorial plane makes an angle of 7.0° with the mean plane of the oxalate ligand. As a result, the binuclear complex displays a chairlike structure.

The lattice structure is stabilized by hydrogen bonding between the amine-N and an O (NO_3) of a neighbouring unit with a distance of 2.855 Å, resulting in a polymeric chain.

1.4.1.4 Description of $[Cu_2(dpyam)_2(\mu\text{-}C_2O_4)(NO_3)_2(CH_3)_2NCOH)_2]$ (V)

The asymmetric unit consists of a non-centrosymmetric dinuclear $[Cu_2(dpyam)_2(C_2O_4)(NO_3)_2(C_3H_7NO)_2]$ molecules. A drawing of the dimeric structure showing the labeling scheme is given in Fig. 6. Selected bond lengths and angles are reported in Table 4, Appendix IB.

The compound **V** has two copper centers bridged by a planar bis(didentate) oxalate ligand. The geometry around each copper(II) ion is considered as an elongated octahedral environment with two nitrogen atoms of dpyam and two oxygen atoms of oxalate bridge (Cu-N/O distances 1.956(7)-2.012(6) Å) in the equatorial plane CuN_2O_2, with the axial sites occupied by an oxygen atom of the dimethylformamide group [Cu-O 2.295(7) and 2.254(7) Å] and the oxygen atom of the nitrato group [Cu-O 2.786 and 2.679 Å], giving an approximately $CuN_2O_2O'O''$ chromophore (Fig. 2). The four basal atoms are not coplanar, showing a slight but significant tetrahedral distortion with dihedral angles of 10.2 and 12.4° formed between the O-Cu-O and N-Cu-N planes for Cu(1) and Cu(2) centers, respectively. The copper atoms are displaced by 0.1259 and 0.1530 Å from the basal planes toward O(5) and O(6) atoms for Cu(1) and Cu(2) centers, respectively in the opposite side. The dimeric entity is slightly folded: the equatorial planes make the angles of 12.5 and 15.4° with the mean plane of the oxalate ligand. As a result, the dinuclear

complex displays a chairlike structure. However, because of the copper atoms, the central Cu-OX-Cu core is planar. The copper-copper separation across the oxalate bridge is 5.212 Å. The axial C_3H_7NO-Cu-ONO_2 angles are 165.9 and 168.6°. The copper atoms deviate by –0.2651 and 0.2570 Å for the Cu(1) and Cu(2), respectively from the oxalate planes.

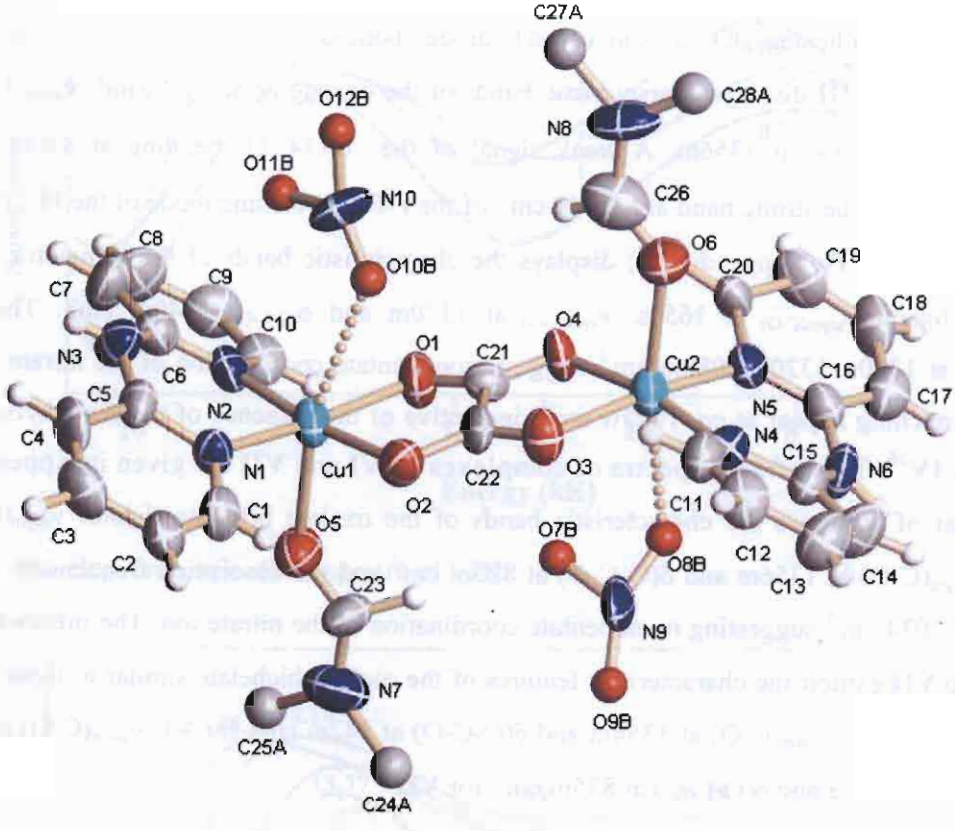

Figure 6 The molecular structure of **V**

The lattice structure is stabilized by hydrogen bonding between the amine-N and the nitrate-O of a neighboring unit with distances of 2.803 – 3.164 Å, resulting in a polymeric chain.

1.4.2 IR spectra

The infrared spectrum of **I** (as in Appendix IC) displays the characteristic bands of the oxalate bridging ligand: ν_{asym}(C-O) at 1649s, ν_{sym}(C-O) at 1374m and δ(O-C-O) at 838m cm^{-1} corresponds to those of other oxalato-bridged copper(II) complexes (Table 6). This indicates that the oxalate ion is present as a bridging quaridentate ligand. The BF_4^- group vibration near 1100

cm^{-1} splitting into a sharp peak at *ca.* 1083 cm^{-1} and a shoulder at *ca.* 1011 cm^{-1}, indicates the BF_4^- ions in **I** involving the hydrogen bonding. A sharp band at *ca.* 3000 cm^{-1} was observed, indicative of the presence of N-H stretching vibrations in this complex. The infrared spectra of complexes **II** and **III** are given in Appendix IC. That of **II** display characteristic bands of the asymmetric oxalate bridging ligand: ν_{asym} (C-O) at 1647s, ν_{sym} (C-O) at 1375m and δ(O-C-O) at 843m cm^{-1}. The ClO_4^- group vibration near 1100 cm^{-1} splitting into three sharp peaks at 1090s, 1116s and 1142s cm^{-1} and, indicates ClO_4^- ions involved hydrogen bonding.

Compound **III** displays characteristic bands of the oxalate bridging ligand: ν_{asym} (C-O) at 1655s and ν_{sym}(C-O) at 1356m. A weak signal of the δ(O-C-O) bending at 850m cm^{-1} is superimposed by the strong band at *ca.* 849 cm^{-1} of the F-P-F stretching mode of the PF_6^- groups.

Compound **IV** (Appendix IC) displays the characteristic bands of the symmetric oxalate bridging ligand $\nu_{asym(C-O)}$ at 1650s, $\nu_{sym(C-O)}$ at 1370m and $\delta_{(O-C-O)}$at 840m cm^{-1}. The bands observed at 1380s, 1320s, 1080m cm^{-1} suggest monodentate coordination of the nitrate ion and the SO stretching appear at *ca.* 1023w cm^{-1}, indicative of the presence of the dimethylsulfoxide ligand in **IV**[26]. The infrared spectra of complexes **V**, **VI** and **VII** are given in Appendix IC.

That of **V** shows the characteristic bands of the oxalate bridging ligand: ν_{asym}(C-O) at 1653s, ν_{sym}(C-O) at 1356m and δ(O-C-O) at 823m cm^{-1} and the absorption frequencies at 1384, 1332 and 1034 cm^{-1} suggesting monodentate coordination of the nitrate ion. The infrared spectra of **VI** and **VII** exhibit the characteristic features of the oxalate bichelate similar to those of **V**: ν_{asym}(C-O) at 1651s, ν_{sym}(C-O) at 1354m and δ(O-C-O) at 842m cm^{-1} for **VI**; ν_{asym}(C-O) at 1659s, ν_{sym}(C-O) at 1361m and δ(O-C-O) at 835m cm^{-1} for **VII**.

1.4.3 Electronic Reflectance spectra

The electronic reflectance spectrum of **I** (Fig. 7) consists of two clearly resolved peaks at 13.97 and 8.70 kK which are very comparable to those of **II** (14.05 and 8.80 kK) and **III** (14.49 and 8.90 kK). These spectra are consistent with the compressed rhombic octahedral stereochemistry and assigned to be the $d_{x^2-y^2} \rightarrow d_{z^2}$ and the d_{xz} , d_{xy}, $d_{yz} \rightarrow d_{z^2}$ transitions.

The electronic reflectance spectra of **IV** and **V** (Fig. 8) show a broad peak center at 14.14 and 14.22 kK, respectively, with a poorly resolved shoulder to low energy at *ca.* 10.18 kK, corresponding to the elongated octahedral geometry. This suggests the assignment of the bands as the d_{xz}, d_{yz}, $d_{xy} \rightarrow d_{x^2-y^2}$ and $d_{z^2} \rightarrow d_{x^2-y^2}$ transitions, respectively. However, there is a comparable

feature in electronic spectra of **VI** and **VII** as in Fig. 8, each adopting a broad band at 13.77 kK, corresponding to the d_{xz}, d_{yz}, d_{xy}, $d_z2 \rightarrow d_{x^2-y^2}$ transition, in agreement with the square pyramidal stereochemistry.

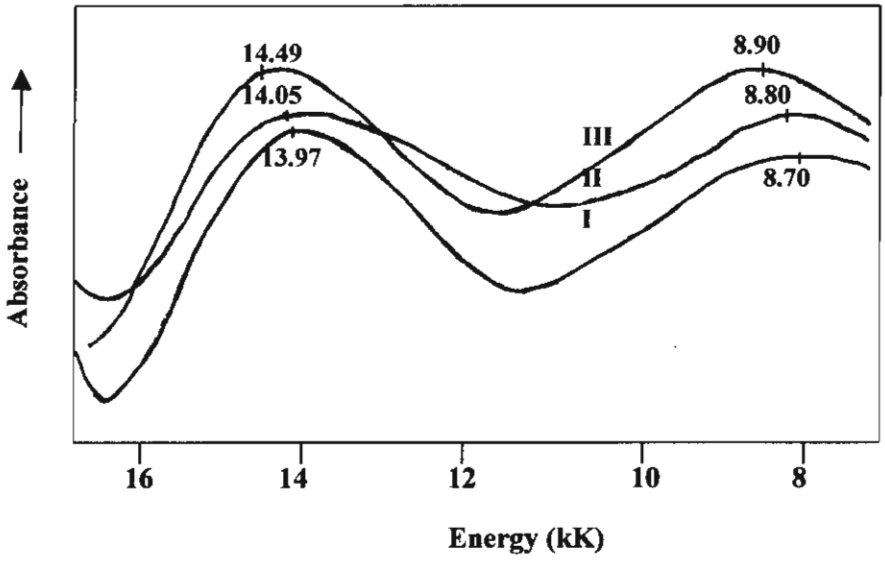

Figure 7 The electronic reflectance spectra of **I-III**

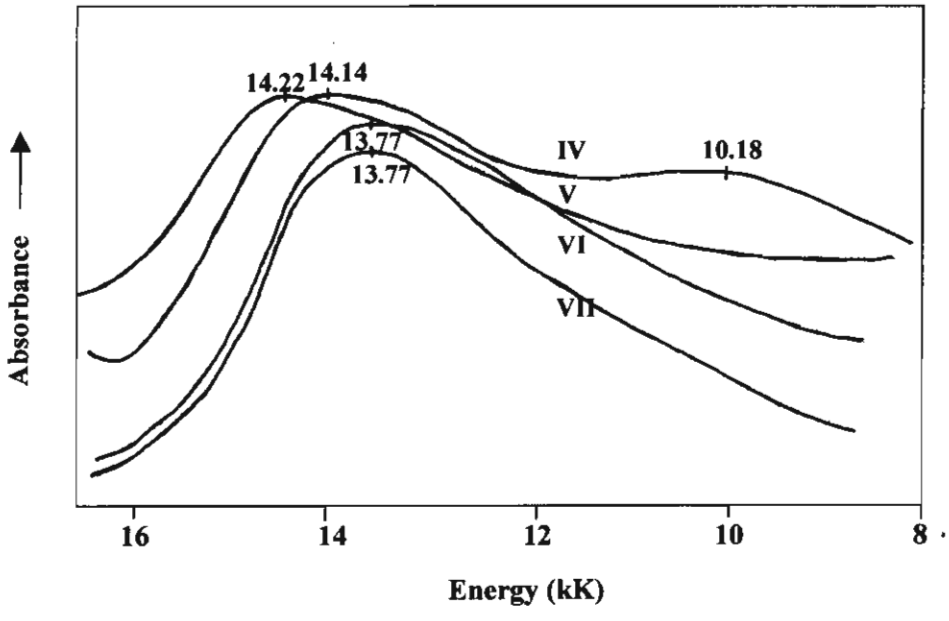

Figure 8 The electronic reflectance spectra of **IV-VII**

1.4.4 EPR spectra

The X-band powder EPR spectrum at room temperature (Appendix ID) of $[Cu_2(dpyam)_4(\mu\text{-}C_2O_4)](BF_4)_2.3H_2O$ (**I**) displays a broad absorption centered around g of 2.14. At the high-field side (g = 1.94) a small shoulder is observed, which is due to a signal from the triplet state with a very small zero field splitting. No half-field signal was observed. Low-temperature (77 K) solid state spectrum of this complex was not sufficiently magnetically diluted as genuine dinuclear spectra. The half-field signal at *ca.* 160 mT of $\Delta M = \pm 2$ transition was observed, which indicates that there is an interaction between two Cu(II) ions within complex **I**. This feature of the EPR bands was also observed in spectra of the analogous μ-oxalato-bridged copper(II) dimer. The EPR spectra of complexes **II** and **III** are given in Appendix ID. The EPR spectrum of complex **II** is similar to that of complex **I** suggesting the magnetic interaction between two copper(II) centers in this dimer. The room temperature X-band powder EPR spectra of compounds **II** and **III** display a broad absorption centered around g of 2.14. At the high-field side (g = approximately 1.94) a small shoulder is observed which is due to a signal from the triplet state with a very small zero-field splitting. No half-field signal was observed at RT. Compounds **II** and **III** were also measured as solids at 77 K, in which cases the signal appears as more resolved with non-split signals at $g_\perp = 2.10$, $g_{//} = 2.27$ for **II** and $g_\perp = 2.05$, $g_{//} = 2.21$ for **III**, corresponding to the pattern of Cu(II) in an elongated geometry, $g_{//} > g_\perp > 2.0$ with the $d_{x^2-y^2}$ ground state. This suggests that the apparent compressed geometry at room temperature could be caused by a dynamic Jahn- Teller effect. This is because compounds **II** and **III** adopt the time averaged structure found crystallographically which arise due to the short time scale of the X-ray technique, but the EPR spectra at 77 K are related to the underlying static axial elongated chromophore. Also the half-field signal at approximately 1600 G, corresponding to $\Delta M \pm 2$ transition was observed, which indicates that indeed a weak interaction between two Cu(II) ions within these compounds is present.

The EPR spectrum at room temperature of $[Cu_2(dpyam)_2(\mu\text{-}C_2O_4)(NO_3)_2((CH_3)_2SO)_2]$ (**IV**) (Appendix ID) displays an asymmetric broad resonance with a center at g = 2.12. The observed triplet signal is not resolved, apparently due to exchange narrowing resulting from nearby triplet molecules in the lattice. Lowering the temperature of the sample to 77 K results in a better resolved spectrum and shows a seven-line hyperfine splitting due to the coupling of the unpaired electrons with two equivalent copper nuclei[7]. A weak resolved signal is observed with $g_\perp = 2.10$,

$g_{//}$ = 2.41, and an average hyperfine spacing A *ca.* 8.8 mT. No half-field signal was observed in this case. So the observed signal is typical for triplet Cu(II) dinuclear in an isolated state. The EPR spectra of complexes **V**, **VI** and **VII** are given in Appendix ID. The room temperature EPR spectrum of **V** appears an asymmetric broad resonance with a center at g = 2.101. The observed triplet signal is not resolved, apparently due to exchange narrowing, resulting from nearby triplet molecules in the lattice. The EPR spectrum recorded at 77 K is better resolved than the room-temperature and shows resolved hyperfine splitting due to the coupling of the unpaired electrons with two equivalent copper nuclei. A weak signal resolved is observed with $g_{//}$ = 2.37 and $g_{\perp}$ = 2.07. The EPR spectra of **VI** and **VII** at room temperature display a broad absorption for monomeric impurity at g= 2.15 for **VI** and 2.16 for **VII**. At 77 K, a seven line copper hyperfine resonance is not resolved with $g_{//}$ = 2.57 and $g_{\perp}$ = 2.11 for **VI**, and $g_{//}$ = 2.45 and $g_{\perp}$ = 2.04 for **VII**, in agreement with the presence of the exchange-couple of unpaired electrons with equivalent copper nuclei.

1.4.5 Magnetic properties and superexchange mechanism

The magnetic susceptibility of $[Cu_2(dpyam)_4(\mu\text{-}C_2O_4)](BF_4)_2.3H_2O$ **(I)** was measured from 5 to 280 K. The temperature dependence of the effective magnetic moment (μ_{eff}) is shown in Fig. 9. At 280 K, μ_{eff} is 2.64 BM, which agrees well with the spin only value of Cu(II) calculated for two uncoupled spin = 1/2 centers. This value slowly increases reaching of 2.80 BM at 5 K, indicating the presence of a very weak ferromagnetically coupled Cu(II) dinuclear compound.

The data for complex **I** was successfully fitted to a modified Bleaney-Bowers expression[27]

$$\chi_m = (2Ng^2\beta^2)[KT-(2zJ'/(3+\exp(-J/KT))]^{-1}[3+\exp(-J/KT)]^{-1}(1-\rho)+ \chi_p\rho$$

for a dinuclear copper(II) complex, where J is the singlet-triplet energy gap defined by the Hamiltonian $H = -JS_AS_B$, with $S_A = S_B = ½$, N, g, β,K and T having their usual meaning, ρ is the percent of non-coupled impurity and zJ' is the interaction between neighbouring dinuclear identities.

Minimization of the expression $R = \Sigma(\chi_{obs}-\chi_{calc})^2/\Sigma\ \chi_{obs}^2$, results in the best fit parameters J = +3.38 cm^{-1}, g = 2.10 and zJ' and ρ = 0 with $R = 2.8\times10^{-3}$, which confirms a very weak ferromagnetic interaction between two Cu(II) ions within this complex.

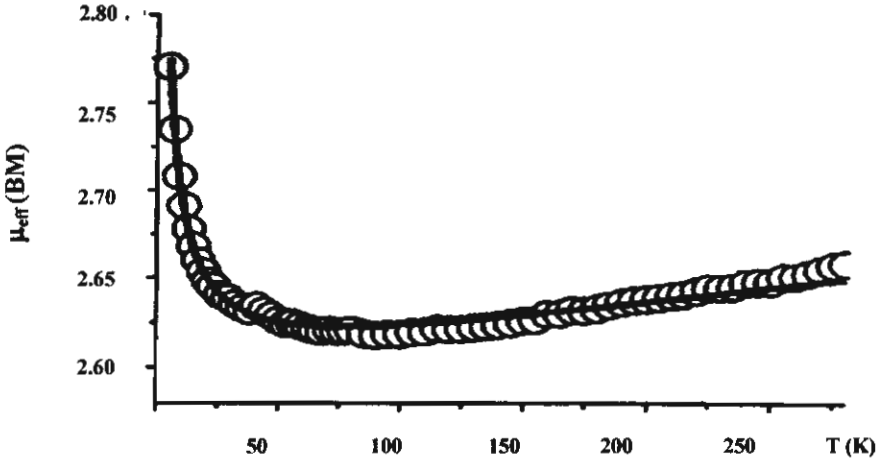

Figure 9 Plots of μ_{eff} vs. T of $[Cu_2(dpyam)_4(\mu\text{-}C_2O_4)](BF_4)_2.3H_2O$ **(I)**

Previous theorethical and experimental works have revealed that the exchange interaction between the copper ions propagated through the oxalate bridge is strongly dependent on the geometry around the copper ions, sensitive to the orientation of the magnetic orbital of each copper(II), relative to the oxalate plane and the bridging mode of the oxalate group, which favours the antiferromagnetic interaction. This interaction is weakened by the not strictly identical coordination geometry around the copper atoms and structural distortions such as the displacement of the copper atom out of the basal plane, the nonplanarity of the Cu-ox-Cu framework and the tetrahedral distortion of the basal plane. That it is well known, the coordinating behavior of the oxalato anion besides the plasticity of the copper(II) ions affords a wide variety of polynuclear copper(II) complexes with oxalato as bridging ligand. Three models predicting the magnetic interactions in oxalato-bridged Cu(II) complexes are shown in Fig. 10. Coordination **mode a**, the unpaired electron is located in a $d_{x^2-y^2}$ type orbital which is contributed from the square planar, square pyramidal or elongated octahedral geometry, with the oxalato anion occupying two basal positions, they are coplanar. The $d_{x^2-y^2}$ magnetic orbitals will be ideally directed toward the oxalate σ orbitals, and the antiferromagnetic interaction will be maximized. However, a variety of factors influencing the interaction in dinuclear complexes, such as, the metal-metal separation, the dihedral angle between the planes containing the magnetic orbitals, the metal bridged ligand bonds and angles, the metal ion stereochemistry, the terminal ligand basicity, etc [J from –41 to –400 cm^{-1}]. For **mode b**, the oxalato bridge is occupying axial and equatorial coordination sites (in short, "axial – equatorial" dimers), the two

metal centered $d_{x^2-y^2}$ magnetic orbitals are parallel but perpendicular to the bridging oxalato ligand, and consequently the magnetic coupling is very weak [J from +3 to –45 cm^{-1}]. Finally, for **mode c**, the magnetic orbitals can be described by d_{z^2} orbitals (which is contributed from the compressed octahedral or trigonal pyramidal geometry) perpendicular to the oxalate σ orbitals. Hence, the magnetic orbitals have a poor overlap with oxalate σ orbitals, leading to very weak and of the ferro- or antiferro-magnetic interaction [J from +2 to –37 cm^{-1}].

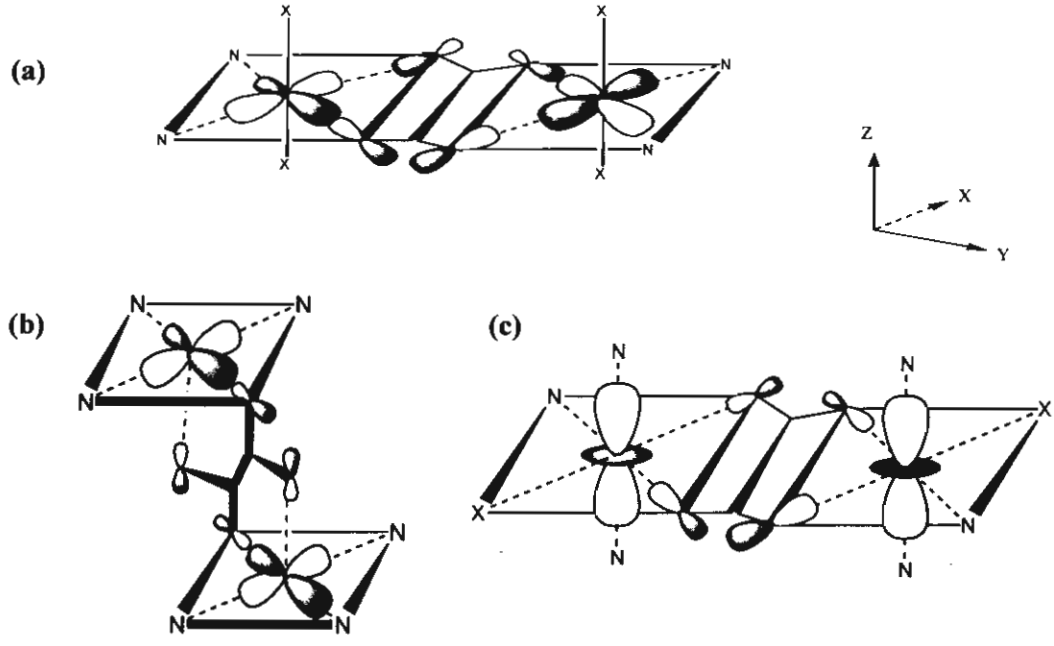

Figure 10 Three models predicting the magnetic interactions in oxalato-bridged Cu(II) complexes, X=O (1) or N (2)

Complexes **I** and **II** involve the compressed rhombic octahedral geometry, which the unpaired electrons of the Cu centers are not in $d_{x^2-y^2}$ orbitals but rather in d_{z^2} orbitals. Therefore magnetic orbitals are perpendicular to the oxalate plane, hence overlap very poorly with the oxalate σ orbitals. This situation is corresponding to the coordination **mode c** and consequently a weakness of the ferromagnetic interaction, with the singlet-triplet energy gap (J) of +3.38 cm^{-1} for **I** and +2.42 cm^{-1} for **II**.

The structure and structural distortions of compound **III** is very comparable to those of compounds **I** and **II**. Thus **III** is suggested to exhibit a very weak ferromagnetic interaction.

However, the room temperature magnetic moments of **I-III** (2.64, 2.62 and 2.55 BM, respectively) are in the typical range of the uncoupled Cu(II) ions at this temperature.

The structural data and magnetic properties of some of the corresponding complexes are compared as in Table 1.

The temperature dependence of the molar magnetic susceptibility χ_m of **IV**, measured on a powdered sample, is shown in Fig. 11. At 280 K, χ_m is equal to $1.6x10^{-3}$ cm^3mol^{-1} and decreases when cooling down and reaches almost zero at about 40 K. From 40 K to 5 K the χ_m increase a little to $0.4x10^{-3}$ cm^3mol^{-1}. The singlet-triplet energy gap (J) was deduced from least-squares fit of the experimental data to the temperature dependence of the molar magnetic susceptibility χ_m expressed according to the Bleany-Bowers equation[27] for isotropic exchange in a copper(II) dimer.

$$\chi_m = (2Ng^2\beta^2)[KT-(2zJ'/(3+\exp(-J/KT))]^{-1}[3+\exp(-J/KT)]^{-1}(1-\rho)+ \chi_p\rho$$

This equation has been modified to take into account admixture of paramagnetic impurity, where the symbols have their usual meaning and ρ is fraction of non-coupled impurity. Minimization of the expression $R = \Sigma(\chi_{obs}-\chi_{calc})^2/\Sigma\ \chi_{obs}^2$, resulted in the best-fit parameters J = -305.1 cm^{-1}, g = 2.14 , zJ' = 0.07 and $\rho = 1x10^{-2}$ with R about 0.6 %, which confirms the strong antiferromagnetic type of the interaction. The measurements were repeated several times, but special in the high temperature area the fit is not so good, resulting in a somewhat high R value.

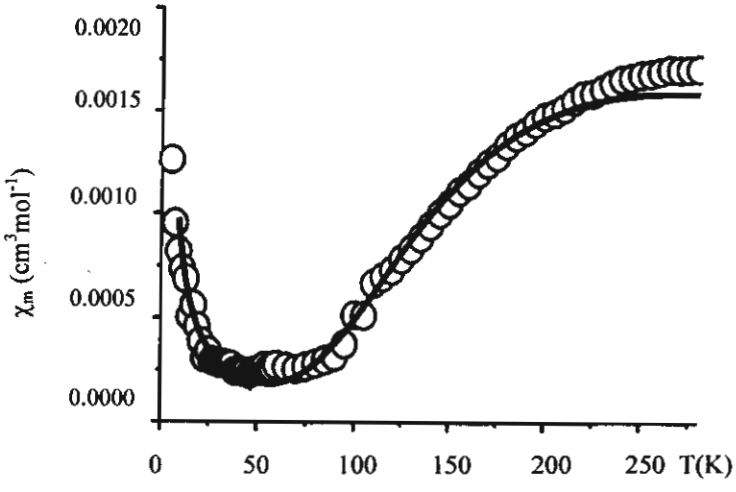

Figure 11 Plots of χ_m vs. T of $[Cu_2(dpyam)_2(C_2O_4)(NO_3)_2((CH_3)_2(SO)_2]$ **(IV)**

Table 1. Structural data and the singlet-triplet energy gap for octahedral oxalato-bridge copper(II) complexes

compound[a]	donor set	local geometry[b]	oxalato-bridged [c] coordination	h_{Cu} (Å)	d_{Cu-Cu} (Å)	dihedral angle[c]	J (cm^{-1})	Ref.
$[Cu_2(dpyam)_4(\mu\text{-}C_2O_4)](BF_4)_2.3H_2O$ **(I)**	$O_2N_2N_2'$	comp.Oct.	eq-eq	-0.05 0.024	5.745	11.4 11.0	3.38	This work
$[Cu_2(dpyam)_4(\mu\text{-}C_2O_4)](ClO_4)_2.3H_2O$ **(II)**	$O_2N_2N_2'$	comp.Oct.	eq-eq	-0.14 0.044	5.752	11.3 11.3	2.42	This work
$[Cu_2(dpyam)_4(\mu\text{-}C_2O_4)](PF_6)_2.2H_2O$ **(III)**	$O_2N_2N_2'$	comp.Oct.	eq-eq	0.028 -0.013	5.737	7.16 5.73	-	This work
$[Cu_2(bpy)_2(\mu\text{-}C_2O_4)(NO_3)_2(H_2O)_2]$ **(VIII)**	$O_2N_2O'O''$	elong.Oct	eq-eq	0.113	5.143	4.6	-382	5
$[Cu_2(mpym)_2(\mu\text{-}C_2O_4)(NO_3)_2(H_2O)_2]$ **(IX)**	$O_2N_2O'O''$	elong.Oct	eq-eq	0.122 0.065	5.217	d	-142	7
$[Cu_2(deen)_2(\mu\text{-}C_2O_4)(ClO_4)_2(H_2O)_2]$ **(X)**	$O_2N_2O'O''$	elong.Oct	eq-eq	d	d	3.88	-300	8
$[Cu_2(tacn)_2(\mu\text{-}C_2O_4)(ClO_4)_2]$ **(XI)**	O_2N_3O'	elong.Oct	eq-eq	0.043 0.049	5.176	d	-41	9
$[Cu_2(bpca)_2(\mu\text{-}C_2O_4)(H_2O)_2].2H_2O$ **(XII)**	O_2N_3O'	elong.Oct	ax-eq	0.048	5.631	d	1.1	6
$[Cu_2(bispicen)_2(\mu\text{-}C_2O_4)](ClO_4)_2$ **(XIII)**	$O_2N_2N'_2$	comp.Oct.	eq-eq	d	5.608	d	2.3	11
$[Cu_2(bispicMe_2en)_2(\mu\text{-}C_2O_4)](ClO_4)_2$ **(XIV)**	$O_2N_2N'_2$	comp.Oct.	eq-eq	d	5.494	d	2.14	11

[a] dpyam = di-2-pyridylamine; bpy = 2,2'-dipyridine; mpym = meripirizole; deen = N,N-diethylethane-1,2-diamine; tacn = 1,4,7-triazacyclononane; bpca = bis(2-pyridylmethyl)1-3,3-propanediamine; bispicen = N,N'-bis(2-pyridylmethyl)-1,2-ethanediamine; bispicMe$_2$en = N,N'-bis(2-pyridylmethyl)-N-N-dimethyl-1,2-ethanediamine, [b] com.Oct = Compressed Octahedral; elong. Oct. = elongated octahedral, [c] dihedral angle between the basal and oxalate planes, [d] = not reported.

Compound **IV** exhibits an elongated octahedral geometry. In this case the unpaired electrons of the Cu centers are in d_{x2-y2} orbitals. There are well oriented to interact with the oxalate σ orbitals, which is consistent with the coordination **mode a** (Fig. 10) and the maximized antiferromagnetic interaction is expected. However, the magnetic exchange interaction may be slightly weakened by the structural distortion such as the displacement of the copper atom out of the basal plane (-0.077 and 0.077 Å), the tetrahedral distortion of the basal plane (7.2°), the copper atom deviation from the oxalate plane (-0.098 and +0.098 Å), and the dihedral angle of 7.0° between the basal plane and the oxalate plane. Thus **IV** exhibits a strongly antiferromagnetic interaction, which is confirmed by the magnetic susceptibility measurements presented above and also with similar cases known in the literature[14, 16, 18].

The structure and structural distortions of compound **V** is very comparable to those of compound **IV**. Thus **V** is predicted to exhibit a very strong antiferromagnetic interaction. However, the room temperature magnetic moments of both compounds (2.03 and 2.16 BM for **IV** and **V**, respectively) are in the typical range for the uncoupled Cu(II) ions at this temperature.

The structural data and magnetic properties of some of the corresponding complexes are compared as in Table 2. Fig. 12 displays the schematic drawing of the copper chromophore geometries for this complex system.

Table 2 Structural data and the singlet-triplet energy gap for oxalato- bridged copper(II) dimers

compounds[a]	donor set	local geometry[b]	oxalato-bridged coordination	h_{Cu} (Å)	d_{Cu-Cu} (Å)	dihedral angle (°)[c]	J (cm^{-1})	Ref.
$[Cu_2(dpyam)_2(\mu\text{-}C_2O_4)(NO_3)_2((CH_3)_2SO)_2]$ **(IV)**	$O_2N_2O'O''$	elong.Oct.	eq-eq	-0.08 0.077	5.220	7	-301	This work
$[Cu_2(dpyam)_2(\mu\text{-}C_2O_4)(NO_3(CH_3)_2NCOH)_2)_2]$ **(V)**	$O_2N_2O'O''$	elong.Oct.	eq-eq	0.125 -0.156	5.213	9.9 12.8	-	This work
$[Cu_2(dpyam)_2(\mu\text{-}C_2O_4)\ Cl_2]$ **(VI)**	O_2N_2Cl	SP	eq-eq	-	-	-	-	This work
$[Cu_2(dpyam)_2(\mu\text{-}C_2O_4)\ Br_2]$ **(VII)**	O_2N_2Br	SP	eq-eq	-	-	-	-	This work
$[Cu_2(bdpm)_2(\mu\text{-}C_2O_4)(H_2O)_2](ClO_4)_2.H_2O$ **(XV)**	O_2N_2O	SP	eq-eq	0.327	5.194	d	-102	9
$[Cu_2(phen)_2(\mu\text{-}C_2O_4)(NO_3)_2$ **(XVI)**	O_2N_2O	SP	eq-eq	0.27	5.158	d	-330	16
$[Cu_2(tmen)_2(\mu\text{-}C_2O_4)(H_2O)_2](ClO_4)_2.1.25H_2O$ **(XVII)**	O_2N_2O	SP	eq-eq	0.147 0.182	5.147	d	-385	7
$[Cu_2(Me_4en)_2(\mu\text{-}C_2O_4)(H_2O)_2](PF_6)_2.2H_2O$ **(XVIII)**	O_2N_2O	SP	eq-eq	0.208	5.232	d	- (μ = 1.4 BM)	19
$[Cu_2(Et_5dien)_2(\mu\text{-}C_2O_4)](PF_6)_2$ **(XIX)**	O_2N_3	SP-TBP	eq-eq	0.218	5.457	d	- (μ = 1.8 BM)	19
$[Cu_2(dien)_2(\mu\text{-}C_2O_4)(NO_3)_2$ **(XX)**	$OO'N_3$	SP	eq-ax	0.138 0.167	5.489	d	-6.5	5
$[Cu_2(bpca)_2(\mu\text{-}C_2O_4)]$ **(XXI)**	$OO'N_3$	SP	eq-ax	-	5.442	d	+1.1	6
$[Cu_2(mpz)_2(\mu\text{-}C_2O_4)(H_2O)_2](PF_6)_2.mpz.3H_2O$ **(XXII)**	O_2N_2O	SP	eq-eq	0.24	5.175	d	-201	12
$[Cu_2(Et2dien)_2(\mu\text{-}C_2O_4)](BPh_4)_2$ **(XXIII)**	$OO'N_2O$	TBP	eq-ax	0.005	5.410	d	-37.4	12

[a] dpyam = di-2-pyridylamine; bdpm = bis(3,5-dimethylparazol-l-yl)methane; phen = 1,10 phenanthroline; tmen = N,N,N',N'-tatramethylethylenediamine; Me_4en = N,N,N',N'- tatramethylendiamine; Et_5dien = N,N,N',N",N"-pentaethylenediamine; bpca =bis(2-pyridylmethyl)1-3,3-propanediamine; mpz = 4-methoxy-2-(5-methoxy 3-methyl-parazol-l-ly)6-methylpyrimidine), [b] elong. Oct. = elongated octahedral; SP = square pyramidal; TBP = trigonal bipyramidal, [c] dihedral angle between the basal and oxalate planes, [d] = not reported.

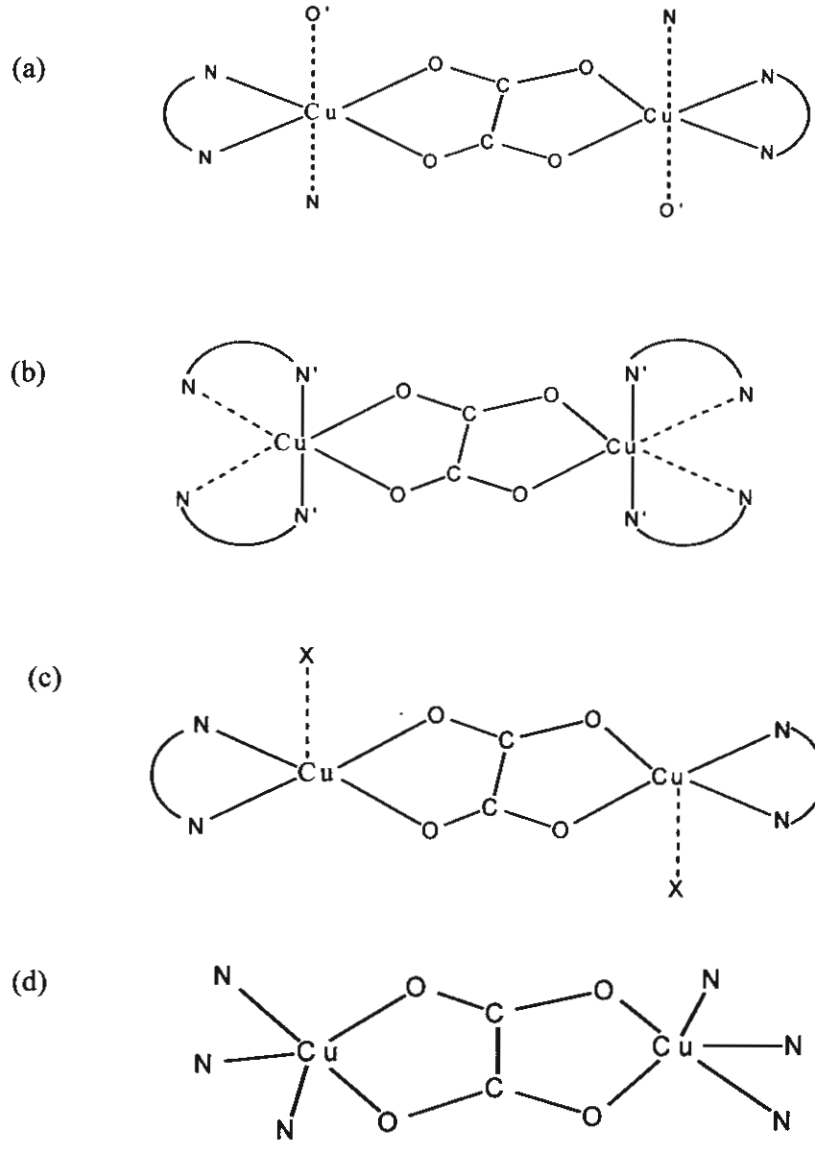

Figure 12 Schematic drawing of

(a) The elongated octahedral CuN_3O_2O' chromophore

(b) The compressed octahedral $CuN_2O_2N_2'$ chromophore

(c) The square-pyramidal CuN_2O_2X chromophore

(d) The trigonal-bipyramidal CuN_3O_2 chromophore

1.4.6 The proposed stereochemistry and magnetic properties of VI and VII

1.4.6.1 Infrared and electronic diffuse reflectance spectra

The infrared spectra of **VI** and **VII** exhibit the characteristic features of the oxalate bichelate similar to those of **V**: ν_{asym}(C-O) at 1651s, ν_{sym}(C-O) at 1354m and δ(O-C-O) at 842m cm^{-1} for **VI**; ν_{asym}(C-O) at 1659s, ν_{sym}(C-O) at 1361m and δ(O-C-O) at 835m cm^{-1} for **VII**.

The electronic diffuse reflectance spectra of **VI** and **VII** show a broad band at 13.37 kK for each compound, corresponding to the d_{z2}, d_{xz}, d_{xy}, d_{yz} $\rightarrow$ d_{x2-y2} transition of the square pyramidal stereochemistry. The proposed stereochemistry of both complexes are given as in Figures 13(a) and (b), respectively.

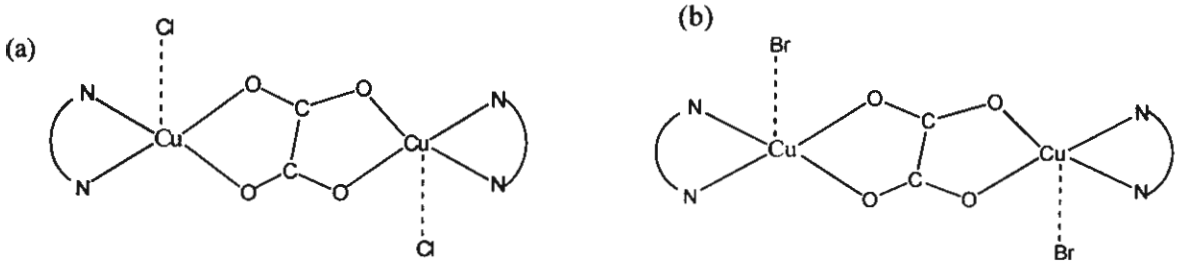

Figure 13 The proposed stereochemistry of (a) $[Cu_2(dpyam)_2(\mu\text{-}C_2O_4)Cl_2]$ **(VI)**, and (b) $[Cu_2(dpyam)_2(\mu\text{-}C_2O_4)Br_2]$ **(VII)**

1.4.6.2 EPR spectra and magnetic properties

The EPR spectra of **VI** and **VII** at room temperature display a broad absorption for monomeric impurity at g= 2.15 for **VI** and 2.16 for **VII**. At 77 K, a seven line copper hyperfine resonance is not resolved with $g_{//} = 2.57$ and $g_{\perp} = 2.11$ for **VI**, and $g_{//} = 2.45$ and $g_{\perp} = 2.04$ for **VII**, in agreement with the presence of the exchange-couple of unpaired electrons with equivalent copper nuclei. The effective magnetic moments at room temperature of complexes **VI** and **VII** were measured to be 2.17 and 2.13 BM, respectively, which are comparable to the values of **IV** and **V** (2.03 and 2.16 BM, respectively). These values are less than the value of 2.45 BM expected for two noninteracting d^9 Cu(II) ions. Therefore complexes **VI** and **VII** are predicted to exhibit a strong antiferromagnetic interaction between copper(II) ions of a dimeric unit.

1.5 Conclusions

The first part of this research sets out to examine and develop the preparative work of a series of dinuclear oxalato-bridged copper(II) complexes with the di-2-pyridylamine as the terminal ligand. The spectroscopic and magnetic characterization, the X-ray crystal structure and the magneto-structural correlation of the complex system are investigated and discussed in comparison with other relevant complexes.

The dinuclear oxalato-bridged copper(II) complexes $[Cu_2(dpyam)_4(\mu\text{-}C_2O_4)](BF_4)_2.3H_2O$ **(I)**, $[Cu_2(dpyam)_4(\mu\text{-}C_2O_4)](ClO_4)_2.3H_2O$ **(II)**, $[Cu_2(dpyam)_4(\mu\text{-}C_2O_4)](PF_6)_2.2H_2O$ **(III)**, $[Cu_2(dpyam)_2(\mu\text{-}C_2O_4)(NO_3)_2((CH_3)_2SO)_2]$ **(IV)**, $[Cu_2(dpyam)_2(\mu\text{-}C_2O_4)(NO_3)_2(CH_3)_2NCOH)_2]$ **(V)**, $[Cu_2(dpyam)_2(\mu\text{-}C_2O_4)Cl_2]$ **(VI)** and $[Cu_2(dpyam)_2(\mu\text{-}C_2O_4)Br_2]$ **(VII)** were prepared directly from the mole ratio in different conditions. Good quality single crystals for X-ray analyses of complexes **I-V** were obtained. All product were analysed by elemental microanalyses and characterized spectroscopically (IR, EPR, solid state VIS). The room temperature magnetic moment of all products and the temperature variable magnetic susceptibilities (5-280 K) of complexes **I**, **II** and **IV** are investigated and discussed together with the magneto-structural correlation and superexchange pathways.

The crystal structures of **I-V** are characterized crystallographically, while those of **VI** and **VII** have been proposed by their spectroscopic properties. Complexes **I-V** contain six-coordinate copper centers bridged by planar oxalate groups from the equatorial position of one chromophore to the equatorial position of the other one. Each copper chromophore in **I-III** exhibits the compressed rhombic octahedral geometry, whereas **IV-V** display an elongated tetragonal octahedral environment. Those of **VI** and **VII** have been proposed from the spectroscopic properties having the square pyramidal geometry of the CuN_2O_2X chromophore.

Compounds **I** and **II** have the singlet-triplet energy gaps J = +3.38 and +2.42 cm^{-1}, respectively, which confirms a very weak ferromagnetic interaction between two Cu(II) ions within these complexes. Both compounds involve the compressed rhombic octahedral geometry, which the unpaired electrons of the Cu centres are not in d_{x2-y2} orbital but rather in d_{z2} orbitals. Therefore, magnetic orbitals are perpendicular to the oxalate plane, hence overlap very poorly with the oxalato σ orbitals, resulting in a weakness of the ferromagnetic interaction. In contrast, **IV** has the J value of -305.1 cm^{-1} which is distinct both in the sign and magnitude of the J value which indicates the strong antiferromagnetic interaction between two Cu(II) centres within this complex. As **IV** exhibits an elongated octahedral geometry, the unpaired electrons of the Cu

centres are in d_{x2-y2} orbitals. Hence, there are well oriented to interact with the oxalate σ orbitals and the maximized antiferromagnetic interaction is expected. However, the magnetic exchange interaction may be slightly weakened by the structural distortion such as the displacement of the copper atom out of the basal plane (-0.077 and 0.077 Å), the tetrahedral distortion of the basal plane (7.2°), the copper atom deviation from the oxalate plane (-0.098 and +0.098 Å), and the dihedral angle of 7.0° between the basal plane and the oxalate plane. It is noted that the structure and structural distortion of **III** is very comparable to those of **I** and **II**, and that of **V** is very similar to that of **IV**. Thus **III** and **V** are predicted to have a very weak ferromagnetic and strong antiferromagnetic interaction, respectively.

Parts of the results of this complex system have been published[28-29].

References

1. Hernández-Molina M, Lorenzo-Luis PA, Ruiz-Pérez C. ***Cryst. Eng. Comm.*** 2001; 16:1-8.
2. Castillo O, Luque A, Iglesias S, Guzmán-Miralles C, Román P. ***Inorg. Chem. Comm.*** 2001; 4: 640-642.
3. Kou H-Z, Liao D-Z, Yang G-M, Cheng P, Jiang Z-H, Yan S-P, Wang G-L,Yao X-K, Wang H-G. ***Polyhedron*** 1998; 18(17): 3193-3199.
4. Núñez H, Timor J-J, Server-Carrió J, Soto L, Escrivá E. ***Inorg. Chim. Acta*** 2001; 318: 8-14.
5. Castillo O, Muga I, Luque A, Gutiérrez-Zorrilla JM, Sertucha J, Vitoria P, Román P. ***Polyhedron*** 1999; 18: 1235-1245.
6. Calatayud ML, Castro I, Sletten J, Lloret F, Julve M. ***Inorg. Chim. Acta*** 2000; 300-302: 846-854.
7. Tuero LS, Garcia-Lozano J, Monto EE, Borja MB, Dahan F, Tuchagues J-P, Legros J-P. ***J. Chem. soc., Dalton Trans*** 1991; 2619-2624.
8. Vicente R, Escuer A, Ferretjans J, Stoeckli-Evans H, Solans X, Font-Bardía M. ***J. Chem. Soc., Dalton Trans*** 1997: 167-171.
9. Zhang L, Bu W-M, Yan S-P, Jiang Z-H, Liao D-Z, Wang GL. ***Ployhedron*** 2000; 19: 1105-1110.
10. Tang J, Gao E, Bu W, Liao D, Yan S, Jiang Z,Wang G. ***J. Mol. Struct.*** 2000; 525: 271-275.
11. Glerup J, Goodson PA, Hodgson DJ, Michelsen K. ***Inorg. Chem.*** 1995; 34: 6255-6264.
12. Alvarez S, Julve M, Verdaguer M. ***Inorg. Chem.*** 1990; 29: 4500-4507.

13. Julve M, Faus J, Verdaguer M, Gleizes A. ***J. Am. Chem. Soc.*** 1984; 106: 8306-8308.
14. Julve M, Verdaguer M, Gleizes A, Philoche-Levisalles M, Kahn O. ***Inorg. Chem.*** 1984; 23: 3808-3818.
15. Hall GR, Duggan DM, Hendrickson DN. ***Inorg. Chem.*** 1975; 8(14): 6255-6264.
16. Bencini A, Fabretti AC, Zanchini C, Zannini P. ***Inorg. Chem.*** 1987; 26: 1445-1449.
17. Julve M, Verdaguer M, Kahn O, Gleizes A, Philoche-Levisalles M. ***Inorg. Chem.*** 1983; 22: 368-370.
18. Soto L, Garcia J, Escriva E, Legros J-P, Tuchagues J-P, Dahan F, Fuertes A. ***Inorg. Chem.*** 1989; 28: 3378-3386.
19. Sletten J. ***Acta Chem. Scand. A*** 1983; 37: 569-578.
20. Bruker. ***SAINT, Data Integration Software, Version 5.6,*** Bruker Analytical X-Ray Systems, Inc., Madison, Wisconsin, USA: 2000.
21. Bruker. ***SADABS, Program for Empirical Absorption correction of Area Detector Data, Version 5.6,*** Bruker Analytical X-Ray Systems, Inc., Madison, Wisconsin, USA: 2000.
22. Bruker. ***SHELXTL (PC-Version): Program Library for the Solution and Molecular Graphics, Version 6.12,*** Bruker Analytical X-Ray Systems, Inc., Madison, Wisconsin, USA: 2000.
23. Sheldrick GM. ***SHELXS-97: Program for the Solution of Crystal Structures***. University of Göttingen; 1997.
24. Sheldrick GM. ***SHELXL-97: Program for the Refinement of Crystal Structures***. University of Göttingen: Germany; 1997.
25. ***Texsan. Single Crystal Structure Analysis Software, Version 1.6, Molecular structure Corporation***, The Woodlands, TX. 77381, USA.1993.
26. Nakamoto K. ***Infrared and raman spectra of inorganic and coordination compounds.*** New York: John Wiley & Sons, Inc; 1997.
27. Abragam A, Bleaney B. ***Electronic Paramagnetic Resonance of Transition Ions.*** Oxford: Clarendon; 1970.
28. Youngme S, van Albada GA, Chaichit N, Gunnasoot P, Kongsaeree P, Mutikainen I, Roubeau O, Reedijk J, Turpeinen U. ***Inorg. Chim. Acta,*** 2003; 353: 119.
29. Youngme S, Gunnasoot P, Chaichit N, Pakawatchai C. ***Trans. Metal Chem.*** 2004; 29: 840.

Part II

Synthesis, Crystal Structure, Spectroscopic and Magnetic Properties of Hydrogenphosphato- bridged Polynuclear Copper(II) Complexes

2

Synthesis, Crystal Structure, Spectroscopic and Magnetic Properties of Hydrogenphosphato- bridged Polynuclear Copper(II) Complexes

2.1 Introduction

The hydrogenphosphate anion is a versatile ligand, having the wide variety of topologies for coordination geometries with transition metal ions. The hydrogenphosphate ion has been proven to be a bridging ligand to design inorganic-organic hybrid materials and many hydrogenphosphato-bridged complexes have been prepared and characterized[1-24]. Ten different coordination modes of hydrogenphosphate ligand have been reported for the hydrogenphosphato transition metal complexes (Fig. 1)[9-24]. The coordination **modes a, b, c** and **f** (Fig. 1a, b, c and f) are commonly observed.

The synthesis of open-framework metal phosphates has been a subject of intense research owing to their interesting structural chemistry and potential applications as ion-exchangers, catalysts, adsorbents, electrical and magnetic properties[2, 11]. A large number of these materials are synthesised in the presence of organic amines as structure directing (templating) agents. Recently, many research activities have focused on the synthesis of organic–inorganic hybrid frameworks, such as phosphates of transition metals[18–19]. As compared with organic ligands, the advantage of using inorganic multidentate anionic ligands in combination with organic polar molecules and ligands is the efficacy of rational design of crystalline solids through their coordinating properties and geometries. So far the most extensively studied bridging organic ligand with transition metals and phosphate is 4,4'-bipyridine[4-8], 2,2'-bipyridine[20] and 1,10-phenanthroline[16] with a number of one-, two- and three- dimensional structures. Now we have extended this research by using the ligand di-2-pyridylamine (abbreviated as dpyam) and have isolated several new phases in such organic–inorganic metal-phosphate systems. In the present study, six new examples of the dpyam-phosphate system, $\{[Cu_3(dpyam)_3(\mu_3,\eta^3\text{-}HPO_4)(\mu_3,\eta^4\text{-}PO_4)(H_2O)](PF_6)\cdot 3H_2O\}_n$ **(I)**, $[Cu(dpyam)(\mu_2,\eta^3\text{-}HPO_4)]_n$ **(II)**, $[Cu(dpyam)(\mu_2,\eta^2\text{-}H_2PO_4)(H_2PO_4)]_2$ **(III)**, $[Cu_4(dpyam)_4(\mu_4,\eta^3\text{-}HPO_4)_2(\mu\text{-}Cl)_2]X_2$, X = Cl $\cdot 6H_2O$ **(IV)** and Br $\cdot 6H_2O$ **(V)** and $[Cu_4(dpyam)_4(\mu_3,\eta^3\text{-}HPO_4)_2(NO_3)_2(H_2O)_2](NO_3)_2\cdot 2H_2O$ **(VI)** are reported.

a. 1L, 1M

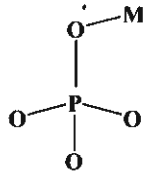

b. 1L, 2M

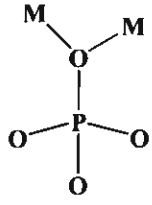

c. 2L, 2M

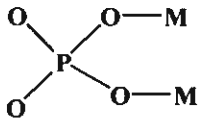

d. 4L, 2M

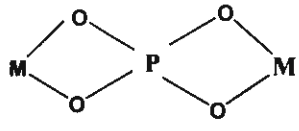

e. 3L, 3M

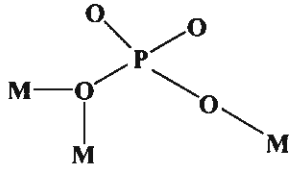

f. 3L, 3M

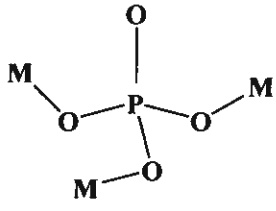

g. 3L, 3M

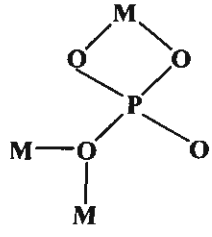

h. 3L, 6M

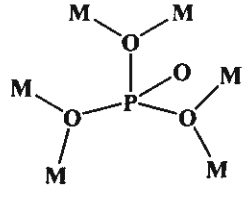

i. 4L, 4M

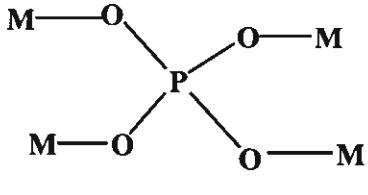

j. 3L, 4M

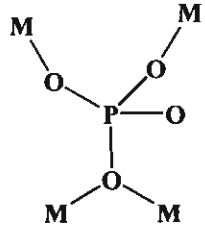

Figure 1 Structurally characterized coordination modes of hydrogenphosphate ($H_nPO_4^{(3-n)-}$) ligand for the hydrogenphosphato transition metal complexes: Where M = metalic and L = ligate

2.2 Aims and Scopes

The objective of the second part is to examine and develop the preparative work of the polynuclear copper(II) complexes containing the hydrogenphosphate oxoanion as a bridging ligand and the di-2-pyridylamine as a chelate didentate terminal ligand. The products are analyzed and characterized by microanalyses, thermogravimetric analysis, their spectroscopic properties (IR, solid state VIS, EPR (room temperature and liquid nitrogen temperature)) and the X-ray crystal structure determined crystallographically. The room temperature magnetic moment and the temperature variable susceptibilities (5-350 K) are measured in order to investigate the magneto-structural correlation together with the superexchange pathways.

2.3 Experimental

2.3.1 Reagents and physical measurements

All reagents are commercial grade materials and were used without further purification. Elemental analyses (C, H, N) were performed by the Microanalytical Service of Science and Technological Research Equipment Center, Chulalongkorn University on Perkin-Elmer PE2400 CHNS/O Analyzer. Copper content was determined on atomic absorption spectrophotometer. IR spectra were recorded with a Spectrum One Perkin-Elmer FT-IR spectrophotometer as KBr pellets in the 4000-450 cm^{-1} spectral range. Solid-state (diffuse reflectance) electronic spectra were recorded as polycrystalline samples on a Perkin-Elmer Lambda2S spectrophotometer over the range 8000–18000 cm^{-1}. Thermogravimetric measurements were performed in Perkin-Elmer system Pyris diamond TG-DTA instrument. The samples were heated at 10°C min^{-1} under dry air in the temperature rang 30-1000°C. X-band powder EPR spectra were obtained on a Jeol RE2x electron spin resonance spectrometer using DPPH (g = 2.0036) as a standard. The room temperature magnetic moments were carried out using a Faraday-type microbalance. Magnetic susceptibility measurements (5-350 K) were carried out using a Quantum Design MPMS-5 5T SQUID magnetometer (measurements carried out at 1000 Gauss). Data were corrected for magnetization of the sample holder and for diamagnetic contributions, which were estimated from the Pascal constants.

2.3.2 Syntheses

$\{[Cu_3(dpyam)_3(\mu_3,\eta^3\text{-}HPO_4)(\mu_3,\eta^4\text{-}PO_4)(H_2O)](PF_6)\cdot 3H_2O\}_n$ (I)

An aqueous solution (30 ml) of copper(II) acetate (0.181 g, 1.0 mmol) was added to a solution of di-2-pyridylamine (0.171 g, 1.0 mmol) in ethanol (15 ml) and followed by an aqueous solution (20 ml) of potassium dihydrogenphosphate (0.272 g, 2.0 mmol) and an aqueous solution (10 ml) of potassium hexafluorophosphate (0.184 g, 1.0 mmol). The resulting green solution was allowed to evaporate at room temperature for two weeks, producing dark green needle crystals of **I**, which were filtered off, washed with mother liquor and were dried in air. Yield ca. 45%. Calc. For $\{[Cu_3(dpyam)_3(\mu_3,\eta^3\text{-}HPO_4)(\mu_3,\eta^4\text{-}PO_4)(H_2O)](PF_6)\cdot 3H_2O\}_n$ **(I)**: C, 32.39; H, 3.26; N, 11.33; Cu, 17.14%. Found : C, 32.69; H, 3.31; N, 11.69; Cu, 17.21 %.

$[Cu(dpyam)(\mu_2,\eta^3\text{-}HPO_4)]_n$ (II)

An aqueous solution (30 ml) of copper(II) nitrate trihydrate (0.241 g, 1.0 mmol) was added to a solution of dpyam (0.171 g, 1.0 mmol) in ethanol (15 ml) and followed by an aqueous solution (20 ml) of potassium dihydrogenphosphate (0.272 g, 2.0 mmol). The resulting green solution was allowed to evaporate at room temperature. After several days, dark green crystals of **II** (*Anal.* Calc. for $[Cu(dpyam)\ (\mu_2,\eta^3\text{-}HPO_4)]_n$: C, 36.32; H, 3.05; N, 12.71; Cu, 19.21%. Found: C, 36.25; H, 2.98; N, 12.67; Cu, 19.28%) were deposited. Yield ca. 45%. Subsequently green needle crystals of $[Cu_4(dpyam)_4(\mu_3,\eta^3\text{-}HPO_4)_2(NO_3)_2(H_2O)_2](NO_3)_2\cdot 2H_2O$ **(VI)** (*Anal.* Calc. for **VI**: C, 33.13; H, 3.19; N, 15.45; Cu, 17.56%. Found: C, 33.20; H, 3.04; N, 15.52; Cu, 17.91%) were deposited in the second crystallization. Yield ca. 30%. Greenish-blue crystals of $[Cu(dpyam)(\mu_2,\eta^2\text{-}H_2PO_4)(H_2PO_4)]_2$ **(III)** were obtained in the final crystallization. They were filtered off, washed with the mother liquid and dried in air. Yield ca. 20%. Calc. For $[Cu(dpyam)(\mu_2,\eta^2\text{-}H_2PO_4)(H_2PO_4)]_2$: C, 28.05; H, 3.03; N, 9.80; Cu, 14.81 %. Found: C, 28.14; H, 2.93; N, 9.74; Cu, 14.37%.

$[Cu(dpyam)(\mu_2,\eta^2\text{-}H_2PO_4)(H_2PO_4)]_2$ (III)

A solution containing di-2-pyridylamine (0.171 g, 1.0 mmol) in ethanol (15 ml) and potassium dihydrogenphosphate (0.272 g, 2.0 mmol) in water (10 ml) was added to an aqueous solution (20 ml) of copper(II) tetrafluoroborate hydrate (0.237 g, 1.0 mmol). The resulting green solution was allowed to evaporate at room temperature. After two weeks, blue green crystals of **III** were obtained, which were filtered off, washed with mother liquor and were dried in air. Yield ca. 40%.

$[Cu_4(dpyam)_4(\mu_4,\eta^3\text{-}HPO_4)_2(\mu\text{-}Cl)_2](Cl)_2{\cdot}6H_2O$ (IV)

Solid potassium dihydrogenphosphate (0.272 g, 2.0 mmol) dissolved in water (20 ml) was added to a warm solution of di-2-pyridylamine (0.171 g. 1.0 mmol) in ethanol (15 ml) in order to avoid precipitation. Its color became greenish by slow addition of an aqueous solution (30 ml) of copper(II) chloride dihydrate (0.170 g, 1.0 mmol). The resulting green solution was allowed to evaporate at room temperature. After several days, green crystals of **IV** were deposited. They were filtered off, washed with mother liquid and air dried. Yield ca. 72%. Calc. For $[Cu_4(dpyam)_4(\mu_4,\eta^3\text{-}HPO_4)_2(\mu\text{-}Cl)_2](Cl)_2{\cdot}6H_2O$: C, 34.79; H, 3.65; N, 12.17; Cu, 18.40 %. Found: C, 34.88; H, 3.42; N, 12.13; Cu, 18.60 %.

$[Cu_4(dpyam)_4(\mu_4,\eta^3\text{-}HPO_4)_2(\mu\text{-}Br)_2](Br)_2{\cdot}6H_2O$ (V)

A solution of potassium dihydrogenphosphate (0.272 g, 2.0 mmol) in 10 ml water was added slowly to a solution containing copper(II) bromide (0.170 g, 1.0 mmol) in 30 ml water and di-2-pyridylamine (0.171 g, 1.0 mmol) in 15 ml ethanol. The resulting green solution was allowed to evaporate at room temperature. After a week, green crystals of **V** were obtained. They were filtered off, washed with mother liquid and air-dried. Yield ca. 68%.Calc. For $[Cu_4(dpyam)_4(\mu_4,\eta^3\text{-}HPO_4)_2(\mu\text{-}Br)_2](Br)_2{\cdot}6H_2O$: C, 32.02; H, 3.16; N, 10.84; Cu, 16.31 %. Found: C, 32.48; H, 2.67; N, 10.78; Cu, 16.41 %.

$[Cu_4(dpyam)_4(\mu_3,\eta^3\text{-}HPO_4)_2(NO_3)_2(H_2O)_2](NO_3)_2{\cdot}2H_2O$ (VI)

Method A. Solid potassium dihydrogenphosphate (0.272 g, 2.0 mmol) was slowly added under continuous stirring to solution containing copper(II) nitratte 2.5hydrate (0.370 g, 1.0 mmol) in water (25 ml) and di-2-pyridylamine (0.171 g, 1.0 mmol) in ethanol (15 ml), yielding a green solution. On slow evaporation for two weeks, green needle crystals of **VI** were obtained. Yield ca. 50%. Subsequently blue green crystals of $[Cu(dpyam)(\mu_2,\eta^2\text{-}H_2PO_4)(H_2PO_4)]_2$ (**III**) were deposited which were filtered off, washed with mother liquid and dried in air. Yield ca. 40%.

Method B. This compound was also prepared successfully following the preparation of the complex $[Cu(dpyam)(\mu_2,\eta^3\text{-}HPO_4)]_n$ (**II**). Yield ca. 30%.

2.3.3 Crystallography

Reflection data of **I** were collected on a 4K Bruker SMART APEX CCD area-detector diffractometer with graphite monochromated Mo Kα radiation (λ= 0.71073 Å) (at a detector distance of 6.0 cm and swing angle of -28°) using SMART program. Raw data frame integration

was performed with SAINT, which also applied correction for Lorentz and polarization effects. Absorption corrections were applied using SADABS, provided an empirical absorption correction and put the standard deviations of measured intensities onto absolute scale. The structures were solved by direct methods. The software package SHELXTL V 6.12 was used for structure solution and structure refinement. All hydrogen atoms were located by difference synthesis and refined isotropically.

Reflection data for **II** and **III** were collected at 298 K while those of **IV**, **V** and **VI** were collected at 273 K on a 1K Bruker SMART CCD area–detector diffractometer using graphite monochromated MoK_α radiation (λ = 0.71073 Å) at a detector distance of 4.5 cm and swing angle of –35°. A hemisphere of the reciprocal space was covered by combination of three sets of exposures; each set had a different ϕ angle (0, 88, 180°) and each exposure of 10 s for **II**, **III** and **IV**, 15 s for **V** and 35s for **VI** covered 0.3° in ω. Data reduction and cell refinements were performed using the program SAINT. An empirical absorption correction by using the SADABS program was applied, which resulted in transmission coefficients ranging from 0.7902 to 1.000, 0.8520 to 1.0000, 0.7123 to 1.0000, 0.7090 to 1.0000 and 0.7891 to 1.0000 for **II-VI**, respectively. The structure was solved by direct methods and refined by full–matrix least–squares method on $(F_{obs})^2$ with anisotropic thermal parameters for all non–hydrogen atoms using the SHELXTL-PC V 6.12 software package. All hydrogen atoms in **II**, **III** and **IV** were located by difference synthesis and refined isotropically except H(22), H(29), H(42), H(52) and H(58) in **IV**. These hydrogen atoms were geometrically fixed and allowed to ride on attached atoms. One water hydrogen atom and two hydrogenphosphate hydrogen atoms of **IV** were unable to locate. For **V** all hydrogen atoms were located and refined isotropically except five water hydrogen atoms which were unable to locate. Two water oxygen atoms of **IV** and **V** are located with site occupancies of 0.5. All hydrogen atoms in **VI** were located by difference synthesis and refined isotropically except for the water hydrogen atoms, which were unable to locate.

2.4 Results and Discussion

2.4.1 Description of the crystal structures

2.4.1.1 Description of $[Cu_3(dpyam)_3(\mu_3,\eta^3\text{-}HPO_4)(\mu_3,\eta^4\text{-}PO_4)(H_2O)](PF_6)\cdot 3H_2O\}_n$ (I)

The structure of **I**, consists of a polynuclear infinite chain structure of $[Cu_3(dpyam)_3(\mu_3,\eta^3\text{-}HPO_4)(\mu_3,\eta^4\text{-}PO_4)(H_2O)]^+$ cations, uncoordinated $[PF_6]^-$ anions and three crystallization water molecules. The structure is depicted in Fig. 2 together with the numbering scheme. Selected bond distances and angles are listed in Table 2, Appendix IIB.

The Cu atoms are bridged unsymmetrically through mixed tridentate hydrogenphosphate and tetradentate phosphate ligands. The HPO_4^{2-} is tridentate, each group bonds monodentately to three Cu(II) ions, giving a μ_3,η^3 coordination mode while PO_4^{3-} which is a tetradentate bridging group, bonds didentately to two Cu(II) ions and monodentately coordinated to the third one giving a novel μ_3,η^4 coordination mode. Complex **I** has mixed stereochemistries of an intermediate geometry between regular trigonal bipyramid and regular square pyramid ($\tau = 0.57$), and a tetrahedrally distorted square-based pyramidal geometry ($\tau = 0.17$ and 0.13) within a polymeric unit. The polynuclear unit involves three independent chromophores: one CuN_2O_3 chromophore of the former geometry and two CuN_2O_2O' chromophores of the latter. The Cu...Cu distances are ranging from 4.408(3) to 5.942(3) Å.

For the five coordinate CuN_2O_3 chromophore with an intermediate geometry ($\tau = 0.57$), slightly distorted towards the trigonal bipyramid, the out-of-plane bond lengths, Cu(1)-N(1) and Cu(1)-O(1), are significantly shorter, with values of 2.008(3) and 1.957(2) Å, compared to those of the in-plane bond lengths, Cu(1)-N(2), Cu(1)-O(6) and Cu(1)-O(1W), with values of 2.027(3), 1.942(2) and 2.191(3) Å, respectively. However, the CuN_2O_2O' chromophore stereochemistry is extremely distorted from regular trigonal pyramidal ($\tau = 0.57$). The O(1)-Cu(1)-N(1) angle of 166.9(1)° is significantly different from 180° and is distorted away from the Cu(1)-O(1W) direction. The in-plane angles, O(6)-Cu(1)-O(1W) (α_1), N(2)-Cu(1)-O(1W) (α_2) and O(6)-Cu(1)-N(2) (α_3), are all significantly different from 120°, namely 119.1(1), 107.7(1) and 132.8(1)°, respectively. The extremely distorted trigonal bipyramidal Cu(1) chromophore is linked to the distorted square pyramidal Cu(2) and Cu(3) chromophores via a HPO_4^{2-} group in an axial-equatorial configuration and via a PO_4^{3-} group in an equatorial-equatorial configuration with an

additional equatorial-axial configuration (pathways Cu(1)-O(6)-P(2)-O(8)-Cu(2) and Cu(1)-O(6)-P(2)- O(8)-Cu(3), respectively). However, if the square pyramidal geometry with the axial bond Cu(1)-O(1W) is considered for the Cu(1) chromophore with τ = 0.57, the equatorial-equatorial configuration is pronounced between Cu(1) and Cu(2) and between Cu(1) and Cu(3) chromophores, leading to the partial contribution to the magnetic interaction through this pathway.

For the remaining two distorted square-based pyramidal chromophores (τ = 0.17 and 0.13), the basal plane consists of two oxygen atoms from different bridging μ_3,η^3-HPO_4 and μ_3,η^4-PO_4 groups, O(7) and O(2A) (1.929(2), 1.920(2) Å) for Cu(2) and O(5) and O(4A) (1.924(2), 1.908(2) Å) for Cu(3) and two nitrogen atoms from a dpyam ligand (1.991(3) and 1.978(3) Å for Cu(2) and 1.985(3) and 1.976(3) Å for Cu(3)). The second oxygen atom (O(8)) from phosphate group is bent towards the Cu(2) and Cu(3) ions to complete the fifth coordination sites in the approximately axial positions at longer distances of 2.912(1) and 2.989(1) Å, respectively. Both Cu ions are liked by the HPO_4^{2-} and PO_4^{3-} groups in an equatorial-equatorial configuration (pathways Cu(3)-O(5)-P(2)-O(7)-Cu(2) and Cu(3)-O(4A)-P(1A)-O(2A)-Cu(2)) with an additional axial-axial configuration (pathway Cu(2)-O(8)- Cu(3)). However, the four in-plane atoms (N(4), N(5), O(2A) and O(7) for Cu(2) chromophore and N(7), N(8), O(4A) and O(5) for Cu(3) chromophore) are not planar with r.m.s. deviations of 0.804 and 0.598 Å. The Cu ion lies above this plane, 0.079 Å for Cu(2) and 0.062 Å for Cu(3) toward O(8). The tetragonality, T = 0.671 and 0.651 based on the changes in bond lengths for both chromophores (T = the mean in-plane bond length/the mean out-of-plane bond length). The τ-values defined to describe the degree of trigonal distortion are 0.13 and 0.17 {$\tau = (\alpha_1-\alpha_2)/60$, where α_1= O(4)-Cu(1)-N(2) and α_2 = O(6)-Cu(1)-N(1)}. As the regular trigonal bipyramid and square-based pyramid have τ values of 1.00 and 0.00, respectively, the stereochemistry of the CuN_2O_2O' chromophore of **I** is best described as extremely tetrahedral-distorted square-based pyramidal, with a slight trigonal distortion rather than square pyramidal distorted trigonal bipyramidal.

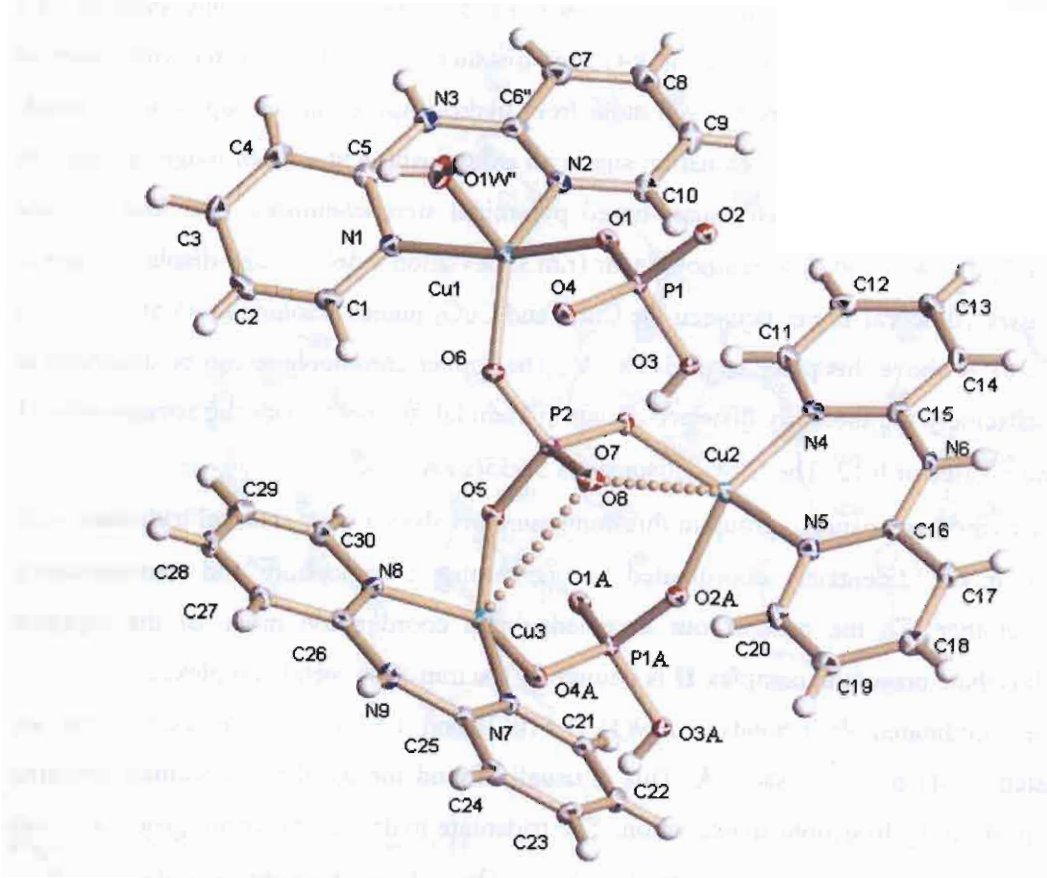

Figure 2 The polymeric structure of **I**

The lattice structure is stabilized by the hydrogen-bonding network N-H...O($W_{uncoor.}$), O(HPO_4^{2-}) and O(PO_4^{3-}), O(HPO_4^{2-})-H...O(PO_4^{3-}), O($W_{coor.}$)-H...O(PO_4^{3-}) and O($W_{uncoor.}$), O($W_{uncoor.}$)-H...O(HPO_4^{2-}), O(PO_4^{3-}), O($W_{uncoor.}$), F(PF_6) and amine group.

2.4.1.2 Description of $[Cu(dpyam)(\mu_2,\eta^3\text{-}HPO_4)]_n$ (II)

The structure is depicted in Fig. 3 together with the numbering scheme. Selected bond distances and angles are listed in Table 3, Appendix IIB. The structure consists of a neutral and polymeric chains of [Cu(dpyam)(μ_2,η^3-HPO_4)] bridged by tridentate hydrogenphosphato ligands. The local molecular structure of the copper atom involves square pyramidal CuN_2O_2O' chromophore in an equatorial-equatorial configuration. The basal plane consists of two oxygen atoms from two equivalent bridging hydrogenphosphato groups and of a dpyam ligand coordinated through two nitrogen atoms. The dpyam ligand chelates in the tetragonal plane,

almost symmetrically, with Cu-N distances of 1.969(1) and 1.994(1) Å, and a bite angle of 92.0 (6)°. The equatorial Cu(1)-O(1) and Cu(1)-O(4) bond distances are slightly shorter with values of 1.946(1) and 1.919(1) Å. The third oxygen atom from hydrogenphosphate group is bent towards the Cu atom to complete a fifth coordination site in an axial position at a much longer distance of 2.719(2) Å, generating a distorted square-based pyramidal stereochemistry. The four in-plane atoms, N(1), N(2), O(1) and O(4) are not planar (r.m.s. deviation 0.562 Å) and display a marked tetrahedral twist (dihedral angles between the CuN_2 and CuO_2 planes amounts to 45.56°). The Cu atom lies 0.202 Å above this plane towards O(2A). The copper chromophore can be described as having an extremely tetrahedrally distorted square pyramidal geometry with the tetragonality, T of 0.720 and τ-value of 0.12. The Cu-Cu distance is 5.955(2) Å.

The hydrogenphosphato group in this compound involves a quite unusual tridentate μ_2,η^3 coordination mode: didentately coordinated to one copper chromophore and monodentately bonded to another. To the best of our knowledge this coordination mode of the bridging hydrogenphosphate present in complex **II** is unique for the transition metal complexes.

The coordinated P=O bonds, 1.519(1), 1.510(2) and 1.531(1) Å, are shorter than the uncoordinated P-OH bond, 1.588(2) Å. This is usually found for the three-coordinate bridging coordination of the hydrogenphosphate anion. The tridentate hydrogenphosphato group involves O-P-O angles ranging from 101.9(1) to 111.7(1)°. The lattice structure is stabilized by a hydrogen-bonding network between the amine N and an oxygen atom of the hydrogenphosphate group with a short contact distance of 2.663(3) Å and between the oxygen atom of the hydrogenphosphate group to the oxygen atom of another phosphatogroup with a contact distance of 2.528(3) Å. The structure contains chains of Cu ions in the c-direction bridged by the HPO_4^{2-} ions in a trigonal way. Two nearest Cu(II) ions are bridged by a tridentate hydrogenphosphate group which is didentately coordinated to one copper(II) ion, and monodentately coordinated to another in an equatorial-equatorial configuration in an unusual bridging coordination mode. The helical arrangement of the Cu-HPO_4 chain is clearly visible in Fig. 3 with the N ligands at the outside stacked in the direction of the 3-fold screw axis.

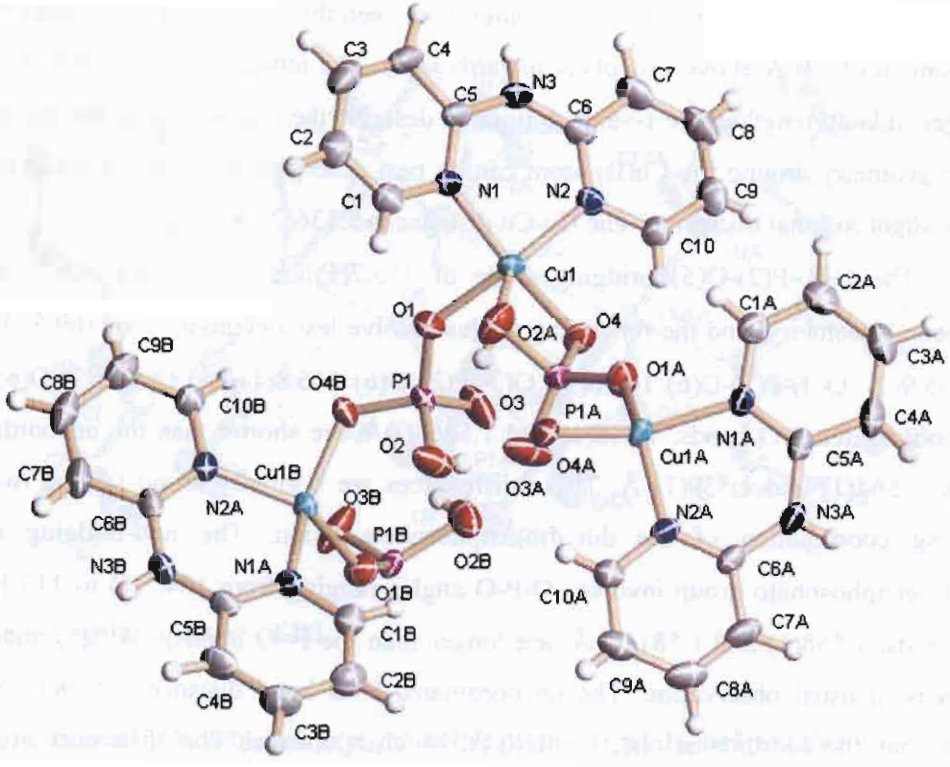

Figure 3 The polymeric structure of **II**

2.4.1.3 Description of $[Cu(dpyam)(\mu_2, \eta^2\text{-}H_2PO_4)(H_2PO_4)]_2$ (III)

The structure is depicted in Fig. 4 together with the numbering scheme. Selected bond distances and angles are listed in Table 4, Appendix IIB. The centrosymmetric dinuclear compound consists of two $[Cu(dpyam)(\mu_2,\eta^2\text{-}H_2PO_4)(H_2PO_4)]$ units being doubly bridged by two didentate dihydrogenphosphato anions. The local molecular structure of the copper atom involves a square pyramidal CuN_2O_2O' chromophore. The basal plane consists of two oxygen atoms of the two bridging dihydrogenphosphato groups, O(5) and O(8A) and of dpyam ligand coordinated through two nitrogen atoms. The dpyam ligand chelates in the square plane, almost symmetrically, with Cu-N distances of 1.991(1) and 1.997(1) Å and a bite angle of 88.1(1)°. The equatorial Cu(1)-O(8A) and Cu(1)-O(5) bond distances are slightly shorter with values of 1.964 (1) and 1.987(1) Å. The fifth axial coordination site is occupied by one oxygen atom of non-bridging monodentate dihydrogenphosphato group at the Cu-O distance of 2.271(1) Å. The four in-plane atoms, N(1), N(2), O(5) and O(8A) are essentially planar, (r.m.s. deviation 0.0598 Å)

with a slightly tetrahedral twist (dihedral angles between the CuN_2 and CuO_2 planes = 14.0°). The Cu atom lies 0.16 Å above this plane towards O(1). The tetragonality, T = 0.874 based on the changes in bond lengths. The τ-value defined to describe the degree of trigonal distortion is 0.12, so the geometry around the Cu(II) atom can be best described as square-based pyramidal, with only a slight trigonal distortion. The Cu-Cu distance is 5.136(2) Å.

The O(8)-P(2)-O(5) bridging angle of 115.7(1)° is larger than 109.5° of the ideal tetrahedral geometry, and the remaining angles involve less deviation from 109.5° [O(5)-P(2)-O (7) 105.9(1), O(5)-P(2)-O(6) 105.6(1), O(7)-P(2)-O(6) 106.8(1) and O(8)-P(2)-O(6) 112.6(1)°]. The coordinated P-O bonds, 1.518(1) and 1.506(1) Å, are shorter than the uncoordinated P-OH bonds, 1.564(1) and 1.559(1) Å. These differences are normally found for the two-coordinate bridging coordination of the dihydrogenphosphate anion. The non-bridging monodentate dihydrogenphosphato group involves O-P-O angles ranging from 104.1(1) to 115.1(1)°. The P-OH bonds, 1.558(1) and 1.581(1) Å, are longer than the P=O bonds, 1.512(1) and 1.519(1) Å, which is in usual observation. The uncoordinated P=O bond distance, 1.519(1) Å, is slightly longer than the coordinated one, 1.511(1) Å, which is unusual. This difference arises from the hydrogen bond involved to the uncoordinated P=O bond. The P=O distances in both the monodentate dihydrogenphosphato group and the dihydrogenphosphato bridge are ranging from 1.506(1) to 1.519(1) Å, while the P-OH bond distances vary from 1.558(1) to 1.581(1) Å. This behavior is consistent with the general observation that P-OH bonds are longer than P=O bonds in primary and secondary phosphates.

The lattice structures are stabilized by a hydrogen bonding network between the amine N and the oxygen atom of the non-bridged dihydrogenphosphate anion with a distance of 3.1603 (19) Å, and between oxygen atoms of different dihydrogenphosphate groups (O···O distances vary from 2.5825(18) to 2.648(2) Å).

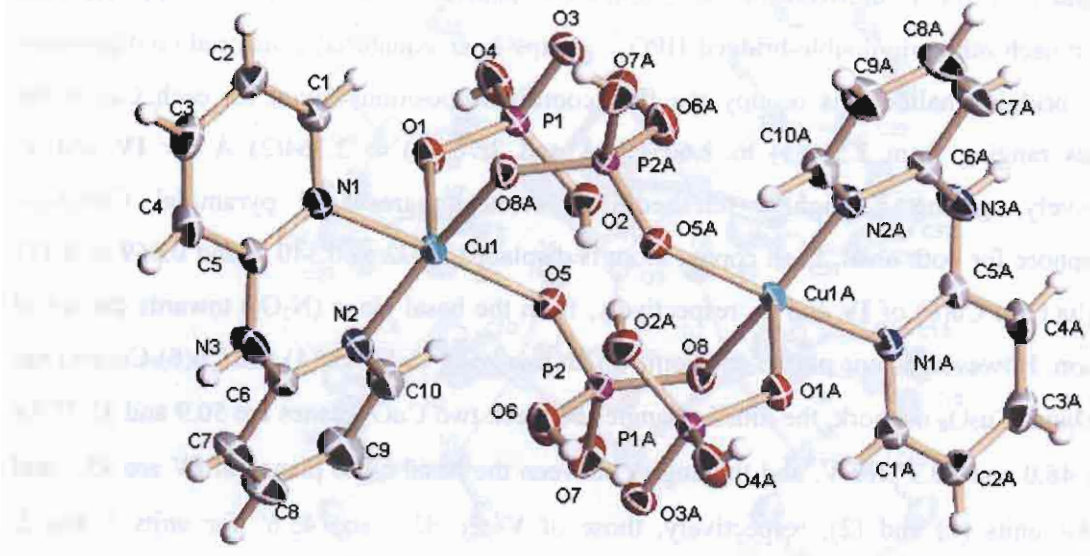

Figure 4 The molecular structure of **III**

2.4.1.4 Description of $[Cu_4(dpyam)_4(\mu_4,\eta^3\text{-}HPO_4)_2(\mu\text{-}Cl)_2](Cl)_2{\cdot}6H_2O$ (IV) and $[Cu_4(dpyam)_4(\mu_4,\eta^3\text{-}HPO_4)_2(\mu\text{-}Br)_2](Br)_2{\cdot}6H_2O$ (V)

The structure of **IV** consists of two independent tetranuclear units of $[Cu_4(dpyam)_4(\mu_4,\eta^3\text{-}HPO_4)_2(\mu\text{-}Cl_2)]^{2+}$, namely units (1) and (2), four chloride anions and twelve lattice water molecules. Unit (1) is situated in a general position, whereas unit (2) is situated on a mirror plane. The unit cell contains four molecules on general positions and two molecules on special positions. Compound **V** is isostructural and involves similar asymmetric unit and similar structure to those of **IV.** An ORTEP plot, together with the numbering scheme of the compounds are shown in Figs. 5 and 6, with relevant distances and angles in Tables 5 and 6, Appendix IIB.

The tetranuclear unit of both compounds consists of two pairs of five coordinated copper (II) ions bridged by two tetrahedral tridentate hydrogenphosphato groups in each molecule. Both HPO_4^{2-} groups coordinate monodentately to each copper(II) ion and bridging via one oxygen to two other Cu(II) ions, giving a μ_4,η^3 coordination mode which is rarely found in the hydrogenphosphate metals. Each copper ion involves an essentially planar square base of the CuN_2O_2X chromophore through the two bridging HPO_4^{2-} groups and a terminal dpyam ligand with a slight tetrahedral twist (evident from the dihedral angles of 18.06,19.38, 5.68, 6.66,23.59 and 6.20° for Cu(1) to Cu(6) chromophores, respectively, for **IV** and 17.63, 19.21, 4.53, 5.40,

22.25 and 5.11° for **V**, between the CuO_2 and CuN_2 planes). Consequently, all copper(II) ions linked to each other via double-bridged HPO_4^{2-} groups in an equatorial-equatorial configuration. Finally, bridging halide ions occupy the fifth coordinate positions (axial for each Cu) at the distances ranging from 2.559(1) to 2.603(1) Å and 2.707(2) to 2.764(2) Å for **IV** and **V**, respectively, giving a slightly tetrahedral-distorted square-based pyramidal CuN_2O_2X chromophore for both units. Each copper atom is displaced 0.072 to 0.340 Å and 0.069 to 0.337 Å for Cu(1) to Cu(6) of **IV** and **V**, respectively, from the basal plane (N_2O_2) towards the apical halide ion. However, as one pair of each unit which involving Cu(3)-Cu(4) and Cu(6)-Cu(6A) has a non-planar Cu_2O_2 network, the dihedral angles between two CuO_2 planes are 50.9 and 51.7° for **IV** and 48.0 and 50.3° for **V**, and the angles between the basal N_2O_2 planes of **IV** are 45.1 and 45.9° for units (1) and (2), respectively, those of **V** are 43.3 and 45.6° for units 1 and 2, respectively, indicating a roof-shaped structure. The τ values vary from 0.020 to 0.053 and 0.001 to 0.071 for **IV** and **V**, respectively, indicating the nearly perfect square-based pyramidal geometry for all CuN_2O_2X chromophores. The Cu...Cu distances in **IV** are ranging from 2.802(1) Å, in the dinuclear units to 5.224(1) Å in the tetranuclear units and those of **V** are ranging from 2.834(1) to 5.2339(1) Å.

The P-OH bonds which are ranging from 1.533(10) to 1.629(10) Å for **V**, are longer than the P-O bonds (1.475(8)-1.599(10) Å **V**), which are in usual observation except those of P(1)-O (3) (1.599(10)Å), P(2)-O(7) (1.589(9)Å), and P(4)-O(12) (1.555(11)Å) in **V**. This arises may be due to the hydrogen bonding between these oxygen atoms and the hydrogen atoms attached to carbon atom from the amine groups. These hydrogen bonds may be co-responsible for the evident longer P-O bonds.

The lattice structure is stabilized by a hydrogen-bonding network (D...A distances) N-H...X(uncoor., 3.246-3.419 Å for **IV** and 3.369-3.542 Å for **V**), O(HPO_4)-H...O(W) (2.590-2.638 Å for **IV** and 2.588-2.700 Å for **V**), and O(W)-H...Br(uncoor., 3.144-3.274 for **IV** and 3.276-3.669 Å for **V**) and O(W)-H...O(W) (2.664 Å for **IV** and 2.664-3.738 Å for **V**).

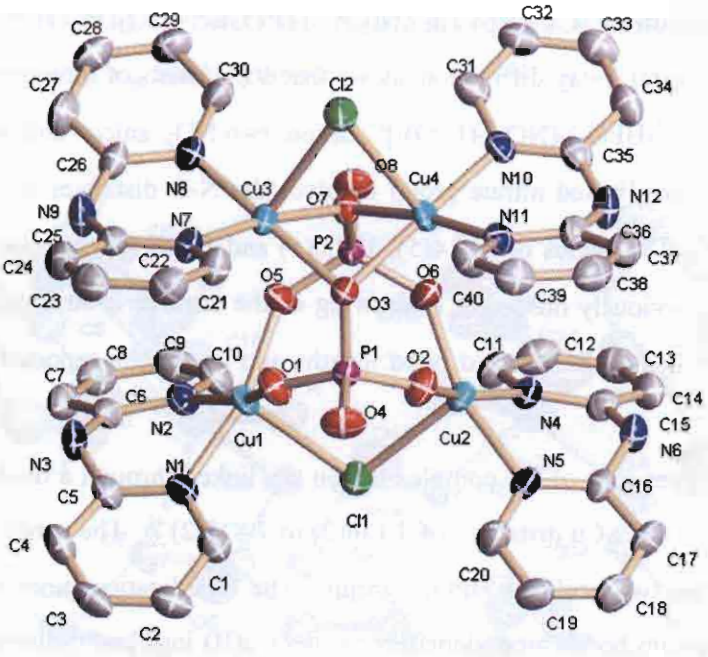

Figure 5 The molecular structure of **IV**

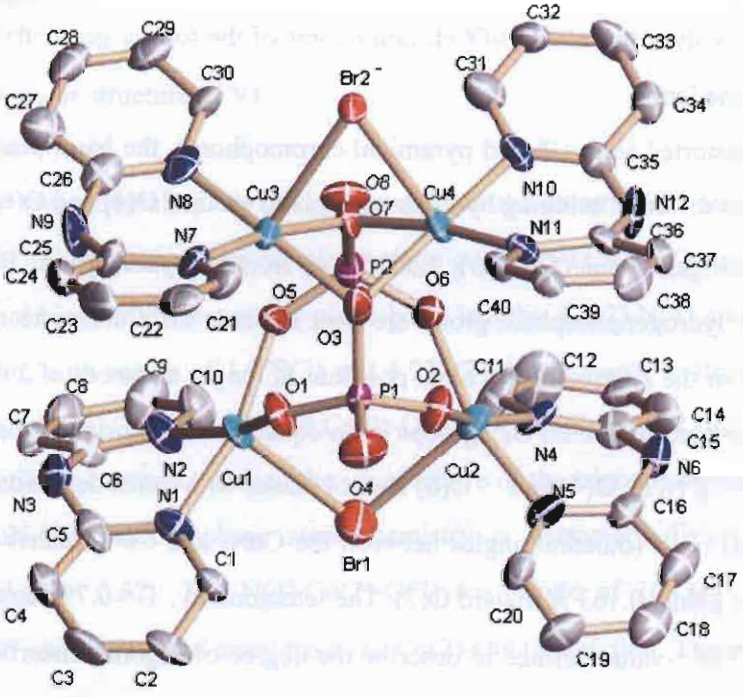

Figure 6 The molecular structure of **V**

2.4.1.5 Description of $[Cu_4(dpyam)_4(\mu_3,\eta^3\text{-}HPO_4)_2(NO_3)_2(H_2O)_2](NO_3)_2 \cdot 2H_2O$ (VI)

Single crystal X-ray diffraction shows that **VI** consists of a centrosymmetric tetranuclear $[Cu_4(dpyam)_4(\mu_3,\eta^3\text{-}HPO_4)_2(NO_3)_2(H_2O)_2]^{2+}$ cation, two NO_3^- anions and two molecules of lattice water. The non-coordinated nitrate group involves the N-O distances of 1.233(5), 1.236(6) and 1.23(5) Å and O-N-O angles of 119.4(5), 120.0(5) and 120.6(5)°, in good agreement with those of the free ion previously observed. A drawing of the tetrameric structure showing the labeling scheme is given in Fig. 7. Selected bond lengths and angles are reported in Table 7, Appendix IIB.

Four copper ions of the complex cation are linked through a double hydrogenphosphate bridge, leading to Cu...Cu distances of 4.136(2) to 7.833(2) Å. The cation is located on a c glide plane through the two bridging HPO_4^{2-} groups. The coordination mode of HPO_4^{2-} is tridentate bridging, each group bonds monodentately to two Cu(II) ions and didentately coordinated to the third one giving a novel μ_3,η^3 coordination mode. Compound **VI** has mixed stereochemistries of a tetrahedral distorted square-based pyramid (τ = 0.32) and an intermediate geometry between regular trigonal bipyramid and regular square pyramid (τ = 0.52) within a tetranuclear unit. The tetranuclear unit involves two CuN_2O_2O' chromophores of the former geometry and two CuN_2O_3 chromophores of the latter.

For two distorted square-based pyramidal chromophores, the basal plane consists of two oxygen atoms from different bridging hydrogenphosphato groups, O(4) and O(6) (1.968(2), 1.972 (2) Å) and two nitrogen atoms (1.967(3), 2.001(3) Å) from a dpyam ligand. The second oxygen atoms from each hydrogenphosphate group are bent towards the Cu ions to complete the fifth coordination sites in the approximately axial positions at longer distances of 2.497(2) Å. Two Cu ions are doubly bridged by the HPO_4^{2-} groups in an equatorial-equatorial configuration. The four in-plane atoms, N(1), N(2), O(4) and O(6) are not planar with r.m.s. deviation of 0.473 Å and a marked tetrahedral twist (dihedral angles between the CuN_2 and CuO_2 planes = 41.2°). The Cu ion lies above this plane, 0.163 Å toward O(7). The tetragonality, T = 0.791 based on the changes in bond lengths. The τ-value defined to describe the degree of trigonal distortion is 0.32. As the regular trigonal bipyramid and square-based pyramid have τ values of 1.00 and 0.00, respectively, the stereochemistry of the CuN_2O_2O' chromophore of **VI** is best described as

extremely tetrahedral-distorted square-based pyramidal with a slight trigonal distortion, rather than square pyramidal distorted trigonal bipyramidal.

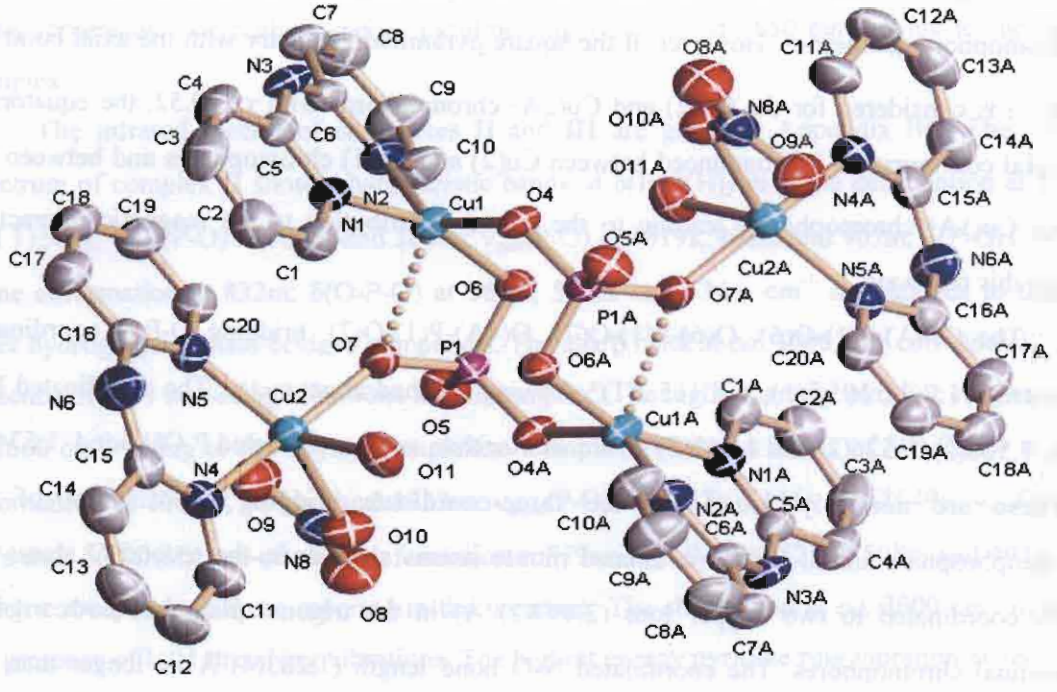

Figure 7 The molecular structure of **VI**

The other two equivalent chromophores within the tetranuclear unit involve a five coordinate CuN_2O_3 chromophore, with an intermediate geometry ($\tau = 0.52$) but slightly distorted towards the trigonal bipyramid. The out-of-plane bond lengths, Cu(2)-N(4) and Cu(2)-O(7), are significantly shorter, with values of 1.979(3) and 1.933(2) Å, compared to those of the in-plane bond lengths, Cu(2)-N(5), Cu(2)-O(10) and Cu(2)-O(11), with values of 2.013(3), 2.145(3) and 2.152(3) Å, respectively, corresponding to the usual nature of the trigonal bipyramidal geometry. However, the CuN_2O_2O' chromophore stereochemistry is extremely distorted from regular trigonal pyramidal ($\tau = 0.52$). The N(4)-Cu(2)-O(7) (α_8) angle of 168.6(1)° is significantly different from 180° and is distorted away from the Cu(2)-O(11) direction. The in-plane angles, N(5)-Cu(2)-O(11) (α_1), N(5)-Cu(2)-O(10) (α_2) and O(10)-Cu(2)-O(11) (α_3), are all significantly different from 120°, namely 131.1(1), 137.5(1) and 91.2(1)°, respectively. A pair of the extremely

distorted trigonal bipyramidal Cu(2) and Cu(2A) chromophores is non-bridged, but each chromophore is linked to the distorted square pyramidal Cu(1) and Cu(1A) chromophores via a HPO_4^{2-} group in an axial-equatorial configuration. Additionally, the axial-axial configuration (pathways Cu(1)-O(7)-Cu(2) and Cu(1A)-O(7A)-Cu(2A)) is also exist between these two types of the chromophore geometries. However, if the square pyramidal geometry with the axial bond Cu (2)-O(11) is considered for the Cu(2) and Cu(2A) chromophores with $\tau = 0.52$, the equatorial-equatorial configuration is pronounced between Cu(2) and Cu(1) chromophores and between Cu (2) and Cu(1A) chromophores, leading to the partial contribution to the magnetic interaction through this pathway.

The O(4A)-P(1)-O(6), O(6)-P(1)-O(7), O(4A)-P(1)-O(7), bridging O-P-O coordinated angles are 111.7(1), 105.3(1), and 115.2(1)° showing tetrahedral geometry. The coordinated P-O bonds, 1.526(2), 1.526(2) and 1.542(2) Å, are shorter than an uncoordinated P-OH bond, 1.574(2) Å. These are normally found for the three-coordinate bridging coordination of the hydrogenphosphate anion. Both coordinated nitrate anions are planar, the second O atoms are weakly coordinated to two copper ions (2.497(2) Å) in the trigonal planes of both trigonal bipyramidal chromophores. The coordinated N-O bond length (1.283(4) Å) is longer than the uncoordinated N-O bonds (1.233(4) and 1.249(4) Å) as well as the larger O-N-O angles of 122.2(3) and 119.5(3)° compared to the uncoordinated O-N-O one (118.3(3)°), corresponding to the typical feature of the monodentate nitrite group.

The lattice structure is stabilized by the hydrogen-bonding network N-H...O(HPO_4), O (HPO_4)-H...O($W_{uncoor.}$) and O($W_{coor.}$)-H...O(HPO_4) and O($W_{coor.}$)-H...O($W_{uncoor.}$).

2.4.2 IR spectra

The infrared spectrum of **I** (as in Appendix IIC) displays the characteristic bands of the hydrogenphosphate bridging ligand: δ(P-O(H)) in-plane deformation at 1240m and 1164m; ν_{asym} (P-O) at 1110s, 1071s and 1056m; ν_{sym}(P-O) at 1015s and 984m; δ(P-O(H)) out-of-plane deformation at 883m; δ(O-P-O) at 558m and 499m cm^{-1} corresponds to those of other hydrogenphosphato-bridged copper(II) complexes. This indicates that the hydrogenphosphate and phosphate ions are present as a bridging of mixed hydrogenphosphate and phosphate ligands. The

PF_6^- group vibration near 900 cm^{-1} splitting into a sharp peak at *ca.* 842 cm^{-1} indicates the PF_6^- ions in **I**. The sharp band at *ca.* 3000 cm^{-1} was observed, indicative of the presence of N-H stretching vibrations in this complex. The occurrence of a strong and broad absorption centered at 3419 cm^{-1} (symmetric and antisymmetric OH stretchings) is consistent with the crystallization water molecules. The highest energy pyridine ring vibration at 1650 cm^{-1} owing to the dpyam complex.

The infrared spectra of complexes **II** and **III** are given in Appendix IIC. The infrared spectrum of complex **II** shows characteristic bands of δ(P-O(H)) in-plane deformation at 1238m and 1156m; ν_{asym}(P-O) at 1092s and 1056s; ν_{sym}(P-O) at 1019s, 968m and 907m; δ(P-OH) out-of-plane deformation at 832m; δ(O-P-O) at 586m, 555m and 534m cm^{-1} corresponds to those of other hydrogenphosphato-bridged complexes. The sharp band at *ca.* 3000 cm^{-1} corresponds to the presence of N-H stretching vibrations in this complex. The highest energy pyridine ring vibration at 1660 cm^{-1} owing to the dpyam complexes. Complex **III** shows bands of δ(P-O(H)) in-plane deformation at 1354w, 1274m and 1232m; ν_{asym}(P-O) at 1157s, 1116s and 1049s; ν_{sym}(P-O) at 977s and; δ(P-O(H)) out-of-plane deformation at 879m; δ(O-P-O) at 525m, 508m and 491m cm^{-1} which corresponds to those reported in the literature. The sharp band at *ca.* 3000 cm^{-1} indicates the presence of N-H stretching vibrations. The highest energy pyridine ring vibration at 1633 cm^{-1} owing to the dpyam complexes.

The infrared spectrum of **IV** (as in Appendix IIC) displays the characteristic bands of the hydrogenphosphate bridging ligand: δ(P-O(H)) in-plane deformation at 1349m and 1235m; ν_{asym} (P-O) at 1159s, 1096s and 1054s; ν_{sym}(P-O) at 1019m, 976m and 936m; δ(O-P-O) at 529m and 511m cm^{-1} corresponds to those of other hydrogenphosphato-bridged copper(II) complexes, Table 2.2. The sharp band at *ca.* 3000 cm^{-1} was observed, indicative of the presence of N-H stretching vibrations in this complex. The crystallisation water molecules are consistent with the occurrence of a strong and broad absorption centered at 3422 cm^{-1} (symmetric and asymmetric OH stretchings). The highest energy pyridine ring vibration at 1630 cm^{-1} owing to the dpyam complexes.

The infrared spectra of complexes **V** and **VI** are given in Appendix IIC. Complex **V** shows characteristic bands of δ(P-O(H)) in-plane deformation at 1354m and 1236m; ν_{asym}(P-O) at 1159s, 1098m and 1054m; ν_{sym}(P-O) at 1019m, 980m and 938m; δ(O-P-O) at 529m and 511m cm^{-1} corresponds to those of other hydrogenphosphato-bridged copper(II) complexes. That of **VI**

shows band of δ(P-O(H)) in-plane deformation at 1238m; ν_{asym}(P-O) at 1156w, 1110s and 1056s; ν_{sym}(P-O) at 1012m; δ(P-O(H)) out-of plane deformation at 842m and δ(O-P-O) at 530w and 506w cm^{-1} corresponds to those of hydrogenphosphate anions and ν_{asym}(N-O) at 1384s and ν_{sym} (N-O) at 1312m cm^{-1} attributed to the coordinated nitrate group. The sharp band at *ca.* 3000 cm^{-1} for **V** and **VI** indicates of the presence of N-H stretching vibrations in these complexes. The occurrence of a strong and broad absorption centered at 3412 cm^{-1} for **V** and at 3429 cm^{-1} for **VI** (symmetric and asymmetric OH stretchings) are consistent with the presence of crystallization water molecules in both complexes. The highest energy pyridine ring vibration at 1633 cm^{-1} for **V** and at 1643 cm^{-1} for **VI** is owing to the dpyam complexes.

2.4.3 Electronic Reflectance spectra

The electronic diffuse reflectance spectrum of **I** (Fig. 8) shows a broad band ranging from 10.02 to 15.60 kK (centred at ca. 12.46 kK) where kK = 1000 cm^{-1}. This observed single broad peak is consistent with the mixed stereochemistries: the distorted square pyramidal geometry (τ = 0.17 and 0.13) which results in a typical main peak around 14.00-15.00 kK and a shoulder around 11.00-12.00 kK, usually observed for the regular square pyramidal geometry and the intermediate five-coordinate geometry (τ = 0.57) which displays a typical single broad peak around 12.00-13.00 kK, usually observed for the intermediate five-coordinated geometry. If the distorted trigonal bipyramidal geometry is considered for the intermediate five-coordinate geometry, a single broad peak appeared at the lower frequency side of a broad band may be assigned as the d_{xy}, d_{xz}, d_{yz}, $d_{x^2-y^2} \rightarrow d_{z^2}$ transition. In addition, that of the distorted square pyramidal geometry which appeared at the higher frequency side of a broad band may be assigned as the d_{z^2}, d_{xy}, d_{xz}, $d_{yz} \rightarrow d_{x^2-y^2}$ transition. However, there is a comparable feature with the electronic spectra of **II** and **III** (Fig. 8), in that **II** also exhibits a main peak at 14.44 kK with a shoulder at 11.20 kK. This observation corresponds to the d_{xy}, $d_{z^2} \rightarrow d_{x^2-y^2}$ transition for the low-energy peak and the d_{xz}, $d_{yz} \rightarrow d_{x^2-y^2}$ transition for the high-energy peak of the distorted square pyramidal geometry usually observed. Complex **III** displays a broad band at ca. 14.88 kK. This observed single broad peak is consistent with the square pyramidal stereochemistry and assigned to be d_{z^2}, d_{xy}, d_{xz}, $d_{yz} \rightarrow d_{x^2-y^2}$ transition.

The electronic diffuse reflectance spectrum of **IV** consists of an unsymmetrical, broad band centered at ca. 14.97 kK (Fig. 9) which is very comparable to that of **V** (14.88 kK) (Fig. 9). This

observed single broad peak is consistent with the square pyramidal stereochemistry and assigned to be the d_{z2}, d_{xy}, d_{xz}, $d_{yz} \rightarrow d_{x2-y2}$ transition. However, there is a comparable feature in electronic spectrum of **VI** (Fig. 9), which also shows a broad band ranging from 11.40 to 13.90 kK (centered at ca. 12.32 kK). The observed single broad peak in **VI** is consistent with the mixed stereochemistries: the distorted square pyramidal geometry (τ = 0.32) with a remarkable tetrahedral twist of the square base which results in the lower frequency of the spectrum as compared to that of the regular square pyramidal geometry (ca. 14.00-15.50 kK) and the intermediate five-coordinate geometry (τ = 0.52) which exhibits a typical single broad peak around 12.00-13.00 kK, usually observed for the intermediate five-coordinate geometry. If the distorted trigonal bipyramidal geometry is favorably considered for the intermediate five-coordinate geometry, a single peak which appeared at the lower frequency side of a broad band may be assigned as the d_{xy}, d_{xz}, d_{yz}, $d_{x2-y2} \rightarrow d_{z2}$ transition. In addition, that of the former geometry that appeared at the higher frequency side of a broad band may be assigned as the d_{z2}, d_{xy}, d_{xz}, $d_{yz} \rightarrow d_{x2-y2}$ transition. Both transitions are superimposed to each other resulting in an observed single broad band.

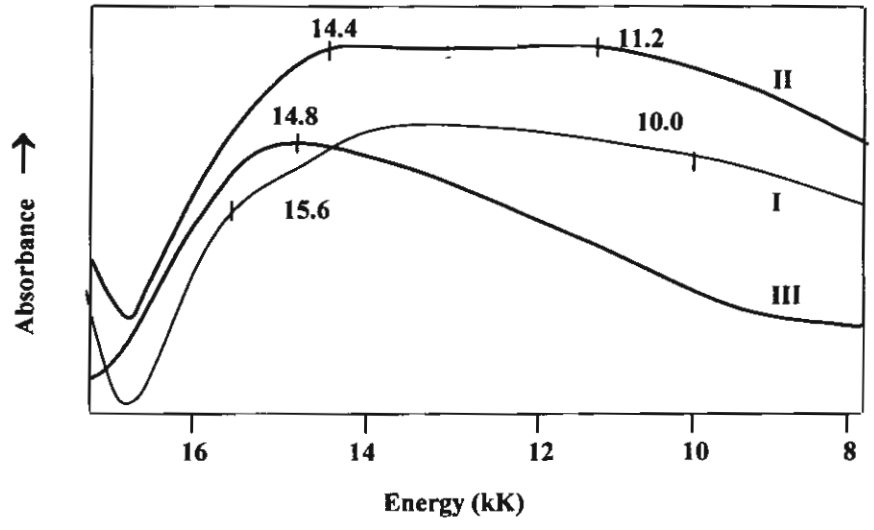

Figure 8 The electronic diffuse reflectance spectra of **I-III**

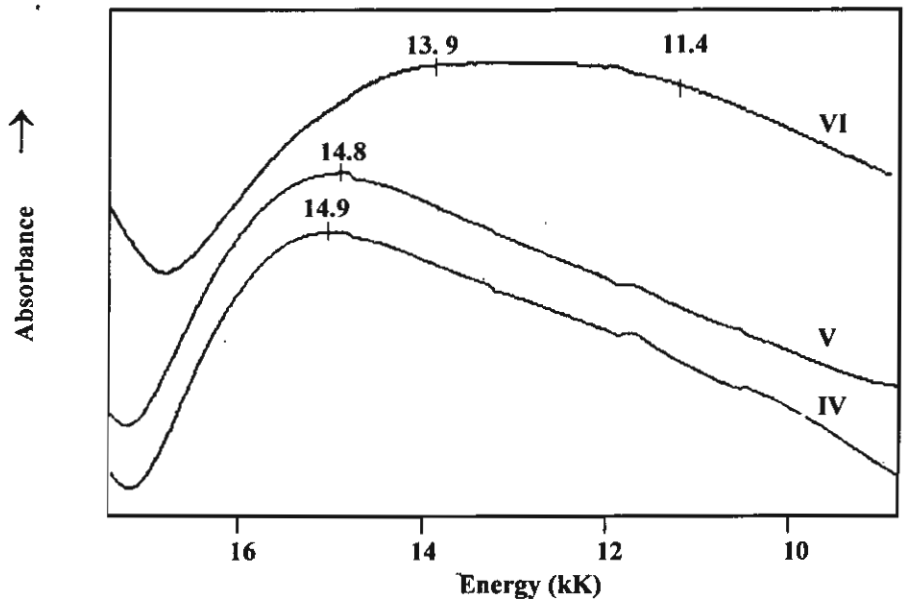

Figure 9 The electronic diffuse reflectance spectra of **IV-VI**

2.4.4 Thermogravimetric analysis

In order to determine the thermal stability of all products, the thermogravimetric analyses of **I-VI** (as in Appendix IID) were carried out in dry air from 30-1000°C using a heating rate of 10°C min^{-1}. The result shows two weight losses, two rather broads. For **I** the first weight loss of about 17.04% occurring in the region 30-300°C corresponds to the loss of hexafluorophosphate anions, dehydration of hydrogenphosphato group and four water molecules (calc. 17.53%) and the second weight loss of 45.24% in the region 300-900°C corresponds to the loss of three amine groups (calc. 46.17%). The final product of the thermal decomposition of **I** is a black powder that appears to be a CuP_2O_7. The thermal behavior of complexes **II** and **III** are given in Appendix IID. The thermogravimetric analysis of **II** and **III** shows two weight losses, two rather broads. The total weight loss of about 53.20% for **II** and 49.40% for **III** occurring in the region 200-850°C corresponds to the loss of water and amine ligand molecules (calc. 54.40% for **II** and 48.40% for **III**, respectively). The final product of the thermal decomposition of **II** and **III** are a black powder that appears to be a CuP_2O_7.

The overall decomposition reactions based on the weight loss data are summarized below:

$$\{[Cu_3(dpyam)_3(\mu_3,\eta^3\text{-}HPO_4)(\mu_3,\eta^4\text{-}PO_4)(H_2O)](PF_6)\cdot 3H_2O\}_n\ (\mathbf{I}) \xrightarrow{-4.5H_2O + PF_6} Cu_3(dpyam)_3P_2O_7 \xrightarrow{-3dpyam} 2\ Cu_2P_2O_7$$

$$[Cu(dpyam)(\mu_2,\eta^3\text{-}HPO_4)]_n\ (\mathbf{II}) \xrightarrow{-1/2H_2O} 1/2\ Cu_2(dpyam)_2P_2O_7 \xrightarrow{-dpyam} 1/2\ Cu_2P_2O_7$$

$$[Cu(dpyam)(\mu_2,\eta^2\text{-}H_2PO_4)(H_2PO_4)]_2\ (\mathbf{III}) \xrightarrow{-4H_2O} Cu_2(dpyam)_2P_2O_7 \xrightarrow{-2dpyam} Cu_2P_2O_7$$

The thermogravimetric analysis of **IV** (as in Appendix IID) shows two weight losses, two rather broads. The first weight loss of about 7.90% occurring in the region 30-100°C corresponds to the loss of twelve water molecules (three from twelve water molecules are considered with site occupancy factor of 0.5, calc. 6.91%) and the second weight loss of 61.90% in the region 150-580°C corresponds to the loss of chloride anions, amine groups and dehydrate of hydrogenphosphato groups (calc. 61.77%). The final product of the thermal decomposition of **IV** is a black powder that appears to be a CuP_2O_7.

The thermal behaviors of complexes **V** and **VI** are given in Appendix IID. The thermogravimetric analysis of **V** is similar to that of complex **IV** suggesting that the total weight loss of about 69.70% corresponds to the loss of water molecules, bromide anions and dehydrate of hydrogenphosphate groups (calc. 71.90%). While complex **VI** shows two weight losses, two rather broads as in the proposed decomposition reactions below. The total weight loss of about 70.30% occurring in the region 100-600°C corresponds to the loss of water and dehydrate of hydrogenphosphate groups, nitrate anions and amine ligand molecules (calc. 70.50%). The final product of the thermal decomposition of **V** and **VI** are also a black powder that appears to be a CuP_2O_7.

The overall decomposition reactions based on the weight loss data are summarized below:

$$2\,[Cu_4(dpyam)_4(\mu\text{-}HPO_4)_2(\mu\text{-}Cl)_2](Cl_2)\cdot 6H_2O\ (\mathbf{IV}) \xrightarrow{-10.5H_2O} 2\,Cu_4(dpyam)_4(HPO_4)_2Cl_4$$

$$\xrightarrow{-8dpyam + 4Cl + 2H_2O} 4\,Cu_2P_2O_7$$

$$2\,[Cu_4(dpyam)_4(\mu\text{-}HPO_4)_2(\mu\text{-}Br)_2](Br_2)\cdot 6H_2O\ (\mathbf{V}) \xrightarrow{-10.5H_2O} 2\,Cu_4(dpyam)_4(HPO_4)_2Br_4$$

$$\xrightarrow{-8dpyam + 4Br + 2H_2O} 4\,Cu_2P_2O_7$$

$$[Cu_4(dpyam)_4(\mu\text{-}HPO_4)_2(H_2O)_2(NO_3)_2](NO_3)_2.2H_2O\ (\mathbf{VI}) \xrightarrow{-4H_2O} Cu_4(dpyam)_4(HPO_4)_2$$

$$(NO_3)_2(NO_3)_2 \xrightarrow{-4dpyam + 4NO_3 + H_2O} 2\,Cu_2P_2O_7$$

2.4.5 EPR spectra

The polycrystalline EPR spectra of $[Cu_3(dpyam)_3(\mu_3,\eta^3\text{-}HPO_4)(\mu_3,\eta^4\text{-}PO_4)(H_2O)](PF_6)\cdot 3H_2O$ (**I**) at both room temperature and liquid nitrogen temperature (77 K) (as in Appendix IIE) are very broad isotropic with g = 2.12 giving no information regarding to the electronic ground state, due to the misalignment of the CuN_2O_2O' chromophores. This single signal can be due to exchange narrowing and also to the compound containing three different copper sites. No half-field signal was observed.

The EPR spectra of complexes **II** and **III** are given in Appendix IIE. The EPR spectrum of compound **II** at room temperature shows an unresolved isotropic signal with g = 2.127. No half-field signal was observed. At liquid nitrogen temperature a more resolved signal is obtained for compound **II** with $g_{//} = 2.291$ and $g_{\perp} = 2.084$. Compound **III** displays an axial signal at both room temperature ($g_{//} = 2.270$ and $g_{\perp} = 2.027$) and liquid nitrogen temperature ($g_{//} = 2.273$ and $g_{\perp} = 2.022$). No triplet signal has been observed. Apparently the dinuclear units in **III** are not isolated from one another, resulting in exchange narrowing. The signals for compounds **II** and **III** are consistent with the d_{x2-y2} ground state and a distorted square-based pyramidal geometry.

The EPR spectra of **IV** (as in Appendix IIE) at both room temperature and liquid nitrogen temperature exhibit four features at 70, 120, 270 and 400 mT and at 50, 110, 250 and 400 mT, respectively. The spectra are qualitatively similar to that reported for other dinuclear copper(II) compounds for other coupled copper(II) pairs with a $|D| > h$. The feature at 270 mT is most

certainly from a mononuclear copper(II) impurity, which is always present in polynuclear species and the weak absorption at low field (120 mT) is the $\Delta M_s = \pm 2$ transition. The presence of the peaks at high field values is as expected when the value of the axial zero-field splitting parameter $|D|$ is larger than the incident quantum (about 0.3 cm^{-1}). At the high-field side (g = 2.004 at both temperatures) a small shoulder is observed, which is due to a signal from the triplet state with a very small zero field splitting, which indicates that there is an interaction between the Cu (II) ions within complex **IV**.

The EPR spectra of complexes **V** and **VI** are also given in Appendix IIE. The EPR spectra of complex **V** is similar to that of complex **IV** suggesting the magnetic interaction between two copper(II) centers in this tetramer. This type of EPR spectrum is also observed in **V**, which shows four features at 60, 135, 270 and 400 mT at room temperature and at 50, 100, 250 and 400 mT at 77 K. While **VI** reveals a very broad isotropic signal with g = 2.13 at room temperature and 77 K giving no information regarding to the electronic ground state, due to the misalignment of the CuN_2O_2O' chromophores. This unresolved signal might be able to be due to exchange narrowing and also to the fact that the compound contains two different copper sites.

2.4.6 Magnetic properties and superexchange mechanism

The magnetic susceptibility of a powdered sample was measured from 5 to 350 K. The magnetic susceptibility plots of $\{[Cu_3(dpyam)_3(\mu_3,\eta^3\text{-}HPO_4)(\mu_3,\eta^4\text{-}PO_4)(H_2O)](PF_6)\cdot 3H_2O\}_n$ **(I)** are depicted in Figs. 10 (a) and (b) in the form of μ_{eff} versus T and χ^{-1} versus T for three Cu(II) ions.

From 350 K to about 30 K the μ_{eff} stays almost constant between 3.1-2.90 BM. This value is lower than the spin-only value of three uncoupled copper(II) S = ½ ions (theoretical value for g = 2, μ_{eff} = 3.88 BM). At about 30 K the μ_{eff} starts to decrease slightly to a value of 1.95 BM at 5 K. This overall behaviour indicates a very weak antiferromagnetic interaction between the Cu(II) ions.

(a)

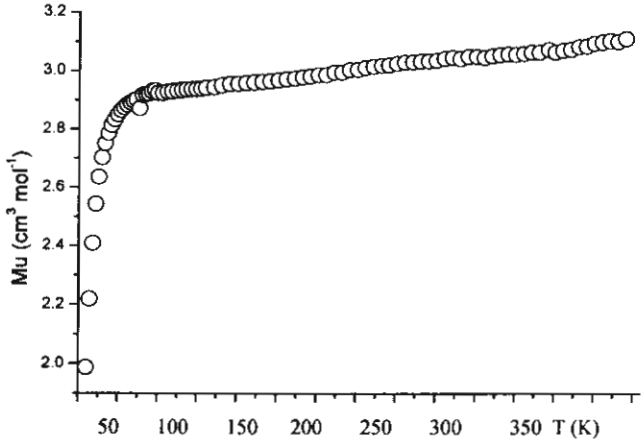

(b)

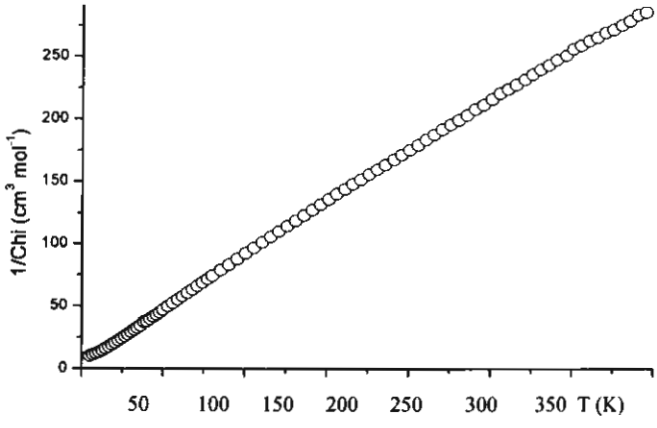

Figure 10 Magnetic susceptibility plot of μ_{eff} versus T (a) and χ^{-1} versus T (b) for compound $[Cu_3(dpyam)_3(\mu_3,\eta^3\text{-}HPO_4)(\mu_3,\eta^4\text{-}PO_4)(H_2O)](PF_6)\cdot 3H_2O\}_n$ **(I)**

The magnetic interaction calculated from Curie-Weiss law out of the χ^{-1} versus T plot, results in a Curie-Weiss constant Θ = -4 K, also indicating a weak antiferromagnetic interaction. This weak interaction can be understood by the fact that the three Cu ions are not equal to each other, the Cu(1) distances to Cu(2) and Cu(3) are large (5.218, 5.942 Å), while the Cu(2)-Cu(3) distance is shorter (4.407 Å), so magnetically it can be also understood as a dinuclear identity which form a polymeric chain via a single Cu ion.

Complex **I** involves both the square pyramidal geometry with an unpaired electron in d_{x2-y2} orbital and an intermediate five-coordinated geometry with an unpaired electron partially delocalized in both d_{x2-y2} and d_{z2} orbitals. In addition, the μ_3,η^3-HPO_4^{2-} and μ_3,η^4-PO_4^{3-} bridges joins copper(II) ions in an equatorial-equatorial and an equatorial-axial configurations between two distorted square pyramidal chromophores and two different geometry chromophores. Hence a weak antiferromagnetic interaction is occurring through the Cu-O-P-O-Cu pathways. The other hydrogenphosphato-bridged complexes with related structures to that of complex **I** are compared as in Table 1.

The magnetic susceptibility plots of complexes **II** and **III** are depicted in Figs 11 and 12 in the form of χ_M and $\chi_M T$ versus T plots. For compound **II**, from 300 K onwards the magnetism is steadily decreasing down to 0.01 $cm^3mol^{-1}K$ at 5 K, indicative for a medium antiferromagnetic coupling between neighbouring Cu(II) ions. The maximum in χ_M, expected for such couplings, is observed at 45 K, and a small Curie tail indicative of paramagnetic impurity is detected below 15 K. The data were fitted using the theoretical expression for a uniform Heisenberg chain. The resulting best fit parameters, corresponding to the full lines were J = -26.20(2) cm^{-1}. For compound **III** the $\chi_M T$ value at 300 K of 0.805 $cm^3mol^{-1}K$, is in agreement with uncoupled spin ½ centres (0.375 $cm^3mol^{-1}K$ per centre with g = 2). Decrease of $\chi_M T$ is observed upon lowering the temperature starting from 50 K down to 0.69 $cm^3\ mol^{-1}K$ at 5 K, which is indicative for a very weak antiferromagnetic interaction. The magnetic data were fitted for two interacting S = ½ centres, based on the general Hamiltonian: $H = -J\ S_1 \cdot S_2$, in which the exchange parameter J is negative for antiferromagetic and positive for ferromagnetic interaction. The data were fitted to the equation given in the literature. Also a Temperature Independent Paramagnetism (TIP) of the Cu(II) ions has been considered. The resulting best fit parameters, corresponding to the full lines were J = -2.85(1) cm^{-1}.

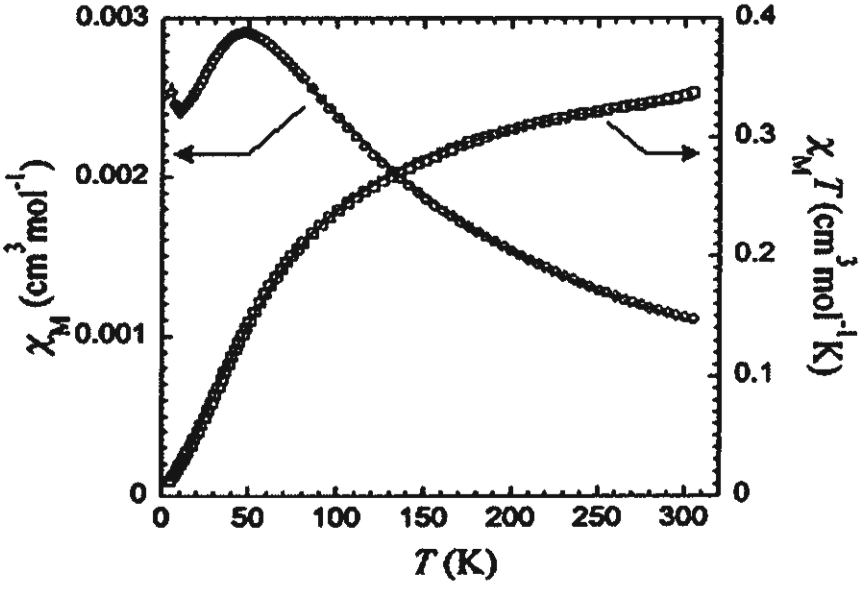

Figure 11 Plots of temperature dependence of the molar magnetic susceptibility χ_M (○) and the $\chi_M T$ product (□) for $[Cu_4(dpyam)_4(\mu_2,\eta^3\text{-}HPO_4)]_n$ **(II)**

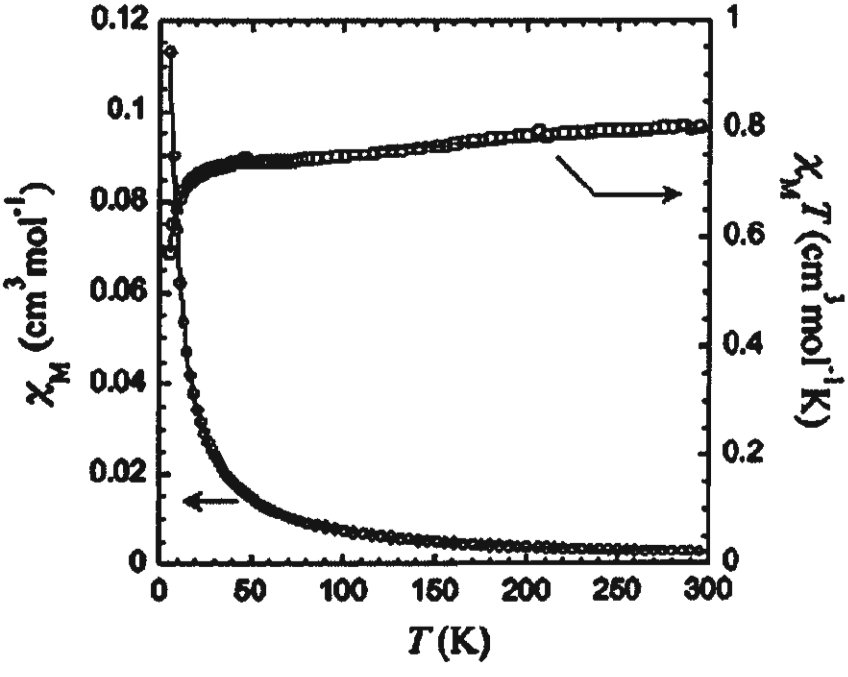

Figure 12 Plots of temperature dependence of the molar magnetic susceptibility χ_M (○) and the $\chi_M T$ product (□) for $[Cu(dpyam)(\mu_2,\eta^2\text{-}H_2PO_4)(H_2PO_4)]_2$ **(III)**

Because of the square pyramidal geometry in compounds **II** and **III** the spin density is mostly in the d_{x2-y2} orbitals of the copper(II) ions. The $H_nPO_4^{(3-n)-}$ bridges, joining the copper atoms in an equatorial-equatorial configuration, the superexchange coupling through the phosphate anion (Cu-O-P-O-Cu) can be expected to be non negligible. The antiferromagnetic couplings found in compounds **II** and **III** are thus in agreement with this structural feature and the large Cu-Cu distances. The compounds together with a number of related complexes **II** and **III** are listed in Table 2 and 3, respectively.

The magnetic susceptibility of a powdered sample for $[Cu_4(dpyam)_4(\mu_4,\eta^3\text{-}HPO_4)_2(\mu\text{-}Cl)_2](Cl)_2\cdot 6H_2O$ **(IV)** was measured from 5 to 350 K. The molar magnetic susceptibility, χ_M, and the product $\chi_M T$ are plotted in Fig. 13.

In this case χ_M gradually increases upon lowering temperature from values at high temperatures in agreement with four uncoupled spin ½ centres. A maximum is reached around 55 K, at which temperature that χ_M decreases sharply. This behaviour is indicative of an antiferromagnetic coupling between some of the copper ions. For simplicity, the two similar tetranuclear units contained in the structure will be considered as identical for the rationalisation of these magnetic properties. Moreover, the diagonal coupling pathways through phosphato groups will also be assumed identical. The magnetic coupling scheme for **IV** proposed in Fig. 14 and the corresponding Hamiltonian writes

$$H = -2J_1(S_A \cdot S_C + S_B \cdot S_D) - 2J_2(S_A \cdot S_B) - 2J_3(S_B \cdot S_C + S_A \cdot S_D) - 2J_4(S_C \cdot S_D) \quad (1)$$

Although the topologies of the compounds differ, this Hamiltonian is identical to one solved for a linear tetranuclear copper compound.

Table 1 Structural and magnetic data of complexes **I-VI** and relevant complexes

[a]*Complex*	*Chromophore*	[b]*Coordination geometry*	[c]τ	[d]*Mode of* $H_xPO_4^{(3-x)-}$	[e]*Bridging configuration*	*J value* (cm^{-1})	*Ref.*
Polynuclear $\{[Cu_3(dpyam)_3(\mu_3,\eta^3\text{-}HPO_4)(\mu_3,\eta^4\text{-}PO_4)(H_2O)](PF_6)\cdot 3H_2O\}_n$ **(I)**	CuN_2O_2O', CuN_2O_3	Dist. SP, TBP	0.17, 0.13, 0.57	3M,3L; 3M,4L	eq-eq, ax-eq	-4.98	This work
$[Cu(dpyam)(\mu,\eta^3\text{-}HPO_4)]_n$ **(II)**	CuN_2O_2O'	dist. SP	0.12	2M,3L	eq-eq, ax-eq	-26.20(2)	This work
$[Cu(phen)(\mu,\eta^2\text{-}HPO_4)(H_2O)_2]_n$ **(1)**	$CuN_2O_2O_2'$	Dist. Oct.	-	2M,2L	ax-ax	-5.86	25
$[Cu_2(bpy)_2(\mu,\eta^2\text{-}HPO_4)(\mu,\eta^1\text{-}H_2PO_4)(\mu,\eta^2\text{-}H_2PO_4)]_n$ **(2)**	CuN_2O_2O'	Dist. SP	0.03, 0.30	2M,2L; 2M,1L	eq-eq, ax-eq	-5.3	26
Dinuclear $[Cu(dpyam)(\mu,\eta^2\text{-}H_2PO_4)(H_2PO_4)]_2$ **(III)**	CuN_2O_2O'	Dist. SP	0,12	1M,1L; 2M,2L	eq-eq	-2.85(1)	This work
Tetranuclear $[Cu_4(dpyam)_4(\mu_4,\eta^3\text{-}HPO_4)_2(\mu\text{-}Cl)_2](Cl)_2\cdot 6H_2O$ **(IV)**	CuN_2O_2O'	Dist. SP	0.020-0.053	4M,3L	eq-eq	22(2), -79(1), 46(4)	This work
$[Cu_4(dpyam)_4(\mu_4,\eta^3\text{-}HPO_4)_2(\mu\text{-}Br)_2](Br)_2\cdot 6H_2O$ **(V)**	CuN_2O_2O'	Dist. SP	0.001-0.071	4M,3L	eq-eq	33(1), -83(1), 12(3)	This work
$[Cu_4(dpyam)_4(\mu_3,\eta^3\text{-}HPO_4)_2(NO_3)_2(H_2O)_2](NO_3)_2\cdot 2H_2O$ **(VI)**	CuN_2O_2O'	Dist. SP, intermediate	0.32^1, 0.49^2	3M,3L	eq-eq, ax-eq	-10.3(1), -5.3(2)	This work
$[Cu_4(phen)_4(\mu_3,\eta^2\text{-}HPO_4)_2(\mu,\eta^2\text{-}H_2PO_4)_2(H_2PO_4)_2].2H_2O$ **(3)**	CuN_2O_2O'	Dist. SP	0.03^1, 0.13^2	1M,1L; 2M,2L; 3M,2L	eq-eq, ax-eq	0.12, -1.32, 0.10	26

[a] Abbreviation: dpyam = di-2-pyridylamine; bpy = 2,2'-bipyridine; phen = 1,10-phenanthroine.
[b] Dist.Oct. = distorted octahedral; Dist.SP = distorted square pyramidal; TBP = trigonal bipyramidal. [c] 1 = Cu(1) chromophore ; 2 = Cu(2) chromophore
[d] M = Metal; L= Ligand [e] ax = axial; eq = equatorial configuration

Table 2 Structural data and electronic spectra of complex **II** and relevant complexes

Complex	Coordination geometry	τ	Chromophore	Tetrago nality	Tetrahedral twist,°	Configuration	J value (cm^{-1})	Ref.
Polymer $[Cu(dpyam)(\mu_3\text{-}HPO_4\text{-}O,O',O'')]_n$ **(II)**	polymeric dist. SP	0.120	CuN_2O_3	0.720	45.5	equatorial-equatorial	-26.20(2)	This work
$Cu(dpyam)(CO_3)]\cdot 3H_2O$ **(1)**	polymeric dist. SP	0.003	$CuN_2O_2O_2'$	0.861	-	axial-equatorial	-	27
$[Cu(dpyam)(H_2O)_2(SO_4)]$ **(2)**	polymeric elong.oct	-	$CuN_2O_2O_2'$	0.815	15.8	axial-axial	-	28
$[Cu(phen)(H_2O)_2(SO_4)]$ **(3)**	polymeric elong.oct	-	$CuN_2O_2O_2'$	0.808	-	axial-axial	-3.8	29
$[Cu(oaoH_2)(H_2O)_2(SO_4)]$ **(4)**	polymeric dist.oct	-	$CuN_2O_2O_2'$	0.832	-	axial-equatorial	-1.0	30
Monomer $[Cu(dpyam)(CO_3)(H_2O)]\cdot 2H_2O$ **(5)**	monomeric dist.SP	0.096	CuN_2O_3	0.899	50.3	-	-	31
$[Cu(tmen)(H_2O)_2(SO_4)]\cdot H_2O$ **(6)**	monomeric dist.SP	0.085	CuN_2O_3	0.908	-	-	-	32
Dimer $[Cu(oaoH_2)(H_2O)(SO_4)]_2$ **(7)**	dinuclear dist.TP	0.145	CuN_2O_3	0.774	-	axial-equatorial	-1.27	30
$[Cu(dpyam)(CO_3)]_2\cdot H_2O$ **(8)**	dinuclear dist.SP	0.220	CuN_2O_3	0.815	5.9[a], 5.1[b]	axial-equatorial	-9.9	33

dpyam = di-2-pyridylamine; bpy = 2,2'-bipyridine; phen = 1,10-phenanthroine; $oaoH_2$; oxamide oxime; tmen = N,N,N',N'-tetramethylethylenediamine; [a]chromophore A ; [b] chromophore B; dist.oct = distorted octahedral; dist.SP = distorted square pyramidal; dist.TP = distorted tetragonal pyramidal

Table 3 Structural data and electronic spectra of complex **III** and relevant complexes

Complex	Coordination geometry	τ	Chromophore	Tetragonality	Tetrahedral twist,°	Bridging configuration	J value (cm^{-1})	Ref.
Dinuclear $[Cu(dpyam)(\mu\text{-}H_2PO_4\text{-}O,O')(H_2PO_4)]_2$ **(III)**	dinuclear SP	0.120	CuN_2O_3	0.874	14.00	equatorial-equatorial	- 2.85(1)	this work
$[Cu(dpyam)(C_6H_3Cl_2OCH_2COO)_2]_2$ **(1)**	dinuclear dist.SP	0.480	CuN_2O_3	0.897	-	axial-equatorial	-0.8	34
$[Cu(dpyam)(ONO\text{-}O,O)(\mu\text{-}ONO\text{-}O)]_2 \cdot 2CH_3CN$ **(2)**	dinuclear dist.SP	0.000	CuN_2O_3	0.813	-	axial-equatorial	-	35
$[Cu_2(dpyam)_2(O_2CH)_4(OH_2)]\cdot H_2O$ **(3)**	dinuclear dist.SP	0.113, 0.096	CuN_2O_3	0.841	16.01,19.35	axial-equatorial	-	36
Monomeric $[Cu(dpyam)(NO_2)_2]$ **(4)**	monomeric dist.oct.	0.020	$CuN_2O_2O_2'$	0.813	31.16	-	-	37
$[Cu(dpyam)(O_2CCH_3)_2]\cdot 2H_2O$ **(5)**	monomeric dist.oct.	-	$CuN_2O_2O_2'$	0.764	34.38	-	-	38
$[Cu(bpy)(NO_3)_2]$ **(6)**	monomeric dist.Oct	-	$CuN_2O_2O_2'$	0.776	27.7	-	-	39
$[Cu(TIMM)(NO_2)_2]$ **(7)**	monomeric dist.Oct	-	$CuN_2O_2O_2'$	0.792	-	-	-	40
$[Cu(BimOBz)(NO_3)_2]$ **(8)**	monomeric dist.Oct	-	$CuN_2O_2O_2'$	0.779	15.6	-	-	41
Polymeric $[Cu(dpyam)(NO_3)_2]$ **(9)**	polymeric elong.oct.	-	$CuN_2O_2O_2'$	0.824, 0.817	7.00, 3.80	-	-	42
$[Cu(dpyam)(NO_3)(O_2CCH_2CH_3)]$ **(10)**	polymeric elong.oct.	-	$CuN_2O_2O_2'$	0.753	-	axial-equatorial	-	43
$[Cu(dpyam)(O_2CCH_3)(O_2ClO_2)]\cdot H_2O$ **(11)**	polymeric elong.oct.	-	$CuN_2O_2O_2'$	0.765	-	axial-axial	-	44

dpyam = di-2-pyridylamine; bpy = 2,2'-bipyridine; TIMM = Tris[2-(1-methyl)imidazolyl]methoxymethane; BimOBz = bis(1-methyl-4,5-diphenylimidaz-2-oyl) (benzyloxy)methane; dist.oct= distorted octahedral; dist.SP = distorted square pyramidal; elong.oct. = elongated octahedral.

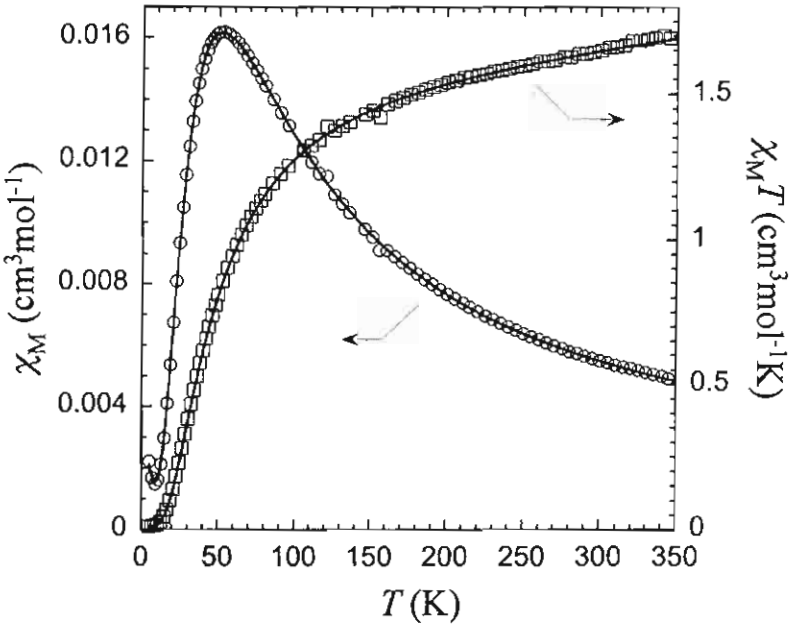

Figure 13 Plots of temperature dependence of the molar magnetic susceptibility χ_M (○) and the $\chi_M T$ product (□) for $[Cu_4(dpyam)_4(\mu_4,\eta^3\text{-}HPO_4)_2(\mu\text{-}Cl)_2](Cl)_2 \cdot 6H_2O$ **(IV)**

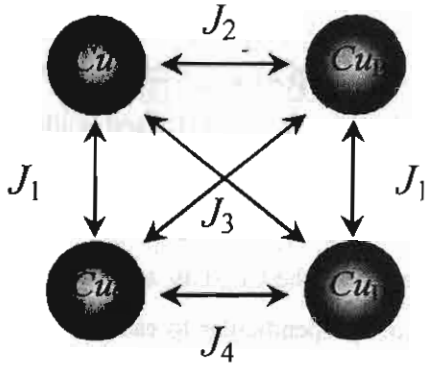

Figure 14 Scheme of the magnetic interactions used in the calculations for $[Cu_4(dpyam)_4(\mu_4,\eta^3\text{-}HPO_4)_2(\mu\text{-}Cl)_2](Cl)_2 \cdot 6H_2O$ **(IV)** and $[Cu_4(dpyam)_4(\mu_4,\eta^3\text{-}HPO_4)_2(\mu\text{-}Br)_2](Br)_2 \cdot 6H_2O$ **(V)**

The energy levels and their spin quantum numbers derived are given in the

$S_1=2$ $E_1=-J_1-J_2/2-J_3-J_4/2$

$S_2=1$ $E_2=J_1-J_2/2+J_3-J_4/2$

$S_3=1$ $E_3=(J_2+J_4)/2+\left[(J_2-J_4)^2+(J_3-J_1)^2\right]^{1/2}$

$S_4=1$ $E_4=(J_2+J_4)/2-\left[(J_2-J_4)^2+(J_3-J_1)^2\right]^{1/2}$

$S_5=0$ $E_5=J_1+J_3+(J_2+J_4)/2+\left[4(J_1^2+J_3^2)+J_2^2+J_4^2-2J_1(J_2+2J_3+J4)-2J_2(J_3-J_4)-2J_3J_4\right]^{1/2}$

$S_6=0$ $E_6=J_1+J_3+(J_2+J_4)/2-\left[4(J_1^2+J_3^2)+J_2^2+J_4^2-2J_1(J_2+2J_3+J4)-2J_2(J_3-J_4)-2J_3J_4\right]^{1/2}$

Considering also that the g values are identical for all copper ions, the molar magnetic susceptibility is then:

$$\chi_M=\frac{N_A g^2\beta^2}{3k_BT}\frac{\sum_i S_i(S_i+1)(2S_i+1)\exp(-E_i/k_BT)}{\sum_i(S_i+1)\exp(-E_i/k_BT)} \qquad (2)$$

A term taking into account a small monomeric paramagnetic impurity was added to this expression and evaluated from the low temperature data as 0.07%. To avoid over-parameterisation, these terms were held constant during the fitting procedure as well as the g value, which was fixed at 2. For this compound, the experimental data were first fitted to eq. 2 letting the coupling constants vary by groups of 2 and 3 and holding the other(s) to 0. This way, it was found first that $2J_3$ had to be negative of the order of -90 K, and second, that the other coupling constants should be positive with J_1 and J_2 of the same order, to obtain a good fit. At this point one has to remark that apart for the Cu_A-Cu_C and Cu_B-Cu_D pairs, the basal planes of the other pairs of copper ions are almost perpendicular to each other. This indicates that the overlap between the spin-rich d_{x2-y2} orbitals of these copper ions cannot be expected to be important. In addition, Cu_C-O-Cu_D angles are close to 90°, value yielding ferromagnetic interaction in alkoxo- or hydroxo- bridged copper dimers. Finally, chloride bridges between Cu_A and Cu_B and Cu_C and Cu_D respectively correspond to the axial coordination site of the copper ions where the spin density is negligible. Therefore, the participation of this pathway to the interactions should be negligible.

Hence the data were then fit by forcing $J_1 = J_2$ and letting the three remaining coupling constants free, starting from $J_3<0$ and J_1 and $J_4>0$. The two sets of best fit parameters,

corresponding to the full lines in Fig. 13, were obtained as $2J_1 = 2J_2 = 22(1)$ cm^{-1}, $2J_3 = -79.4(7)$ cm^{-1}, $2J_4 = 46(3)$ cm^{-1}. This concludes that the compound presents a singlet ground state with a first excited triplet state at E_4-E_6 (eg. 76 cm^{-1}) above it. The molar magnetic susceptibilities of complexes **V** and **VI** are depicted in Figs. 15 and 16.

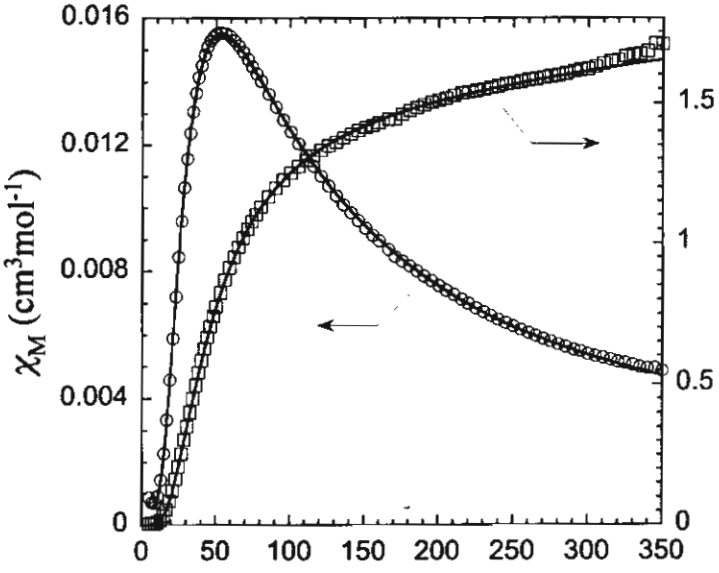

Figure 15 Plots of temperature dependence of the molar magnetic susceptibility χ_M (○) and the $\chi_M T$ product (□) for $[Cu_4(dpyam)_4(\mu_4,\eta^3\text{-}HPO_4)_2(\mu\text{-}Br)_2](Br)_2 \cdot 6H_2O$ **(V)**

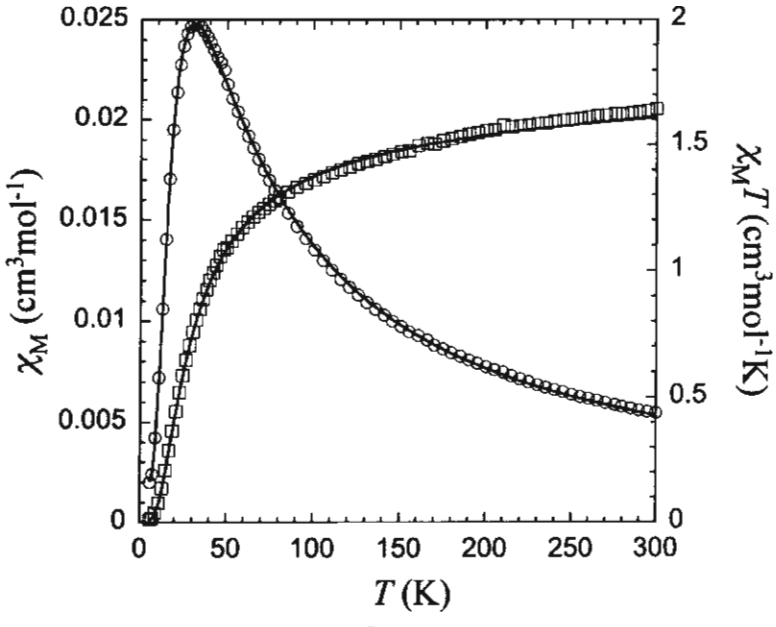

Figure 16 Plots of temperature dependence of the molar magnetic susceptibility χ_M (○) and the $\chi_M T$ product (□) for $[Cu_4(dpyam)_4(\mu_3,\eta^3\text{-}HPO_4)_2(NO_3)_2(H_2O)_2](NO_3)_2 \cdot 2H_2O$ **(VI)**

Compound **V** is isostructural with compound **IV** and involves a similar asymmetric unit and similar distorted square pyramidal geometry. Hence the data were then fit by forcing $J_1 = J_2$ and letting the three remaining coupling constants free, starting from $J_3<0$ and J_1 and $J_4>0$. The two sets of best fit parameters, corresponding to the full lines were obtained as $2J_1 = 2J_2 = 33.3(7)$ cm^{-1}, $2J_3 = -83.1(5)$ cm^{-1}, $2J_4 = 12(2)$ cm^{-1}. This concludes that the compound presents a singlet ground state with a first excited triplet state at E_4-E_6 (and 84 cm^{-1}) above it.

Fig. 17 shows the magnetic interaction scheme of **VI**, which was used for the fitting procedure and is based on the assumption that the magnetic coupling of the outer Cu ions (Cu(1)-Cu(2), Cu(1)-Cu(2A)) is identical. This is understandable as the main difference lies in a long Cu-O apical bond, where no spin density is expected. The corresponding Hamiltonian is then :

$$H = -J_1\left(S_1 \cdot S_2 + S_1 \cdot S_{2'} + S_{1'} \cdot S_2 + S_{1'} \cdot S_{2'}\right) - J_2\left(S_2 \cdot S_{2'}\right)$$

Applying the Kambe vector coupling method with $S_A = S_1+S_{1'}$ and $S_B = S_2+S_{2'}$ (1 is for outer magnetic Cu-Cu interaction and 2 for inner magnetic Cu-Cu interaction, see Fig. 17) yields the following expression for the energy levels:

$$E(S_T,S_A,S_B)=-\frac{J_1}{2}\left(S_T(S_T+1)-S_A(S_A+1)-S_B(S_B+1)\right)-\frac{J_2}{2}\left(S_B(S_B+1)\right)$$

and after inserting in the van Vleck equation the expression for the molar susceptibility :

$$\chi_{tetra}=(1-p)\frac{Ng^2\beta^2}{k_BT}\frac{\left[2+2\exp\left(\frac{J_2}{k_BT}\right)+10\exp\left(\frac{(J_1+J_2)}{k_BT}\right)\right]}{\left[4+3\exp\left(\frac{J_2}{k_BT}\right)+5\exp\left(\frac{(J_1+J_2)}{k_BT}\right)+\exp\left(\frac{-2J_1+J_2}{k_BT}\right)\right]}+\frac{4\times0.375\times p}{T}+TIP$$

which includes terms to take into account: Temperature Independent Paramagnetism (TIP) and a monomeric paramagnetic impurity (p). Fitting the experimental data to this expression yields the full lines corresponding to the parameters g = 1.99(1), J_1 = -20.4(1) cm^{-1}, J_2 = -10.1(2) cm^{-1}. In light of the longer distance of the inner Cu-Cu ions (Cu(1)-Cu(1A)) in contrary to the outer Cu-Cu distance (Cu(1)-Cu(2)), the found J values seem to be reasonable.

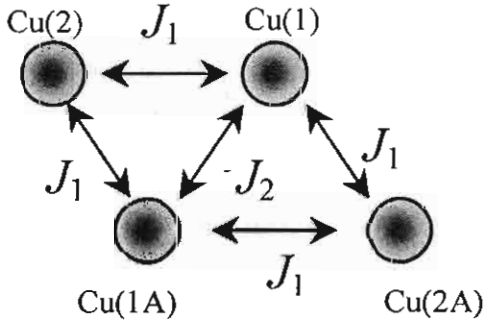

Figure 17 Scheme of the magnetic interactions used in the calculations for $[Cu_4(dpyam)_4(\mu_3,\eta^3\text{-}HPO_4)_2(NO_3)_2(H_2O)_2](NO_3)_2\cdot2H_2O$ **(VI)**

Because of the square pyramidal geometry in compounds **IV** and **V** the spin density is mostly in the $d_{x^2-y^2}$ orbitals of the copper(II) ions. The $H_nPO_4^{(3-n)-}$ bridges join the copper atoms in an equatorial-equatorial configuration, the superexchange coupling through the phosphate anion (Cu-O-P-O-Cu) can be expected to be non negligible. The antiferromagnetic couplings found in compounds **IV** and **V** are thus in agreement with this structural feature and the large Cu-Cu distances. The magnetic susceptibility measurements (5-350 K) reveal an antiferromagnetic interaction. While the phosphate bridges in compound **VI** join the copper atoms in an equatorial-equatorial and an equatorial-axial modes between two distorted square pyramidal chromophores

with an unpaired electron in $d_{x^2-y^2}$ orbital and link the copper atoms in an axial-equatorial mode between an intermediate five-coordinate chromophore and a distorted square pyramidal chromophore with an unpaired electron partially delocalized in both $d_{x^2-y^2}$ and d_{z^2} orbitals for an intermediate five-coordinate chromophore. Hence, a weak antiferromagnetic interaction is occurring through the Cu-O-P-O-Cu pathways.

2.5 Conclusions

The second part of this research sets out to examine and develop the preparative work of a series of polynuclear hydrogenphosphato-bridged copper(II) complexes with di-2-pyridylamine (dpyam) ligand. The spectroscopic and magnetic characterization, the crystal structure determination and the magneto-structural correlation of this complex system are investigated and discussed.

The polynuclear hydrogenphosphato-bridged copper(II) complexes $\{[Cu_3(dpyam)_3(\mu_3,\eta^3\text{-}HPO_4)(\mu_3,\eta^4\text{-}PO_4)(H_2O)](PF_6)\cdot 3H_2O\}_n$ **(I)**, $[Cu(dpyam)(\mu_2,\eta^3\text{-}HPO_4)]_n$ **(II)**, $[Cu(dpyam)(\mu_3,\eta^3\text{-}H_2PO_4)(H_2PO_4)]_2$ **(III)**, $[Cu_4(dpyam)_4(\mu_4,\eta^3\text{-}HPO_4)_2(\mu\text{-}Cl)_2](Cl)_2\cdot 6H_2O$ **(IV)**, $[Cu_4(dpyam)_4(\mu_4,\eta^3\text{-}HPO_4)_2(\mu\text{-}Br)_2](Br)_2\cdot 6H_2O$ **(V)** and $[Cu_4(dpyam)_4(\mu_3,\eta^3\text{-}HPO_4)_2(NO_3)_2(H_2O)_2](NO_3)_2\cdot 2H_2O$ **(VI)** were prepared directly from the mole ratio in various solvents. All products were analyzed by elemental microanalyses and TG-DTA and characterized spectroscopically (IR, EPR, solid state and VIS). The X-ray crystal structures of all products are determined and reported in details in comparison with those of the related complexes.

Complexes **I** and **II** exhibit polymeric chains of the $[Cu_3(dpyam)_3(\mu_3,\eta^3\text{-}HPO_4)(\mu_3,\eta^4\text{-}PO_4)(H_2O)]^+$ cation and $[Cu(dpyam)(\mu_2,\eta^3\text{-}HPO_4)]$ unit, respectively with the novel bridging coordination modes $\mu_3,\eta^3\text{-}HPO_4$ and $\mu_3,\eta^4\text{-}PO_4$ for **I** and $\mu_2,\eta^3\text{-}HPO_4$ for **II**. The trimeric unit in **I** involves two CuN_2O_2O' chromophores with a tetrahedrally distorted square-based pyramidal geometry (τ = 0.17 and 0.13) and a CuN_2O_3 chromophore with an intermediate five-coordinate geometry (τ = 0.57). Complex **II** displays a distorted square-based pyramidal geometry of the CuN_2O_2O' chromophore with τ = 0.12. Complex **III** is a dinuclear compound consisting of the $\mu_2,\eta^2\text{-}H_2PO_4$ bridge and the monodentate H_2PO_4 group with a distorted square pyramidal CuN_2O_2O' chromophore (τ = 0.12). Complexes **IV**, **V** and **VI** are tetranuclear compounds consisting of the tetrameric units $[Cu_4(dpyam)_4(\mu_4,\eta^3\text{-}HPO_4)_2(\mu\text{-}Cl)_2]^{2+}$, $[Cu_4(dpyam)_4(\mu_4,\eta^3\text{-}HPO_4)_2(\mu\text{-}Br)_2]^{2+}$ and $[Cu_4(dpyam)_4(\mu_3,\eta^3\text{-}HPO_4)_2(NO_3)_2(H_2O)_2]^{2+}$, respectively. Complexes **IV** and **V** are isostructural, both having the $\mu_4,\eta^3\text{-}HPO_4$ bridging coordination mode with the halide bridges. Each copper(II) environment involves a range of the distorted square pyramidal geometry of CuN_2O_2X chromophores with τ = 0.02-0.05 for **IV** and τ = 0.001-0.07 for **V**. Complex **VI** exhibits two different geometries, a tetrahedrally distorted square-based pyramid (τ = 0.32) of two CuN_2O_2O' chromophores and an intermediate five-coordinate geometry

(τ = 0.52) of the other two CuN_2O_3 chromophores with an unprecedented μ_4,η^3-HPO_4 bridging coordination mode.

The magnetic interaction in **I** calculated from Curie-Weiss law out of the χ^{-1} versus T plot, results in a Curie-Weiss constant Θ = -4 K, also indicating a weak antiferromagnetic interaction. This weak interaction can be understood by the fact that the three Cu ions are not equal to each other, the Cu(1) distances to Cu(2) and Cu(3) are large (5.218, 5.942 Å), while the Cu(2)-Cu(3) distance is shorter (4.407 Å), so magnetically it can be also understood as a dinuclear identity which form a polymeric chain via a single Cu ion. Compounds **II** and **III** have the singlet-triplet energy gaps J = -26.20(2) and -2.85(1) cm^{-1}, respectively, which confirm the medium and weak antiferromagnetic interactions, respectively between neighboring Cu(II) ions. Because of the square pyramidal geometry in **II** and **III** the spin density is mostly in the d_{x2-y2} orbitals of the copper(II) ions. Although the $H_nPO_4^{(3-n)-}$ bridges, join the copper atoms in an equatorial-equatorial configuration, both square bases are not parallel in the same plane with an anti-anti or syn-anti configuration of the $H_nPO_4^{(3-n)-}$ bridges. Consequently, the superexchange coupling through the phosphate anion (Cu-O-P-O-Cu) can be expected to be non negligible. The antiferromagnetic couplings found in **II** and **III** are thus in agreement with this structural feature and the large Cu-Cu distances. Compound **IV** has the singlet-triplet energy gaps $2J_1 = 2J_2 = 22(1)$ cm^{-1}, $2J_3 = -79.4(7)$ cm^{-1}, $2J_4 = 46(3)$ cm^{-1} for different pathways. Those of **V** are $2J_1 = 2J_2 = 33.3$ (7) cm^{-1}, $2J_3 = -83.1(5)$ cm^{-1}, $2J_4 = 12(2)$ cm^{-1}. This concludes that both compounds present a singlet ground state. Compound **VI** has the singlet-triplet energy gaps $J_1 = -20.4(1)$ cm^{-1} and $J_2 = -10.1(2)$ cm^{-1}. In light of the longer distance of the inner Cu-Cu ions (Cu(1)-Cu(2)), the found J values seem to be reasonable. The phosphate bridges in **VI** join copper atoms in an equatorial-equatorial modes between two distorted square pyramidal chromophores which have a marked tetrahedral twist of the square bases and the large Cu-Cu distance and link the copper atoms in the equatorial-axial and axial-axial configuration modes between two different geometries (τ = 0.32 and 0.52). The antiferromagnetic interaction found in **VI** is thus in agreement with this structural feature.

The results of all products obtained in this complex series have been published[25, 45-49].

References

1. Lii K.-H, Huang Y.-F, Zima V, Huang C.-Y, Lin H.-M, Jiang Y.-C, Liao F.-L, Wang S.-L. ***Chem. Mater.*** 1998; 10: 2599.
2. Cheetham A.K, Férey G, Loiseau T. ***Angew. Chem. Int. Ed.*** 1999; 38: 3268.
3. Kitagawa S, Kondo M. ***Bull. Chem. Soc. Jpn.*** 1998; 71: 1739.
4. Chui S.S.-Y, Lo S.M.-F, Charmant J. P.H, Orpen A.G, Williams I.D. ***Science*** 1999; 283: 1148.
5. Kagan C. R, Mitzi D. B, Dimitrakopoulos C. D. ***Science*** 1999; 286: 945.
6. Batten S. R, Robson R. ***Angew. Chem., Int. Ed. Engl.*** 1998; 37: 1460.
7. Zaworotko M. J. ***Angew. Chem., Int. Ed. Engl.*** 1998; 37: 1211.
8. Hagrman D, Hammond R.P, Haushalter R.C, Zubieta J. ***Chem. Mater.*** 1998; 10: 2091.
9. Hagrman P.J, Hagrman D, Zubieta J. ***Angew. Chem. Int. Ed.*** 1999; 38: 2638.
10. Choudhury A, Natarajan S, Rao C.N.R. ***J. Solid State Chem.*** 1999; 146: 538.
11. Choudhury A, Natarajan S. ***J. Mater. Chem.*** 1999; 9: 3113.
12. Choudhury A, Natarajan S, Rao C.N.R. ***Chem.-A Eur. J.*** 2000; 6: 1168.
13. Chang W.-J, Lin H.-M, Lii K.-H. ***J. Solid State Chem.*** 2000; 157: 233.
14. Tsai Y.-M, Wang S.-L, Huang C.-H, Lii K.-H. ***Inorg. Chem.*** 1999; 38: 4183.
15. Do J, Bontchev R.P, Jacobson A.J. ***Chem. Mater.*** 2001; 13: 2601.
16. Finn R.C, Zubieta J. ***J. Phy. Chem. Solids.*** 2001; 62: 1513.
17. Zhang X.-M, Tong M.-L, Feng S.-H, Chen X.-M. ***J. Chem. Soc. Dalton Trans.*** 2001; 2069.
18. Finn R.C, Zubieta J. ***J. Chem. Soc. Dalton Trans.*** 2000; 16: 856.
19. Zhang X.-M, Wu H.-S, Gao S, Chen X.-M. ***J. Solid State Chem.*** 2003; 176: 69.
20. Chang W.-J, Chen C.-Y, Lii K.-H. ***J. Solid State Chem.*** 2003; 172: 6.
21. Lin Z.-E, Zhang J, Sun Y.-Q, Yang G.-Y. ***Inorg. Chem.*** 2004; 43: 797.
22. Zhang Y, Haushalter R.C, Zubieta J. ***Inorg. Chim. Acta.*** 1997; 260: 105.
23. Lin C.-H, Wang S.-L. ***Inorg. Chem.*** 2001; 40: 2918.
24. Lu Y, Wang E, Yuan M, Luan G, Li Y, Zhang H, Hu C, Yao Y, Qin Y, Chen Y. ***J. Chem. Soc. Dalton Trans.*** 2000; 3029.
25. Youngme S, Phuengphai P, Pakawatchai C, van Albada GA, Tanase S, Mutikainen I, Turpeinen U, Reedijk J. ***Inorg. Chem. Commun.*** 2005; 8: 335.
26. Youngme S, Phuengphai P, Pakawatchai C, van Albada GA, Tanase S, Mutikainen I, Turpeinen U, Reedijk J. ***Polyhedron*** 2006; inpress.

27. Sletten J, ***Acta Chem. Scand., Sect. A*** 1984; 38: 491.
28. Youngme S, Chaichit N, Pakawatchai C, Booncoon S, ***Polyhedron*** 2002; 21: 1279.
29. Xu L, Wang E, Peng J, Huang R. ***Inorg. Chem. Commun.*** 2003; 6: 740.
30. Endres H, Nöthe D, Rossato E, Hatfield WE. ***Inorg. Chem.*** 1984; 23: 3467.
31. Akhter P, Fitzsimons P, Hathaway B. ***Acta Crystallogr., Sect. C*** 1991; 47 308.
32. Balvich J, Fivizzani KP, Pavkovic SF, Brown JN. ***Inorg. Chem.*** 1976; 15 71.
33. Youngme S, Chaichit N, Kongsaeree P, van Albada GA, Reedijk J. ***Inorg. Chim. Acta*** 2001; 20: 232.
34. Psomas G, Raptopoulou CP, Iordanidis L, Dendrinou- Samara C, Tangoulis V, Kessissoglou DP. ***Inorg. Chem.*** 2000; 39: 3042.
35. Camus A, Marsich N, Lanfredi AMM, Ugozzoli F, Massera C. ***Inorg. Chim. Acta*** 2000; 309: 1.
36. Youngme S, Somjitsripunya W, Chinnakali K, Chantrapromma S, Fun HK. ***Polyhedron*** 1999; 18: 857.
37. Youngme S, Tonpho S, Chinnakali K, Chantrapromma S, Fun HK. ***Polyhedron*** 1999; 18: 851.
38. Youngme S, Pakawatchai C, Fun HK, Chinnakali K. ***Acta Crystallogr., Sect. C*** 1998; 54: 1586.
39. Tadsanaprasittipol A, Kraatz HB, Enright GD. ***Inorg. Chim. Acta*** 1998; 278: 143.
40. Stibrany RT, Potenza JA, Schugar HJ. ***Inorg. Chim. Acta*** 1996; 243: 33.
41. Bhalla R, Helliwell M, Garner CD. ***Inorg. Chem.*** 1997; 36: 2944.
42. Youngme S, Chaichit N, Damnatara K. ***Polyhedron*** 2002; 21: 943.
43. Youngme S, Pakawatchai C, Fun HK. ***Acta Crystallogr., Sect. C*** 1998; 54: 451.
44. Ray N, Tyagi S, Hathaway BJ. ***Acta Crystallogr., Sect. B*** 1982; 38: 1574.
45. Youngme S, Phuengphai P, Chaichit N, Pakawatchai C, van Albada GA, Roubeau O, Reedijk J. ***Inorg. Chim. Acta*** 2004; 357: 3603.
46. Youngme S, Phuengphai P, Pakawatchai C, van Albada GA, Roubeau O, Reedijk J. ***Inorg. Chim. Acta*** 2005; 358: 849.
47. Youngme S, Phuengphai P, Chaichit N, Pakawatchai C, van Albada GA, Reedijk J. ***Inorg. Chim. Acta*** 2005; 358: 2125.
48. Youngme S, Phuengphai P, Chaichit N, van Albada GA, Roubeau O, Reedijk J. ***Inorg. Chim. Acta*** 2005; 358: 2262.

49. Phuengphai P, Youngme S, Pakawatchai C, van Albada GA, Quesada M, Reedijk J. ***Inorg. Chem. Commun.*** 2005; 9: 147.

Part III

Synthesis, Crystal Structure, Spectroscopic and Magnetic Properties of Dinuclear Formato-bridged Copper(II) Compounds

3

Synthesis, Crystal Structure, Spectroscopic and Magnetic Properties of Dinuclear Formato-Bridged Copper(II) Compounds

3.1 Introduction

The triply-bridged dinuclear copper(II) carboxylato complexes involving didentate chelate ligand are reported in the literature[1-14]. These complexes exhibit many types of bridging conformations of the carboxylato bridges (Fig. 1) and various geometries of copper(II) ions. The previous reports have established that the type (antiferromagnetic or ferromagnetic) and magnitude of magnetic exchange interaction are influenced by the bridge identity, the coordination geometry of copper(II) ion, the Cu···Cu separation, the bond angles at the bridging atoms, the dihedral angle between the planes containing the copper(II) ions and the copper-bridging ligand bond lengths[3]. Among the copper(II) carboxylato complexes, the copper(II) acetates form a large family with many structurally characterized complexes for which magnetic and spectroscopic properties have been measured. In contrast, a closely related structure in formate and propionate families is rarely reported. Because of the variety of the geometries displayed by the copper(II) ion and also because of the structurally dependent magnetic properties, an attempt has been made to prepare the copper(II) complexes containing the chelate di-2-pyridylamine (dpyam) ligand and involving the formato bridge. The triply-bridged dinuclear copper(II) complexes $[Cu_2(dpyam)_2(\mu\text{-}O_2CH)(\mu\text{-}OH)(\mu\text{-}OCH_3)](ClO_4)$ **(I)**, $[Cu_2(dpyam)_2(\mu\text{-}O_2CH)(\mu\text{-}OH)_2](ClO_4)\cdot H_2O$ **(II)**, $[Cu_2(dpyam)_2(\mu\text{-}O_2CH)(\mu\text{-}OOCH)(\mu\text{-}OH)](PF_6)$ **(III)**, $[Cu_2(dpyam)_2(\mu\text{-}O_2CH)(\mu\text{-}OH)(\mu\text{-}Cl)](ClO_4)\cdot 0.5H_2O$ **(IV)**, $[Cu_2(dpyam)_2(\mu\text{-}O_2CH)(\mu\text{-}OH)(\mu\text{-}Cl)](PF_6)$ **(V)** and $[Cu_2(dpyam)_2(\mu\text{-}O_2CH)(\mu\text{-}OH)(\mu\text{-}Cl)](BF_4)$ **(VI)** are reported.

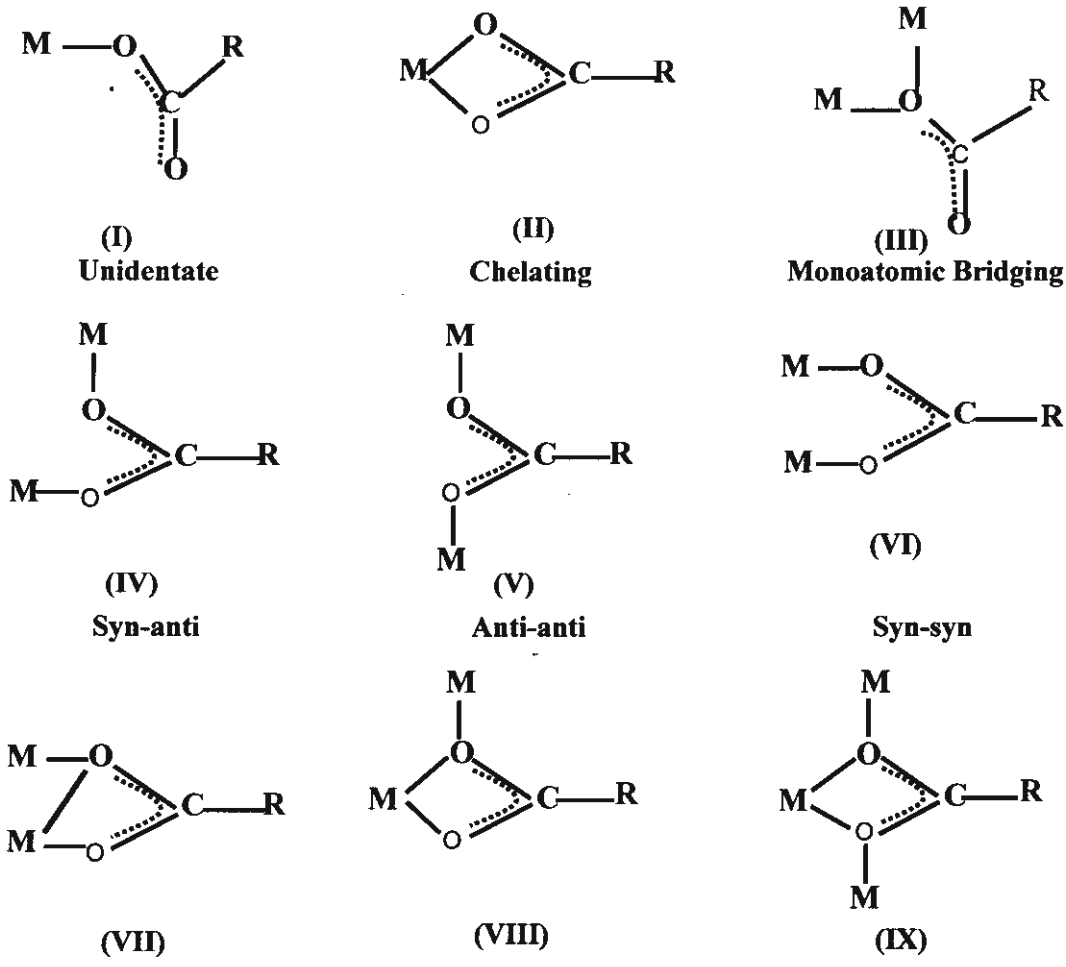

Figure 1 Different coordination modes of carboxylato ligand

3.2 Aims and Scopes

The objective of the third part of this research is to examine and develop the preparation work of the dinuclear copper(II) complexes containing the formate as a bridging ligand and the di-2-pyridylamine as a chelate didentate terminal ligand. The products are characterized by elemental analyses and their spectroscopic properties (IR, solid state VIS, EPR (room temperature and liquid nitrogen temperature)). The molecular and crystal structures were determined by X-ray diffraction method. The room temperature magnetic moment and the temperature variable susceptibilities (5-350 K) were measured and the magneto-structural correlation together with the superexchange pathways are investigated and discussed in comparison with other relevant complexes.

3.3 Experimental

3.3.1 Reagents and physical measurements

All reagents are commercial grade materials and were used without further purification. Elemental analyses(C, H, N) were performed by the Microanalytical Service of Science and Technological Research Equipment Center, Chulalongkorn University on Perkin-Elmer PE2400 CHNS/O Analyzer. Copper content was determined on atomic absorption spectrophotometer. IR spectra were recorded with a Biorad FTS-7/PC FTIR spectrophotometer as KBr pellets/and or as nujol mulls in the 4000 – 450 cm^{-1} spectral range. Solid-state (diffuse reflectance) electronic spectra were recorded as polycrystalline samples on a Perkin-Elmer Lambda2S spectrophotometer over the range 8000–18000 cm^{-1}. X-band powder EPR spectra were obtained on a Jeol RE2x electron spin resonance spectrometer using DPPH (g = 2.0036) as a standard. Magnetic susceptibility measurements (5-280 K) were carried out using a Quantum Design MPMS-5 5T SQUID magnetometer (measurements carried out at 1000 Gauss). Data were corrected for magnetization of the sample holder and for diamagnetic contributions, which were estimated from the Pascal constants.

3.3.2 Syntheses

$[Cu_2(dpyam)_2(\mu\text{-}O_2CH)(\mu\text{-}OH)(\mu\text{-}OCH_3)](ClO_4)$ (I)

A hot methanol solution (10 ml) containing dpyam (0.171 g, 1.0 mmol) was added to a hot aqueous solution (10 ml) of $Cu(ClO_4)_2{\cdot}6H_2O$ (0.371 g, 1.0 mmol), after which solid HCOONa (0.272 g, 4.0 mmol) was added. The resulting green solution was allowed to evaporate at room temperature. After one week, green polygon-shape crystals of **I** were obtained which were filtered off, washed with the mother liquid and air-dried. Yield ca. 80%. Calc. for $[Cu_2(dpyam)_2(\mu\text{-}O_2CH)(\mu\text{-}OH)(\mu\text{-}OCH_3)](ClO_4)$ **(I)**: C, 39.92; H, 3.50; N, 12.70; Cu, 19.20%. Found: C, 39.80; H, 3.62; N, 12.90; Cu, 18.99%.

$[Cu_2(dpyam)_2(\mu\text{-}O_2CH)(\mu\text{-}OH)_2](ClO_4){\cdot}H_2O$ (II)

A hot methanol solution (10 ml) of dpyam (0.171 g, 1.0 mmol) was added to a hot aqueous solution (20 ml) of $Cu(COOH)_2$ (0.154 g, 1.0 mmol). Then a solid of HCOONa (0.204 g, 3.0 mmol) was added, followed by a solid of $NaClO_4$ (0.195 g, 1.0 mmol). The green powder immediately formed, after which the mixture was warmed and the methanol solution (10 ml) and the aqueous solution (10 ml) were added, yielding a clear green solution. On slow evaporation at room temperature for two weeks, the product **II** was isolated as blue rod-shape crystals. They were filtered off, washed with the mother liquid and air-dried. Yield

ca. 30%. Calc. for $[Cu_2(dpyam)_2(\mu\text{-}O_2CH)(\mu\text{-}OH)_2](ClO_4)\cdot H_2O$ **(II)**: C, 37.87; H, 3.48; N, 12.62; Cu, 19.08%. Found: C, 37.59; H, 3.33; N, 12.53; Cu, 18.87%.

$[Cu_2(dpyam)_2(\mu\text{-}O_2CH)(\mu\text{-}OOCH)(\mu\text{-}OH)](PF_6)$ (III)

This complex was prepared by adding a hot DMSO solution (5 ml) of dpyam (0.171 g, 1.0 mmol), to a hot aqueous solution (10 ml) of $Cu(COOH)_2$ (0.154 g, 1.0 mmol), after which a hot methanol solution (10 ml) of KPF_6 (0.184 g, 1.0 mmol) was added. The resulting green solution was allowed to evaporate at room temperature. After two weeks, green hexagon-shape crystals of **III** were obtained which were filtered off, washed with the mother liquid and air-dried. Yield ca. 75%. Calc. for $[Cu_2(dpyam)_2(\mu\text{-}O_2CH)(\mu\text{-}OOCH)(\mu\text{-}OH)](PF_6)$: C, 36.62; H, 2.93; N, 11.65; Cu, 17.62%. Found: C, 36.13; H, 2.58; N, 11.81; Cu, 17.12%.

$[Cu_2(dpyam)_2(\mu\text{-}O_2CH)(\mu\text{-}OH)(\mu\text{-}Cl)](ClO_4)\cdot 0.5H_2O$ (IV)

A hot DMF solution (20 ml) of dpyam (0.171 g, 1.0 mmol) was added to a hot aqueous solution (10 ml) of $CuCl_2\cdot 2H_2O$ (0.171 g, 1.0 mmol). Then a hot aqueous solution (10 ml) of HCOONa (0.136 g, 2.0 mmol) was added to the mixture yielding a dark green solution, after which the solid $KClO_4$ (0.416 g, 3.0 mmol) was added. The resulting green solution was allowed to evaporate at room temperature. After a month, green polygon-shape crystals of **IV** were formed which were filtered off, washed with the mother liquid and air-dried. Yield ca. 75%. Calc. for $[Cu_2(dpyam)_2(\mu\text{-}O_2CH)(\mu\text{-}OH)(\mu\text{-}Cl)](ClO_4)\cdot 0.5H_2O$: C, 37.34; H, 3.13; N, 12.44; Cu, 18.82%. Found: C, 37.66; H, 3.40; N, 12.50; Cu, 18.49%.

$[Cu_2(dpyam)_2(\mu\text{-}O_2CH)(\mu\text{-}OH)(\mu\text{-}Cl)](PF_6)$ (V)

A hot DMF solution (10 ml) of dpyam (0.171 g, 1.0 mmol) was added to a hot DMF solution (10 ml) of $CuCl_2\cdot 2H_2O$ (0.171 g, 1.0 mmol). Then solid HCOONa (0.136 g, 2.0 mmol) was added to the mixture yielding a brown solution. Its color became green by addition of an aqueous solution (5 ml) of KPF_6 (0.184 g, 1.0 mmol). After a month, green hexagon-shape crystals of **V** were obtained, which were filtered off, washed with the mother liquid and air-dried. Yield ca. 81%. Calc. for $[Cu_2(dpyam)_2(\mu\text{-}O_2CH)(\mu\text{-}OH)(\mu\text{-}Cl)](PF_6)$ **(V)**: C, 35.43; H, 2.83; N, 11.81; Cu, 17.85%. Found: C, 35.65; H, 2.71; N, 11.61; Cu, 17.71%.

$[Cu_2(dpyam)_2(\mu\text{-}O_2CH)(\mu\text{-}OH)(\mu\text{-}Cl)](BF_4)$ (VI)

This complex was prepared by adding a hot DMF solution (10 ml) of dpyam (0.171 g, 1.0 mmol) to a hot aqueous solution (10 ml) of $CuCl_2\cdot 2H_2O$ (0.171 g, 1.0 mmol), then an aqueous solution (5 ml) of HCOONa (0.136 g, 2.0 mmol) was added. The resultant solution was then warmed and a solid of $NaBF_4$ (0.329 g, 3.0 mmol) was added. The resulting green solution was allowed to evaporate at room temperature. After two weeks, green polygon-

shape crystals of **VI** were formed which were filtered off, washed with the mother liquid and air-dried. Yield ca. 76%. Calc. for $[Cu_2(dpyam)_2(\mu\text{-}O_2CH)(\mu\text{-}OH)(\mu\text{-}Cl)](BF_4)$: C, 38.58; H, 3.08; N, 12.85; Cu, 19.44%. Found: C, 38.11; H, 3.24; N, 12.57; Cu, 19.12%.

3.3.3 Crystallography

Five expected complexes **I-V** are obtained and have been crystallographically characterized to be a dinuclear copper(II) complexes containing formato bridged while **VI** was characterized spectroscopically because the crystals of this complex were not of good enough quality to carry out a single-crystal X-ray diffraction structure determination.

Reflection data of **I-V** complexes were collected on a 4K Bruker SMART APEX CCD area-detector diffractometer with graphite monochromated Mo Kα radiation (λ= 0.71073 Å) (at a detector distance of 6.0 cm and swing angle of -28°) using SMART program. Raw data frame integration was performed with SAINT, which also applied correction for Lorentz and polarization effects. An empirical absorption correction by using the SADABS program was applied, which resulted in transmission coefficients ranging from 0.654 to 1.000, 0.8520 to 1.000, 0.7123 to 1.000, 0.773 to 1.000 and 0.7891 to 1.000 for **I-V**, respectively. The structure was solved by direct methods and refined by full–matrix least–squares method on $(F_{obs})^2$ with anisotropic thermal parameters for all non–hydrogen atoms except disordered O atoms of the ClO_4^- group and disordered F atoms of the PF_6^- groups using the SHELXTL-PC V 6.12 software package. The O atoms of the ClO_4^- group of **I** and **II** showed disorder; the occupancies of the disordered positions were initially refined and later fixed at 0.45 and 0.55 for **I** and 0.50 and 0.50 for **II**. The O atoms of the ClO_4^- group of **IV** also showed disorder. Attempts to model disordered positions into two sets are unsuccessful. However, their thermal parameters are substantially reasonable. For the structure determination of **III** and **V**, the two F atoms of each PF_6^- group showed disorder; the occupancies of the disordered positions were initially refined and later fixed at 0.47 and 0.53 for **III** and 0.49 and 0.51 for **V**. Furthermore, for **III**, one O atom of a formato group is also disordered and refined with site occupancies of 0.5. All hydrogen atoms of the dpyam ligands in **I** and **III** including one of formato ligand in **I** were geometrically fixed and allowed to ride on the attached atoms. Those of the bridging hydroxo and bridging methoxo groups in **I**, the bridging hydroxo and two bridging formato groups in **III** were located geometrically. All hydrogen atoms in **II**, **IV** and **V** were located geometrically and refined isotropically. The crystal and refinement details for complexes **I-V** are listed in Appendix IIIA.

3.4 Results and Discussion

3.4.1 Description of the crystal structures

3.4.1.1 Description of $[Cu_2(dpyam)_2(\mu\text{-}O_2CH)(\mu\text{-}OH)(\mu\text{-}OCH_3)](ClO_4)$ (I)

Complex **I** is a dinuclear unit copper(II) complex bridging by three different ligands. The structure of **I** consists of symmetric dinuclear $[Cu_2(dpyam)_2(\mu\text{-}O_2CH)(\mu\text{-}OH)(\mu\text{-}OCH_3)]^+$ cations with a single ClO_4^- counteranion. This unit is depicted in Fig. 2 together with the numbering scheme. Selected bond distances and angles are listed in Appendix IIIB.

Each copper(II) ion involves a CuN_2O_3 chromophore. The coordination geometry around each copper(II) ion is distorted trigonal bipyramidal ($\tau = 0.61$). The structure index is defined as $\tau = (\beta\text{-}\alpha)/60$, where β and α are the largest coordination angles[15]. The three longer bonds in the trigonal planar plane are a nitrogen atom of the dpyam ligand (Cu-N(2) distance 2.010(4) Å), an oxygen atom of the bridging formato ligand (Cu-O(3) distance 2.175(3) Å) and an oxygen atom of the bridging methoxo ligand (Cu-O(2) distance 2.169(5) Å). The two shorter bonds in the axial positions involve the other nitrogen atom of the dpyam ligand (Cu-N(1) distance 1.961(4) Å) and an oxygen atom of the bridging hydroxo ligand (Cu-O(1) distance 1.918(4) Å). This is typical for the trigonal bipyramidal geometry. The formate anion bridges two copper atoms in a syn-syn arrangement. The Cu-Cu distance is 3.023(1) Å. The bridging Cu(1)-O(1)-Cu(1A) and Cu(1)-O(2)-Cu(1A) angles are 104.0(3) and 88.3(2)°, respectively. The dpyam ligands are essentially planar, with only a dihedral angle of 6.9° between the individual pyridine rings. The bite angles of the dpyam ligands (N-Cu-N, 91.4 (2)°) are only slightly greater than 90°.

The lattice is further stabilized by hydrogen bonding between the amine N and the oxygen atom of bridging formato group with a N···O contact of 2.869 Å.

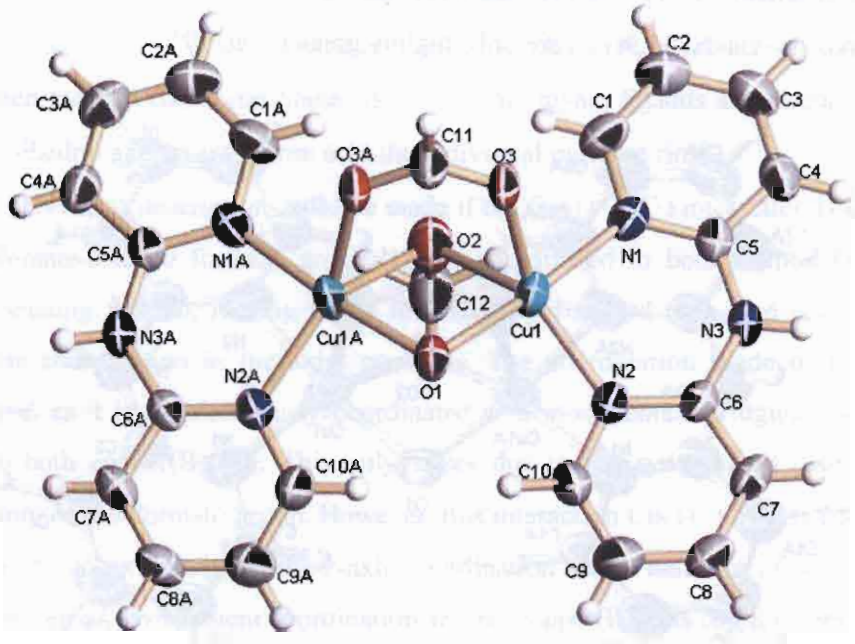

Figure 2 The molecular structure of **I**

3.4.1.2 Description of $[Cu_2(dpyam)_2(\mu\text{-}O_2CH)(\mu\text{-}OH)_2](ClO_4)\cdot H_2O$ (II)

The structure of **II** consists of a symmetric dinuclear $[Cu_2(dpyam)_2(\mu\text{-}O_2CH)(\mu\text{-}OH)_2]^+$ cation, with ClO_4^- counter anions. This unit is depicted in Fig. 3, together with the numbering scheme. Selected bond distances and angles are listed in Appendix IIIB.

Both copper(II) ions of the complex cation are linked through double hydroxo and a formato bridges, leading to a Cu–Cu distance of 2.902(1) Å. The coordination environment around each copper(II) ion can be best described as tetrahedrally distorted square pyramidal CuN_2O_2O' chromophore with a τ value of 0.27. The four shorter bonds in the basal plane involve two nitrogen atoms of the dpyam ligand (Cu-N 2.005(3) and 2.030(3) Å), two oxygen atoms of bridging hydroxo ligands (Cu-O 1.952(3) and 1.955 Å). An oxygen atom of the triatomic bridging formato ligand completes five-coordination at Cu(1) atom (Cu-O(3) 2.345 (3) Å), consistent with the typical square pyramidal geometry. The four basal atoms are not coplanar, showing a significant tetrahedral distortion with a dihedral angle of 23.8° formed between CuO_2 and CuN_2 planes and the copper atom is displaced by 0.189 Å from the basal plane toward the O(3) atom. The dinuclear unit is slightly planar and the dihedral angle between the basal N_2O_2 planes is 14.4°. The bridging Cu(1)-O(1)-Cu(1A) and Cu(1)-O(2)-Cu (1A) are 95.8(1) and 96.0(1)°, respectively. The dpyam ligands are essentially planar with

small dihedral angles of 6.6° between the individual pyridine rings. The bite angles of the dpyam ligands (N–Cu–N, 91.9(1)°) are only slightly greater than 90°.

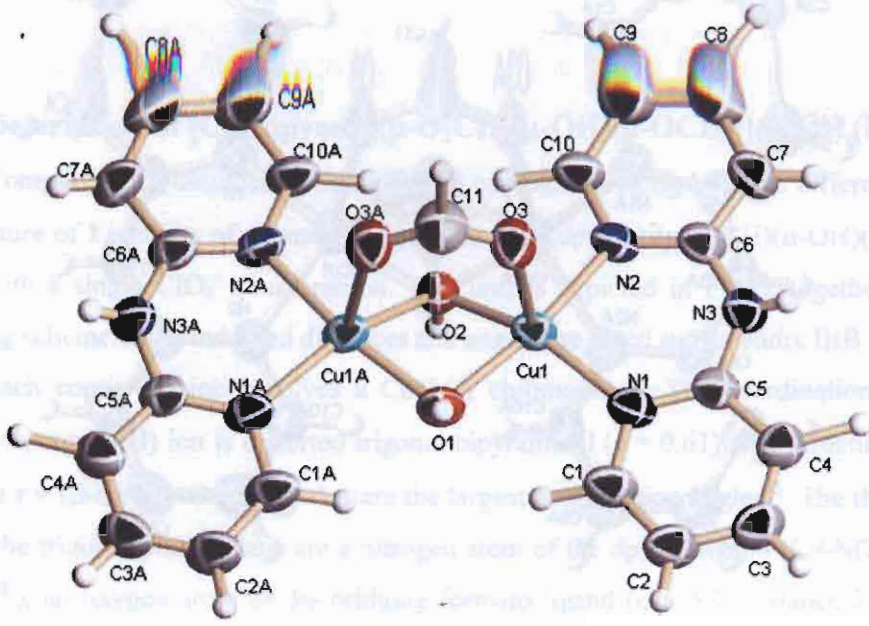

Figure 3 The molecular structure of **II**

3.4.1.3 Description of $[Cu_2(dpyam)_2(\mu\text{-}O_2CH)(\mu\text{-}OOCH)(\mu\text{-}OH)](PF_6)$ (III)

Complex **III** is made up of one-half $[Cu(dpyam)(\mu\text{-}O_2CH)_2(\mu\text{-}OH)]^+$ moiety, which the other half being inversion related and a disordered PF_6^- anion. This unit is depicted in Fig. 4 together with the numbering scheme. Selected bond distances and angles are listed in Appendix IIIB.

The formato ligands, which one of them is in a disordered position, in **III** exhibit different coordination mode. Both copper(II) ions within the dinuclear unit are bridged by three ligands, i.e. a hydroxo group and two formato ligands, which one formato ligand is in a familiar didentate syn,syn η^1: η^1: μ_2-bridging mode and the other is in the monoatomic bridging mode. A terminal dpyam ligand completes five coordination at each copper atom, which has a distorted trigonal bipyramidal geometry (τ = 0.59) of the CuN_2O_3 chromophore. An oxygen atom of the monoatomic bridged formato ligand (Cu(1)-O(2) 2.144(6) Å), an oxygen atom of the η^1: η^1: μ_2-bridging formato ligand (Cu(1)-O(4) 2.200(3) Å) and a nitrogen atom of the dpyam ligand (Cu(1)-N(2) 2.029(4) Å) comprise the trigonal plane. These equatorial distances are considerably longer than the two axial bonds occupied by an oxygen atom of the bridging hydroxo ligand (Cu(1)-O(1) 1.934(5) Å) and another nitrogen atom of the dpyam ligand (Cu(1)-N(1) 1.972(4) Å) corresponding to the typical environment of the

trigonal bipyramidal geometry. The Cu···Cu separation is 3.113(5) Å. The bridging Cu(1)-O (1)-Cu(1A), Cu(1)-O(2)-Cu(1A) angles are 107.2(4), 93.1(4)°, respectively. The dihedral angle between the two equatorial planes is 90.3°. The dpyam ligands are essentially planar, with only a dihedral angle varies from 6.1° the individual pyridine rings.

An alternative description could be made if the Cu(1)···O(3) interaction is considered. The monodentate-bridged formato group is also coordinated to both copper(II) ions in a didentate chelating fashion, leading to the tetrahedrally-distorted elongated octahedral with off-the-z-axis coordination in the axial positions. The coordination mode of this formato group is novel as it is simultaneously coordinated as a monodentate bridging and didentate chelating to both copper(II) ion. This only arises due to the symmetrical disorder of the second O atom of this formato group. However, this interaction Cu(1)···O(3) is considered to be weak due to an extremely-off-the-z-axis coordination and a half site of the O(3) atom. Hence, the preferred environment coordination around copper(II) ions could be best described as a distorted trigonal bipyramidal geometry.

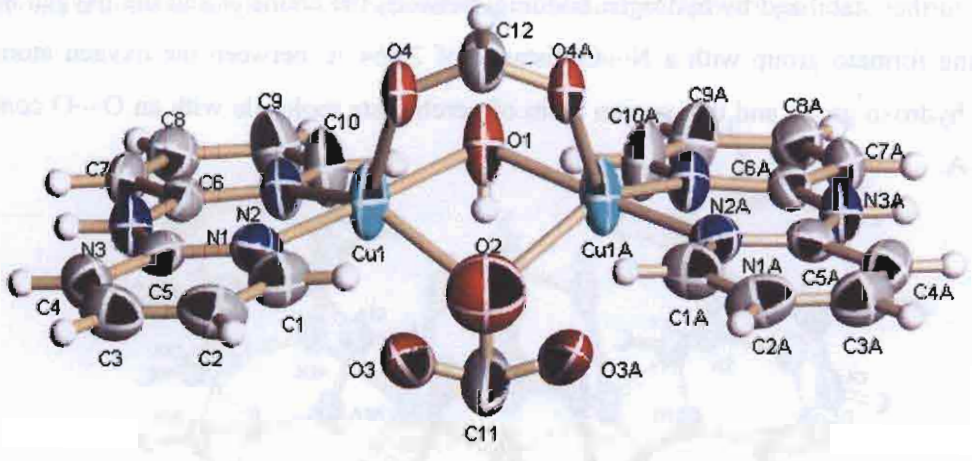

Figure 4 The molecular structure of **III**

The lattice is further stabilized by hydrogen bonding: between the amine N and the oxygen atom of bridging formato group with a N···O contact of 2.917 Å, between the carbon atom of dpyam ligand and the fluoride atom of PF_6^- anion with C···F distance of 3.099 Å.

3.4.1.4 Description of $[Cu_2(dpyam)_2(\mu\text{-}O_2CH)(\mu\text{-}OH)(\mu\text{-}Cl)](ClO_4)\cdot 0.5H_2O$ (IV)

The structure of **IV** consists of symmetric dinuclear $[Cu_2(dpyam)_2(\mu\text{-}O_2CH)(\mu\text{-}OH)(\mu\text{-}Cl)]^+$ cation, a ClO_4^- counter anion and half a molecule of lattice water. This unit is depicted in Fig. 5 together with the used numbering scheme. Selected bond distances and angles are listed in Appendix IIIB.

In the dinuclear unit the copper(II) ions are triply bridged through three different ligands, i.e. formate, chloride and hydroxide anions. Each copper(II) center is coordinated by two oxygen atoms and an chloride atom of the triple bridges and two nitrogen atoms of a dpyam ligand, leading to the five–coordinated, distorted trigonal bipyramidal geometry with CuN_2O_2Cl chromophore (τ = 0.60). The trigonal plane consists of a nitrogen atom of the dpyam ligand (Cu–N(2) distance 2.027(2) Å), a bridging chloro ligand (Cu–Cl(1) distance 2.478(2) Å) and an oxygen atom of the bridging formato ligand (Cu–O(2) distance 2.158(1) Å). The apical coordination sites are occupied by another nitrogen atom of the dpyam ligand (Cu–N(1) distance 1.975(1) Å) and an oxygen atom of the bridging hydroxo group (Cu–O(1) distance 1.916(1) Å). The Cu-Cu distance is 3.036(1) Å. The bridging Cu(1)-O(1)-Cu(1A) and Cu(1)-Cl(1)-Cu(1A) angles are 104.8(1) and 75.6(1)°, respectively. The dpyam ligands are planar, the dihedral angle between the individual pyridine rings is as low as 6.6°. The lattice is further stabilized by hydrogen bonding: between the amine N and the oxygen atom of bridging formato group with a N····O distance of 2.864 Å, between the oxygen atom of bridging hydroxo group and the oxygen atom of perchlorate molecule with an O····O contact of 2.922 Å.

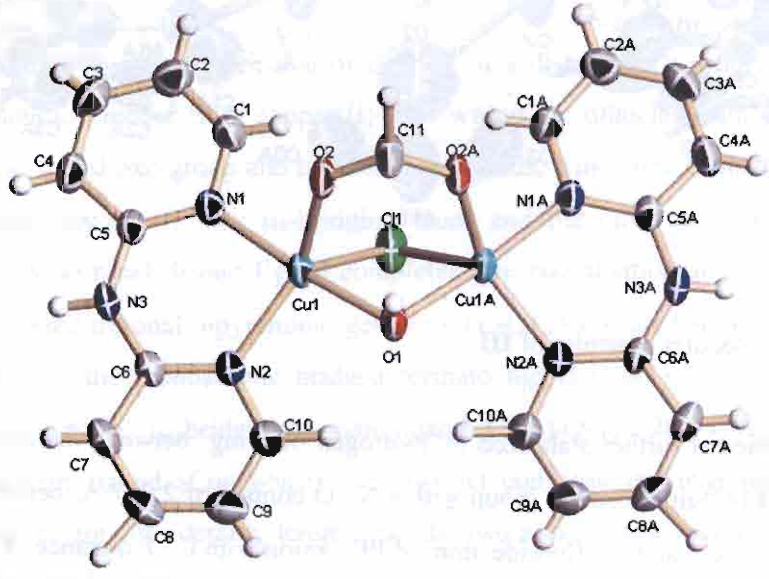

Figure 5 The molecular structure of **IV**

3.4.1.5 Description of $[Cu_2(dpyam)_2(\mu\text{-}O_2CH)(\mu\text{-}OH)(\mu\text{-}Cl)](PF_6)$ (V)

The structure of compound **V** is made up of a centrosymmetric dinuclear $[Cu_2(dpyam)_2(\mu\text{-}O_2CH)(\mu\text{-}OH)(\mu\text{-}Cl)]^+$ cation and a disordered PF_6^- counteranion. This unit is depicted in Fig. 6 together with the numbering scheme. Selected bond distances and angles are listed in Appendix IIIB.

Each copper(II) ion has a distorted trigonal bipyramidal geometry (τ = 0.72, the structure index is defined as $\tau = (\beta\text{-}\alpha)/60$, where β and α are the largest coordination angles), of the CuN_2O_2Cl chromophore, with a nitrogen atom of the dpyam ligand (Cu(1)-N(1) 2.031 (3) Å), an oxygen atom of the bridging formato ligand (Cu(1)-O(1) 2.183(2) Å) and a bridging chloro ligand (Cu(1)-Cl(1) 2.451(1) Å) forming the trigonal plane. The axial site of each copper(II) atom is occupied by another nitrogen atom of the dpyam ligand (Cu(1)-N(2) 1.983(2) Å) and an oxygen atom of the hydroxo ligand (Cu(1)-O(2) 1.918(2) Å, which are shorter than those of the equatorial plane corresponding to the typical environment of the trigonal bipyramidal geometry. The symmetric syn, syn-coordinated formato ligand bridges the two equatorial planes, leading to a Cu···Cu distance of 3.061(5) Å. The dihedral angle between the equatorial planes is 86.8°. The bridging angles (Cu(1)-O(2)-Cu(1A) and Cu(1)-Cl (1)-Cu(1A) are 105.9(1) and 77.2(1)°, respectively. The dpyam ligands are essentially planar, with only a dihedral angle of 4.4° between the individual pyridine rings.

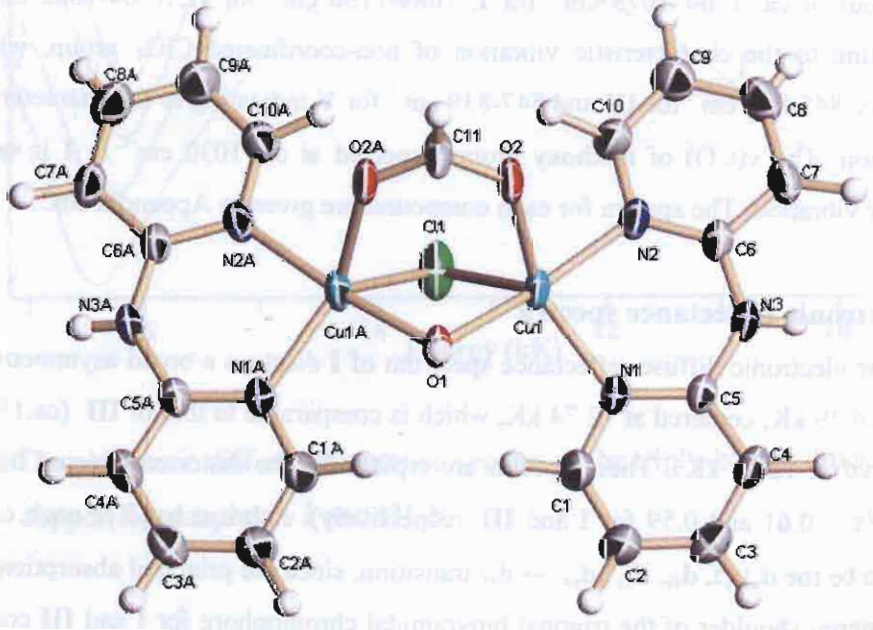

Figure 6 The molecular structure of **V**

The lattice is further stabilized by hydrogen bonding: between the amine N and the oxygen atom of bridging formato group with a N···O distance 2.857 Å, between the oxygen atom of bridging hydroxo group and the fluoride atom of PF_6^- anion with O···F contact of 2.961 Å.

3.4.2 IR spectra

The infrared spectra display a broad band at 3467, 3500, 3580, 3449 and 3563 cm^{-1} for **I-V**, respectively, which can be assigned to the bridging OH vibrations of the hydroxo bridged. The spectra also exhibit the broad and intense bands at 1570 cm^{-1} for **I** and **IV**, 1571 cm^{-1} for **II** and **V** corresponding to the $\nu_{as}(COO^-)$ vibration and a medium broad band at 1344 cm^{-1} for I, 1350 cm^{-1} for **II**, 1357 cm^{-1} for **IV** and 1354 cm^{-1} for **V** corresponding to the ν_s (COO^-) vibration, the difference Δ [$\Delta = \nu_{as}(COO^-) - \nu_s(COO^-)$; 226 cm^{-1} for **I**, 220 cm^{-1} for **II**, 213 cm^{-1} for **IV** and 217 cm^{-1} for **V**] is close to that of NaO_2CH (201 cm^{-1}) as expected for the triatomic bridging coordination mode of the formate group within a dinuclear species. Due to the formato bridges in **III** are present in different coordination modes, two $\nu_{as}(COO^-)$ 1603, 1586 cm^{-1} and two ν_s (COO^-) 1411, 1346 cm^{-1} bands are observed in the IR spectrum. The bands at 1603, 1346 cm^{-1} (Δ = 257 cm^{-1}) are assigned to the stretching modes of the monoatomic formato bridges. The vibrations observed at 1586, 1411 cm^{-1} (Δ = 175 cm^{-1}) are consistent with the triatomic carboxylato bridge. Moreover, the spectra exhibit the broad and intense bands at ca. 1104–1078 cm^{-1} for **I**, 1089-1100 cm^{-1} for **II**, 1104-1082 cm^{-1} for **IV** corresponding to the characteristic vibration of non-coordinated ClO_4^- group, while those appear at ca. 845-840 cm^{-1} for **III** and 847-839 cm^{-1} for **V** indicating to the characteristic band of PF_6^- anion. The ν(CO) of methoxy group expected at ca. 1030 cm^{-1} in **I** is masked by perchlorate vibration. The spectra for each compound are given in Appendix IIIC.

3.4.3 Electronic reflectance spectra

The electronic diffuse reflectance spectrum of **I** displays a broad asymmetric band at ca. 12.20-14.49 kK, centered at 12.74 kK, which is comparable to that of **III** (ca.11.49-14.60 kK, centered at 12.81 kK). These spectra are typical for the distorted trigonal bipyramidal geometry (τ = 0.61 and 0.59 for **I** and **III**, respectively). A broad band of each complex is assigned to be the d_{x2-y2}, d_{xy}, d_{xz}, $d_{yz} \rightarrow d_{z2}$ transition, since the principal absorption peak and a higher energy shoulder of the trigonal bipyramidal chromophore for **I** and **III** could not be resolved. A regular trigonal bipyramidal geometry is usually characterized by an asymmetric broad peak at ca. 11.50 kK with a possible high-energy shoulder at ca. 14.50 kK. The

principal absorption may be assigned as a $d_{x2-y2} \rightarrow d_{z2}$ transition, with the high-energy shoulder assigned as a $d_{xz} \approx d_{yz} \rightarrow d_{z2}$. The spectra of **IV** and **V** show broad asymmetric peaks at approximately 11.96 and 11.98 kK, respectively, with some evidences for a possible high-energy shoulders at ca. 14.29 and ca. 14.30 kK consistent with the distorted trigonal bipyramidal geometry (τ = 0.60 for **IV** and 0.72 for **V**). The principal absorption may be assigned as a $d_{x2-y2} \rightarrow d_{z2}$ transition, with the high-energy shoulder assigned as a $d_{xz} \approx d_{yz} \rightarrow d_{z2}$.

The electronic diffuse reflectance spectrum of **II** show a broad band centered at 13.99 kK. This observed single broad peak is consistent with the tetrahedrally-distorted square pyramidal stereochemistry[4-10] and assigned to be the d_{z2}, d_{xy}, d_{xz}, d_{yz}, $\rightarrow d_{x2-y2}$ transition.

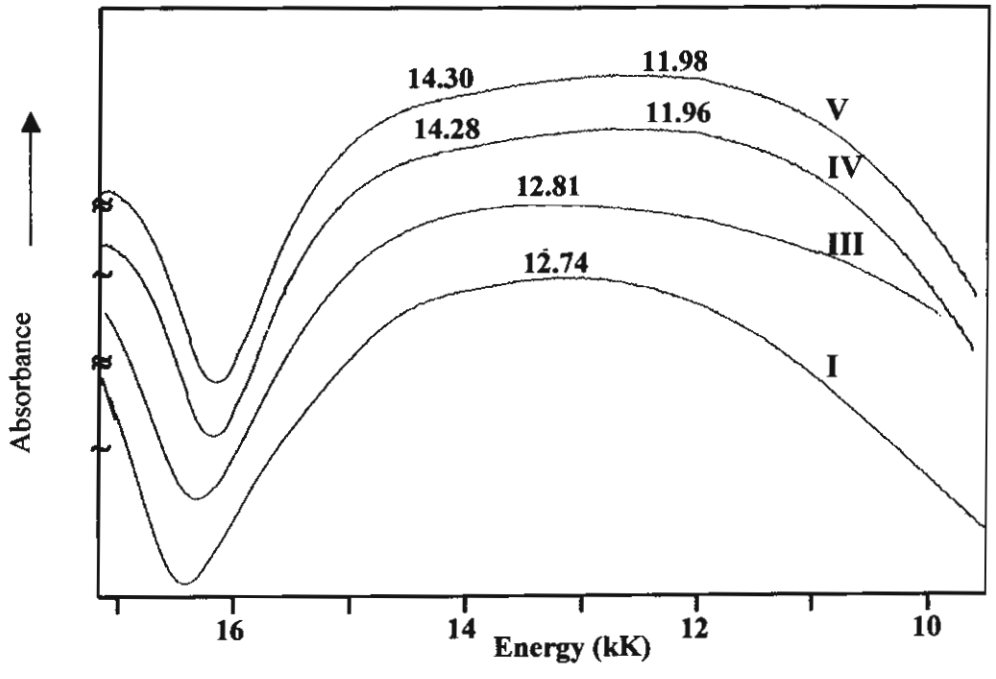

Figure 7 The electronic diffuse reflectance spectra of the triply-bridge dinuclear copper(II) complexes **I** and **III-V**

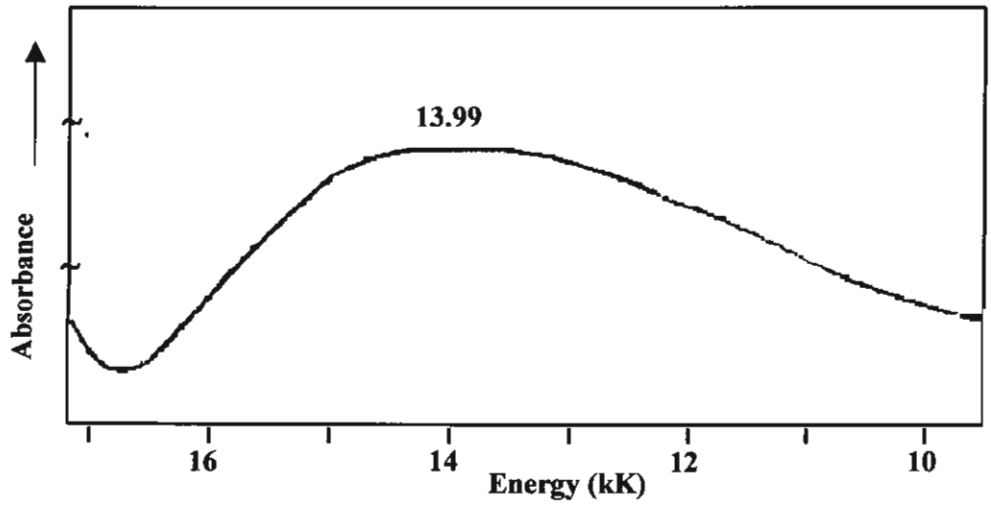

Figure 8 The electronic diffuse reflectance spectra of the triply-bridge dinuclear copper(II) complexes $[Cu_2(dpyam)_2(\mu\text{-}O_2CH)(\mu\text{-}OH)_2](ClO_4)\cdot H_2O$ **(II)**

3.4.4 EPR spectra

The X-band polycrystalline EPR spectra of $[Cu_2(dpyam)_2(\mu\text{-}O_2CH)(\mu\text{-}OH)(\mu\text{-}OCH_3)](ClO_4)$ **(I)** (Appendix IIID) at room temperature and liquid nitrogen temperature (77 K) are either very weak and display an isotropic copper(II) signal at 2.10 and 2.10, respectively, while a triplet state signal at g ≈6.96 (≈160 mT) are not observed properly. The former feature is most certainly from a monomeric Cu(II) impurity, which is always present in dinuclear species. The isotropic-typed EPR of the almost compounds spectra give no information regarding to the ground state, due to the misalignment of the CuN_2O_3 chromophore. A triplet state signal usually attributed to intramolecular exchange interaction between two unpair electrons of copper atoms, $\Delta M_s = \pm 2$ transition. The room temperature and 77 K EPR spectra of complexes $[Cu_2(dpyam)_2(\mu\text{-}O_2CH)(\mu\text{-}OOCH)(\mu\text{-}OH)](PF_6)$ **(III)**, $[Cu_2(dpyam)_2(\mu\text{-}O_2CH)(\mu\text{-}OH)(\mu\text{-}Cl)](ClO_4)\cdot 0.5H_2O$ **(IV)** and $[Cu_2(dpyam)_2(\mu\text{-}O_2CH)(\mu\text{-}OH)(\mu\text{-}Cl)](PF_6)$ **(V)** also indicated isotropic signal, while those of $[Cu_2(dpyam)_2(\mu\text{-}O_2CH)(\mu\text{-}OH)_2](ClO_4)\cdot H_2O$ **(II)** is silent. The spectra for each compound are given in Appendix IIID.

3.4.5 Magnetic properties and superexchange mechanism

The effective magnetic moment (μ_{eff}) measuring by the Faraday method at room temperature are 2.50, 2.54, 2.50 and 2.53 μ_B for **I**, **III**, **IV** and **V**, respectively, which is close to the normal value (2.45 μ_B) of the uncoupled d^9 copper(II) ions suggesting noninteraction between the copper(II) centers in dimeric complexes at room temperature.

The magnetic properties of compounds **I** and **IV** mutually show a very similar behaviour and are depicted in in the form of μ_{eff} *versus* T for two copper(II) ions (Figs. 9 and 10 respectively), also in the form of μ_{eff} versus T for two Cu(II) ions. At 280 K, μ_{eff} is 2.561 μ_B for compound **I** (2.781 μ_B for compound **IV**) which agrees well with the spin-only value of Cu(II) calculated for two uncoupled spin =1/2 centres. Upon cooling, it raises gradually to reach 2.741 μ_B and 2.97 at 30 K, for compounds **I** and **IV**, respectively. This is typical for a ferromagnetically coupled Cu(II) dinuclear compound. Below that temperature, μ_{eff} then diminishes till a value of 2.631 μ_B at 5 K for compound **I** (2.76 for compound **IV**), which may originate from intermolecular antiferromagnetic interactions, or from zero-field splitting of the S = 1 state of the dinuclear species.

The theoretical expression for the magnetic susceptibility for two interacting S = 1/2 centres, which is based on the general Hamiltonian[16], is $H_{ex} = -JS_1S_2$, in which the exchange parameter J is negative for antiferromagnetic and positive for ferromagnetic interaction. The magnetic data were fitted to the equation given in the literature for dinuclear copper compounds

$$\chi_m = (2Ng^2\beta^2)[kT-(2\,zJ'/(3+\exp(-J/kT)))]^{-1}\,[3+\exp(-J/kT)]^{-1}\,(1-p)+\chi_m p + \text{TIP}$$

in which N, g, β, k and T have their usual meanings. The parameter p denotes the fraction of paramagnetic impurity in the sample and zJ' the interaction between neighboring dinuclear identities. A temperature independent paramagnetism (TIP) was also considered and fixed at 60 x 10^{-6} per copper ion. The best fit was obtained with the following values: J = 62.5 cm^{-1}, g = 1.99, zJ' = -3.80 cm^{-1}, p = 0.06, with a final R of 1.4 x 10^{-3} (Fig. 9). For compound **IV**, these values are J = 79.1 cm^{-1}, g = 2.14, zJ' = -4.27 cm^{-1}, p = 0.025, with a final R of 1.6 x 10^{-3} (Fig. 10).

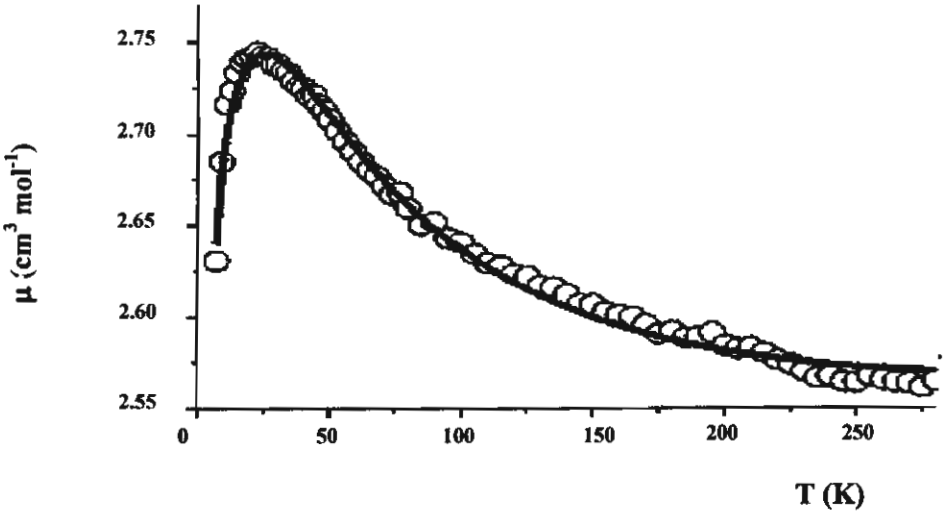

Figure 9 A plot of the temperature dependence of μ_{eff} *vs.* T for compound **I**

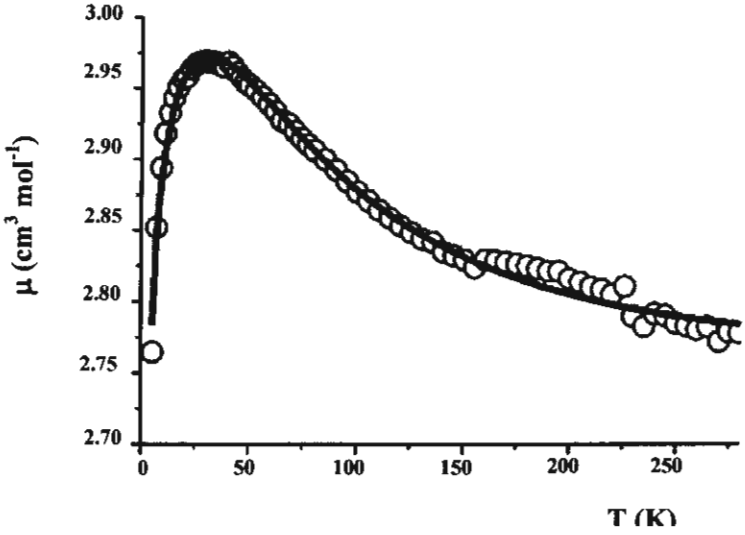

Figure 10 A plot of the temperature dependence of μ_{eff} *vs.* T for compound **IV**

The magnetic properties compounds **III** and **V** mutually show a very similar behaviour. At 280 K μ_{eff} is 2.45 μ_B for compound **III** (2.45 μ_B, for **V**) which agrees reasonable with the spin-only value of Cu(II) calculated for two uncoupled spin = ½ centres. Upon cooling it raises gradually to reach 2.59 and 2.60 at around 30 K, for compounds **III** and **V**, respectively. This is typical for a ferromagnetically coupled Cu(II) dinuclear compound. Below that temperature, μ_{eff} then diminishes till a value around 2.45 μ_B at 5 K for compounds **III** and **V**, which may originate from intermolecular antiferromagnetic interactions, or from zero-field splitting of the S = 1 state of the dinuclear species.

The theoretical expression for the magnetic susceptibility for two interacting S = 1/2 centres, which is based on the general Hamiltonian is: $H_{ex} = -JS_1S_2$, in which the exchange parameter J, is negative for antiferromagnetic and positive for ferromagnetic interaction. The magnetic data were fitted to the equation given in the literature for dinuclear copper compounds

$$\chi_m = (2Ng^2\beta^2)[kT-(2\,zJ'/(3 + \exp(-J/kT)))]^{-1}\,[3 + \exp(-J/kT)]^{-1}\,(1-p) + \chi_M p + \text{TIP}$$

in which N, g, β, k and T have their usual meanings. The parameter p denotes the fraction of paramagnetic impurity in the sample and zJ' the interaction between neighbouring dinuclear identities. A temperature independent paramagnetism (TIP) was also considered and fixed at 60 x 10^{-6} per copper ion.

The best fit was obtained for compound **III** with the following values: J = 30.8 cm^{-1}, g = 1.95, zJ'= -8.29 cm^{-1}, p = 0.00, with a final R of 3.0 x 10^{-3} (Fig. 11). For compound **V**

these values are J = 36.7 cm^{-1}, g = 1.95, zJ'= -6.32 cm^{-1}, p = 0.06, with a final R of 5.7 x 10^{-3} (Fig. 12).

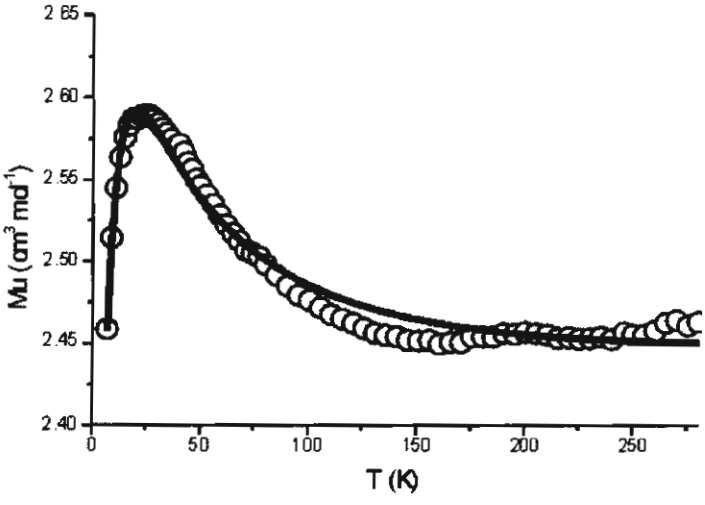

Figure 11 A plot of the temperature dependence of μ_{eff} *vs.* T for compound **III**

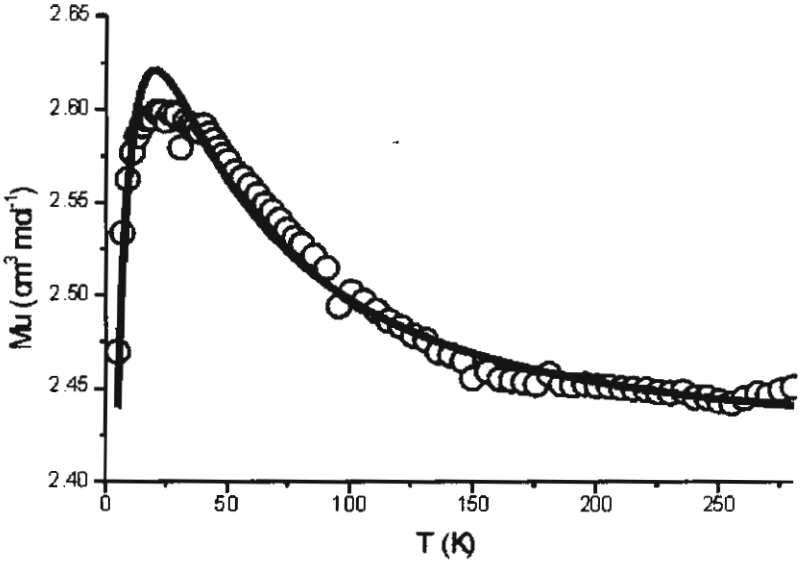

Figure 12 A plot of the temperature dependence of μ_{eff} *vs.* T for compound **V**

The obvious explanation for the triply-bridged dinuclear copper(II) complexes lies in the fact that the most complexes have a distorted square pyramidal stereochemistry with d_{x2-y2} ground states. A hydroxo ligand bridges from an equatorial position at one copper(II) ion to an equatorial positions at the other and contribute the antiferromagnetic interaction, which is

the general trend for increased antiferromagnetic coupling with increasing hydroxide bridge angle. The considerably reduced antiferromagnetic contribution is attributed to the reduced σ overlap between the oxygen p orbital and the copper(II) $d_{x^2-y^2}$ orbital. This relation would be expected for the intermediate geometry with possibly some mixture of the d_{z^2} character in the axial position that reduce electron density in the $d_{x^2-y^2}$ orbital. A change in electron density of the magnetic orbital can have a pronounced effect on the sign and magnitude of a magnetic exchange interaction.

The coordination geometry around each copper(II) ion of **I**, **III**, **IV** and **V** is distorted trigonal bipyramidal, which the unpaired electron resides primarily in d_{z^2} orbital with orientation along the apical hydroxo bridging ligand. In this case a major σ pathway via (Cu-OH-Cu) is possible for the electron delocalization via the d_{z^2} magnetic orbitals, corresponding to the weak or strong ferromagnetic interaction (Fig. 13). The unpair electron of first copper ion couple with an electron in p-orbital of oxygen atom and the unpair electron of second copper ion couple with an electron in other p-orbital of oxygen atom resulting to two unpair electrons in p-orbital. A strong magnetic interaction requires both good σ orientation of the magnetic orbitals and good superexchange properties of the bridging atom(s). Therefore this case indicates a moderate ferromagnetic exchange.

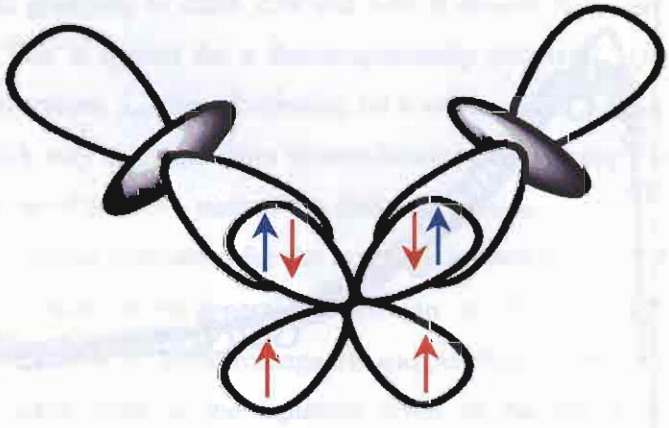

Figure 13 The proposed superexchange mechanism in **I** through oxygen p-orbitals of hydroxo bridging ligand

It should be noted that when the copper(II) geometry is close to regular square pyramidal, an often strong antiferromagnetic interaction will be predominant, but a reduction of an antiferromagnetic contribution will be observed when the geometry becomes closer to trigonal bipyramidal (Table 1).

The complex $[Cu_2(dpyam)_2(\mu\text{-}O_2CH)(\mu\text{-}OH)_2](ClO_4)\cdot H_2O$ **(II)** exhibits a distorted square pyramidal geometry, which the unpaired electron is located in a $d_{x^2-y^2}$ type orbital. The

$d_{x^2-y^2}$ magnetic orbital in **II** is directed toward the dihydroxo-bridged, the Cu-O-Cu angles of 95.8 and 96.0°. For these bridging angles, a moderate antiferromagnetic coupling (J = -122.54 cm^{-1}) should be expected following Hodgson and Hatfield's linear relationship[17] which is usually applied successfully for the planar dihydroxo bridge complexes (Fig. 14).

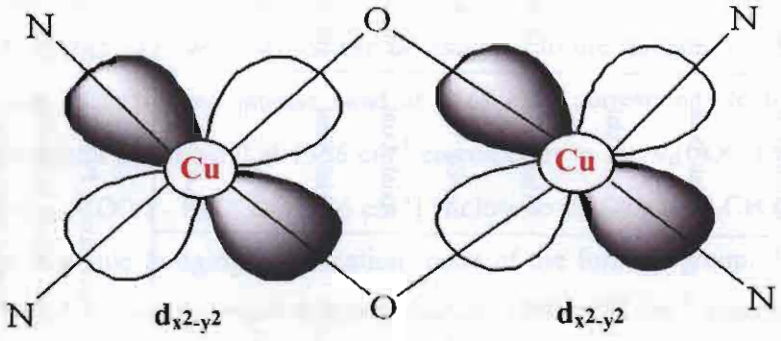

Figure 14 The proposed superexchange mechanism in **II** through oxygen p-orbitals of hydroxo bridges

Table 1 Structural and magnetic data for triply-bridged dinuclear copper(II) complexes

Compound[a]	Coordination geometry[b]	τ	Chromophore	μ-OH position[c]	Cu-OH-Cu (°)	J (cm^{-1})	Ref.
$[Cu_2(dpyam)_2(\mu\text{-}O_2CH)(\mu\text{-}OH)(\mu\text{-}OCH_3)](ClO_4)$ **(I)**	Dist. TBP.	0.61	CuN_2O_3	Axial/Axial	104.0	62.5	This work
$[Cu_2(dpyam)_2(\mu\text{-}O_2CH)_2(\mu\text{-}OH)](PF_6)$ **(III)**	Dist. TBP.	0.59	CuN_2O_3	Axial/Axial	107.2	30.8	This work
$[Cu_2(dpyam)_2(\mu\text{-}O_2CH)(\mu\text{-}OH)(\mu\text{-}Cl)](ClO_4)\cdot 0.5H_2O$ **(IV)**	Dist. TBP.	0.60	CuN_2O_2Cl	Axial/Axial	104.7	79.1	This work
$[Cu_2(dpyam)_2(\mu\text{-}O_2CH)(\mu\text{-}OH)(\mu\text{-}Cl)](PF_6)$ **(V)**	Dist. TBP.	0.72	CuN_2O_2Cl	Axial/Axial	105.9	36.7	This work
$[Cu_2(bpy)_2(\mu\text{-}OH)(\mu\text{-}H_2O)(\mu\text{-}O_2CCH_3)](ClO_4)_2$	Dist. Spy.	0.14, 0.25[f]	CuN_2O_3	Eq./Eq	103.8	19.3	3
$[Cu_2(\mu\text{-EtBITP})(\mu\text{-}OH)(\mu\text{-}Cl)Cl_2]\cdot DMF$	intermediate[d]	0.58, 0.55[f]	CuN_2Cl_2O	Axial/Axial	104.7	-260	11
$[Cu_2(\mu\text{-PTP})(\mu\text{-}OH)(\mu\text{-}Cl)Cl_2]\cdot 2CH_3CN$	intermediate[d]	0.51	CuN_2Cl_2O	Axial/Axial	106.2	-296	12
$[Cu_2(\mu\text{-PAP})(\mu\text{-}OH)(\mu\text{-}IO_3)(IO_3)_2]\cdot 4H_2O$	Dist. Spy.[e]	0.40	CuN_2O_3	Eq/Eq	113.8	-283	12, 13
$[Cu_2(\mu\text{-PAP})(\mu\text{-}OH)(\mu\text{-}SO_4)Cl]\cdot 2H_2O$	Dist. Spy.	0.35, 0.37[f]	CuN_2O_3	Eq./Eq	115.5	-532	14

[a] Abbreviations: dpyam = di-2-pyridylamine; bpy = 2,2'-bipyridine; EtBITP = 3,6-bis(2-benzimidazolylthio)pyridazine; PTP = 3,6-bis(2-pyridylthio)phthalazine; PAP = 1,4-bis-(2-pyrodyl amino)phthalazine), [b] Dist. TBP = distorted trigonal bipyramidal, Dist. Spy. = distorted square pyramidal, [c] Eq. = Equatorial, [d] Trigonality (τ). According to the τ value of 0.58 and 0.55, the preferred geometry should be intermediate towards distorted trigonal bipyramidal.,

[e] Average trigonality (τ_{av}). According to the τ value of 0.40, the preferred geometry should be intermediate towards distorted square pyramidal.

[f] Calculated from the known structural parameters.

3.4.6 The proposed stereochemistry of $[Cu_2(dpyam)_2(\mu\text{-}O_2CH)(\mu\text{-}OH)(\mu\text{-}Cl)](BF_4)$ (VI)

3.4.6.1 The stoichiometry and IR spectrum

The stoichiometry of the complex $[Cu_2(dpyam)_2(\mu\text{-}O_2CH)(\mu\text{-}OH)(\mu\text{-}Cl)](BF_4)$ **(VI)** has been characterized by microanalyses. The infrared spectrum of **VI** (Appendix IIIC) exhibits a broad band at 3455 cm^{-1}, which can be assigned to the bridging OH vibrations of the hydroxo group. A broad and intense band at 1562 cm^{-1} corresponds to the $\nu_{as}(COO^-)$ vibration and a medium broad band at 1356 cm^{-1} corresponds to the $\nu_s(COO^-)$ vibration, the difference Δ [$\Delta = \nu_{as}(COO^-) - \nu_s(COO^-)$; 206 cm^{-1}] is close to that for NaO_2CH (201 cm^{-1}) as expected for the triatomic bridging coordination mode of the formate group. The spectrum also displays a broad and intense band at approximately 1090-1083 cm^{-1}, consistent with the characteristic peak of BF_4^- anion. This spectrum is comparable to those of **IV** and **V** suggesting the comparable functional groups in these complexes except that of the ClO_4^- and PF_6^- in **IV** and **V**, respectively.

3.4.6.2 The electronic diffuse reflectance spectrum

The electronic diffuse reflectance spectrum of **VI** (Fig. 15) displays a broad asymmetric band at ca. 11.56-12.76 kK, centered at 12.74 kK, corresponding to the distorted trigonal bipyramidal copper(II) stereochemistry. This feature is assigned to be the d_{x2-y2}, d_{xy}, d_{xz}, $d_{yz} \rightarrow d_{z2}$ transition.

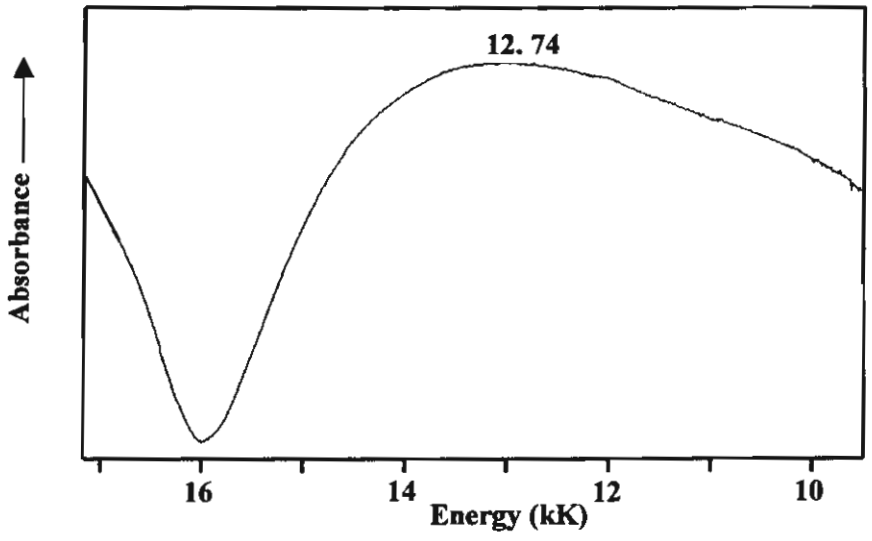

Figure 15 The electronic diffuse reflectance spectrum of $[Cu_2(dpyam)_2(\mu\text{-}O_2CH)(\mu\text{-}OH)(\mu\text{-}Cl)](BF_4)$ **(VI)**

3.4.6.3 The EPR spectrum

The X-band polycrystalline EPR spectra of **VI** (Appendix IIID) at room temperature and liquid nitrogen temperature (77 K) are either very weak and display an isotropic copper (II) signal at 2.09 and 2.10, respectively. These spectra give no information regarding to the ground state (Appendix IIID).

Taken together, microanalysis and infrared spectrum suggest the stoichiometry of $[Cu_2(dpyam)_2(\mu\text{-}O_2CH)(\mu\text{-}OH)(\mu\text{-}Cl)](BF_4)$ **(VI)** which is consistent with the formato complex. The electronic properties of **VI** are consistent with a distorted trigonal bipyramidal geometry. The isotropic-type EPR spectra give no information regarding to the electronic ground state. Consequently, the possible stereochemistry for **VI** is suggested as shown in Fig. 16.

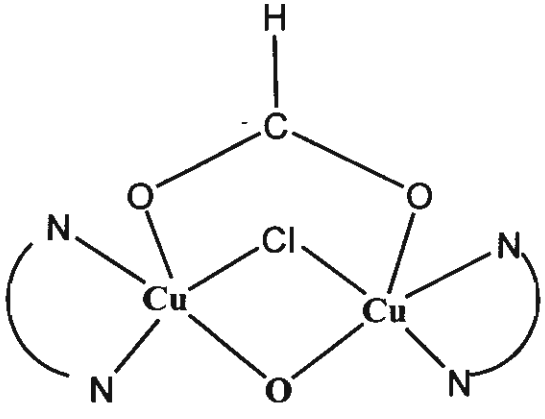

Figure 16 Suggested possible stereochemistry of $[Cu_2(dpyam)_2(\mu\text{-}O_2CH)(\mu\text{-}OH)(\mu\text{-}Cl)](BF_4)$ **(VI)**

3.4.6.4 Magnetic properties and superexchange mechanism

The effective magnetic moment (μ_{eff}) of **VI** measuring by the Faraday method at room temperature is 2.43 μ_B, which is close to the normal value (2.45 μ_B) of the uncoupled d^9 copper(II) ions suggesting noninteraction between the copper(II) centers in a dimeric unit at room temperature. However, the ferromagnetic behavior is expected for this complex at low temperature which occurs via the Cu-O-Cu pathway similar to those of the closely related complexes, $[Cu_2(dpyam)_2(\mu\text{-}O_2CH)(\mu\text{-}OH)(\mu\text{-}OCH_3)](ClO_4)$ **(I)**, $[Cu_2(dpyam)_2(\mu\text{-}O_2CH)(\mu\text{-}OOCH)(\mu\text{-}OH)](PF_6)$ **(III)**, $[Cu_2(dpyam)_2(\mu\text{-}O_2CH)(\mu\text{-}OH)(\mu\text{-}Cl)](ClO_4)\cdot 0.5H_2O$ **(IV)** and $[Cu_2(dpyam)_2(\mu\text{-}O_2CH)(\mu\text{-}OH)(\mu\text{-}Cl)](PF_6)$ **(V)**.

3.5 Conclusions

The triply-bridged dinuclear copper(II) carboxylato complexes $[Cu_2(dpyam)_2(\mu\text{-}O_2CH)(\mu\text{-}OH)(\mu\text{-}OCH_3)](ClO_4)$ **(I)**, $[Cu_2(dpyam)_2(\mu\text{-}O_2CH)_2(\mu\text{-}OH)](PF_6)$ **(III)**, $[Cu_2(dpyam)_2(\mu\text{-}O_2CH)(\mu\text{-}OH)(\mu\text{-}Cl)](ClO_4)\cdot 0.5H_2O$ **(IV)** and $[Cu_2(dpyam)_2(\mu\text{-}O_2CH)(\mu\text{-}OH)(\mu\text{-}Cl)](PF_6)$ **(V)** have been synthesized from their components by the mole ratio method. The crystal structures of all four complexes were determined by X-ray crystallography in this laboratory. All complexes involve the five coordinate distorted trigonal bipyramidal copper(II) ion stereochemistry. The copper(II) environment in **I** and **III** are similar with CuN_2O_3 chromophore, while **IV** and **V** display the CuN_2O_2Cl chromophore. The formato bridging ligands in **I, IV** and **V** are in a familiar didentate syn,syn η^1: η^1: μ_2-bridging mode. Whereas two formato ligands in **III** exhibit different coordination modes, which one formato ligand is in a familiar didentate syn,syn η^1: η^1: μ_2-bridging mode and the other is in the monoatomic bridging mode.

All complexes have the magnetic d_{z2} orbitals with lobe directed toward the bridging hydroxo group, which is positioned in the apical site of each trigonal bipyramidal copper(II) chromophore. This feature should cause the superexchange pathway that can occur through this bridging ligand contributing to a ferromagnetic interaction between two copper(II) ions.

Complex **VI** has been characterized by spectroscopy and microanalysis to be the triply-bridged dinuclear copper(II) formato complex, $[Cu_2(dpyam)_2(\mu\text{-}O_2CH)(\mu\text{-}OH)(\mu\text{-}Cl)](BF_4)$ **(VI)**. The suggested coordination environment around copper(II) ion involves a distorted trigonal bipyramidal geometry. The expected magnetic behavior is ferromagnetic interaction due to the Cu-OH-Cu superexchange pathway.

The magnetic properties of compounds **I** and **IV** mutually show a very similar behaviour with the singlet-triplet energy gaps (J) of +62.5 and +79.1 cm^{-1}, respectively and the very similar structure is also found **III** and **V** with J values of +30.8 and +36.7 cm^{-1}. The ferromagnetic interaction in the latter two compounds is smaller than that of the former two compounds, resulting in the conclusion that the bigger the bridging Cu-O(H)-Cu angle and the longer the Cu-Cu distance, the smaller the ferromagnetic interaction is found. It is noted that the τ values in the studied ranges do not affect the magnitude of exchange interaction. The coordination geometry around each copper(II) ion of **I, III, IV** and **V** is distorted trigonal bipyramidal, which the unpaired electron resides primarily in d_{z2} orbital with orientation along the apical hydroxo bridging ligand. In this case a major σ pathway via (Cu-OH-Cu) is possible for the electron delocalization via the d_{z2} magnetic orbitals, corresponding to the weak or strong ferromagnetic interaction. The unpair electron of first copper ion couples with

an electron in p-orbital of oxygen atom and the unpair electron of second copper ion couples with an electron in the other p-orbital of oxygen atom resulting in the existence of two parallel unpair electrons, each from different p-orbitals. A strong magnetic interaction requires both good σ orientation of the magnetic orbitals and good superexchange properties of the bridging atom(s). Therefore, these complexes contribute a moderate ferromagnetic exchange. It should be noted that when the copper(II) geometry is close to regular square pyramidal, an often strong antiferromagnetic interaction will be predominant, but a reduction of an antiferromagnetic contribution will be observed when the geometry becomes closer to trigonal bipyramidal. Compound **II** exhibits the distinct copper(II) environment, a distorted square pyramidal geometry, as compared to other complexes which the unpaired electron is located in a d_{x2-y2} type orbital. The d_{x2-y2} magnetic orbital in **II** is directed toward both hydroxo bridges, the Cu-O-Cu angles of 95.8 and 96.0°. For these bridging angles, a moderate antiferromagnetic coupling ($J = -122.54\ cm^{-1}$) should be expected following Hodgson and Hatfield's linear relationship which is usually applied successfully for the planar dihydroxo-bridged complexes.

References

1. Towle DK, Hoffmann SK, Hatfield WE, Singh P, Chaudhuri P. ***Inorg. Chem.*** 1988; 27: 394.
2. Wojtczak WA, Hampden-Smith MJ, Duesler EN. ***Inorg. Chem.*** 1998; 37: 1781.
3. Christou G, Perlepes SP, Libby E, Folting K, Huffman JC, Webb RJ, Hendrickson DN. ***Inorg. Chem.*** 1990; 29: 3657.
4. Perlepes SP, Huffman JC, Christou G. ***Polyhedron*** 1991; 10: 2301.
5. Perlepes SP, Huffman JC, Christou G. ***Polyhedron*** 1995; 14: 1073.
6. Neels A, Stoeckli-Evans H, Escuer A, Vicente R. ***Inorg. Chim. Acta*** 1997; 260: 189-198.
7. Graham B, Hearn MTW, Junk PC, Kepert CM, Mabbs FE, Moubaraki B, Murray KS, Spiccia L. ***Inorg. Chem.*** 2001; 40: 1536.
8. Rajendiran TM, Kannappan R, Venkatesan R, Rao PS, Kandaswamy M. ***Polyhedron*** 1999; 18: 3085.
9. Chadjistamatis I, Terzis A, Raptopoulou CP, Perlepes SP. ***Inorg. Chem. Com.*** 2003; 6: 1365.
10. Lubben M, Hage R, Meetsma A, Büma K, Feringa BL. ***Inorg. Chem.*** 1995; 34: 2217.
11. Thompson LK, Mandal SK, Rosenberg L. ***Inorg. Chim. Acta.*** 1987; 133: 81.
12. Chen L, Thompson LK, Bridson JN. ***Inorg. Chim. Acta.*** 1996; 244: 87.
13. Thompson LK, Lee FL, Gabe EJ. ***Inorg. Chem.*** 1988; 27: 39.
14. Thompson LK, Hanson AW, Ramaswamy BS. ***Inorg. Chem.*** 1984; 23: 2459.
15. Addison AW, Rao TN, Reedijk J, Van Rijn J, Verschoor GC ***J. Chem. Soc., Dalton Trans.*** 1984; 1349.
16. Kahn O. ***Molecular Magnetism.*** Cambridge: VCH Publishers; 1993.
17. Haddad MS, Wilson SR, Hodgson DJ, Hendrickson DN. ***J. Am. Chem. Soc.*** 1981; 103: 384.

OUTPUT OF THE RESEARCH

M.Sc. Students

1. Miss Pimprapun Gunnasoot: (1999-2002), "The Synthesis, Crystal Structure, Spectroscopic and Magnetic Properties of Dinuclear Oxalato-bridged Copper(II) Complexes Containing the 2,2′-Bipyridylamine Ligand" Master of Science Thesis in Chemistry, Graduate School, Khon Kaen University.
2. Mr. Pongthipun Phuengphai: (2001-2004), "Structural Diversity of Hydrogenphosphato-bridged Polynuclear Copper(II) Complexes Containing the di-2-pyridylamine: Synthesis Spectroscopic and Magnetic Properties" Master of Science Thesis in Chemistry, Graduate School, Khon Kaen University. Khon Kaen University Thesis Good Achievement Award in 2006.
3. Miss Chatkeaw chailuecha: (2001-2004), "The Synthesis, Crystal Structure, Spectroscopic and Magnetic Properties of Dinuclear Triply-bridged Copper(II) Compounds Containing the Di-2-pyridylamine Ligand with the Carboxylato Bridge" Master of Science Thesis in Chemistry, Graduate School, Khon Kaen University. Khon Kaen University Thesis Distinguished Achievement Award in 2006.

PUBLICATION PAPERS

1. S. Youngme, G.A. van Albada, N. Chaichit, P. Gunnasoot, P. Kongsaeree, I. Mutikainen, O. Roubeau, J. Reedijk, U. Turpeinen, "Synthesis, Spectroscopic Characterization, X-ray Crystal Structure and Magnetic Properties of Oxalato-bridged Copper(II) Dinuclear Complexes with Di-2-pyridylamine", ***Inorg. Chim. Acta***, 2003, **353**, 119-128.
2. S. Youngme, C. Chailuecha, N. Chaichit, "The novel dinuclear doubly and tripy-bridged copper(II) compound with monoatomic bridges", ***Polyhedron***, 2004, **23**, 1641-1647.
3. S. Youngme, C. Chailuecha, G.A. van Albada, C. Pakawatchai, N. Chaichit, J. Reedijk, "Synthesis, crystal structure, spectroscopic and magnetic properties of doubly and triply bridged dinuclear copper(II) compounds containing di-2-pyridylamine as a ligand", ***Inorg. Chim. Acta***, 2004, **357**, 2532-2542.
4. S. Youngme, P. Phuengphai, N. Chaichit, C. Pakawatchai, G.A. van Albada, O. Roubeau, J. Reedijk, "The coordination chemistry of mono(di-2-pyridylamine) copper(II) complexes with monovalent and divalent oxoanions: Crystal structure, spectroscopic and magnetic properties

of dinuclear $[Cu(L)(\mu\text{-}H_2PO_4)(H_2PO_4)]_2$ and polynuclear $[Cu(L)(\mu_3\text{-}HPO_4)]_n$", ***Inorg. Chim. Acta***, 2004, **357**, 3603-3612.

5. S. Youngme, P. Gunnasoot, N. Chaichit, C. Pakawatchai " New examples of dinuclear copper (II) complexes with ferromagnetic and antiferromagnetic interactions mediated by bridging oxalato group: structures and magnetic properties of $[Cu_2L_4(\mu\text{-}C_2O_4)](PF_6)_2(H_2O)_2$ and $[Cu_2L_2(\mu\text{-}C_2O_4)(NO_3)_2(CCH_3)_2N(OH)_2]$ (L = di-2-pyridylamine)" ***Trans. Metal Chem.***, 2004, **29**, 840-846.
6. S. Youngme, P. Phuengphai, N. Chaichit, G.A. van Albada, O. Roubeau, J. Reedijk "An unprecedented tetranuclear Cu(II) cluster, exclusively bridged by two μ_3,η^3-hydrogenphosphate anions. Synthesis, structure, and magnetic properties" ***Inorg. Chim. Acta***, 2005, **358**, 849-853.
7. S. Youngme, C. Chailuecha, G.A. van Albada, C. Pakawatchai, N. Chaichit, J. Reedijk "Dinuclear triply-bridged copper(II) compounds containing carboxylato bridges and di-2-pyridylamine as a ligand. Synthesis, crystal structure, spectroscopic and magnetic properties" ***Inorg. Chim. Acta***, 2005, **358**, 1068-1078.
8. S. Youngme, P. Phuengphai, N. Chaichit, G.A. van Albada, O. Roubeau, J. Reedijk "A novel tetranuclear hydrogenphosphate-bridged Cu(II) cluster. Synthesis, structure, spectroscopy and magnetism of $[Cu_4(dpyam)_4(\mu_4, \eta^3\text{-}HPO_4)_2(\mu\text{-}X)_2]X_2(H_2O)_6$ (X = Cl, Br)" ***Inorg. Chim. Acta***, 2005, **358**, 2262-2268.
9. S. Youngme, P. Phuengphai, C. Pakawatchai, G.A. van Albada, S. Tanase, I. Mutikainen, U. Turpeinen, Jan Reedijk "A copper(II) chain compound with hydrogenphosphate bridges organized in a double-chain structure. Synthesis, structure and magnetic properties of $[Cu(1,10\text{-phenanthroline})(\mu\text{-}HPO_4)(H_2O)_2]_n$" ***Inorg. Chem. Commun.***, 2005, **8**, 335-338.
10. S. Youngme, P. Phuengphai, C. Pakawatchai, G.A. van Albada, J. Reedijk "A novel polymeric trinuclear-based μ_3-phosphato-bridged Cu(II) complex containing two different types of monophosphate. Synthesis, structure and magnetism of $\{[Cu_3(di\text{-}2\text{-}pyridylamine)_3(\mu_3, \eta^3\text{-}HPO_4)(\mu_3, \eta^4\text{-}PO_4)(H_2O)](PF_6)(H_2O)_3\}_n$" ***Inorg. Chim. Acta***, 2005, **358**, 2125-2128.
11. S. Youngme, P. Phuengphai, N. Chaichit, G.A. van Albada, S. Tanase, J. Reedijk "Synthesis, crystal structure and magnetic properties of a polynuclear Cu(II) complex: *catena*-poly[aqua (di-2-pyridylamine)copper(II)(μ-formato-*O,O'*)nitrate]" ***Inorg. Chim. Acta***, 2005, **358**, 3267-3271.

12. P. Phuengphai, **S. Youngme**, C. Pakawatchai, G.A. van Albada, M. Quesada and J. Reedijk "Synthesis, crystal structure and magnetic properties of an unexpected new coordination Cu (II) compound, containing two different phosphato-bridged dinuclear units; $[Cu_2(phen)_2(\mu\text{-}H_2PO_4\text{-}O,O')_2(H_2PO_4)_2][Cu_2(phen)_2(\mu\text{-}H_2PO_4\text{-}O,O')(\mu\text{-}H_2PO_4\text{-}O)(\mu\text{-}HPO_4\text{-}O)]_2(H_2O)_9$(phen = 1,10-phenanthroline)", ***Inorg. Chem. Commun.***, 2006, **9**, 147-151.

Presentations

1. P. Gunnasoot, S. Youngme, N. Chaichit "The chemistry of dinatrato-di-2-pyridylamine copper(II). Crystal structures of *catena*-Poly[[(di-2-pyridylamine)(nitrato-0,0′)copper (II)]-μ-nitrato-0:0′] and Bis(nitrato-0,0′)(di-2-pyridylame)copper(II) Dihydrate" ***Oral presented at the 27th Congress on Science and Technology of Thailand***, Hatyai, Songkhla, Thailand. 16-18 October 2001.
2. P. Gunnasoot, S. Youngme, N. Chaichit, and J. Reedijk "Synthesis, Crystal Structure, Spectroscopic and Magnetic Properties of Oxalato Bridged Dinuclear Copper(II) Compound with Di-2-pyridylamine as a Ligand " ***Oral presented at the 28th Congress on Science and Technology of Thailand***, Bangkok, Thailand. 24-26 October 2002.
3. P. Gunnasoot, S. Youngme, N. Chaichit, "Synthesis, Crystal Structure, Spectroscopic and Magnetic Properties of Dinuclear Oxalato-Bridged Copper(II) Containing the 2,2'-Bipyridylamine as a Ligand " ***Oral*** *presented at the 5th Symposium on Graduate Research KKU,* Khon Kaen, Thailand. 20 January 2002. Oral presented distinguished achievement award.
4. P. Gunnasoot, S. Youngme, N. Chaichit "Synthesis, Crystal structure, Spectroscopy and Magnetic Properties of Oxalato-Bridged Copper(II) Complexes with Di-2-pyridylamine" ***Oral*** *presented at the 1st PERCH Annual Scientific Congress,* Chonburi, Thailand. 12-15 May 2002.
5. P. Phuengphai, S. Youngme, N. Chaichit "Synthesis, spectroscopic properties and crystal structure of polynuclear copper (II) complexes containing the di-2-pyridylamine and hydrogenphosphate ligands" ***Oral presented at the 29th Congress on Science and Technology of Thailand***, Khon Kaen, Thailand. 20-22 October 2003.
6. C. Chailuecha, S. Youngme, C. Pakawatchai "Synthesis, crystal structures, spectroscopic and magnetic properties of the doubly- and triply-bridged dinuclear copper(II) compounds containing the di-2-pyridylamine ligand" ***Poster*** *presented at the 29th*

Congress on Science and Technology of Thailand, Khon Kaen, Thailand. 20-22 October *2003.*

7. P. Phuengphai, S. Youngme, N. Chaichit "Synthesis, Spectroscopic Properties and Crystal stricture of Polynuclear Copper(II) Containing the Di-2-pyridylamine and Hydrogenphosphate Ligands" ***Poster*** *presented at the 2nd PERCH Annual Scientific Congress,* Chonburi, Thailand. 11-14 May 2003. Poster presented distinguished achievement award.
8. C. Chailuecha, S. Youngme, C. Pakawatchai "Synthesis, Crystal structure, Spectroscopic and Magnetic Properties of Roof-shaped formato-bridged Dinuclear Copper(II) Compounds Containing the Di-2-pyridylamine Ligand" ***Poster*** *presented at the 2nd PERCH Annual Scientific Congress,* Chonburi, Thailand. 11-14 May 2003. Poster presented distinguished achievement award.
9. P. Phuengphai, S. Youngme, N. Chaichit "The coordination chemistry of mono(di-2-pyridylamine) copper(II) complexes with monovalent and divalent oxoanions: Crystal structure and spectroscopic and magnetic properties of dinuclear $[Cu(L)(\mu\text{-}H_2PO_4)(H_2PO_4)]_2$ and polynuclear $[Cu(L)(\mu_3\text{-}HPO_4)]_n$" ***Poster*** *presented at the 7th Symposium on Graduate Research KKU,* Khon Kaen, Thailand. 20 January 2004. Poster presented distinguished achievement award.
10. C. Chailuecha, S. Youngme, C. Pakawatchai "Synthesis, crystal structure, spectroscopic and magnetic properties of doubly- and triply-bridged dinuclear copper(II) compounds containing di-2-pyridylamine as a ligand" ***Poster*** *presented at the 7th Symposium on Graduate Research KKU,* Khon Kaen, Thailand. 20 January 2004.
11. P. Phuengphai, S. Youngme, N. Chaichit "Structural Diversity of Hydrogenphosphato-bridged Polynuclear Copper(II) Complexes Containing the Di-2-pyridylamine: Synthesis, Spectroscopic and Magnetic Properties" ***Oral*** *presented at the 3rd PERCH Annual Scientific Congress,* Chonburi, Thailand. 9-12 May 2004.
12. C. Chailuecha, S. Youngme, C. Pakawatchai "Synthesis, Crystal structure, Spectroscopic and Magnetic Properties of Dinuclear Triply-bridged Dinuclear Copper(II) Compounds Containing the Di-2-pyridylamine Ligand with Carboxylato Bridge" ***Oral*** *presented at the 3rd PERCH Annual Scientific Congress,* Chonburi, Thailand. 9-12 May 2004. Oral presented distinguished achievement award.

13. S. Youngme, N. Chaichit, C. Pakawatchai, A.L. Spek, J. Reedijk "Planar and Roof-shaped Hydroxo-bridged Dinuclear Copper(II) Complexes: Structures, Magnetic Properties and Phase Transitions" ***Invited speaker*** *at the 4th PERCH Annual Scientific Congress,* Chonburi, Thailand. 8-11 May 2005.

14. S. Youngme, J. Phatchimkun, N. Chaichit, G.A. van Albada, S. Tanase, J. Reedijk "The coordination Chemistry of mono(di-2-pyridylamine) copper(II) complexes with monovalent oxoanions: Crystal structure and magnetic properties of polynuclear [Cu(L)(μ-O_2CH)(OH_2)]$_n$(NO_3)$_n$" ***Oral*** *presented at* the 20th International Conference on Coordination and Bioinorganic Chemistry, Smolenice, Slovakia. 5-10 June 2005.

APPENDICES

APPENDIX IA

Crystal and Refinement Data for

$[Cu_2(dpyam)_4(\mu\text{-}C_2O_4)]X_2$, X = BF_4^- (I), ClO_4^- (II) and PF_6^- (III)

and $[Cu_2(dpyam)_2(\mu\text{-}C_2O_4)Y_2]$, Y = NO_3^-·DMSO (IV),

NO_3^-·DMF (V), Cl^- (VI) and Br^- (VII)

Table 1 Crystal and refinement data for complexes **I-V**

Complexes	I	II	III	IV	V
Molecular formula	$[Cu_2(dpyam)_4(\mu\text{-}C_2O4)](BF_4)_2(H_2O)_3$	$[Cu_2(dpyam)_4(\mu\text{-}C_2O_4)](ClO_4)_2(H_2O)_3$	$[Cu_2(dpyam)_4(\mu\text{-}C_2O_4)](PF_6)_2(H_2O)_2$	$[Cu_2(dpyam)_2(\mu\text{-}C_2O_4)NO_3)_2((CH_3)_2SO)_2]$	$[Cu_2(dpyam)_2(\mu\text{-}C_2O_4)(NO_3)_2(CH_3)_2NCOH)_2]$
Molecular weight	1126.5	1152.8	1223.86	837.76	412.85
T(K)	293(2)	293(2)	293(2)	297.76	293(2)
Crystal system	Triclinic	Triclinic	Monoclinic	Triclinic	Triclinic
Space group	P-1	P-1	$P2_1/c$	P-1	P-1
a (Å)	9.629(2)	9.599(2)	8.5712(2)	8.719(0)	8.353(2)
b (Å)	11.170(2)	11.206(2)	11.3170(2)	8.980692)	9.100(2)
c (Å)	12.381(2)	12.480(3)	25.8680(5)	11.421(0)	12.245(3)
α (°)	73.81(2)	73.22(3)	90	68.58(0)	72.035(4)
β (°)	78.15(2)	77.84(3)	82.6150(10)	77.79(0)	75.228(4)
γ (°)	76.59(2)	76.88(3)	90	80.58(0)	78.552(4)
V ($Å^3$)	1229.7(2)	1236.5(4)	2488.39	808.87(1)	848.8(4)
Z	1	1	2	1	2
D_{calc} ($g\ cm^{-3}$)	1.516	1.542	1.633	1.720	1.615
μ (*mm*)	0.956	1.046	1.025	3.495	1.330
F (000)	569	588	1236	428	422
Crystal size (mm)	0.33 x 0.45 x 0.75	0.30 x 0.42 x 0.45	0.25 x 0.30 x 0.43	0.35 x 0.35 x 0.22	0.303 x 0.253 x 0.106
Reflection collected	9078	4834	17857	3171	7532
Unique reflections	7711 (R_{int} = 0.0179)	4834 (R_{int} = 0.0000)	7076 (R_{int} = 0.0487)	2964 (R_{int} = 0.0281)	3939 (R_{int} = 0.0150)
Observed ref. [I>2σ(I)]	6519	4349	7695	2828	6045
Data/restraints /parameter	7711/3/679	4834/3/694	7076/2/474	2964/0/228	3939/0/373
Goodness-of-fit	1.020	1.076	1.139	1.247	1.061
Final R indices [I>2σ(I)]	R1 = 0.0464, wR_2 = 0.1401	R1 = 0.0383, wR_2 = 0.1079	R1 = 0.0606, wR_2 = 0.1480	R1 = 0.0512, wR_2 = 0.1363	R1 = 0.0407, wR_2 = 0.1120
R indices (all data)	R1 = 0.0547, wR_2 = 0.1497	R1 = 0.0442, wR_2 = 0.1170	R1 = 0.0878, wR_2 = 0.1614	R1 = 0.060747, wR_2 = 0.1615	R1 = 0.0459, wR_2 = 0.1161
Largest difference peak and hole ($e\ Å^{-3}$)	0.946 and – 0.455	0.854 and – 0.472	1.058 and – 0.424	0.968 and – 0.554	0.676 and – 0.494

$$R = \Sigma||F_o| - |F_c||/\Sigma|F_o||,\quad R_w = [\Sigma w\{|F_o| - |F_c|\}^2/w|F_o|^2]^{1/2}$$

APPENDIX IB

Selected Bond Lengths (Å) and Angles (°) for

$[Cu_2(dpyam)_4(\mu\text{-}C_2O_4)]X_2$, X = BF_4^- (I), ClO_4^- (II) and PF_6^- (III)

and $[Cu_2(dpyam)_2(\mu\text{-}C_2O_4)Y_2]$, Y = NO_3^-·DMSO (IV),

NO_3^-· DMF (V), Cl^- (VI) and Br^- (VII)

Table 2
Selected bond lengths (Å) and angles (°) with e.s.d.s. in parentheses of $[Cu_2(dpyam)_4(C_2O_4)](BF_4)_2(H_2O)_3$ **(I)** and $[Cu_2(dpyam)_4(C_2O_4)](ClO_4)_2(H_2O)_3$ **(II)**

	(I)	**(II)**
Bond lengths		
Cu(1)-N(1)	2.008(8)	2.020(9)
Cu(1)-N(2)	2.111(7)	2.136(8)
Cu(1)-N(4)	2.024(6)	2.000(8)
Cu(1)-N(5)	2.134(8)	2.095(8)
Cu(1)-O(1)	2.229(8)	2.141(10)
Cu(1)-O(2)	2.252(8)	2.305(9)
Cu(2)-N(7)	2.021(8)	2.010(9)
Cu(2)-N(8)	2.145(7)	2.141(9)
Cu(2)-N(10)	2.006(7)	2.025(8)
Cu(2)-N(11)	2.094(6)	2.107(8)
Cu(2)-O(3)	2.208(9)	2.225(9)
Cu(2)-O(4)	2.189(8)	2.229(8)
Cu(1)-Cu(2)	5.745(3)	5.752(3)
Bond angles		
N(1)-Cu(1)-N(4)	173.4(3)	175.4(3)
N(2)-Cu(1)-O(1)	170.7(3)	165.8(3)
N(5)-Cu(1)-O(2)	166.0(2)	171.4(3)
N(2)-Cu(1)-N(5)	97.1(3)	97.5(3)
O(1)-Cu(1)-O(2)	74.8(2)	74.7(3)
N(7)-Cu(2)-N(10)	175.5(3)	173.2(4)
N(8)-Cu(2)-O(3)	166.1(2)	168.9(3)
N(11)-Cu(2)-O(4)	170.1(3)	166.8(3)
N(8)-Cu(2)-N(11)	97.6(3)	97.3(3)
O(3)-Cu(2)-O(4)	73.9(3)	73.7(3)

Table 3
Selected bond lengths (Å) and angles (°) with e.s.d.s. in parentheses of $[Cu_2(dpyam)_4(C_2O_4)](PF_6)_2(H_2O)_2$ **(III)**

Cu(1)-N(4)	1.992(10)	Cu(1)-N(2)	1.995(9)
Cu(1)-O(1)	2.029(9)	Cu(1)-N(5)	2.049(7)
Cu(1)-N(1)	2.191(6)	Cu(1)-O(2)	2.424(6)
Cu(2)-N(8)	1.979(9)	Cu(2)-O(4)	2.025(8)
Cu(2)-N(7)	2.027(7)	Cu(2)-N(11)	2.098(8)
Cu(2)-N(10)	2.249(8)	Cu(2)-O(3)	2.448(8)
Cu(1)...Cu(2)	5.737(2)		

N(4)-Cu(1)-N(2)	93.0(4)	N(4)-Cu(1)–O(1)	174.7(3)
N(2)-Cu(1)-O(1)	86.6(4)	N(4)-Cu(1)-N(5)	87.1(3)
N(2)-Cu(1)-N(5)	170.4(3)	O(1)-Cu(1)-N(5)	92.5(3)
N(4)-Cu(1)-N(1)	96.8(3)	N(2)-Cu(1)-N(1)	87.4(3)
O(1)-Cu(1)-N(1)	88.4(3)	N(5)-Cu(1)-N(1)	102.1(3)
N(4)-Cu(1)-O(2)	99.7(3)	N(2)-Cu(1)-O(2)	88.6(3)
O(1)-Cu(1)-O(2)	75.0(3)	N(5)-Cu(1)-O(2)	82.0(3)
N(1)-Cu(1)-O(2)	163.1(3)	N(8)-Cu(2)–O(4)	90.9(3)
N(8)-Cu(2)-N(7)	88.7(4)	O(4)-Cu(2)–N(7)	173.8(3)
N(8)-Cu(2)-N(1)1	171.5(4)	O(4)-Cu(2)-N(11)	89.4(3)
N(7)-Cu(2)-N(11)	90.1(3)	N(8)-Cu(2)–N(10)	101.5(3)
O(4)-Cu(2)-N(10)	87.2(3)	N(7)-Cu92)-N(10)	98.9(4)
N(11)-Cu(2)-N(10)	87.0(3)	N(8)-Cu(2)–O(3)	79.9(4)
O(4)-Cu(2)-O(3)	75.0(2)	N(7)-Cu(2)-O(3)	98.8(3)
N(11)-Cu(2)-O(3)	91.9(3)	N(10)-Cu(2)-O(3)	162.2(3)

Table 4
Selected bond lengths (Å) and angles (°) with e.s.d.s. in parentheses of $[Cu_2(dpyam)_2(C_2O_4)(NO_3)_2((CH_3)_2SO)_2]$ **(IV)**

Bond lengths

Cu(1)-N(1)	1.986(2)	Cu(1)-N(2)	2.002(2)
Cu(1)-O(1)	1.998(2)	Cu(1)-O(2)	1.994(2)
Cu(1)-O(3)	2.331(2)	Cu(1)-O(4)	2.502(2)
Cu(1)-Cu(1A)	5.220(2)		

Bond angles

N(1)-Cu(1)-O(2)	92.3(2)	N(1)-Cu(1)-O(1)	174.3(8)
O(2)-Cu(1)-O(1)	82.2(7)	N(1)-Cu(1)-N(2)	93.3(2)
O(2)-Cu(1)-N(2)	170.9(3)	O(1)-Cu(1)-N(2)	91.8(7)
N(1)-Cu(1)-O(3)	88.2(6)	O(2)-Cu(1)-O(3)	93.5(7)
O(1)-Cu(1)-O(3)	93.5(5)	O(4)-Cu(1)-N(1)	86.6(7)
O(4)-Cu(1)-N(2)	85.5(7)	O(4)-Cu(1)-O(1)	91.7(7)
O(4)-Cu(1)-O(2)	87.7(7)	O(4)-Cu(1)-O(3)	74.8(7)

Symmetry code: A= -x, -y+1, -z.

Table 5
Selected bond lengths (Å) and angles (°) with e.s.d.s. in parentheses of $[Cu_2(dpyam)_2(\mu\text{-}C_2O_4)(NO_3)_2((CH_3)_2NCOH)_2]$ (V)

Cu(1)-N(2)	1.979(7)	Cu(1)-N(1)	1.990(6)
Cu(1)-O(2)	2.005(6)	Cu(1)-O(1)	2.012(6)
Cu(1)-O(5)	2.254(7)	Cu(2)-N(4)	1.956(7)
Cu(1)-O(10B)	2.786(2)	Cu(1)-O(8B)	2.679(2)
Cu(2)-N(5)	1.973(7)	Cu(2)-O(4)	1.978(5)
Cu(2)-O(3)	2.002(6)	Cu(2)-O(6)	2.295(7)
Cu(1)...Cu(2)	5.212(2)		

N(2)-Cu(1)-N(1)	90.8(3)	N(2)-Cu(1)-O(2)	173.1(3)
N(1)-Cu(1)-O(2)	92.1(2)	N(2)-Cu(1)-O(1)	93.2(2)
N(1)-Cu(1)-O(1)	170.4(3)	O(2)-Cu(1)-O(1)	82.9(2)
N(2)-Cu(1)-O(5)	89.2(3)	N(1)-Cu(1)-O(5)	92.7(3)
O(2)-Cu(1)-O(5)	96.8(2)	O(1)-Cu(1)-O(5)	96.1(3)
N(4)-Cu(2)-N(5)	92.1(3)	N(4)-Cu(2)-O(4)	170.6(3)
N(5)-Cu(2)-O(4)	92.8(2)	N(4)-Cu(2)-O(3)	91.0(3)
N(5)-Cu(2)-O(3)	169.2(3)	O(4)-Cu(2)-O(3)	82.8(2)
N(4)-Cu(2)-O(6)	90.0(3)	N(5)-Cu(2)-O(6)	93.0(3)
O(4)-Cu(2)-O(6)	97.8(2)	O(3)-Cu(2)-O(6)	97.4(3)

Symmetry code: B= x, y, z-1

APPENDIX IC

The Infrared Spectra for

$[Cu_2(dpyam)_4(\mu\text{-}C_2O_4)]X_2$, X = BF_4^- (I), ClO_4^- (II) and PF_6^- (III) and $[Cu_2(dpyam)_2(\mu\text{-}C_2O_4)Y_2]$, Y = NO_3^- DMSO (IV), NO_3^- DMF (V), Cl^- (VI) and Br^- (VII)

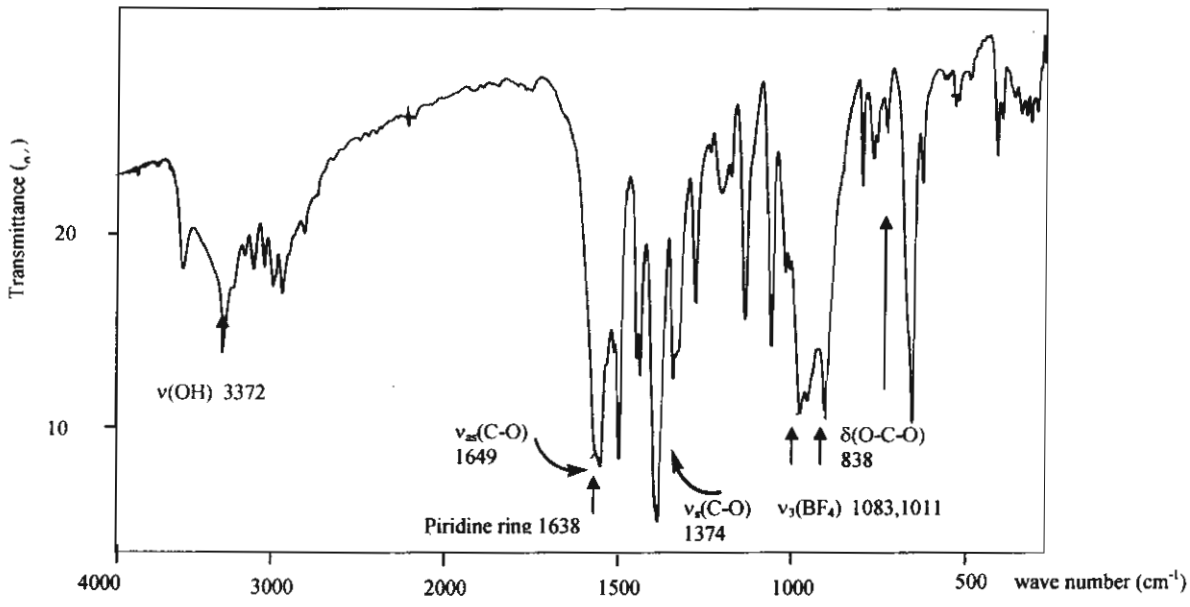

(a) The IR spectrum of $[Cu_2(dpyam)_4(\mu\text{-}C_2O_4)](BF_4)_2.3H_2O$ **(I)**

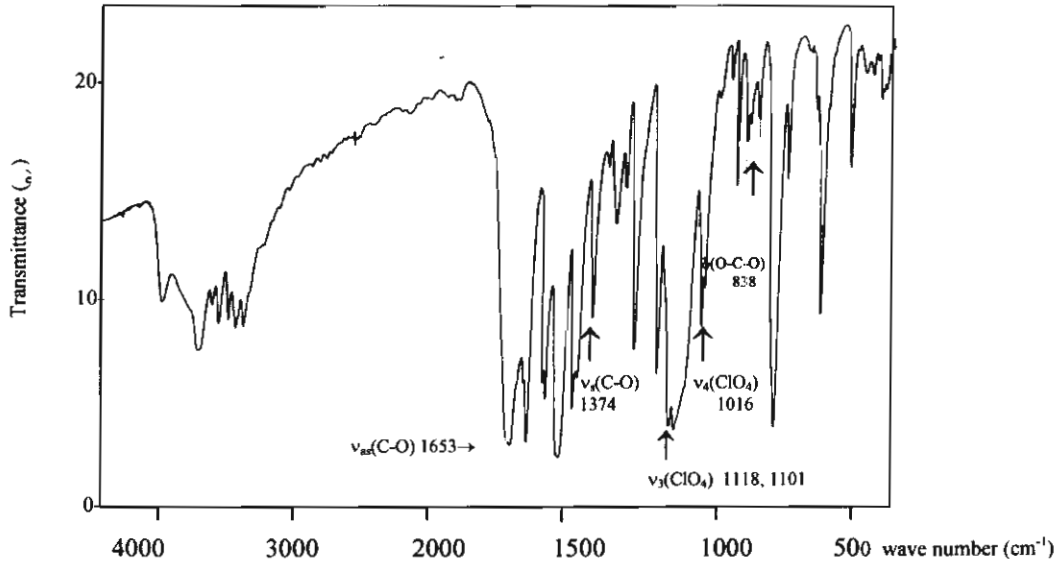

(b) The IR spectrum of $[Cu_2(dpyam)_4(\mu\text{-}C_2O_4)_2](ClO_4)_2.3H_2O$ **(II)**

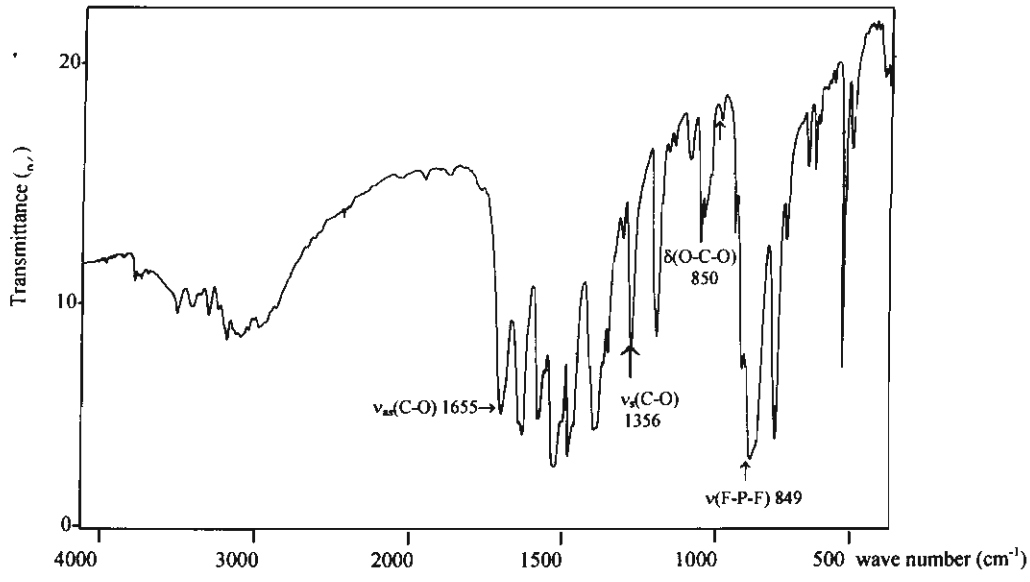

(c) The IR spectrum of $[Cu_2(dpyam)_4(\mu\text{-}C_2O_4)_2](PF_6)_2.2H_2O$ **(III)**

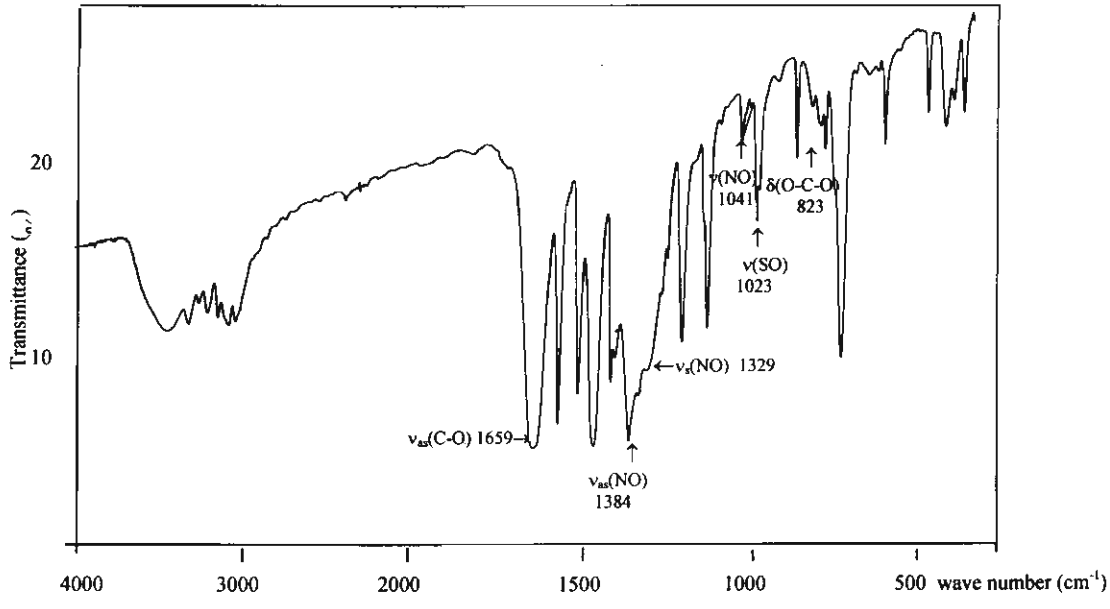

(d) The IR spectrum of $[Cu_2(dpyam)_2(\mu\text{-}C_2O_4)(NO_3)_2((CH_3)_2SO)_2)_2]$ **(IV)**

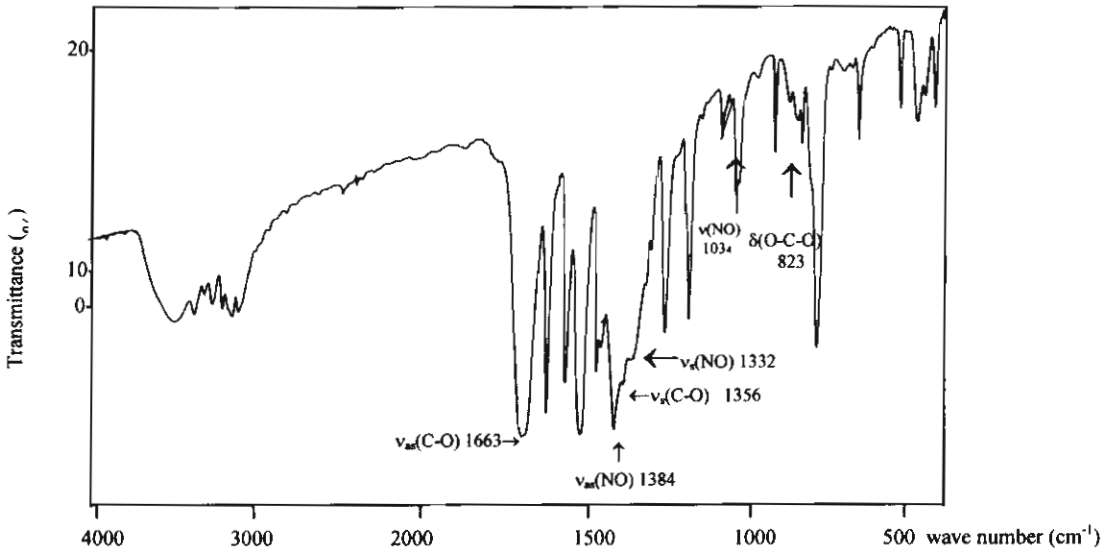

(e) The IR spectra of $[Cu_2(dpyam)_2(\mu\text{-}C_2O_4)(NO_3)_2(CH_3)_2NCOH)_2]$ **(V)**

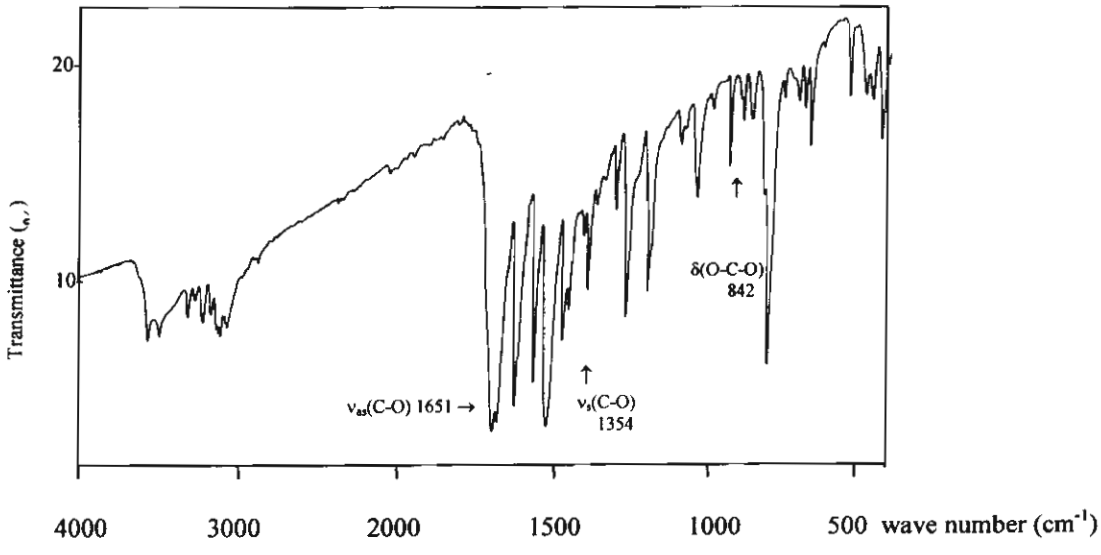

(f) The IR spectrum of $[Cu_2(dpyam)_2(\mu\text{-}C_2O_4)(Cl)_2]$ **(VI)**

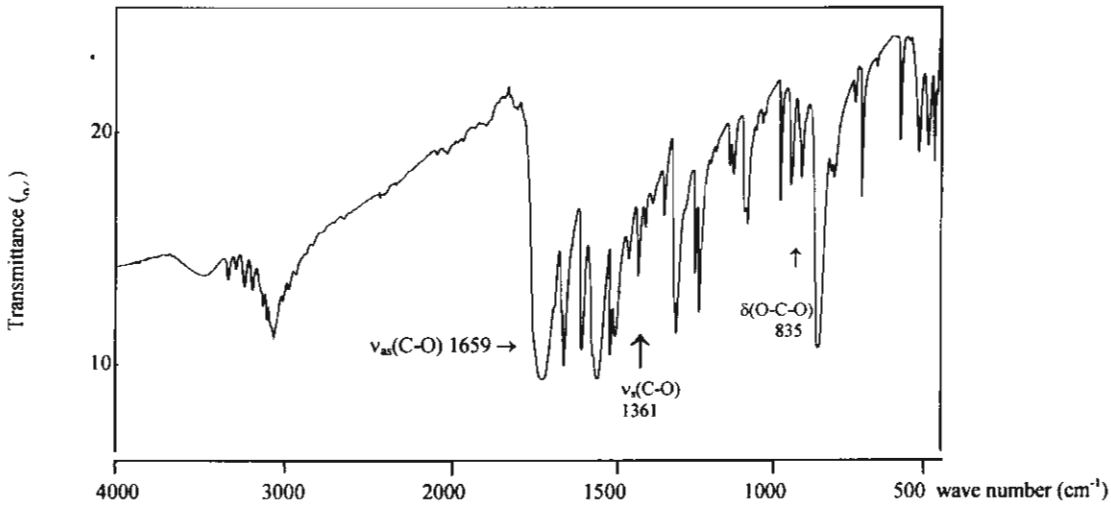

(g) The IR spectrum of $[Cu_2(dpyam)_2(\mu\text{-}C_2O_4)(Br)_2]$ **(VII)**

APPENDIX ID

The EPR Spectra for

$[Cu_2(dpyam)_4(\mu\text{-}C_2O_4)]X_2$, X = BF_4^- (I), ClO_4^- (II) and PF_6^- (III) and $[Cu_2(dpyam)_2(\mu\text{-}C_2O_4)Y_2]$, Y = NO_3^- DMSO (IV), NO_3^- DMF (V), Cl^- (VI) and Br^- (VII)

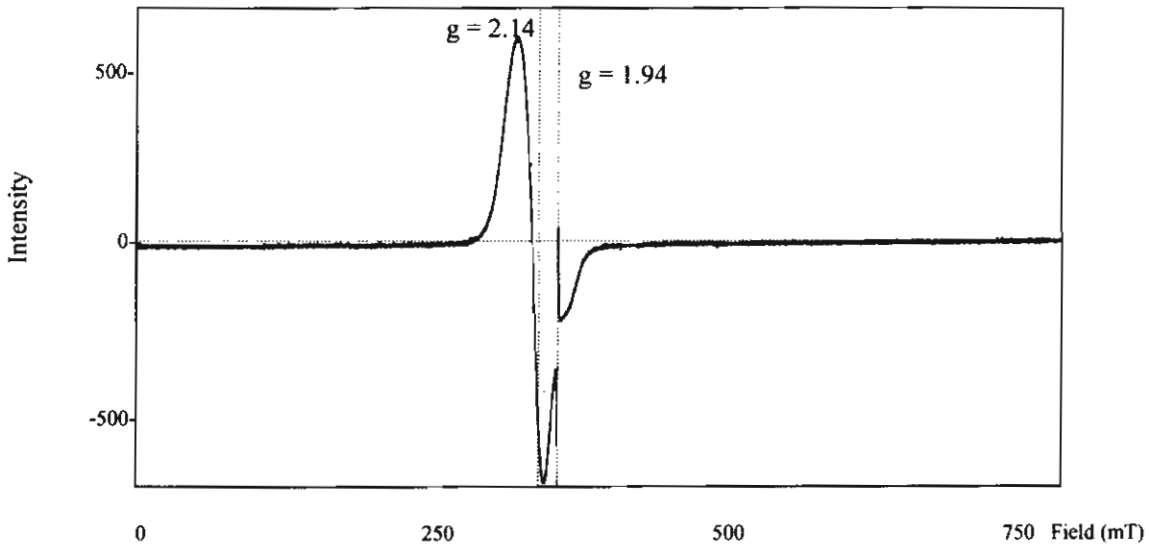

(a) The EPR spectrum at room temperature of $[Cu_2(dpyam)_4(\mu\text{-}C_2O_4)_2](BF_4)_2.3H_2O$ **(I)**

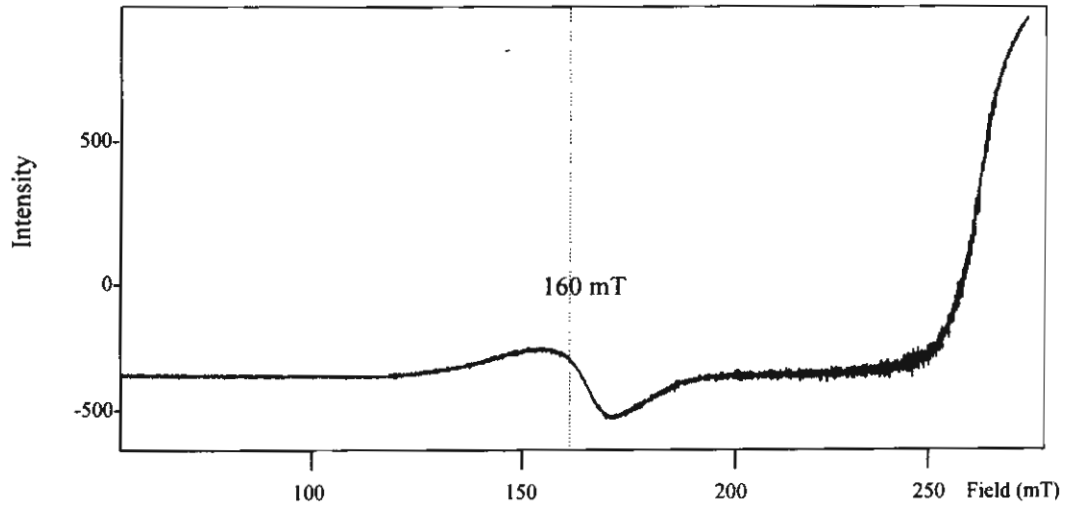

(b) The EPR spectrum at 77 K of $[Cu_2(dpyam)_4(\mu\text{-}C_2O_4)_2](BF_4)_2.3H_2O$ **(I)**

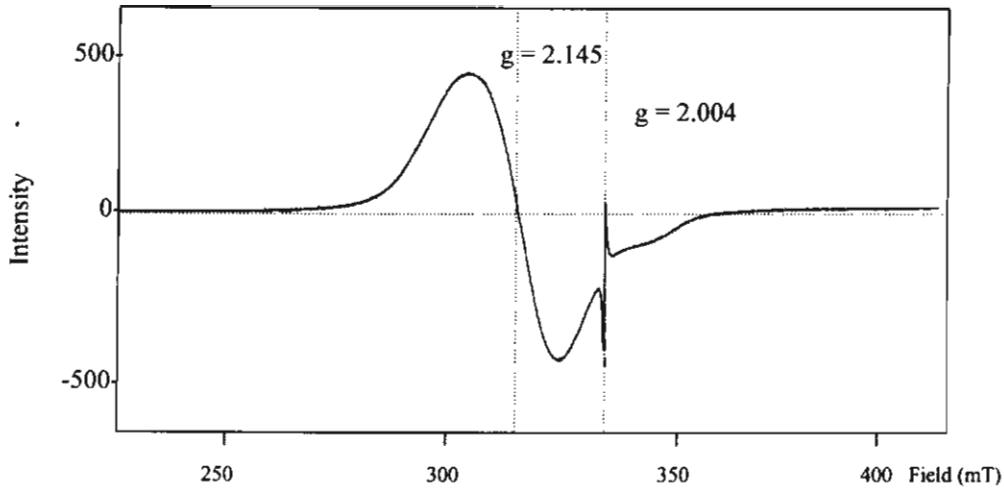

(c) The EPR spectrum at room temperature of $[Cu_2(dpyam)_4(\mu\text{-}C_2O_4)_2](ClO_4)_2.3H_2O$ **(II)**

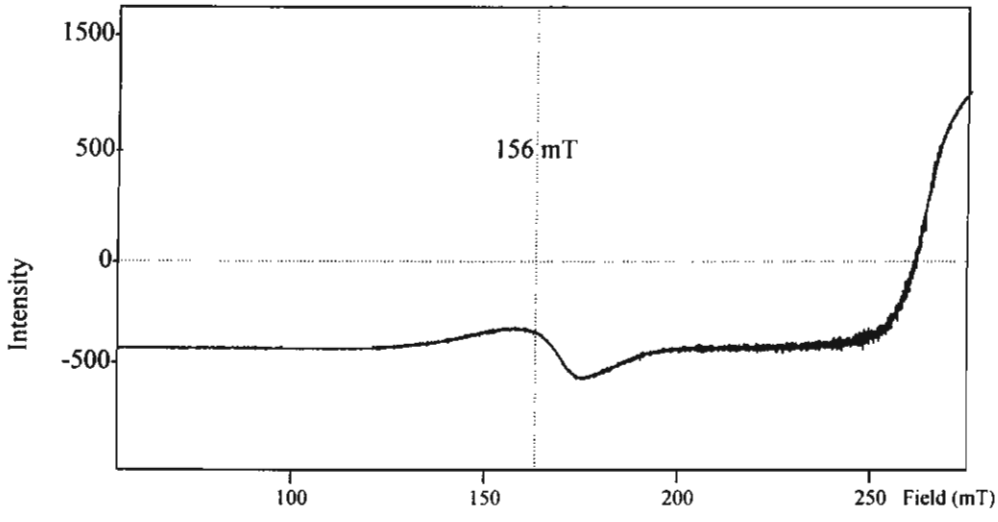

(d) The EPR spectrum at 77 K of $[Cu_2(dpyam)_4(\mu\text{-}C_2O_4)_2](ClO_4)_2.2H_2O$ **(II)**

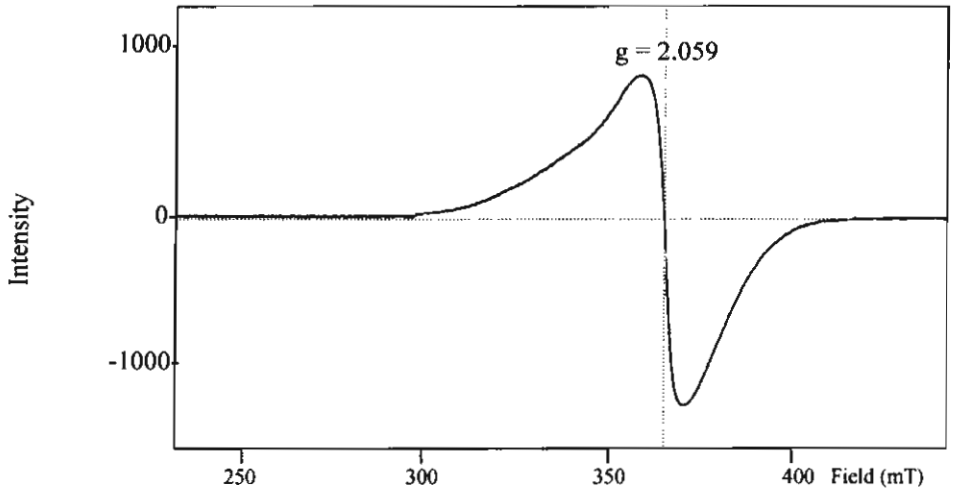

(e) The EPR spectrum at room temperature of $[Cu_2(dpyam)_4(\mu\text{-}C_2O_4)_2](PF_6)_2.2H_2O$ **(III)**

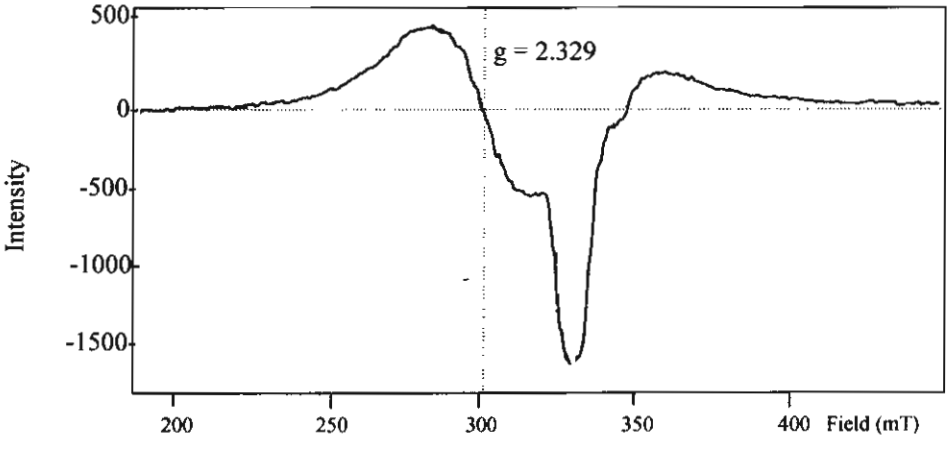

(f) The EPR spectrum at 77 K of $[Cu_2(dpyam)_4(\mu\text{-}C_2O_4)_2](PF_6)_2.2H_2O$ **(III)**

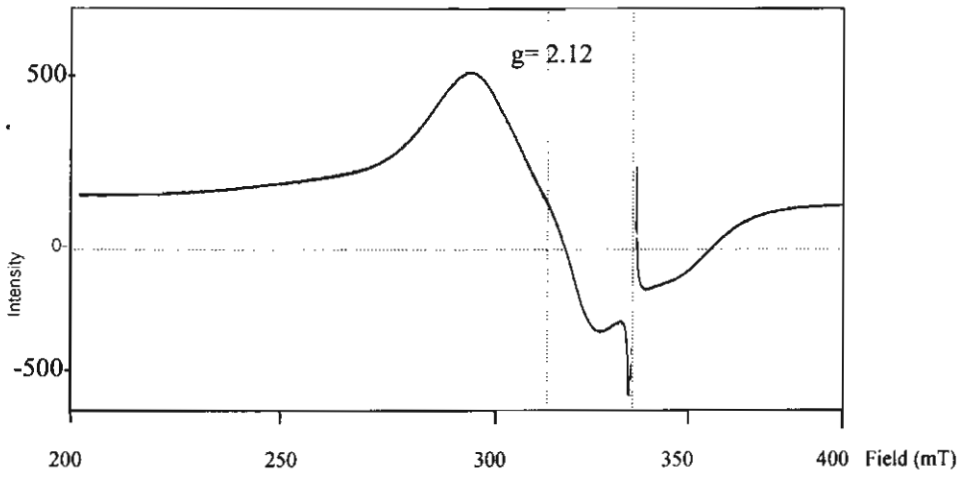

(g) The EPR spectrum at room temperature of $[Cu_2(dpyam)_2(C_2O_4)(NO_3)_2((CH_3)_2(SO)_2]$ **(IV)**

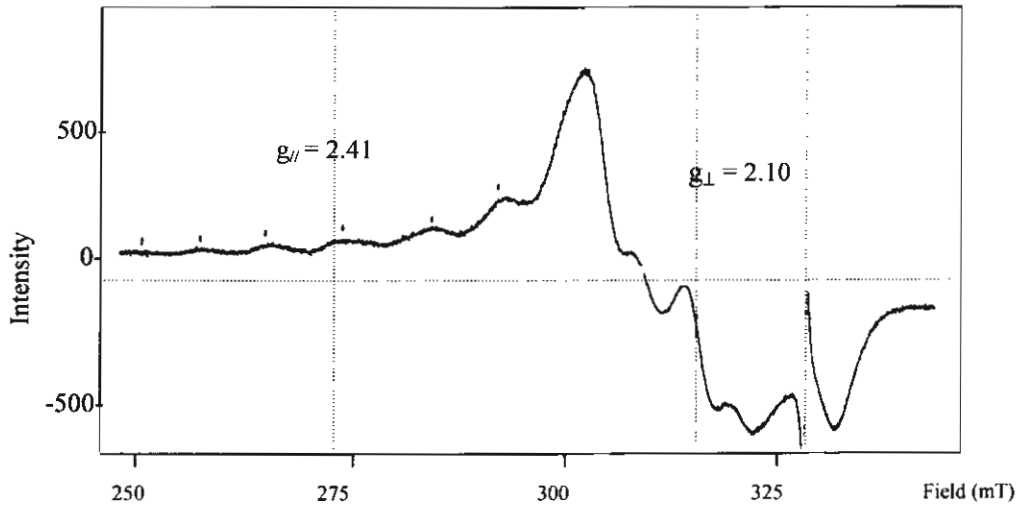

(h) The EPR spectrum at 77 K of $[Cu_2(dpyam)_2(C_2O_4)(NO_3)_2((CH_3)_2(SO)_2]$ **(IV)**

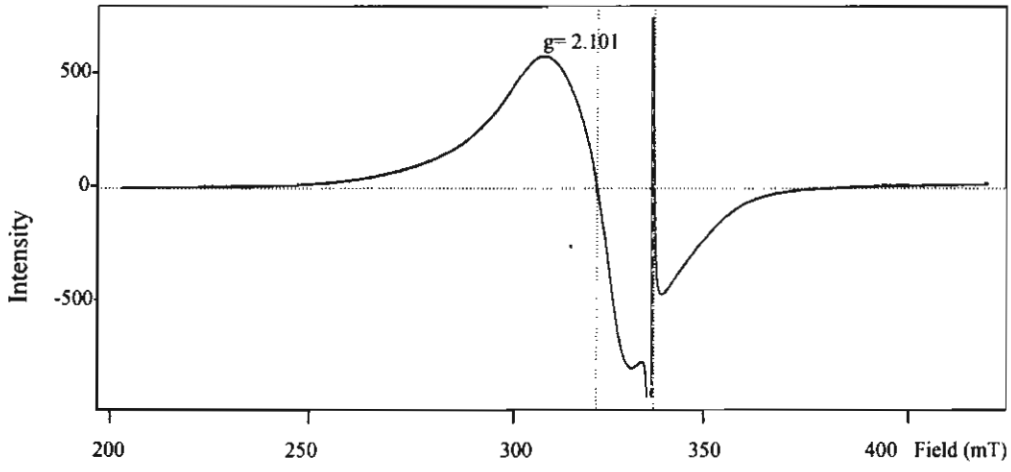

(i) The EPR spectrum at room temperature of $[Cu_2(dpyam)_2(\mu\text{-}C_2O_4)(NO_3)((CH_3)_2NCOH)_2]$ **(V)**

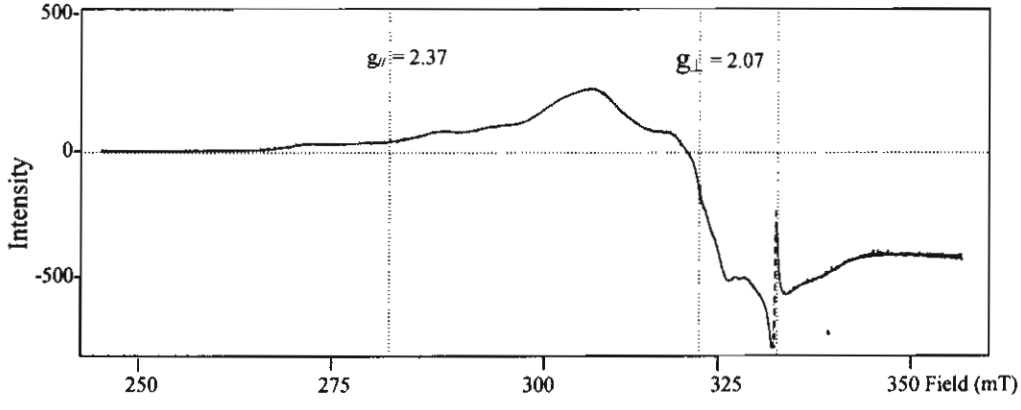

(j) The EPR spectrum at 77 K of $[Cu_2(dpyam)_2(\mu\text{-}C_2O_4)(NO_3)((CH_3)_2NCOH)_2]$ **(V)**

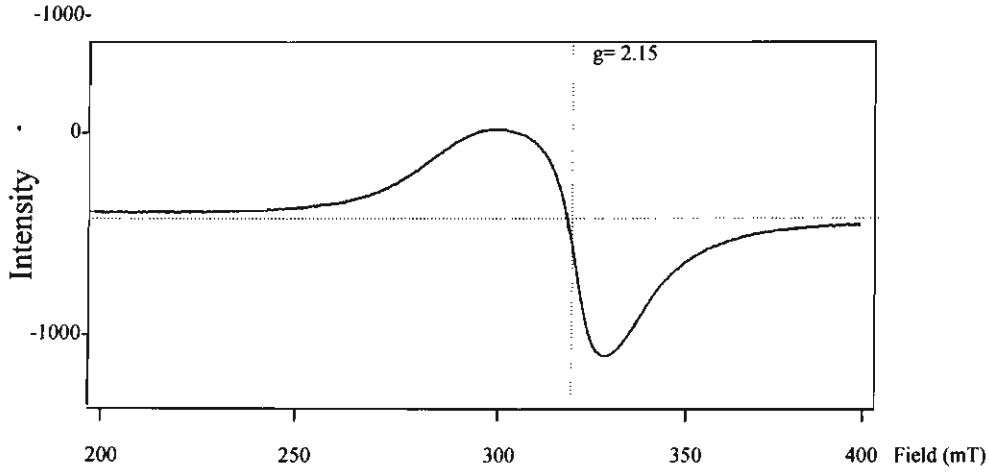

(k) The EPR spectrum at room temperature of $[Cu_2(dpyam)_2(\mu\text{-}C_2O_4)Cl_2]$ **(VI)**

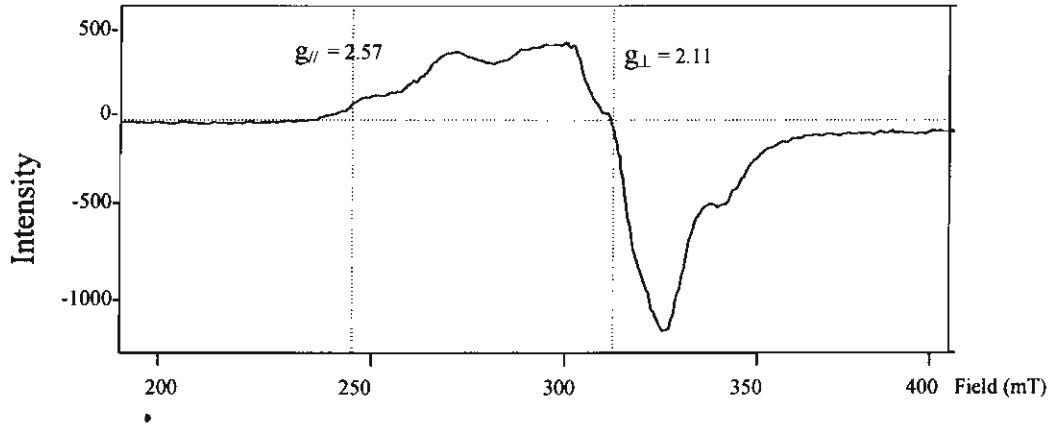

(l) The EPR spectrum at 77 K of $[Cu_2(dpyam)_2(\mu\text{-}C_2O_4)Cl_2]$ **(VI)**

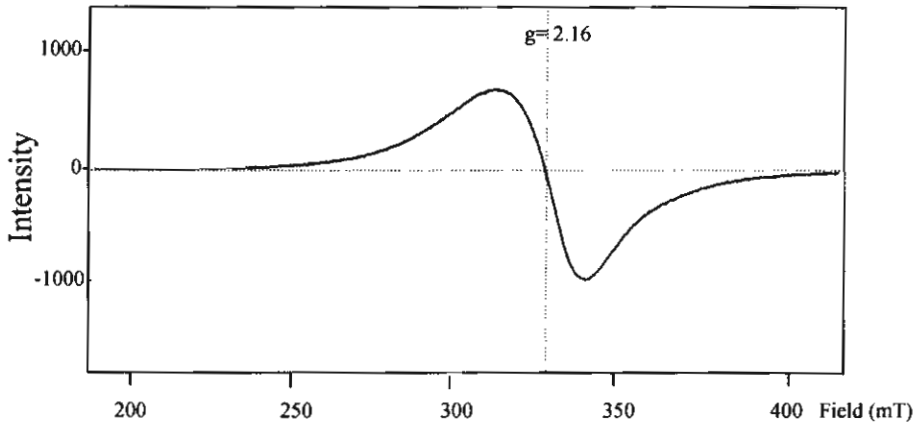

(m) The EPR spectrum at room temperature of $[Cu_2(dpyam)_2(\mu\text{-}C_2O_4)Br_2]$ **(VII)**

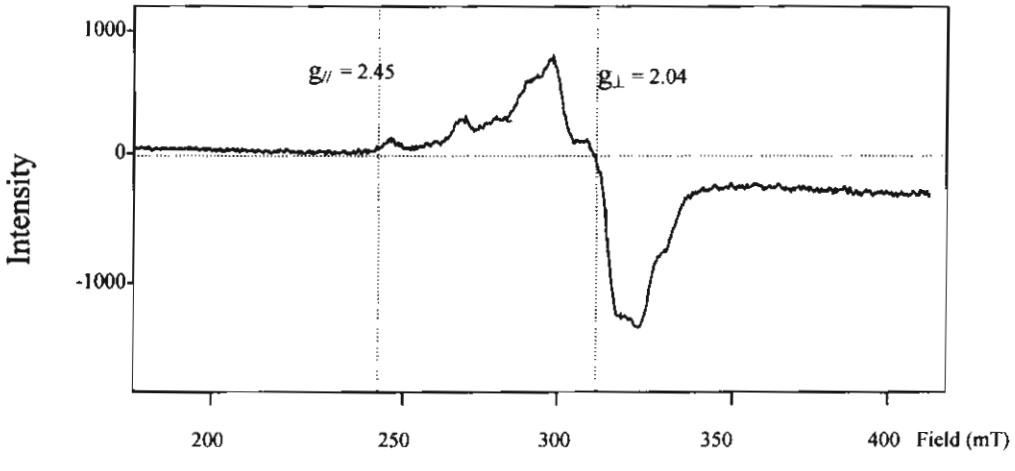

(n) The EPR spectrum at 77 K of $[Cu_2(dpyam)_2(\mu\text{-}C_2O_4)Br_2]$ **(VII)**

APPENDIX IIA

Crystal and Refinement Data for

$\{[Cu_3(dpyam)_3(\mu_3,\eta^3\text{-}HPO_4)(\mu_3,\eta^4\text{-}PO_4)(H_2O)](PF_6)\cdot 3H_2O\}_n$ (I)

$[Cu(dpyam)(\mu_2,\eta^3\text{-}HPO_4)]_n$ (II),

$[Cu(dpyam)(\mu_2,\eta^2\text{-}H_2PO_4)(H_2PO_4)]_2$ (III),

$[Cu_4(dpyam)_4(\mu_4,\eta^3\text{-}HPO_4)_2(\mu\text{-}Cl)_2](Cl)_2\cdot 6H_2O$ (IV),

$[Cu_4(dpyam)_4(\mu_4,\eta^3\text{-}HPO_4)_2(\mu\text{-}Br)_2](Br)_2\cdot 6H_2O$ (V) and

$[Cu_4(dpyam)_4(\mu_3,\eta^3\text{-}HPO_4)_2(NO_3)_2(H_2O)_2](NO_3)_2\cdot 2H_2O$ (VI)

Table 1 Crystal and refinement data for complexes **I-V**

Complexes	**I**	**II**	**III**	**IV**	**V**	**VI**
Formula weight	{[Cu_3(dpyam)$_3$ (μ_3,η^3 -HPO_4)(μ_3,η^4-PO_4) (H_2O)](PF_6)·3H_2O}$_n$ (**I**)	[Cu(dpyam)(μ_2,η^3-HPO_4)]$_n$ (**II**)	[Cu(dpyam) (μ_2,η^2-H_2PO_4) (H_2PO_4)]$_2$ (**III**)	[Cu_4(dpyam)$_4$(μ_4,η^3 -HPO_4)$_2$(μ-Cl)$_2$] (Cl)$_2$·6H_2O (**IV**)	[Cu_4(dpyam)$_4$(μ_4,η^3-HPO_4)$_2$(μ-Br)$_2$] (Br)$_2$·6H_2O (**V**)	[Cu_4(dpyam)$_4$(μ_3,η^3-HPO_4)$_2$(NO_3)$_2$ (H_2O)$_2$](NO_3)$_2$· 2H_2O (**VI**)
Molecular weight	1112.21	330.72	857.44	1380.85	1558.67	1451.02
T(K)	100(2) K	293(2)	293(2)	273(2)	273(2)	273(2)
Crystal system	Triclinic	Trigonal	Triclinic	monoclinic	monoclinic	monoclinic
Space group	P-1	P3/2	P-1	*Cm*	*Cm*	*C2/c*
a (Å)	7.4301(5)	9.6644(1)	8.0347(1)	16.3150(3)	16.4716(3)	28.4236(10)
b (Å)	15.9715(10)	9.6644(1)	10.0264(1)	48.2777(4)	49.3270(4)	9.7305(10)
c (Å)	17.4521(10)	10.6841(2)	10.5912(1)	12.5824(2)	12.6314(2)	22.7510(2)
α (°)	67.9970(10)	90	83.217(1)	90	90	90
β (°)	85.2240(10)	90	70.490(1)	125.9980(10)	126.2060(10)	118.183(10)
γ (°)	79.7430(10)	120	69.356(1)	90	90	90
V ($Å^3$)	1889.2(2) $Å^3$	864.21(2)	752.58(2)	8017.99(12)	8281.1(2)	5546.37(8)
Z	2	2	2	*4*	*4*	*8*
D_{calc} (*g* cm^{-3})	1.955 g.cm^{-3}	1.271	1.892	1.761	1.904	1.584
μ (mm)	1.907	1.365	1.712	1.908	4.548	1.650
F (000)	1122	334	434	4320	4752	2680
Crystal size (mm)	0.24 × 0.12 × 0.08	0.28 × 0.30 × 0.20	0.15 × 0.35 × 0.50	0.25 x 0.30 x 0.73	0.23 x 0.24 x 0.35	0.10 x 0.33 x 0.05
Reflection collected	16764	6496	5631	30204	31126	19678
Unique reflections	8741	3042	4101	17411	18172	7885
Observed ref. [I>2σ(I)]				11833		
Data/restraints /parameter	8741 / 0 / 712	3042/1/212	4101/0/269	17411 / 2 / 1306	18172/2/1085	7885/0/472
Goodness-of-fit	1.043	1.030	1.065	1.044	1.019	1.047
Final R indices	R1 = 0.0458,	*R1* = 0.0186	*R1* = 0.0261	R1 = 0.0364,	*R1* = 0.0796	*R1* = 0.0511
[I>2σ(I)]	wR2= 0.0903	*wR2* = 0.0451	*wR2* = 0.0752	wR2 = 0.0914	*wR2* = 0.01949	*wR2* = 0.0961
R indices (all data)	R1 = 0.0611, wR2= 0.0964	*R1* = 0.0192 *wR2* = 0.0452	*R1* = 0.0281 *wR2* = 0.0759	R1 = 0.0448, wR2 = 0.0981	*R1* = 0.11481 *wR2* = 0.2255	*R1* = 0.0977 *wR2* = 0.1144
Largest difference peak and hole (e $Å^{-3}$)	0.618,-0.508	0.252,-0.321	0.580,-0.509	1.981,-0.604	6.603,-1.298	0.956,-0.536

$$R = \Sigma||F_o| - |F_c||/\Sigma|F_o|, \quad R_w = [\Sigma w\{|F_o| - |F_c|\}^2/w|F_o|^2]^{1/2}$$

APPENDIX IIB

Selected Bond Lengths (Å) and Angles (°) for

$\{[Cu_3(dpyam)_3(\mu_3,\eta^3\text{-}HPO_4)(\mu_3,\eta^4\text{-}PO_4)(H_2O)](PF_6)\cdot 3H_2O\}_n$ (I)

$[Cu(dpyam)(\mu_2,\eta^3\text{-}HPO_4)]_n$ (II),

$[Cu(dpyam)(\mu_2,\eta^2\text{-}H_2PO_4)(H_2PO_4)]_2$ (III),

$[Cu_4(dpyam)_4(\mu_4,\eta^3\text{-}HPO_4)_2(\mu\text{-}Cl)_2](Cl)_2\cdot 6H_2O$ (IV),

$[Cu_4(dpyam)_4(\mu_4,\eta^3\text{-}HPO_4)_2(\mu\text{-}Br)_2](Br)_2\cdot 6H_2O$ (V) and

$[Cu_4(dpyam)_4(\mu_3,\eta^3\text{-}HPO_4)_2(NO_3)_2(H_2O)_2](NO_3)_2\cdot 2H_2O$ (VI)

Table 2 Selected bond lengths (Å) and angles (°) with e.s.d.s. in parentheses of $\{[Cu_3(dpyam)_3(\mu_3,\eta^3\text{-}HPO_4)(\mu_3,\eta^4\text{-}PO_4)(H_2O)](PF_6)\cdot 3H_2O\}_n$ **(I)**

Cu(3)-O(4A)	1.908(2)	Cu(3)-O(5)	1.924(2)
Cu(3)-N(8)	1.976(3)	Cu(3)-N(7)	1.985(3)
Cu(2)-O(2A)	1.920(2)	Cu(2)-O(7)	1.929(2)
Cu(2)-N(5)	1.978(3)	Cu(2)-N(4)	1.991(3)
Cu(1)-O(6)	1.942(2)	Cu(1)-O(1)	1.957(2)
Cu(1)-N(1)	2.008(3)	Cu(1)-N(2)	2.027(3)
Cu(1)-O(1W)	2.191(3)	P(2)-O(6)	1.515(2)
P(2)-O(8)	1.541(2)	P(2)-O(5)	1.547(2)
P(2)-O(7)	1.560(2)	P(1)-O(2)	1.516(2)
P(1)-O(4)	1.523(2)	P(1)-O(1)	1.524(2)
P(1)-O(3)	1.601(2)		
O(4A)-Cu(3)-O(5)	91.3(1)	O(4A)-Cu(3)-N(8)	148.0(1)
O(5)-Cu(3)-N(8)	94.4(1)	O(4A)-Cu(3)-N(7)	94.9(1)
O(5)-Cu(3)-N(7)	155.8(1)	N(8)-Cu(3)-N(7)	92.7(1)
O(2A)-Cu(2)-O(7)	98.7(1)	O(2A)-Cu(2)-N(5)	91.6(1)
O(7)-Cu(2)-N(5)	150.7(1)	O(2A)-Cu(2)-N(4)	140.3(1)
O(7)-Cu(2)-N(4)	97.1(1)	N(5)-Cu(2)-N(4)	92.1(1)
O(6)-Cu(1)-O(1)	97.3(1)	O(6)-Cu(1)-N(1)	91.9(1)
O(1)-Cu(1)-N(1)	166.9(1)	O(6)-Cu(1)-N(2)	132.8(1)
O(1)-Cu(1)-N(2)	91.6(1)	N(1)-Cu(1)-N(2)	89.0(1)
O(6)-Cu(1)-O(1W)	119.1(1)	O(1)-Cu(1)-O(1W)	85.4(1)
N(1)-Cu(1)-O(1W)	82.0(1)	N(2)-Cu(1)-O(1W)	107.7(1)
O(6)-P(2)-O(8)	111.2(1)	O(6)-P(2)-O(5)	108.9(1)
O(8)-P(2)-O(5)	108.8(1)	O(6)-P(2)-O(7)	110.4(1)
O(8)-P(2)-O(7)	107.6(1)	O(5)-P(2)-O(7)	109.9(1)
O(2)-P(1)-O(4)	113.0(1)	O(2)-P(1)-O(1)	112.4(1)
O(4)-P(1)-O(1)	114.3(1)	O(2)-P(1)-O(3)	102.6(1)
O(4)-P(1)-O(3)	105.1(1)	O(1)-P(1)-O(3)	108.3(1)

Table 3 Selected bond lengths (Å) and angles (°) with e.s.d.s. in parentheses of [Cu(dpyam)(μ_2,η^3-HPO_4)]$_n$ **(II)**

Cu(1)-O(4)	1.919(1)	Cu(1)-O(1)	1.946(1)
Cu(1)-N(1)	1.969(1)	Cu(1)-N(2)	1.994(1)
P(1)-O(3)	1.510(1)	P(1)-O(1)	1.519(1)
P(1)-O(4)A	1.531(1)	P(1)-O(2)	1.588(2)
Cu(1)-O(2)A	2.719(3)	Cu(1)-Cu(1)A	5.955(2)
O(4)-Cu(1)-O(1)	101.6(1)	O(4)-Cu(1)-N(1)	149.7(1)
O(1)-Cu(1)-N(1)	91.4(1)	O(4)-Cu(1)-N(2)	93.6(1)
O(1)-Cu(1)-N(2)	142.6(1)	O(1)-Cu(1)-N(2)	92.0(1)
O(3)-P(1)-O(1)	111.7(1)	O(3)-P(1)-O(4)A	111.1(1)
O(1)-P(1)-O(4)A	111.6(1)	O(3)-P(1)-O(2)	110.7(1)
O(1)-P(1)-O(2)	109.3(1)	O(4)A-P(1)-O(2)	101.9(1)

Symmetry code: A = –x+y+1, -x+1,z+1/3

Table 4 Selected bond lengths (Å) and angles (°) with e.s.d.s. in parentheses of $[Cu(dpyam)(\mu_2,\eta^2\text{-}H_2PO_4)(H_2PO_4)]_2$ **(III)**

Cu(1)-O(8A)	1.964(1)	Cu(1)-O(5)	1.987(1)
Cu(1)-N(1)	1.991(1)	Cu(1)-N(2)	1.997(1)
Cu(1)-O(1)	2.271(1)	P(1)-O(1)	1.512(1)
P(1)-O(3)	1.519(1)	P(1)-O(4)	1.558(1)
P(1)-O(2)	1.581(1)	P(2)-O(8)	1.506(1)
P(2)-O(5)	1.518(1)	P(2)-O(7)	1.558(1)
P(2)-O(6)	1.564(1)	Cu(1)-Cu(1)A	5.136(2)
O(8)A-Cu(1)-O(5)	89.7(1)	O(8)A-Cu(1)-N(1)	89.0(1)
O(5)-Cu(1)-N(1)	174.1(1)	O(8)A-Cu(1)-N(2)	167.0(1)
O(5)-Cu(1)-N(2)	91.8(1)	N(1)-Cu(1)-N(2)	88.1(1)
O(8)A-Cu(1)-O(1)	96.0(1)	O(5)-Cu(1)-O(1)	91.9(1)
N(1)-Cu(1)-O(1)	94.1(1)	N(2)-Cu(1)-O(1)	96.8(1)
O(1)-P(1)-O(3)	115.1(1)	O(1)-P(1)-O(4)	112.2(1)
O(3)-P(1)-O(4)	106.9(1)	O(1)-P(1)-O(2)	109.2(1)
O(3)-P(1)-O(2)	108.5(1)	O(4)-P(1)-O(2)	104.1(1)
O(8)-P(2)-O(5)	115.6(1)	O(8)-P(2)-O(7)	109.6(1)
O(5)-P(2)-O(7)	105.9(1)	O(8)-P(2)-O(6)	112.6(1)
O(5)-P(2)-O(6)	105.6(1)	O(7)-P(2)-O(6)	106.8(1)
P(2)-O(5)-Cu(1)	130.9(1)	P(1)-O(1)-Cu(1)	122.9(1)

Symmetry code: A = -x+1, -y+1, -z+1

Table 5 Selected bond lengths (Å) and angles (°) with e.s.d.s. in parentheses of $[Cu_4(dpyam)_4(\mu_4,\eta^3\text{-}HPO_4)_2(\mu\text{-}Cl)_2](Cl)_2\cdot 6H_2O$ **(IV)**

Cu(6)-N(17)	1.962(4)	Cu(6)-N(16)	1.965(4)
Cu(6)-O(9)	2.011(3)	Cu(6)-O(12)	2.021(3)
Cu(6)-Cl(4)	2.604(3)	Cu(6)-Cu(6A)	2.802(3)
Cu(5)-O(10)	1.947(3)	Cu(5)-O(13)	1.966(3)
Cu(5)-N(14)	1.993(4)	Cu(5)-N(13)	2.012(4)
Cu(5)-Cl(3)	2.560(3)	Cu(4)-N(10)	1.970(4)
Cu(4)-N(11)	1.982(4)	Cu(4)-O(7)	2.012(3)
Cu(4)-O(3)	2.026(3)	Cu(4)-Cl(2)	2.592(3)
Cu(3)-N(8)	1.971(4)	Cu(3)-N(7)	1.981(4)
Cu(3)-O(7)	2.012(3)	Cu(3)-O(3)	2.030(3)
Cu(3)-Cl(2)	2.598(3)	Cu(3)-Cu(4)	2.816(3)
Cu(2)-O(6)	1.950(3)	Cu(2)-O(2)	1.969(3)
Cu(2)-N(5)	1.996(4)	Cu(2)-N(4)	2.009(4)
Cu(2)-Cl(1)	2.556(3)	Cu(1)-O(5)	1.948(3)
Cu(1)-O(1)	1.965(3)	Cu(1)-N(1)	1.993(3)
Cu(1)-N(2)	2.001(4)	Cu(1)-Cl(1)	2.551(3)
P(3)-O(11)	1.565(4)	P(3)-O(10)	1.509(3)
P(3)-O(9)	1.553(5)	P(4)-O(12)	1.558(4)
P(4)-O(13)	1.512(3)	P(2)-O(6)	1.503(3)
P(4)-O(14)	1. 587(5)	P(2)-O(7)	1.560(3)
P(2)-O(5)	1.504(3)	P(1)-O(2)	1.499(3)
P(2)-O(8)	1.580(3)	P(1)-O(3)	1.563(3)
P(1)-O(1)	1.501(3)	Cu(5)-Cu(5A)	3.917(3)
P(1)-O(4)	1.584(3)	Cu(6)-Cu(6A)	2.802(1)
Cu(1)-Cu(2)	3.882(3)	Cu(5A)-Cu(6A)	5.232(3)
Cu(3)-Cu(4)	2.8163(6)	Cu(2)-Cu(4)	4.027(3)
N(17)-Cu(6)-N(16)	91.4(2)	O(10)-Cu(5)-O(13)	91.8(2)
N(16)-Cu(6)-O(9)	171.7(2)	O(10)-Cu(5)-N(14)	164.0(2)
N(17)-Cu(6)-O(12)	172.9(2)	O(13)-Cu(5)-N(13)	162.5(2)
O(9)-Cu(6)-O(12)	78.9(2)	N(14)-Cu(5)-N(13)	87.4(2)
N(10)-Cu(4)-N(11)	90.6(2)	O(6)-Cu(2)-O(2)	91.6(2)
N(11)-Cu(4)-O(7)	171.6(2)	O(6)-Cu(2)-N(5)	162.6(2)
N(10)-Cu(4)-O(3)	173.3(2)	O(2)-Cu(2)-N(4)	164.8(2)
O(7)-Cu(4)-O(3)	79.0(2)	N(5)-Cu(2)-N(4)	87.3(2)
N(8)-Cu(3)-N(7)	91.3(2)	O(5)-Cu(1)-O(1)	91.6(2)
N(7)-Cu(3)-O(7)	171.7(2)	O(5)-Cu(1)-N(1)	164.5(2)
N(8)-Cu(3)-O(3)	173.4(2)	O(1)-Cu(1)-N(2)	161.3(2)
O(7)-Cu(3)-O(3)	78.9(2)	N(1)-Cu(1)-N(2)	87.1(2)

Table 6 Selected bond lengths (Å) and angles (°) with e.s.d.s. in parentheses of $[Cu_4(dpyam)_4(\mu_4,\eta^3\text{-}HPO_4)_2(\mu\text{-}Br)_2](Br)_2\cdot 6H_2O$ **(V)**

Br(4)-Cu(6)	2.766(2)	O(10)- Cu(5)- N(13)	163.3(4)
Cu(6)- N(16)	1.960(9)	O(13)- Cu(5)- N(13)	87.9(4)
Cu(6)- N(17)	1.977(9)	N(14)- Cu(5)- N(13)	87.5(4)
Cu(6)- O(12)	2.039(8)	N(10)- Cu(4)- N(11)	90.9(4)
Cu(6)- O(9)	2.045(7)	N(10)- Cu(4)- O(7)	97.2(4)
Cu(6)- Cu(6A)	2.834(2)	N(11)- Cu(4)- O(7)	170.8(4)
Cu(5)- O(10)	1.937(9)	N(10)- Cu(4)- O(3)	174.2(4)
Cu(5)- O(13)	1.974(9)	N(10)- Cu(4)- Cu(3)	132.8(3)
Cu(5)- N(14)	2.008(10)	N(11)- Cu(4)- Cu(3)	130.6(3)
Cu(5)- N(13)	2.019(10)	O(5)- Cu(1)- N(1)	165.3(4)
Cu(5)- Br(3)	2.7077(19)	O(1)- Cu(1)- N(2)	162.3(4)
Cu(4)- N(10)	1.981(10)	O(2)- Cu(2)- O(6)	91.8(4)
Cu(4)- N(11)	1.998(10)	O(2)- Cu(2)- N(5)	88.6(4)
Cu(4)- O(7)	2.005(7)	O(6)- Cu(2)- N(5)	164.5(4)
Cu(4)- O(3)	2.029(8)	O(2)- Cu(2)- N(4)	164.9(4)
Cu(4)- Br(2)	2.7450(19)	N(8)- Cu(3)- O(7)	97.4(4)
Cu(4)- Cu(3)	2.8507(17)	N(8)- Cu(3)- N(7)	90.9(4)
Cu(1)- O(1)	1.974(7)	O(7)- Cu(3)- N(7)	170.8(4)
Cu(1)- O(5)	1.988(8)	N(8)- Cu(3)- O(3)	175.1(4)
Cu(1)- N(1)	2.003(10)	O(7)- Cu(3)- O(3)	78.6(3)
Cu(1)- N(2)	2.021(10)	N(7)- Cu(3)- O(3)	92.9(4)
Cu(1)- Br(1)	2.7154(19)	N(8)- Cu(3)- Cu(4)	132.8(3)
Cu(2)- O(2)	1.970(8)	O(7)- Cu(3)- Cu(4)	44.7(2)
Cu(2)- O(6)	1.979(8)	N(7)- Cu(3)- Cu(4)	130.0(3)
Cu(2)- N(5)	1.987(10)	O(3)- Cu(3)- Cu(4)	45.4(2)
Cu(2)- N(4)	2.023(9)	Cu(4)- Br(2)- Cu(3)	62.40(5)
Cu(2)- Br(1)	2.7199(19)	O(13)- P(4)- O(13A)	115.3(7)
Cu(3)- N(8)	1.984(10)	O(13)- P(4)- O(12)	111.3(4)
Cu(3)- O(7)	1.993(7)	O(13)- P(4)- O(14)	108.0(5)
Cu(3)- N(7)	2.005(10)	O(12)- P(4)- O(14)	101.9(7)
Cu(3)- O(3)	2.033(8)	O(10)- P(3)- O(10A)	115.8(7)
Cu(3)- Br(2)	2.7577(18)	O(10)- P(3)- O(9)	109.8(4)
P(4)- O(13)	1.506(8)	O(10)- P(3)- O(11)	110.3(4)
P(4)- O(12)	1.555(11)	O(9)- P(3)- O(11)	99.8(8)
P(4)- O(14)	1.612(12)	O(5)- P(2)- O(6)	116.7(6)
P(3)- O(10)	1.523(8)	O(5)- P(2)- O(7)	111.4(4)
P(3)- O(9)	1.529(11)	O(6)- P(2)- O(7)	110.6(5)
P(3)- O(11)	1.544(14)	O(5)- P(2)- O(8)	107.1(5)
P(2)- O(5)	1.475(8)	O(6)- P(2)- O(8)	106.3(5)
P(2)- O(6)	1.492(8)	O(7)- P(2)- O(8)	103.7(5)
P(2)- O(7)	1.589(9)	O(1)- P(1)- O(2)	117.9(5)
P(2)- O(8)	1.629(10)	O(1)- P(1)- O(4)	109.6(5)
P(1)- O(1)	1.497(7)	O(2)- P(1)- O(4)	109.5(5)
P(1)- O(2)	1.510(7)	O(2)- P(1)- O(3)	108.2(5)
P(1)- O(4)	1.533(10)	O(4)- P(1)- O(3)	102.3(6)
P(1)- O(3)	1.599(10)		
N(17)- Cu(6)- O(12)	173.1(4)		
N(16)- Cu(6)- O(9)	173.2(4)		
O(13)- Cu(5)- N(14)	165.0(4)		

Table 7 Selected bond lengths (Å) and angles (°) with e.s.d.s. in parentheses of $[Cu_4(dpyam)_4(\mu_3,\eta^3\text{-}HPO_4)_2(NO_3)_2(H_2O)_2](NO_3)_2\cdot 2H_2O$ **(VI)**

Cu(1)-O(6)	1.972(2)	Cu(1)-O(4)	1.968(2)
Cu(1)-N(1)	1.967(2)	Cu(1)-N(2)	2.001(3)
Cu(1)-O(7)	2.497(2)	Cu(2)-O(7)	1.933(2)
Cu(2)-N(5)	2.013(3)	Cu(2)-N(4)	1.979(3)
Cu(2)-O(10)	2.145(2)	Cu(2)-O(11)	2.152(3)
Cu(2)-O(9)	2.743(2)	Cu(1)...Cu(2)	4.136(2)
Cu(1)...Cu(2A)	4.895(2)	Cu(1)...Cu(1A)	4.560(2)
Cu(2)...Cu(2A)	7.833(2)	P(1)-O(7)	1.525(2)
P(1)-O(4A)	1.526(2)	P(1)-O(6)	1.542(2)
P(1)- O(5)	1.574(2)	N(8)-O(8)	1.233(4)
N(8)-O(9)	1.249(4)	N(8)-O(10)	1.283(3)
N(1)-Cu(1)-O(6)	161.7(1)	O(4)-Cu(1)-N(2)	142.4(1)
O(6)-Cu(1)-N(2)	95.3(1)	O(7)-Cu(2)-N(5)	90.6(1)
N(5)-Cu(2)-N(4)	89.6(1)	O(7)-Cu(2)-O(10)	91.8(1)
N(5)-Cu(2)-O(10)	137.5(1)	N(4)-Cu(2)-O(10)	95.5(1)
O(7)-Cu(2)-O(11)	86.4(1)	N(5)-Cu(2)-O(11)	131.1(1)
N(4)-Cu(2)-O(11)	84.7(1)		

A; –x +2, -y, -z +1

APPENDIX IIC

The Infrared Spectra for

$\{[Cu_3(dpyam)_3(\mu_3,\eta^3\text{-}HPO_4)(\mu_3,\eta^4\text{-}PO_4)(H_2O)](PF_6)\cdot 3H_2O\}_n$ (I)

$[Cu(dpyam)(\mu_2,\eta^3\text{-}HPO_4)]_n$ (II),

$[Cu(dpyam)(\mu_2,\eta^2\text{-}H_2PO_4)(H_2PO_4)]_2$ (III),

$[Cu_4(dpyam)_4(\mu_4,\eta^3\text{-}HPO_4)_2(\mu\text{-}Cl)_2](Cl)_2\cdot 6H_2O$ (IV),

$[Cu_4(dpyam)_4(\mu_4,\eta^3\text{-}HPO_4)_2(\mu\text{-}Br)_2](Br)_2\cdot 6H_2O$ (V) and

$[Cu_4(dpyam)_4(\mu_3,\eta^3\text{-}HPO_4)_2(NO_3)_2(H_2O)_2](NO_3)_2\cdot 2H_2O$ (VI)

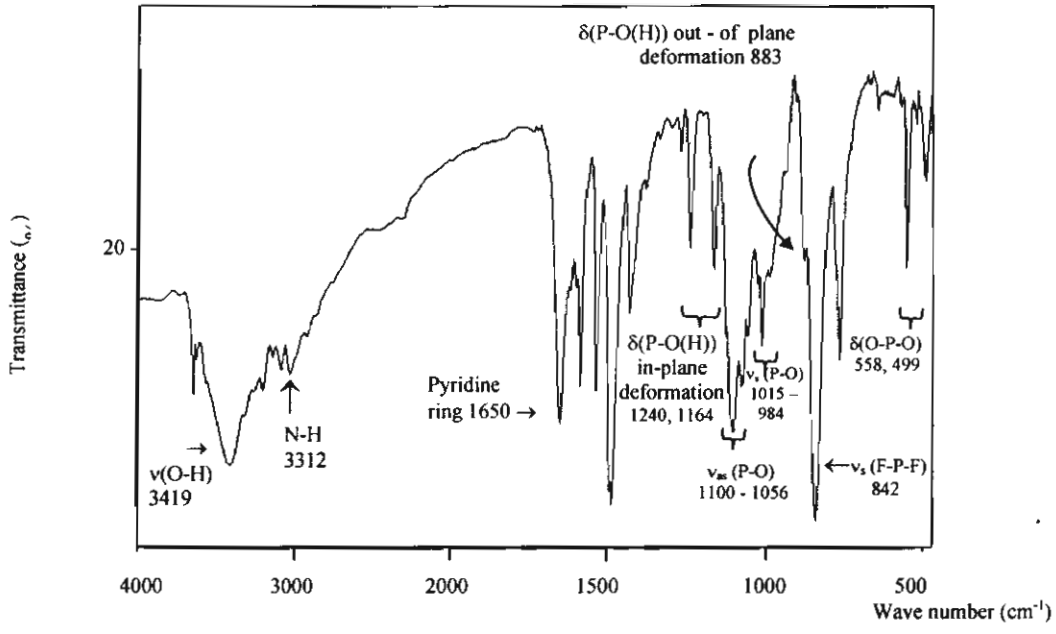

(a) The infrared spectrum of $\{[Cu_3(dpyam)_3(\mu_3,\eta^3\text{-}HPO_4)(\mu_3,\eta^4\text{-}PO_4)(H_2O)](PF_6)\cdot 3H_2O\}_n$ **(I)**

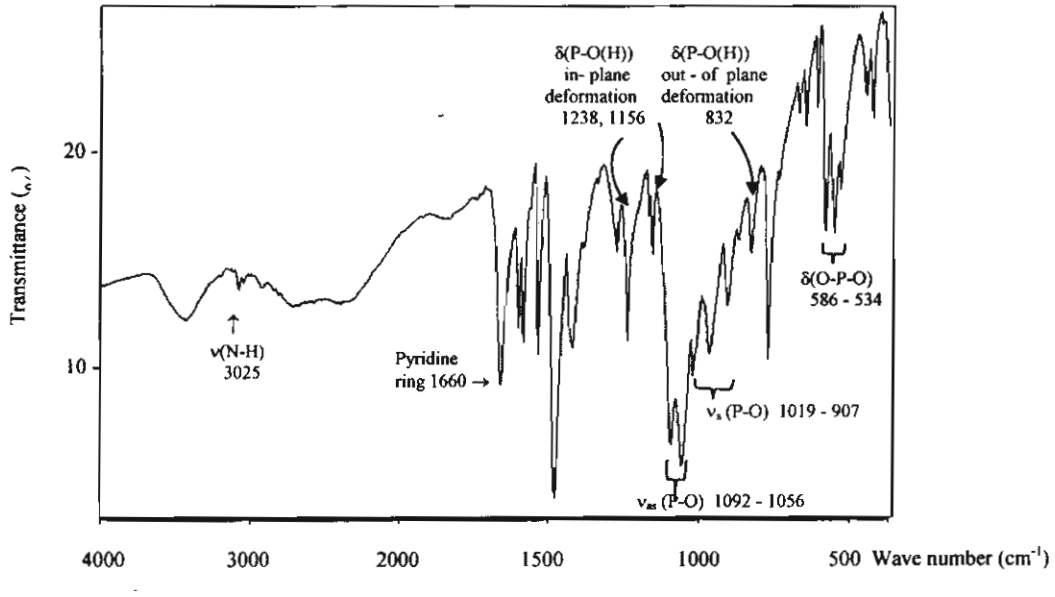

(b) The IR spectrum of $[Cu(dpyam)(\mu_2,\eta^3\text{-}HPO_4)]_n$ **(II)**

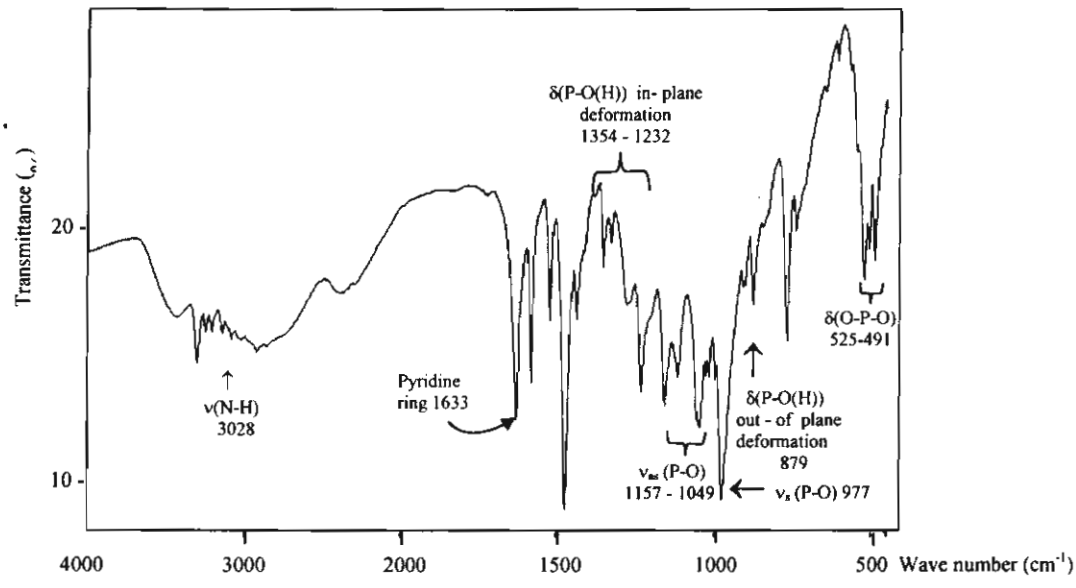

(c) The IR spectrum of $[Cu(dpyam)(\mu_2,\eta^2\text{-}H_2PO_4)(H_2PO_4)]_2$ **(III)**

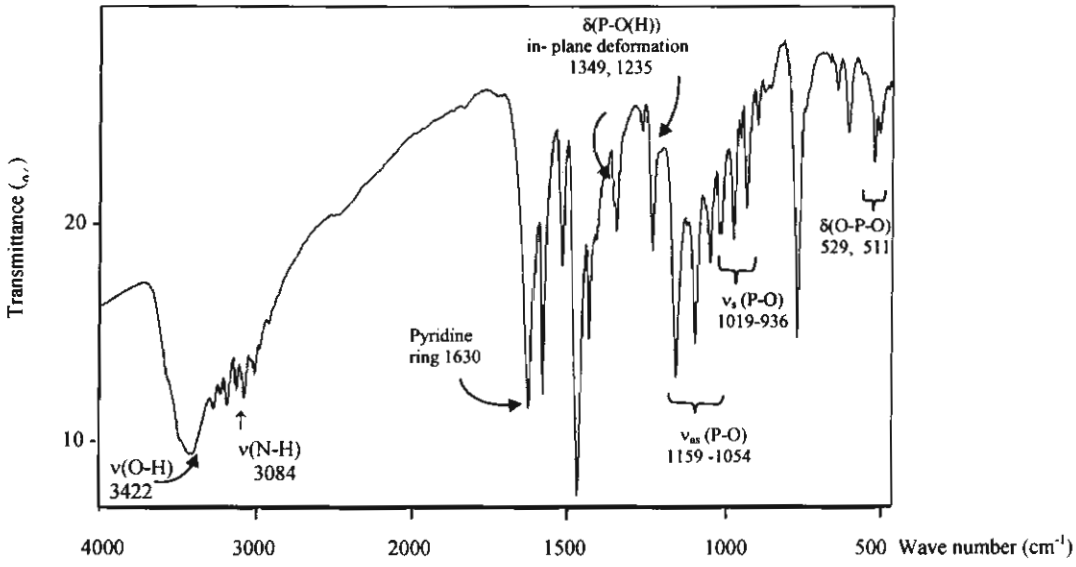

(d) The infrared spectrum of $[Cu_4(dpyam)_4(\mu_4,\eta^3\text{-}HPO_4)_2(\mu\text{-}Cl)_2](Cl)_2\cdot 6H_2O$ **(IV)**

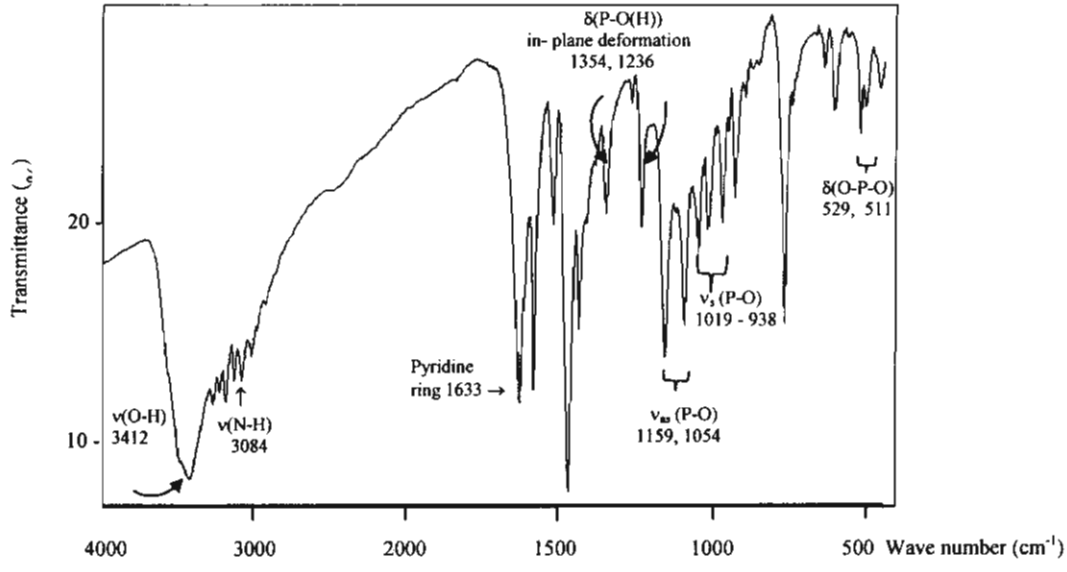

(e) The IR spectrum of $[Cu_4(dpyam)_4(\mu_4,\eta^3\text{-}HPO_4)_2(\mu\text{-}Br)_2](Br)_2{\cdot}6H_2O$ **(V)**

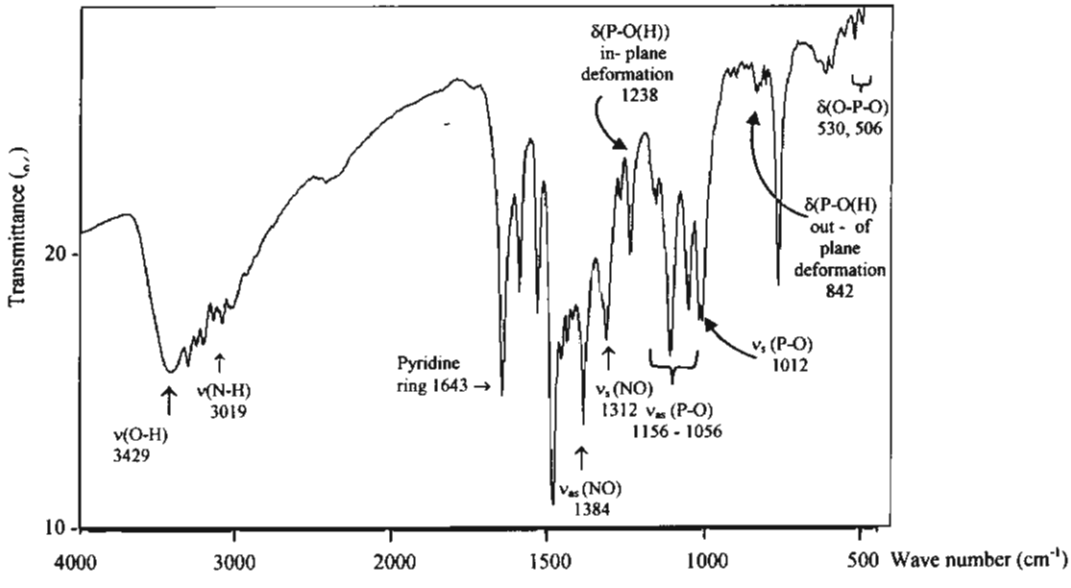

(f) The IR spectrum of $[Cu_4(dpyam)_4(\mu_3,\eta^3\text{-}HPO_4)_2(NO_3)_2(H_2O)_2](NO_3)_2{\cdot}2H_2O$ **(VI)**

APPENDIX IID

The Thermal Analysis for

$\{[Cu_3(dpyam)_3(\mu_3,\eta^3\text{-}HPO_4)(\mu_3,\eta^4\text{-}PO_4)(H_2O)](PF_6)\cdot 3H_2O\}_n$ (I)

$[Cu(dpyam)(\mu_2,\eta^3\text{-}HPO_4)]_n$ (II),

$[Cu(dpyam)(\mu_2,\eta^2\text{-}H_2PO_4)(H_2PO_4)]_2$ (III),

$[Cu_4(dpyam)_4(\mu_4,\eta^3\text{-}HPO_4)_2(\mu\text{-}Cl)_2](Cl)_2\cdot 6H_2O$ (IV),

$[Cu_4(dpyam)_4(\mu_4,\eta^3\text{-}HPO_4)_2(\mu\text{-}Br)_2](Br)_2\cdot 6H_2O$ (V) and

$[Cu_4(dpyam)_4(\mu_3,\eta^3\text{-}HPO_4)_2(NO_3)_2(H_2O)_2](NO_3)_2\cdot 2H_2O$ (VI)

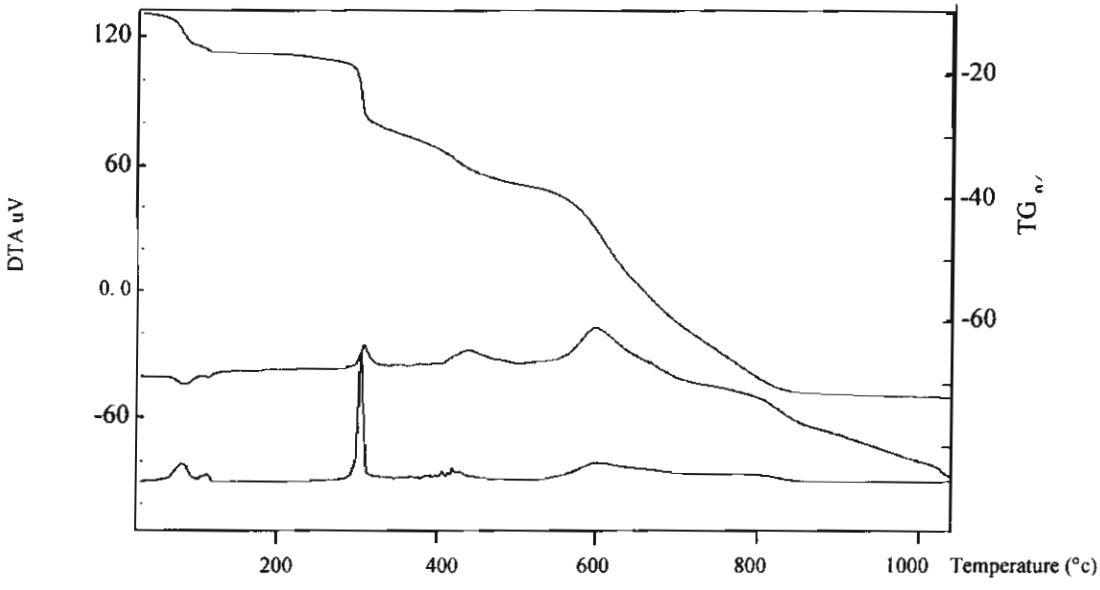

(a) The TG-DTA curve of $\{[Cu_3(dpyam)_3(\mu_3,\eta^3\text{-}HPO_4)(\mu_3,\eta^4\text{-}PO_4)(H_2O)](PF_6)\cdot 3H_2O\}_n$ **(I)**

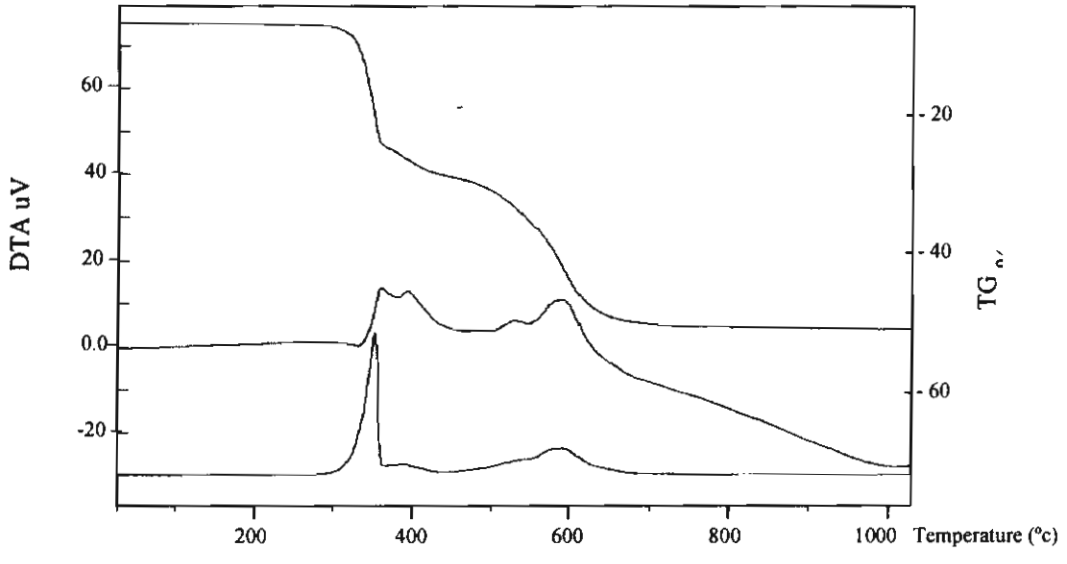

(b) The TG-DTA curve of $[Cu(dpyam)(\mu_2,\eta^3\text{-}HPO_4)]_n$ **(II)**

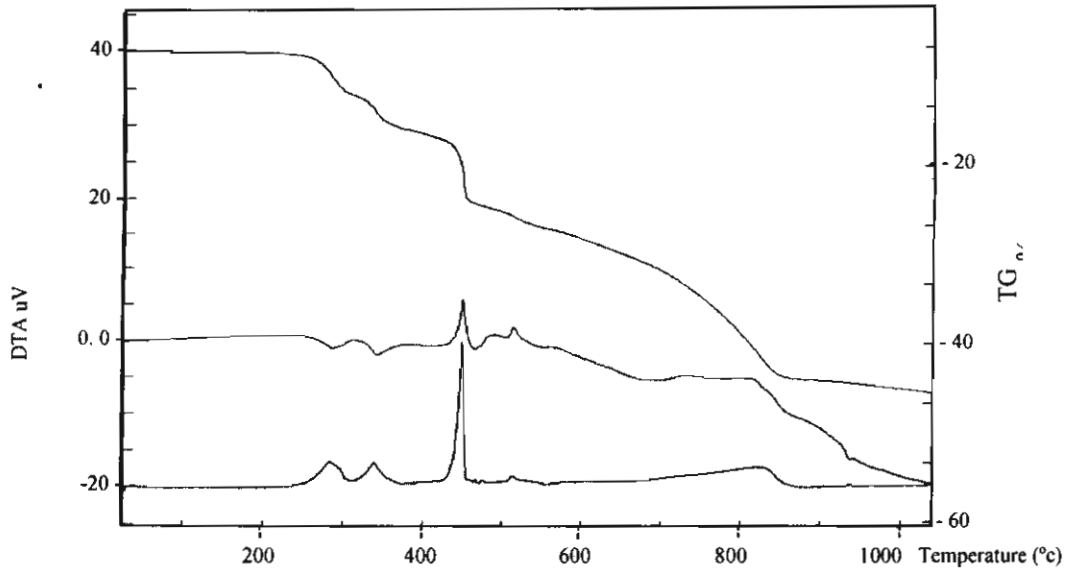

(c) The TG-DTA curve of $[Cu(dpyam)(\mu_2,\eta^2\text{-}H_2PO_4)(H_2PO_4)]_2$ **(III)**

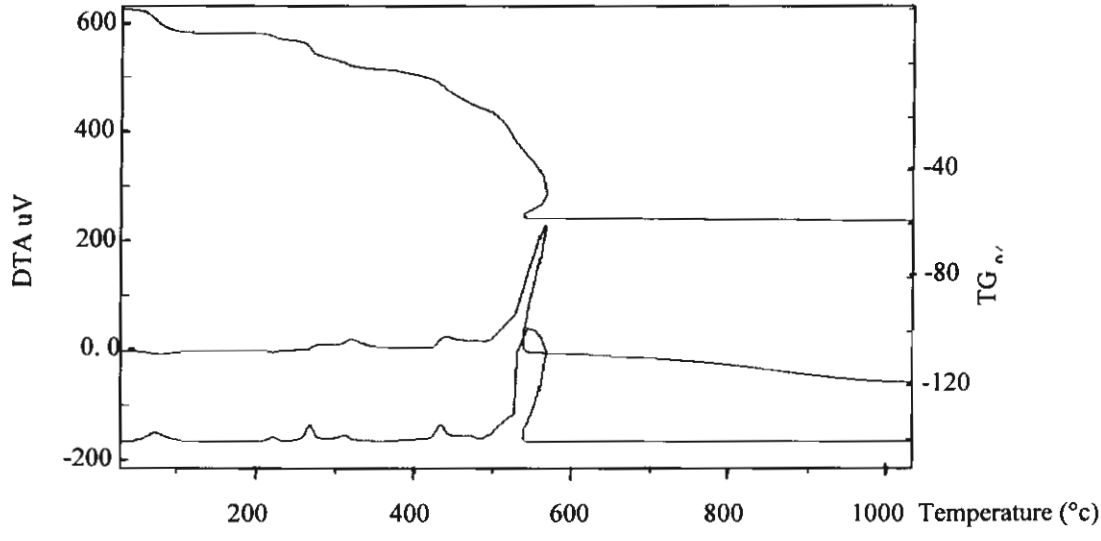

(d) The TG-DTA curve of $[Cu_4(dpyam)_4(\mu_4,\eta^3\text{-}HPO_4)_2(\mu\text{-}Cl)_2](Cl)_2{\cdot}6H_2O$ **(IV)**

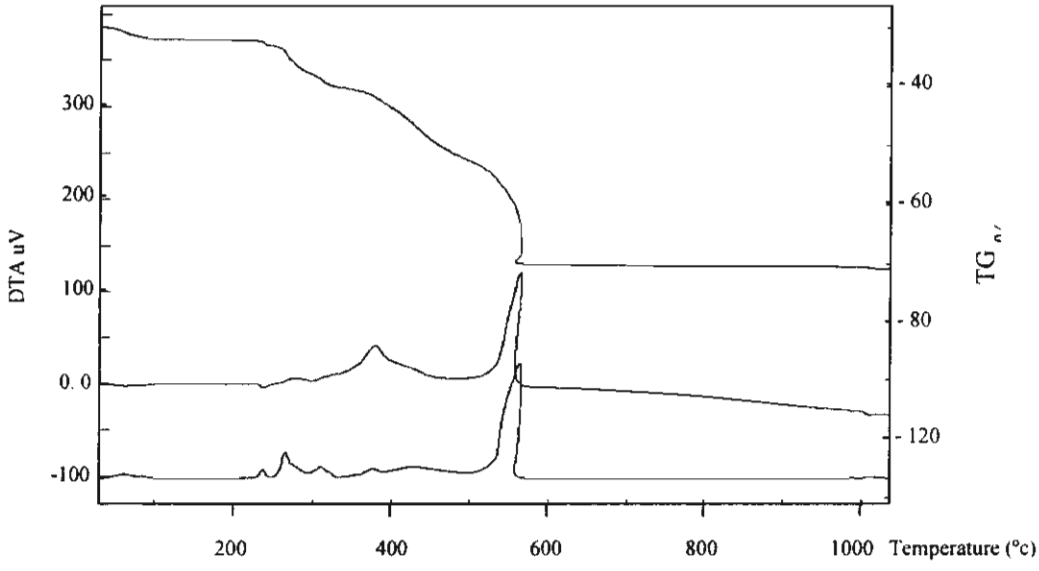

(e) The TG-DTA curve of $[Cu_4(dpyam)_4(\mu_4,\eta^3\text{-}HPO_4)_2(\mu\text{-}Br)_2](Br)_2 \cdot 6H_2O$ **(V)**

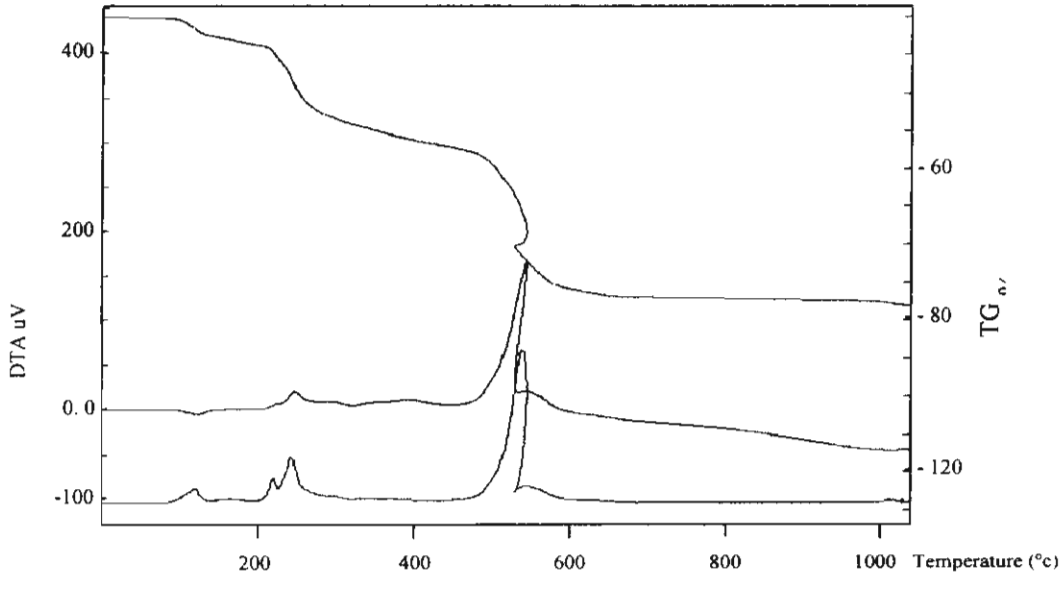

(f) The TG-DTA curve of $[Cu_4(dpyam)_4(\mu_3,\eta^3\text{-}HPO_4)_2(NO_3)_2(H_2O)_2](NO_3)_2 \cdot 2H_2O$ **(VI)**

APPENDIX IIE

The EPR Spectra for

$\{[Cu_3(dpyam)_3(\mu_3,\eta^3\text{-}HPO_4)(\mu_3,\eta^4\text{-}PO_4)(H_2O)](PF_6)\cdot 3H_2O\}_n$ (I)

$[Cu(dpyam)(\mu_2,\eta^3\text{-}HPO_4)]_n$ (II),

$[Cu(dpyam)(\mu_2,\eta^2\text{-}H_2PO_4)(H_2PO_4)]_2$ (III),

$[Cu_4(dpyam)_4(\mu_4,\eta^3\text{-}HPO_4)_2(\mu\text{-}Cl)_2](Cl)_2\cdot 6H_2O$ (IV) ,

$[Cu_4(dpyam)_4(\mu_4,\eta^3\text{-}HPO_4)_2(\mu\text{-}Br)_2](Br)_2\cdot 6H_2O$ (V) and

$[Cu_4(dpyam)_4(\mu_3,\eta^3\text{-}HPO_4)_2(NO_3)_2(H_2O)_2](NO_3)_2\cdot 2H_2O$ (VI)

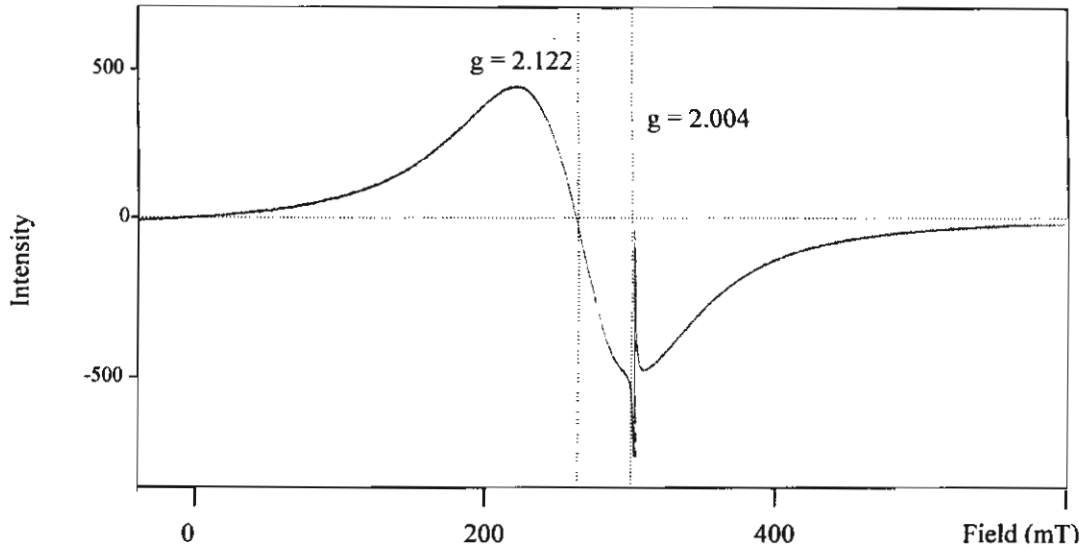

(a) The EPR spectrum at room temperature of $\{[Cu_3(dpyam)_3(\mu_3,\eta^3\text{-}HPO_4)(\mu_3,\eta^4\text{-}PO_4)(H_2O)](PF_6)\cdot 3H_2O\}_n$ **(I)**

(b)

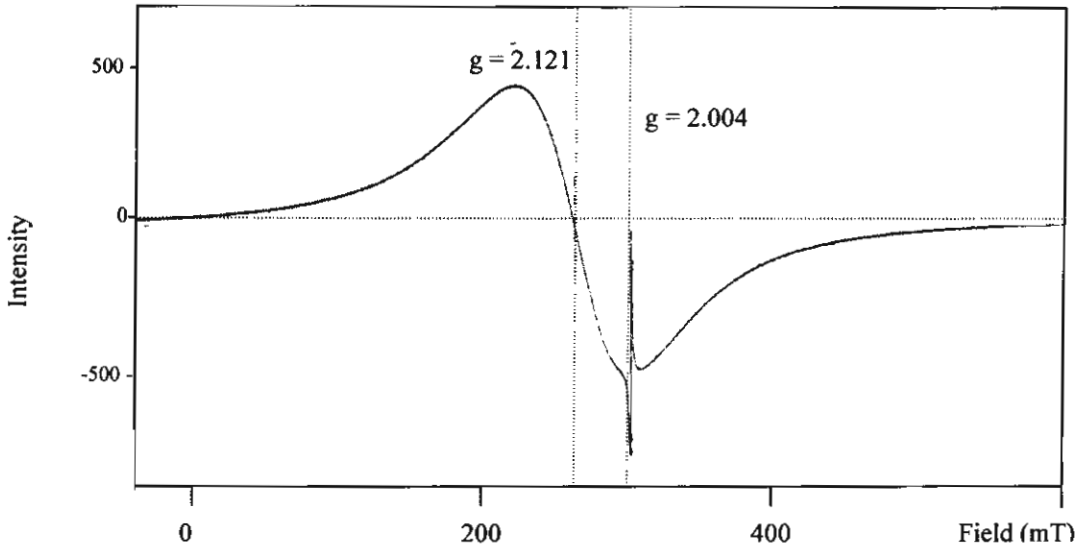

(b) The EPR spectrum at 77K of $\{[Cu_3(dpyam)_3(\mu_3,\eta^3\text{-}HPO_4)(\mu_3,\eta^4\text{-}PO_4)(H_2O)](PF_6)\cdot 3H_2O_n$ **(I)**

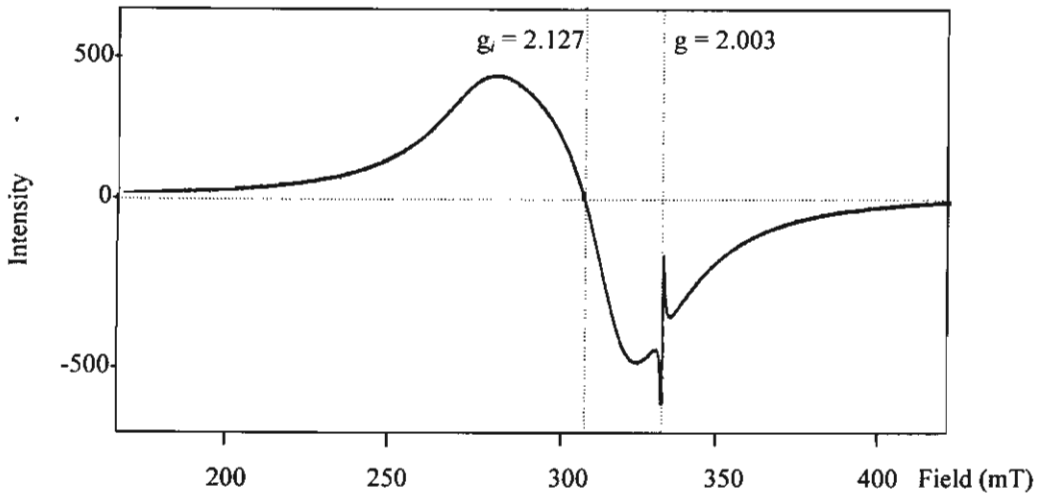

(c) The EPR spectrum at room temperature of $[Cu(dpyam)(\mu_2,\eta^3\text{-}HPO_4)]_n$ **(II)**

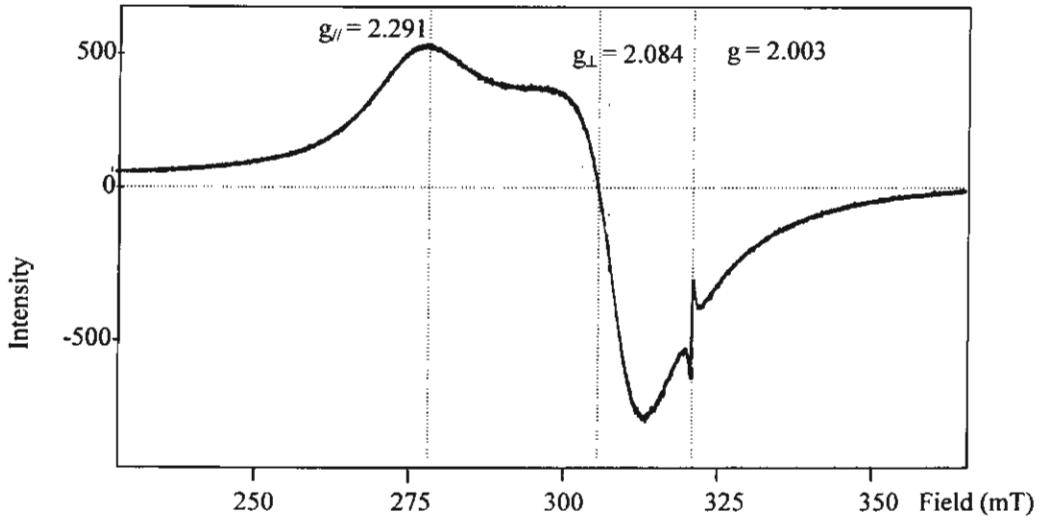

(d) The EPR spectrum at 77K of $[Cu(dpyam)(\mu_2,\eta^3\text{-}HPO_4)]_n$ **(II)**

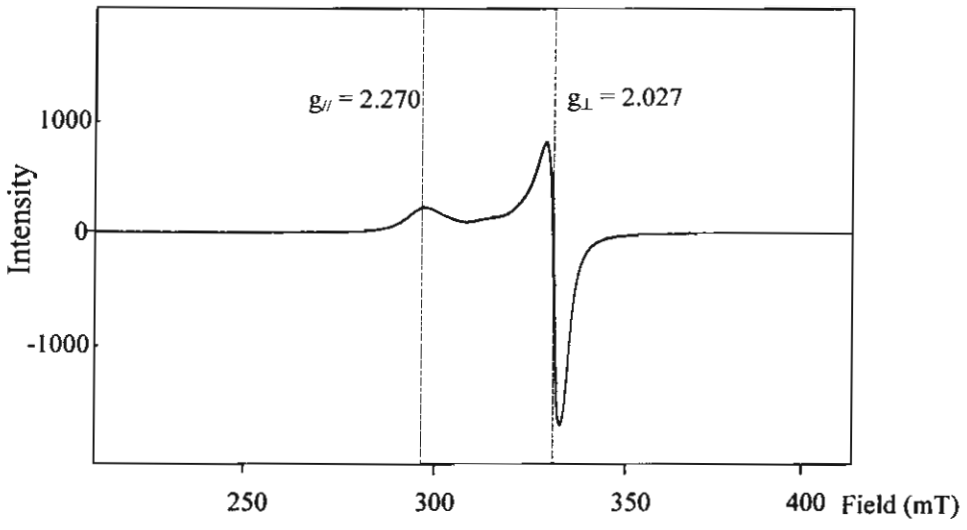

(e) The EPR spectrum at room temperature of $[Cu(dpyam)(\mu_2,\eta^2\text{-}H_2PO_4)(H_2PO_4)]_2$ **(III)**

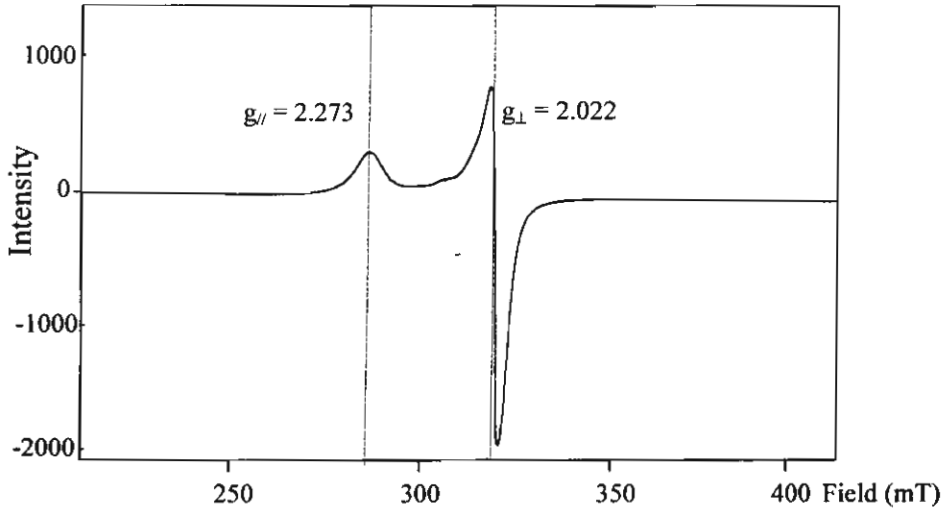

(f) The EPR spectrum at 77K of $[Cu(dpyam)(\mu_2,\eta^2\text{-}H_2PO_4)(H_2PO_4)]_2$ **(III)**

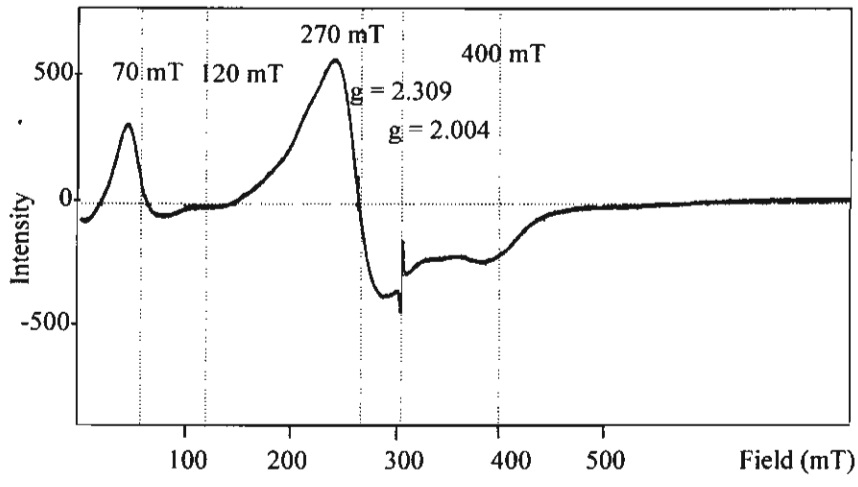

(g) The EPR spectrum at room temperature of $[Cu_4(dpyam)_4(\mu_4,\eta^3\text{-}HPO_4)_2(\mu\text{-}Cl)_2](Cl)_2{\cdot}6H_2O$ **(IV)**

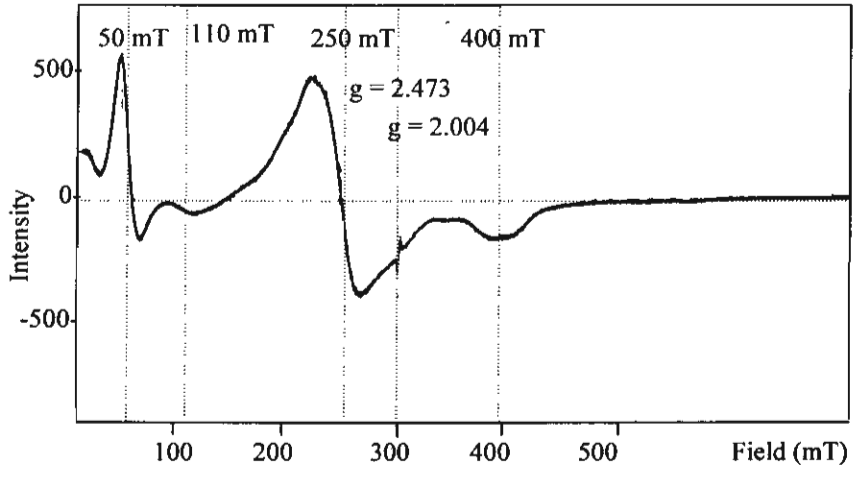

(h) The EPR spectrum at 77K of $[Cu_4(dpyam)_4(\mu_4,\eta^3\text{-}HPO_4)_2(\mu\text{-}Cl)_2](Cl)_2{\cdot}6H_2O$ **(IV)**

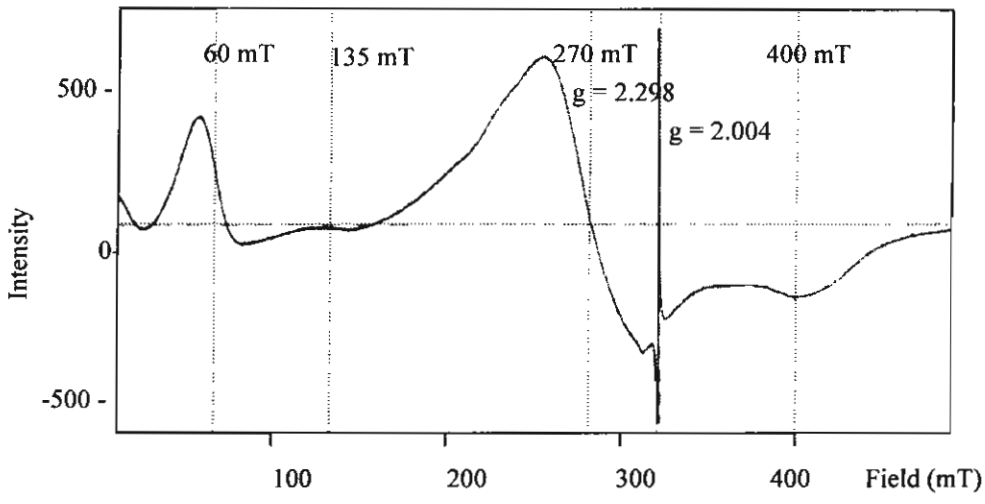

(i) The EPR spectrum at room temperature of $[Cu_4(dpyam)_4(\mu_4,\eta^3\text{-}HPO_4)_2(\mu\text{-}Br)_2](Br)_2{\cdot}6H_2O$ **(V)**

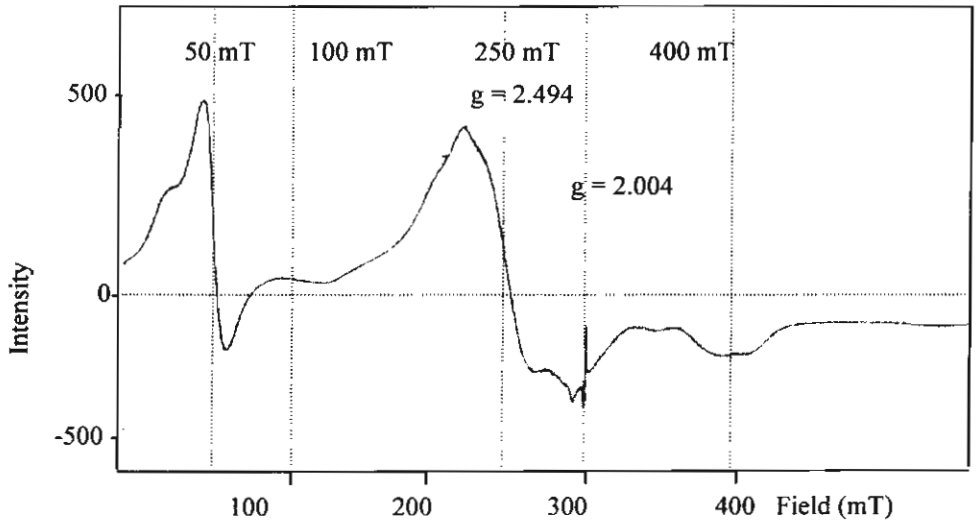

(j) The EPR spectrum at 77K of $[Cu_4(dpyam)_4(\mu_4,\eta^3\text{-}HPO_4)_2(\mu\text{-}Br)_2](Br)_2{\cdot}6H_2O$ **(V)**

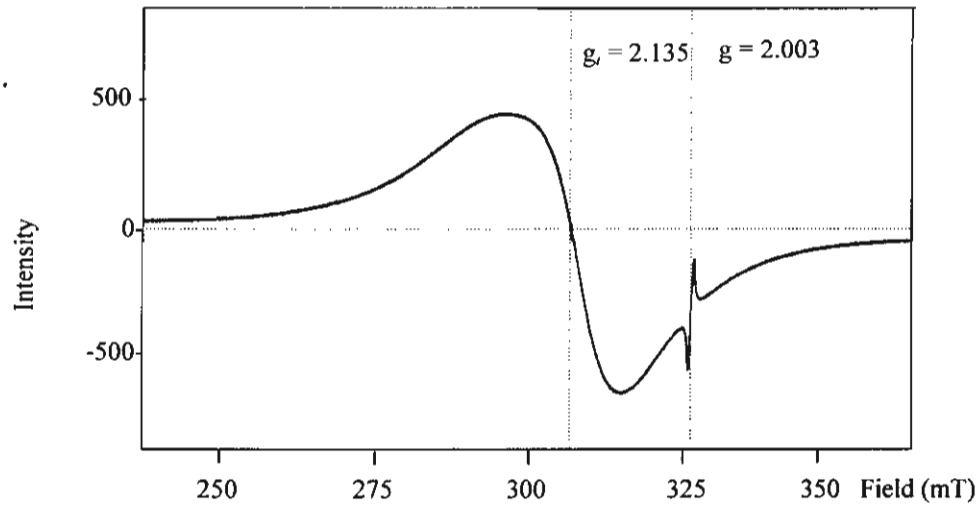

(k) The EPR spectrum at room temperature of $[Cu_4(dpyam)_4(\mu_3,\eta^3\text{-}HPO_4)_2(NO_3)_2(H_2O)_2](NO_3)_2{\cdot}2H_2O$ **(VI)**

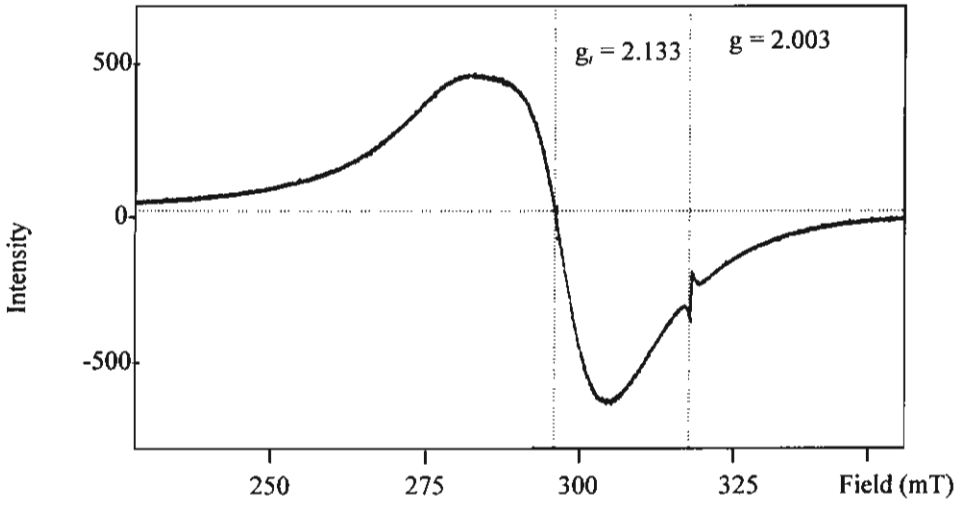

(l) The EPR spectrum at 77K of $[Cu_4(dpyam)_4(\mu_3,\eta^3\text{-}HPO_4)_2(NO_3)_2(H_2O)_2](NO_3)_2{\cdot}2H_2O$ **(VI)**

APPENDIX IIIA

Crystal and Refinement Data for

$[Cu_2(dpyam)_2(\mu\text{-}O_2CH)(\mu\text{-}OH)(\mu\text{-}OCH_3)](ClO_4)$ (I)

$[Cu_2(dpyam)_2(\mu\text{-}O_2CH)(\mu\text{-}OH)_2](ClO_4)\cdot H_2O$ (II)

$[Cu_2(dpyam)_2(\mu\text{-}O_2CH)(\mu\text{-}OOCH)(\mu\text{-}OH)](PF_6)$ (III)

$[Cu_2(dpyam)_2(\mu\text{-}O_2CH)(\mu\text{-}OH)(\mu\text{-}Cl)](ClO_4)\cdot 0.5H_2O$ (IV)

and $[Cu_2(dpyam)_2(\mu\text{-}O_2CH)(\mu\text{-}OH)(\mu\text{-}Cl)](PF_6)$ (V)

Table 1 Crystal and refinement data for complexes **I-V**

Complex	**I**	**II**	**III**	**IV**	**V**
Molecular Formula	$[Cu_2(dpyam)_2(\mu\text{-}O_2CH)(\mu\text{-}OH)(\mu\text{-}OCH_3)](ClO_4)$	$[Cu_2(dpyam)_2(\mu\text{-}O_2CH)(\mu\text{-}OH)_2](ClO_4).H_2O$	$[Cu_2(dpyam)_2(\mu\text{-}O_2CH)_2(\mu\text{-}OH)](PF_6)$	$[Cu_2(dpyam)_2(\mu\text{-}O_2CH)(\mu\text{-}OH)(\mu\text{-}Cl)](ClO_4).0.5H_2O$	$[Cu_2(dpyam)_2(\mu\text{-}O_2CH)(\mu\text{-}OH)(\mu\text{-}Cl)](PF_6)$
Molecular weight	661.99	665.98	721.50	675.43	771.94
Temperature/K	293(2)	293(2)	293(2)	293(2)	293(2)
Crystal system	Orthorhombic	Monoclinic	Orthorhombic	Orthorhombic	Orthorhombic
Space group	$Cmc2_1$	C2/m	$Cmc2_1$	$Cmc2_1$	$Cmc2_1$
a (Å)	16.7872(13)	14.3312(5)	17.011(43)	16.8229(3)	16.8665(1)
b (Å)	8.0793(7)	16.8446(7)	8.031(2)	7.8066(2)	7.829(1)
c (Å)	18.7410(15)	12.4728(5)	19.258(5)	19.2753(0)	19.4941(1)
α	90	90	90	90	90
β	90	120.97	90	90	90
γ	90	90	90	90	90
Volume/$Å^3$	2541.8(4)	2581.72(17)	2631.1(11)	2531.42(10)	2574.22(4)
Z	4	4	4	4	4
Density (calculated)/$g.cm^{-3}$	1.693	1.713	1.821	1.746	1.837
Absorption coefficient (μ)/mm^{-1}	1.837	1.813	1.767	1.946	1.900
F(000)	1312	1352	1448	1344	1424
Crystal size/mm	0.08x0.20x0.30	0.05x0.10x0.38	0.05x0.12x0.25	0.13x0.33x0.40	0.13x0.28x0.33
No. reflection collected	10804	9714	11030	9109	9380
No. unique reflections	3124 (R_{int}=0.0226)	3851 (R_{int}=0.0351)	3180 (R_{int}=0.0355)	3640 (R_{int}=0.0208)	3725 (R_{int}=0.0224)
Data/restraints/parameter	3124/1/206	3851/0/221	3180/1/234	3640/1/230	3725/1/234
GOF	1.095	1.022	1.022	1.007	1.033
Final R indices [I>2σ(I)]	R1=0.0571, wR2=0.1668	R1=0.0609, wR2=0.1571	R1=0.0515, wR2=0.1194	R1=0.0278, wR2=0.0707	R1=0.0387, wR2=0.1073
R indices (all data)	R1=0.0625, wR2=0.1734	R1=0.0936, wR2=0.1796	R1=0.0699, wR2=0.1296	R1=0.0322, wR2=0.0731	R1=0.0441, wR2=0.1115
Largest diff. peak and hole/$e.Å^{-3}$	0.979, -0.419	1.037, -0.884	0.669, -0.468	0.388, -0.373	0.651, -0.672

$$R = \Sigma||F_o| - |F_c||/\Sigma|F_o|, \quad R_w = [\Sigma w\{|F_o| - |F_c|\}^2/w|F_o|^2]^{1/2}$$

APPENDIX IIB

Selected Bond Lengths (Å) and Angles (°) for

$[Cu_2(dpyam)_2(\mu\text{-}O_2CH)(\mu\text{-}OH)(\mu\text{-}OCH_3)](ClO_4)$ (I)

$[Cu_2(dpyam)_2(\mu\text{-}O_2CH)(\mu\text{-}OH)_2](ClO_4)\cdot H_2O$ (II)

$[Cu_2(dpyam)_2(\mu\text{-}O_2CH)(\mu\text{-}OOCH)(\mu\text{-}OH)](PF_6)$ (III)

$[Cu_2(dpyam)_2(\mu\text{-}O_2CH)(\mu\text{-}OH)(\mu\text{-}Cl)](ClO_4)\cdot 0.5H_2O$ (IV) and

$[Cu_2(dpyam)_2(\mu\text{-}O_2CH)(\mu\text{-}OH)(\mu\text{-}Cl)](PF_6)$ (V)

Table 1 Selected bond lengths (Å) and angles (°) with e.s.d.s. in parentheses for $[Cu_2(dpyam)_2(\mu\text{-}O_2CH)(\mu\text{-}OH)(\mu\text{-}OCH_3)](ClO_4)$ **(I)**

Cu(1)-N(1)	1.961(4)	Cu(1)-O(2)	2.169(5)
Cu(1)-N(2)	2.010(4)	Cu(1)-O(3)	2.175(3)
Cu(1)-O(1)	1.918(4)	Cu(1)-Cu(1A)	3.023(1)
O(2)-C(12)	1.196(1)	O(3)-C(11)	1.257(4)
O(1)-Cu(1)-O(2)	81.9(2)	N(1)-Cu(1)-Cu(1A)	138.2(1)
O(1)-Cu(1)-O(3)	88.5(2)	N(1)-Cu(1)-N(2)	91.1(2)
O(1)-Cu(1)-N(1)	173.8(1)	N(2)-Cu(1)-O(2)	133.0(3)
O(1)-Cu(1)-N(2)	93.7(2)	N(2)-Cu(1)-O(3)	135.7(2)
O(1)-Cu(1)-Cu(1A)	38.0(1)	N(2)-Cu(1)-Cu(1A)	125.3(1)
O(2)-Cu(1)-O(3)	91.1(2)	Cu(1)-O(1)-Cu(1A)	104.0(3)
O(2)-Cu(1)-Cu(1A)	45.8(1)	Cu(1)-O(2)-Cu(1A)	88.3(2)
O(3)-Cu(1)-Cu(1A)	79.7(1)	C(11)-O(3)-Cu(1)	126.5(3)
N(1)-Cu(1)-O(2)	95.6(2)	O(3)-C(11)-O(3A)	126.6(6)
N(1)-Cu(1)-O(3)	86.9(2)		

Symmetry code: A = -x, y, z

Table 2 Selected bond lengths [Å] and angles [°] with e.s.d.s. in parentheses of $[Cu_2(dpyam)_2(\mu\text{-}O_2CH)(\mu\text{-}OH)_2](ClO_4).H_2O$ **(II)**

Cu(1)-N(1)	2.003(3)	Cu(1)-O(2)	1.952(3)
Cu(1)-N(2)	2.005(3)	Cu(1)-O(3)	2.345(3)
Cu(1)-O(1)	1.955(3)	Cu(1)-Cu(1A)	2.9027(10)
O(1)-Cu(1)-O(2)	79.55(13)	N(1)-Cu(1)-O(2)	156.04(16)
O(1)-Cu(1)-O(3)	89.07(15)	N(1)-Cu(1)-O(3)	102.81(13)
O(1)-Cu(1)-N(1)	95.88(13)	N(1)-Cu(1)-N(2)	91.92(15)
O(1)-Cu(1)-N(2)	172.20(13)	N(2)-Cu(1)-O(2)	93.28(13)
O(2)-Cu(1)-O(3)	100.62(14)	N(2)-Cu(1)-O(3)	89.25(13)
C(11)-O(3)-Cu(1)	124.4(3)	O(3)-C(11)-O(3A)	127.6(6)
Cu(1)-O(1)-Cu(1A)	95.89(17)	Cu(1)-O(2)-Cu(1A)	96.09(17)

Symmetry code: A = -x+2, y, z

Table 3 Selected bond lengths [Å] and angles [°] with e.s.d.s. in parentheses of $[Cu_2(dpyam)_2(\mu\text{-}O_2CH)(\mu\text{-}OOCH)(\mu\text{-}OH)](PF_6)$ **(III)**

Cu(1)-N(1)	1.972(4)	Cu(1)-O(2)	2.144(6)
Cu(1)-N(2)	2.029(4)	Cu(1)-O(4)	2.200(3)
Cu(1)-O(1)	1.934(5)	Cu(1)-Cu(1A)	3.113(5)
Cu(1)-O(3)	2.246(5)		
O(1)-Cu(1)-O(2)	78.2(2)	N(1)-Cu(1)-O(2)	100.5(2)
O(1)-Cu(1)-O(4)	96.6(2)	N(1)-Cu(1)-O(4)	87.2(1)
O(1)-Cu(1)-N(1)	173.6(2)	N(1)-Cu(1)-N(2)	91.7(1)
O(1)-Cu(1)-N(2)	93.3(2)	N(2)-Cu(1)-O(2)	138.3(3)
O(2)-Cu(1)-O(4)	89.7(3)	N(2)-Cu(1)-O(4)	130.9(1)
C(12)-O(4)-Cu(1)	127.4(4)	O(4)-C(12)-O(4A)	127.5(7)
Cu(1)-O(1)-Cu(1A)	107.2(4)	Cu(1)-O(2)-Cu(1A)	93.1(4)

Symmetry code: A = -x+2, y, z

Table 4 Selected bond lengths [Å] and angles [°] with e.s.d.s. in parentheses of $[Cu_2(dpyam)_2(\mu\text{-}O_2CH)(\mu\text{-}OH)(\mu\text{-}Cl)](ClO_4)\cdot 0.5H_2O$ **(IV)**

Cu(1)-N(1)	1.975(1)	Cu(1)-O(1)	1.916(2)
Cu(1)-N(2)	2.027(2)	Cu(1)-O(2)	2.158(1)
Cu(1)-Cl(1)	2.478(2)	Cu(1)-Cu(1A)	3.036(1)
O(1)-Cu(1)-N(1)	173.8(1)	N(1)-Cu(1)-Cl(1)	96.4(1)
O(1)-Cu(1)-N(2)	94.1(1)	N(1)-Cu(1)-Cu(1A)	138.0(1)
O(1)-Cu(1)-O(2)	88.1(1)	N(2)-Cu(1)-O(2)	133.6(1)
O(1)-Cu(1)-Cl(1)	82.5(1)	N(2)-Cu(1)-Cl(1)	119.1(1)
O(1)-Cu(1)-Cu(1A)	37.6(1)	N(2)-Cu(1)-Cu(1A)	126.3(1)
O(2)-Cu(1)-Cl(1)	107.2(1)	Cu(1)-O(1)-Cu(1A)	104.8(1)
O(2)-Cu(1)-Cu(1A)	79.4(1)	Cu(1)-Cl(1)-Cu(1A)	75.6(1)
N(1)-Cu(1)-N(2)	91.7(1)	C(11)-O(2)-Cu(1)	126.8(1)
N(1)-Cu(1)-O(2)	86.4(1)	O(2)-C(11)-O(2 A)	127.1(3)

Symmetry code: A = -x+2, y, z

Table 5 Selected bond lengths [Å] and angles [°] with e.s.d.s. in parentheses of $[Cu_2(dpyam)_2(\mu\text{-}O_2CH)(\mu\text{-}OH)(\mu\text{-}Cl)](PF_6)$ **(V)**

Cu(1)-N(1)	2.031(3)	Cu(1)-O(1)	2.183(2)
Cu(1)-N(2)	1.983(2)	Cu(1)-O(2)	1.918(2)
Cu(1)-Cl(1)	2.451(1)	Cu(1)-Cu(1A)	3.061(5)
O(1)-Cu(1)-N(1)	130.6(1)	N(1)-Cu(1)-Cl(1)	124.1(1)
O(1)-Cu(1)-N(2)	86.7(1)	N(2)-Cu(1)-O(2)	173.8(1)
O(1)-Cu(1)-O(2)	87.3(1)	N(2)-Cu(1)-Cl(1)	97.7(1)
O(1)-Cu(1)-Cl(1)	104.8(1)	Cu(1)-O(2)-Cu(1A)	105.9(1)
O(2)-Cu(1)-Cl(1)	82.3(1)	Cu(1)-Cl(1)-Cu(1A)	77.2(1)
N(1)-Cu(1)-N(2)	91.8(1)	C(11)-O(1)-Cu(1)	127.5(2)
N(1)-Cu(1)-O(2)	93.2(1)	O(1)-C(11)-O(1A)	126.5(4)

Symmetry code: A = -x+1, y, z

APPENDIX IIIC

The infrared spectra for

$[Cu_2(dpyam)_2(\mu\text{-}O_2CH)(\mu\text{-}OH)(\mu\text{-}OCH_3)](ClO_4)$ (I)

$[Cu_2(dpyam)_2(\mu\text{-}O_2CH)(\mu\text{-}OH)_2](ClO_4)\cdot H_2O$ (II)

$[Cu_2(dpyam)_2(\mu\text{-}O_2CH)(\mu\text{-}OOCH)(\mu\text{-}OH)](PF_6)$ (III)

$[Cu_2(dpyam)_2(\mu\text{-}O_2CH)(\mu\text{-}OH)(\mu\text{-}Cl)](ClO_4)\cdot 0.5H_2O$ (IV)

$[Cu_2(dpyam)_2(\mu\text{-}O_2CH)(\mu\text{-}OH)(\mu\text{-}Cl)](PF_6)$ (V) and

$[Cu_2(dpyam)_2(\mu\text{-}O_2CH)(\mu\text{-}OH)(\mu\text{-}Cl)](BF_4)$ (VI)

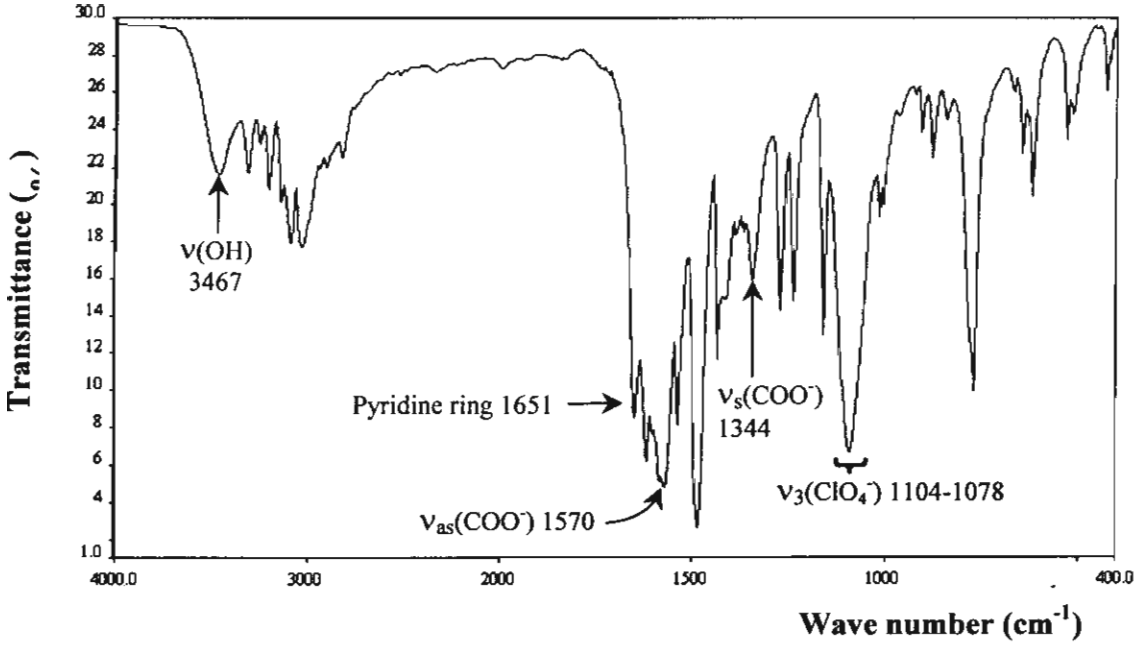

(a) IR spectrum of $[Cu_2(dpyam)_2(\mu\text{-}O_2CH)(\mu\text{-}OH)(\mu\text{-}OCH_3)](ClO_4)$ **(I)**

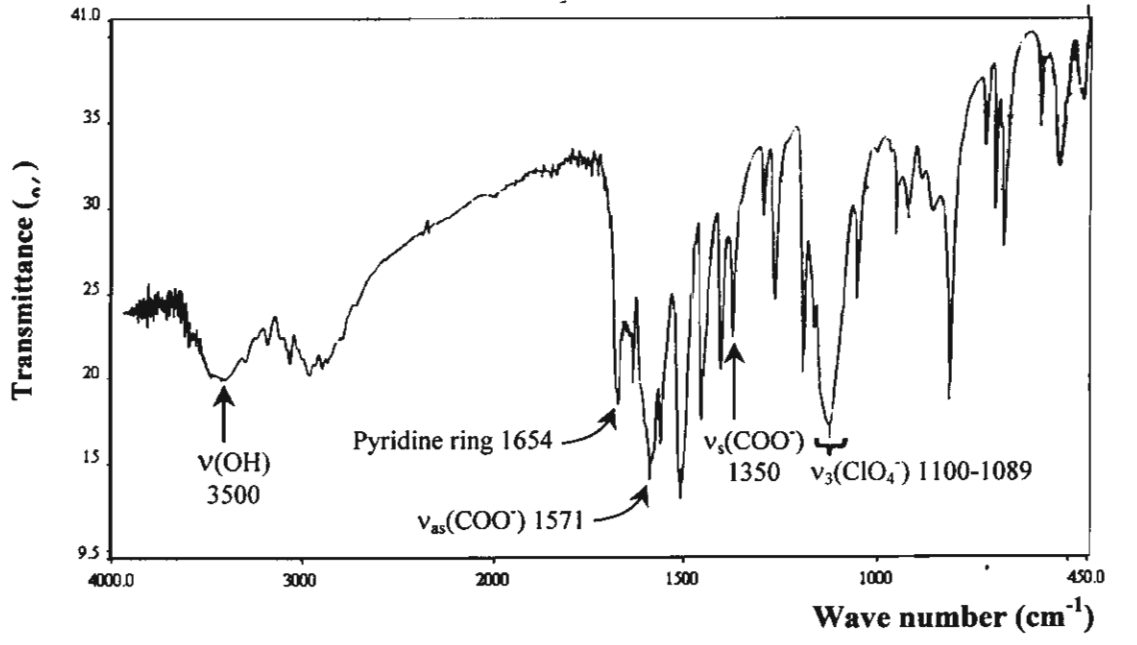

(b) IR spectrum of $[Cu_2(dpyam)_2(\mu\text{-}O_2CH)(\mu\text{-}OH)_2](ClO_4)\cdot H_2O$ **(II)**

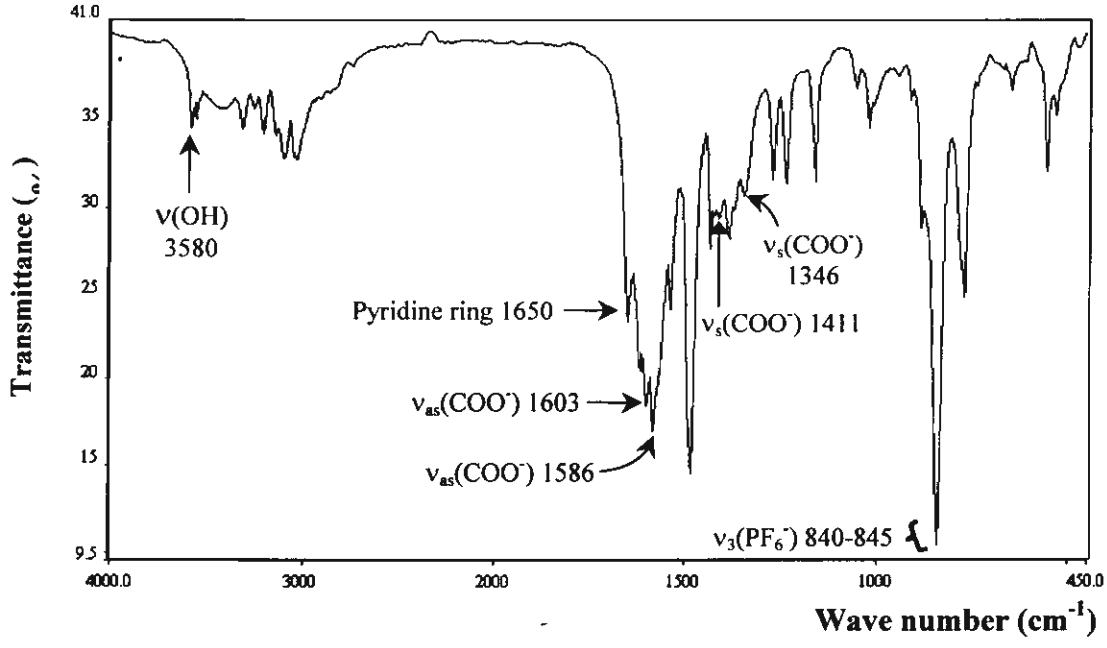

(c) IR spectrum of $[Cu_2(dpyam)_2(\mu\text{-}O_2CH)(\mu\text{-}OOCH)(\mu\text{-}OH)](PF_6)$ **(III)**

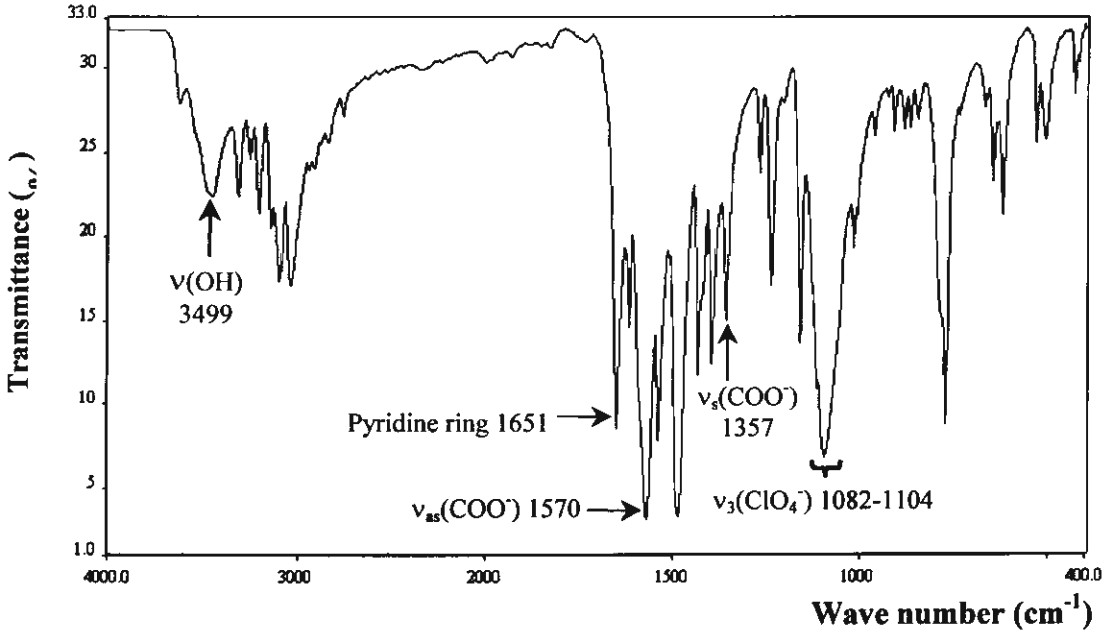

(d) IR spectrum of $[Cu_2(dpyam)_2(\mu\text{-}O_2CH)(\mu\text{-}OH)(\mu\text{-}Cl)](ClO_4)\cdot 0.5H_2O$ **(IV)**

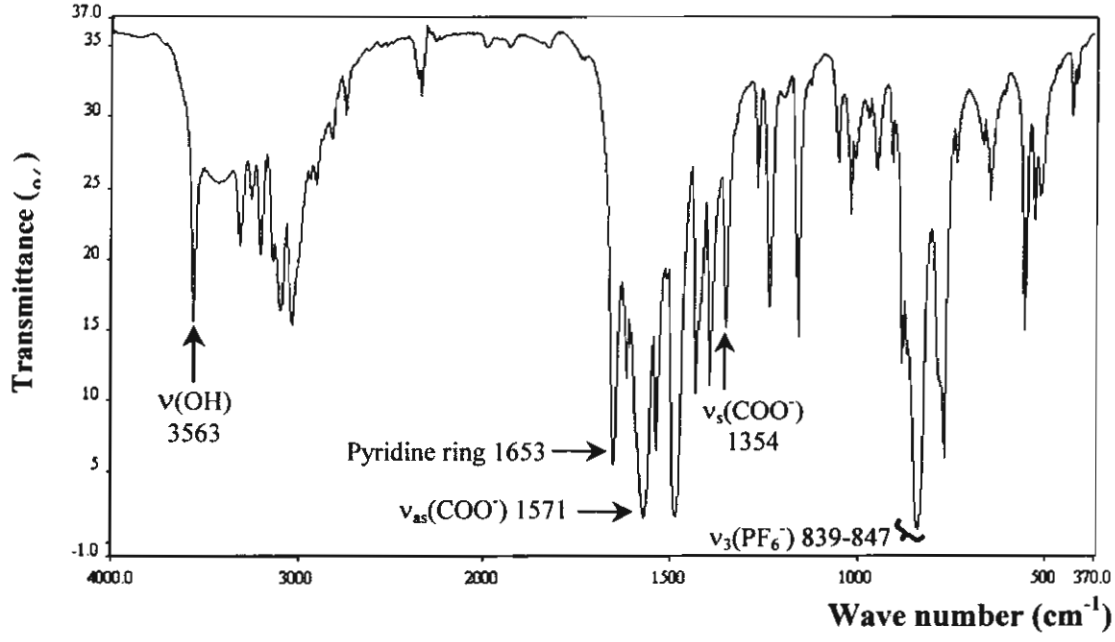

(e) IR spectrum of $[Cu_2(dpyam)_2(\mu\text{-}O_2CH)(\mu\text{-}OH)(\mu\text{-}Cl)](PF_6)$ **(V)**

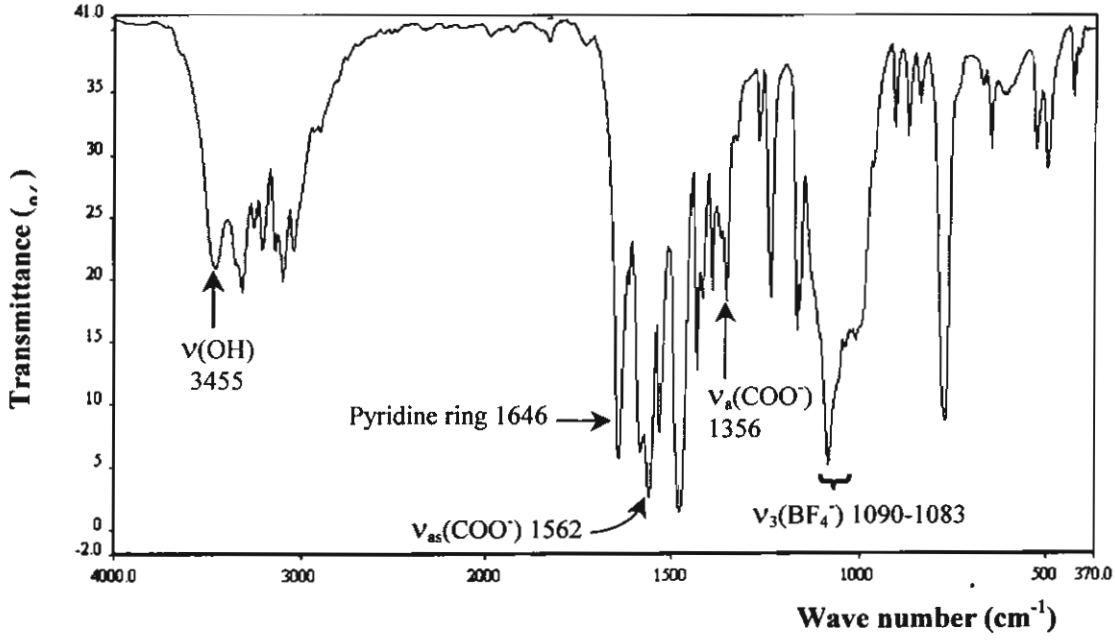

(f) IR spectrum of $[Cu_2(dpyam)_2(\mu\text{-}O_2CH)(\mu\text{-}OH)(\mu\text{-}Cl)](BF_4)$ **(VI)**

APPENDIX IIID

The EPR spectra for

$[Cu_2(dpyam)_2(\mu\text{-}O_2CH)(\mu\text{-}OH)(\mu\text{-}OCH_3)](ClO_4)$ (I)

$[Cu_2(dpyam)_2(\mu\text{-}O_2CH)(\mu\text{-}OH)_2](ClO_4)\cdot H_2O$ (II)

$[Cu_2(dpyam)_2(\mu\text{-}O_2CH)(\mu\text{-}OOCH)(\mu\text{-}OH)](PF_6)$ (III)

$[Cu_2(dpyam)_2(\mu\text{-}O_2CH)(\mu\text{-}OH)(\mu\text{-}Cl)](ClO_4)\cdot 0.5H_2O$ (IV)

$[Cu_2(dpyam)_2(\mu\text{-}O_2CH)(\mu\text{-}OH)(\mu\text{-}Cl)](PF_6)$ (V)

and $[Cu_2(dpyam)_2(\mu\text{-}O_2CH)(\mu\text{-}OH)(\mu\text{-}Cl)](BF_4)$ (VI)

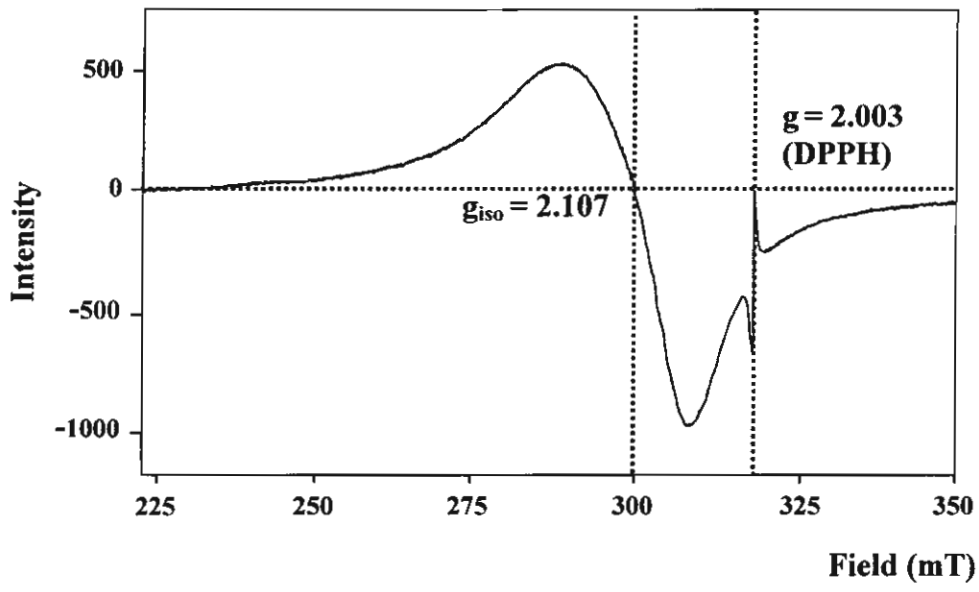

(a) The EPR spectrum at room temperature of $[Cu_2(dpyam)_2(\mu\text{-}O_2CH)(\mu\text{-}OH)(\mu\text{-}OCH_3)](ClO_4)$ **(I)**

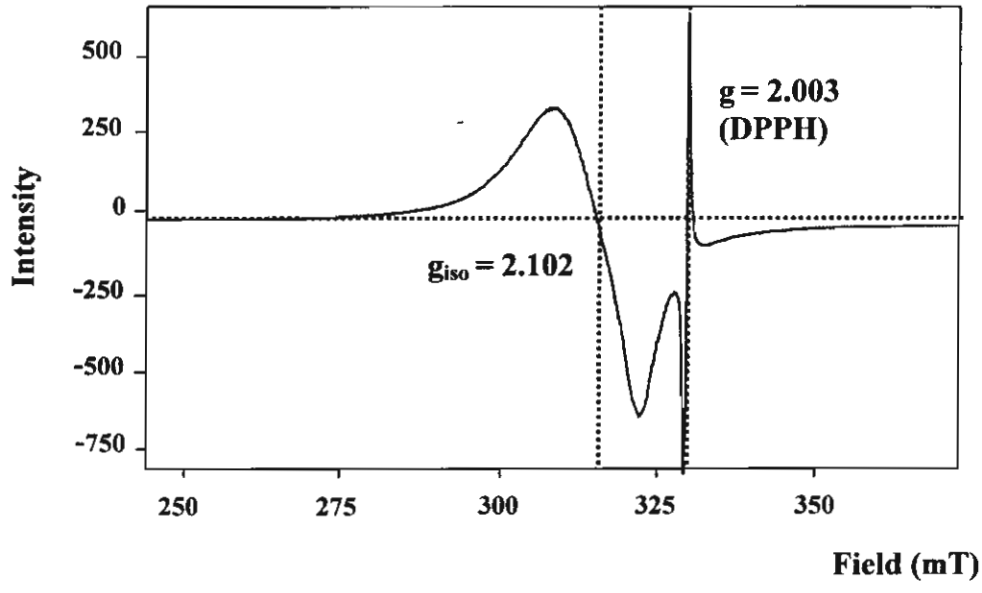

(b) The EPR spectrum at 77 K of $[Cu_2(dpyam)_2(\mu\text{-}O_2CH)(\mu\text{-}OH)(\mu\text{-}OCH_3)](ClO_4)$ **(I)**

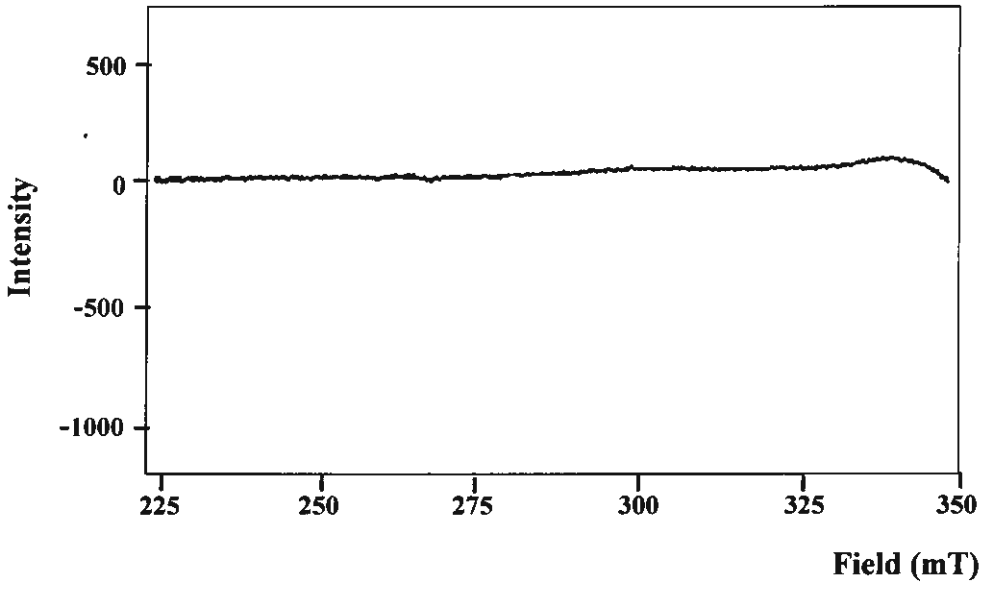

(c) The EPR spectrum at room temperature of $[Cu_2(dpyam)_2(\mu\text{-}O_2CH)(\mu\text{-}OH)_2](ClO_4)\cdot H_2O$ **(II)**

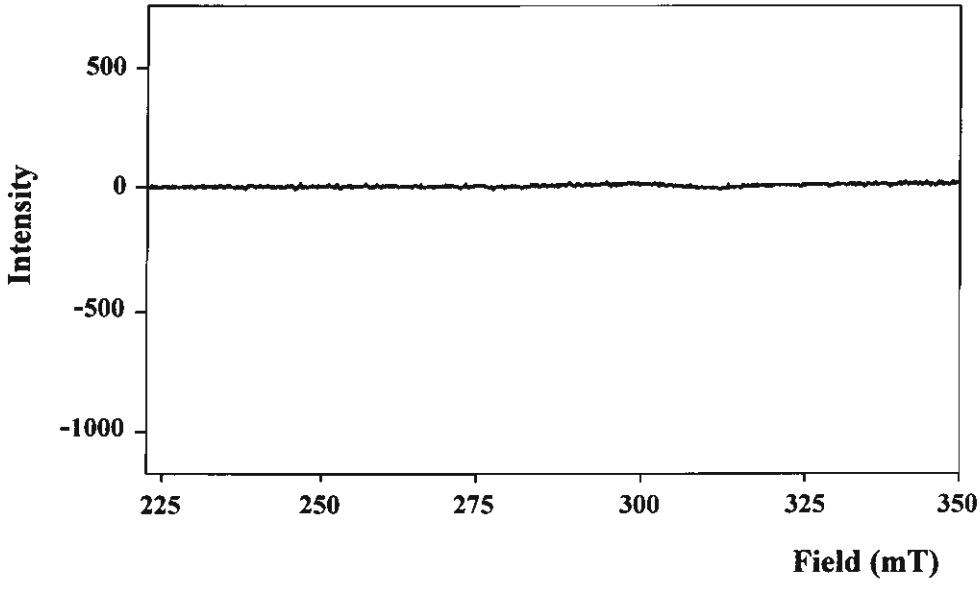

(d) The EPR spectrum at 77 K of $[Cu_2(dpyam)_2(\mu\text{-}O_2CH)(\mu\text{-}OH)_2](ClO_4)\cdot H_2O$ **(II)**

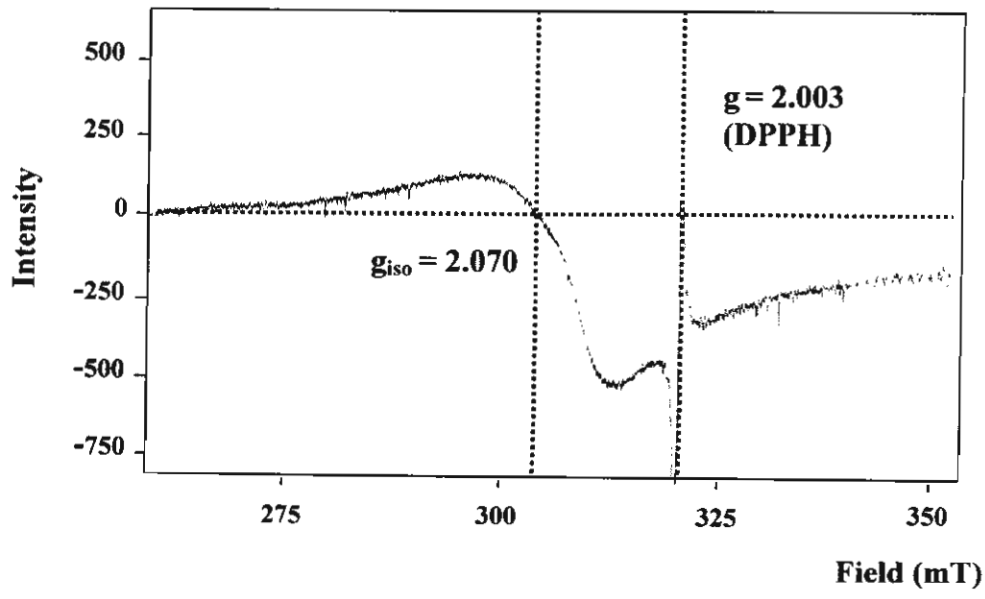

(e) The EPR spectrum at room temperature of $[Cu_2(dpyam)_2(\mu\text{-}O_2CH)(\mu\text{-}OOCH)(\mu\text{-}OH)](PF_6)$ **(III)**

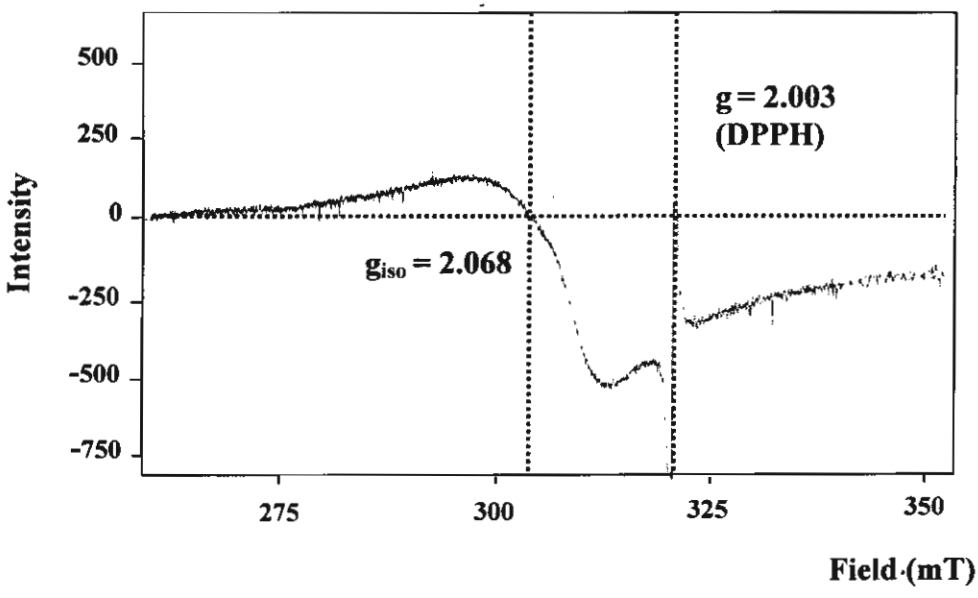

(f) The EPR spectrum at 77 K of $[Cu_2(dpyam)_2(\mu\text{-}O_2CH)(\mu\text{-}OOCH)(\mu\text{-}OH)](PF_6)$ **(III)**

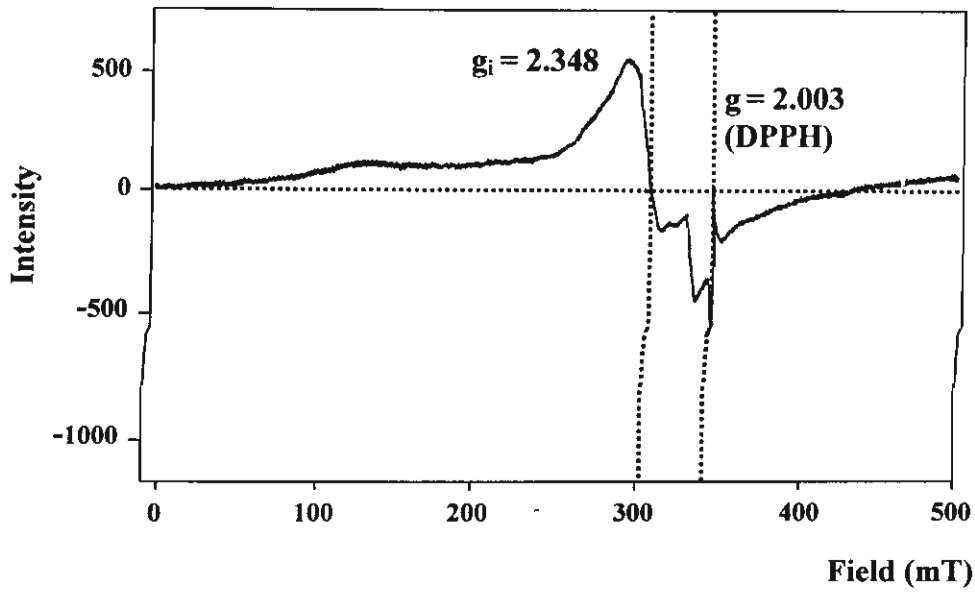

(g) The EPR spectrum at room temperature of $[Cu_2(dpyam)_2(\mu\text{-}O_2CH)(\mu\text{-}OH)(\mu\text{-}Cl)](ClO_4)\cdot 0.5H_2O$ **(IV)**

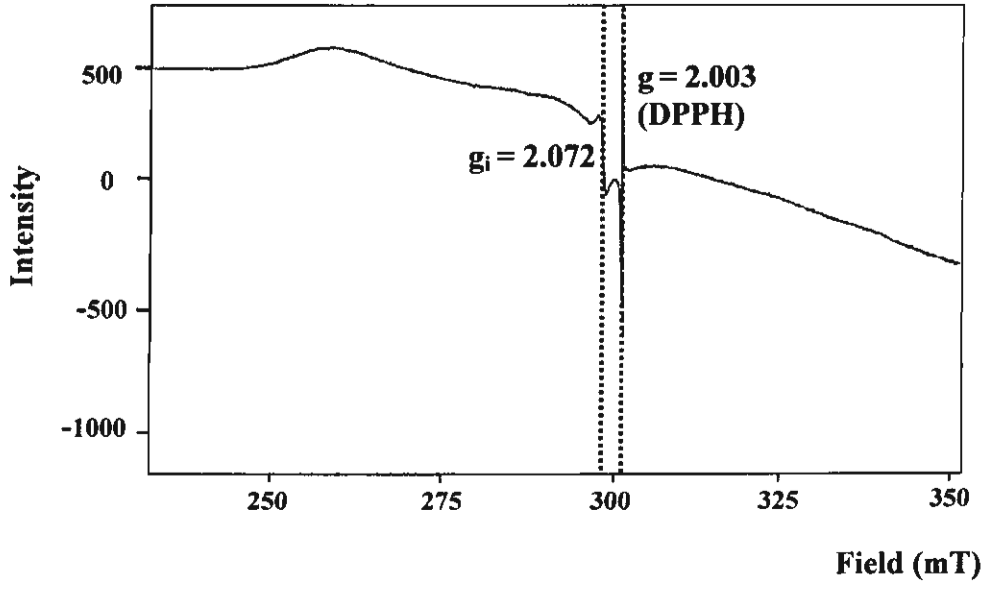

(h) The EPR spectrum at 77 K of $[Cu_2(dpyam)_2(\mu\text{-}O_2CH)(\mu\text{-}OH)(\mu\text{-}Cl)](ClO_4)\cdot 0.5H_2O$ **(IV)**

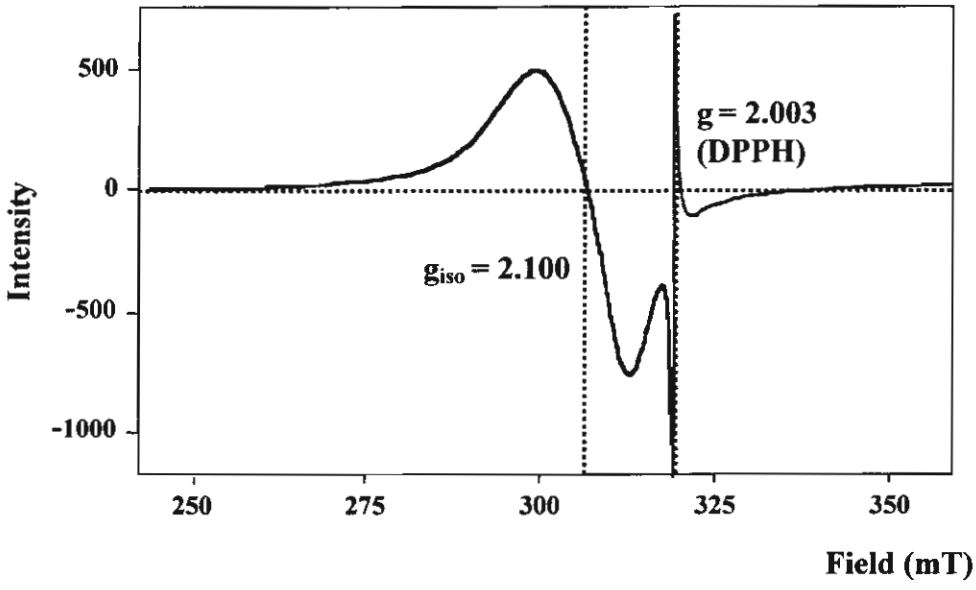

(i) The EPR spectrum at room temperature of $[Cu_2(dpyam)_2(\mu\text{-}O_2CH)(\mu\text{-}OH)(\mu\text{-}Cl)](PF_6)$ (V)

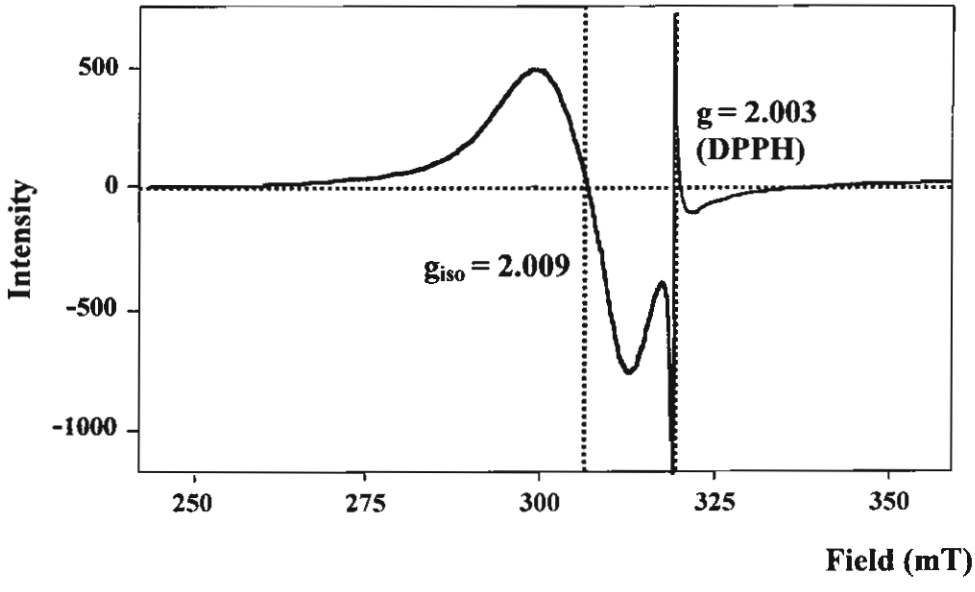

(j) The EPR spectrum at 77 K of $[Cu_2(dpyam)_2(\mu\text{-}O_2CH)(\mu\text{-}OH)(\mu\text{-}Cl)](PF_6)$ (V)

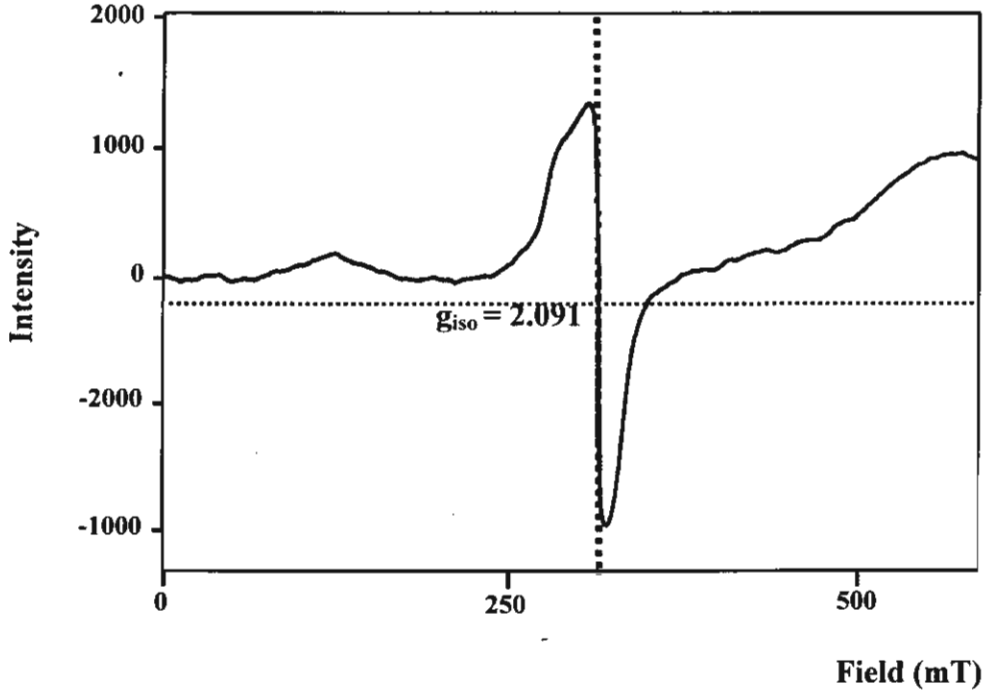

(k) The EPR spectrum at room temperature of $[Cu_2(dpyam)_2(\mu\text{-}O_2CH)(\mu\text{-}OH)(\mu\text{-}Cl)](BF_4)$ **(VI)**

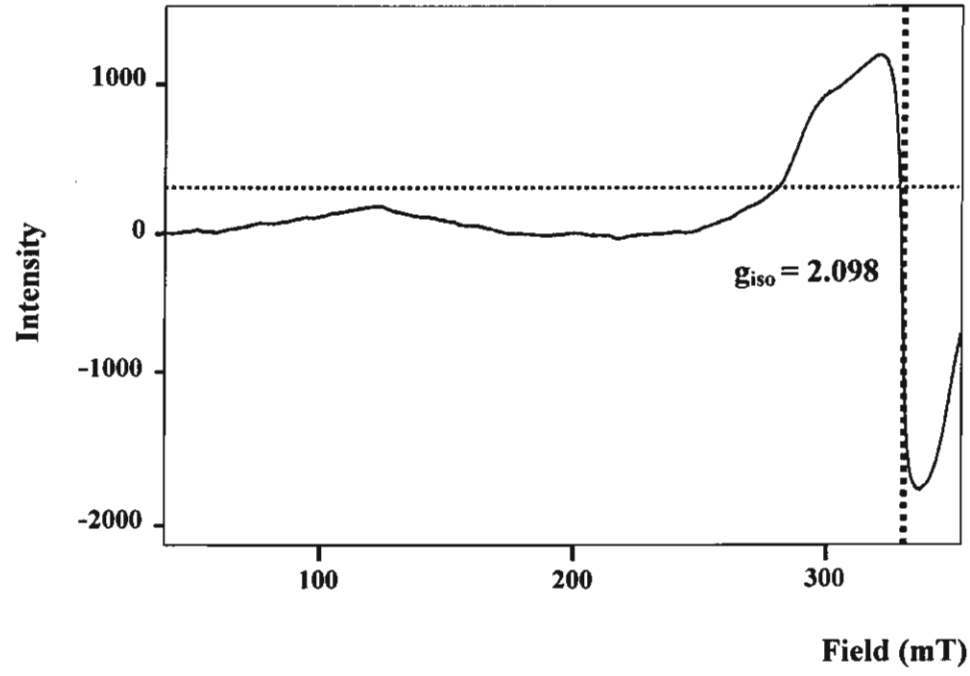

(l) The EPR spectrum at 77 K of $[Cu_2(dpyam)_2(\mu\text{-}O_2CH)(\mu\text{-}OH)(\mu\text{-}Cl)](BF_4)$ **(VI)**

APPENDIX IV

PUBLICATION PAPERS

PUBLICATION PAPERS OF PART I

Available online at www.sciencedirect.com
SCIENCE DIRECT®
Inorganica Chimica Acta 353 (2003) 119–128
Inorganica Chimica Acta
www.elsevier.com/locate/ica

Synthesis, spectroscopic characterization, X-ray crystal structure and magnetic properties of oxalato-bridged copper(II) dinuclear complexes with di-2-pyridylamine

Sujittra Youngme [a,*], Gerard A. van Albada [d], Narongsak Chaichit [b], Pimprapun Gunnasoot [a], Palangpon Kongsaeree [c], Ilpo Mutikainen [e], Olivier Roubeau [d], Jan Reedijk [d], Urho Turpeinen [e]

[a] Department of Chemistry, Faculty of Science, Khon Kaen University, Khon Kaen 40002, Thailand
[b] Department of Physics, Faculty of Science and Technology, Thammasat University Rangsit, Pathumthani 12121, Thailand
[c] Department of Chemistry, Faculty of Science, Mahidol University, Bangkok 10400, Thailand
[d] Gorlaeus Laboratories, Leiden Institute of Chemistry, Leiden University, P.O. Box 9502, 2300 RA Leiden, The Netherlands
[e] Department of Chemistry, Laboratory of Inorganic Chemistry, P.O. Box 55 (A.I.Virtasen aukio 1), 00014 University of Helsinki, Helsinki, Finland

Received 28 October 2002; accepted 4 February 2003

Abstract

The syntheses and characterization of a series of dinuclear μ-oxalato copper(II) complexes of the general type $[(NN)_{1\text{ or }2}Cu(C_2O_4)Cu(NN)_{1\text{ or }2}]^{2+}$, where NN = didentate dpyam (di-2-pyridylamine) ligand, are described. The crystal structures of three representative complexes have been determined. The dinuclear-oxalate bridged compounds $[Cu(dpyam)_4(C_2O_4)](ClO_4)_2(H_2O)_3$ **(1)** and $[Cu_2(dpyam)_4(C_2O_4)](BF_4)_2(H_2O)_3$ **(2)** crystallize in the non-centrosymmetric triclinic space group $P\bar{1}$ which are isomorphous and isostructural. The compound $[Cu_2(dpyam)_2(C_2O_4)(NO_3)_2((CH_3)_2SO)_2]$ **(3)** crystallizes in the centrosymmetric monoclinic space group $P\bar{1}$ with all Cu-oxalate contacts in the equatorial plane. All three complexes contain six-coordinate copper centres bridged by planar bis-didentate oxalate groups from the equatorial position of one chromophore to the equatorial position of the other one. Both chromophores in **1** and **2** exhibit the compressed octahedral Cu(II) geometry, while **3** displays an elongated octahedral Cu(II) environment. The IR, ligand field and EPR measurements are in agreement with the structures found. The magnetic susceptibility measurements, measured from 5 to 280 K, revealed a very weak ferromagnetic interaction between the Cu(II) atoms for compound **1** and **2**, with a singlet–triplet energy gap (J) of 2.42 and 3.38 cm^{-1}, for compounds **1** and **2**, respectively. Compound **3** has a strong antiferromagnetic interaction with a J of -305.1 cm^{-1}, in agreement with coplanarity of the magnetic orbitals.

Keywords: Copper(II) complexes; Crystal structures; μ-Oxalato dimers; Magnetic properties; EPR

1. Introduction

In the past decades, there has been a great deal of interest in the magneto-structural studies of transition metal atoms [1–40] with polyatomic bridging ligands both in the experimental and theoretical points of view. The oxalate ion is well known to be an appropriate bridging ligand to design magnetic materials and many oxalato-bridged complexes have been prepared and characterized [2–36]. Eight different bridging modes (Scheme 1) have been observed for the oxalato group in the oxalato copper(II) complexes [1–4].

A number of dinuclear copper complexes with an oxalato bridge, generally formulated as $[(NN)Cu(\mu\text{-}C_2O_4)Cu(NN)]X_n$, where NN is a chelating ligand, and X is a counter anion or a solvent molecule, have been structurally characterized [5–14,36]. Analysis of the structural factors that influence the magnitude of the magnetic interactions allowed to tune the value of the singlet–triplet energy gap (J values) in oxalato-bridged dinuclear Cu(II) complexes from approximately 0 to approximate -400 cm^{-1} by playing on the nature of

* Corresponding author. Fax: +66-43-243-338.
E-mail address: sujittra@kku.ac.th (S. Youngme).

0020-1693/03/$ - see front matter © 2003 Elsevier B.V. All rights reserved.
doi:10.1016/S0020-1693(03)00207-X

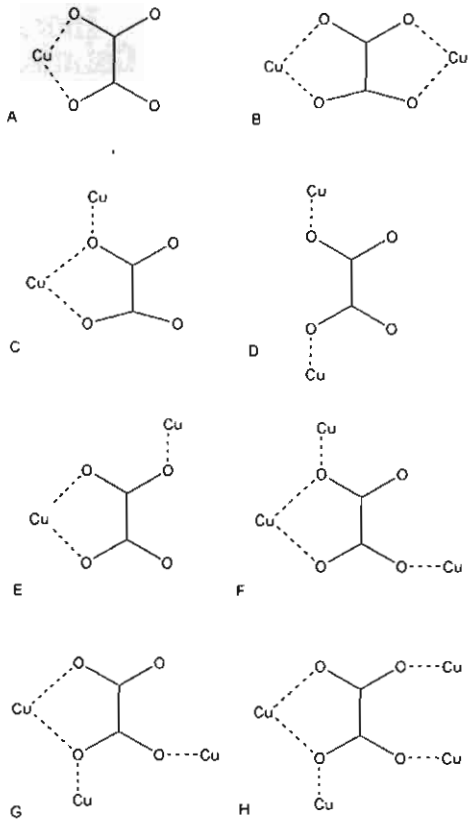

Scheme 1. Different coordination modes of oxalate ligands known for oxalato copper (II) complexes.

the terminal ligand (tridentate and/or didentate nitrogen donors) or of the counter ions, taking advantage of the plasticity effect of the Cu(II) coordination sphere [5,19,21]. Previous theoretical and experimental works [5,6,16–21] have revealed that the exchange interaction between the copper ions propagated through the oxalate bridge is strongly dependent on the geometry around the copper ions, sensitive to the orientation of the magnetic orbital of each Cu(II) relative to the oxalate plane and the bridging mode of the oxalate group. The actual role of this ligand modification is to realign the metal magnetic orbital relative to the oxalate σ orbital as the magnetic exchange pathway is dominated by interactions between the metal $d_{x^2-y^2}$ orbitals and the oxalate σ orbitals.

In most cases, the copper ions present a square-pyramidal structure with two oxygen atoms of oxalate bridge and two nitrogen atoms of the diamine occupying the base of the pyramid and the counter anion or a solvent molecule occupying the axial position. Some compounds present an additional bond to X, giving rise to elongated octahedral coordination. In the literature compounds have been reported which have a square-pyramidal and elongated octahedral geometries in which one of the oxalate oxygen atoms is in the basal plane and the other oxygen is apical [4,5,10,12–14,19] and others having a trigonal-bipyramidal geometry around the copper atoms [15].

It is extremely difficult to control the value of structural parameters during the synthetic process and great difficulties are faced to establish the magneto-structural correlation. In order to extend the investigation by modifying the terminal ligand to the more flexible, nitrogen donor didentate dpyam ligand, we now describe the synthesis, the crystal structure, and the magnetic properties of three new μ-oxalato Cu(II) complexes, $[Cu_2(dpyam)_4(C_2O_4)](ClO_4)_2(H_2O)_3$ (1), $[Cu_2(dpyam)_4(C_2O_4)](BF_4)_2(H_2O)_3$ (2) and $[Cu_2(dpyam)_2(C_2O_4)(NO_3)_2((CH_3)_2SO)_2]$ (3). The ligand dipyam has been selected primarily because of the fact that it also has a N–H H-bond donor function that might interfere with the oxalate bridging ligand.

2. Experimental

2.1. Reagents and physical measurements

All reagents are commercial grade materials and were used without further purification. Elemental analyses(C, H, N) were performed by the Microanalytical Service of Science and Technological Research Equipment Centre, Chulalongkorn University on Perkin–Elmer PE2400 CHNS/O Analyzer. Copper content was determined on atomic absorption spectrophotometer.

IR spectra were recorded with a Biorad FTS-7/PC FTIR spectrophotometer as KBr pellets/and or as Nujol mulls in the 4000–450 cm^{-1} spectral range. Solid-state (diffuse reflectance) electronic spectra were recorded as polycrystalline samples on a Perkin–Elmer Lambda2S spectrophotometer over the range 8000–18 000 cm^{-1}. X-band powder EPR spectra were obtained on a JEOL RE2x electron spin resonance spectrometer using DPPH ($g = 2.0036$) as a standard. Magnetic susceptibility measurements (5–280 K) were carried out using a Quantum Design MPMS-5 5T SQUID magnetometer (measurements carried out at 1000 Gauss). Data were corrected for magnetization of the sample holder and for diamagnetic contributions, which were estimated from the Pascal constants.

2.2. Syntheses

Caution! Although the perchlorate salt described in this work do not appear to be sensitive to shock. This material, like all perchlorate salts can be potentially explosive with organic solvents. Only a small amount of material should be prepared, and it should be handled with caution.

2.2.1. $[Cu_2(dpyam)_4(\mu\text{-}C_2O_4)](ClO_4)_2(H_2O)_3$ (1)

Compound **1** was prepared by adding a hot methanol solution (40 ml) of dpyam (0.342 g, 2.0 mmol) to a hot aqueous solution (60 ml) of $Cu(ClO_4)_2$ (0.371 g, 1.0 mmol). The mixture was heated at approximately 70 °C with continuous stirring for 10 min, then solid $Na_2C_2O_4$ (0.134 g, 1.0 mmol) was added. The resulting hot solution was filtered off to remove any impurities. After standing at room temperature (r.t.) for a week, green needle-like crystals of **1** were obtained. Yield approximately 75%. *Anal.* Calc. for $C_{42}H_{42}Cl_2Cu_2N_{12}O_{15}$: C, 43.76; H, 3.67; Cu, 11.03; N, 14.58. Found: C, 43.69; H, 3.60; Cu, 11.10; N, 14.61%.

2.2.2. $[Cu_2(dpyam)_4(\mu\text{-}C_2O_4)](BF_4)_2(H_2O)_3$ (2)

A solution containing dpyam (0.342 g, 2.0 mmol) in ethanol (20 ml) and $Na_2C_2O_4$ (0.068 g, 0.5 mmol) in water (10 ml) was added to a solution of $Cu(BF_4)_2$ (0.237 g, 1 mmol) in water (10 ml). The resulting green solution was allowed to evaporate at r.t. After 2 weeks, green crystals of $[Cu_2(dpyam)_4(\mu\text{-}C_2O_4)](BF_4)_2(H_2O)_3$ (**2**) were obtained which were filtered off, washed with water and were dried in air. Yield approximately 60%. *Anal.* Calc. for $C_{42}H_{42}B_2Cu_2F_8N_{12}O_7$: C, 44.74; H, 3.76; Cu, 11.27; N, 14.90. Found: C, 44.82; H, 3.68; Cu, 11.33; N, 14.85%.

2.2.3. $[Cu_2(dpyam)_2(\mu\text{-}C_2O_4)(NO_3)_2((CH_3)_2SO)_2]$ (3)

Compound **3** was prepared by adding a hot dimethylsulfoxide (10 ml) of dpyam (0.342 g, 2.0 mmol) to hot aqueous solution containing $Cu(NO_3)_2(H_2O)_{2.5}$ (0.465 g, 2.0 mmol) and $H_2C_2O_4$ (0.126 g, 1 mmol) in dimethylsulfoxide (23 ml). The green solution was allowed to evaporate at r.t. After a week, green crystals of $[Cu_2(dpyam)_2(\mu\text{-}C_2O_4)(NO_3)_2(dmso)_2]$ (**3**) formed which were filtered off, washed with mother liquor and air-dried. Yield approximately 95%. *Anal.* Calc. for $C_{26}H_{30}Cu_2N_8O_{12}S_2$: C, 37.27; H, 3.61; Cu, 15.17; N, 13.37. Found: C, 37.34; H, 3.55; Cu, 15.12; N, 13.44%.

2.3. Crystallography

Reflection data for **1** were collected using an Enraf–Nonius MACH3 diffractometer with Mo Kα radiation($\lambda = 0.70183$ Å) at 298 K. An absorption correction was performed by using the Psi-scan program, which resulted in transmission coefficients ranging from 0.917 to 1.000. The structure was solved by direct methods using SHELXS-97 [40] and refined by the least-squares method F^2_{obs} using SHELXL-97 [41]. The non-hydrogen atoms were located on the E map or successive Fourier difference syntheses and anisotropically refined. All other hydrogen atoms were geometrically fixed and allowed to ride on the attached atoms except the water hydrogen atoms, which could not be located at all. One of the perchlorate groups showed disorder which was resolved in two sets with occupancies of 0.5 for both conformers.

Reflection data for **2** were collected at 298 K on a 1K Bruker SMART CCD area-detector diffractometer using graphite monochromated Mo Kα radiation ($\lambda =$ 0.71073 Å) at a detector distance of 4.5 cm and swing angle of −35°. A hemisphere of the reciprocal space was covered by combination of three sets of exposures; each set had a different ϕ angle (0, 88, 180°) and each exposure of 10 s covered 0.3° in ω. Data reduction and cell refinements were performed using the program SAINT [42]. An empirical absorption correction by using the SADABS [43] program was applied, which resulted in transmission coefficients ranging from 0.659 to 1.000. The structure was solved by direct methods and refined by full-matrix least-squares method on F^2_{obs} with anisotropic thermal parameters for all non-hydrogen atoms using the SHELXTL-PC V 5.03 software package [44]. All hydrogen atoms were geometrically fixed and allowed to ride on the attached atoms. Two BF_4^- groups and three water molecules are disordered with site occupancies of 0.5 for both conformers. The hydrogen atoms of the lattice water molecules could not be located at all.

A crystal of compound **3** was selected and mounted to a glass fiber using the oil-drop method. Data were collected on a Rigaku AFC-7S diffractometer (graphite-monochromated Mo Ka radiation, ω–2θ scans). The intensity data were corrected for Lp, for absorption (psi-scan absorption correction) and extinction. The structures were solved by direct methods. The programs TEXSAN [45], SHELXS-97 [50], SHELXL-97 [41] were used for data reduction, structure solution and structure refinement, respectively. Refinement of F^2 was done against all reflections. The weighted R factor, wR, and goodness of fit S are based on F^2. Conventional R factors, R, are based on F, with F set to zero for negative F^2. All non-H atoms were refined anisotropically. The H atoms were introduced in calculated positions and refined with fixed geometry with respect to their carrier atoms.

The molecular graphics were created by using SHELXTL-PC [44]. The crystal and refinement details for compounds **1**–**3** are listed in Table 1.

3. Results and discussion

3.1. Description of $[Cu_2(dpyam)_4(C_2O_4)]X_2(H_2O)_3$ ($X=(ClO_4)$ (1) and (BF_4) (2))

The structures of **1** and **2** are made up of oxalate bridged non-centrosymmetric dinuclear cations $[(dpyam)_2Cu(C_2O_4)Cu(dpyam)_2]^{2+}$, non-coordinating ClO_4^- and BF_4^- anions and water molecules of crystallization. The structures are depicted in Figs. 1

Table 1
Crystal and refinement data for complexes **1**, **2** and **3**

Complex	**1**	**2**	**3**
Molecular formular	$[Cu_2(dpyam)_4(C_2O_4)](ClO_4)_2(H_2O)_3$	$[Cu_2(dpyam)_4(C_2O_4)](BF_4)_2(H_2O)_3$	$[Cu_2(dpyam)_2(C_2O_4)NO_3)_2((CH_3)_2SO)_2$
Molecular weight	1152.8	1126.5	837.76
T (K)	293(2)	293(2)	297.76
Crystal system	triclinic	triclinic	triclinic
Space group	P_1	P_1	$P\bar{1}$
a (Å)	9.599(2)	9.629(2)	8.719(0)
b (Å)	11.206(2)	11.170(2)	8.980(9)
c (Å)	12.480(3)	12.381(2)	11.421(0)
α (°)	73.22(3)	73.81(2)	68.58(0)
β (°)	77.84(3)	78.15(2)	77.79(0)
γ (°)	76.88(3)	76.59(2)	80.58(0)
V (Å^3)	1236.5(4)	1229.7(2)	808.87(1)
Z	1	1	1
D_{calc} (g cm^{-3})	1.542	1.516	1.720
μ (mm)	1.046	0.956	3.495
F (000)	588	569	428
Crystal size (mm)	0.30 × 0.42 × 0.45	0.33 × 0.45 × 0.75	0.35 × 0.35 × 0.22
Reflection collected	4834	9078	3171
Unique reflections	4834 ($R_{int} = 0.0000$)	7711 ($R_{int} = 0.0179$)	2964 ($R_{int} = 0.0281$)
Observed ref. [$I > 2\sigma(I)$]	4349	6519	2828
Data/restraints/parameter	4834/3/694	7711/3/679	2964/0/228
Goodness-of-fit	1.076	1.020	1.247
Final R indices [$I > 2\sigma(I)$]	$R_1 = 0.0383$, $wR_2 = 0.1079$	$R_1 = 0.0464$, $wR_2 = 0.1401$	$R_1 = 0.0512$, $wR_2 = 0.1363$
R indices (all data)	$R_1 = 0.0442$, $wR_2 = 0.1170$	$R_1 = 0.0547$, $wR_2 = 0.1497$	$R_1 = 0.060747$, $wR_2 = 0.1615$
Largest difference peak and hole (e Å^{-3})	0.854, −0.472	0.946, −0.455	0.968, −0.554

and **2** together with the numbering scheme. Selected bond distances and angles are listed in Table 2.

Compounds **1** and **2** are found to be isomorphous and isostructural, the copper coordination spheres in both complexes display a identical environment. Each copper atom in **1** and **2** has a compressed rhombic octahedral coordination geometry with the equatorial plane formed by two nitrogen atoms from a dpyam ligand and two oxalate–oxygen atoms (Cu–N distances vary from 2.095(8) to 2.141(9) Å and from 2.094(6) to 2.145(7) Å, for **1** and **2** respectively, while Cu–O distances vary

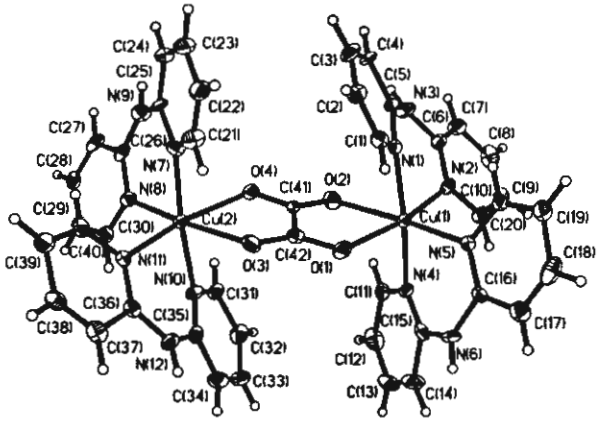

Fig. 1. ORTEP 50% probability plot of the cation in $[Cu(dpyam)_4(C_2O_4)](ClO_4)_2(H_2O)_3$ (**1**)

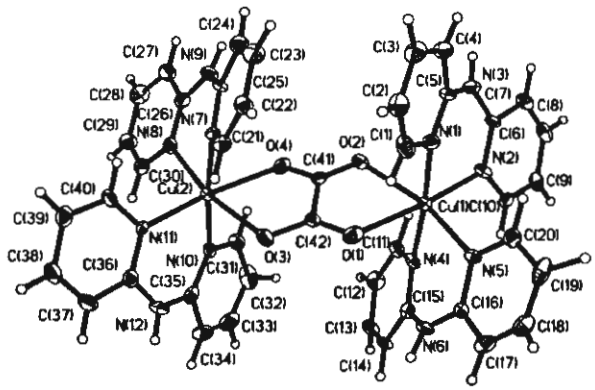

Fig. 2. ORTEP 50% probability plot of the cation in $[Cu_2(dpyam)_4(C_2O_4)](BF_4)_2(H_2O)_3$ (**2**)

from 2.141(10) to 2.305(9) and from 2.189(8) to 2.252(8), for **1** and **2**, respectively). The axial positions are occupied by the other nitrogen atoms of the dpyam ligand (Cu–N distances vary from 2.000(8) to 2.025(8) and from 2.006(7) to 2.024(6) Å, for **1** and **2**, respectively), resulting in the rather unique $CuN_2O_2N_2'$ (4+2) chromophore. This axially-compressed octahedral (2+4) geometry is uncommon as most of other dinuclear μ-oxalatodicopper(II) complexes found in literature have five-coordinate geometries. This geometry has only been previously observed in the dinuclear oxalato-bridged Cu^{II} complexes with a tetradentate terminal ligand [11].

Table 2
Selected bond lengths (Å) and angles (°) with e.s.d.s. in parentheses of $[Cu_2(dpyam)_4(C_2O_4)](ClO_4)_2(H_2O)_3$ (1) and $[Cu_2(dpyam)_4(C_2O_4)](BF_4)_2(H_2O)_3$ (2)

	(1)	(2)
Bond lengths		
Cu(1)–N(1)	2.020(9)	2.008(8)
Cu(1)–N(2)	2.136(8)	2.111(7)
Cu(1)–N(4)	2.000(8)	2.024(6)
Cu(1)–N(5)	2.095(8)	2.134(8)
Cu(1)–O(1)	2.141(10)	2.229(8)
Cu(1)–O(2)	2.305(9)	2.252(8)
Cu(2)–N(7)	2.010(9)	2.021(8)
Cu(2)–N(8)	2.141(9)	2.145(7)
Cu(2)–N(10)	2.025(8)	2.006(7)
Cu(2)–N(11)	2.107(8)	2.094(6)
Cu(2)–O(3)	2.225(9)	2.208(9)
Cu(2)–O(4)	2.229(8)	2.189(8)
Cu(1)–Cu(2)	5.752(3)	5.745(3)
Bond angles		
N(1)–Cu(1)–N(4)	175.4(3)	173.4(3)
N(2)–Cu(1)–O(1)	165.8(3)	170.7(3)
N(5)–Cu(1)–O(2)	171.4(3)	166.0(2)
N(2)–Cu(1)–N(5)	97.5(3)	97.1(3)
O(1)–Cu(1)–O(2)	74.7(3)	74.8(2)
N(7)–Cu(2)–N(10)	173.2(4)	175.5(3)
N(8)–Cu(2)–O(3)	168.9(3)	166.1(2)
N(11)–Cu(2)–O(4)	166.8(3)	170.1(3)
N(8)–Cu(2)–N(11)	97.3(3)	97.6(3)
O(3)–Cu(2)–O(4)	73.7(3)	73.9(3)

This geometry arise due to the flexible nature of the dpyam ligand compared to the bpy, phen or other didentate chelate ligands which are found to have a square-pyramidal structure with the counter anion or solvent molecule occupying the axial position and the general formula of $[(NN)Cu(\mu\text{-}C_2O_4)Cu(NN)]X_n$, (in which X = counter anion or solvent molecule) [5–14]. Some compounds of this formula present an additional bond to X, giving rise to an axially-elongated octahedral geometry [5–10]. In addition, the compounds **1** and **2** are two rare examples of 2+4 compressed rhombic coordination resulting from a pseudo Jahn–Teller effect. As in almost all the cases of observed Jahn–Teller compression examined in detail to date, the apparent compression is due to dynamic interconversion between two of the possible axial elongations [51,52].

For compound **1**, the lattice is similarity further stabilized by hydrogen bonding between the amine-N and O_{ClO4} (N···O distances 3.059–3.334 Å) and O_{water} (N···O distances 2.828–2.843 Å) and between the O_{water} and O_{ClO4} (O···O distance 3.094 Å) and $O_{oxalate}$ (O···O distance 3.002 Å).

For compound **2**, the lattice is stabilized by hydrogen bonding between the amine-N and F_{BF4} (N···F distances 2.974–3.189 Å) and O_{water} (N···O distances 2.750–2.923 Å)

3.2. Description of $[Cu_2(dpyam)_2(C_2O_4)(NO_3)_2((CH_3)_2SO)_2]$ (3)

The structure of **3** consists of centrosymmetric $[Cu_2(dpyam)_2(\mu\text{-}C_2O_4)(NO_3)_2((CH_3)_2SO)_2]$ molecules. This unit is depicted in Fig. 3 together with the numbering scheme. Selected bond distances and angles are listed in Table 3.

The geometry around the copper atom can be considered as an elongated tetragonal octahedral environment with the equatorial plane formed by two nitrogen atoms of dpyam ligand and two oxygen atoms of the oxalate bridge (Cu–N/O distances vary from 1.986(2) to 2.002(2) Å), with the axial sites occupied by an oxygen atom of the nitrato group (Cu–O 2.502(2) Å) and the oxygen atom of the dimethylsulfoxide group (Cu–O 2.331(2) Å]. The copper–copper distance is 5.220(2) Å. The axial O_2NO–Cu–$OS(CH_3)_2$ angle is 174.8(7)° and the four donor atoms on the equatorial plane are not perfectly planar, showing a small tetrahedral distortion, with a dihedral angle of 7.2° formed between the O–Cu–O and N–Cu–N planes. The copper atoms are displaced by 0.0770 Å from the basal planes toward O(4).

The lattice is further stabilized by hydrogen bonding between the amine-N and an O_{NO3} of a neighbouring unit with a distance of 2.8551 Å, resulting in a polymeric chain.

3.3. Structure comparisons

The compounds **1** and **2** are found to be isomorphous and isostructural, and have compressed rhombic octahedral $CuN_2O_2N'_2$ chromophores. The most similarity to the stereochemistry of both complexes are found in the oxalato-bridged dimers $[Cu_2(bispicen)_2(C_2O_4)]$-

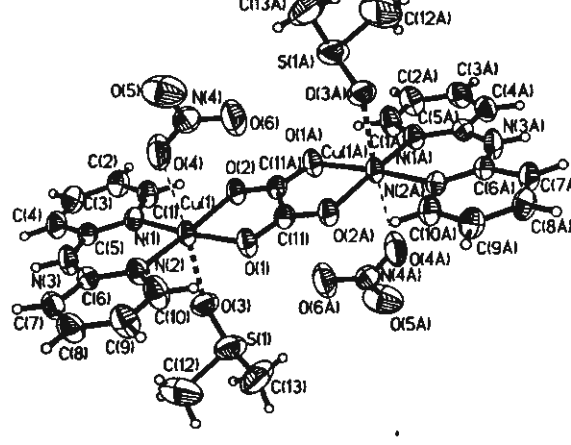

Fig. 3. ORTEP 50% probability plot of $[Cu_2(dpyam)_2(C_2O_4)(NO_3)_2((CH_3)_2SO)_2]$ (3) Atoms with an 'A' are generated by an inversion centre.

Table 3
Selected bond lengths (Å) and angles (°) with e.s.d.s. in parentheses for $[Cu_2(dpyam)_2(C_2O_4)(NO_3)_2((CH_3)_2SO)_2]$ (3)

Bond lengths			
Cu(1)–N(1)	1.986(2)	Cu(1)–N(2)	2.002(2)
Cu(1)–O(1)	1.998(2)	Cu(1)–O(2)	1.994(2)
Cu(1)–O(3)	2.331(2)	Cu(1)–O(4)	2.502(2)
Cu(1)–Cu(1A)	5.220(2)		
Bond angles			
N(1)–Cu(1)–O(2)	92.3(2)	N(1)–Cu(1)–O(1)	174.3(8)
O(2)–Cu(1)–O(1)	82.2(7)	N(1)–Cu(1)–N(2)	93.3(2)
O(2)–Cu(1)–N(2)	170.9(3)	O(1)–Cu(1)–N(2)	91.8(7)
N(1)–Cu(1)–O(3)	88.2(6)	O(2)–Cu(1)–O(3)	93.5(7)
O(1)–Cu(1)–O(3)	93.5(5)	O(4)–Cu(1)–N(1)	86.6(7)
O(4)–Cu(1)–N(2)	85.5(7)	O(4)–Cu(1)–O(1)	91.7(7)
O(4)–Cu(1)–O(2)	87.7(7)	O(4)–Cu(1)–O(3)	74.8(7)

Symmetry code: A = $-x, -y+1, -z$.

$(ClO_4)_2$ (**9**), $[Cu_2(bispicMe_2en)_2(C_2O_4)](ClO_4)_2$ (**10**), which have the compressed octahedral $CuN_2O_2N_2'$ chromophores (see Table 4). Related complexes are $[Cu_2(bpy)_2(C_2O_4)(NO_3)_2(H_2O)_2]$ (**4**), $[Cu_2(mpym)_2(C_2O_4)(NO_3)_2(H_2O)_2]$ (**5**), $[Cu_2(deen)_2(C_2O_4)(ClO_4)_2(H_2O)_2]$ (**6**),and $[Cu_2(tacn)_2(C_2O_4)(ClO_4)_2]$ (**7**) (Table 4), which have an elongated octahedral $CuN_2O_2O'O''$ and CuN_3O_2O chromophores, respectively, similar to the $CuN_2O_2O'O''$ chromophore geometry of **3**. There is some similarity to other dinuclear μ-oxalato dicopper(II) complexes which exhibit a square-pyramidal structure with two oxygen atoms of oxalate bridge and two nitrogen atoms of the diamine occupying the base of the pyramid and the counter anion or a solvent molecule occupying the axial position [12–14]. There are some differences to the elongated octahedral complex $[Cu_2(bpca)_2(C_2O_4)(H_2O)_2](H_2O)_2$ (**8**) involving the oxalato-bridged occupying axial and equatorial coordination sites and the trigonal bipyramidal complex $[Cu_2(Et_5dien)_2(C_2O_4)](BPh_4)_2]$ (in which Et_5dien is 1,1,4,7,7-pentaethylenetriamine) [15].

The coordination around the Cu ion of **1**, **2** can be best described as an axially-compressed octahedral (2+4) geometry [11], and differs from those of **3**, **4**, **5**, **6**, **7** which have an axially-elongated octahedral (4+2) geometry [5–10].

3.4. IR and electronic spectra

3.4.1. IR spectra

The IR spectra of **1** and **2** display characteristic bands of the asymmetric oxalate bridging ligand [6,8–10]: $\nu_{asym\ (C-O)}$ at 1647s, $\nu_{sym\ (C-O)}$ at 1375m and $\delta_{(O-C-O)}$ at 843m cm^{-1} for **1**; $\nu_{asym\ (C-O)}$ at 1642s, $\nu_{sym\ (C-O)}$ at 1370m and $\delta_{(O-C-O)}$ at 845m cm^{-1} for **2**. The ClO_4^- group vibration near 1100 cm^{-1} splitting into three sharp peaks at 1090s, 1116s and 1142s cm^{-1} and the BF_4^- group vibration near 1100 cm^{-1} splitting into a sharp

Table 4
Structural data and magnetic properties for 10 selected oxalato-bridged Cu(II) complexes

Compound[a]	Donor set	Geometry[b]	Oxalato-bridged Coordination	d_{Cu-Cu} (Å)	Dihedral angle[c]	Mode of magnetic interaction	J (cm^{-1})	Ref.
$[Cu_2(dpyam)_4(C_2O_4)](ClO_4)_2(H_2O)_3$ (**1**)	$O_2N_2N_2'$	com. Oct	eq–eq	5.752	11.3/11.3	c	2.42	this work
$[Cu_2(dpyam)_4(C_2O_4)](BF_4)_2(H_2O)_3$ (**2**)	$O_2N_2N_2'$	com. Oct	eq–eq	5.745	11.4/11.0	c	3.38	this work
$[Cu_2(dpyam)_2(C_2O_4)(NO_3)_2(DMSO)_2]$ (**3**)	$O_2N_2O'O$	elong. Oct	eq–eq	5.22	7	a	−305	this work
$[Cu_2(bpy)_2(C_2O_4)(NO_3)_2(H_2O)_2]$ (**4**)	$O_2N_2O'O''$	elong. Oct	eq–eq	5.143	4.6	a	−382	[5]
$[Cu_2(mpym)_2(C_2O_4)(NO_3)_2(H_2O)_2]$ (**5**)	$O_2N_2O'O''$	elong. Oct	eq–eq	5.217	d	a	−142	[7]
$[Cu_2(deen)_2(C_2O_4)(ClO_4)_2(H_2O)_2]$ (**6**)	$O_2N_2O'O''$	elong. Oct	eq–eq	d	3.88	a	−300	[8]
$[Cu_2(tacn)_2(C_2O_4)(ClO_4)_2]$ (**7**)	O_2N_3O'	elong. Oct	eq–eq	5.176	d	a	−41	[9]
$[Cu_2(bpca)_2(C_2O_4)(H_2O)_2](H_2O)_2$ (**8**)	O_2N_3O'	elong. Oct	ax–eq	5.631	d	b	1.1	[10]
$[Cu_2(bispicen)_2(C_2O_4)](ClO_4)_2$ (**9**)	$O_2N_2N_2'$	com. Oct	eq–eq	5.608	d	c	2.3	[11]
$[Cu_2(bispicMe_2en)_2(C_2O_4)](ClO_4)_2$ (**10**)	$O_2N_2N_2'$	com. Oct	eq–eq	5.494	d	c	2.14	[11]

[a] dpyam = di-2-pyridylamine; bpy = 2,2′-dipyridine; mpym = meripirizole; deen = *N*,*N*-diethylethane-1,2-diamine; tacn = 1,4,7-triazacyclononane; bpca = bis(2-pyridylmethyl)1-3,3-propanediamine; bispicen = *N*,*N*′-bis(2-pyridylmethyl)-1,2-ethanediamine; bispicMe2en = N,N′-bis(2-pyridylmethyl)-N-N-dimethyl-1,2-ethanediamine.
[b] com.Oct = compressed octahedral; elong. Oct = elongated octahedral.
[c] Dihedral angle between the basal and oxalate planes.
[d] Not reported.

peak at 1075 cm^{-1} and a shoulder at approximately 1055 cm^{-1}, indicates ClO_4^- ions in **1** and BF_4^- ions in **2** involved hydrogen bonding [46,47].

Compound **3** displays the characteristic bands of the symmetric oxalate bridging ligand $\nu_{asym(C-O)}$ at 1650s, $\nu_{sym(C-O)}$ at 1370m and $\delta_{(O-C-O)}$at 840m cm^{-1}. The bands observed at 1380s, 1320s,1080m cm^{-1} suggest monodentate coordination of the nitrate ion [6] and the SO stretching appear at approximately 1023w cm^{-1}, indicative of the presence of the dimethylsulfoxide ligand in **3** [48].

3.4.2. Electronic spectra

The electronic reflectance spectra of **1** and **2** consist of two clearly resolved peaks at 14 050 and 8800 cm^{-1} for **1** and 13 970 and 8700 cm^{-1} for **2**. These spectra are consistent with the compressed rhombic octahedral stereochemistry and assigned to be the $d_{x^2-y^2} \rightarrow d_{z^2}$ and the d_{xz}, d_{xy}, $d_{yz} \rightarrow d_{z^2}$ transitions. That of **3** has a broad peak center at 14700 cm^{-1}, with a poorly resolved shoulder to low energy at approximately 10600 cm^{-1}, corresponding to the elongated octahedral geometry. This suggests the assignment of the bands as the d_{xz}, d_{yz}, $d_{xy} \rightarrow d_{x^2-y^2}$ and $d_{z^2} \rightarrow d_{x^2-y^2}$ transitions, respectively.

3.5. EPR and Magnetic properties

The room temperature X-band powder EPR spectra of compounds **1** and **2** display a broad absorption centered around g of 2.14. At the high-field side (g = approximately 1.94) a small shoulder is observed which is due to a signal from the triplet state with a very small zero-field splitting. No half-field signal was observed at RT.

Both compounds were also measured as solids at 77 K, in which cases the signal appears as more resolved with non-split signals at $g_\perp = 2.10$, $g_\parallel = 2.27$ for **1** and $g_\perp = 2.10$, $g_\parallel = 2.33$ for **2**, corresponding to the pattern of Cu(II) in an elongated geometry, $g_\parallel > g_\perp > 2.0$ with the $d_{x^2-y^2}$ ground state. This suggest that the apparent compressed geometry at room temperature could be caused by a dynamic Jahn–Teller effect [51,52]. This is because compounds **1** and **2** adopt the time averaged structure found crystallographically which arise due to the short time scale of the X-ray technique, but the EPR spectra at 77 K are related to the underlying static axial elongated chromophore [51,52]. Also the half-field signal at approximately 1600 G, corresponding to $\Delta M = \pm 2$ transition was observed, which indicates that indeed a weak interaction between two Cu(II) ions within these compounds is present.

Compound **3**, measured as a powdered solid displays at RT an asymmetric broad resonance with a center at $g = 2.12$. The observed triplet signal is not resolved, apparently due to exchange narrowing resulting from nearby triplet molecules in the lattice. At 77 K a weak resolved signal is observed, with bands assigned for H_{z1} at 2691 G, H_{x1y1} at 3014 G, H_{x2y2} at 3218 G and H_{z2} at 3316 G. On the low field side of the $\Delta M = \pm 1$ signal of compound **3** a seven-line Cu hyperfine resonance centered at $g = 2.44$, with an average spacing of 88 G, is observed. The seventh line of this pattern is obscured by the intense signal of the perpendicular component. Such a seven-line pattern, is evidence for the parallel $\Delta M = \pm 1$ transition and indicative for a small zero-field splitting parameter, D [49,50,53–56]. No half-field signal was observed in this case. So the observed signal is typical for triplet Cu(II) dinuclear in an isolated state with D = approximately 0.03 cm^{-1} [49,50].

From the magnetic susceptibility (vide infra) at 77 K the compound is almost diamagnetic, so the observed resonances are likely to originate from a small paramagnetic impurity and a small amount of triplet signal thermally accessible at 77 K.

The exchange interaction between the copper ions via the oxalate bridge is known to be strongly dependent on the geometry around the Cu ions, the orientation of the magnetic orbitals in respect to the oxalate plane and the bridging mode of the oxalate group, which favours the antiferromagnetic interaction [5,6,16–21]. This interaction is weakened by structural distortions, such as the displacement of the copper atom out of the basal plane, the non-planarity of the Cu–ox–Cu framework and the tetrahedral distortion of the basal plane.

In compounds **1** and **2** the short Cu–L bonds result in magnetic orbitals that do not coincide with the oxalate ligand plane and therefore any significant antiferromagnetic interaction is not present. Instead a weak ferromagnetic interaction is seen and this agrees well to related systems from literature [10,11].

The magnetic susceptibility of the powdered compounds were measured from 5 to 280 K. At 280 K μ_{eff} is 2.62 μ_B for **1** (2.64 μ_B for **2**) which agrees well with the spin-only value of Cu(II) calculated for two uncoupled spin = 1/2 centres. Upon cooling these values are staying almost constant between about 2.64 and 2.61 μ_B until at about 50 K it raises gradually to reach 2.77 μ_B at 5 K for **1** (2.80 μ_B for **2**). This is typical for a very weak ferromagnetically coupled Cu(II) dinuclear compound. To reproduce this behaviour the theoretical expression of the magnetic susceptibility of spin = 1/2 dimer, arising from the hamiltonian $H = -J\ S_1 \cdot S_2$, has been considered, including possible intermolecular interactions, in the molecular-field approximation ([53], p. 132): $\chi_m = (2Ng^2\beta^2)[kT-(2\ zJ'/(3+\exp(-J/kT)))]^{-1}\ [3+\exp(-J/kT)]^{-1}\ (1-p)+\chi_p p$ where J is the singlet–triplet energy gap (negative value for antiferromagetic and positive value for ferromagnetic interaction) and N, g, β, k and T have their usual meanings. The parameter p denotes the molar fraction of paramagnetic impurity in the sample ([53], p. 107) and zJ' the interaction between neighbouring dinuclear identities.

Minimisation of the expression $R = \Sigma(\chi_{obs} - \chi_{calc})^2/\Sigma \chi^2_{obs}$, resulted in the best-fit parameters $J = 2.42$ cm^{-1}, $g = 2.12$ and zJ' and $p = 0$ with $R = 4.8 \times 10^{-4}$ for compound **1** (see Fig. 4(a)) and $J = 3.38$ cm^{-1}, $g = 2.10$ and zJ' and $p = 0$ with $R = 2.8 \times 10^{-3}$ for compound **2** (see Fig. 4(b)), which confirms the ferromagnetic type of the intradimer interaction.

The dinuclear unit is slightly folded in a chair from and the dihedral angles between the basal and the oxalate planes and the Cu–Cu distance are 5.752 Å in **1** and 5.745 Å in **2**. The magnetic orbitals are perpendicular to the oxalate plane, so the overlap of the Cu(II) orbitals do not coincide with the oxalate σ orbitals. This situation is corresponding to the coordinate *mode c* (Scheme 2) and consequently (as in fact the value of the exchange coupling (J) in a Cu(II) dimer is decomposed in two terms, of which one is antiferromagnetic (J_{AF}) and the other is ferromagnetic (J_F) according to $J = J_{AF} + J_F$)) when the antiferromagnetic term is almost zero, the ferromagnetic term is predominant, which is confirmed by the susceptibility measurements presented above.

The temperature dependence of the molar magnetic susceptibility χ_M of **3**, measured on a powdered sample, is shown in Fig. 5 down to 5 K. At 280 K, χ_M is equal to 1.6×10^{-3} cm^3 mol^{-1} and decreases when cooling down and reaches almost zero at about 40 K. From 40 to 5 K the χ_M increases a little to 0.4×10^{-3} cm^3 mol^{-1}. The susceptibility data were fitted using the formula mentioned earlier with minimisation of the expression $R = \Sigma(\chi_{obs} - \chi_{calc})^2/\Sigma \chi^2_{obs}$ and resulted in the best-fit parameters $J = -305$ cm^{-1}, $g = 2.14$ and $zJ' = 0.07$ and $p = 1 \times 10^{-2}$ with $R = 0.6\%$, which confirms the strong antiferromagnetic type of the interaction. The measurements were repeated several times, but special in the high temperature area the fit is not so good, resulting in a somewhat high R value.

Compound **3** exhibits an elongated octahedral geometry and in this case the Cu(II) orbitals interact with the oxalate σ orbitals, which is consistent with the coordinated *mode a* (Scheme 2) and a strong antiferromagnetic interaction is expected, which is confirmed by the magnetic susceptibility measurements presented above and also with similar cases known in the literature [5,8].

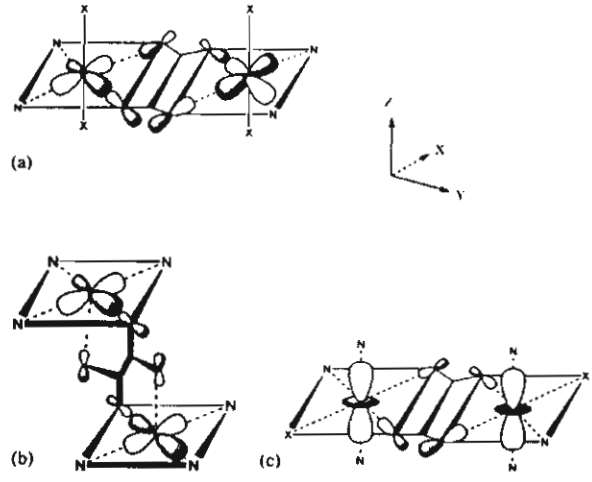

Scheme 2. Three models predicting the magnetic interactions in oxalato-bridged Cu(II) complexes (X–O (**1**) or N (**2**)).

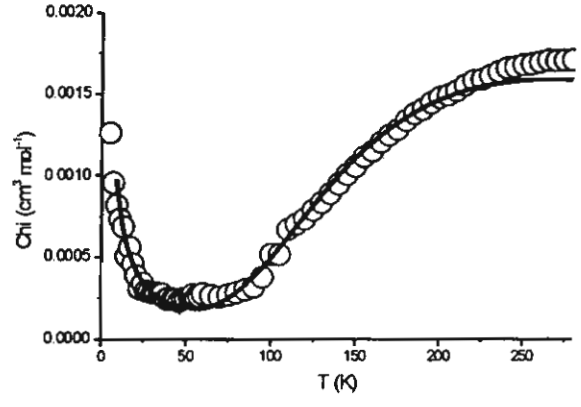

Fig. 5. Temperature dependence of χ_M vs. T for compound **3**. The solid lines represent the calculated curve (see text).

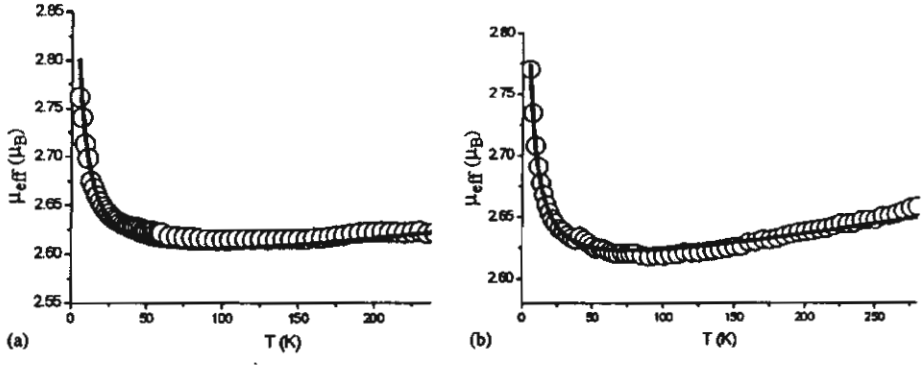

Fig. 4. Temperature dependence of μ_{eff} vs. T for compound **1** (a) and compound **2** (b). The solid lines represent the calculated curve (see text).

4. Conclusions

Three new Cu(II) dinuclear oxalate bridged compounds are presented in this study with the ligand dpyam together with their spectroscopic and magnetic results. Compounds **1** and **2** display a compressed rhombic octahedral geometry, with asymmetrically bound oxalato ligands and have a weak ferromagnetic interaction between the Cu(II) atoms. On the other hand compound **3** has an elongated tetragonal octahedral geometry with a symmetric oxalato bridge and displays a strong antiferromagnetic interaction.

5. Supplementary material

Crystallographic data (excluding structure factors) for the structures in this paper have been deposited with the Cambridge Crystallographic Data Centre, CCDC No. 194972–74 for structures **1**, **2** and **3**, respectively. Copies of the data can be obtained free of charge on application to The Director, CCDC, 12 Union Road, Cambridge CB2 1EZ, UK (fax: (internat.) +44-1223-336-033, e-mail: deposit@ccdc.cam.ac.uk or www: http://www.ccdc.cam.ac.uk).

Acknowledgements

The authors (S.Y, N.C, P.G, P.K) would like to thank the Thailand Research Fund and Khon Kaen University for research grant. Support of the Postgraduate Education and Research Program in Chemistry is also gratefully acknowledged. The work described in the present paper has been supported by the Leiden University Study group WFMO (Werkgroep Fundamenteel Materialen Onderzoek). Part of the work has been supported financially by the Graduate Research School Combination 'Catalysis'.

References

[1] M. Hernández-Molina, P.A. Lorenzo-Luis, C. Ruiz-Pérez, Cryst. Eng. Comm. (2001) article #16.
[2] O. Castillo, A. Luque, S. Iglesias, C. Guzmán-Miralles, P. Román, Inorg. Chem. Comm. 4 (2001) 640.
[3] H.Z. Kou, D.Z. Liao, G.M. Yang, P. Cheng, Z.H. Jiang, S.P Yan, G.L. Wang, X.K. Yao, H.G. Wang, Polyhedron 18 (1998) 3193.
[4] H. Núñez, J.J. Timor, J. Server-Carrió, L. Soto, E. Escrivá, Inorg. Chim. Acta. 318 (2001) 8.
[5] O. Castillo, I. Muga, A. Luque, J.M. Gutierrez-Zorrilla, J. Sertucha, P. Vitoria, P. Román, Polyhedron 18 (1999) 1235.
[6] J. Tang, E. Gao, W. Bu, D. Liao, S. Yan, Z. Jiang, G. Wang, J. Mol. Struct. 525 (2000) 271.
[7] L.S. Tuero, J. Garcia-Lozano, E.E. Monto, M.B. Borja, F. Dahan, J.P. Tuchagues, J.P. Legros, J. Chem. Soc., Dalton Trans. (1991) 2619.
[8] R. Vicente, A. Escuer, J. Ferretjans, H. Stoeckli-Evans, X. Solans, M. Font-Bardía, J. Chem. Soc., Dalton Trans. (1997) 167.
[9] L. Zhang, W.-M. Bu, S.-P. Yan, Z.-H. Jiang, D.-Z. Liao, G.-L. Wang, Polyhedron 19 (2000) 1105.
[10] M.L. Calatayud, I. Castro, J. Sletten, F. Lloret, M. Julve, Inorg. Chim. Acta. 300–302 (2000) 846.
[11] J. Glerup, P.A. Goodson, D.J. Hodgson, K. Michelsen, Inorg. Chem. 34 (1995) 6255.
[12] M. Julve, M. Verdaguer, A. Gleizes, M. Philoche-Levisalles, O. Kahn, Inorg. Chem. 23 (1984) 3808.
[13] G.R. Hall, D.M. Duggan, D.N. Hendrickson, Inorg. Chem. 14 (1975) 1956.
[14] Y. Akhriff, J. Server-Carrió, A. Sancho, J. Garcia-Lozano, E. Escrivá, J.V. Folgado, L. Soto, Inorg. Chem. 38 (1999) 1174.
[15] T.R. Felthouse, E.J. Laskowski, D.N. Hendrickson, Inorg. Chem. 16 (1977) 1077.
[16] J. Cano, P. Alemany, S. Alvarez, M. Verdaguer, E. Ruiz, Chem. Eur. J. 4 (1998) 476.
[17] J. Cabrero, N.B. Amor, C. de Graaf, F. Illas, R. Caballol, J. Phys. Chem., A. 104 (2000) 9983.
[18] O. Castillo, A. Luque, F. Lloret, P. Román, Inorg. Chem. Comman. 4 (2001) 350.
[19] Z. Smékal, Z. Trávnícek, F. Lloret, J. Marek, Polyhedron 18 (1999) 2787.
[20] O. Castillo, A. Luque, P. Román, F. Lloret, M. Julve, Inorg. Chem. 40 (2001) 5526.
[21] O. Castillo, A. Luque, M. Julve, F. Lloret, P. Román, Inorg. Chim. Acta 315 (2001) 9.
[22] H. Oshio, U. Nagashima, Inorg. Chem. 31 (1992) 3295.
[23] Z. Smekal, P. Thornton, Z. Šindelár, R. Klicka, Polyhedron 17 (1998) 1631.
[24] S. Decurtins, H.W. Schmalle, P. Schneuwly, L.M. Zheng, J. Ensling, A. Hauser, Inorg. Chem. 34 (1995) 5501.
[25] G.D. Munno, M. Julve, F. Nicolo, F. Lloret, J. Faus, R. Ruiz, E. Sinn, Angew. Chem., Int. Ed. Engl. 32 (1993) 613.
[26] R. Vicente, A. Escuer, X. Solans, M. Font-Bardia, J. Chem. Soc., Dalton Trans. (1996) 1835.
[27] A. Gleizes, M. Julve, M. Verdaguer, J.A. Real, J. Faus, X. Solans, J. Chem. Soc., Dalton Trans. (1992) 3209.
[28] S.K. Chattopadhyay, T.C.W. Mak, B.S. Luo, L.K. Thompson, A. Rana, S. Ghosh, Polyhedron 14 (1995) 3661.
[29] O. Castillo, A. Luque, J. Sertucha, P. Román, F. Lloret, Inorg. Chem. 39 (2000) 6142.
[30] J. Suárez-Varela, J.M. Domingue-Vera, E. Colacio, J.C. Avila-Rosón, M.A. Hidalgo, D. Martin-Ramos, J. Chem. Soc., Dalton Trans. (1995) 2143.
[31] H.Y. Shen, W.M. Bu, E.Q. Gao, D.Z. Liao, Z.H. Jiang, S.P. Yan, G.L. Wang, Inorg. Chem. 39 (2000) 396.
[32] M. Andruh, R. Melanson, C.V. Stager, F.D. Rochon, Inorg. Chim. Acta 251 (1996) 309.
[33] P. Román, C. Guzmán-Miralles, A. Luque, J.I. Beitia, J. Cano, F. Lloret, M. Julve, S. Alvarez, Inorg. Chem. 35 (1996) 3741.
[34] O. Castillo, A. Luque, M. Julve, F. Lloret, P. Román, Inorg. Chim. Acta 324 (2001) 141.
[35] Z. Smekal, J. Kameníček, P. Klasová, G. Wrzeszcz, Z. Šindelář, P. Kopel, Z. Zák, Polyhedron 21 (2002) 1203.
[36] M. Du, Y.-M. Guo, X.-H. Bu, Inorg. Chim Acta 335 (2002) 136.
[37] J.Y. Lu, M.A. Lawandy, J. Li, T. Yuen, C.L. Lin, Inorg. Chem. 38 (1999) 2695.
[38] I. Castro, J. Faus, M. Julve, M.C. Muñoz, W. Diaz, X. Solans, Inorg. Chim. Acta 179 (1991) 59.
[39] J. Novosad, A.C. Messimeri, C.D. Papadimitriou, P.G. Veltsistas, J.D. Woollins, Trans. Metal Chem. 25 (2000) 664.
[40] G.M. Sheldrick, SHELXS-97, Program for the solution of crystal structures, University of Göttingen, Germany, 1997.

[41] G.M. Sheldrick, SHELXL-97, Program for the refinement of crystal structures, University of Göttingen, Germany, 1997.
[42] SAINT, Data Integration Software, Version 4.0, Bruker AXS, Inc., Madison, WI, 1997.
[43] G.M. Sheldrick, SADABS, Program for empirical absorption correction of area detector data, University of Göttingen, Germany, 1996.
[44] SHELXTL 5.03 (PC-Version), Program library for the solution and molecular graphics, Siemens Analytical Instruments Division, Madison, WI, 1995.
[45] TEXSAN, Single Crystal Structure Analysis Software, Version 1.6, Molecular Structure Corporation, The Woodlands, TX, 77381, USA, 1993.
[46] S. Youngme, C. Pakawatchai, W. Somjitsripunya, S. Chantrapromma, K. Chinnakali, H.K. Fun, Inorg. Chim. Acta. 303 (2000) 181.
[47] S. Youngme, N. Chaichit, P. Kongsaeree, G.A. van Albada, J. Reedijk, Inorg. Chim. Acta 324 (2001) 232.
[48] K. Nakamoto, Infared and Raman Spectra of Inorganic and Coordination Compounds, 5 (Part B), Wiley, New york, (1997) 102.
[49] V.T. Kasumov, F. Köksal, Z. Anorg. Allg. Chem. 627 (2001) 2553.
[50] E. Wasserman, L.C. Snyder, W.A. Yager, J. Chem. Phys. 25 (1964) 1763.
[51] B.J. Hathaway, M. Duggan, A. Murphy, J. Mullane, C. Power, A. Walsh, B. Walsh, Coord. Chem. Rev. 36 (1981) 267.
[52] B.J. Hathaway, Struct. Bonding (Berlin) 57 (1984) 203.
[53] O. Kahn, Molecular Magnetism, VCH Publishers, New York, (1993) 107, 132.
[54] J. Reedijk, B. Nieuwenhuijse, Recl. Trav. Chim. Pays-Bas 91 (1972) 533.
[55] G.J.A.A. Koolhaas, W.L. Driessen, J. Reedijk, J.L. van der Plas, R.A.G. de Graaff, D. Gatteschi, H. Kooijman, A.L. Spek, Inorg. Chem. 35 (1996) 1509.
[56] M. Korabik, M. Materny, W. Surga, T. Glowiak, J. Mrozinski, J. Mol. Struct. 443 (1998) 255.

Transition Metal Chemistry 29: 840–846, 2004.

Dinuclear copper(II) complexes with ferromagnetic and antiferromagnetic interactions mediated by a bridging oxalato group: structures and magnetic properties of $[Cu_2L_4(\mu\text{-}C_2O_4)](PF_6)_2(H_2O)_2$ and $[Cu_2L_2(\mu\text{-}C_2O_4)(NO_3)_2((CH_3)_2NCOH)_2]$ (L = di-2-pyridylamine)

Sujittra Youngme* and Pimprapun Gunnasoot
Department of Chemistry, Faculty of Science, Khon Kaen University, Khon Kaen 40002, Thailand

Narongsak Chaichit
Department of Physics, Faculty of Science and Technology, Thammasat University Rangsit, Pathumthani 12121, Thailand

Chaveng Pakawatchai
Department of Chemistry, Faculty of Science, Prince of Songkla University, Hatyai, Songkla 90112, Thailand

Received 15 April 2004; accepted 04 May 2004

Abstract

Two dinuclear Cu^{II} complexes of formula $[Cu_2(dpyam)_4(\mu\text{-}C_2O_4)](PF_6)_2(H_2O)_2$ *(1)* and $[Cu_2(dpyam)_2(\mu\text{-}C_2O_4)(NO_3)_2(DMF)_2]$ *(2)* (dpyam = di-2-pyridylamine) have been synthesized and their spectroscopic and magnetic properties characterized. Complex *(1)* crystallizes in the non-centrosymmetric monoclinic space group Pc, while *(2)* crystallizes in the non-centrosymmetric triclinic space group P1. Compound *(1)* involves the compressed octahedral Cu^{II} environment, whereas *(2)* exhibits an elongated octahedral Cu^{II} geometry. Both complexes contain six-coordinate metal centers bridged by planar bis-didentate oxalate group. The geometry, spectroscopic properties and the effective magnetic moment of *(1)* are very close to those of the recently published $[Cu_2(dpyam)_4(\mu\text{-}C_2O_4)](ClO_4)_2(H_2O)_3$ and $[Cu_2(dpyam)_4(\mu\text{-}C_2O_4)](BF_4)_2(H_2O)_3$. Thus *(1)* is expected to exhibit a very weak ferromagnetic interaction between the Cu^{II} centers which is confirmed by EPR spectrum. Those of *(2)* are comparable to those of the recently published $[Cu_2(dpyam)_2(\mu\text{-}C_2O_4)(NO_3)_2(DMSO)_2]$. Therefore a strong antiferomagnetic interaction is expected. The effective magnetic moment at room temperature of *(1)* was measured to be 2.55 BM/dimer, which agrees with the spin only value of Cu^{II}, 2.45 BM calculated for two uncoupled spin = 1/2 centers. In *(2)* the room temperature effective magnetic moment of 2.16 BM/dimer indicates the partial spin paring by antiferromagnetic coupling. This is confirmed by the e.p.r. spectrum and is explained as a result of the magnetic interaction between the coplanar $d_{x^2-y^2}$ orbitals on the two copper atoms.

Introduction

It is now well-known that oxalato bridges can propagate magnetic exchange interactions between paramagnetic metal ions. A number of dinuclear copper complexes with an oxalato bridge, generally formulated as $[(NN)_{1\text{ or }2}Cu(\mu\text{-}C_2O_4)Cu(NN)_{1\text{ or }2}]X_n$, where NN is a chelating ligand, and X is a counter anion or a solvent molecule, have been structurally characterized [1–11] in the past decades.

The previous paper describes the crystal structure, spectroscopic properties and magneto-structural correlation of complexes $[Cu_2(dpyam)_4(\mu\text{-}C_2O_4)](ClO_4)_2(H_2O)_3$, $[Cu_2(dpyam)_4(\mu\text{-}C_2O_4)](BF_4)_2(H_2O)_3$ and $[Cu_2(dpyam)_2(\mu\text{-}C_2O_4)(NO_3)_2(DMSO)_2]$ [12]. The exchange interaction between the copper ions *via* the oxalate bridge is known to be strongly dependent on the geometry around the copper ions, which sensitive to nature of counter anions and terminal ligands. In order to extend the investigation by modifying to other counter ions, this paper reports the synthesis, the results of the structure determination and the magnetic properties of two new μ-oxalato copper(II) complexes, $[Cu_2(dpyam)_4(\mu\text{-}C_2O_4)](PF_6)_2(H_2O)_2$ *(1)* and $[Cu_2(dpyam)_2(\mu\text{-}C_2O_4)(NO_3)_2(DMF)_2]$ *(2)*.

Experimental

Materials and physical measurements

All reagents are commercial grade materials and were used without further purification. Elemental analyses (C, H, N) were performed by the microanalytical Service

* Author for correspondence

of Science and Technological Research Equipment Center, Chulalongkorn University on Perkin-Elmer PE2400 CHNS/O Analyzer. The copper content was determined on an atomic absorption spectrophotometer.

I.r. spectra were recorded with a Spectrum One Perkin-Elmer FTIR spectrophotometer as KBr pellets and, or as Nujol mulls in the 4000–450 cm^{-1} spectral range. Solid-state (diffuse reflectance) electronic spectra were recorded as polycrystalline samples on a Perkin-Elmer Lambda2S spectrophotometer over the 8000–18,000 cm^{-1} range. X-band powder e.p.r. spectra were obtained on a JEOL RE2x electron spin resonance spectrometer using DPPH ($g = 2.0036$) as a standard. The room temperature magnetic susceptibility measurements were carried out on a Faraday-type microbalance. The apparatus was calibrated with $Hg[Co(NCS)_4]$. Data were corrected for magnetization of the sample holder and for diamagnetic contributions, which were estimated from the Pascal constants and the temperature independent paramagnetism was estimated to be 60×10^{-6} cm^3 mol^{-1} per copper(II) ion.

Synthesis of complexes (1) and (2)

Complex (1)

Method A. Compound *(1)* was prepared by adding a solution (10 cm^3) of oxalic acid (0.063 g, 0.5 mmol) to a suspension of $CuCo_3$ (0.221 g, 1.0 mmol) in H_2O (10 cm^3). The mixture was added to a solution containing di-2-pyridylamine (0.342 g, 2.0 mmol) in EtOH (20 cm^3) and potassium hexafluorophosphate (0.184 g, 1.0 mmol) in H_2O (10 cm^3). The resulting blue solution was filtered to remove impurities. After two weeks, green crystals of *(1)* were obtained. They were filtered off, washed with mother liquor and were dried in air. Yield approximately 60%. (Found: C, 41.4; H 3.4; Cu, 10.3; N, 13.7. $C_{42}H_{40}P_2Cu_2F_{12}N_{12}O_6$ calcd.: C, 41.15; H, 3.3; Cu, 10.4; N, 13.7%)

Method B. Compound *(1)* was prepared by adding an aqueous solution (25 cm^3) of $CuSO_4 \cdot 5H_2O$ (0.249 g, 1.0 mmol) to a solution of hexafluorophosphate (0.184 g, 1.0 mmol) in H_2O (20 cm^3), followed by a solution of sodium oxalate (0.124 g, 1 mmol) in H_2O (10 cm^3) and a solution of di-2-pyridylamine (0.171 g, 1.0 mmol) in MeOH (20 cm^3). The resulting green solution was allowed to stand at room temperature for two weeks to produce green crystals of *(1)*. The crystals were separated by filtration and washed with the mother liquor. Yield *ca.* 50%. Calcd.: $C_{42}H_{40}P_2Cu_2F_{12}N_{12}O_6$: C, 41.15; H, 3.29; Cu, 10.37; N, 13.71%. Found: C, 41.26; H 3.41; Cu, 10.20; N, 13.65%.

Complex (2)

A solution containing di-2-pyridylamine (0.342 g, 2.0 mmol) in dimethylformamide (10 cm^3) was added to a solution containing $Cu(NO_3)_2 \cdot 3H_2O$ (0.482 g, 2.0 mmol) in DMF (20 cm^3) and sodium oxalate (0.068 g, 0.5 mmol) in H_2O (10 cm^3). Then DMF (30 cm^3) was added to the resulting green solution which was filtered to remove impurities. After 4 months, green crystals of *(2)* were obtained, which were filtered off, washed with the mother liquor and air-dried. Yield *ca.* 70%. Calcd.: $C_{28}H_{32}Cu_2N_{10}O_{12}$: C, 40.6; H, 3.9; Cu, 15.35; N, 16.92. Found: C, 40.5; H, 3.8; Cu, 15.3; N, 16.8.

Found: C, 40.5; H, 3.8; Cu, 15.3; N, 16.8 $C_{28}H_{32}Cu_2N_{10}O_{12}$ calcd.: C, 40.5; H, 3.9; Cu, 15.35; N, 16.9%.

Crystallographic data collection and structure determination of complexes (1) and (2)

Reflection data for *(1)* were collected at 298 K on a 1 K Bruker SMART CCD area-detector diffractometer using graphite monochromated MoK_α radiation ($\lambda = 0.71073$ Å) at a detector distance of 4.5 cm and swing angle of −35°. A hemisphere of the reciprocal space was covered by a combination of three sets of exposures; each set had a different ϕ angle (0°, 88°, 180°) and each exposure of 30 S covered 0.3° in ω. Data reduction and cell refinement were performed using the program SAINT [13]. An empirical absorption correction by using the SADABS [14] program was applied, which resulted in transmission coefficients ranging from 0.5054 to 1.0000. The structure was solved by direct methods and refined by full-matrix least-squares method on F^2_{obs} with anisotropic thermal parameters for all non-hydrogen atoms using the SHELXTL-PC V 6.1 software package [15]. All hydrogen atoms were geometrically fixed and allowed to ride on the attached atoms. One of the hydrogen atoms of each lattice water molecule could not be located and the hexafluorophosphate groups are well ordered.

Reflection data of *(2)* were collected on a 4 K Bruker SMART APEX CCD area-detector diffractometer with graphite monochromated MoK_α radiation ($\lambda = 0.71073$ Å) (at a detector distance of 6.0 cm and swing angle of −28°) using SMART program. Raw data frame integration was performed with SAINT [13], which also applied correction for Lorentz and polarization effects. Absorption corrections were applied using SADABS [14], provided an empirical absorption correction and put the standard deviations of measured intensities onto absolute scale. The structures were solved by direct methods. The software package SHELXTL V 6.12 [15] was used for structure solution and structure refinement. All non-H atoms were refined anisotropically except the nitrate-O atoms and the methyl-C atoms of DMF. The H atoms were introduced in calculated positions and refined with fixed geometry with respect to their carrier atoms. The nitrate groups are disordered with site occupancies of 0.48 and 0.52 for both conformers. Both methyl groups of the DMF ligands are also disordered with site occupancies of 0.44 and 0.56 for both conformers and some of the methyl hydrogen atoms could not be located.

The molecular graphics were created by using SHELXTL-PC [15]. The crystal and refinement details for compounds *(1)* and *(2)* are listed in Table 1. Selected bond lengths and angles are given in Table 2.

Crystallographic data for the structures in this paper have been deposited with the Cambridge Crystallographic Data Centre as supplementary publication CCDC No. 227148 and 227149 for structures 1 and 2, respectively. Copies of the data can be obtained free of charge from The Director, CCDC, 12 Union Road, Cambridge CB2 1EZ, UK (fax: +44-1223-336033; e-mail: deposit@ccdc.cam.ac.uk, www:http://www.ccdc.cam.ac.uk).

Result and discussion

Crystal structure of $[Cu_2(dpyam)_4(C_2O_4)](PF_6)_2(H_2O)_2$ (1)

The structure of *(1)* consists of a noncentrosymmetric dinuclear $[(dpyam)_2Cu(C_2O_4)Cu(dpyam)_2]^{2+}$ cation, two non-coordinated PF_6^- anions and two crystallization water molecules. An ORTEP plot, together with the numbering scheme of the compound is shown in Figure 1, with relevant distances and angles in Table 2.

The chromophore of *(1)* is very similar to the recently published compounds $[Cu_2(dpyam)_4(C_2O_4)](ClO_4)_2(H_2O)_3$ and $[Cu_2(dpyam)_4(C_2O_4)](BF_4)_2(H_2O)_3$ [12]. The two copper(II) ions of the complex cation are linked through an oxalato bridge, leading to a Cu...Cu distance of 5.737(2) Å. The copper atoms are involved in the rather unique $CuN_2O_2N'_2$ (4 + 2) chromophore, and lie in the uncommon compressed rhombic octahedral environment. The equatorial coordination positions are occupied by two oxalate oxygen atoms and two nitrogen atoms of the dpyam ligand (Cu—O and Cu—N distances range from 1.992 to 2.448 Å) and the other two nitrogen atoms from each dpyam ligand in axial positions (Cu—N bond lengths in the 1.979–2.098 Å range). There is a very slight tetrahedral distortion of the equatorial planes [dihedral angles between CuN_2 and CuO_2 planes = 3.2° and 1.2° for Cu(1) and Cu(2) centers, respectively], therefore both four-donor atoms basal planes are planar [r.m.s.d's = 0.0263 and 0.0028 Å] and the copper atoms are displaced by 0.0350 and 0.0168 Å from the basal planes toward N(5) and N(11) atoms for the Cu(1) and Cu(2) centers, respectively. The two basal planes are parallel to each other with dihedral angle of 1.4°. The oxalate divalent anion is planar (r.m.s.d = 0.0132) and it bridges the two copper atoms in the nearly symmetric mode of coordination. The copper atoms deviate by 0.2339, −0.1947 Å for the Cu(1) and Cu(2), respectively, from the oxalate plane. The dimeric entity is slightly folded in a chair form, the basal planes make the angles of 7.2° and 5.7° and with the oxalate mean plane.

The lattice is similarly further stabilized by hydrogen bonding between amine-N and F_{PF6} (N—O distances 3.075–3.391 Å) and O_{water} (N—O distances 2.952–

Table 1. Crystal and refinement data for complexes *(1)* and *(2)*

Complexes	*(1)*	*(2)*
Molecular formula	$[Cu_2(dpyam)_4(\mu\text{-}C_2O_4)](PF_6)_2(H_2O)_2$	$[Cu_2(dpyam)_2(\mu\text{-}C_2O_4)(NO_3)_2(CH_3)_2NCOH)_2]$
Molecular weight	1226.86	829.73
T(K)	293(2)	293(2)
Crystal system	Monoclinic	Triclinic
Space group	Pc	P1
a (Å)	8.5712(2)	8.353(2)
b (Å)	11.3170(2)	9.100(2)
c (Å)	25.8680(5)	12.245(3)
α (°)	90	72.035(4)
β (°)	82.6150(10)	75.228(4)
γ (°)	90	78.552(4)
V (Å^3)	2488.39	848.8(4)
Z	2	1
D_{calc} (g cm^{-3})	1.637	1.623
μ (mm)	1.025	1.330
F(000)	1238	426
Crystal size (mm)	0.25 × 0.30 × 0.43	0.303 × 0.253 × 0.106
Reflection collected	17,865	7532
Unique reflections	10,999 (R_{int} = 0.0407)	6784 (R_{int} = 0.0101)
Observed ref. [$I > 2\sigma(I)$]	7695	6045
Data/restraints/parameter	10,999/2/707	6784/3/534
Goodness-of-fit	1.035	1.063
Final R indices [$I > 2\sigma(I)$]	$R1$ = 0.0657, wR_2 = 0.1686	$R1$ = 0.0377, wR_2 = 0.1011
R indices (all data)	$R1$ = 0.0944, wR_2 = 0.1921	$R1$ = 0.0434, wR_2 = 0.1067
Largest difference peak and hole (e Å^{-3})	1.093 and −0.665	0.365 and −0.389

$R = \sum||F_o|-|F_c||/\sum|F_o||$, $R_w = \{\sum w\{|F_o|-|F_c|\}^2/w|F_o|^2\}^{1/2}$.

Table 2. Selected bond lengths (Å) and angles (°) with e.s.d.s. in parentheses of *(1)* and *(2)*

$[Cu_2(dpyam)_4(\mu\text{-}C_2O_4)](PF_6)_2(H_2O)_2$ *(1)*					
Cu(1)—N(4)	1.992(10)	Cu(1)—N(2)	1.995(9)	Cu(1)—O(1)	2.029(9)
Cu(1)—N(5)	2.049(7)	Cu(1)—N(1)	2.191(6)	Cu(1)—O(2)	2.424(6)
Cu(2)—N(8)	1.979(9)	Cu(2)—O(4)	2.025(8)	Cu(2)—N(7)	2.027(7)
Cu(2)—N(11)	2.098(8)	Cu(2)—N(10)	2.249(8)	Cu(2)—O(3)	2.448(8)
Cu(1)...Cu(2)	5.737(2)				
N(4)—Cu(1)—N(2)	93.0(4)	N(4)—Cu(1)—O(1)	174.7(3)		
N(2)—Cu(1)—O(1)	86.6(4)	N(4)—Cu(1)—N(5)	87.13)		
N(2)—Cu(1)—N(5)	170.4(3)	O(1)—Cu(1)—N(5)	92.5(3)		
N(4)—Cu(1)—N(1)	96.8(3)	N(2)—Cu(1)—N(1)	87.4(3)		
O(1)—Cu(1)—N(1)	88.4(3)	N(5)—Cu(1)—N(1)	102.1(3)		
N(4)—Cu(1)—O(2)	99.7(3)	N(2)—Cu(1)—O(2)	88.6(3)		
O(1)—Cu(1)—O(2)	75.0(3)	N(5)—Cu(1)—O(2)	82.0(3)		
N(1)—Cu(1)—O(2)	163.1(3)	N(8)—Cu(2)—O(4)	90.9(3)		
N(8)—Cu(2)—N(7)	88.7(4)	O(4)—Cu(2)—N(7)	173.8(3)		
N(8)—Cu(2)—N(1)1	171.5(4)	O(4)—Cu(2)—N(11)	89.4(3)		
N(7)—Cu(2)—N(11)	90.1(3)	N(8)—Cu(2)—N(10)	101.5(3)		
O(4)—Cu(2)—N(10)	87.2(3)	N(7)—Cu92)—N(10)	98.9(4)		
N(11)—Cu(2)—N(10)	87.0(3)	N(8)—Cu(2)—O(3)	79.9(4)		
O(4)—Cu(2)—O(3)	75.0(2)	N(7)—Cu(2)—O(3)	98.8(3)		
N(11)—Cu(2)—O(3)	91.9(3)	N(10)—Cu(2)—O(3)	162.2(3)		
$[Cu_2(dpyam)_2(\mu\text{-}C_2O_4)(NO_3)_2((CH_3)_2NCOH)_2]$ *(2)*					
Cu(1)—N(2)	1.979(7)	Cu(1)—N(1)	1.990(6)	Cu(1)—O(2)	2.005(6)
Cu(1)—O(1)	2.012(6)	Cu(1)—O(5)	2.254(7)	Cu(2)—N(4)	1.956(7)
Cu(1)—O(10B)	2.786(2)	Cu(1)—O(8B)	2.679(2)	Cu(2)—N(5)	1.973(7)
Cu(2)—O(4)	1.978(5)	Cu(2)—O(3)	2.002(6)	Cu(2)—O(6)	2.295(7)
Cu(1)...Cu(2)	5.212(2)				
N(2)—Cu(1)—N(1)	90.8(3)	N(2)—Cu(1)—O(2)	173.1(3)		
N(1)—Cu(1)—O(2)	92.1(2)	N(2)—Cu(1)—O(1)	93.2(2)		
N(1)—Cu(1)—O(1)	170.4(3)	O(2)—Cu(1)—O(1)	82.9(2)		
N(2)—Cu(1)—O(5)	89.2(3)	N(1)—Cu(1)—O(5)	92.7(3)		
O(2)—Cu(1)—O(5)	96.8(2)	O(1)—Cu(1)—O(5)	96.1(3)		
N(4)—Cu(2)—N(5)	92.1(3)	N(4)—Cu(2)—O(4)	170.6(3)		
N(5)—Cu(2)—O(4)	92.8(2)	N(4)—Cu(2)—O(3)	91.0(3)		
N(5)—Cu(2)—O(3)	169.2(3)	O(4)—Cu(2)—O(3)	82.8(2)		
N(4)—Cu(2)—O(6)	90.0(3)	N(5)—Cu(2)—O(6)	93.0(3)		
O(4)—Cu(2)—O(6)	97.8(2)	O(3)—Cu(2)—O(6)	97.4(3)		

Symmetry code: *B*; *x*, *y*, *z*−1.

2.965 Å) and between the O_{water} and F_{PF6} (O—F distance 3.088 Å) and $O_{oxalate}$ (O—O distances 2.956–3.348 Å).

Crystal structure of $[Cu_2(dpyam)_2(\mu\text{-}C_2O_4)(NO_3)_2(C_3H_7NO)_2]$ *(2)*

The asymmetric unit consists of a non-centrosymmetric dinuclear $[Cu_2(dpyam)_2(C_2O_4)(NO_3)_2(C_3H_7NO)_2]$ molecules. A drawing of the dimeric structure showing the labeling scheme is given in Figure 2. Selected bond lengths and angles are reported in Table 2.

Compound *(2)* has two copper centers bridged by a planar bis(didentate) oxalate ligand. The geometry around each copper(II) ion is considered as an elongated octahedral environment with two nitrogen atoms of dpyam and two oxygen atoms of oxalate bridge (Cu—N/O distances 1.956(7)–2.012(6) Å) in the equatorial plane CuN_2O_2, with the axial sites occupied by an oxygen atom of the DMF group [Cu—O 2.295(7) and 2.254(7) Å] and the oxygen atom of the nitrato group [Cu—O 2.786 and 2.679 Å], giving an approximately $CuN_2O_2O'O''$ chromophore (Figure 2). The four basal atoms are not coplanar, showing a slight but significant tetrahedral distortion with dihedral angles of 10.2° and 12.4° formed between the O—Cu—O and N—Cu—N planes for Cu(1) and Cu(2) centers, respectively. The copper atoms are displaced by 0.1259 and 0.1530 Å from the basal planes toward O(5) and O(6) atoms for Cu(1) and Cu(2) centers, respectively in the opposite side. The dimeric entity is slightly folded: the equatorial planes make the angles of 12.5° and 15.4° with the mean plane of the oxalate ligand. As a result, the dinuclear complex displays a chairlike structure. However, because of the copper atoms, the central Cu—OX—Cu core is planar (see Figure 2). The copper–copper separation across the oxalate bridge is 5.212 Å. The axial C_3H_7NO—Cu—O-NO_2 angles are 165.9° and 168.6°. The copper atoms deviate by −0.2651 and 0.2570 Å for the Cu(1) and Cu(2), respectively from the oxalate planes.

The lattice structure is stabilized by hydrogen bonding between the amine-N and the nitrate-O of a neighboring

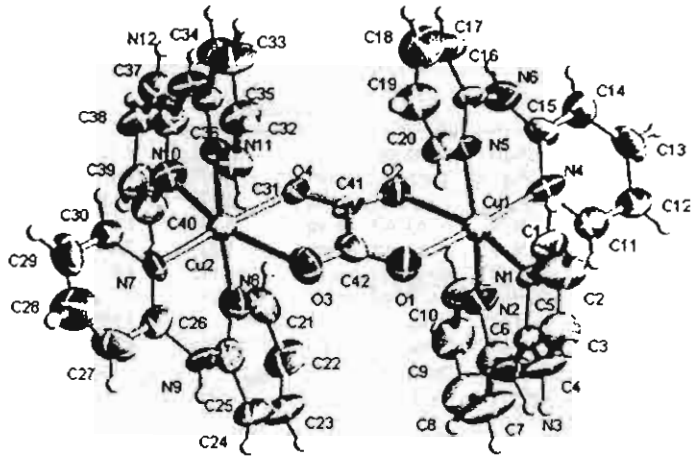

Fig. 1. ORTEP 50% probability plot of the cation in $[Cu_2(dpyam)_4(\mu\text{-}C_2O_4)](PF_6)_2(H_2O)_2$ *(1)*.

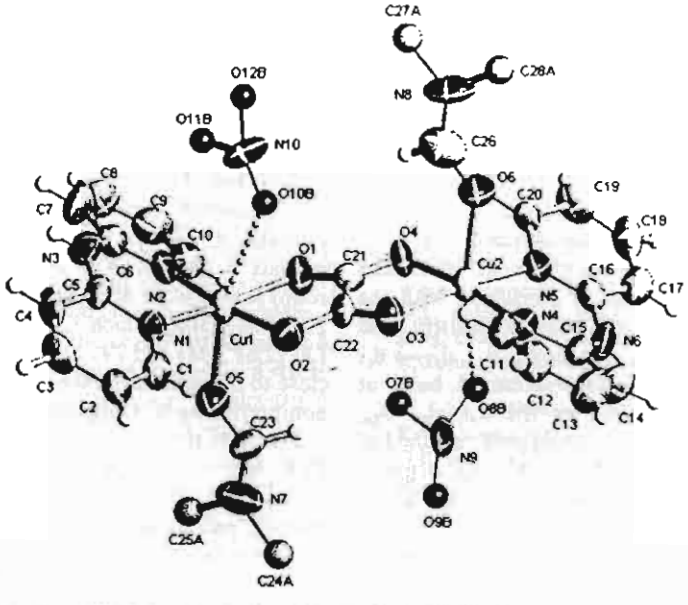

Fig. 2. ORTEP 50% probability plot of $[Cu_2(dpyam)_2(\mu\text{-}C_2O_4)(NO_3)_2((CH_3)_2NCOH)_2]$ *(2)*.

unit with distances of 2.803–3.164 Å, resulting in a polymeric chain.

Structure comparisons

The chromophore of *(1)* is very similar to the recently published compounds $[Cu_2(dpyam)_4(C_2O_4)](ClO_4)_2(H_2O)_3$ *(3)* and $[Cu_2(dpyam)_4(C_2O_4)](BF_4)_2(H_2O)_3$ *(4)* [12], Table 3 which exhibit the compressed octahedral $CuN_2O_2N_2$ chromophore. The axially compressed octahedral (2 + 4) geometry was rarely found in dinuclear-μ-oxalatodicopper(II) complexes. This geometry has only been previously observed in the dinuclear oxalato-bridged copper (II) complexes with a tetradentate-terminal ligand [7] and differs from compounds *(2)*, and *(5–10)* (Table 3) which exhibit axially-elongated (4 + 2) structure. The compounds *(1)*, *(3)* and *(4)* are three rare examples of 2 + 4 compressed rhombic coordination with a didentate-terminal ligand resulting from a pseudo Jahn–Teller effect. As in almost all the cases of observed Jahn–Teller compression examined in detail to date, the apparent compression is due to dynamic interconvertion between two of the possible axial elongation [16, 17]. There is some similarity to other dinuclear-μ-oxalatodicopper(II) complexes which exhibit a square-pyramidal structure with two oxygen atoms

Table 3. Structural data and magnetic properties for *12* selected oxalato-bridged Cu(II) complexes

Compounds[a]	Donor set	Geometry[b]	Oxalato-bridged Coordination	d_{Cu-Cu} (Å)	Dihedral angle[c]	Mode of magnetic interaction	J (cm^{-1})	Ref.
$[Cu_2(dpyam)_4(\mu\text{-}C_2O_4)](PF_6)_2 \cdot 2H_2O$ *(1)*	$O_2N_2N'_2$	comp. oct	eq–eq	5.737	7.16/5.73	c	–	This work
$[Cu_2(dpyam)_2(\mu\text{-}C_2O_4)(NO_3)_2(DMF)_2]$ *(2)*	$O_2N_2O'O$	elong. oct	eq–eq	5.213	9.9/12.8	a	–	This work
$[Cu_2(dpyam)_4(\mu\text{-}C_2O_4)](ClO_4)_2 \cdot 3H_2O$ *(3)*	$O_2N_2N'_2$	comp. oct	eq–eq	5.752	11.3/11.3	c	2.42	[12]
$[Cu_2(dpyam)_4(\mu\text{-}C_2O_4)](BF_4)_2 \cdot 3H_2O$ *(4)*	$O_2N_2N'_2$	comp. oct	eq–eq	5.745	11.4/11.0	c	3.38	[12]
$[Cu_2(dpyam)_2(\mu\text{-}C_2O_4)(NO_3)_2(DMSO)_2]$ *(5)*	$O_2N_2O'O$	elong. oct	eq–eq	5.22	7.0	a	−305	[12]
$[Cu_2(bpy)_2(\mu\text{-}C_2O_4)(NO_3)_2(H_2O)_2]$ *(6)*	$O_2N_2O'O''$	elong. oct	eq–eq	5.143	4.6	a	−382	[1]
$[Cu_2(mpym)_2(\mu\text{-}C_2O_4)(NO_3)_2(H_2O)_2]$ *(7)*	$O_2N_2O'O''$	elong. oct	eq–eq	5.217	d	a	−142	[3]
$[Cu_2(deen)_2(\mu\text{-}C_2O_4)(ClO_4)_2(H_2O)_2]$ *(8)*	$O_2N_2O'O''$	elong. oct	eq–eq	d	3.88	a	−300	[4]
$[Cu_2(tacn)_2(\mu\text{-}C_2O_4)(ClO_4)_2]$ *(9)*	O_2N_3O'	elong. oct	eq–eq	5.176	d	a	−41	[5]
$[Cu_2(bpca)_2(\mu\text{-}C_2O_4)(H_2O)_2](H_2O)_2$ *(10)*	O_2N_3O'	elong. oct	ax–eq	5.631	d	b	1.1	[6]
$[Cu_2(bispicen)_2(\mu\text{-}C_2O_4)](ClO_4)_2$ *(11)*	$O_2N_2N'_2$	comp. oct	eq–eq	5.608	d	c	2.3	[7]
$[Cu_2(bispicMe_2en)_2(\mu\text{-}C_2O_4)](ClO_4)_2$ *(12)*	$O_2N_2N'_2$	comp. oct	eq–eq	5.494	d	c	2.14	[7]

[a] dpyam – di-2-pyridylamine; bpy – 2,2′-dipyridine; mpym – meripirizole; deen – *N,N*-diamine; tacn – 1,4,7-triazacyclonone; bpca – bis(2-pyridylmethyl)1-3,3-propanediamine; bispicen – *N,N′*-bis(2-pyridylmethyl)-1,2-ethanediamine; bispicMe$_2$en – *N,N′*-bis(2-pyridylmethyl)-*N-N*-dimethyl-1,2-ethanediamine.

[b] comp.oct – compressed octahedral; elong. oct – elongated octahedral.

[c] Dihedral angle between the basal and oxalate planes.

[d] Not reported.

of oxalate bridge and two nitrogen atoms of the diamine occupying the base of the pyramid and the counter anion or a solvent molecule occupying the axial position-[1–10].

Spectroscopic properties

The electronic diffuse reflectance spectrum of *(1)* consists of two clearly resolved peaks at 14.49 and 8.90×10^3 cm^{-1}. This spectrum is consistent with the compressed rhombic octahedral stereochemistry and assigned to be the $d_{x^2-y^2} \rightarrow d_{z^2}$ and the $d_{xz},d_{xy}, d_{yz} \rightarrow d_{z^2}$ transitions. Compound *(2)* shows a broad band at 14.22×10^3 cm^{-1}, corresponding to the d_{z^2}, d_{xz}, d_{xy}, $d_{yz} \rightarrow d_{x^2-y^2}$ transition of the elongated octahedral stereochemistry. The i.r. spectrum of *(1)* displays characteristic bands of the oxalate bridging ligand [2, 4–6]: ν_{asym}(C—O) at 1655s and ν_{sym}(C—O) at 1356 m. A weak signal of the δ(O—C—O) bending at 850 m cm^{-1} is superimposed by the strong band at *ca.* 849 cm^{-1} of the F–P–F stretching mode of the PF_6^- groups. That of *(2)* shows the characteristic bands of the oxalate bridging ligand: ν_{asym}(C—O) at 1653s, ν_{sym}(C—O) at 1356 m and δ(O—C—O) at 823 m cm^{-1} and the absorption frequencies at 1384, 1332 and 1034 cm^{-1} suggesting monodentate coordination of the nitrate ion.

The polycrystalline powder e.p.r. spectrum at room temperature of compound *(1)* displays a broad absorption centered around g of 2.09. No half-field signal was observed at room temperature. Complex *(1)* was also measured as solids at 77 K, in which the signal appears as more resolved at $g_\perp = 2.05$, $g_{//} = 2.21$, corresponding to the pattern of Cu(II) in an elongated geometry, $g_{//} > g_\perp > 2.0$ with the $d_{x^2-y^2}$ ground state. This suggests that the apparent compressed geometry at room temperature could be caused by a dynamic Jahn–Teller effect [16, 17]. This is because compound *(1)* adopts the time averaged structure found crystallographically which arises due to the short time scale of the X-ray technique, but the e.p.r. spectra at 77 K are related to the underlying static axial elongated chromophore [16, 17]. Also the half-field signal at approximately 1600 G, corresponding to $\Delta M = \pm 2$ transition was observed, which indicates that indeed a weak interaction between two Cu(II) ions within these compounds is present. The effective magnetic moment at room temperature of compound *(1)* was measured to be 2.55 BM/dimer, which is comparable to the values of *(3)* (2.62 BM) and *(4)* (2.64 BM) [12]. These values are close to the spin only value of 2.45 BM expected for two noninteracting d^9 Copper(II) ions.

The structure, structural distortions, electronic and EPR spectra and the effective magnetic moment of compound *(1)* are very comparable to those of the recently published compounds *(3)* and *(4)*. The magnetic orbitals (d_{z^2}) are perpendicular to the oxalate plane, so the overlap of the oxalate σ orbitals. This situation is corresponding to the coordination mode C, Scheme 1 and consequently a very weak ferromagnetic interaction is expected for *(1)*, based on the previously reported singlet-triplet energy gap (J) of 2.42 cm^{-1} for *(3)* and +3.38 cm^{-1} for *(4)* [12].

The room temperature e.p.r. spectrum of *(2)* appears to be an asymmetric broad resonance with a center at $g = 2.10$. The observed triplet signal is not resolved, apparently due to exchange narrowing, resulting from nearby triplet molecules in the lattice. That of *(2)* recorded at 77 K is better resolved than the room-temperature and shows resolved hyperfine resonances on the low field side of the $\Delta M = \pm 1$ signal due to the coupling of the unpaired electrons with two equivalent copper nuclei and is indicative for a small zero-field splitting. So the observed signal is typical for triplet copper (II) dinuclear in an isolated state [18, 19] with a

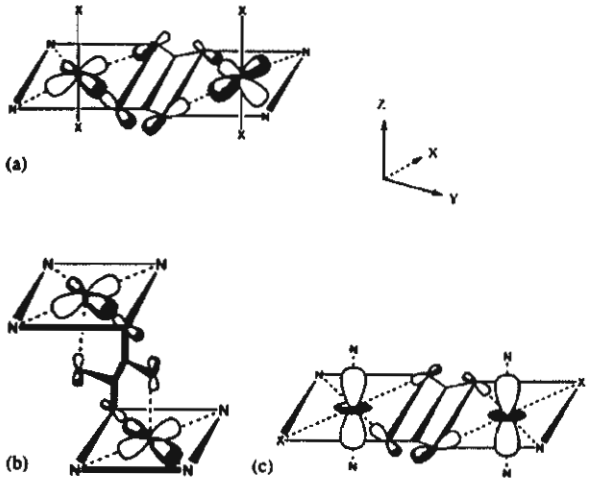

Scheme 1. Three models predicting the magnetic interaction in oxalato-bridged Cu(II) complexes [X = O *(1)* or N *(2)*].

small amount of triplet signal thermally accessible at 77 K. The weak signals resolved are observed with $g_{//}$ *ca.* 2.37 and $g_{\perp}$ *ca.* 2.07, are likely to originate from a small paramagnetic impurity. The room temperature magnetic moment of *(2)* is 2.16 BM/dimer, which is smaller than the value of 2.45 BM expected for two noninteracting d^9 Cu(II) ions and is expected to become almost diamagnetic as confirmed by the EPR spectrum at 77 K.

The structure of *(2)* displays an elongated tetragonal octahedral, which is very similar to that of the recently published [12] compound $[Cu_2(dpyam)_2(C_2O_4)(NO_3)_2(DMSO)_2]$ *(5)*. In this case the copper(II) magnetic orbital ($d_{x^2-y^2}$) interacts with the oxalate σ orbital, which consistent with the coordination mode a, Scheme 1. Compound *(5)* was found to display a strong antiferromagnetic interaction with a singlet-triplet gap(J) of -305.1 cm^{-1}. Therefore compound *(2)* is expected to exhibit a strong antiferromagnetic interaction between copper(II) ions of a dimeric unit, which is confirmed by the effective magnetic moment and e.p.r. spectrum.

Conclusions

Dimeric copper (II) complexes of the form $[(dpyam)_{1\text{ or }2}Cu(\mu\text{-}C_2O_4)Cu(dpyam)_{1\text{ or }2})]X_2$, have been characterized by spectroscopic and magnetic results. Compound *(1)* displays the compressed octahedral copper(II) geometry with asymmetrically bound oxalate ligand, which is similar to those the recently published compounds $[Cu_2(dpyam)_4(C_2O_4)](ClO_4)_2(H_2O)_3$ *(3)* and $[Cu_2(dpyam)_4(C_2O_4)](BF_4)_2(H_2O)_3$ *(4)*. Thus *(1)* is expected to exhibit a very weak ferromagnetic interaction. On the other hand compound *(2)* has an elongated tetragonal octahedral geometry with a symmetric oxalate bridge which is very similar to the recently characterized compound $[Cu_2(dpyam)_2(C_2O_4)(NO_3)_2(DMSO)_2]$ *(5)*. Therefore a strong antiferromagnetic interaction is expected for the compound *(2)*. These conclusions have been confirmed structurally and spectroscopically as well as the efficient magnetic moment. This work confirms that the exchange interaction between the copper(II) ions propagated through the oxalate bridge is strongly dependent on the geometry around the copper ions, sensitive to the orientation of the magnetic orbital of each copper(II), relative to the oxalate plane and the bridging mode of the oxalate group.

Acknowledgements

The authors would like to thank The Thailand Research Fund and Khon Kaen University for a research grant. Support of the Postgraduate Education and Research Program in Chemistry is also gratefully acknowledged. The work described in the present paper has been supported by the Leiden University Study group WFMO (Werkgroep Fundamenteel MaterialenOnderzoek).

References

1. O. Castillo, I. Muga, A. Luque, J.M. Gutierrez-Zorrilla, J. Sertucha, P. Vitoria and P. Román, *Polyhedron*, **18**, 1235 (1999).
2. J. Tang, E. Gao, W. Bu, D. Liao, S. Yan, Z. Jiang and G. Wang, *J. Mol. Struct.*, **525**, 271 (2000).
3. L.S. Tuero, J. Garcia-Lozano, E.E. Monto, M.B. Borja, F. Dahan, J.P. Tuchagues and J.P. Legros, *J. Chem. Soc., Dalton Trans.*, 2619 (1991).
4. R. Vicente, A. Escuer, J. Ferretjans, H. Stoeckli-Evans, X. Solans and M. Font-Bardía, *J. Chem. Soc., Dalton Trans.*, 167 (1997).
5. L. Zhang, W.-M. Bu, S.-P. Yan, Z.-H. Jiang, D.-Z. Liao and G.-L. Wang, *Polyhedron*, **19**, 1105 (2000).
6. M.L. Calatayud, I. Castro, J. Sletten, F. Lloret and M. Julve, *Inorg. Chim. Acta.*, **300–302**, 846 (2000).
7. J. Glerup, P.A. Goodson, D.J. Hodgson and K. Michelsen, *Inorg. Chem.*, **34**, 6255 (1995).
8. M. Julve, M. Verdaguer, A. Gleizes, M. Philoche-Levisalles and O. Kahn, *Inorg. Chem.*, **23**, 3808 (1984).
9. G.R. Hall, D.M. Duggan and D.N. Hendrickson, *Inorg. Chem.*, **14**, 1956 (1975).
10. Y. Akhriff, J. Server-Carrió, A. Sancho, J. Garcia-Lozano, E. Escrivá, J.V. Folgado and L. Soto, *Inorg. Chem.*, **38**, 1174 (1999).
11. M. Du, Y.-M. Guo and X.-H. Bu, *Inorg. Chim Acta*, **335**, 136 (2002).
12. S. Youngme, G.A. Albada, N. Chaichit, P. Gunnasoot, P. Kongsaeree, I. Mutikainen, O. Roubeau, J. Reedijk and U. Turpeinen, *Inorg. Chim. Acta.*, **353**, 119 (2003).
13. SAINT, Data Integration Software, Version 6.12, Bruker AXS, Inc., Madison, WI, 1997.
14. G.M. Sheldrick, SADABS, Program for empirical absorption correction of area detector data, University of Göttingen, Germany, 1996.
15. SHELXTL 6.1 (PC-Version), Program library for the solution and molecular graphics, Siemens Analytical Instruments Division, Madison, WI, U.S.A.
16. B.J. Hathaway, M. Duggan, A. Murphy, J. Mullane, C. Power, A. Waslsh and B. Walsh, *Coord. Chem. Rev.*, **36**, 267 (1981).
17. B.J. Hathaway, *Struct. Bonding (Berlin)*, **57**, 203 (1984).
18. V.T. Kasumov, F. Köksal and Z. Anorg *Allg. Chem.*, **627**, 2553 (2001).
19. E. Wasserman, L.C. Snyder and W.A. Yager, *J. Chem. Phys.*, **25**, 1763 (1964).

PUBLICATION PAPERS OF PART II

Available online at www.sciencedirect.com
SCIENCE DIRECT
Inorganica Chimica Acta 357 (2004) 3603–3612
Inorganica Chimica Acta
www.elsevier.com/locate/ica

The coordination chemistry of mono(di-2-pyridylamine) copper(II) complexes with monovalent and divalent oxoanions: crystal structure, spectroscopic and magnetic properties of dinuclear $[Cu(L)(\mu\text{-}H_2PO_4)(H_2PO_4)]_2$ and polynuclear $[Cu(L)(\mu_3\text{-}HPO_4)]_n$

Sujittra Youngme [a,*], Pongthipun Phuengphai [a], Narongsak Chaichit [b], Chaveng Pakawatchai [c], Gerard A. van Albada [d], Olivier Roubeau [e], Jan Reedijk [d]

[a] Department of Chemistry, Faculty of Science, Khon Kaen University, Khon Kaen 40002, Thailand
[b] Department of Physics, Faculty of Science and Technology, Thammasat University Rangsit, Pathumthani 12121, Thailand
[c] Department of Chemistry, Faculty of Science, Prince of Songkla University, Hatyai, Songkla 90112, Thailand
[d] Leiden Institute of Chemistry, Gorlaeus Laboratories, Leiden University, P.O. Box 9502, 2300 RA Leiden, The Netherlands
[e] Centre de Recherche Paul Pascal – CNRS, 115 avenue du dr. A. Schweitzer, 33600 Pessac, France

Received 5 February 2004; accepted 17 April 2004
Available online 20 July 2004

Abstract

The crystal structures of two copper(II) complexes containing the ligand di-2-pyridylamine (dpyam) with monovalent $H_2PO_4^-$ and divalent HPO_4^{2-} oxoanions, $[Cu(dpyam)(\mu\text{-}H_2PO_4\text{-}O,O')(H_2PO_4)]_2$ (**1**) and $[Cu(dpyam)(\mu_3\text{-}HPO_4\text{-}O,O',O'')]_n$ (**2**), are reported and determined by X-ray crystallography. The dinuclear Cu(II) complex **1** was obtained by the reaction of dpyam with $Cu(NO_3)_2 \cdot 3H_2O$ and KH_2PO_4 in a water–ethanol (45/55) mixture. The molecules are linked into dinuclear units by two bridging didentate dihydrogenphosphate groups (*endolexo*) in an equatorial–equatorial configuration giving a slightly distorted square pyramidal stereochemistry. The Cu–Cu contact distance of 5.136(2) Å is unusually large due to the *exolendo* binding of the phosphate bridges. Complex **2** is a polymeric copper(II) derivative with helical $[Cu(HPO_4)]_3$ units surrounded by dpyam ligands and stabilized by intermolecular hydrogen bonds. Two nearest Cu(II) ions are bridged by a tridentate hydrogenphosphate group which is didentately coordinated to one copper(II) ion, and monodentately coordinated to another in an equatorial–equatorial configuration in an unusual bridging coordination mode. Each copper(II) ion in **2** exhibits a tetrahedrally distorted square-based geometry with the third oxygen atom (Cu–O = 2.719(3) Å), from the hydrogenphosphate group weakly bound in an approximately axial position giving an extremely tetrahedrally distorted square-based pyramidal CuN_2O_2O' chromophore. The magnetic susceptibility measurements (5–300 K) reveals an antiferromagnetic interaction with J values of −2.85(1) and −26.20(2) cm^{-1} for complexes **1** and **2**, respectively. Some magneto-structural trends are discussed, along with their EPR and electronic reflectance spectra and compared with those of related complexes.

Keywords: Crystal structures; Copper(II) complexes; Dihydrogenphosphate complexes; Di-2-pyridylamine complexes

1. Introduction

The variety of complexes of copper(II) and didentate mono(chelating) ligand with monovalent and divalent oxoanions may be grouped in many classes for each type of oxoanions depending on the coordinating nature [1–23]. Complexes with monovalent oxoanions formulated as $Cu(chelate)(anion1)_2(H_2O)_n$ or $Cu(chelate)(anion1)(anion2)(H_2O)_n$ (in which anion1 and/or anion2 = NO_2^-, NO_3^-, ClO_4^-, $CH_3CH_2COO^-$, CH_3COO^- or $HCOO^-$) were found to exhibit four classes of local molecular structures, as summarized in

*Corresponding author. Tel.: +66-43-202-22241; fax :+66-43-202-373.
E-mail address: sujittra@kku.ac.th (S. Youngme).

0020-1693/$ - see front matter © 2004 Elsevier B.V. All rights reserved.
doi:10.1016/j.ica.2004.04.027

Scheme 1. These four classes can be described as follows: Class A: monomeric tetrahedrally distorted elongated octahedron with an extremely asymmetric didentate coordination of both oxoanions [1–12]; Class B: polymeric elongated tetragonal (or rhombic) octahedron with the nearly symmetric didentate coordination of a basal oxoanion and the bridging didentate coordination in the axial positions of the second one [12–15]; Class C: polymeric tetrahedrally distorted square pyramid with non-bridging monodentate and bridging didentate oxoanions [16] and Class D: dinuclear tetrahedrally distorted square pyramid with non-bridging monodentate and bridging didentate oxoanions [8,17].

Complexes with divalent oxoanions formulated as Cu(chelate)(anion)$(H_2O)_n$ (in which anion = CO_3^{2-} and

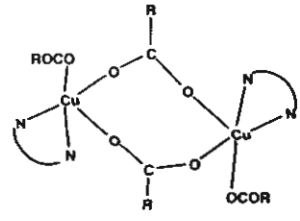

$[Cu_2(dpyam)_2(C_6H_3Cl_2OCH_2COO)_4]$(**3**) [30]

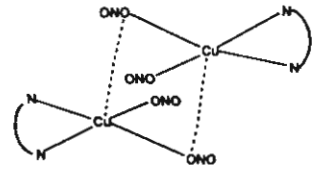

$[Cu_2(dpyam)_2(ONO)_2(\mu\text{-}ONO)_2]\cdot 2CH_3CN$ (**4**) [8]

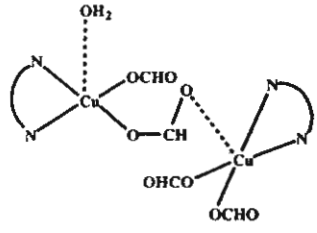

$[Cu_2(dpyam)_2(OH_2)(O_2CH)_4]\cdot H_2O$(**5**) [17]

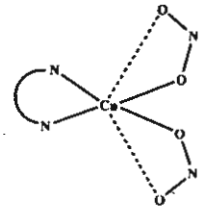

$[Cu(dpyam)(NO_2)_2]$(**6**) [7]

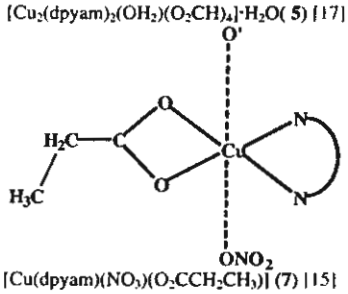

$[Cu(dpyam)(NO_3)(O_2CCH_2CH_3)]$ (**7**) [15]

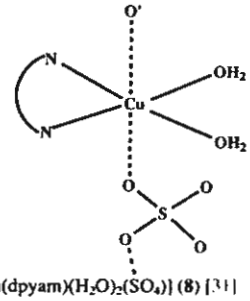

$[Cu(dpyam)(H_2O)_2(SO_4)]$ (**8**) [31]

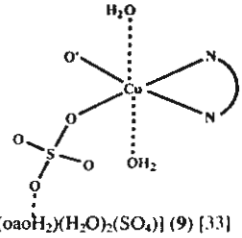

$[Cu(oaoH_2)(H_2O)_2(SO_4)]$ (**9**) [33]

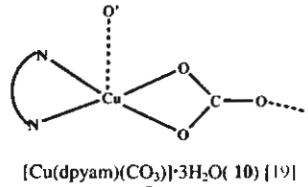

$[Cu(dpyam)(CO_3)]\cdot 3H_2O$(**10**) [19]

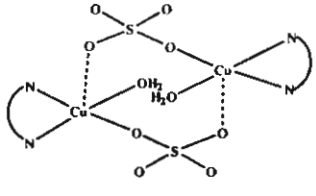

$[Cu_2(oaoH_2)_2(H_2O)_2(SO_4)_2]$(**11**) [32]

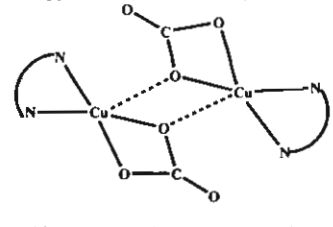

$[Cu_2(dpyam)_2(CO_3)_2]\cdot H_2O$(**12**) [23]

Scheme 1. Representation of the coordination modes described to date for the mono(chelate) copper(II) complexes with monovalent and divalent oxoanions.

SO_4^{2-}) exhibit five classes of local molecular structures, namely: Class A: monomeric distorted square-based pyramid with didentate oxoanion [18]; Class B: polymeric distorted square-based pyramid with bridging tridentate oxoanions [19]; Class C: monomeric square-based pyramid with monodentate oxoanion [20]; Class D: polymeric elongated octahedron with bridging didentate oxoanions [21,22]; Class E: dinuclear distorted square-based pyramid with double bridges of tridentate oxoanions [23].

We now extended our studies towards mono-, di- and trivalent tetraoxophosphate anions. In this study, the compounds [Cu(dpyam)(μ-H_2PO_4-O,O′)(H_2PO_4)]$_2$ (1) and [Cu(dpyam)(μ_3-HPO_4-O,O′,O″)]$_n$ (2) have been synthesized and characterized. They contain monovalent $H_2PO_4^-$ and divalent HPO_4^{2-} oxoanions and their X-ray structures, spectroscopic properties and magnetic behaviour are investigated and discussed in the context of a magneto-structural correlation study. These two structures appear to belong to class D and class B, for 1 and 2, respectively.

2. Experimental

2.1. General

All reagents were commercial grade materials and were used without further purification. Elemental analyses (C, H, N) were determined on a Perkin–Elmer PE2400 CHNS/O Analyzer by the Microanalytical Service of Science and Technological Research Equipment Centre, Chulalongkorn University.

2.2. Syntheses of the compounds

2.2.1. [Cu(dpyam)(μ-H_2PO_4-O,O′)(H_2PO_4)]$_2$ (1) and [Cu(dpyam)(μ_3-HPO_4-O,O′,O″)]$_n$ (2)

An aqueous solution (30 ml) of $Cu(NO_3)_2 \cdot 3H_2O$ (0.241 g, 1.0 mmol) was added to a solution of dpyam (0.171 g, 1.0 mmol) in ethanol (15 ml) and followed by an aqueous solution (20 ml) of potassium dihydrogenphosphate (0.272 g, 2.0 mmol). The resulting green solution was allowed to evaporate at room temperature. After several days, dark green crystals of [Cu(dpyam)(μ_3-HPO_4-O,O′,O″)]$_n$ (2) (*Anal.* Calc. for $C_{10}H_{10}CuN_3O_4P$: C, 36.32; H, 3.05; N, 12.71. Found: C, 36.25; H, 2.98; N, 12.67%) were deposited. Yield: ca. 40%. Subsequently, green needle crystals of [Cu_4(dpyam)$_4$(μ_3,η^3-HPO_4)$_2$(NO_3)$_2$(H_2O)$_2$](NO_3)$_2 \cdot 2H_2O$ (*Anal.* Calc. for $C_{40}H_{46}Cu_4N_{16}O_{24}P_2$: C, 33.13; H, 3.19; N, 15.45. Found: C, 33.20; H, 3.04; N, 15.52%) were deposited in the second crystallization. Yield: ca. 30%. This complex was obtained as a side product and has also been characterized crystallographically (to be published separately). Greenish-blue crystals of [Cu(dpyam)(μ-H_2PO_4-O,O′)(H_2PO_4)]$_2$ (1) were obtained in the final crystallization. They were filtered off, washed with the

Table 1
Crystal and refinement data for complexes 1 and 2

Complex	1	2
Molecular formula	$C_{20}H_{26}Cu_2N_6O_{16}P_4$	$C_{10}H_{10}CuN_3O_4P$
Molecular weight	857.44	330.72
T (K)	293(2)	293(2)
Crystal system	triclinic	trigonal
Space group	$P\bar{1}$	$P3/2$
a (Å)	8.0347(1)	9.6644(1)
b (Å)	10.0264(1)	9.6644(1)
c (Å)	10.5912(1)	10.6841(2)
α (°)	83.217(1)	90
β (°)	70.490(1)	90
γ (°)	69.356(1)	120
V (Å^3)	752.58(2)	864.21(2)
Z	2	2
D_{calc} (g cm^{-3})	1.892	1.271
μ (mm^{-1})	1.712	1.365
F(000)	434	334
Crystal size (mm)	0.15×0.35×0.50	0.28×0.30×0.20
θ Range (°)	2.04–30.48	2.43–30.48
Number of reflections collected	5631	6496
Number of unique reflections	4101	3042
Data/restraints/parameter	4101/0/269	3042/1/212
Goodness-of-fit	1.065	1.030
Final R indices [$I > 2\sigma(I)$]	$R_1 = 0.0261$, $wR_2 = 0.0752$	$R_1 = 0.0186$, $wR_2 = 0.0451$
R indices (all data)	$R_1 = 0.0281$, $wR_2 = 0.0759$	$R_1 = 0.0192$, $wR_2 = 0.0452$
Largest difference peak and hole (e Å^{-3})	0.580 and −0.509	0.252 and −0.321

$R = \sum ||F_o| - |F_c|| / \sum |F_o||$, $R_w = [\sum w\{|F_o| - |F_c|\}^2 / w|F_o|^2|]^{1/2}$.

mother liquid and dried in air. Yield: ca. 20%. (*Anal.* Calc. for $C_{20}H_{26}Cu_2N_6O_{16}P_4$: C, 28.05; H, 3.03; N, 9.80. Found: C, 28.14; H, 2.93; N, 9.74%).

2.3. Crystal structure analyses

Reflection data for complexes **1** and **2** were collected at 293 K on a 1K Bruker SMART CCD area-detector diffractometer using graphite monochromated Mo Kα radiation ($\lambda = 0.71073$ Å). Data reduction and cell refinements were performed using the program SAINT [24]. An empirical absorption correction by using the SADABS [25] program was applied, which resulted in transmission coefficients ranging from 0.790 to 1.000 for **1** and from 0.854 to 1.000 for **2**. The structures ware solved by direct methods and refined by full-matrix least-squares method on $(F_{obs})^2$ with anisotropic thermal parameters for all non-hydrogen atoms using the SHELXTL-PC V 6.12 [26] software package. All hydrogen atoms in **1** and **2** were located by difference synthesis and refined isotropically. The molecular graphics were created by using SHELXTL-PC. The crystal and refinement details for **1** and **2** are listed in Table 1.

2.4. Physical measurements

IR spectra were recorded on a Spectrum One Perkin–Elmer FT-IR spectrophotometer as KBr pellets in the 4000–450 cm^{-1} spectral range. Diffuse reflectance measurements from 9090 to 20 000 cm^{-1} were recorded as polycrystalline samples using a Perkin–Elmer Lambda 2S spectrophotometer equipped with an intergrating sphere attachment. Barium sulfate was used as the reflectance standard. X-band powder EPR spectra were recorded on a JEOL RE2X electron spin resonance spectrometer using DPPH ($g = 2.0036$) as a standard. Magnetic susceptibility measurements (5–300 K) were carried out using a Quantum Design MPMS-5 5T SQUID magnetometer (measurements carried out at 1000 G) performed at Leiden University. Data were corrected for magnetization of the sample holder and for diamagnetic contributions, which were estimated from the Pascal constants.

3. Results and discussion

3.1. Description of the crystal structures

3.1.1. $[Cu(dpyam)(\mu\text{-}H_2PO_4\text{-}O,O')(H_2PO_4)]_2$ (1)

The structure is depicted in Fig. 1 together with the numbering scheme. Selected bond distances and angles are listed in Table 2. The centrosymmetric dinuclear compound consists of two [Cu(dpyam)(μ-H_2PO_4-O,O′)(H_2PO_4)] units being doubly bridged by two didentate dihydrogenphosphato anions. The local molecular structure of the copper atom involves a square pyramidal CuN_2O_2O' chromophore. The basal plane consists of two oxygen atoms of the two bridging dihydrogenphosphato groups, O(5) and O(8A) and of dpyam ligand coordinated through two nitrogen atoms. The dpyam ligand chelates in the square plane, almost symmetrically, with Cu–N distances of 1.991(1) and 1.997(1) Å and a bite angle of 88.1(1)°. The equatorial Cu(1)–O(8A) and Cu(1)–O(5) bond distances are slightly shorter with values of 1.964(1) and 1.987(1) Å. The fifth axial coordination site is occupied by one oxygen atom of non-bridging monodentate dihydrogenphosphato group at the Cu–O distance of 2.271(1) Å. The four in-plane atoms, N(1), N(2), O(5) and O(8A) are essentially planar (r.m.s. deviation 0.0598 Å), with a slightly tetrahedral twist (dihedral angles between the CuN_2 and CuO_2 planes = 14.0°). The Cu atom lies 0.16 Å above this plane towards O(1). The tetragonality, $T = 0.874$ based on the changes in bond lengths (T = the mean in-plane bond length/the mean out-of-plane bond length). The τ-value

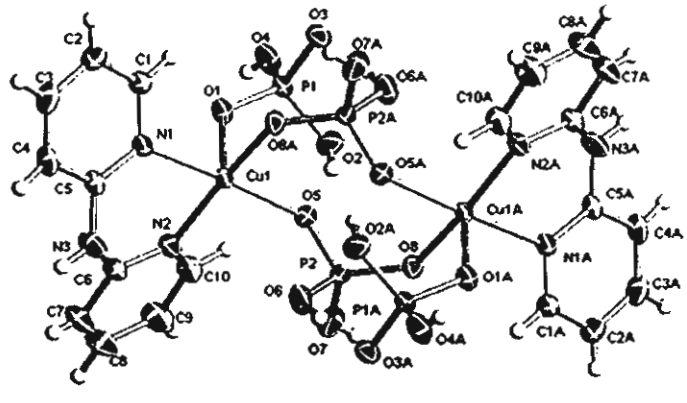

Fig. 1. ORTEP 50% probability plot of [Cu(dpyam)(μ-H_2PO_4)(H_2PO_4)]$_2$ (1). H-atoms are omitted for clarity. Atoms with an "A" are generated by an inversion centre.

Table 2
Selected bond lengths (Å) and angles (°) with e.s.d.s. in parentheses of compound **1**

Bond lengths			
Cu(1)–O(8)A	1.964(1)	Cu(1)–O(5)	1.987(1)
Cu(1)–N(1)	1.991(1)	Cu(1)–N(2)	1.997(1)
Cu(1)–O(1)	2.271(1)	P(1)–O(1)	1.512(1)
P(1)–O(3)	1.519(1)	P(1)–O(4)	1.558(1)
P(1)–O(2)	1.581(1)	P(2)–O(8)	1.506(1)
P(2)–O(5)	1.518(1)	P(2)–O(7)	1.558(1)
P(2)–O(6)	1.564(1)	Cu(1)–Cu(1)A	5.136(2)
Bond angles			
O(8)A–Cu(1)–O(5)	89.7(1)	O(8)A–Cu(1)–N(1)	89.0(1)
O(5)–Cu(1)–N(1)	174.1(1)	O(8)A–Cu(1)–N(2)	167.0(1)
O(5)–Cu(1)–N(2)	91.8(1)	N(1)–Cu(1)–N(2)	88.1(1)
O(8)A–Cu(1)–O(1)	96.0(1)	O(5)–Cu(1)–O(1)	91.9(1)
N(1)–Cu(1)–O(1)	94.1(1)	N(2)–Cu(1)–O(1)	96.8(1)
O(1)–P(1)–O(3)	115.1(1)	O(1)–P(1)–O(4)	112.2(1)
O(3)–P(1)–O(4)	106.9(1)	O(1)–P(1)–O(2)	109.2(1)
O(3)–P(1)–O(2)	108.5(1)	O(4)–P(1)–O(2)	104.1(1)
O(8)–P(2)–O(5)	115.6(1)	O(8)–P(2)–O(7)	109.6(1)
O(5)–P(2)–O(7)	105.9(1)	O(8)–P(2)–O(6)	112.6(1)
O(5)–P(2)–O(6)	105.6(1)	O(7)–P(2)–O(6)	106.8(1)
P(2)–O(5)–Cu(1)	130.9(1)	P(1)–O(1)–Cu(1)	122.9(1)

D–H···A (°)	D–H (Å)	H···A (Å)	D···A (Å)	D–H···A (°)
Hydrogen-bonding parameters				
N(3)–H(5)···O(3) [$x, 1+y, z$]	0.82(2)	2.362(19)	3.1603(19)	165(2)
O(4)–H(41)···O(1) [$-x, 1-y, 2-z$]	0.57(3)	2.02(3)	2.5825(18)	169(6)
O(6)–H(61)···O(3) [$1-x, 1-y, 1-z$]	0.79(3)	1.84(3)	2.631(2)	172(3)
O(7)–H(71)···O(3) [$1+x, y, z$]	0.62(4)	2.05(4)	2.648(2)	164(5)

Symmetry code: A, $-x+1, -y+1, -z+1$.

defined to describe the degree of trigonal distortion is 0.12 (τ describes the relative amount of trigonality; $\tau = 0$ for square pyramid and $\tau = 1$ for trigonal bipyramid) [27], so the geometry around the Cu(II) atom can be best described as square-based pyramidal, with only a slight trigonal distortion. The Cu–Cu distance is 5.136(2) Å.

The O(8)–P(2)–O(5) bridging angle of 115.7(1)° is larger than 109.5° of the ideal tetrahedral geometry, and the remaining angles involve less deviation from 109.5° [O(5)–P(2)–O(7) 105.9(1)°, O(5)–P(2)–O(6) 105.6(1)°, O(7)–P(2)–O(6) 106.8(1)° and O(8)–P(2)–O(6) 112.6(1)°]. The coordinated P–O bonds, 1.518(1) and 1.506(1) Å, are shorter than the uncoordinated P–OH bonds, 1.564(1) and 1.559(1) Å. These differences are normally found for the two-coordinate bridging coordination of the dihydrogenphosphate anion [28]. The non-bridging monodentate dihydrogenphosphato group involves O–P–O angles ranging from 104.1(1)° to 115.1(1)°. The P–OH bonds, 1.558(1) and 1.581(1) Å, are longer than the P=O bonds, 1.512(1) and 1.519(1) Å, which is in usual observation. The uncoordinated P=O bond distance, 1.519(1) Å, is slightly longer than the coordinated one, 1.511(1) Å, which is unusual. This difference arises from the hydrogen bond involved to the uncoordinated P=O bond. The P=O distances in both the monodentate dihydrogenphosphato group and the dihydrogenphosphato bridge are ranging from 1.506(1) to 1.519(1) Å, while the P–OH bond distances vary from 1.558(1) to 1.581(1) Å. This behaviour is consistent with the general observation that P–OH bonds are longer than P=O bonds in primary and secondary phosphates [28].

The lattice structures are stabilized by a hydrogen bonding network between the amine N and the oxygen atom of the non-bridged dihydrogenphosphate anion with a distance of 3.160(1) Å, and between oxygen atoms of different dihydrogenphosphate groups (O···O distances vary from 2.582(1) to 2.648(2) Å). Details of hydrogen bonding are given in Table 2 and a projection of the lattice is shown in Fig. 2.

3.1.2. *[Cu(dpyam)(μ_3-HPO$_4$-O,O′,O″)]$_n$ (2)*

The structure is depicted in Fig. 3 together with the numbering scheme. Selected bond distances and angles are listed in Table 3. The structure consists of a neutral and polymeric chains of [Cu(dpyam)(μ_3-HPO$_4$-O,O′,O″)] bridged by tridentate hydrogenphosphato ligands. The local molecular structure of the copper atom involves square pyramidal CuN_2O_2O' chromophore in an equatorial–equatorial configuration. The basal plane consists of two oxygen atoms from two equivalent bridging hydrogenphosphato groups and of a dpyam ligand coordinated through two nitrogen atoms. The dpyam ligand chelates in the tetragonal plane, almost symmetrically, with Cu–N distances of 1.969(1) and

Fig. 2. Showing the lattice structure of complex 1.

1.994(1) Å, and a bite angle of 92.0(6)°. The equatorial Cu(1)–O(1) and Cu(1)–O(4) bond distances are slightly shorter with values of 1.946(1) and 1.919(1) Å. The third oxygen atom from hydrogenphosphate group is bent towards the Cu atom to complete a fifth coordination site in an axial position at a much longer distance of 2.719(2) Å, generating a distorted square-based pyramidal stereochemistry. The four in-plane atoms, N(1), N(2), O(1) and O(4) are not planar (r.m.s. deviation 0.562 Å) and display a marked tetrahedral twist (dihedral angles between the CuN_2 and CuO_2 planes amounts to 45.56°). The Cu atom lies 0.202 Å above this plane towards O(2A). The copper chromophore can be described as having an extremely tetrahedrally distorted square pyramidal geometry with the tetragonality, T of 0.720 and τ-value of 0.12. The Cu–Cu distance is 5.955(2) Å.

The hydrogenphosphato group in this compound involves a quite unusual tridentate μ-κ-O,O′,O″ coordination mode: didentately coordinated to one copper chromophore and monodentately bonded to another. To the best of our knowledge, this coordination mode of the bridging hydrogenphosphate present in complex **2** is unique for the transition metal complexes.

The coordinated P=O bonds, 1.519(1), 1.510(2) and 1.531(1) Å, are shorter than the uncoordinated P–OH bond, 1.588(2) Å. This is usually found for the three-coordinate bridging coordination of the hydrogenphosphate anion [29]. The tridentate hydrogenphosphato group involves O–P–O angles ranging from 101.9(1)° to 111.7(1)°. The lattice structure is stabilized by a hydrogen-bonding network between the amine N and an oxygen atom of the hydrogenphosphate group with a short contact distance of 2.663(3) Å and between the oxygen atom of the hydrogenphosphate group to the oxygen atom of another hydrogenphosphato group with a contact distance of 2.528(3) Å. The structure contains chains of Cu ions in the c-direction bridged by the HPO_4^{2-} ions in a trigonal way. Two nearest Cu(II) ions are bridged by a tridentate hydrogenphosphate group which is didentately coordinated to one copper(II) ion, and monodentately coordinated to another in an equatorial–equatorial configuration in an unusual bridging coordination mode. The helical arrangement of the Cu–HPO_4 chain is clearly visible in Fig. 4 with the N ligands at the outside stacked in the direction of the three-fold screw axis.

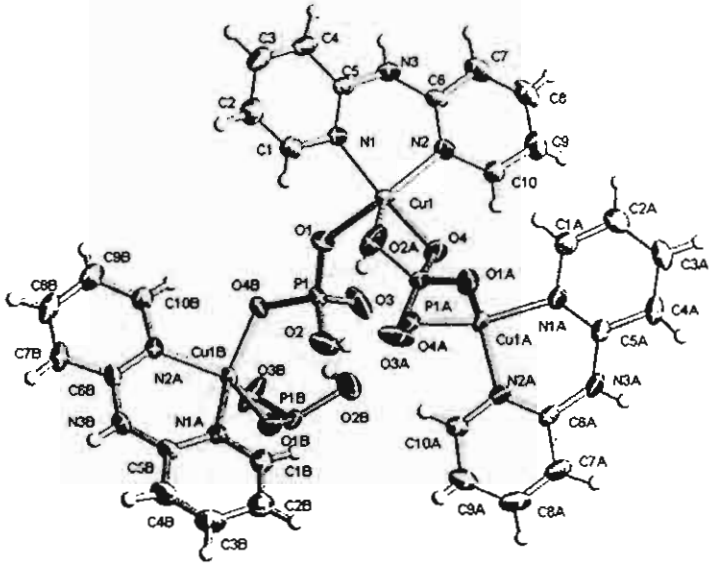

Fig. 3. ORTEP 50% probability plot of the cation in $[Cu(dpyam)(\mu_3\text{-}HPO_4)]_n$ (**2**). H-atoms are omitted for clarity. Atoms with an "A" and "B" are generated by symmetry operations.

Table 3
Selected bond lengths (Å) an angles (°) with e.s.d.s. in parentheses of compound **2**

Bond lengths			
Cu(1)–O(4)	1.919(1)	Cu(1)–O(1)	1.946(1)
Cu(1)–N(1)	1.969(1)	Cu(1)–N(2)	1.994(1)
P(1)–O(3)	1.510(1)	P(1)–O(1)	1.519(1)
P(1)–O(4)A	1.531(1)	P(1)–O(2)	1.588(2)
Cu(1)–O(2)A	2.719(3)	Cu(1)–Cu(1)A	5.955(2)
Bond angles			
O(4)–Cu(1)–O(1)	101.6(1)	O(4)–Cu(1)–N(1)	149.7(1)
O(1)–Cu(1)–N(1)	91.4(1)	O(4)–Cu(1)–N(2)	93.6(1)
O(1)–Cu(1)–N(2)	142.6(1)	O(1)–Cu(1)–N(2)	92.0(1)
O(3)–P(1)–O(1)	111.7(1)	O(3)–P(1)–O(4)A	111.1(1)
O(1)–P(1)–O(4)A	111.6(1)	O(3)–P(1)–O(2)	110.7(1)
O(1)–P(1)–O(2)	109.3(1)	O(4)A–P(1)–O(2)	101.9(1)

Symmetry code: A, $x+y+1, -x+1, z+1/3$.

3.2. Structural comparison

The square pyramidal CuN_2O_2O' chromophore of complex **1** corresponds to the square pyramidal CuN_2O_2O' chromophore observed from the copper environments of the known dinuclear structures; $[Cu_2(dpyam)_2(C_6H_3Cl_2OCH_2\text{-}COO)_4]$ (**3**) [30], $[Cu_2(dpyam)_2(ONO\text{-}O,O')_2(\mu\text{-}ONO\text{-}O)_2]\cdot 2CH_3CN$ (**4**) [8] and $[Cu_2(dpyam)_2(OH_2)(O_2CH)_4]\cdot H_2O$ (**5**) [17] (Table 4 and Scheme 1). The structure of **1** and **3**, confirms the two-coordinate bridging coordination of oxoanions in equatorial–equatorial and axial–equatorial configurations, respectively. Additionally, there are some differences in the five-coordinate distortion ($\tau = 0.12$ and 0.48 for **1** and **3**, respectively), along with the tetragonality $T = 0.874$ and 0.897 for **1** and **3**, respectively. The CuN_2O_2O' chromophore of **1** is best described as square-based pyramidal with a slight trigonal distortion, while that of **3** can be described as having an intermediate geometry between regular square pyramid and trigonal bipyramidal. The nitrite groups in **4** act as two non-bridging monodentate anions and two bridging monodentate anions while the formate groups in **5** act as three non-bridging monodentate anions and a single bridging didentate anion. The copper atoms in **4** and **5** are bridged by oxoanion in an axial–equatorial configuration that is different from the equatorial–equatorial configuration in **1**. The monomeric Cu(II) complexes shows tetrahedrally distorted elongated tetragonal-octahedral geometry with the long off-the-z-axis coordination of the second oxygen atoms from each OXO^- ligand in the axial positions (complex **6**). While an important feature of the structures of polymeric complexes is the two-coordinate bridging coordination of the oxoanion, which shows an unsymmetrical bonding to the Cu atom in the elongated rhombic octahedral configuration (complex **7**).

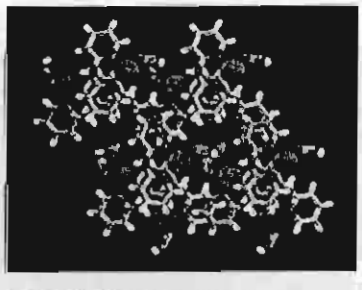

Fig. 4. Showing the lattice structure of complex **2**.

The polymeric structure of complex **2** is comparable to those of complexes with divalent sulfate anion $[Cu(dpyam)(H_2O)_2(SO_4)]$ (**8**) [31], $[Cu(en)(H_2O)_2(SO_4)]$ [21], $[Cu(bpy)(H_2O)_2(SO_4)]$ [22], $[Cu(phen)(H_2O)_2(SO_4)]$ [32], and $[Cu(oaoH_2)(H_2O)_2(SO_4)]$ (**9**) [33] all having a polymeric structure with bridging didentate sulfate groups and coordinated water and are also comparable to the compound with a divalent carbonate group $[Cu(dpyam)(CO_3)]\cdot 3H_2O$ (**10**) [34] (see Scheme 1 and Table 5). The Cu atoms in **10** are bridged by the carbonate anion in an axial–equatorial configuration, while in complex **2** the Cu atoms are bridged by the HPO_4^{2-} oxoanion in an equatorial–equatorial configuration. However, they differ from the square-pyramidal monomeric complexes, $[Cu(tmen)(H_2O)_2(SO_4)]\cdot H_2O$ [20], $[Cu(dpyam)(CO_3)(H_2O)]\cdot 2H_2O$ [18] which contains a monodentate sulfate and didentate carbonate anion, respectively. The dinuclear complexes $[Cu(oaoH_2)(H_2O)(SO_4)]_2$ (**11**) [33] and $[Cu(dpyam)(CO_3)]_2(H_2O)$ (**12**) [23] have a square pyramidal structure with bridging didentate sulfate and carbonate groups in an axial–equatorial configuration.

3.3. EPR spectra and magnetic properties

The polycrystalline EPR spectrum of compound **1** reveals at room temperature and at 77 K an axial signal with $g_{\parallel} = 2.32$ and $g_{\perp} = 2.07$. For compound **2** at room temperature an unresolved isotropic signal is obtained with $g = 2.13$. At 77 K a more resolved signal is obtained for compound **2** with $g_{\parallel} = 2.29$ and $g_{\perp} = 2.08$. The signals for both compounds are consistent with the $d_{x^2-y^2}$ ground state and a distorted square-based pyramidal geometry. No triplet signal has been observed. Apparently, the dinuclear units in **1** are not isolated from one another, resulting in exchange narrowing.

The magnetic susceptibility of powdered samples were measured from 5 to 300 K. The magnetic properties of compound **1** are given in Fig. 5 in the form of χ_M and $\chi_M T$ versus T plots. The $\chi_M T$ value at 300 K of 0.805 $cm^3\ mol^{-1}\ K$, is in agreement with uncoupled spin 1/2 centres (0.375 $cm^3\ mol^{-1}\ K$ per centre with $g = 2$). Decrease of $\chi_M T$ is observed upon lowering the temperature starting from 50 K down to 0.69 $cm^3\ mol^{-1}\ K$ at 5 K, which is indicative for a very weak antiferromagnetic interaction.

Table 4
Structural data and electronic spectra of complex **1** and relevant complexes

Complex	Coordination geometry	τ	Chromophore	Tetragonality	Tetrahedral twist (°)	Bridging configuration	*J* value (cm^{-1})	References
Dinuclear								
$[Cu(dpyam)(\mu\text{-}H_2PO_4\text{-}O,O')(H_2PO_4)]_2$ (**1**)	dinuclear SP	0.120	CuN_2O_3	0.874	14.00	equatorial–equatorial	−2.85(1)	this work
$[Cu(dpyam)(C_6H_3Cl_2OCH_2COO)_2]_2$ (**3**)	dinuclear dist.SP	0.480	CuN_2O_3	0.897		axial–equatorial	−0.8	[30]
$[Cu(dpyam)(ONO\text{-}O,O)(\mu\text{-}ONO\text{-}O)]_2 \cdot 2CH_3CN$ (**4**)	dinuclear dist.SP	0.000	CuN_2O_3	0.813		axial–equatorial		[8]
$[Cu_2(dpyam)_2(O_2CH)_4(OH_2)] \cdot H_2O$ (**5**)	dinuclear dist.SP	0.113, 0.096	CuN_2O_3	0.841	16.01, 19.35	axial–equatorial		[17]
Monomeric								
$[Cu(dpyam)(NO_2)_2]$ (**6**)	monomeric dist.oct.	0.020	$CuN_2O_2O'_2$	0.813	31.16			[7]
$[Cu(dpyam)(O_2CCH_3)_2] \cdot 2H_2O$	monomeric dist.oct.		$CuN_2O_2O'_2$	0.764	34.38			[6]
$[Cu(bpy)(NO_3)_2]$	monomeric dist.oct		$CuN_2O_2O'_2$	0.776	27.7			[9]
$[Cu(TIMM)(NO_2)_2]$	monomeric dist.oct		$CuN_2O_2O'_2$	0.792				[11]
$[Cu(BimOBz)(NO_3)_2]$	monomeric dist.oct		$CuN_2O_2O'_2$	0.779	15.6			[12]
Polymeric								
$[Cu(dpyam)(NO_3)_2]$	polymeric elong.oct.		$CuN_2O_2O'_2$	0.824, 0.817	7.00, 3.80			[10]
$[Cu(dpyam)(NO_3)(O_2CCH_2CH_3)]$ (**7**)	polymeric elong.oct.		$CuN_2O_2O'_2$	0.753		axial–equatorial		[15]
$[Cu(dpyam)(O_2CCH_3)(O_2ClO_2)] \cdot H_2O$	polymeric elong.oct.		$CuN_2O_2O'_2$	0.765		axial–axial		[13]

dpyam, di-2-pyridylamine; bpy, 2,2′-bipyridine; TIMM, Tris[2-(1-methyl)imidazolyl]methoxymethane; BimOBz, bis(1-methyl-4,5-diphenylimidaz-2-oyl)(benzyloxy)methane; dist.oct., distorted octahedral; dist.SP, distorted square pyramidal; elong.oct., elongated octahedral.

The magnetic data were fitted for two interacting $S = 1/2$ centres, based on the general Hamiltonian [34a]: $H = -JS_1 \cdot S_2$, in which the exchange parameter J is negative for antiferromagnetic and positive for ferromagnetic interaction. The data were fitted to the equation given in the literature [34a]. Also a temperature independent paramagnetism (TIP) of the Cu(II) ions has been considered. The resulting best fit parameters, corresponding to the full lines in Fig. 5, were $J = -2.85(1)$ cm^{-1} and $TIP = 0.85 \times 10^{-5}$ cm^3 mol^{-1} with g fixed to 2.00.

The magnetic properties of compound **2** are given in Fig. 6 in the form of χ_M and $\chi_M T$ versus T plots. From 300 K onwards the magnetism is steadily decreasing down to 0.01 cm^3 mol^{-1} K at 5 K, indicative for a medium antiferromagnetic coupling between neighbouring Cu(II) ions. The maximum in χ_M, expected for such couplings, is observed at 45 K, and a small Curie tail indicative of paramagnetic impurity is detected below 15 K. The data were fitted using the theoretical expression for a uniform Heisenberg chain [34]. The possibility of a percentage of paramagnetic impurity (p) and the TIP of the Cu(II) ions have been also taken into account. The resulting best fit parameters, corresponding to the full lines in Fig. 6 were $J = -26.20(2)$ cm^{-1}, $g = 1.98(1)$, $TIP = 1 \times 10^{-5}$ cm^3 mol^{-1} and $p = 0.3(1)\%$.

Because of the square pyramidal geometry in compounds **1** and **2** the spin density is mostly in the $d_{x^2-y^2}$ orbitals of the copper(II) ions. The $H_nPO_4^{(3-n)-}$ bridges, joining the copper atoms in an equatorial–equatorial configuration, the superexchange coupling through the phosphate anion (Cu–O–P–O–Cu) can be expected to be non-negligible. The antiferromagnetic couplings found in compounds **1** and **2** are thus in agreement with this structural feature and the large Cu–Cu distances.

3.4. Electronic and IR spectra

The electronic diffuse reflectance spectrum of **1** shows a broad band at 14.9×10^3 cm^{-1}. This observed single broad peak is consistent with the square pyramidal stereochemistry and assigned to be d_{z^2}, d_{xy}, d_{xz}, $d_{yz} \rightarrow d_{x^2-y^2}$ transition. Complex **2** exhibits a main peak at 14.4×10^3 cm^{-1} with a shoulder at 11.2×10^3 cm^{-1}. The transitions may be assigned as the d_{xy}, $d_{z^2} \rightarrow d_{x^2-y^2}$ transition for the low-energy peak and the d_{xz}, $d_{yz} \rightarrow d_{x^2-y^2}$ transition for the high-energy peak.

Table 5
Structural data and electronic spectra of complex **2** and relevant complexes

Complex	Coordination geometry	τ	Chromophore	Tetragonality	Tetrahedral twist (°)	Configuration	*J* value (cm^{-1})	References
Polymer								
$[Cu(dpyam)(\mu_3\text{-}HPO_4\text{-}O,O',O'')]_n$ **(2)**	polymeric dist.SP	0.120	CuN_2O_3	0.720	45.5	equatorial–equatorial	−26.20(2)	this work
$Cu(dpyam)(CO_3)\cdot 3H_2O$ **(8)**	polymeric dist. SP	0.003	CuN_2O_2O'	0.861		axial–equatorial		[19]
$[Cu(dpyam)(H_2O)_2(SO_4)]$ **(9)**	polymeric elong.oct		$CuN_2O_2O'_2$	0.815	15.8	axial–axial		[31]
$[Cu(phen)(H_2O)_2(SO_4)]$	polymeric elong. oct		$CuN_2O_2O'_2$	0.808		axial–axial	−3.8	[32]
$[Cu(oaoH_2)(H_2O)_2(SO_4)]$ **(10)**	polymeric dist.oct		$CuN_2O_2O'_2$	0.832		axial–equatorial	−1.0	[33]
Monomer								
$[Cu(dpyam)(CO_3)(H_2O)]\cdot 2H_2O$	monomeric dist.SP	0.096	CuN_2O_3	0.899	50.3			[18]
$[Cu(tmen)(H_2O)_2(SO_4)]\cdot H_2O$	monomeric dist.SP	0.085	CuN_2O_3	0.908				[20]
Dimer								
$[Cu(oaoH_2)(H_2O)(SO_4)]_2$ **(11)**	dinuclear dist.TP	0.145	CuN_2O_3	0.774		axial–equatorial	−1.27	[33]
$[Cu(dpyam)(CO_3)]_2\cdot H_2O$ **(12)**	dinuclear dist.SP	0.220	CuN_2O_3	0.815	5.9[a], 5.1[b]	axial–equatorial	−9.9	[23]

dpyam, di-2-pyridylamine; bpy, 2,2′-bipyridine; phen, 1,10-phenanthroline; $oaoH_2$, oxamide oxime; tmen, *N*,*N*,*N*′,*N*′-tetramethylethylenediamine; dist.oct., distorted octahedral; dist.SP, distorted square pyramidal; dist.TP, distorted tetragonal pyramidal.
[a] Chromophore A.
[b] Chromophore B.

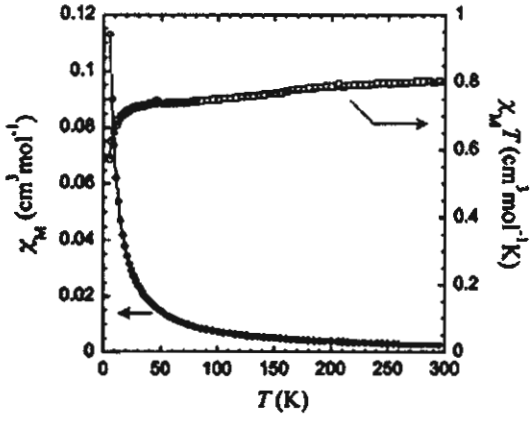

Fig. 5. Plots of temperature dependence of the molar magnetic susceptibility χ_M (○) and the $\chi_M T$ product (□) for compound **1**. The solid lines represent the calculated curves for the parameters $J = -2.85(1)$ cm^{-1} (see text).

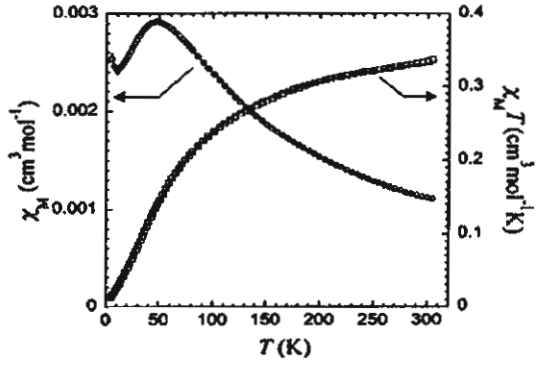

Fig. 6. Plots of temperature dependence of the molar magnetic susceptibility χ_M (○) and the $\chi_M T$ product (□) for compound **2**. The solid lines represent the calculated curves for the parameters $J = -26.20(2)$ cm^{-1}, $g = 1.98(1)$ (see text).

The infrared spectrum of complex **1** shows bands at ca. 1353; 1330, 1112 and 1049; 975 and 881 cm^{-1} and a broad band at ca. 522–488 cm^{-1} characteristic of P–O–H in-plane deformation, ν(P–O), ν(P–O–(H)) and δ(O–P–O), respectively, which corresponds to the literature [28,35–38]. The IR spectrum of complex **2** shows two strong and one medium band at 1092, 1056 and 968 cm^{-1}, characteristic of a ν(P–O). The δ(O–P–O) vibrations are found at 585 and 555 cm^{-1} [39–41].

4. Conclusions

In this study, two Cu(II) compounds with the ligand dipyam containing phosphato bridges are synthesized and characterized and have both a weakly distorted

square pyramidal geometry. Compound **1** is a dinuclear compound bridged by two phosphato anions. The Cu–Cu interaction is very weak antiferromagnetic ($J = -2.85(1)$ cm^{-1}) and is generated via the phosphato bridge. Compound **2** is a polynuclear compound bridged by a phosphato group which is didentately coordinated to one copper atom and monocoordinated to the next copper atom. The magnetic interaction is weak antiferromagnetic ($J = -26.20(2)$ cm^{-1}) and occurs also via the phosphato group in the Cu chain.

5. Supplementary material

Crystallographic data for the structures in this paper have been deposited with the Cambridge Crystallographic Data Centre as supplementary publication CCDC Nos. 230043 and 230044 for structures **1** and **2**, respectively. Copies of the data can be obtained free of charge from The Director, CCDC, 12 Union Road, Cambridge CB2 1EZ, UK (fax: +44-1223-336033; e-mail: deposit@ccdc.cam.ac.uk, www:http://www.ccdc.cam.ac.uk).

Acknowledgements

The authors thank the Thailand Research Fund and Khon Kaen University for a research grant. Support of the Postgraduate Education and Research Program in Chemistry is also gratefully acknowledged. The work described in the present paper has been supported by the Leiden University Study group WFMO (Werkgroep Fundamenteel Materialen Onderzoek).

References

[1] I.M. Procter, B.J. Hathaway, P.G. Hodgson, Inorg. Nucl. Chem. 34 (1972) 3689.
[2] S.F. Pavkovic, D. Miller, Acta Crystallogr., Sect. B 33 (1977) 2894.
[3] D.L. Lewis, D.J. Hodgson, Inorg. Chem. 12 (1973) 2935.
[4] F.S. Stephens, J. Chem. Soc. A (1969) 2081.
[5] M.C. Munoz, J.M. Lazaro, J. Faus, M. Julve, Acta Crystallogr., Sect. C 49 (1993) 1756.
[6] S. Youngme, C. Pakawatchai, H.K. Fun, K. Chinnakali, Acta Crystallogr., Sect. C 54 (1998) 1586.
[7] S. Youngme, S. Tonpho, K. Chinnakali, S. Chantrapromma, H.K. Fun, Polyhedron 18 (1999) 851.
[8] A. Camus, N. Marsich, A.M.M. Lanfredi, F. Ugozzoli, C. Massera, Inorg. Chim. Acta 309 (2000) 1.
[9] A. Tadsanaprasittipol, H.B. Kraatz, G.D. Enright, Inorg. Chim. Acta 278 (1998) 143.
[10] S. Youngme, N. Chaichit, K. Damnatara, Polyhedron 21 (2002) 943.
[11] R.T. Stibrany, J.A. Potenza, H.J. Schugar, Inorg. Chim. Acta 243 (1996) 33.
[12] R. Bhalla, M. Helliwell, C.D. Garner, Inorg. Chem. 36 (1997) 2944.
[13] N. Ray, S. Tyagi, B.J. Hathaway, Acta Crystallogr., Sect. B 38 (1982) 1574.
[14] S. Aduldecha, B.J. Hathaway, Acta Crystallogr., Sect. C 47 (1991) 84.
[15] S. Youngme, C. Pakawatchai, H.K. Fun, Acta Crystallogr., Sect. C 54 (1998) 451.
[16] T.D. Coombs, B.J. Brisdon, C.P. Curtis, M.F. Mahon, S.A. Brewer, C.R. Willis, Polyhedron 20 (2001) 2935.
[17] S. Youngme, W. Somjitsripunya, K. Chinnakali, S. Chantrapromma, H.K. Fun, Polyhedron 18 (1999) 857.
[18] P. Akhter, P. Fitzsimons, B. Hathaway, Acta Crystallogr., Sect. C 47 (1991) 308.
[19] J. Sletten, Acta Chem. Scand., Sect. A 38 (1984) 491.
[20] J. Balvich, K.P. Fivizzani, S.F. Pavkovic, J.N. Brown, Inorg. Chem. 15 (1976) 71.
[21] M. Dunai-Jurio, M.A. Porai-Koshits, Chem. Zvesti 20 (1966) 783.
[22] J.C. Tedenac, N.D. Phung, C. Avinens, M. Maurin, Inorg. Nucl. Chem. 38 (1976) 85.
[23] S. Youngme, N. Chaichit, P. Kongsaeree, G.A. van Albada, J. Reedijk, Inorg. Chim. Acta 20 (2001) 232.
[24] Siemens. SAINT 1997, Version 4: Software Reference Manual, Siemens Analytical X-Ray Systems Inc., Madison, WI, 1997.
[25] G.M. Sheldrick, SADABS: Program for Empirical Absorption Correction of Area Dectector Data, University of Göttingen, Göttingen, Germany, 1997.
[26] Siemens. SHELXTL 1997, Version 5: Reference Manual, Siemens Analytical X-Ray Systems, Inc., Madison, WI, 1997.
[27] A.W. Addison, T.N. Rao, J. Reedijk, J. van Rijn, G.C. Verschoor, J. Chem. Soc., Dalton Trans. (1984) 1349.
[28] A.M. Krogh Andersen, P. Norby, J.C. Hanson, T. Vogt, Inorg. Chem. 37 (1998) 876.
[29] T.R. Jenson, R.G. Hazell, T. Vosegaard, H.J. Jakobsen, Inorg. Chem. 39 (2000) 2026.
[30] G. Psomas, C.P. Raptopoulou, L. Iordanidis, C. Dendrinou-Samara, V. Tangoulis, D.P. Kessissoglou, Inorg. Chem. 39 (2000) 3042.
[31] S. Youngme, N. Chaichit, C. Pakawatchai, S. Booncoon, Polyhedron 21 (2002) 1279.
[32] L. Xu, E. Wang, J. Peng, R. Huang, Inorg. Chem. Commun. 6 (2003) 740.
[33] H. Endres, D. Nöthe, E. Rossato, W.E. Hatfield, Inorg. Chem. 23 (1984) 3467.
[34] (a) O. Kahn, Molecular Magnetism, VCH, New York, 1993; (b) J.W. Hall, W.E. Marsh, R.R. Weller, W.E. Hatfield, Inorg. Chem. 20 (1981) 1033.
[35] M. Roca, P. Amorós, J. Cano, M.D. Marcos, J. Alamo, A. Beltrán-Porter, D. Beltrán-Porter, Inorg. Chem. 37 (1998) 3167.
[36] Z. Bircsak, W.T.A. Harrison, Inorg. Chem. 37 (1998) 3204.
[37] J.E. Johnson, T.A. Beineke, R.A. Jacobson, J. Chem. Soc. A (1971) 1371.
[38] C.-H. Lin, S.-L. Wang, Inorg. Chem. 40 (2001) 2918.
[39] W. Liu, Y. Liu, Z. Shi, W. Pang, J. Mater. Chem. 10 (2000) 1451.
[40] Y. Zhang, R.C. Haushalter, J. Zubieta, Inorg. Chim. Acta 260 (1997) 105.
[41] A.C. Chapman, L.E. Thirlwell, Spectrochim. Acta 20 (1964) 937.

Available online at www.sciencedirect.com
SCIENCE DIRECT®
Inorganica Chimica Acta 358 (2005) 849–853
Inorganica Chimica Acta
www.elsevier.com/locate/ica

Note

An unprecedented tetranuclear Cu(II) cluster, exclusively bridged by two μ_3,η^3-hydrogenphosphate anions: synthesis, structure, and magnetic properties

Sujittra Youngme [a,*], Pongthipun Phuengphai [a], Narongsak Chaichit [b], Gerard A. van Albada [c], Olivier Roubeau [d], Jan Reedijk [c]

[a] *Department of Chemistry, Faculty of Science, Khon Kaen University, Khon Kaen 40002, Thailand*
[b] *Department of Physics, Faculty of Science and Technology, Thammasat University Rangsit, Pathumthani 12121, Thailand*
[c] *Leiden Institute of Chemistry, Gorlaeus Laboratories, Leiden University, P.O. Box 9502, 2300 RA Leiden, The Netherlands*
[d] *Centre de Recherche Paul Pascal – CNRS, 115 avenue du dr. A. Schweitzer, 33600 Pessac, France*

Received 27 August 2004; accepted 22 September 2004

Abstract

A novel tetranuclear μ_3,η^3-HPO_4^{2-} Cu(II) complex with a new coordination mode of a hydrogenphosphato bridge, $[Cu_4(\text{di-2-pyridylamine})_4(\mu_3,\eta^3\text{-}HPO_4)_2(H_2O)_2(NO_3)_2](NO_3)_2(H_2O)_2$ has been synthesised and characterised structurally, spectroscopically and magnetically. The geometry around the Cu(II) ions is distorted square pyramidal for Cu1 and an intermediate between square pyramidal and trigonal pyramidal. The magnetic susceptibility measurements have been fit for a weak antiferromagnetic interaction of $J = -10.3(1)$ cm^{-1} between outer Cu ions and $J = -5.3(2)$ cm^{-1} between inner Cu atoms.

Keywords: Tetranuclear complexes; Copper(II) cluster; Hydrogenphosphate complexes; Di-2-pyridylamine; Magnetism

1. Introduction

In the past few years, the design and synthesis of inorganic–organic hybrid materials have been increasingly developed for their potential application in the fields of catalysts, biology, electrical conductivity, magnetism and photochemistry [1]. A number of polynuclear hydrogenphosphate-bridged metal systems have been structurally characterised [2] in relation to bioinorganic models [3] and the relationship between the hydrogenphosphato bridging mode and magnetic properties [4]. In recent years, many researches have focused on the synthesis of inorganic–organic hybrid frameworks containing the phosphate anion (and derivatives) in a bridging mode [5–9]. Very recently, a tetranuclear compound with 2,2′-bipyridine and a μ_4-PO_4 bridging mode was published; however, the bridge also contained a bridging carbonate anion [10].

To obtain more insight into bridging phosphate anions, we now extended that study using the ligand di-2-pyridylamine (abbreviated as dpyam). In the present study, an unprecedented hydrogenphosphato-bridging Cu(II) complex, $[Cu_4(dpyam)_4(\mu_3,\eta^3\text{-}HPO_4)_2(H_2O)_2(NO_3)_2](NO_3)_2(H_2O)_2$ (**1**), with different coordination geometries of the hydrogenphosphato bridges, is described and investigated structurally and magnetically. To the best of our knowledge, this is also the first Cu(II) tetranuclear compound with a (μ_3,η^3-HPO_4-O′,O′,O″) phosphate binding mode.

* Corresponding author. Tel.: +66043202222-41; fax: +66043202373.
E-mail address: sujittra@kku.ac.th (S. Youngme).

0020-1693/$ - see front matter © 2004 Elsevier B.V. All rights reserved.
doi:10.1016/j.ica.2004.09.031

2. Experimental

2.1. Materials and measurements

All reagents were commercial grade materials and were used without further purification. Elemental analyses (C, H, N) were determined on a Perkin–Elmer PE2400 CHNS/O Analyser. IR spectra were recorded on a Spectrum One Perkin–Elmer FT-IR spectrophotometer as KBr pellets in the 4000–450 cm^{-1} spectral range. Diffuse reflectance measurements from 9090 to 20 000 cm^{-1} were recorded as polycrystalline samples using a Perkin–Elmer Lambda 2S spectrophotometer equipped with an integrating sphere attachment. Barium sulfate was used as the reflectance standard. X-band powder EPR spectra were recorded on a JEOL RE2x electron spin resonance spectrometer using DPPH ($g = 2.0036$) as a standard. Magnetic susceptibility measurements (5–300 K) were carried out using a Quantum Design MPMS-5 5T SQUID magnetometer (measurements carried out at 1000 Gauss). Data were corrected for magnetisation of the sample holder and for diamagnetic contributions, which were estimated from the Pascal constants.

2.2. Synthesis of the compound 1

2.2.1. $[Cu_4(dpyam)_4(\mu_3,\eta^3\text{-}HPO_4)_2(NO_3)_2(H_2O)_2](NO_3)_2(H_2O)_2$

An aqueous solution (30 ml) of $Cu(NO_3)_2{\cdot}3H_2O$ (0.24 g, 1.0 mmol) was added to a solution of di-2-pyridylamine (0.17 g, 1.0 mmol) in ethanol (15 ml) and followed by an aqueous solution (20 ml) of potassium dihydrogenphosphate (0.27 g, 2.0 mmol). The green solution was allowed to slowly evaporate at room temperature. After several days, dark green crystals were deposited, which have been characterised as being the compound $[Cu(dpyam)(\mu\text{-}HPO_4)]_n$. After filtration, the remaining solution was allowed to evaporate in the open air and after a few days green needle shaped crystals of complex **1** were deposited in a yield of 56%. The crystals were filtered, washed with the mother liquid and dried in air. Elemental *Anal.* Calc. for $C_{40}H_{46}Cu_4N_{16}O_{24}P_2$: C, 33.13; H, 3.19; N, 15.45. Found: C, 33.20; H, 3.04; N, 15.52%. The infrared spectrum of **1** exhibits strong bands at 1384 cm^{-1} [ν_{as}(NO)], 1313 cm^{-1} [ν(NO)] and 1111, 1056 and 1012 cm^{-1} [ν(P–O)].

2.3. Crystallography

Crystal data: $C_{40}H_{42}Cu_4N_{16}O_{24}P_2$, monoclinic, space group *C2/c*, $a = 28.4236(1)$, $b = 9.7305(1)$, $c = 22.7510(2)$ (Å), $\beta = 118.183(10)°$, $V = 5546.38(9)$ $Å^3$, $\mu = 1.667$ mm^{-1}, $Z = 4$ and $R1 = 0.051$ for 7885 reflections. Reflection data for complex **1** were collected at 273 K on a 1K Bruker SMART CCD area-detector diffractometer. Data reduction and cell refinements were performed using the program SAINT [11]. The structure was solved by direct methods and refined by full-matrix least-squares method on $(F_{obs})^2$ with anisotropic thermal parameters for all non-hydrogen atoms using the SHELXTL-PC [12] software package. All hydrogen atoms were located by difference synthesis and refined isotropically except for the lattice water hydrogen atoms (4 H atoms), which could not be located and are also not fixed. The molecular graphics were created by using SHELXTL-PC [12]. CCDC Reference No. 233865. See http://www.ccdc.cam.ac.uk for crystallographic data in CIF format.

3. Results and discussion

3.1. Crystal structure of $[Cu_4(dpyam)_4(\mu_3,\eta^3\text{-}HPO_4)_2(NO_3)_2(H_2O)_2](NO_3)_2(H_2O)_2$ (1)

A plot of the structure is depicted in Fig. 1 with selected bond distances and angles in Table 1. The crystal structure obtained consists of a centrosymmetric tetranuclear $[Cu_4(dpyam)_4(\mu_3,\eta^3\text{-}HPO_4)_2(NO_3)_2(H_2O)_2]^{2+}$ cation, two non-coordinating NO_3^- anions and two molecules of lattice water. The four copper ions of the tetranuclear identity are linked through a double hydrogenphosphate bridge, with internal Cu···Cu distances varying from 4.136(2) to 7.833(2) Å. The cation is located on an inversion centre located in between the two bridging HPO_4^{2-} groups. The coordination mode of HPO_4^{2-} is tridentate bridging, each anion is bonded monodentately to two Cu(II) ions and didentately coordinated to a third Cu ion resulting in a novel μ_3,η^3 coordination mode. The two different Cu ions have a different chromophore (CuN_2O_2O' chromophore for Cu1 and a CuN_2O_3 chromophore for Cu2).

The geometry around Cu1 can be best described as distorted square pyramidal with the basal plane formed by 2 nitrogen atoms of a dpyam ligand (Cu–N distances 1.967(3) and 2.001(3) Å) and two oxygen atoms from different bridging hydrogenphosphato groups (Cu–O distances 1.968(2) and 1.972(2) Å). The apical position is occupied by an oxygen atom of one of the bridging hydrogenphosphate groups (Cu1–O7 2.497(2) Å). The angles of the basal plane are 161.77(12) and 142.43(12)°, while the four in-plane atoms (N1, N2, O4 and O6) are not planar (rms deviation of 0.473 Å) and have a marked tetrahedral twist (dihedral angles between the CuN_2 and CuO_2 planes) of 41.2°. The Cu ion lies 0.163 Å above this plane towards O(7). The distortion parameter τ, defined to describe the degree of trigonal distortion is 0.32 (a regular trigonal bipyramid (TBP) and square-based pyramid (SP) have τ values of 1.00 and 0.00, respectively [13]). The two Cu1 ions are doubly bridged by a HPO_4^{2-} anion in an equatorial–

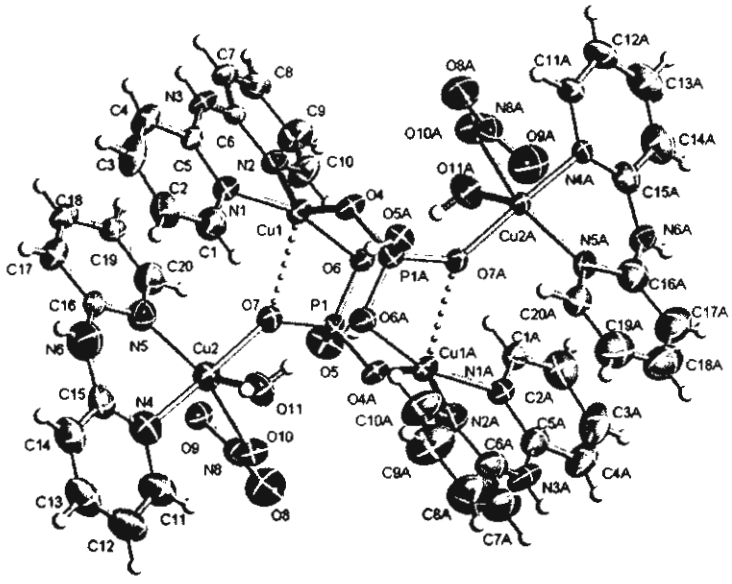

Fig. 1. Thermal ellipsoid plot (50% probability) of **1**. Atoms with an "A" are generated by symmetry operation $-x+2$, $-y$, $-z+1$. The uncoordinating nitrate anions and lattice water molecules are omitted for clarity.

Table 1
Selected bond lengths (Å) and angles (°) with esd in parentheses of compound **1**

Cu(1)–O(6)	1.972(2)	Cu(1)–O(4)	1.968(2),
Cu(1)–N(1)	1.967(2)	Cu(1)–N(2)	2.001(3)
Cu(1)–O(7)	2.497(2)	Cu(2)–O(7)	1.933(2)
Cu(2)–N(5)	2.013(3)	Cu(2)–N(4)	1.979(3)
Cu(2)–O(10)	2.145(2)	Cu(2)–O(11)	2.152(3)
Cu(2)–O(9)	2.743(2)	Cu(1)–Cu(2)	4.136(2)
Cu(1)–Cu(2)A	4.895(2)	Cu(1)–Cu(1)A	4.560(2)
Cu(2)–Cu(2)A	7.833(2)		
N(1)–Cu(1)–O(6)	161.7(1)	O(4)–Cu(1)–N(2)	142.4(1)
O(6)–Cu(1)–O(7)	110.4(1)	O(7)–Cu(1)–N(2)	106.2(1)
N(5)–Cu(2)–O(10)	137.6(1)	N(5)–Cu(2)–O(11)	131.1(1)
N(4)–Cu(2)–O(7)	168.6(1)		

Hydrogen-bonding parameters

D–H···A	D–H (Å)	H···A (Å)	D···A (Å)	D–H···A (°)
N(3)–H(5)···O(4) [$-x$, $1-y$, $1-z$]	0.77(5)	2.26(5)	2.918(4)	144(5)
N(6)–H(15)···O(2) [$1/2-x$, $3/2-y$, $1-z$]	0.73(4)	2.18(4)	2.904(6)	172(4)
O(11)–H(21)···O(1) [x, $2-y$, $1/2+z$]	0.65(6)	2.22(6)	2.813(5)	153(7)
O(11)–H(22)···O(6) [$-x$, $2-y$, $1-z$]	0.79(6)	1.93(6)	2.718(5)	175(5)
O(5)–H(23)···O(1W) [$-1+x$, $1+y$, z]	0.79(5)	1.82(5)	2.608(5)	173(5)

equatorial configuration. Cu2 is linked to Cu1 via O7 of P1.

The geometry around the Cu2 ion is distorted TBP with the trigonal plane formed by the nitrogen atom of a dpyam ligand (Cu–N distance 2.013(3) Å) and two oxygen atoms, one from a water molecule and one from a coordinating nitrate anion (Cu–O distances 2.145(3), 2.152(4) Å). The angles of the trigonal plane are 137.56(11) and 131.15(12)°. The apical positions are occupied by a N-atom of the dpyam ligand (Cu–N 1.979(3) Å) and an oxygen atom of a bridging hydrogenphosphato group (Cu–O 1.933(2) Å) with an angle of 168.64(12)°. These shorter distances as compared to those in the trigonal plane are typical for TBP geometry. The distortion parameter τ for Cu2 is 0.49, so in fact it is an intermediate between TBP and SP.

The lattice structure is stabilised by a hydrogen-bonding network between the N atom of the dpyam ligand and oxygen atoms of a hydrogenphosphato group and a nitrate anion (N···O distances 2.918(4), 2.904(6) Å); between the coordinated water oxygen atom and the oxygen atoms of a hydrogenphosphato

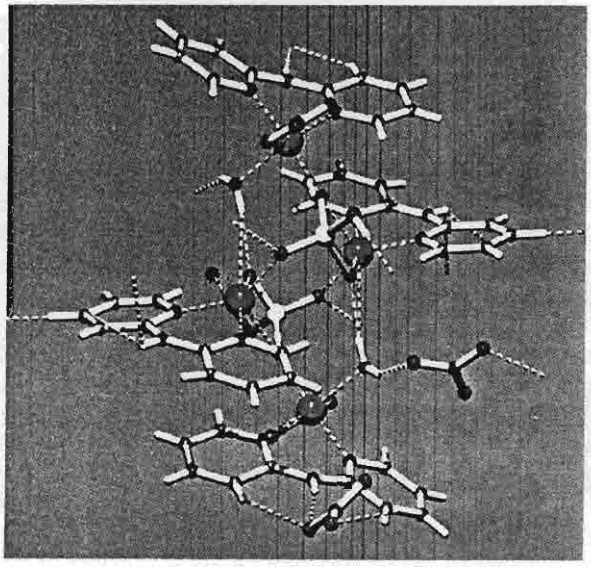

Fig. 2. Hydrogen bonding of **1**.

group and a nitrate anion (O···O distances 2.813(5), 2.718(5) Å) and finally a quite strong bond between an oxygen atom of a hydrogenphosphato group and the oxygen atom of the non-coordinated water molecule (O···O distance only 2.608(5) Å). Details of the hydrogen bonds are given in Table 1 and a H-bonding picture is presented in Fig. 2.

3.2. Spectroscopy and magnetism

The diffuse reflectance spectrum of **1** measured as a solid shows a broad split band with a maximum at 11.4 and 13.9×10^3 cm^{-1}, which can be considered as normal transitions for TBP to SP geometries [14].

The polycrystalline EPR spectrum of compound **1** reveals a very broad isotropic signal with g at around 2.11 (RT and 77 K). This broad unresolved signal can be due to exchange narrowing and also to the fact that the compound contains two different copper sites. No signals for triplet species are observed.

The magnetic susceptibility of a powdered sample was measured from 5 to 300 K. The magnetic properties of the complex are depicted in Fig. 3 in the form of χ_m versus T and $\chi_m T$ versus T. Fig. 4 shows the magnetic interaction scheme, which was used for the fitting procedure and is based on the assumption that the magnetic coupling between outer and inner Cu ions is identical for all Cu1–Cu2, Cu1–Cu2A, Cu1A–Cu2A and Cu1 A–Cu2 pairs. This is understandable, as the Cu–Cu distances and the O–P–O bridging pathway are very similar. The corresponding Hamiltonian is then

$$H = -J_1(S_{Cu1}\cdot S_{Cu2} + S_{Cu1}\cdot S_{Cu2A} + S_{Cu1A}\cdot S_{Cu2} + S_{Cu1A}\cdot S_{Cu2}) - J_2(S_{Cu1}\cdot S_{Cu1A}).$$

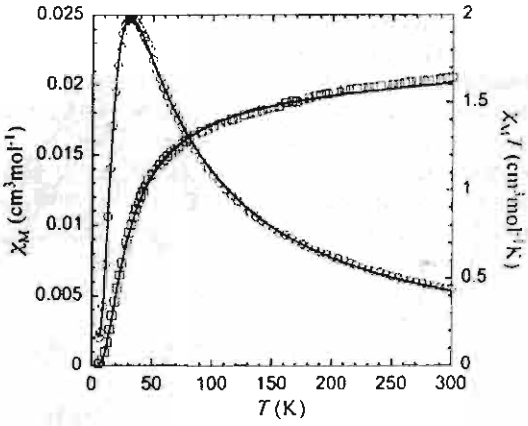

Fig. 3. Temperature dependence of the molar magnetic susceptibility χ_M (○) and the $\chi_M T$ product (□) for compound **1**. The solid lines represent the calculated curves for $J_1 = -10.3(1)$ cm^{-1}, $J_2 = -5.3(2)$ cm^{-1} (see text).

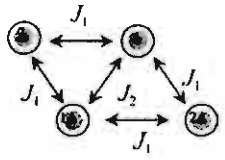

Fig. 4. Scheme of the magnetic interactions used in the calculations, using atom labelling from the structural data (see text).

Applying the Kambe vector coupling method with $S_A = S_{Cu2} + S_{Cu2A}$ and $S_B = S_{Cu1} + S_{Cu1A}$ (J_1 represents the Cu–Cu outer–inner magnetic interaction and J_2 the Cu–Cu inner–inner magnetic interaction, see Fig. 4) yields the following expression for the energy levels:

$$E(S_T, S_A, S_B) = -\frac{J_1}{2}(S_T(S_T+1) - S_A(S_A+1) - S_B(S_B+1)) - \frac{J_2}{2}(S_B(S_B+1))$$

and after inserting in the van Vleck equation [15] the expression for the molar susceptibility

$$\chi_{tetra} = (1-p)\frac{Ng^2\beta^2}{k_BT} \times \frac{\left[2+2\exp\left(\frac{J_2}{k_BT}\right)+10\exp\left(\frac{(J_1+J_2)}{k_BT}\right)\right]}{\left[4+3\exp\left(\frac{J_2}{k_BT}\right)+5\exp\left(\frac{(J_1+J_2)}{k_BT}\right)+\exp\left(\frac{-2J_1+J_2}{k_BT}\right)\right]} + \frac{4\times 0.375\times p}{T} + \mathrm{TIP},$$

which includes terms to take into account the temperature independent paramagnetism (TIP) and a monomeric paramagnetic impurity (p). Fitting the experimental data to this expression yields the full lines in Fig. 3 corresponding to the parameters $g = 2.01(1)$,

$J_1 = 10.3(1)$ cm^{-1}, $J_2 = -5.3(2)$ cm^{-1} and $p = 0.060(3)\%$. The TIP was kept at a constant of 2.0×10^{-4} cm^3 mol^{-1}. The fitted g value does not correspond completely with the g value obtained by EPR, but as the EPR gives a very broad unresolved signal no accuracy can be given on that observed EPR g value.

The phosphate bridges in the title compound are all in an equatorial–equatorial mode, (type I) for Cu1–Cu1A, SP–SP geometry; an equatorial–axial mode (type II) for Cu1–Cu2A and Cu1A–Cu2, SP–TBP geometry; and an axial–axial mode (type III) for Cu1–Cu2 and Cu1A–Cu2A, SP–TBP geometry, while the unpaired electron is usually in the $d_{x^2-y^2}$ for SP geometry and delocalised in d_z^2 for the TBP geometry. The delocalised efficiency of the unpaired electrons expected for inner Cu-ions (Cu1–Cu1A, SP geometry) and outer Cu ions (Cu2, Cu2A, TBP geometry) is remarkably diminished due to the distorted SP with a remarkable tetrahedral twist of the square base for the inner Cu-ions and the significantly distorted TBP (in fact an intermediate five-coordinated geometry) for the outer Cu-ions, resulting in a weaker overlap between magnetic orbitals, and therefore in a weaker antiferromagnetic interaction. The fact that $J_1 > J_2$ is thus due to differences in the Cu–O–P–O–Cu pathways and therefore the type II pathway seems slightly more efficient. However, the precise geometry of the phosphate bridge is likely to have an influence on the exchange parameters. Moreover, indeed the shortest Cu–Cu distance between inner Cu ions (4.56 Å) is larger than that between inner and outer Cu ions (4.13 Å). Detailed correlation of these structural effects with the magnetic exchange parameters requires other comparable compounds with phosphate bridges, which is under current investigation.

4. Conclusions

A tetranuclear Cu(II) compound with an unique (μ_3,η^3-HPO_4–O′,O′,O″) binding mode has been described. The compound shows a weak antiferromagnetic interaction. Parameters determined for the exchange intercation between the outer Cu ions are $J = -10.3(1)$ cm^{-1} and $J = -5.3(2)$ cm^{-1} for the inner Cu ions.

Acknowledgements

The authors thank The Thailand Research Fund and Khon Kaen University for a research grant. Support of the Postgraduate Education and Research Program in Chemistry (Thailand) is also gratefully acknowledged. The work described in the present paper has been supported by the Leiden University Study group WFMO (Werkgroep Fundamenteel MaterialenOnderzoek). Support of the NRSC Catalysis (a Research School Combination of HRSMC and NIOK, Netherlands) is kindly acknowledged.

References

[1] A.K. Cheetham, G. Ferey, T. Loiseau, Angew. Chem. Int. Ed. 38 (1999) 3286, and references cited therein.
[2] K.-H. Lii, Y.-F. Huang, Inorg. Chem. 38 (1999) 1348.
[3] R.C. Finn, J. Zubieta, J. Phys. Chem. Solids 62 (2001) 1513.
[4] M. Yuan, E. Wang, Y. Lu, Y. Li, C. Hu, N. Hu, H. Jai, Inorg. Chem. Commun. 5 (2002) 505.
[5] W.-J. Chang, C.-Y. Chen, K.-H. Lii, J. Solid State Chem. 172 (2003) 6.
[6] Z. Shi, S. Feng, L. Zhang, G. Yang, J. Hua, Chem. Mater. 12 (2000) 2930.
[7] R. Murugavel, M. Sathiyendiran, R. Pothiraja, M.G. Walawalkar, T. Mallah, E. Riviére, Inorg. Chem. 43 (2004) 945.
[8] Y. Moreno, A. Vega, S. Ushak, R. Baggio, O. Peña, E. Le Fur, J.-Y. Pivan, E. Spodine, J. Mater. Chem. 13 (2003) 2381.
[9] B. Moubaraki, K.S. Murray, J.D. Ranford, X. Wang, Y. Xu, Chem. Commun. (1998) 353.
[10] R.P. Doyle, P.E. Kruger, B. Moubaraki, K.S. Murray, M. Nieuwenhuyzen, J. Chem. Soc., Dalton Trans. (2003) 4230.
[11] Siemens, SAINT, Version4 Software Reference Manual, Siemens Analytical X-Ray Systems, Inc., Madison, WI, USA, 1996.
[12] Siemens, SHELXTL, Version 5 Reference Manual, Siemens Analytical X-Ray Systems, Inc., Madison, WI, USA, 1996.
[13] A.W. Addison, T.N. Rao, J. Reedijk, J. van Rijn, G.C. Verschoor, J. Chem. Soc., Dalton Trans. (1984) 1349.
[14] B.J. Hathaway, in: G. Wilkinson, R.D. Gill, J.A. McCleverty (Eds.), Comprehensive Coordination Chemistry, 5, Pergamon Press, Oxford, 1987.
[15] J.H. van Vleck, The Theory of Electric and Magnetic Susceptibilities, Oxford University Press, Oxford, 1932.

Available online at www.sciencedirect.com
SCIENCE DIRECT®
Inorganica Chimica Acta 358 (2005) 2125–2128
Inorganica Chimica Acta
www.elsevier.com/locate/ica

Note

A novel polymeric trinuclear-based μ_3-phosphato-bridged Cu(II) complex containing two different types of monophosphate. Synthesis, structure and magnetism of $\{[Cu_3(\text{di-2-pyridylamine})_3(\mu_3,\eta^3\text{-}HPO_4)(\mu_3,\eta^4\text{-}PO_4)(H_2O)](PF_6)(H_2O)_3\}_n$

Sujittra Youngme [a,*], Pongthipun Phuengphai [a], Chaveng Pakawatchai [b], Gerard A. van Albada [c], Jan Reedijk [c]

[a] Department of Chemistry, Faculty of Science, Khon Kaen University, Khon Kaen 40002, Thailand
[b] Department of Chemistry, Faculty of Science, Prince of Songkla University, Hatyai, Songkla 90112, Thailand
[c] Leiden Institute of Chemistry, Gorlaeus Laboratories, Leiden University, P.O. Box 9502, 2300 RA Leiden, The Netherlands

Received 27 July 2004; accepted 19 December 2004
Available online 11 February 2005

Abstract

A novel trinuclear-based polymeric Cu(II) complex with uniquely bridged $H_xPO_4^{(3-x)-}$ anions, $[Cu_3(\text{di-2-pyridylamine})_3(\mu_3,\eta^3\text{-}HPO_4)(\mu_3,\eta^4\text{-}PO_4)(H_2O)](PF_6)(H_2O)_3\}_n$ **1** has been synthesized and characterised. Each Cu(II) ion in the polynuclear unit is linked by hydrogenphosphato and phosphato bridges showing μ_3, η^3-HPO_4^{2-} and an unprecedented μ_3, η^4-PO_4^{3-} coordination mode. Two different coordination geometries around the Cu(II) ions are found in the polynuclear unit: an intermediate geometry between square pyramidal and trigonal bipyramidal and a tetrahedrally distorted square-based pyramidal geometry. The Cu ··· Cu distances vary from 4.408(3) to 5.942(3) Å. From variable magnetic susceptibility measurements (5–250 K) a weak antiferromagetic interactions between the Cu(II) ions in the trinuclear unit with an exchange parameter of $J = -4.98\ cm^{-1}$ and a very weak antiferromagnetic interaction between neighbouring units with $zJ' = -1.49\ cm^{-1}$ are observed.

Keywords: Copper(II) complexes; Hydrogenphosphate complexes; Di-2-pyridylamine; Magnetism

1. Introduction

Recently, many research activities have focused on the synthesis of new open-framework metal phosphates, owing to their diverse structural chemistry and potential applications [1–3]. In the context of building open frameworks, it is also possible to use organic molecules in the skeleton. As compared with inorganic phosphates, the organic molecules have larger sizes of polyhedral centres and a wide variety of means of intramolecular connection. The organic components can greatly affect the connecting patterns of inorganic polyhedra, thus providing a method for the synthesis of new materials [4–6]. The synthesis of metal–phosphate complexes containing organic didentate chelating ligands has been investigated recently [7,8]. We have now extended the study by using the didentate ligand di-2-pyridylamine (abbreviated dpyam) and $H_nPO_4^{(3-n)-}$ oxoanions, to obtain complexes with different nuclearity and different

* Corresponding author. Tel. +66 43 202 22241; fax: +66 43 202 373.
E-mail address: sujittra@kku.ac.th (S. Youngme).

0020-1693/$ - see front matter © 2005 Elsevier B.V. All rights reserved.
doi:10.1016/j.ica.2004.12.043

coordinating and bridging modes of $H_xPO_4^{(3-x)-}$ ion. In the present study the synthesis, structural characterisation and magnetic properties of the polynuclear compound $\{[Cu_3(dpyam)_3(\mu_3,\eta^4\text{-}PO_4)(\mu_3,\eta^3\ HPO_4)(H_2O)](PF_6)(H_2O)_3\}_n$ (**1**) is reported. The unique 1-D structure is built up from the copper(II) ion, dpyam and two different $H_xPO_4^{(3-x)-}$ bridges with a novel coordination mode.

2. Experimental

2.1. Experimental

An aqueous solution (30 ml) of $Cu(COOCH_3)_2$ (0.18 g, 1.0 mmol) was added to a solution of di-2-pyridylamine (0.17 g, 1.0 mmol) in ethanol (15 ml) and followed by an aqueous solution (20 ml) of potassium dihydrogenphosphate (0.27 g, 2.0 mmol) and an aqueous solution (10 ml) of potassium hexafluorophosphate (0.18 g, 1.0 mmol). The resulting green solution was allowed to evaporate at room temperature for 2 weeks, producing dark green needle crystals of **1** (*Anal.* Calc. for $C_{30}H_{36}Cu_3F_6N_9O_{12}P_3$: C, 32.4; H, 3.3; N, 11.3. Found: C, 32.7; H, 3.3; N, 11.4%). IR (KBr; cm^{-1}): 3411 m, 1195 s, 1100 s, 1074 s, 1015 m, 984 w, 842 s, 768 s, 558 m, 499 w. X-band powder EPR spectrum was obtained on a JEOL RE2X electron spin resonance spectrometer with DPPH ($g = 2.0036$) as a reference. Magnetic susceptibility measurements were carried out using a Quantum design MPMS-5 5T SQUID magnetometer (measurements carried out at 1000 G). Data were corrected for magnetization of the sample holder and for diamagnetic contributions, which were estimated from the Pascal constants.

2.1.1. Crystal data

$C_{30}H_{36}Cu_3F_6N_9O_{12}P_3$, triclinic, space group $P\bar{1}$, $a = 7.4301(5)$, $b = 15.9715(10)$, $c = 17.4521(11)$ (Å), $\alpha = 67.9970(10)°$, $\beta = 85.2240(10)°$, $\gamma = 79.7430(10)°$, $V = 1889.2(2)$ (Å^3), $\mu = 1.955$ Mg/m^3 and $R_1 = 0.0458$ for 7116 reflections. Reflection data for complex **1** were collected on a 1K Bruker SMART CCD area-detector diffractometer. Data reduction and cell refinements were performed using the program SAINT [9]. The structure was solved by direct methods and refined by full-matrix least-squares method on $(F_{obs})^2$ with anisotropic thermal parameters for all non-hydrogen atoms using the SHELXTL-PC V 6.12 [10] software package. All hydrogen atoms were located by difference synthesis and refined isotropically. The molecular graphics were created by using SHELXTL-PC [10]. CCDC reference number 240395 (see crystallographic data in CIF format, e-mail: deposit@ccdc.cam.ac.uk, www: http://www.ccdc.cam.ac.uk).

3. Results and discussion

The structure of **1** (Fig. 1) consists of a polynuclear infinite chain structure of $[Cu_3(dpyam)_3(\mu_3,\eta^4\text{-}PO_4)(\mu_3,\eta^3\text{-}HPO_4)(H_2O)]^+$ cations, uncoordinated PF_6^- anions and lattice water molecules.

The Cu atoms are bridged unsymmetrically through mixed tridentate hydrogenphosphate and tetradentate phosphate ligands. The tridentate HPO_4^{2-} anion coordinates monodentately to three different Cu(II) ions, resulting in a μ_3,η^3 coordination mode. The tetradentate PO_4^{3-} anion coordinates didentately to two different Cu(II) ions and monodentately to a third Cu(II) ion, resulting in a μ_3,η^4 coordination mode.

The five-coordinated CuN_2O_3 chromophore around the Cu1 ion is obtained by two nitrogen atoms of a dpyam ligand (Cu–N distances 2.008(3), 2.027(3) Å), two oxygen atoms of two different hydrogenphosphate anions (Cu–O distances 1.957(2), 1.942(2) Å) and an oxygen of a coordinated water molecule (Cu–O distance 2.191(3) Å). The largest angle (O1–Cu1–N1) is 166.93(11)°, while the angles of the trigonal plane are 132.82(12)°, 119.12(11)° and 107.70(12)°.

The distortion of a square pyramidal coordination sphere can be described by the structural parameter τ, which indicates the relative amount of trigonality ($\tau = 0$ for a pure square pyramid (sp) and $\tau = 1$ for a trigonal bipyramid (tbp) [11]). In this case $\tau = 0.57$, so the geometry can be described as an intermediate between sp and tbp.

The other two Cu(II) ions have both a distorted square-pyramidal geometry. The basal plane of Cu2 consists of two oxygen atoms from different bridging μ_3,η^3-HPO_4 and μ_3,η^4-PO_4 anions (Cu–O distances 1.929(2), 1.920(2) Å) and two nitrogen atoms from a dpyam ligand (Cu–N distances 1.991(3), 1.978(3) Å). The apical position is formed by an oxygen atom from a didentate coordinated phosphate group at a semi-coordination distance of 2.912(1) Å. The basal angles are 150.69(12)° and 140.26(12)°, resulting in a τ value of 0.17.

The geometry of Cu3 is almost the same as Cu2 with the basal plane consisting of two oxygen atoms from different bridging μ_3,η^3-HPO_4 and μ_3,η^4-PO_4 anions (Cu–O distances (1.924(2), 1.908(2) Å) and two nitrogen atoms from a dpyam ligand (Cu–N distances 1.976(3), 1.985(3) Å). The apical position is formed by an oxygen atom from a didentate coordinated phosphate group at a semi-coordination distance of 2.989(1) Å. The basal angles are 155.82(11)° and 148.04(12)°, resulting in a τ value of 0.13. The square-pyramidal geometry is quite distorted as the four in-plane atoms (N4, N5, O2A, O7 for Cu2 and N7, N8, O4A, O5 for Cu3) are not planar with an extremely high r.m.s. deviations of 0.804 and 0.598 Å, respectively. The Cu ion lies 0.079 Å for Cu2 and 0.062 Å for Cu3 above this plane towards

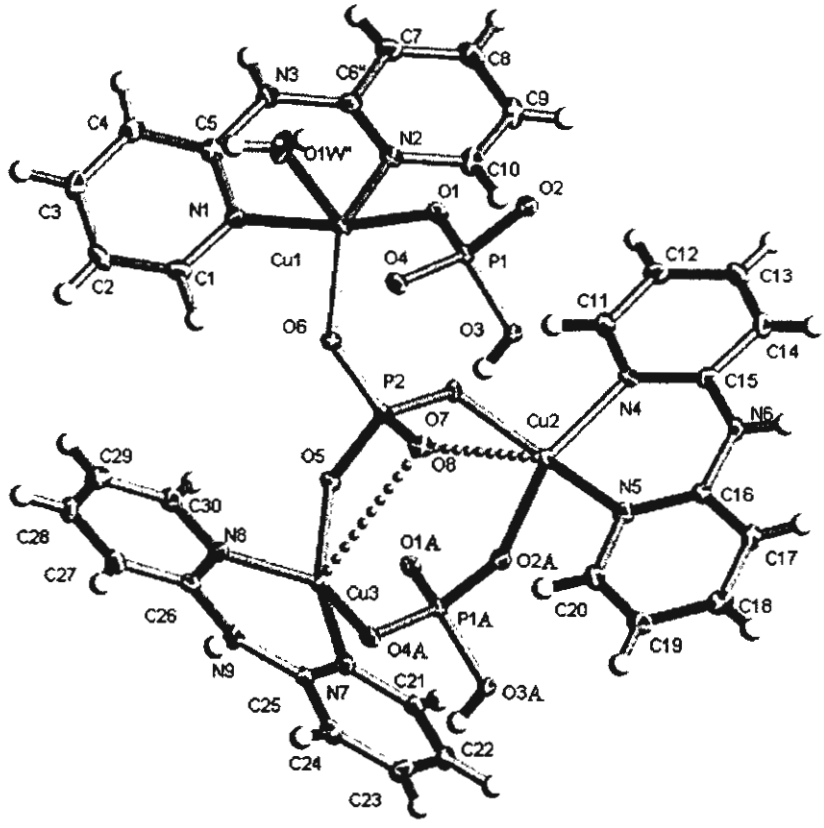

Fig. 1. Thermal ellipsoid (50% probability) plot of the title compound. The uncoordinating PF_6 anion and the lattice water molecules are omitted for clarity. Selected bond lengths (Å) and angles (°) Cu(1)–O(6) 1.942(2), Cu(1)–O(1) 1.957(2), Cu(1)–N(1) 2.008(3), Cu(1)–N(2) 2.027(3), Cu(1)–O(1W) 2.191(3), Cu(2)–O(2A) 1.920(2), Cu(2)–O(7) 1.929(2), Cu(2)–N(5) 1.978(3), Cu(2)–N(4) 1.991(3), Cu(2)–O(8) 2.912(1), Cu(3)–O(4A) 1.908(2), Cu(3)–O(5) 1.924(2), Cu(3)–N(8) 1.976(3), Cu(3)–N(7) 1.985(3), Cu(3)–O(8) 2.989(1), O(6)–Cu(1)–O(1) 97.3(1), O(1)–Cu(1)–N(1) 166.9(1), O(6)–Cu(1)–N(2) 132.8(1), O(6)–Cu(1)–O(1W) 119.1(1), N(2)–Cu(1)–O(1W) 107.6(1), O(7)–Cu(2)–N(5) 150.6(1), O(2A)–Cu(2)–N(4) 140.2(1), O(4A)–Cu(3)–N(8) 148.0(1), O(5)–Cu(3)–N(7) 155.8(1), Cu1–Cu2 5.218, Cu1–Cu3 5.942, Çu2–Cu3 4.407(7). $A = -x + 2, -y, -z + 1$.

O8. The origin of this distortion is the small value for the angles O5–Cu3–O8 and O7–Cu2–O8 (56.61° and 58.09°, respectively).

The lattice structure is stabilised by a hydrogen-bonding network interaction with N···O distances of 2.807–2.914 Å, O···O distances of 2.544–2.982 Å and O···F distances from 2.936 to 3.113 Å.

The diffuse reflectance spectrum of **1** measured as a solid shows a broad band centred at about $12.5 \times 10^3\ cm^{-1}$, which can be considered as normal for the presence of both trigonal bipyramidal to square-pyramidal geometries [12].

The polycrystalline EPR spectrum of compound **1** reveals at RT and 77 K a very broad isotropic signal with $g = 2.12$. This single signal may be due to exchange narrowing and also to the fact that the compound contains three different copper sites, with different g-tensor orientations.

The magnetic susceptibility of a powdered sample was measured from 5 to 250 K. The magnetic properties

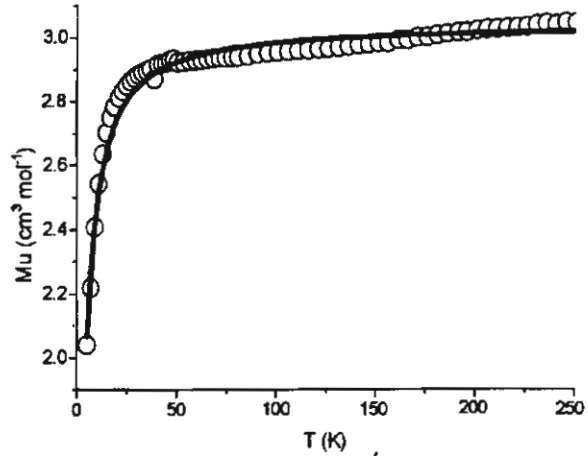

Fig. 2. A plot for compound **1** of temperature dependence of μ_{eff} vs. T is shown; the solid line represents the calculated curve for the parameters $J = -4.98\ cm^{-1}$, $g = 2.03$ and $zJ' = -1.49\ cm^{-1}$, see text.

of the complex are depicted in Fig. 2 in the form of μ_{eff} versus T for three Cu(II) ions.

From 250 K to about 30 K the μ_{eff} stays almost constant between 3.1–2.90 BM. This value is somewhat lower than the spin-only value of three uncoupled copper(II) $S = 1/2$ ions (theoretical value for $g = 2$, $\mu_{eff} = 3.88$ BM). At about 30 K the μ_{eff} starts to decrease slightly to a value of 1.95 BM at 5 K. This overall behaviour indicates a very weak antiferromagnetic interaction between the Cu(II) ions. The magnetic data were fitted to the theoretical expression for the magnetic susceptibility of a triangular trinuclear system, considering the following Hamiltonian for the description of the magnetic interactions: $\mathbf{H} = -J_{12}\ (\mathbf{S_1} \cdot \mathbf{S_2}) - J_{13}(\mathbf{S_1} \cdot \mathbf{S_3}) - J_{23}\ (\mathbf{S_2} \cdot \mathbf{S_3})$.

Although the Cu(II) triangle in compound **1** is not strictly equilateral, we considered identical g tensors and exchange integrals J_{ij} for the three copper(II) ions. This is because using the general expression for an asymmetrical triangular system does not give direct access to the exchange parameters [13], they are then related to each other, without increasing the quality of the fit in this particular case. The expression for the molar susceptibility is then derived from the above Hamiltonian as used before in the literature [14–16].

The common exchange parameter is denoted as J and parameter zJ' introduces intercluster magnetic interactions, with z nearest neighbours. A Temperature Independent Paramagnetism (TIP) was also considered and fixed at 60×10^{-6} per copper. Minimising the function $R = \sum(\chi_{obs} - \chi_{calc})^2 / \sum \chi^2_{obs}$, the best fit was obtained for $J = -4.98\ cm^{-1}$, $g = 2.03$ and $zJ' = -1.49\ cm^{-1}$, with $R = 8 \times 10^{-3}$.

The phosphate bridges in the title compound are in an equatorial–equatorial mode for Cu1–Cu2 and Cu1–Cu3, TBP-SP and the hydrogenphosphate links Cu2 and Cu3 in an equatorial-equatorial mode of the square pyramidal environment. The unpaired electron is usually in the $d_{x^2-y^2}$ for the square pyramidal geometry and delocalized in d_z^2 for the trigonal bipyramidal environment. As the Cu1 environment is extremely distorted trigonal bipyramidal (in fact an intermediate five-coordinated geometry) and Cu2 and Cu3 are in an extremely tetrahedral distorted square-based pyramidal environment, hence remarkable diminish the delocalized efficiency of the unpaired electrons resulting from a weaker overlap between magnetic orbitals, and therefore a weaker antiferromagnetic interaction is observed. Moreover, the three Cu ions are far away from each other (distances vary from 4.407 to 5.942 Å).

So far such Cu(II) compounds with phosphato bridges of which also the magnetic interaction reported have been rare and more examples will be required for magneto-structural correlations in such compounds.

Acknowledgements

The authors thank The Thailand Research Fund and Khon Kaen University for a research Grant. Support of the Postgraduate Education and Research Program in Chemistry in Thailand is also gratefully acknowledged. The work described in the present paper has been supported by the Leiden University Study group WFMO (Werkgroep Fundamenteel MaterialenOnderzoek).

References

[1] R.C. Haushalter, L.A. Mundi, Chem. Mater. 4 (1992) 31.
[2] K.-H. Lii, Y.-F. Huang, V. Zima, C.-Y. Huang, H.-M. Lin, Y.-C. Jiang, F.-L. Liao, S.-L. Wang, Chem. Mater. 10 (1998) 2599.
[3] A.K. Cheetham, G. Férey, T. Loiseau, Angew. Chem., Int. Ed. 38 (1999) 3268.
[4] S.T. Wilson, B.M. Lock, C.A. Messina, T.R. Cannan, E.M. Flanigen, J. Am. Chem. Soc. 104 (1982) 1146.
[5] R.C. Haushalter, L.A. Mundi, Chem. Mater. 4 (1992) 31.
[6] O.M. Yaghi, G. Li, H. Li, Nature 378 (1995) 703.
[7] R.C. Finn, J. Zubieta, J. Chem. Soc., Dalton Trans. (2002) 856.
[8] R.C. Finn, J. Zubieta, J. Phys. Chem. Solids 62 (2001) 1513.
[9] Siemens. SAINT 1997, Version4 Software Reference Manual, Siemens Analytical X-ray Systems, Inc., Madison, WI, USA, 1997.
[10] Siemens. SHELXTL 1997, Version 6.12 Reference Manual, Siemens Analytical X-Ray Systems, Inc., Madison, WI, USA, 1997.
[11] A.W. Addison, T.N. Rao, J. Reedijk, J. van Rijn, G.C. Verschoor, J. Chem. Soc., Dalton Trans. (1984) 1349.
[12] B.J. Hathaway, in: G. Wilkinson, R.D. Gill, J.A. McCleverty (Eds.), Comprehensive Coordination Chemistry, 5, Pergamon Press, Oxford, 1987.
[13] O. Kahn, Molecular Magnetism, VCH Publ., NY, 1993, references citied therein.
[14] A. Bencini, C. Benelli, A. Dei, D. Gatteschi, Inorg. Chem. 24 (1984) 695.
[15] G.A. van Albada, I. Mutikainen, O.S. Roubeau, U. Turpeinen, J. Reedijk, Eur. J. Inorg. Chem. (2000) 2179.
[16] G.A. van Albada, I. Mutikainen, O.S. Roubeau, U. Turpeinen, J. Reedijk, Inorg. Chim. Acta 331 (2002) 208.

Available online at www.sciencedirect.com
SCIENCE DIRECT®
Inorganica Chimica Acta 358 (2005) 2262–2268
Inorganica Chimica Acta
www.elsevier.com/locate/ica

A novel tetranuclear hydrogenphosphate-bridged Cu(II) cluster. Synthesis, structure, spectroscopy and magnetism of $[Cu_4(dpyam)_4(\mu_4,\eta^3\text{-}HPO_4)_2(\mu\text{-}X)_2]X_2(H_2O)_6$ (X = Cl, Br)

Sujittra Youngme [a,*], Pongthipun Phuengphai [a], Narongsak Chaichit [b], Gerard A. van Albada [c], Olivier Roubeau [d], Jan Reedijk [c]

[a] *Department of Chemistry, Faculty of Science, Khon Kaen University, Khon Kaen 40002, Thailand*
[b] *Department of Physics, Faculty of Science and Technology, Thammasat University Rangsit, Pathumthani 12121, Thailand*
[c] *Leiden Institute of Chemistry, Gorlaeus Laboratories, Leiden University, P.O. Box 9502, 2300 RA Leiden, The Netherlands*
[d] *Centre de Recherche Paul Pascal – CNRS, 115 avenue du dr. A. Schweitzer, 33600 Pessac, France*

Received 18 August 2004; accepted 21 January 2005

Abstract

Two novel tetranuclear $\mu_4,\eta^3\text{-}HPO_4^{2-}Cu(II)$ compounds with an unprecedented mode of a hydrogenphosphato bridge, $[Cu_4(dpyam)_4(\mu_4,\eta^3\text{-}HPO_4)_2(\mu\text{-}X)_2]^{2+}$ (in which dpyam = di-2-pyridylamine and X = Cl (**1**), Br (**2**)) have been synthesised and characterised structurally and magnetically. The Cu(II) ions in the structures each display a square-pyramidal geometry, with two tridentate hydrogenphosphato groups bridging four copper atoms in a μ_4,η^3 coordination mode which is rarely found in hydrogenphosphate metal compounds. Each (different) pair of Cu(II) ions is additionally bridged by halide ions, with relatively long Cu–X distances (2.551(3)–2.604(3) Å for **1** and 2.707(1)–2.766(2) Å for **2**) and subsequently also a small Cu–X–Cu angle (65.7(1)° and 65.1(1)° for **1** and 61.6(1)° and 62.4(1) for **2**) and a large Cu–X–Cu angle (95.5(1)° and 96.5(1)° for **1** and 91.1(1)° and 92.6(1)° for **2**). Cu···Cu distances in the tetranuclear units varies from 2.802(3) to 5.232(3) Å for **1** and from 2.834(1) to5.233(1) Å in **2**. The lattice structures are stabilised by extensive intermolecular hydrogen bonds. The magnetic susceptibility measurements down to 5 K revealed a weak ferromagnetic interaction between the outer pairs of Cu(II) ions which vary from 22 to 46 cm^{-1} in **1** and 12 to 33 cm^{-1} in **2** and a moderately strong antiferromagnetic interaction between the inner Cu(II) ions of -79 cm^{-1} in **1** and -83 cm^{-1} in **2**, via the Cu–O–P–O–Cu pathway.

Keywords: Tetranuclear complexes; Copper (II) cluster; Hydrogenphosphate complexes; Di-2-pyridylamine; Magnetism

1. Introduction

The synthesis of open-framework metal phosphates has been a subject of intense research owing to their interesting structural chemistry and potential applications as ion-exchangers, catalysts and adsorbents [1–3]. A large number of these materials are synthesised in the presence of organic amines as structure directing (templating) agents. Recently, many research activities have focused on the synthesis of organic–inorganic hybrid frameworks, such as phosphates of transition metals [4–7]. As compared with organic ligands, the advantage of using inorganic multidentate anionic ligands in combination with organic polar molecules and ligands is the efficacy of rational design of crystalline solids through their coordinating properties and geometries. So far the most extensively studied bridging

* Corresponding author. Tel.: +66043202222-41; fax: +66043202373.
E-mail address: sujittra@kku.ac.th (S. Youngme).

0020-1693/$ - see front matter © 2005 Elsevier B.V. All rights reserved.
doi:10.1016/j.ica.2005.01.019

organic ligand with transition metals and phosphate is 4,4′-bipyridine with a number of one-, two- and three-dimensional structures [4–8]. With ligands like 2,2′-bipyridine [9] and 1,10-phenanthroline [10] the number of such new organic–inorganic hybrid compounds are rare. Now we have extended this research by using the ligand di-2-pyridylamine (abbreviated as dpyam) and have isolated several new phases in such organic–inorganic metal-phosphate systems. In the present study, two novel examples of the dpyam-phosphate system, $[Cu_4(dpyam)_4(\mu_4,\eta^3\text{-}HPO_4)_2(\mu\text{-}Cl)_2]Cl_2(H_2O)_6$ (**1**) and $[Cu_4(dpyam)_4(\mu_4,\eta^3\text{-}HPO_4)_2(\mu\text{-}Br)_2]Br_2(H_2O)_6$ (**2**) are reported.

Both compounds were prepared as green crystals from potassium dihydrogenphosphate, dpyam and copper halide in ethanol under ambient conditions and characterised by elemental analysis and infrared spectroscopy. Also the magnetic susceptibility has been studied. The two new compounds have a μ_4-HPO_4 bridging system, which is to the best of our knowledge only reported once [11] and in that case the copper (II) atoms are also bridged by a carbonato ligand. This is the first case reported for a tetranuclear Cu(II) system bridged only by μ_4-HPO_4 and halide anions.

2. Experimental

2.1. Synthesis of the compounds

Solid KH_2PO_4 (0.27 g, 2.0 mmol) dissolved in water (20 ml) was added to a warm solution of di-2-pyridylamine (0.17 g, 1.0 mmol) in ethanol (15 ml) yielding a pale-yellow solution. The colour became greenish by slow addition of an aqueous solution (30 ml) of $CuCl_2 \cdot 2H_2O$ (0.17 g, 1.0 mmol). The resulting green solution was allowed to evaporate at room temperature. After several days, green crystals of **1** were deposited. They were filtered off, washed with the mother liquid and air-dried. Compound **2** was prepared similarly to that of **1** using $CuBr_2$ (0.22 g,1.0 mmol) as starting material. Yield approx. 67%. Elemental analyses of the bulk powders, as used for the measurements: Compound **1** ($Cu_4(dpyam)_4(HPO_4)_2(Cl)_2](Cl)_2(H_2O)_{5.5}$): *Anal.* Calc. for $C_{40}H_{49}Cu_4N_{12}O_{13.5}Cl_4P_2$: C, 35.02; H, 3.60; N, 12.25. Found: C, 34.88; H, 3.42; N, 12.13%. Compound **2**: $Cu_4(dpyam)_4(HPO_4)_2(Br)_2](Br)_2(H_2O)_{5.5}$; *Anal.* Calc. for $C_{40}H_{49}Cu_4N_{12}O_{13.5}\ Br_4P_2$: C, 31.00; H, 3.18; N, 10.84. Found: C, 31.61; H, 2.96; N, 10.79%.

2.2. Physical measurements

IR spectra were recorded on a Spectrum One Perkin–Elmer FT-IR spectrophotometer as KBr pellets in the 4000–450 cm^{-1} spectral range. Diffuse reflectance measurements from 9090 to 20 000 cm^{-1} were recorded as polycrystalline samples using a Perkin–Elmer Lambda 2S spectrophotometer equipped with an integrating sphere attachment. Barium sulfate was used as the reflectance standard. X-band powder EPR spectra were recorded on a JEOL RE2x electron spin resonance spectrometer using DPPH ($g = 2.0036$) as a standard. Magnetic susceptibility measurements (5–350 K) were carried out using a Quantum Design MPMS-5 5T SQUID magnetometer (measurements carried out at 0.1 T). Data were corrected for magnetisation of the sample holder and for diamagnetic contributions, which were estimated from the Pascal constants.

2.3. Crystal structure analyses

Reflection data for complexes **1** and **2** were collected at 293 K on a 1K Bruker SMART CCD area-detector diffractometer using graphite monochromated Mo Kα radiation ($\lambda = 0.71073$ Å). Data reduction and cell refinements were performed using the program SAINT [12]. The structures were solved by direct methods and refined by full-matrix least-squares method on $(F_{obs})^2$ with anisotropic thermal parameters for all non-hydrogen atoms using the SHELXTL-PC V 6.12 [13] software package. All hydrogen atoms in **1** were located by difference synthesis and refined isotropically except H(22), H(29), H(42), H(52) and H(58). These hydrogen atoms were geometrically fixed and allowed to ride on attached atoms. One water hydrogen atom and one hydrogenphosphate hydrogen atom of **1** were unable to locate and also not fixed. For **2**, all hydrogen atoms were located and refined isotropically except five water hydrogen atoms, which were unable to locate and also not fixed. Two water oxygen atoms of both compounds were disordered and were refined with site occupancies of 0.5. Moreover, two water oxygen atoms of both compounds were refined with site occupation factor of 0.5. The molecular graphics were created by using SHELXTL-PC [13]. Crystallographic data for both structures are presented in Table 1.

3. Results and discussion

3.1. Description of the structures

The asymmetric unit of **1** and **2** consists of one and a half units of $[Cu_4(dpyam)_4(\mu_4,\eta^3\text{-}HPO_4)_2(\mu\text{-}X)_2]X_2$ (X = Cl, Br) and 12 lattice water molecules, two of which having site occupation factor of 0.5. Both structures are isostructural. Structures **1** and **2** involve two crystallographically independent, but very similar tetranuclear units of $[Cu_4(dpyam)_4(\mu_4,\eta^3\text{-}HPO_4)_2(\mu\text{-}X)_2]^{2+}$. One unit of each structure with the atomic numbering system is presented in Figs. 1 and 2, for compounds **1** and **2**, respectively. The second unit of compounds **1**

Table 1
Crystallographic data for compounds 1 and 2

Complex	1	2
Molecular formula	$[Cu_4(dpyam)_4(HPO_4)_2(Cl)_2](Cl)_2(H_2O)_6$	$[Cu_4(dpyam)_4(HPO_4)_2(Br)_2](Br)_2(H_2O)_6$
Empirical formula	$C_{60}H_{79}Cu_6N_{18}O_{23}Cl_6P_3$	$C_{60}H_{79}Cu_6N_{18}O_{23}Br_6P_3$
Formula weight	2107.26	2374.02
T (K)	273(2)	273(2)
Crystal system	monoclinic	monoclinic
Space group	*Cm*	*Cm*
a (Å)	16.3150(2)	16.4716(3)
b (Å)	48.2777(1)	49.3270(4)
c (Å)	12.5824(1)	12.6314(2)
β (°)	125.9980(10)	126.2060(10)
V (Å^3)	8017.99(12)	8281.1(2)
Z	4	4
D_{cal} (g cm^{-3})	1.746	1.904
μ (mm^{-1})	1.907	4.548
$F(0\,0\,0)$	4280	4712
Crystal size (mm)	$0.33 \times 0.45 \times 0.75$	$0.23 \times 0.24 \times 0.35$
θ (°)	1.60–30.55	1.59–30.43
Number of reflections collected	30 204	31 126
Number of unique reflections	17 411	18 172
Number of observed references $[I > 2\sigma(I)]$	11 833	10 280
T_{max} and T_{min}	1.000 and 0.712	1.000 and 0.709
Data/restraints/parameter	17 411/2/1306	18 172/2/1090
Goodness-of-fit	1.044	1.019
Final R indices $[I > 2\sigma(I)]$	$R_1 = 0.0364$, $wR_2 = 0.0914$	$R_1 = 0.0796$, $wR_2 = 0.1949$
R indices (all data)	$R_1 = 0.0448$, $wR_2 = 0.0981$	$R_1 = 0.1148$, $wR_2 = 0.2255$
Largest difference peak and hole (e Å^{-3})	1.981 and −0.604	6.603 and −1.298

$R = \sum ||F_o| - |F_c|| / \sum |F_o||$, $R_w = [\sum w\{|F_o| - |F_c|\}^2 / w|F_o|^2]^{1/2}$.

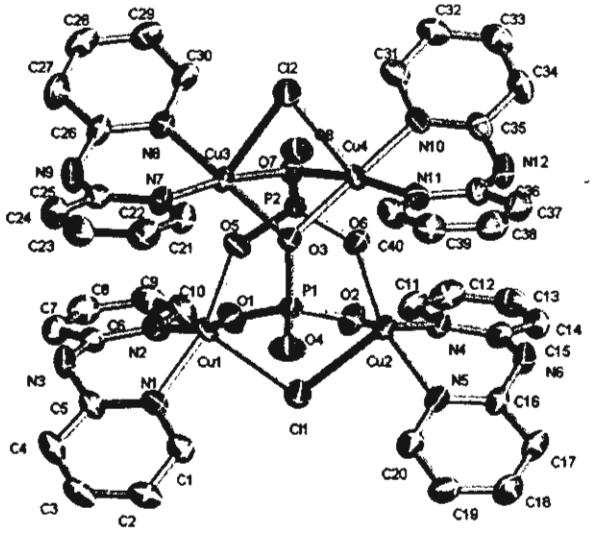

Fig. 1. Thermal ellipsoid plot of the first unit of compound 1 with labeling scheme. Hydrogen atoms, the uncoordinating chloride atoms and the lattice water molecules are omitted for clarity.

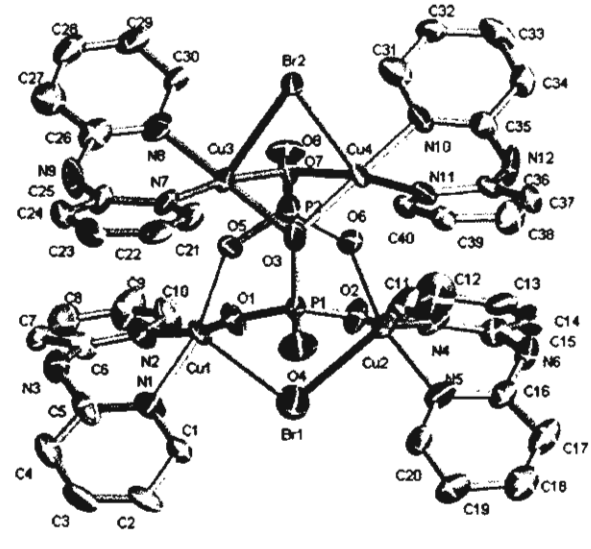

Fig. 2. Thermal ellipsoid plot of the first unit of compound 2 with labeling scheme. Hydrogen atoms, the uncoordinating bromide atoms and the lattice water molecules are omitted for clarity.

and 2 is given as supplementary material (Figs. S1 and S2). Selected bond lengths and angles are given in Table 2. The first unit of each compound is situated on a general position, whereas the second unit is situated on a mirror plane. The unit cell contains four molecules on general positions and two molecules on special positions.

Each tetranuclear unit of both compounds consists of two pairs of five-coordinated copper (II) ions bridged by two tetrahedral tridentate hydrogenphosphato groups in

Table 2
Selected distances and angles for compounds **1** and **2**

	1	2
Bond lengths		
Cu(6)–N(17)	1.962(4)	1.977(9)
Cu(6)–N(16)	1.965(4)	1.960(9)
Cu(6)–O(9)	2.011(3)	2.045(7)
Cu(6)–O(12)	2.021(3)	2.039(8)
Cu(6)–X(4)	2.604(1)	2.766(2)
Cu(5)–O(10)	1.947(3)	1.937(9)
Cu(5)–O(13)	1.966(3)	1.974(9)
Cu(5)–N(14)	1.993(4)	2.008(10)
Cu(5)–N(13)	2.012(4)	2.019(10)
Cu(5)–X(3)	2.560(1)	2.708(1)
Cu(4)–N(10)	1.970(4)	1.981(10)
Cu(4)–N(11)	1.982(4)	1.998(10)
Cu(4)–O(7)	2.012(3)	2.005(7)
Cu(4)–O(3)	2.026(3)	2.029(8)
Cu(4)–X(2)	2.592(1)	2.745(1)
Cu(3)–N(8)	1.971(4)	1.984(10)
Cu(3)–N(7)	1.981(4)	2.005(10)
Cu(3)–O(7)	2.012(3)	1.993(7)
Cu(3)–O(3)	2.030(3)	2.033(8)
Cu(3)–X(2)	2.598(1)	2.757(1)
Cu(2)–O(6)	1.950(3)	1.979(8)
Cu(2)–O(2)	1.969(3)	1.970(8)
Cu(2)–N(5)	1.996(4)	1.987(10)
Cu(2)–N(4)	2.009(4)	2.023(9)
Cu(2)–X(1)	2.556(1)	2.720(1)
Cu(1)–O(5)	1.948(3)	1.988(8)
Cu(1)–O(1)	1.965(3)	1.974(7)
Cu(1)–N(1)	1.993(3)	2.003(10)
Cu(1)–N(2)	2.001(4)	2.021(10)
Cu(1)–X(1)	2.551(1)	2.715(1)
Cu(1)–Cu(2)	3.781(1)	3.881(1)
Cu(3)–Cu(4)	2.816(1)	2.851(1)
Cu(2)–Cu(4)	4.027(3)	4.028(1)
Cu(1)–Cu(3)	4.069(3)	4.036(1)
Cu(5)–Cu(6)	4.072(3)	4.035(1)
Cu(5)–Cu(5A)	3.820(1)	3.918(1)
Cu(5A)–Cu(6A)	5.224(1)	5.234(1)
Cu(6)–Cu(6A)	2.802(1)	2.834(1)
Bond angles		
N(16)–Cu(6)–O(9)	171.7(2)	173.2(4)
N(17)–Cu(6)–O(12)	172.9(2)	173.1(4)
O(10)–Cu(5)–N(14)	164.0(2)	165.0(4)
O(13)–Cu(5)–N(13)	162.5(2)	163.3(4)
N(11)–Cu(4)–O(7)	171.6(2)	170.8(4)
N(10)–Cu(4)–O(3)	173.3(2)	174.2(4)
N(7)–Cu(3)–O(7)	171.7(2)	170.8(4)
N(8)–Cu(3)–O(3)	173.4(2)	175.1(4)
O(6)–Cu(2)–N(5)	162.6(2)	164.5(4)
O(2)–Cu(2)–N(4)	164.8(2)	164.9(4)
O(5)–Cu(1)–N(1)	164.5(2)	165.3(4)
O(1)–Cu(1)–N(2)	161.3(2)	162.3(4)
Cu(1)–X(1)–Cu(2)	95.5(1)	91.1(1)
Cu(3)–X(2)–Cu(4)	65.7(1)	62.4(1)
Cu(5)–X(3)–Cu(5A)	96.5(1)	92.6(1)
Cu(6)–X(4)–Cu(6A)	65.1(1)	61.6(1)

Symmetry code: $A = -x, -y + 1, -z$, and X = Cl and Br for **1** and **2**, respectively.

each molecule. Both HPO_4^{2-} groups coordinate monodentately to one copper (II) ion and bridging via one oxygen to two other Cu(II) ions, yielding a very rare μ_4,η^3 coordination mode. Each copper ion has a planar square base with a CuN_2O_2X chromophore consisting of two oxygen atoms of two bridging HPO_4^{2-} groups (Cu–O distances vary from 1.947(3) to 2.030(3) Å) and two nitrogen atoms of a dpyam ligand (Cu–N distances vary from 1.962(4) to 2.012(4) Å). The axial position is occupied by a bridging halide anion (Cu–Cl distances vary from 2.559(1) to 2.604(1) Å and Cu–Br distances vary from 2.708(1) to 2.766(2) Å), thus giving a slightly tetrahedrally distorted square-based pyramidal CuN_2O_2X chromophore for both units in compounds **1** and **2**.

Consequently, all copper (II) ions are linked to each other via double-bridged HPO_4^{2-} groups in an equatorial–equatorial configuration. Each copper atom is displaced 0.072 to 0.340 Å and 0.069 to 0.337 Å for Cu(1) to Cu(6) of **1** and **2**, respectively, from the basal plane (N_2O_2) towards the apical halide ion. The τ value (τ describes the relative amount of trigonality; $\tau = 0$ for square pyramid and $\tau = 1$ for trigonal bipyramidal [14]) vary from 0.020 to 0.053 and 0.001 to 0.071 for compounds **1** and **2**, respectively, indicating a nearly perfect square-based pyramidal geometry for all CuN_2O_2X chromophores.

The Cu···Cu distances in the tetranuclear units vary from 2.802(1) to 5.224(1) Å in **1** and from 2.834(2) to 5.234(1) Å in compound **2**.

Each tetranuclear unit has a unique structure with a short Cu–Cu distance (2.816(1) and 2.802(1) Å for **1** and 2.834(1) and 2.851(1) Å for**2**) and a long Cu–Cu distance (3.781(1) and 3.820(1) Å for **1** and 3.881(1) and 3.918(1) for **2**). Consequently, the units have also a small Cu–X–Cu angle (65.7(1)° and 65.1(1)° for **1** and 61.6(1)° and 62.4(1) for **2**) and a large Cu–X–Cu angle (95.5(1)° and 96.5(1)° for **1** and 91.1(1)° and 92.7(1)° for **2**). See Table 2 for details.

The lattice structure is stabilised by a complicated hydrogen-bonding network between oxygen atoms of the hydrogenphosphato groups and oxygen atoms of uncoordinated water molecules (O···O distances vary from 2.587(1) to 2.639(1) Å for **1**, and from 2.587(1) to 2.591(1) Å for **2**) and between oxygen atoms of different water molecules (O···O distances vary from 2.664(1) to 2.845(1) Å for **1** and from 2.588(1) to 2.695(1) Å for **2**). Also hydrogen bond contacts are observed between the O and N atoms and the halide ions (distances vary from 3.139(1) to 3.420(1) Å for **1** and from 3.276(1) to 3.542(1) Å for **2**).

3.2. Electronic and infrared spectra

The electronic diffuse reflectance spectra of **1** and **2** consist of an unsymmetrical, broad band centred around 15.0×10^3 and $14.9 \times 10^3\ cm^{-1}$, respectively, consistent with the square-pyramidal stereochemistry [15].

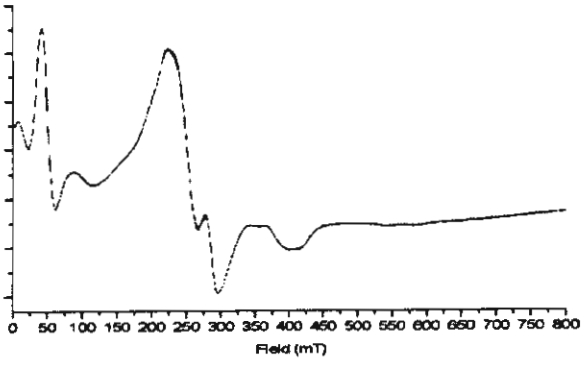

Fig. 3. X-band EPR spectrum (solid) of **1** measured at 77 K.

The infrared spectra of both compounds exhibit strong bands for the phosphato anions [16,17] at 1159, 1098 and 980 cm^{-1} [ν(P–O)] and 529 and 511 cm^{-1} [δ(O–P–O)] for **1** and 1159, 1096 and 976 cm^{-1} [ν(P–O)] and 529 and 511 cm^{-1} [δ(O–P–O) for **2**.

3.3. EPR spectroscopy

The X-band polycrystalline powder EPR spectra of compound **1**, measured from 0 to 800 mT at 77 K (see Fig. 3), revealed a triplet spectrum with some large and less large features at about 50, 90, 225, 280 and 350 mT. Also two very weak signals occur at about 540 and 580 indicating that different Cu(II) species are present. This type of spectrum can be compared with some other tetranuclear copper (II) compounds with a $D > h\nu$ (about 0.3 cm^{-1}) [18,19]. The absorption at low field is most probably the $\Delta M_s = \pm 2$ transition, while the absorption around 280 mT can be attributed to the $\Delta M_s = \pm 1$ transition. For such complicated tetranuclear species, a single-crystal EPR analysis would be required to establish the exact zero-field splitting parameters; this is outside the scope of this investigation. The EPR spectrum of **2** at 77 K and both spectra at RT are presented as supplementary material as Figs. S3, S4 and S5, respectively.

3.4. Magnetic susceptibility

The magnetisation of powdered samples of **1** and **2** were measured from 5 to 350 K in an applied field of 0.1 T. The resulting molar magnetic susceptibility, χ_M and the product $\chi_M T$ are plotted in Figs. 4 and 5 for compounds **1** and **2**, respectively.

In both cases χ_M gradually increases upon lowering temperature from values at high temperatures in agreement with four uncoupled spin = 1/2 centres. A maximum is reached around 55 K, at which temperature χ_M decreases sharply. This behaviour is indicative of an antiferromagnetic coupling between some of the copper ions in **1** and **2**. For simplicity, the two similar tetranuclear units contained in the structures **1** and **2** will be considered as identical for the rationalisation of these magnetic properties. Moreover, the diagonal coupling pathways through phosphato groups (J_3 in Fig. 6) will also be assumed identical. These approximations result in the magnetic coupling scheme proposed in Fig. 6, in which the letters A, B, C and D correspond to the structural labelling of the Cu atoms (see Figs. 1 and 2). The Cu_A–Cu_B (J_2) interaction (Cu3–Cu4 in Fig. 1 with the Cu–O–Cu bridge) represents the shortest distance (about 2.8 Å), the Cu_C–Cu_D (J_4) interaction (Cu1–Cu2 in Fig. 2 with the Cu–O–P–O–Cu bridge) represents the long distance (about 3.8 Å), while the Cu_A–Cu_C and Cu_B–Cu_D (J_1) interaction (Cu3–Cu1 and

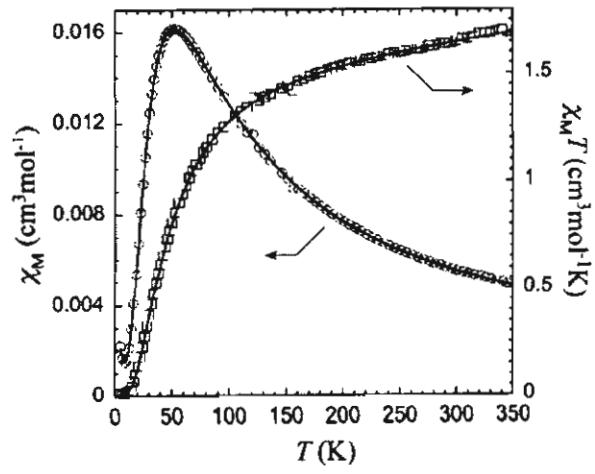

Fig. 4. Plots of temperature dependence of the molar magnetic susceptibility χ_M (○) and the $\chi_M T$ product (□) for compound **1**. The solid lines represent the calculated curves (see text).

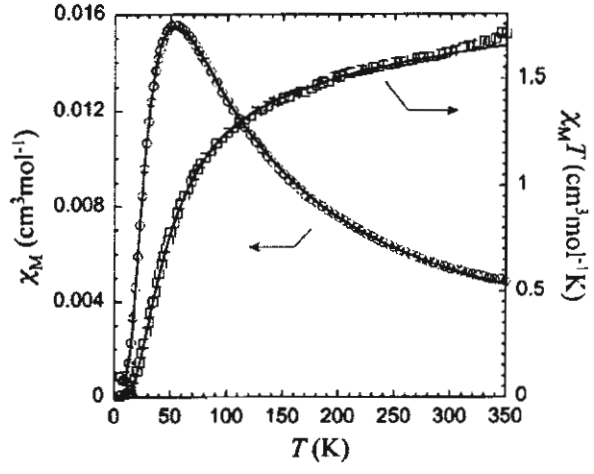

Fig. 5. Plots of temperature dependence of the molar magnetic susceptibility χ_M (○) and the $\chi_M T$ product (□) for compound **2**. The solid lines represent the calculated curves (see text).

Cu4–Cu2, respectively, in Fig. 1) have the longest distance of about 4.07 Å.

The corresponding Hamiltonian writes:

$$H = -2J_1(S_A \cdot S_C + S_B \cdot S_D) - 2J_2(S_A \cdot S_B) - 2J_3(S_B \cdot S_C + S_A \cdot S_D) - 2J_4(S_C \cdot S_D). \quad (1)$$

Although the topologies of the compounds differ, this Hamiltonian is identical to one solved for a linear tetranuclear copper compound [20,21].

The energy levels and their spin quantum numbers (used in the fitting procedure) which were derived are as follows:

$$S_1 = 2: \quad E_1 = -J_1 - J_2/2 - J_3 - J_4/2,$$

$$S_2 = 1: \quad E_2 = J_1 - J_2/2 + J_3 - J_4/2,$$

$$S_3 = 1: \quad E_3 = (J_2 + J_4)/2 + \left[(J_2 - J_4)^2 + (J_3 - J_1)^2\right]^{1/2},$$

$$S_4 = 1: \quad E_4 = (J_2 + J_4)/2 - \left[(J_2 - J_4)^2 + (J_3 - J_1)^2\right]^{1/2},$$

$$S_5 = 0: \quad E_5 = J_1 + J_3 + (J_2 + J_4)/2 + \left[4(J_1^2 + J_3^2) + J_2^2 + J_4^2 - 2J_1(J_2 + 2J_3 + J4) - 2J_2(J_3 - J_4) - 2J_3J_4\right]^{1/2},$$

$$S_6 = 0: \quad E_6 = J_1 + J_3 + (J_2 + J_4)/2 - \left[4(J_1^2 + J_3^2) + J_2^2 + J_4^2 - 2J_1(J_2 + 2J_3 + J4) - 2J_2(J_3 - J_4) - 2J_3J_4\right]^{1/2}.$$

Considering also that the g values are identical for all copper ions, the molar magnetic susceptibility is then

$$\chi_M = \frac{N_A g^2 \beta^2}{3k_B T} \frac{\sum_i S_i(S_i+1)(2S_i+1)\exp(-E_i/k_B T)}{\sum_i (S_i+1)\exp(-E_i/k_B T)}. \quad (2)$$

A term taking into account a small monomeric paramagnetic impurity was added to this expression and evaluated from the low temperature data as little as 0.05% and 0.06% for **1** and **2**, respectively. To avoid over-parameterisation, these terms were held constant during the fitting procedure as well as the g value, which was fixed at 2; this is a quite normal value for Cu(II) species. For both compounds, the experimental data were first fitted to Eq. (2) letting the coupling constants vary by groups of 2 and 3 and holding the other(s) to 0. In this way, it was found first that J_3 had to be negative (antiferromagnetic) of the order of $-60\,cm^{-1}$, and secondly, that the other coupling constants should be positive (ferromagnetic) with J_1 and J_2 of the same order, to obtain a good fit. At this point, one has to remark that these findings are in correct agreement with the structural data. Indeed, apart for the Cu_A–Cu_C and Cu_B–Cu_D pairs, the basal planes of the other pairs of copper ions are almost perpendicular to each other. This geometry indicates that the overlap between the spin-rich d_{x2-y2} orbitals of these copper ions cannot be expected to be important. In addition, Cu_A–O–Cu_B angles are close to 90°, a value yielding ferromagnetic interaction in dinuclear alkoxo- or hydroxo-bridged copper dimers [22,23]. Finally, halide bridges between Cu_A and Cu_B and Cu_C and Cu_D correspond to the axial coordination site of the copper ions where the spin density is negligible. Therefore, the participation of this pathway to the interactions should be negligible.

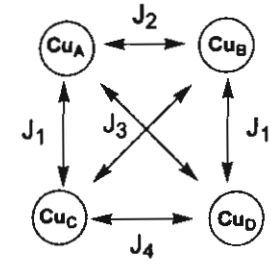

Fig. 6. Scheme of the magnetic interactions used in the calculations (see text).

So with the initial experiments stated above the data were fit by forcing $J_1 = J_2$ and letting the three remaining coupling constants free, starting from $J_3 < 0$ and J_1 and $J_4 > 0$. The two sets of best fit parameters, corresponding to the full lines in Figs. 4 and 5 were obtained as $2J_1 = 2J_2 = 22(2)\,cm^{-1}$, $2J_3 = -79(1)\,cm^{-1}$, $2J_4 = 46(4)\,cm^{-1}$ and $2J_1 = 2J_2 = 33(1)\,cm^{-1}$, $2J_3 = -83(1)\,cm^{-1}$, $2J_4 = 12(3)\,cm^{-1}$, for compounds **1** and **2**, respectively. Their magnetic behaviour is thus dominated by a medium antiferromagnetic interaction occurring through the diagonal phosphato bridges (J_3), resulting in a singlet ground state with a first excited triplet state at, e.g., 76 and $84\,cm^{-1}$ above it (see energy-level scheme above).

4. Conclusions

In summary, two novel tetranuclear μ_4, η^3-HPO_4^{2-}-bridged copper(II) complexes have been synthesised and reported in this study. These structures show a μ_4,η^3-bridging coordination mode which is rarely found in hydrogenphosphate metals compounds and these are the first structures reported with a μ_4-HPO_4 and halide system and these systems provide a new opportunity to study the coordination mode of hydrogenphosphate groups in relation with the magnetic behaviour. The magnetic properties are dominated by a moderately strong antiferromagnetic interaction via the Cu–O–P–O–Cu pathway between the diagonal (inner) Cu ions (Cu_1–Cu_4, Cu_2–Cu_3 pairs), but a weak ferromagnetic

interaction is observed between the outer Cu ions (Cu_3–Cu_4 and Cu_1–Cu_2 pairs).

Acknowledgments

The authors thank The Thailand Research Fund and Khon Kaen University for a research grant. Support of the Postgraduate Education and Research Program in Chemistry is also gratefully acknowledged. The work described in the present paper has been supported by the Leiden University Study group WFMO (Werkgroep Fundamenteel Materialen Onderzoek).

Appendix A. Supplementary data

The thermal ellipsoid plots of the second crystallographic units of compound **1** and compound **2** and their EPR spectra of **2** at 77 K and of **1** and **2** at RT are presented as supplementary material. Crystallographic data for the structures in this paper have been deposited with the Cambridge Crystallographic Data Centre as supplementary publication CCDC Nos. 233926 and 233927 for structures **1** and **2**, respectively. Copies of the data can be obtained free of charge from The Director, CCDC, 12 Union Road, Cambridge CB2 1EZ, UK (fax: +44-1223-336033; e-mail: deposit@ccdc.cam.ac.uk, www: http://www.ccdc.cam.ac.uk). Supplementary data associated with this article can be found, in the online version, at doi:10.1016/j.ica.2005.01.019.

References

[1] A.K. Cheetham, G. Ferey, T. Loiseau, Angew. Chem., Int. Ed. 38 (1999) 3286.
[2] K.-H. Lii, Y.-F. Huang, V. Zima, C.-Y. Huang, H.-M. Lin, Y.-C. Jiang, F.-L. Liao, S.-L. Wang, Chem. Mater. 10 (1998) 2599.
[3] P.J. Hagrman, D. Hagrman, J. Zubieta, Angew. Chem., Int. Ed. 38 (1999) 2638.
[4] H.-M. Lin, K.-H. Lii, Y.-C. Jiang, S.-L. Wang, Chem. Mater. 11 (1999) 519.
[5] C.-Y. Chen, P.P. Chu, K.-H. Lii, Chem. Commun. (1999) 1473.
[6] Z.A.D. Lethbridge, P. Lightfoot, J. Solid State Chem. 143 (1999) 58.
[7] A. Choudhury, S. Natarajan, C.N.R. Rao, J. Solid State Chem. 146 (1999) 538.
[8] L.-I. Hung, S.-L. Wang, H.-M. Kao, K.-H. Lii, Inorg. Chem. 41 (2002) 3929.
[9] W.-J. Chang, C.-Y. Chen, K.-H. Lii, J. Solid State Chem. 172 (2003) 6.
[10] R.C. Finn, J. Zubieta, J. Phys. Chem. Solid 62 (2001) 1513.
[11] G. De Munno, M. Julve, F. Lotret, M. Verdaguer, A. Caneschi, Inorg. Chem. 34 (1999) 157.
[12] Bruker (2000). SAINT (version 5.6), Bruker AXS Inc., Madison, Wisconsin, USA.
[13] Bruker (2000). SHELXTL (version 6.12), Bruker AXS Inc., Madison, Wisconsin, USA.
[14] A.W. Addison, T.N. Rao, J. Reedijk, J. van Rijn, G.C. Verschoor, J. Chem. Soc., Dalton Trans. (1984) 1349.
[15] B.J. Hathaway, in: G. Wilkinson, R.D. Gill, J.A. McCleverty (Eds.), Comprehensive Coordination Chemistry, vol. 5, Pergamon Press, Oxford, 1987.
[16] Y. Zhang, R.C. Haushalter, J. Zubieta, Inorg. Chim. Acta 260 (1997) 105.
[17] A.C. Chapman, L.E. Thirlwell, Spectrochim. Acta 20 (1964) 937.
[18] T.E. Machonkin, P. Mukherjee, M.J. Henson, T.D.P. Stack, E.I. Solomon, Inorg. Chim. Acta 341 (2002) 39.
[19] P. Chaudhuri, I. Karpenstein, M. Winter, M. Lengen, C. Butzlaff, E. Bill, A.X. Trautwein, U. Flörke, H.-J. Haupt, Inorg. Chem. 32 (1999) 888.
[20] B. Chiari, O. Piovesana, T. Tarantelli, P.F. Zanazzi, Inorg. Chem. 32 (1993) 4834.
[21] A.N. Papadopoulos, V. Tangoulis, C.P. Raptopoulou, A. Terzis, D.P. Kessissoglu, Inorg. Chem. 35 (1996) 559.
[22] H. Crawford, H.W. Richardson, J.R. Wasson, D.J. Hodgson, W.E. Hatfield, Inorg. Chem. 15 (1976) 2107.
[23] L. Merz, W. Haase, J. Chem. Soc., Dalton Trans. (1980) 875.

Available online at www.sciencedirect.com
SCIENCE DIRECT®
Inorganic Chemistry Communications 8 (2005) 335–338
INORGANIC CHEMISTRY COMMUNICATIONS
www.elsevier.com/locate/inoche

A copper(II) chain compound with hydrogenphosphate bridges organized in a double-chain structure. Synthesis, structure and magnetic properties of [Cu(1,10-phenanthroline)(μ-HPO_4)(H_2O)$_2$]$_n$

Sujittra Youngme [a,*], Pongthipun Phuengphai [a], Chaveng Pakawatchai [b], Gerard A. van Albada [c], Stefania Tanase [c], Ilpo Mutikainen [d], Urho Turpeinen [d], Jan Reedijk [c]

[a] *Department of Chemistry, Faculty of Science, Khon Kaen University, Khon Kaen 40002, Thailand*
[b] *Department of Chemistry, Faculty of Science, Prince of Songkla University, Hatyai, Songkla 90112, Thailand*
[c] *Leiden Institute of Chemistry, Gorlaeus Laboratories, Leiden University, PO Box 9502, 2300 RA Leiden, The Netherlands*
[d] *Laboratory of Inorganic Chemistry, Department of Chemistry, PO Box 55 (A.I.Virtasen aukio 1), 00014 University of Helsinki, Finland*

Received 25 November 2004; accepted 13 January 2005

Abstract

A new Cu(II) chain compound, [Cu(1,10-phenanthroline)(μ-HPO_4)(H_2O)$_2$]$_n$ **1** has been synthesized hydrothermally and structurally characterized by elemental analysis, IR, EPR spectrum and single-crystal X-ray diffraction. The Cu(II) ion is tetragonally coordinated with a phen ligand and two aqua ligands in the equatorial plane (Cu–N distance 2.006(2) Å and Cu–O distance 1.969(2) Å) and hydrogenphosphates as axial ligands (Cu–O distance 2.470(2) Å), thereby forming a linear chain. The crystal lattice is formed from antiparallel chains, kept together by relatively strong phosphate–water H-bonds (intra- and intermolecular) with O···O contacts of 2.615(3) and 2.672(3) Å and by interpenetrated stacking of the phen ligands with other chains. The magnetic susceptibility measurements (5–300 K) agrees with a weak antiferromagnetic chain interaction between the Cu centers with J value of -5.86 cm^{-1}.

Keywords: Hydrothermal synthesis; Copper(II); Polymeric; One-dimensional chain; Magnetic properties

Open-framework materials have been of interest because of their traditional use in catalysis, separation, and ion exchange and their potential applications as hybrid composite materials in nonlinear optical and sensing applications [1]. Recently much research has focused on the synthesis of inorganic–organic hybrid frameworks using HPO_4^{2-} and derivative ions as bridging [2,3] and both monodentate coordinating and bridging modes of HPO_4^{2-} and derivative ions have been investigated. Complexes of copper(II) and didentate mono(chelate) ligand with divalent oxoanions may be grouped in classes for each type of oxoanions depending on the coordinating nature. Complexes with divalent oxoanions formulated as Cu(LL)(A)(H_2O)$_n$, where LL = chelating didentate ligand and A = CO_3^{2-} and SO_4^{2-} have been divided into five classes of local molecular structures, viz.: (I) mononuclear distorted square-based pyramids with a didentate oxoanion [4]; (II) polymeric distorted square-based pyramids with a bridging tridentate oxoanion [5]; (III) mononuclear

* Corresponding author. Tel.: +6604320222241; Fax : +66 43 243 338/02373.
E-mail address: sujittra@kku.ac.th (S. Youngme).

1387-7003/$ - see front matter © 2005 Elsevier B.V. All rights reserved.
doi:10.1016/j.inoche.2005.01.018

square-based pyramids with a monodentate oxoanion [6]; (IV) polymeric elongated octahedron with bridging didentate oxoanions [7–10]; (V) dinuclear distorted square-based pyramid with double bridges of tridentate oxoanions [11]. With 2,2′-bipyridine (bipy) [12,13] or 1,10-phenanthroline (phen) [14] as the chelating ligand LL, such organic–inorganic hybrid compounds have hardly been synthesized so far. Since some copper(II) complexes with phen ligands have shown to be of interest to catalysis and biochemistry [15], it appeared of interest to prepare Cu(II)–phen coordination polymers with phosphates. So far the presence of one-dimensional interdigitation by phen stacks structures in a copper(II) coordination polymer has been rarely reported [16,17]. In this study we describe the hydrothermal synthesis and crystal structure of a double-chain coordination polymer with the formula $[Cu(phen)(H_2O)_2(\mu\text{-}HPO_4)]_n$ **1**. The spectroscopic properties and magnetic behavior are investigated and discussed.

Compound **1** was synthesized from the reaction mixture of $Cu(NO_3)_2 \cdot 3H_2O$ (0.241 g, 1.0 mmol), 1,10-phenanthroline (0.198 g, 1.0 mmol), $NaH_2PO_4 \cdot H_2O$ (0.175 g, 1.0 mmol) and H_2O (12 ml). The resulting solution was stirred in air for 5 min and transfer into a reactor bomb and heated at 160 °C for 120 h. Blue crystals of **1** were recovered in 55% yield after filtration, washing with water and drying on air. Anal. Calc. for $C_{12}H_{13}CuN_2O_6P$: C, 38.36; H, 3.46; N, 7.45%. Found: C, 38.41; H, 3.53; N, 7.48%. FT-IR data (cm^{-1}): 3415(m), 3051(w), 1601(m), 1497(w), 1474(m), 1447(s), 1319(w), 1250(w), 1176(s), 1076(s), 1032(w), 1001(m), 959(s), 888(s), 772(s), 730(m), 637(w), 618(w), 510(s) cm^{-1}.

A plot of the structure together with the numbering system is shown in Fig. 1. The structure of **1** consists of a chain of $[Cu(phen)(H_2O)_2(\mu\text{-}HPO_4)]$ units. The geometry around the copper(II) ion, which has a $CuN_2O_2O_2'$ chromophore, can be best described as tetragonally distorted octahedral. The basal plane consists of two pyridyl nitrogen atoms from the phen ligand (Cu–N distance 2.006(2) Å) and two oxygen atoms from a water molecule (Cu–O distance 1.969(2) Å). These basal planes are linked into an infinite chain by the didentate bridging hydrogenphosphate group. The two donor atoms from the almost symmetrically bridging hydrogenphosphate groups occupy the axial positions above and below the CuN_2O_2 planes, with a Cu–O distance of 2.470(2) Å. The axial O–Cu–O angle is 178.48(6)°.

The most interesting feature of **1** is its one-dimensional double chain structure. These two one-dimensional chains are antiparallel to each other along the a axis of the cell. Relatively strong hydrogen bonds exist between the oxygen atoms of the phosphate anions and the oxygen atoms of different water molecules with O···O distance of 2.615(3) and 2.672(3) Å, thereby keeping the chains together in pairs. See also Table 1 and Fig. 2 for details.

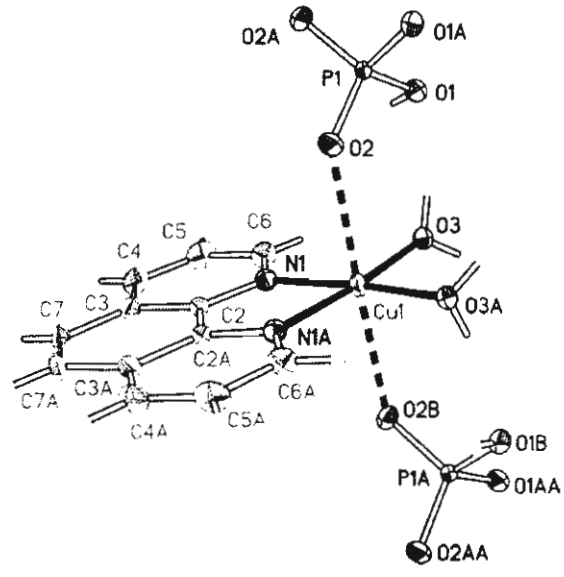

Fig. 1. Thermal ellipsoid plot (50% probability) of $[Cu(phen)(H_2O)_2(\mu\text{-}HPO_4)]_n$ **1**. Atoms marked with an "A", "B" or "AA" are generated by an inversion centre. Selected bond lengths (Å) and angles (°): Cu(1)–O(2) 2.470(2), Cu(1)–O(3) 1.969(2), Cu(1)–N(1) 2.006(2), P(1)–O(1) 1.484(2), P(1)–O(2) 1.461(2) and O(2)–Cu(1)–O(3) 86.09(8), O(2)–Cu(1)–N(1) 88.83(8), O(2)–Cu(1)–O(2B) 178.48(6), O(2)–Cu(1)–O(3A) 92.88(8), O(2)–Cu(1)–N(1A) 92.32(8), O(3)–Cu(1)–N(1) 91.99(9), O(3)–Cu(1)–O(3A) 94.11(8), O(3)–Cu(1)–N(1A) 173.76(9), N(1)–Cu(1)–N(1A) 81.94(9). Symmetry codes B: $-x, y, 1/2-z$.

Table 1
The geometry of hydrogen bonding (Å, °)

D–H···A	D–H	H···A	D···A	D–H···A
O(3)–H(31)···O(1)	0.857	1.759	2.615(3)	179.0
O(3)–H(32)···O(1) [$x,-y,1/2+z$]	0.846	1.844	2.672(3)	165.8

It appears that the hydrogen bonding between the two chains plays an important role in the formation of this double-chain structure.

The phen ligands are located nearly parallel to the equatorial plane of copper(II) center and perpendicular to the chain extension direction. The distance between the closest two phen planes on a mono-chain is 7.022 Å. In the lattice, each phen ligand on a mono-chain is interpenetrated into the interspaces of the closest two phen ligands of another chain. Obviously, the lattice structure in **1** results in that all molecular planes of phen are nearly parallel in stacks. The shortest distance between two phen rings in **1** is 3.533 Å.

The polymeric structure of **1** is comparable to those of complexes with a carbonate anion $[Cu(dpyam)(CO_3)](H_2O)_3$ (in which dpyam = di-2-pyridylamine) [5] or with a sulfate group as an anion, like $[Cu(dpyam)(H_2O)_2(SO_4)]$ [9], $[Cu(ethylenediamine)(H_2O)_2(SO_4)]$ [7], $[Cu(bpy)(H_2O)_2(SO_4)]$ [8], $[Cu(oxamideoxime)(H_2O)_2(SO_4)]$ [18] and completely isomorphous with

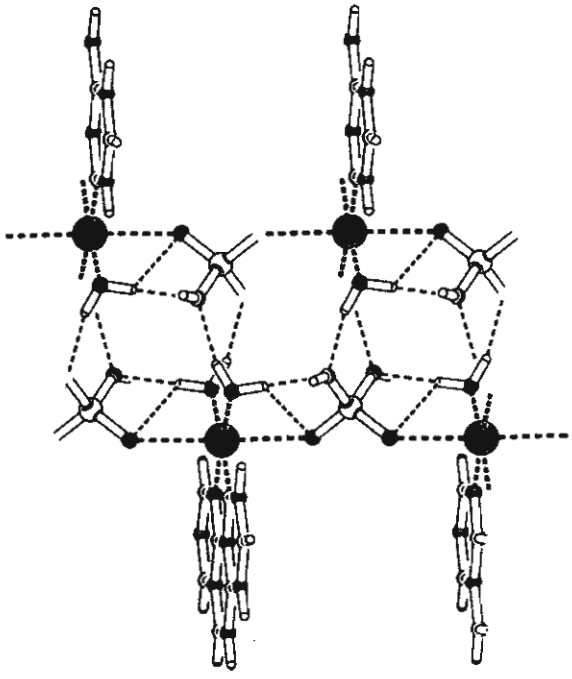

Fig. 2. View of the hydrogen bond system.

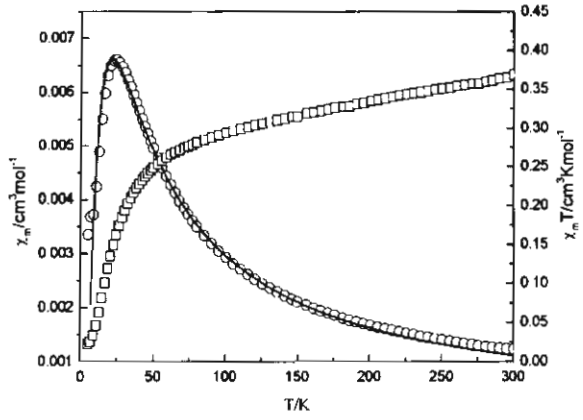

Fig. 3. A plot of temperature dependence of $\chi_M T$ vs. T [□] and χ_M vs. T [○] for compound **1**. The solid lines represents the calculated curve for the parameters $J = -5.86\ cm^{-1}$, $g = 2.00$ (see text).

the compound $[Cu(phen)(H_2O)_2(SO_4)]$ [10]. The only difference is the phosphate group, which has a H donor atom present.

The EPR spectrum of compound **1** reveals, at RT and at 77 K, the same axial signal with a $g_\perp$ of 2.08 and $g_\parallel$ of 2.24, which is in agreement with a (distorted) octahedral geometry [19]. No hyperfine splitting is resolved.

The magnetisation of a powdered sample of **1** was measured from 5 to 300 K in an applied field of 0.1 T. The resulting molar magnetic susceptibility, χ_M, and the product $\chi_M \times T$ are plotted in Fig. 3. At 300 K, the compound exhibits a $\chi_M T$ value of $0.369\ cm^3\ mol^{-1}\ K$, which is close to the theoretical value expected for one noncoupled Cu(II) center with $S = 1/2$ ($\chi_M T = 0.375\ cm^3\ mol^{-1}\ K$). On lowering the temperature, the $\chi_M T$ value decreases until it reaches a value of about $0.03\ cm^3\ mol^{-1}\ K$, a behavior indicative of an antiferromagnetic coupling between two Cu centers.

The temperature dependence of χ_M was then fitted using the equation for a uniformly spaced copper(II) linear chain [20]. A Temperature Independent Paramagnetism (TIP) of $60 \times 10^{-6}\ cm^3\ mol^{-1}$ per Cu(II) ion has been used. The best fit of the experimental magnetic susceptibility data (solid line in Fig. 3) was obtained using the magnetic parameters $g = 2.00$, $J = -5.86\ cm^{-1}$, with $R = 1.6 \times 10^{-5}$.

Any magnetic interaction via the phosphate O–P–O bridge should be very weak, also because the unpaired electrons are in orbitals perpendicular to the chain. The present value may in addition have contributions from the hydrogen bonds. The J value found is in agreement with the weak antiferromagnetic interaction observed in the related compounds $[Cu(phen)(H_2O)_2(SO_4)]$ [10] and $[Cu(oxamideoxime)(H_2O)_2(SO_4)]$ [18], which have a sulfate O–S–O bridge in the axial direction and which have J values of -3.8 and $-1.0\ cm^{-1}$, respectively.

Supplementary material

Crystal data for **1**: $C_{12}H_{13}CuN_2O_6P$, Monoclinic, *C2/c* (No.15), $a = 14.870(2)$, $b = 13.83304(18)$, $c = 7.0220(9)$ Å, $\beta = 108.630(2)$ Å, $V = 1368.5(3)$ Å^3, $T = 293(2)$ K, $Z = 4$, $D_c = 1.824\ Mg\ m^{-3}$, $\mu = 1.745\ mm^{-1}$, $F(0\ 0\ 0) = 764$, k(Mo Kα) = 0.71073 Å. A total of 5,776 reflections were measured in the setting angles $2.06° < h < 28.28°$ by x scan method, of which 1633 were independent reflections. The crystal structure was solved by direct method, and refined by full-matrix least squares on F^2. Empirical absorption corrections were applied, which resulted in transmission coefficients ranging from 0.7403 to 1.000 for **1**. The structure was solved by direct methods and refined by full-matrix least squares method on $(F_{obs})^2$ with anisotropic thermal parameters for all nonhydrogen atoms using the SIR2002 and SHELXL-97 software package, and converging to $R_1 = 0.0388$ and $wR_2 = 0.0944$ [$I > 2\sigma(I)$]. CCDC-256479 contains the supplementary crystallographic data for this paper. These data can be obtained free of charge at www.ccdc.cam.ac.uk/conts/retrieving.html [or from the Cambridge Crystallographic Data Center (CCDC), 12 Union Road, Cambridge CB2 1EZ, UK; fax: +44(0)1223 336033; e-mail: deposit@ccdc.cam.ac.uk].

Acknowledgements

The authors thank The Thailand Research Fund and Khon Kaen University for a research Grant. Support of the Postgraduate Education and Research Program in Chemistry (Thailand) is also gratefully acknowledged. The work described in the present paper has been supported by the Leiden University Study group WFMO (Werkgroep Fundamenteel MaterialenOnderzoek).

References

[1] A.K. Cheetham, G. Ferey, T. Loiseau, Angew. Chem., Int. Ed. 38 (1999) 268.
[2] R. Finn, J. Zubieta, Chem. Commun. (2000) 1321.
[3] Y. Lu, E. Wang, M. Yuan, G. Luan, Y. Li, H. Zhang, C. Hu, Y. Yao, Y. Qin, Y. Chen, J. Chem. Soc., Dalton Trans. (2002) 3029.
[4] P. Akhter, P. Fitzsimons, B. Hathaway, Acta Crystallogr C 47 (1991) 308.
[5] J. Sletten, Acta Chem. Scand. A 38 (1984) 491.
[6] J. Balvich, K.P. Fivizzani, S.F. Pavkovic, J.N. Brown, Inorg. Chem. 15 (1976) 71.
[7] M. Dunai-Jurio, M.A. Porai-Koshits, Chem. Zvesti 20 (1966) 783.
[8] J.C. Tedenac, N.D. Phung, C. Avinens, M. Maurin, Inorg. Nucl. Chem. 38 (1976) 85.
[9] S. Youngme, N. Chaichit, C. Pakawatchai, S. Booncoon, Polyhedron 21 (2002) 1279.
[10] L. Xu, E. Wang, J. Peng, R. Huang, Inorg. Chem. Commun. 6 (2003) 740.
[11] S. Youngme, N. Chaichit, P. Kongsaeree, G.A. van Albada, J. Reedijk, Inorg. Chim. Acta 20 (2001) 232.
[12] Y. Zhang, R.C. Haushalter, J. Zubieta, Inorg. Chim. Acta 260 (1997) 105.
[13] W.-J. Chang, C.-Y. Chen, K.-H. Lii, J. Solid State Chem. 172 (2003) 6.
[14] X.-M. Zhang, M.-L. Tong, S.-H. Feng, X.-M. Chen, J. Chem. Soc., Dalton Trans. (2001) 2069.
[15] (a) G.L. Cheng, C.P. Hu, S.K. Ying, Macromol. Rapid Commun. 20 (1999) 303;
(b) S.A. Ross, M. Pitie, B. Meunier, Eur. J. Inorg. Chem. 1999 (1999) 557.
[16] (a) J. Tao, Y. Zhang, M. Tong, X. Chen, T. Yuen, C.L. Lin, X. Huang, J. Li, Chem. Commun. 13 (2002) 1342;
(b) J.Y. Lu, A.M. Babb, Inorg. Chem. 40 (2001) 3261;
(c) Z. Shi, S. Feng, Y. Sun, J. Hua, Inorg. Chem. 40 (2001) 5312;
(d) P. Gamez, P. Hoog, O. Roubeau, M. Lutz, W.L. Driessen, A.L. Spek, J. Reedijk, Chem. Commun. (2002) 1488;
(e) G. Murphy, C. Murphy, B. Murphy, B. Hathaway, J. Chem. Soc., Dalton Trans. (1997) 2653;
(f) H. Matsushima, H. Hamada, K. Watanabe, M. Koikawa, T. Tokii, J. Chem. Soc., Dalton Trans. (1999) 971;
(g) C. Ruiz-Perez, J. Sauchiz, M.H. Molina, F. Lioret, M. Julve, Inorg. Chem. 39 (2000) 1363;
(h) D. Hagrman, R.C. Hausualter, J. Zubieta, Chem. Mater. 10 (1998) 361.
[17] M.J. Zaworotko, Chem. Commun. (2001) 1.
[18] H. Endres, D. Noethe, E. Rossato, W.E. Hatfield, Inorg. Chem. 23 (1984) 3467.
[19] B.J. Hathaway, in: G. Wilkinson, R.D. Gill, J.A. McCleverty (Eds.), Comprehensive Coordination Chemistry, 5, Pergamon Press, Oxford, 1987.
[20] W.E. Hatfield, J. Appl. Phys. 52 (1981) 1985.

Available online at www.sciencedirect.com
SCIENCE DIRECT
Inorganic Chemistry Communications 9 (2006) 147–151
INORGANIC CHEMISTRY COMMUNICATIONS
www.elsevier.com/locate/inoche

Synthesis, crystal structure and magnetic properties of an unexpected new coordination Cu(II) compound, containing two different phosphato-bridged dinuclear units; $[Cu_2(phen)_2(\mu\text{-}H_2PO_4\text{-}O,O')_2(H_2PO_4)_2][Cu_2(phen)_2(\mu\text{-}H_2PO_4\text{-}O,O')(\mu\text{-}H_2PO_4\text{-}O)(\mu\text{-}HPO_4\text{-}O)]_2(H_2O)_9$(phen = 1,10-phenanthroline)

Pongthipun Phuengphai [a], Sujittra Youngme [b,*], Chaveng Pakawatchai [c], Gerard A. van Albada [d], Manuel Quesada [d], Jan Reedijk [d]

[a] *Chemistry Program, Faculty of Science and Technology, Surindra Rajabhat University, Surin 32000, Thailand*
[b] *Department of Chemistry, Faculty of Science, Khon Kaen University, Khon Kaen 40002, Thailand*
[c] *Department of Chemistry, Faculty of Science, Prince of Songkla University, Hatyai, Songkla 90112, Thailand*
[d] *Leiden Institute of Chemistry, Gorlaeus Laboratories, Leiden University, P.O. Box 9502, 2300 RA Leiden, The Netherlands*

Received 20 September 2005; accepted 17 October 2005
Available online 1 December 2005

Abstract

The crystal structure of a copper(II) complex containing the ligand 1,10-phenanthroline (phen) with mono- and di-dentate $H_2PO_4^-$ and monodentate HPO_4^{2-} oxoanions, $[Cu_2(phen)(\mu\text{-}H_2PO_4\text{-}O,O')_2(H_2PO_4)_2][Cu_2(phen)_2(\mu\text{-}H_2PO_4\text{-}O,O')(\mu\text{-}H_2PO_4\text{-}O)(\mu\text{-}HPO_4\text{-}O)]_2(H_2O)_9$, is reported and determined by X-ray crystallography. Two crystallographically independent dinuclear units with different bridging properties of (di)hydrogenphosphato anions are found in this compound.

The two Cu(II) ions in the first unit, $[Cu_2(phen)(\mu\text{-}H_2PO_4\text{-}O,O')_2(H_2PO_4)_2]$, are bridged by two didentate bridging dihydrogenphosphato monoanions and also contains two non-bridging monovalent dihydrogenphosphato anions. The geometry of the Cu(II) ions is square pyramidal with a Cu–Cu distance of 5.043(3) Å.

The two Cu(II) ions in the second unit, $[Cu_2(phen)_2(\mu\text{-}H_2PO_4\text{-}O,O')(\mu\text{-}H_2PO_4\text{-}O)(\mu\text{-}HPO_4\text{-}O)]$, are bridged by three different hydrogenphosphate anions; a didentate bridging dihydrogenphosphate monoanion, a monodentate dihydrogenphosphate bridging monoanion and a monodentate hydrogenphosphate dianion. This bridging mode is unique and has not been reported so far for dinuclear Cu(II) compounds. The geometry of the Cu(II) ions in this second unit is distorted square pyramidal and the Cu–Cu distance is 3.074(3) Å.

The magnetic susceptibility measurement (5–300 K) have been fitted with two different J values. A weak antiferromagnetic interaction between the Cu ions in one dinuclear unit with $J_1 = -8.2\,cm^{-1}$ and a very weak ferromagnetic interaction between the Cu ions in the other dinuclear unit with $J_2 = 0.96\,cm^{-1}$, allow an acceptable fit.

Keywords: Crystal structure; Copper(II); Dihydrogenphosphate complex; Magnetic properties

Open-framework materials are of considerable interest due to their rich structural chemistry and potential applications in catalysis, separation and ion exchange [1,2]. One class of these materials concerns aluminophosphates, commonly known as AlPOs [3]. Many of these compounds exhibit novel microporous structures. Two notable recent examples are VPI-5 and JDF-20, containing extra-large 18- and 20-ring channels, respectively [4,5]. Recently, others and we have focused on the synthesis of inorganic–organic hybrid compounds by incorporating organic ligands in the structure of copper phosphates [6–11]. Compared with

* Corresponding author. Fax: +66 43 243 338.
E-mail address: sujittra@kku.ac.th (S. Youngme).

1387-7003/$ - see front matter © 2005 Elsevier B.V. All rights reserved.
doi:10.1016/j.inoche.2005.10.020

inorganic ligands, organic multidentate ligands possess more rich coordination sites and a wide variety of shapes.

To obtain more insight into bridging phosphate anions, we have extended our study using the ligand 1,10-phenanthroline (abbreviated as phen). In the present study, a mixed hydrogenphosphato-bridging Cu(II) complex, $[Cu_2(phen)(\mu\text{-}H_2PO_4\text{-}O,O')_2(H_2PO_4)_2][Cu_2(phen)_2(\mu\text{-}H_2PO_4\text{-}O,O')(\mu\text{-}H_2PO_4\text{-}O)(\mu\text{-}HPO_4\text{-}O)]_2(H_2O)_9$, containing two crystallographically independent molecules with different coordination modes of (di)hydrogenphosphato bridges, is described and investigated structurally and magnetically. The unit cell of the title compound contains two crystallographically independent dinuclear units, one unit $[Cu_2(phen)_2(\mu\text{-}H_2PO_4)_2(H_2PO_4)_2]$ (unit A) and two units of $[Cu_2(phen)_2(\mu\text{-}H_2PO_4)_2(\mu\text{-}HPO_4)]_2$ (unit B). Also nine water molecules, of which one is disordered, are present in the unit cell. The dihydrogenphosphato bridges in the two crystallographically independent units are totally different in coordination modes. The first dinuclear moiety, $[Cu_2(phen)(\mu\text{-}H_2PO_4\text{-}O,O')_2(H_2PO_4)_2]$ (unit A, Fig. 1(a))

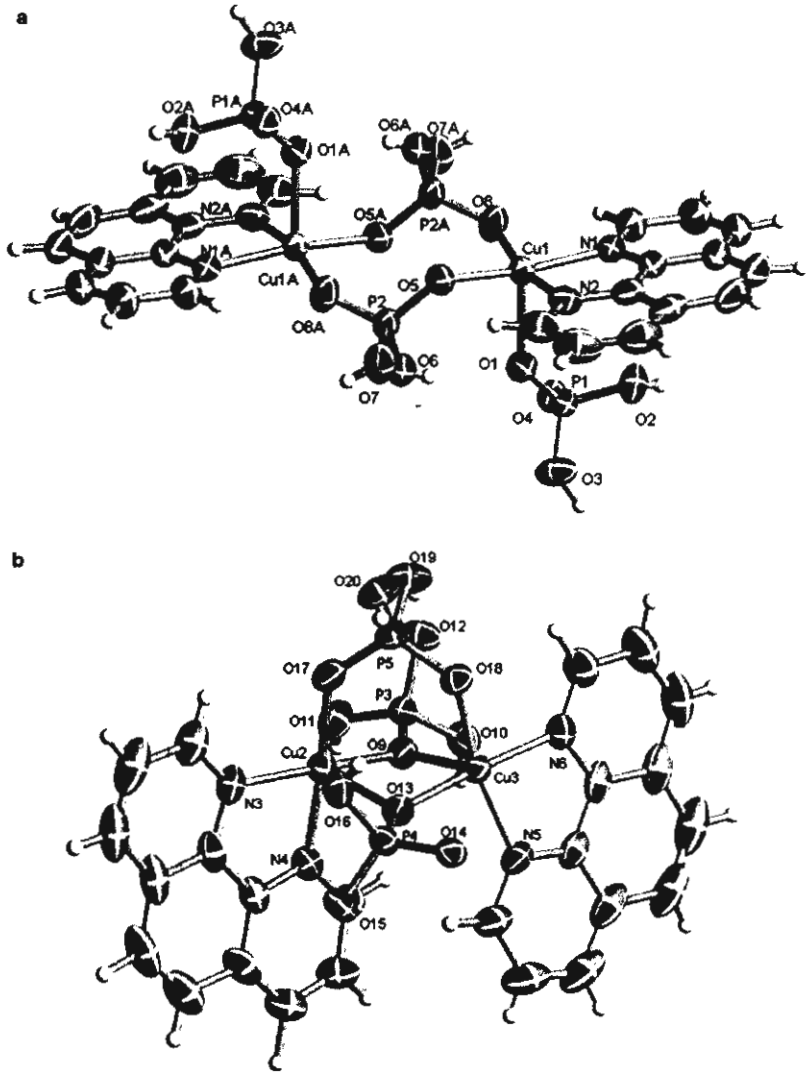

Fig. 1. The molecular structure of $[Cu_2(phen)(\mu\text{-}H_2PO_4O,O')_2(H_2PO_4)_2][Cu_2(phen)_2(\mu\text{-}H_2PO_4\text{-}O,O')(\mu\text{-}H_2PO_4\text{-}O)(\mu\text{-}HPO_4\text{-}O)]_2(H_2O)_8$, the uncoordinating water molecules are omitted for clarity. (a) The structure of $[Cu_2(phen)(\mu\text{-}H_2PO_4O,O')_2(H_2PO_4)_2]$ (unit A). Selected bond distances (Å) and angles: Cu(1)–N(1) 2.015(3), Cu(1)–N(2) 2.021(3), Cu(1)–O(1) 2.230(3), Cu(1)–O(5) 1.949(3), Cu(1)–O(8) 1.928(3), Cu(1)–Cu(1A) 5.043(3), O(1)–Cu(1)–O(5) 94.0(1), O(1)–Cu(1)–O(8) 99.9(1), O(1)–Cu(1)–N(1) 96.5(1), O(1)–Cu(1)–N(2) 92.4(1), O(5)–Cu(1)–O(8) 94.9(1), O(5)–Cu(1)–N(1) 167.8(1), O(5)–Cu(1)–N(2) 91.8(1), O(8)–Cu(1)–N(1) 89.6(1), O(8)–Cu(1)–N(2) 165.6(1). $A = -x+2, -y+2, -z$. (b) The structure of $[Cu_2(phen)_2(\mu\text{-}H_2PO_4\text{-}O,O')(\mu\text{-}H_2PO_4\text{-}O)(\mu\text{-}HPO_4\text{-}O)]$ (unit B). Selected bond distances (Å) and angles (°): Cu(2)–N(3) 1.996(3), Cu(2)–N(4) 1.997(3), Cu(2)–O(9) 2.288(3), Cu(2)–O(13) 1.930(2), Cu(2)–O(17) 1.950(2), Cu(3)–N(5) 2.011(3), Cu(3)–N(6) 1.995(3), Cu(3)–O(9) 1.945(2), Cu(3)–O(13) 2.261(3), Cu(3)–O(18) 1.937(3), Cu(2)–Cu(3) 3.074(3), O(9)–Cu(2)–O(13) 84.0(1), O(9)–Cu(2)–O(17) 93.0(1), O(9)–Cu(2)–N(3) 95.8(1), O(9)–Cu(2)–N(4) 98.9(1), O(13)–Cu(2)–O(17) 91.8(1), O(13)–Cu(2)–N(3) 176.0(1), O(13)–Cu(2)–N(4) 93.5(1), O(17)–Cu(2)–N(3) 92.2(1), O(17)–Cu(2)–N(4) 167.5(1), O(9)–Cu(3)–O(13) 84.4(1), O(9)–Cu(3)–O(18) 92.4(1), O(9)–Cu(3)–N(5) 93.2(1), O(9)–Cu(3)–N(6) 171.4(1), O(13)–Cu(3)–O(18) 92.6(1), O(13)–Cu(3)–N(5) 86.6(1), O(13)–Cu(3)–N(6) 102.5(1), O(18)–Cu(3)–N(5) 174.2(1), O(18)–Cu(3)–N(6) 92.4(1), Cu(2)–O(9)–Cu(3) 92.8(1), Cu(2)–O(13)–Cu(3) 94.0(1). $A = -x+2, -y+2, -z$

is doubly bridged by two didentate dihydrogenphosphato anions. The geometry of the Cu(II) ions is square pyramidal (τ value of 0.04; the τ value describes the relative amount of trigonality; $\tau = 0$ for square pyramid and $\tau = 1$ for trigonal bipyramidal) [12]. The basal plane of CuN_2O_2O' chromophore consists of two oxygen atoms of the two bridging dihydrogenphosphato groups, O(5) and O(8) (Cu–O distances of 1.949(3) and 1.928(3) Å) and two nitrogen atoms of a phen ligand (Cu–N distances of 2.015(3), 2.021(3) Å). The fifth axial coordination site is occupied by one oxygen atom of non-bridging monodentate dihydrogenphosphato group at the Cu–O(1) distance of 2.230(3) Å. The basal angles are 167.8(1)° and 165.6(1)°. The four in-plane atoms, N(1), N(2), O(5) and O(8) are essentially planar (r.m.s. deviation 0.098 Å), with a slightly tetrahedral twist (dihedral angles between the CuN_2 and CuO_2 planes 16.1°). The Cu atom lies 0.197 Å above this plane towards O(1). The Cu···Cu distance is 5.043(3) Å. The coordinated P–O bonds, 1.498(3) and 1.502(3) Å, are shorter than the uncoordinated P–OH bonds, 1.548(3) and 1.567(3) Å. These differences are normally found for the two-coordinate bridging coordination of dihydrogenphosphate anion [13]. The non-bridging monodentate dihydrogenphosphato group involves O–P–O angles ranging from 106.7(1) to 115.3(1) Å. The P–OH bonds, 1.563(3) and 1.572(3) Å, are longer than the P=O bonds, 1.495(3) and 1.570(3) Å, which is in usual observation.

The second unit, $[Cu_2(phen)_2(\mu\text{-}H_2PO_4\text{-}O,O')(\mu\text{-}H_2PO_4\text{-}O)(\mu\text{-}HPO_4\text{-}O)]$ (unit B, Fig. 1(b)), is slightly asymmetric and bridged by three different hydrogenphosphate anions: a didentate bridging dihydrogenphosphate anion, a monodentate bridging dihydrogenphosphate anion and a monodentate bridging hydrogenphosphate anion. This mode is unique and not reported so far for dinuclear Cu(II) compounds.

The geometry of the Cu(II) ions is distorted square pyramidal (τ value of 0.14 and 0.004 for Cu2 and Cu3, respectively) and the Cu–Cu distance is 3.074(3) Å. The basal plane of the CuN_2O_2O' chromophore of each Cu(II) ion consists of two nitrogen atoms of a phen ligand (Cu–N distances vary from 1.995(4) to 2.011(3) Å), one oxygen atom of a didentate bridging dihydrogenphosphato anion (Cu–O distances 1.937(3), 1.950(3) Å) and an oxygen atom of a monodentate bridging dihydrogenphosphato anion (Cu(3)–O(9) distance 1.945(3) Å) or of a monodentate bridging hydrogenphosphato anion (Cu(2)–O(13) distance 1.930(2) Å). The basal angles are 167.5(1)°, 176.0(1)° and 171.4(1)°, 174.2(1)° for Cu2 and Cu3, respectively. The fifth axial coordination site is occupied by an oxygen atom of monodentate hydrogenphosphato anion (Cu(3)–O(13) distance 2.261(3) Å) or of a monodihydrogenphosphato anion (Cu(2)–O(9) distance 2.288(3) Å). The four basal atoms show a small tetrahedral distortion with a dihedral angle of 11.5° and 7.5° formed between CuO_2 and CuN_2 planes and the copper atoms are displaced by −0.095 and −0.047 Å from the basal plane towards the O(9) and O(13) atoms.

The lattice structure is stabilized by a complicated hydrogen bonding network between the oxygen atom of the non-bridged dihydrogenphosphate anion and oxygen atoms of the bridged dihydrogenphosphate anion in unit A and unit B ($O_{(H2PO4)}\cdots O_{(\mu\text{-}H_2PO4)}$ distances 2.602(1), 2.532–2.692(1) Å, respectively); between oxygen atom of dihydrogenphosphate group of unit A and water oxygen atom ($O_{(\mu\text{-}H_2PO4)}\cdots O_{(water)}$ distance 2.564(1) Å); between oxygen atoms of different dihydrogenphosphate groups of unit B ($O_{(\mu\text{-}H_2PO4)}\cdots O_{(\mu\text{-}H_2PO4)}$ distance 2.547(1) Å) and between oxygen atoms of dihydrogenphosphate groups and hydrogenphosphate group of unit B ($O_{(\mu\text{-}H_2PO4)}\cdots O_{(\mu\text{-}HPO_4)}$ distances 2.461(1)–2.584(1) Å). The unique bridging mode using three different phosphates is clearly stabilized by this H bonding pattern.

The electronic diffuse reflectance spectrum shows a broad band at 14,400 cm^{-1}. This single broad peak is consistent with the square pyramidal stereochemistry and assigned to be d_{z^2}, d_{xy}, d_{xz}, $d_{yz} \rightarrow d_{x^2y^2}$ transition [14].

The polycrystalline EPR spectrum of the powdered compound reveals at room temperature and at 77 K an axial signal with $g_{\parallel} = 2.27$ and $g_{\perp} = 2.05$, respectively. These signals are consistent with the $d_{x^2-y^2}$ ground state and resulting from a distorted square-based pyramidal geometry. No strong triplet signals have been observed. However, at around 160 mT a very weak "half-field" signal is observed, indicative for dinuclear compounds.

The magnetic susceptibility of a powdered sample was measured from 5 to 250 K. The magnetic properties are given in Fig. 2 in the form of a χT vs. T (a) and χ vs. T plots (b). In the χT curve, at 250 K, the χT value is 2.088 $cm^3\,mol^{-1}$ K, close to that expected for six uncoupled copper centres ($\chi T = 2.25\ cm^3\,mol^{-1}$ K, $g = 2$). As the temperature is decreased the value remains constant until 50 K, where a decrease begins, pointing at a weak antiferromagnetic interaction. This is confirmed by the fact that no maximum is observed in the χ vs. T plot.

Two crystallographically different dinuclear units form the unit cell with a total of six coppers, 2 in unit A and

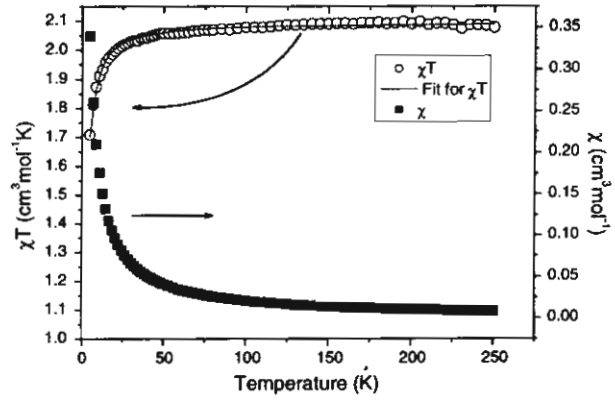

Fig. 2. Plot of χ and χT versus T for the title compound. The solid lines represent the calculated curve for the parameter $J_1 = -8.2\ cm^{-1}$ and $J_2 = 0.96\ cm^{-1}$ (see text).

2×2 in unit B. The following Hamiltonian was considered to fit the magnetic data: $H = -J_1 S_a S_b - 2 \cdot J_2 S_c S_d$, in which J_1 is the interaction in the dinuclear unit A and J_2 that in the dinuclear unit B. As they are independent units, each may have its own coupling constant. Considering an identical g value for the four different coppers and including standard temperature independent paramagnetism, the molar magnetic susceptibility is, based on a Bleaney–Bowers equation [15], described by

$$\chi = 2N_A g^2 \beta^2 / 3k_B T[1/(3 + \exp(-J_1/K_B T)) + 2/(3 + \exp(-J_2/K_B T))] + \text{TIP}.$$

The best set of parameters that fits the magnetic data are: $J_1 = -8.2\ \text{cm}^{-1}$, $J_2 = 0.96\ \text{cm}^{-1}$ and $g = 1.92$. TIP was kept constant with a value of 60×10^{-4} per copper atom. The g value is somewhat lower than expected. This may be due to the small quantity of the sample which was measured. The low values for the coupling constants indicate very weak interactions between the coppers in both dinuclear units. For the unit bridged by two dihydrogenophosphate anions (unit A), the negative value of J_1 implies that the interaction is antiferromagnetic. As the two coppers have a square pyramidal (SP) geometry, their magnetic orbital is $d_{x^2-y^2}$. The angle between these orbitals is about 180°. This and the fact that they are both in the same plane explain the antiferromagnetic interaction. The weakness of the interaction can also be due to the long distance between the two coppers. J_2 (unit B) is on the contrary positive. The magnetic orbitals of the coppers are again $d_{x^2-y^2}$, as the coppers have SP geometry. One of the anions is bridging the two coppers through their magnetic orbitals, but in this case, they are parallel to each other, thus no interaction is expected. A rather complicated explanation of the ferromagnetic interaction alights and DFT calculations will be needed for a better comprehension of this parameter.

The very weak (anti)ferromagnetic couplings found in the title compound is in agreement with this structural feature and the large Cu–Cu distances and is also in agreement with the earlier observed compound, $[Cu(dpyam)(\mu\text{-}H_2PO_4)(H_2PO_4)]_2$, with a J_1 value of $-8.2\ \text{cm}^{-1}$ [6]. The unusual ferromagnetism observed for the second unit could be further investigated with DFT calculations, which is out of the scope of this study.

Supplementary material

Crystal data: $C_{72}H_{71}Cu_6N_{12}O_{49}P_{10}$ ($M_w = 2579.4$), Monoclinic, $P2(1)/n$, $a = 11.9784(5)$, $b = 31.1685(14)$, $c = 13.3329(6)$ Å, $\beta = 101.5570(10)°$, $V = 4876.9(4)$ Å^3, $T = 293(2)$ K, $Z = 2$, $D_c = 1.757$;Mg/m^3, $\mu = 1.553\ \text{mm}^{-1}$, $F(000) = 2606.0$, k(Mo Kα) = 0.71073 Å, 42,866 reflections measured ($3.07° < h < 25.03°$), 11,666 unique ($R_{int} = 0.0578$), $R_1 = 0.0497$, $wR_2 = 0.1240$. Reflection data were collected on a 1K Bruker SMART CCD area-detector diffractometer. Data reduction and cell refinements were performed using the program SAINT [16]. The structure was solved by direct methods and refined by full-matrix least-squares method on $(F_{obs})^2$ with anisotropic thermal parameters for all non-hydrogen atoms using the SHELXTL-PC [17] software package. All hydrogen atoms were located and refined isotropically except 13 water hydrogen atoms, which were unable to locate and also not fixed. One water oxygen atom was disordered and refined with site occupancies of 0.50 and 0.50. The location of the H20O belonging to O20 is influenced by the disordered atom O3W (two positions, no hydrogen atoms could be located nor fixed) to which it forms weak hydrogen bonds. The molecular graphics were created by using SHELXTL-PC [17]. CCDC No. 284274. See http://www.ccdc.cam.ac.uk for crystallographic data in CIF format.

Synthesis: The compound was synthesized by adding an aqueous solution (15 ml) of $Cu(ClO_4)_2(H_2O)_6$ (0.19 g, 0.5 mmol) to a solution of phen (0.10 g, 0.5 mmol) in ethanol (10 ml) and followed by an aqueous solution (10 ml) of potassium dihydrogenphosphate (0.14 g, 1.0 mmol). The resulting blue-green solution was allowed to evaporate at room temperature. After several days, bluish-green crystals were deposited. Yield: ca. 55%. They were filtered off, washed with the mother liquid and dried in air. Anal Calc. for $C_{72}H_{84}Cu_6N_{12}O_{49}P_{10}$ (M_w: 2592.5): C, 33.4; H, 3.3; N, 6.5. Found: C, 32.9; H, 3.0; N, 6.5%. FT-IR data (cm^{-1}): 1167s, 1109s and 1078(s), ν_{as}(P–O); 946s, ν_s(P–O); 893m, 886m and 856s, δ (P–O(H)) out-of-plane deformation; 596m, 535s, and 509s, δ (O–P–O).

Acknowledgements

The authors thank The Thailand Research Fund and Khon Kaen University for a research grant. Support of the Postgraduate Education and Research Program in Chemistry is also gratefully acknowledged. The work described in the present paper has been supported by the Leiden University Study group WFMO (Werkgroep Fundamenteel Materialen Onderzoek).

Supplementary material

Supplementary data associated with this article can be found, in the online version, at doi:10.1016/j.inoche.2005.10.020.

References

[1] A.K. Cheetham, G. Ferey, T. Loiseau, Angew. Chem. Int. Ed. 38 (1999) 3268.
[2] M.E. Davis, Nature 417 (2002) 813.
[3] S.T. Wilson, B.M. Lok, C.A. Messina, T.R. Cannan, E.M. Flanigen, J. Am. Chem. Soc. 104 (1982) 1146.
[4] M.E. Davis, C. Saldarriaga, C. Montes, J.M. Garces, C. Crowder, Nature 331 (1988) 698.
[5] Q. Huo, R. Xu, S. Li, Z. Ma, J.M. Thomas, R.H. Jones, A.M. Chippindale, J. Chem. Soc., Chem. Commun. (1992) 875.

[6] S. Youngme, P. Phuengphai, N. Chaichit, G.A. van Albada, O. Roubeau, J. Reedijk, Inorg. Chim. Acta 7 (2004) 3603.
[7] S. Youngme, P. Phuengphai, N. Chaichit, G.A. van Albada, O. Roubeau, J. Reedijk, Inorg. Chim. Acta 358 (2005) 2262.
[8] S. Youngme, P. Phuengphai, N. Chaichit, G.A. van Albada, O. Roubeau, J. Reedijk, Inorg. Chim. Acta 358 (2005) 849.
[9] S. Youngme, P. Phuengphai, C. Pakawatchai, G.A. van Albada, S. Tanase, I. Mutikainen, U. Turpeinen, J. Reedijk, Inorg. Chem. Commun. 8 (2005) 335.
[10] Z.-E. Lin, J. Zhang, Y.-Q. Sun, G.-Y. Yang, Inorg. Chem. 43 (2004) 797.
[11] R.C. Finn, J. Zubieta, J. Phys. Chem. Solids 62 (2001) 1513.
[12] A.W. Addison, T.N. Rao, J. Reedijk, J. van Rijn, G.C. Verschoor, J. Chem. Soc., Dalton Trans. (1984) 1349.
[13] A.M. Krogh Andersen, P. Norby, J.C. Hanson, T. Vogt, Inorg. Chem. 37 (1998) 876.
[14] B.J. Hathaway, in: G. Wilkinson, R.D. Gill, J.A. McCleverty (Eds.), Comprehensive Coordination Chemistry, vol. 5, Pergamon Press, Oxford, 1987 (Chapter 53).
[15] O. Kahn, Molecular Magnetism, VCH Publishers, New York, 1993.
[16] Siemens, SAINT 1996, Version4 Software Reference Manual, Siemens Analytical X-Ray Systems, Inc., Madison, WI, USA, 1996.
[17] Siemens, SHELXTL 1996, Version 5 Reference Manual, Siemens Analytical X-Ray Systems, Inc., Madison, WI, USA, 1996.

PUBLICATION PAPERS OF PART III

Available online at www.sciencedirect.com
SCIENCE DIRECT®
Polyhedron 23 (2004) 1641–1647
POLYHEDRON
www.elsevier.com/locate/poly

The novel dinuclear doubly and triply bridged copper(II) compound with monoatomic bridges

Sujittra Youngme [a,*], Chatkaew Chailuecha [a], Narongsak Chaichit [b]

[a] Department of Chemistry, Faculty of Science, Khon Kaen University, Khon Kaen 40002, Thailand
[b] Department of Physics, Faculty of Science and Technology, Thammasat University Rangsit, Pathumthani 12121, Thailand

Received 8 January 2004; accepted 29 March 2004
Available online 30 April 2004

Abstract

The planar dihydroxo-bridged $[Cu_2(dpyam)_2(\mu\text{-}OH)_2I_2]\cdot 2H_2O$ **(1)** and the roof-shaped trihydroxo-bridged $[Cu_2(dpyam)_2(\mu\text{-}OH)_3]Cl\cdot 3H_2O$ **(2)** (in which dpyam = di-2-pyridylamine) dinuclear copper(II) compounds have been synthesized and their crystal structures determined by X-ray crystallographic methods. All of compounds are being centrosymmetric molecule. Compound **1** contains a dinuclear $[I(dpyam)Cu(\mu\text{-}OH)_2Cu(dpyam)I]^+$ unit with a strictly planar CuO_2 network, dihedral angle between the CuO_2 planes of 180°. Each copper(II) ion is in a tetrahedrally distorted square pyramidal coordination geometry of the CuN_2O_2I chromophore with a dihedral angle 19.3° between the CuN_2 and CuO_2 planes. In the dinuclear $[(dpyam)Cu(\mu\text{-}OH)_3Cu(dpyam)]^+$ unit of compound **2**, the triply bridged Cu(II) ions show a distorted square pyramidal coordination. The fifth apical ligand is a longer bonded bridging OH^- group, at distance of 2.433(4) Å, which joins the basal CuN_2O_2 planes in a roof-shaped configuration with a dihedral angle of 142.5°. The Cu–Cu distance is 2.803(7) Å.

Keywords: Copper(II) complexes; Crystal structure; Dihydroxo-bridged; Roof-shaped; Triply bridged

1. Introduction

In the last three decades, the dinuclear doubly bridged copper(II) compounds with nitrogen donor ligand and monoatomic bridges have been received much attention especially the di-μ-hydroxo-bridged copper(II) systems which have been studied widely both from experimental and theoretical points of view, since the magnetostructural correlations described by Hatfield et al. [1] for the Cu–O–Cu bridging angle and spin coupling constant ($2J$) between the metal centers. More recently, these correlations have been extended by Ruiz et al. [2,3]. However, the structure characterized of the triply bridged copper(II) compounds containing nitrogen donor didentated chelate ligand and monoatomic bridges are less reported. So far only a few closely related structures, $[Cu_2(dpyam)_2(\mu\text{-}OH)_2(\mu\text{-}OH_2)]Cl_2\cdot 2H_2O$ [4], $[Cu_2(dpyam)_2(\mu\text{-}OMe)_2(\mu\text{-}Cl)]Cl\cdot MeOH$ [5] and $[Cu_2(dpyam)_2(\mu\text{-}OH)_2(\mu\text{-}OH_2)]Br_2\cdot 2H_2O$ [6] (in which dpyam = di-2-pyridylamine) are reported in the literature. In order to extend the investigation on this series of compounds an attempt has been made to prepare the novel planar di-μ-hydroxo-bridged copper(II) compound, $[Cu_2(dpyam)_2(\mu\text{-}OH)_2I_2]\cdot 2H_2O$ **(1)**, and the novel dinuclear copper(II) compounds containing three monoatomic bridges with homospecies, $[Cu_2(dpyam)_2(\mu\text{-}OH)_3]Cl\cdot 3H_2O$ **(2)**. Their IR, EPR and electronic spectra have been investigated and discussed, along with structural and spectral comparisons with those of other relevant compounds.

2. Experimental

2.1. Materials and measurements

Di-2-pyridylamine were purchased as commercial chemicals from Aldrich. All reagents are commercial grade

* Corresponding author. Tel.: +66-043-20222241; fax: +66-043-202373.
E-mail address: sujittra@kku.ac.th (S. Youngme).

0277-5387/$ - see front matter © 2004 Elsevier Ltd. All rights reserved.
doi:10.1016/j.poly.2004.03.021

materials and were used without further purification. Elemental analyses (C, H, N) were determined on a Perkin–Elmer PE 2400 CHNS/O Analyzer by Microanalytical Service of Science and Technological Research Equipment Center, Chulalongkorn University.

IR spectra were recorded on a Biorad FTS-7/PC FT-IR and a Perkin–Elmer Spectrum One FT-IR spectrophotometer for compounds **1** and **2**, respectively as KBr disc in the 4000–450 cm^{-1} spectral range. Solid-state (diffuse reflectance) electronic spectra were measured as polycrystalline samples on a Perkin–Elmer Lambda2S spectrophotometer, over the range 8000–18000 cm^{-1}. The X-band powder EPR spectra were obtained on polycrystalline samples at room temperature and 77 K with a JEOL RE2X electron spin resonance spectrometer by Microanalytical Service of Science and Technological Research Equipment Center, Chulalongkorn University.

2.2. Synthesis of compound 1

2.2.1. $[Cu_2(dpyam)_2(\mu\text{-}OH)_2I_2]\cdot 2H_2O$ (1)

The hot aqueous solution (5 ml) of KI (0.166 g, 1.0 mmol) was added to a hot aqueous solution (5 ml) of $Cu(NO_3)_2\cdot 3H_2O$ (0.121 g, 0.5 mmol). Then a hot acetone solution (8 ml) of dpyam (0.086 g, 0.5 mmol) was added to the mixture yielding a green solution. Its color became greenish-blue by slow addition of an aqueous solution (10 ml) of NaOH (0.020 g, 0.5 mmol) and the blue precipitate formed in a few minutes. The precipitate was filtered off and recrystallized in a hot aqueous solution. After two weeks, blue-plate crystals of compound **1** were obtained. *Anal.* Calc. for $C_{20}H_{24}Cu_2I_2N_6O_4$: C, 30.28; H, 3.05; N, 10.59. Found: C, 30.35; H, 3.12; N, 10.40%.

2.3. Synthesis of compound 2

2.3.1. $[Cu_2(dpyam)_2(\mu\text{-}OH)_3]Cl\cdot 3H_2O$ (2)

This compound was prepared by adding a hot acetone solution (10 ml) of dpyam (0.171 g, 1.0 mmol) to a hot aqueous solution (30 ml) of $CuCl_2\cdot 2H_2O$ (0.170 g, 1.0 mmol) yielding a turquoise green solution. Its color became blue by slow addition of an aqueous solution (10 ml) of NaOH (0.039 g, 1.0 mmol). This solution was allowed to evaporate at room temperature. After several days, bluish-purple crystals of compound **2** were obtained which were filtered off, washed with mother liquor and air-dried. *Anal.* Calc. for $C_{20}H_{27}ClCu_2N_6O_6$: C, 41.70; H, 4.72; N, 14.59. Found: C, 41.67; H, 4.81; N, 14.53%.

2.4. Crystallography

The X-ray single-crystal data for two compounds were collected at 298 and 293 K for compounds **1** and **2**, respectively on a 1 K Bruker SMART CCD area-detector diffractometer using graphite monochromated Mo Kα radiation ($\lambda = 0.71073$ Å) at a detector distance of 4.5 cm and swing angle of −35°. A hemisphere of the reciprocal space was covered by combination of three sets of exposures; each set had a different ϕ angle (0°, 88°, 180°) and each exposure of 40 s covered 0.3° in ω. Data reduction and cell refinements were performed using the program SAINT [7]. An empirical absorption correction by using the SADABS [8] program was applied, which resulted in transmission coefficients ranging from 0.741 to 1.000 for compound **1**, 0.752 to 1.000 for compound **2**.

The structures were solved by direct methods and refined by full matrix least-squares method on $(F_{obs})^2$ with anisotropic thermal parameters for all non-hydrogen atoms using the SHELXTL-PC V 6.12 software package [9]. All hydrogen atoms were located geometrically and refined isotropically except those of a hydroxo group and two molecules of lattice water for **2**.

The molecular graphics were created by using SHELXTL-PC [9] package. The crystal and refinement details for compounds **1** and **2** are listed in Table 1. Selected bond lengths and angles are given in Tables 2 and 3.

3. Results and discussion

3.1. Crystal structure of $[Cu_2(dpyam)_2(\mu\text{-}OH)_2I_2]\cdot 2H_2O$ (1)

The structure of compound **1** consists of a centrosymmetric dinuclear $[Cu_2(dpyam)_2(\mu\text{-}OH)_2I_2]$ unit and two molecules of lattice water. This unit is depicted in Fig. 1, together with the numbering scheme, with selected distances and angles listed in Table 2. Both copper(II) atoms of the complex are linked through the double hydroxo bridges. Each copper(II) atom has a distorted square pyramidal coordination, $\tau = 0.04$ (the structure index is defined as $\tau = (\beta - \alpha)/60$, where β and α are the largest coordination angles [10,11]), with the basal plane, CuN_2O_2 chromophore, comprised of two nitrogen atoms from a terminal dpyam ligand (Cu(1)–(N1) distance of 2.007(3) and Cu(1)–N(2) distance of 2.006(3) Å) and two oxygen atoms from two hydroxo groups (Cu(1)–O(1) distance of 1.967(2) and Cu(1)–O(1A) distance of 1.960(2) Å). The fifth apical coordination site of each copper(II) atom is occupied by an I atom (Cu–I distance of 3.040 Å) to complete the distorted square pyramidal CuN_2O_2I chromophore. However, the Cu–I distance is too long for even weak semi-coordination. The basal planes are slightly deviated from planarity with a distinct tetrahedral twist, evident from the dihedral angle of 19.3° between CuN_2 and CuO_2 planes. The Cu–Cu separation within the dinuclear unit is 2.988(7) Å, while the bridging Cu(1)–

Table 1
Crystal and refinement data for complexes **1** and **2**

Complex	(1)	(2)
Molecular formula	$[Cu_2(dpyam)_2(\mu\text{-}OH)_2I_2]\cdot 2H_2O$	$[Cu_2(dpyam)_2(\mu\text{-}OH)_3]Cl\cdot 3H_2O$
Molecular weight	793.33	610.02
T (K)	293(2)	293(2)
Crystal system	triclinic	orthorhombic
Space group	$P\bar{1}$	$Cmc2_1$
a (Å)	9.191	15.690
b (Å)	9.440(2)	8.629
c (Å)	9.472(2)	18.249
α (°)	111.54	90
β (°)	97.08(10)	90
γ (°)	108.84(10)	90
V (Å^3)	695.66(2)	2470.85(5)
Z	1	4
D_{calc} (g cm^{-3})	1.980	1.626
μ (mm^{-1})	3.792	1.877
$F(000)$	402	1228
Crystal size (mm)	0.05 × 0.20 × 0.25	0.23 × 0.45 × 0.10
Number of reflections collected	5226	9012
Number of unique reflections [R_{int}]	3810 [0.0165]	3593 [0.0408]
Data/restraints/parameter	3810/0/219	3593/1/181
Goodness-of-fit	1.012	1.123
Final R indices [$I > 2\sigma(I)$]	$R_1 = 0.0345$, $wR_2 = 0.0824$	$R_1 = 0.0408$, $wR_2 = 0.1386$
R indices (all data)	$R_1 = 0.0483$, $wR_2 = 0.0904$	$R_1 = 0.0453$, $wR_2 = 0.1427$
Largest difference peak and hole (e Å$_3$)	0.963, −1.010	1.539, −0.402

Table 2
Selected bond lengths [Å] and angles [°] with e.s.d.s. in parentheses of $[Cu_2(dpyam)_2(\mu\text{-}OH)_2I_2]\cdot 2H_2O$ (**1**)

Bond lengths				
Cu(1)–N(1)		2.007(3)	Cu(1)–O(1)	1.967(2)
Cu(1)–N(2)		2.006(3)	Cu(1)–O(1A)	1.960(2)
Cu(1)–I(1)		3.040(5)	Cu(1)–Cu(1A)	2.988(7)
Bond angles				
O(1)–Cu(1)–O(1A)		80.93(11)	O(1A)–Cu(1)–I(1)	99.75(9)
O(1)–Cu(1)–N(1)		93.51(10)	N(1)–Cu(1)–N(2)	89.31(11)
O(1)–Cu(1)–N(2)		166.55(12)	N(1)–Cu(1)–I(1)	95.83(8)
O(1)–Cu(1)–I(1)		97.48(8)	N(2)–Cu(1)–I(1)	95.30(9)
O(1A)–Cu(1)–N(1)		164.oo(12)	Cu(1)–O(1)– Cu(1A)	99.07(11)
O(1A)–Cu(1)–N(2)		92.82(10)		
Hydrogen bonds	D-H	H...A	D...A	D-H...A
N(3) – H(5)...O(3)[a]	0.79	2.13	2.9156	173
O(1) – H(10)...O(2)[b]	0.53	2.25	2.7500	157
O(3) – H(13)...O(1)[c]	0.62	2.40	2.8474	130

$A = -x, -y+1, -z$.
[a] $[1-x, 2-y, -z]$.
[b] $[-x, 1-y, -z]$.
[c] $[1-x, 1-y, -z]$.

O(1)–Cu(1A) angle is 99.1(11)°. Each copper atom is displaced toward the apical I atom of 0.243 Å from the basal N_2O_2 plane. The dinuclear unit is exactly planar, a dihedral angle between two CuO_2 planes is 180° and that between the basal N_2O_2 planes is 180° (see Fig. 3). The bite angle of the dpyam ligand N(1)–Cu(1)–N(2) of 89.3(11)° is only slightly less than 90° but the O(1)–Cu(1)–O(1A) angle of 80.9(11)° is significantly less than 90°. The individual pyridine rings are planar, and the dpyam ligand is non-planar, dihedral angle of 27.2° occurs between the individual pyridine rings.

The lattice is further stabilized by a hydrogen bonding between the amine N and the oxygen atom of lattice water molecule with N···O contact of 2.916 Å ; between the oxygen atom of bridging hydroxo group and the oxygen atom of lattice water molecules with O···O contacts of 2.750–2.847 Å.

Table 3
Selected bond lengths [Å] and angles [°] with e.s.d.s. in parentheses of $[Cu_2(dpyam)_2(\mu\text{-}OH)_3]Cl \cdot 3H_2O$ (2)

Bond lengths				
Cu(1)–N(1)		1.995(3)	Cu(1)–O(1)	1.942(3)
Cu(1)–N(2)		2.006(3)	Cu(1)–O(2)	1.953(3)
Cu(1)–O(3)		2.433(4)	Cu(1)–Cu(1A)	2.803(7)
Bond angles				
O(1)–Cu(1)–O(2)		81.1(2)	N(1)–Cu(1)–N(2)	91.79(13)
O(1)–Cu(1)–O(3)		78.8(2)	N(1)–Cu(1)–O(3)	102.05(14)
O(1)–Cu(1)–N(1)		174.6(2)	N(2)–Cu(1)–O(3)	104.44(14)
O(1)–Cu(1)–N(2)		93.17(14)	Cu(1)–O(1)–Cu(1A)	92.4(2)
O(2)–Cu(1)–O(3)		76.4(2)	Cu(1)–O(2)–Cu(1A)	91.7(2)
O(2)–Cu(1)–N(1)		93.88(14)	Cu(1)–O(3)–Cu(1A)	70.34(13)
O(2)–Cu(1)–N(2)		174.0(2)		
Hydrogen bonds	D-H	H...A	D...A	D-H...A
N(3) – H(5)...Cl(1)[a]	0.86	2.39	3.2518	176
O(2) – H(11)...Cl(1)[b]	0.63	2.59	3.2283	178
O(3) – H(12)...Cl(1)	0.52	2.66	3.1756	174

$A = -x+2, y, z$.
[a] $[x, -1+y, z]$.
[b] $[1/2+x, -1/2+y, z]$.

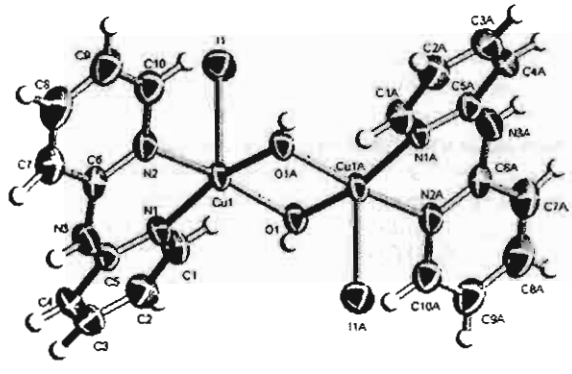

Fig. 1. ORTEP 50% probability plot of the cation in $[Cu_2(dpyam)_2(\mu\text{-}OH)_2I_2] \cdot 2H_2O$ (1) Atoms with an "A" are generated by a mirror plane.

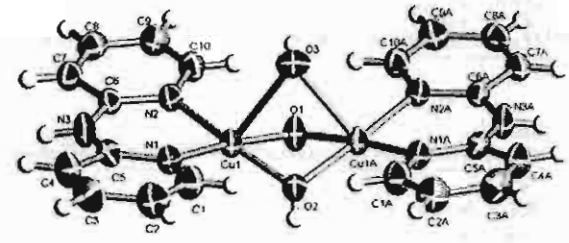

Fig. 2. ORTEP 50% probability plot of the cation in $[Cu_2(dpyam)_2(\mu\text{-}OH)_3]Cl \cdot 3H_2O$ (2) Atoms with an "A" are generated by a mirror plane.

3.2. Crystal structure of $[Cu_2(dpyam)_2(\mu\text{-}OH)_3]Cl \cdot 3H_2O$ (2)

The structure of compound **2** is made up of a dinuclear $[Cu_2(OH)_3(dpyam)]^+$ cation, an uncoordinated Cl^- anion and three crystallisation water molecules. This unit is depicted in Fig. 2, together with the numbering scheme, with selected distances and angles listed in Table 3. The cation is located on a mirror plane through the three bridging OH^- groups. The whole cationic unit and the copper environment are the rooftop configuration. Compound **2** involves a triplyhydroxo-bridged structure with a square pyramidal CuN_2O_2O' chromophore, the fifth axial position is occupied by a longer bonded bridging OH^- group with a distance of 2.433(3) Å. The copper atom is displaced from the basal plane towards the apical oxygen by 0.035 Å. The Cu(1)–N(1) and Cu(1)–N(2) distances are

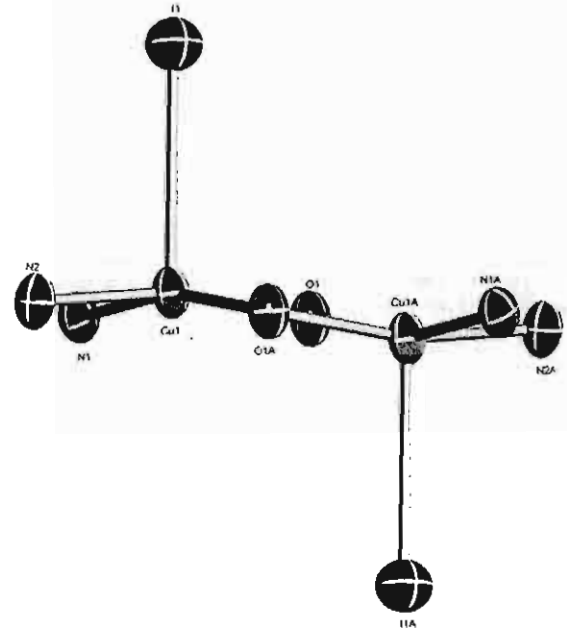

Fig. 3. The chromophore of $[Cu_2(dpyam)_2(\mu\text{-}OH)_2I_2] \cdot 2H_2O$ (1).

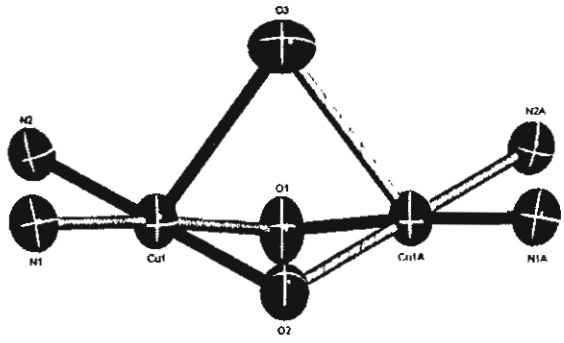

Fig. 4. The chromophore of $[Cu_2(dpyam)_2(\mu\text{-}OH)_3]Cl \cdot 3H_2O$ (2).

1.995(3) and 2.006(3) Å, respectively. The average Cu–O (hydroxo bridge) distance of 1.948 Å is slightly shorter and very close to those observed in the corresponding di-hydroxo bridged copper(II) dimers [5,6,12,13]. The CuN_2O_2 chromophore is planar with a slight tetrahedral twist, dihedral angle of 2.8° between the CuN_2 and CuO_2 planes, but the Cu_2O_2 network is not planar, a dihedral angle between the CuO_2 planes is 142.5° (see Fig. 4). The Cu–Cu distance is 2.803(1) Å. The bridging Cu–O(1)–Cu and Cu–O(2)–Cu angles are 92.4(2)° and 91.7(2)°, respectively, which are not in the range normally found for the planar dihydroxo-bridged copper(II) dimers. The dpyam ligand as a whole is nearly planar and involves a dihedral angle of 9.1° between the individual pyridine rings.

The lattice is stabilized by a hydrogen bonding between the amine N and the chloride atom with N···Cl distance of 3.252 Å and between the oxygen atom of bridging hydroxo group and the chloride atom with O···Cl contacts of 3.176–3.228 Å.

3.3. Spectral characterization

The infrared spectra of compounds **1** and **2** show a broad band at 3460 and 3400 cm^{-1}, respectively which can be assigned to the bridging OH vibrations of the hydroxo bridge and/or lattice water.

The electronic diffuse reflectance spectrum of compound **1** shows a broad band centered at 15 120 cm^{-1}. This observed single broad peak is consistent with the tetrahedrally distorted square pyramidal stereochemistry and assigned to be the $d_{z^2}, d_{xy}, d_{xz}, d_{yz} \rightarrow d_{x^2-y^2}$ transition [14,15]. The reflectance spectrum of **2** displays a broad band and a lower energy shoulder at the frequencies of 17 800 and 14 600(sh) cm^{-1}. The relatively higher energy of this triply bridged dimer is unusual for the square pyramidal geometry. However, they are consistent with those observed for the relevant bipy complexes [16] and the $d_{xy}, d_{yz} \rightarrow d_{x^2-y^2}$ and $d_{xz}, d_{z^2} \rightarrow d_{x^2-y^2}$ transitions are assigned for a broad band and a lower energy shoulder, respectively.

The X-band polycrystalline EPR spectrum of compound **1**, at room temperature, displays a weak signal at ~320 mT ($g_i = 2.078$), while a triplet state signal at ~100–160 mT ($g_i = 6.964$) is not observed properly. The former feature is most certainly from a monomeric Cu(II) impurity, which is always present in dinuclear species. Compound **2** exhibits an intense signal at ~101 mT ($g_i = 6.695$) and a weaker signal at ~307 mT ($g_i = 2.220$). The latter is attributed to the monomeric impurity while the former is usually attributed to intramolecular exchange interaction between copper(II) ions, $\Delta Ms = \pm 2$ transition [17,18].

Compound **1** is planar (dihedral angle of 180° between the CuO_2 planes) and involves the Cu–O–Cu angle of 99.1° expecting a moderate antiferromagnetic coupling ($J = -116$ cm^{-1}) following Hodgson and Hatfield's linear relationship [1,18]. However, the experimental value of singlet-triplet energy gap ($2J$) would be smaller than the predicted value. The difference could be due to the deviation from planarity of the CuN_2O_2 plane with a tetrahedral twist between CuN_2 and CuO_2 planes, which may reduce the orthogonality of the copper(II) $d_{x^2-y^2}$ (or d_{xy}) orbital with the bridging hydroxo groups [4]. The most relevant compound $[Cu_2(dpyam)_2(\mu\text{-}OH)_2Br_2] \cdot 4H_2O$ also involves a double hydroxo bridge and an observed J value of -48.6 cm^{-1}, while the predicted value was as high as -116 cm^{-1} [6]. On the other hand compound **2** has the roof-shaped hydroxo bridge network with a dihedral angle of 142.5° between the CuO_2 planes and the Hatfield's linear relationship, which arises from studies of planar $Cu_2(OH)_2$ cores, is not valid then. The related structure, $[Cu_2(dpyam)_2(\mu\text{-}OH)_2(\mu\text{-}OH_2)]Br_2 \cdot 2H_2O$ compound exhibits $J = -0.6$ cm^{-1}.

3.4. Structure comparison

There are five dihydroxo-bridged copper(II) dimers containing the dpyam ligand: $[Cu_2(dpyam)_2(\mu\text{-}OH)_2Br_2] \cdot 4H_2O$ **(3)**, $[Cu_2(dpyam)_2(\mu\text{-}OH)_2(FBF_3)_2]$ **(4)**, $[Cu_2(dpyam)_2(\mu\text{-}OH)_2(ONO_2)_2]$ **(5)**, $[Cu_2(dpyam)_2(\mu\text{-}OH)_2(\mu\text{-}OH_2)]Cl_2 \cdot 2H_2O$ **(6)** and $[Cu_2(dpyam)_2(\mu\text{-}OH)_2(\mu\text{-}OH_2)]Br_2 \cdot 2H_2O$ **(7)** have been structurally reported [4–6,12]. In the known dimer structures, three copper environments are observed: rhombic coplanar [19], CuN_2O_2, square-based pyramidal, CuN_2O_2X [18,20], and elongated rhombic octahedral [21,22], $CuN_2O_2X_2$. Compounds **1**, **3**, **4** and **5** involve the planar dihydroxo-bridged copper(II) dimer, all exhibit the square pyramidal CuN_2O_2X chromophore geometry. Compound **1** involves the square-based pyramidal CuN_2O_2I chromophores which are very comparable to the CuN_2O_2Br, CuN_2O_2F and CuN_2O_2O' chromophores in **3**, **4** and **5**, respectively. The fifth axial distances of 3.040(5) Å in compound **1** are much longer than those of 2.803(2) and 2.804(2), 2.745(7), 2.400(1) and 2.500(1) Å in

compounds **3**, **4** and **5**, respectively. The marked tetrahedral twists of the CuN_2O_2 chromophores in compound **1** and also in compounds **3**, **4** and **5** (dihedral angle of 19.3°, 21.8° and 21.4°, 24.0°, 20.7° and 16.7°, respectively) are less usual. However, the Cu_2O_2 network in these compounds is planar and the planarities of both the CuN_2O_2 chromophore and the Cu_2O_2 unit for each compound are not many different. Consequently, the Cu–Cu separation of 2.988(7) Å in compound **1** is more similar in compounds **3**, **4** and **5** (2.993(2); 2.919(5) and 2.954(2) Å, respectively). The Cu–O–Cu bridging angle of 99.1 Å in compound **1** is comparable to that of compounds **3**, **4** and **5** (98.1° and 100.1°, 99.3°, 99.4° and 98.9°, respectively). There are a significant difference observed in the Cu to N_2O_2 mean plane distances, those of compounds **1** and **3** (0.243, 0.273 Å, respectively) are longer than those of compounds **4** and **5** (0.022; 0.079 and 0.142 Å, respectively) arising from a very weak interaction in the sixth position of the chromophore provided from the other F atom of the BF_4^- group in compound **4** and the other O atom of the NO_3^- group in compound **5**. However, these sixth distances are between 3.0–4.0 Å. The structural data of compounds **1**, **3**, **4** and **5** have revealed that the bigger in the bite N–Cu–N angle (98.3°, 88.6° and 88.9°, 99.3°, 98.9° and 99.4°, respectively), the bigger the bridging Cu–O–Cu angle is observed. Consequently, the Cu–O–Cu angles in the parent dpyam complexes are bigger (>97.5°) than those of the corresponding bipy complexes (<97.5°). This feature is also observed in other corresponding dimers involving the other terminal ligand. This concludes that the terminal ligand other than the anion and solvent molecule influences the magnitude of the Cu–O–Cu angle.

The most interesting and unusual feature in structure of compound **2** is that this is the triply bridged dinuclear compound with a roof-shaped bridge, the dihedral angle between the CuO_2 planes is far from 180°. Each hydroxo group is symmetrically bound, with Cu–O(1) bond slightly shorter than Cu–O(2) bond. The bridging angles in compound **2** are significantly less than those found in the planar dihydroxo-bridged copper (II) dimers and are not in the usual range 95°–105°, normally found for these dimers [23–25]. So far, compound **2** represents the second structurally characterized examples of a triply bridged dinuclear copper(II) compound containing three monoatomic bridges with homospecies. The first one has been pointed out for the known $Cs_3[Cu_2Cl_7(H_2O)_2]$ compound [26], containing three Cl^- anions bridging two copper atoms separated by 3.45 Å. The related structures of the roof-shaped dinuclear copper(II) containing three monoatomic bridges are $[Cu_2(dpyam)_2(\mu\text{-}OH)_2(\mu\text{-}OH_2)]Cl_2 \cdot 2H_2O$ (**6**) and $[Cu_2(dpyam)_2(\mu\text{-}OH)_2(\mu\text{-}OH_2)]Br_2 \cdot 2H_2O$ (**7**) and $[Cu_2(dpyam)_2(\mu\text{-}OMe)_2(\mu\text{-}Cl)]Cl \cdot MeOH$ (**8**). The cations present in compounds **2**, **6**, **7** and **8** show a similar structure, they exhibit the metal centres in a square pyramidal configuration with in-plane configuration of a dpyam ligand and of two bridging O atoms and involve in similar CuO_2Cu roof-top angles (142.5°, 140.6°, 135.8°, 144.3°, respectively). Also the in-plane Cu–N and Cu–O distances are similar to each other and the Cu–Cu separations are quite comparable (2.803, 2.797, 2.849, 2.792 Å, respectively). The cations differ, however, in the nature of the fifth bridging ligand, which is a hydroxo group in compound **2**, a water molecule in compounds **6** and **7**, and a bigger chloride anion in compound **8**.

4. Conclusion

In comparison to the planar di-μ-hydroxo-bridged complexes significant differences are observed. The dihedral angle between the CuO_2 planes of the dihydroxo-bridged dimers becomes near 180°, while their CuN_2O_2 chromophores are not planar with a distinct tetrahedral twist (except that for the octahedral geometry). On the other hand, the planarity of the square planes for each CuN_2O_2 chromophore with a slight tetrahedral twist is observed in the triply bridged dimers. Due to bending in the molecule, the Cu–Cu distances (2.792–2.849 Å) in the triply bridged complexes are significantly shorter than those of the planar dihydroxo-bridged complexes (2.870–3.000 Å). However, these distances are typical in the range previously observed, 2.80–3.00 Å [1,27]. There is an additional remarkable difference observed, the bridging Cu–O–Cu angles (91.0°–94.7°) in the roof-shaped dimers are significantly smaller than 95.0° while in the planar dihydroxo-bridged dimers, these angles are in the range 95.0°–104.1°.

5. Supplementary material

Crystallographic data (excluding structure factors) for the structures in this paper have been deposited with the Cambridge Crystallographic Data Centre as supplementary publication no.CCDC-223620, 223621, for structures **1** and **2**, respectively. Copies of the data can be obtained free of charge on application to CCDC, 12 Union Road, Cambridge CB2 1EZ, UK (fax: (international) +44-1223-336-033, e-mail: deposit@ccdc.cam.ac.uk or www: http://www.ccdc.cam.ac.uk).

Acknowledgements

The authors would like to thank The Thailand Research Fund and Khon Kaen University for research grant. Support of the Postgraduate Education and Research Program in Chemistry is also gratefully acknowledged.

References

[1] V.H. Crawford, H.W. Richardson, J.R. Wasson, D.J. Hodgson, W.E. Hatfield, Inorg. Chem. 15 (1976) 2107.
[2] E. Ruiz, P. Alemany, S. Alvarez, J. Cano, Inorg. Chem. 36 (1997) 3683.
[3] E. Ruiz, P. Alemany, S. Alvarez, J. Cano, J. Am. Chem. Soc. 119 (1997) 1297.
[4] L.P. Wu, M.E. Keniry, B.J. Hathaway, Acta Cryst. C48 (1992) 35.
[5] N. Marsich, A. Camus, F. Ugozzoli, A.M.M. Lanfredi, Inorg. Chim. Acta 236 (1995) 117.
[6] S. Youngme, G.A. van Albada, O. Roubeau, C. Pakawatchai, N. Chaichit, J. Reedijk, Inorg. Chim. Acta 342 (2003) 48.
[7] Siemens. SAINT. 1996, Version4 Software Reference Manual, Siemens Analytical X-Ray Systems, Inc., Madison, WI, USA.
[8] G.M. Sheldrick, SADABS, Program for Empirical Absorption correction of Area Dectector Data, University of Göttingen, Göttingen, Germany, 1996.
[9] Bruker. XSHELL. 1999, Version 6.12 Reference Manual, Bruker AXS, Inc., Madison, WI, USA.
[10] A.W. Addison, T.N. Rao, J. Reedijk, J. van Rijn, G.C. Verschoor, J. Chem. Soc., Dalton Trans. (1984) 1349.
[11] M. Brophy, G. Murphy, C. O'Sullivan, B. Hathaway, B. Murphy, Polyhedron 18 (1999) 611.
[12] S. Youngme, W. Somjitsripunya, K. Chinnakali, S. Chantrapromma, H.K. Fun, Polyhedron 18 (1999) 857.
[13] S. Youngme, G.A. van Albada, H. Kooijman, O. Roubeau, W. Somjitsripunya, A.L. Spek, C. Pakawatchai, J. Reedijk, Eur. J. Inorg. Chem. (2002) 2367.
[14] G. Murphy, C. Murphy, B. Murphy, B. Hathaway, J. Chem. Soc., Dalton Trans. (1997) 2653.
[15] G. Murphy, C. O'Sullivan, B. Murphy, B. Hathaway, Inorg. Chem. 37 (1998) 240.
[16] C.M. Harris, E. Sinn, W.R. Walker, P.R. Woolliams, Aust. J. Chem. 21 (1968) 631.
[17] G. De Munno, M. Julve, F. Lloret, J. Faus, M. Verdaguer, A. Caneschi, Inorg. Chem. 34 (1995) 157.
[18] G.A. van Albada, I. Mutikainen, W.J.J. Smeets, A.L. Spek, U. Turpeinen, J. Reedijk, Inorg. Chim. Acta 327 (2002) 134.
[19] M.F. Charlot, S. Jeannin, Y. Jeannin, O. Kahn, J. Lucrece-Abaul, J. Martin-Frere, Inorg. Chem. 18 (1979) 1675.
[20] J.M. Seco, U. Amador, M.J. González Garmendia, Polyhedron 18 (1999) 3605.
[21] G.A.van Albada, I. Mutikainen, U. Turpeinen, J. Reedijk, Inorg. Chim. Acta 324 (2001) 273.
[22] S. Amani Komaei, G.A. van Albada, J.G. Haasnoot, H. Kooijman, A.L. Spek, J. Reedijk, Inorg. Chim. Acta 286 (1999) 24.
[23] I. Castro, M. Julve, G.D. Munno, G. Bruno, J.A. Real, F. Lloret, J. Faus, J. Chem. Soc., Dalton Trans. (1992) 1739.
[24] I. Castro, M. Julve, G.D. Munno, G. Bruno, J.A. Real, F. Lloret, J. Faus, J. Chem. Soc., Dalton Trans. (1992) 47.
[25] P.J. Hay, J.C. Thibeault, R. Hoffmann, J. Am. Chem. Soc. 97 (1975) 4884.
[26] V.W. Vogt, H. Haas, Acta Cryst., Sect. B. (1971) 1521.
[27] B.J. Hathaway, Comprehensive co-ordination chemistry. in: G. Wilkinson (Editor in Chief), R.D. Gillard, J.A. McCleverty (Executive Editors), The Synthesis, Reactions, Properties and Applications of Co-ordination Compounds, vol. 5, Sec. 53, Pergamon Press, Oxford, 1987; pp. 533–774.

Available online at www.sciencedirect.com
SCIENCE DIRECT
Inorganica Chimica Acta 357 (2004) 2532–2542
Inorganica Chimica Acta
www.elsevier.com/locate/ica

Synthesis, crystal structure, spectroscopic and magnetic properties of doubly and triply bridged dinuclear copper(II) compounds containing di-2-pyridylamine as a ligand ☆

Sujittra Youngme [a,*], Chatkaew Chailuecha [a], Gerard A. van Albada [b], Chaveng Pakawatchai [c], Narongsak Chaichit [d], Jan Reedijk [b]

[a] Department of Chemistry, Faculty of Science, Khon Kaen University, Khon Kaen 40002, Thailand
[b] Leiden Institute of Chemistry, Gorlaeus Laboratories, Leiden University, P.O. Box 9502, 2300 RA Leiden, The Netherlands
[c] Department of Chemistry, Faculty of Science, Prince of Songkla University, Hatyai, Songkla 90112, Thailand
[d] Department of Physics, Faculty of Science and Technology, Thammasat University Rangsit, Pathumthani 12121, Thailand

Received 8 October 2003; accepted 21 January 2004
Available online 19 March 2004

Abstract

The dihydroxo-bridged dinuclear copper(II) compound $[Cu_2(dpyam)_2(\mu\text{-}OH)_2]I_2$ (1) and the triply bridged dinuclear copper(II) compounds with a formato bridge $[Cu_2(dpyam)_2(\mu\text{-}O_2CH)(\mu\text{-}OH)(\mu\text{-}OMe)](ClO_4)$ (2) and $[Cu_2(dpyam)_2(\mu\text{-}O_2CH)(\mu\text{-}OH)(\mu\text{-}Cl)](ClO_4)\cdot 0.5H_2O$ (3) (in which dpyam = di-2-pyridylamine) have been synthesized and their crystal structures determined by X-ray crystallographic methods. All three compounds are either centrosymmetric, or have a symmetry plane in the molecule. Compound 1 contains the $[Cu_2(dpyam)_2(\mu\text{-}OH)_2]^+$ unit and iodide anions. Each copper(II) ion is in a slightly tetrahedrally distorted square planar coordination with the square plane consisting of two nitrogen atoms of the dpyam ligand and two bridging hydroxo groups. The Cu–I distances of 3.321 Å are quite long and only involve a weak semi-coordination. Compound 2 contains a triply bridged dinuclear copper(II) species, the coordination environment around each copper(II) ion involves a distorted trigonal-bipyramidal CuN_2O_3 chromophore. In the dinuclear unit of compound 3, the triply bridged copper(II) ions show a distorted trigonal-bipyramidal coordination of the CuN_2O_2Cl chromophore. The Cu–Cu distances are 2.933(2), 3.023(1) and 3.036(1) Å for compounds 1, 2 and 3, respectively.

The magnetic susceptibility measurements, measured from 5 to 280 K, revealed a weak antiferromagnetic interaction between the Cu(II) atoms for compound 1 with a singlet–triplet energy gap (J) of -15.3 cm^{-1}, whereas compounds 2 and 3 are ferromagnetic with $J = 62.5$ and 79.1 cm^{-1}, respectively.

Keywords: Copper(II) complexes; Crystal structure; Formato-bridged; Triply bridged; Magnetic properties

1. Introduction

The magneto-structural characterization of ligand-bridged dinuclear copper(II) compounds have received much attention during the past several years [1,2]. The planar dihydroxo-bridged and the triply bridged copper(II) dinuclear species are extensively studied, because of the magnetic interaction between two unpaired electrons [3–19]. For the dihydroxo-bridged copper(II) dinuclear species, the linear correlation between the Cu–O–Cu bridging angle and the singlet–triplet energy gap (J) was first observed by Hodgson and co-workers [3]. An antiferromagnetic interaction is found when the Cu–O–Cu angle is larger than 97.5°, but when the Cu–O–Cu angle is smaller than 97.5°, a ferromagnetic interaction would be expected. Several theoretical approaches were applied to understand the behavior of the antiferromagnetic and ferromagnetic interaction of such dihydroxo-bridged copper(II) dinuclear species [4–11].

☆ Supplementary data associated with this article can be found, in the online version, at doi:10.1016/j.ica.2004.01.039.

* Corresponding author. Fax: +66-43-243-338.
E-mail address: sujittra@kku.ac.th (S. Youngme).

0020-1693/$ - see front matter © 2004 Elsevier B.V. All rights reserved.
doi:10.1016/j.ica.2004.01.039

The magnetic interaction in the triply bridged dinuclear copper(II) complexes can occur via bridging ligands in various pathways, which depend on the type of the bridging ligand, monoatomic and polyatomic bridge for example, and the coordination geometry of the copper(II) center [12–19]. For the square-pyramidal geometry, the magnetic orbital for the copper(II) center is the $d_{x^2-y^2}$ orbital which lies along the basal plane. Therefore, a superexchange interaction between two copper(II) ions is usually observed through the ligands which are located in the same equatorial plane. If the geometry of the copper(II) ion is trigonal-bipyramidal the unpaired spin density is along the *z*-axis, i.e., in the d_{z^2} orbital, that can overlap with the apical-positioned bridging ligands. The magnitude of magnetic interaction is primarily governed by an overlap of two magnetic orbitals centered on the nearest-neighbour copper(II) ions. The present work is focused on the various types of overlapping interactions between the ligand atomic orbital and the copper(II) d orbitals. For this purpose, a dihydroxo-bridged $[Cu_2(dpyam)_2](\mu\text{-}OH)_2]I_2$ **(1)** and two triply bridged dinuclear copper(II) compounds $[Cu_2(dpyam)_2(\mu\text{-}O_2CH)(\mu\text{-}OH)(\mu\text{-}OMe)](ClO_4)$ **(2)** and $[Cu_2(dpyam)_2(\mu\text{-}O_2CH)(\mu\text{-}OH)(\mu\text{-}Cl)](ClO_4)\cdot 5H_2O$ **(3)** are synthesized with the ligand di-2-pyridylamine and characterized by spectroscopy and X-ray crystallography; also magnetic measurements are performed on the compounds.

2. Experimental

2.1. Reagents and physical measurements

The ligand di-2-pyridylamine and all reagents are commercial grade materials and were used without further purification. Elemental analyses (C, H, N) were determined on a Perkin–Elmer PE 2400 CHNS/O Analyzer by Microanalytical Service of Science and Technological Research Equipment Center, Chulalongkorn University.

IR spectra were recorded on a Perkin–Elmer Spectrum One FT-IR spectrophotometer as KBr disc in the 4000–450 cm^{-1} spectral range. Solid-state (diffuse reflectance) electronic spectra were measured as polycrystalline samples on a Perkin–Elmer Lambda2S spectrophotometer, within the range 8000–18 000 cm^{-1}. The X-band powder EPR spectra were obtained on polycrystalline samples at room temperature and 77 K with a JEOL RE2X electron spin resonance spectrometer with DPPH ($g = 2.0036$) as a reference. Magnetic susceptibility measurements (5–280 K) were carried out using a Quantum design MPMS-5 5T SQUID magnetometer (measurements carried out at 1000 Gauss) performed at Leiden University. Data were corrected for magnetization of the sample holder and for diamagnetic contributions, which were estimated from the Pascal constants.

2.2. Syntheses

2.2.1. $[Cu_2(dpyam)_2(\mu\text{-}OH)_2]I_2$ (1)

A hot aqueous solution (5 ml) of KI (0.166 g, 1.0 mmol) was added to a hot aqueous solution (5 ml) of $Cu(NO_3)_2\cdot 3H_2O$ (0.121 g, 0.5 mmol). Then, a hot acetone solution (10 ml) of dpyam (0.086 g, 0.5 mmol) was added to the mixture yielding a green solution. Its color became greenish-blue by slow addition of an aqueous solution (10 ml) of NaOH (0.020 g, 0.5 mmol) and a blue precipitate formed within a few minutes. The precipitate was filtered off and recrystallized from a hot aqueous solution. After a month, blue crystals of compound **1** were obtained. *Anal.* Calc. for $C_{20}H_{20}Cu_2I_2N_6O_2$: C, 31.7; H, 2.7; N, 11.1. Found: C, 31.9; H, 2.4; N, 11.3%.

2.2.2. $[Cu_2(dpyam)_2(\mu\text{-}O_2CH)(\mu\text{-}OH)(\mu\text{-}OMe)](ClO_4)$ (2)

This compound was prepared by adding a hot ethanolic solution (10 ml) of dpyam (0.171 g, 1.0 mmol) to a hot aqueous solution (10 ml) of $Cu(ClO_4)\cdot 6H_2O$ (0.371 g, 1.0 mmol), after which solid HCOONa (0.272 g, 4.0 mmol) was added. The resulting green solution was allowed to evaporate at room temperature. After one week, green crystals of compound **2** were obtained which were filtered off, washed with the mother liquid and air-dried. *Anal.* Calc. for $C_{22}H_{23}ClCu_2N_6O_8$: C, 39.9; H, 3.5; N, 12.7. Found: C, 39.8; H, 3.6; N, 12.9%.

2.2.3. $[Cu_2(dpyam)_2(\mu\text{-}O_2CH)(\mu\text{-}OH)(\mu\text{-}Cl)](ClO_4)\cdot 0.5H_2O$ (3)

A hot DMF solution (20 ml) of dpyam (0.171 g, 1.0 mmol) was added to a hot aqueous solution (10 ml) of $CuCl_2$ (0.135 g, 1.0 mmol). Then, a hot aqueous solution (10 ml) of HCOONa (0.136 g, 2.0 mmol) was added to the mixture yielding a dark green solution, after which the solid $KClO_4$ (0.416 g, 3.0 mmol) was added. The resulting dark green solution was allowed to evaporate at room temperature. After a month, dark green crystals of compound **3** were formed which were filtered off, washed with the mother liquid and air-dried. *Anal.* Calc. for $C_{21}H_{21}Cl_2Cu_2N_6O_{7.5}$: C, 37.3; H, 3.1; N, 12.4. Found: C, 37.7; H, 3.4; N, 12.5%.

2.3. Crystallography

The X-ray single-crystal data for three compounds were collected at 293 K on a 1 K Bruker SMART CCD area-detector diffractometer using graphite monochromated Mo Kα radiation ($\lambda = 0.71073$ Å) at a detector distance of 4.5 cm and swing angle of −35°. Data

reduction and cell refinements were performed using the program SAINT [20]. An empirical absorption correction by using the SADABS [21] program was applied, which resulted in transmission coefficients ranging from 0.701 to 1.000 for **1**, 0.654 to 1.000 for **2** and 0.773 to 1.000 for **3**.

The structures were solved by direct methods and refined by full-matrix least-squares method on $(F_{obs})^2$ with anisotropic thermal parameters for all non-hydrogen atoms except O atoms of the disordered perchlorate group in **2** using the SHELXTL-PC V 6.12 software package [22]. The O atoms of the perchlorate group of **2** showed high disorder; the occupancies of the disordered positions were initially refined and later fixed at 0.45 and 0.55, respectively. The O atoms of the percholrate group of **3** also showed disorder. Attempts to model disordered positions into two sets are unsuccessful. However, their thermal parameters are substantially reasonable. All hydrogen atoms in **1** and **3** were located geometrically and refined isotropically. In **2**, all hydrogen atoms of the formate and dpyam ligands were geometrically fixed and allowed to ride on the attached atoms, those of the bridging hydroxo and bridging methoxo groups were located geometrically.

The molecular structure pictures were created by using SHELXTL-PC [22] package. The crystal and refinement details for compounds **1**, **2** and **3** are listed in Table 1.

3. Results and discussion

3.1. Description of $[Cu_2(dpyam)_2(\mu\text{-}OH)_2]I_2$ (1)

The structure of compound **1** consists of a centrosymmetric dinuclear $[Cu_2(dpyam)_2(\mu\text{-}OH)_2]^{2+}$ cation, with iodide counter anions. This unit is depicted in Fig. 1, together with the numbering scheme, with selected distances and angles listed in Table 2. Both copper(II) ions of the complex cation are linked through the double hydroxo bridges, leading to a Cu–Cu distance of 2.933(2) Å. Each copper(II) ion is in a tetrahedrally distorted square-planar coordination environment consisting of a CuN_2O_2 chromophore, which has two bridging hydroxo groups and a terminal dpyam ligand coordinated through their nitrogen atoms. A dihedral angle of 21.9° is present between the CuO_2 and CuN_2 planes. The apical Cu–I distance (3.321(5) Å) is too long to be considered as coordination (semi-coordination only). The fact that the copper(II) ions are lifted from the N_2O_2 planes, toward the I^- ions by 0.122 Å is a further indication for the semi-coordination. The Cu–O distances (1.935(5) and 1.937(5) Å) are slightly shorter than the Cu–N distances (2.006(5) and 2.007(5) Å). The bridging Cu–O–Cu angles are 98.5(2)°, greater than 97.5°, hence an antiferromagnetic coupling between copper(II) ions is predicted from Hodgson and Hatfield equation [3]. The dpyam ligands are essentially planar

Table 1
Crystal and refinement data for complexes **1**, **2** and **3**

Complex	1	2	3
Molecular formula	$[Cu_2(dpyam)_2(\mu\text{-}OH)_2]I_2$	$[Cu_2(dpyam)_2(\mu\text{-}O_2CH)(\mu\text{-}OH)(\mu\text{-}OMe)](ClO_4)$	$[Cu_2(dpyam)_2(\mu\text{-}O_2CH)(\mu\text{-}OH)(\mu\text{-}Cl)](ClO_4)\cdot 0.5H_2O$
Molecular weight	757.30	661.99	675.43
T (K)	293(2)	293(2)	273(2)
Crystal system	triclinic	orthorhombic	orthorhombic
Space group	$P\bar{1}$	$Cmc2_1$	$Cmc2_1$
a (Å)	7.28690(10)	16.7872(13)	16.8229(3)
b (Å)	9.3274(3)	8.0793(7)	7.8066(2)
c (Å)	9.5968(3)	18.7410(15)	19.2753(0)
α (°)	101.345(2)	90	90
β (°)	96.997(2)	90	90
γ (°)	109.985(2)	90	90
V (Å^3)	588.23(3)	2541.8(4)	2531.42(10)
Z	1	4	4
D_c (g cm^3)	2.138	1.693	1.749
μ (mm^{-1})	4.462	1.837	1.946
$F(000)$	362	1312	1344
Crystal size (mm)	0.08 × 0.08 × 0.20	0.08 × 0.20 × 0.30	0.13 × 0.33 × 0.40
Number of reflections collected	4407	10 804	9109
Number of unique reflections	3210 (R_{int} = 0.0246)	3124 (R_{int} = 0.0226)	3640 (R_{int} = 0.0208)
Data/restraints/parameter	3210/0/185	3124/1/206	3640/1/230
Goodness-of-fit	1.089	1.095	1.007
Final R indices [$I > 2\sigma(I)$]	R_1 = 0.0542, wR_2 = 0.0972	R_1 = 0.0571, wR_2 = 0.1668	R_1 = 0.0278, wR_2 = 0.0707
R indices (all data)	R_1 = 0.0965, wR_2 = 0.1168	R_1 = 0.0625, wR_2 = 0.1734	R_1 = 0.0322, wR_2 = 0.0731
Largest difference peak and hole (e Å^3)	1.182, −0.894	0.979, −0.419	0.388, −0.373

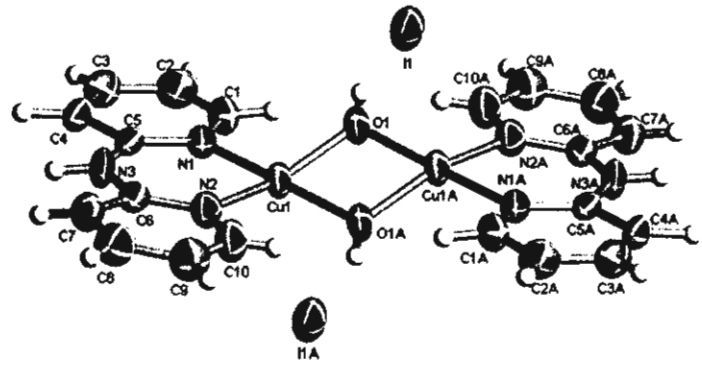

Fig. 1. ORTEP 50% probability plot of the cation in $[Cu_2(dpyam)_2(\mu\text{-}OH)_2]I_2$ (1) Atoms with an "A" are generated by a mirror plane.

Table 2
Selected bond lengths (Å) and angles (°) with e.s.d.s. in parentheses of $[Cu_2(dpyam)_2(\mu\text{-}OH)_2]I_2$ (1)

Cu(1)–N(1)	2.006(5)	Cu(1)–O(1)	1.937(5)
Cu(1)–N(2)	2.007(5)	Cu(1)–O(1A)	1.935(5)
Cu(1A)···I(1)	3.321(5)	Cu(1)–Cu(1A)	2.933(2)
O(1)–Cu(1)–N(1)	94.2(2)	O(1A)–Cu(1)–O(1)	81.5(2)
O(1)–Cu(1)–N(2)	158.6(3)	N(1)–Cu(1)–Cu(1A)	134.5(4)
O(1)–Cu(1)–Cu(1A)	40.7(2)	N(1)–Cu(1)–N(2)	92.6(2)
O(1A)–Cu(1)–N(1)	171.7(2)	N(2)–Cu(1)–Cu(1A)	131.3(2)
O(1A)–Cu(1)–N(2)	94.0(2)	Cu(1A)–O(1)–Cu(1)	98.5(2)
O(1A)–Cu(1)–Cu(1A)	40.7(2)		

A, $[-x+1, -y+1, -z+1]$.

with small dihedral angles of 4.8° between the individual pyridine rings. The bite angles of the dpyam ligands (N–Cu–N, 92.6(2)°) are only slightly greater than 90°.

3.2. Description of $[Cu_2(dpyam)_2(\mu\text{-}O_2CH)(\mu\text{-}OH)(\mu\text{-}OMe)](ClO_4)$ (2)

Compound **2** is a dinuclear unit copper(II) complex bridging by three different ligands. The structure of compound **2** consists of symmetric dinuclear $[Cu_2(dpyam)_2(\mu\text{-}O_2CH)(\mu\text{-}OH)(\mu\text{-}OMe)]^+$ cations with a single ClO_4^- counteranion. This unit is depicted in Fig. 2 together with the numbering scheme, with selected distances and angles listed in Table 3. Each copper(II) ion involves a CuN_2O_3 chromophore. The coordination geometry around each copper(II) ion is distorted trigonal-bipyramidal ($\tau = 0.65$). The structure index is defined as $\tau = (\beta - \alpha)/60$, where β and α are the largest coordination angles [23,24]. The three longer bonds in the trigonal planar plane are a nitrogen atom of the dpyam ligand (Cu–N(2) distance 2.010(4) Å), an oxygen atom of the bridging formato ligand (Cu–O(3) distance 2.175(3) Å) and an oxygen atom of the bridging methoxo ligand (Cu–O(2) distance 2.169(5) Å). The two shorter bonds in the axial positions involve the other nitrogen atom of the dpyam ligand (Cu–N(1) distance 1.961(4) Å) and an oxygen atom of the bridging hydroxo

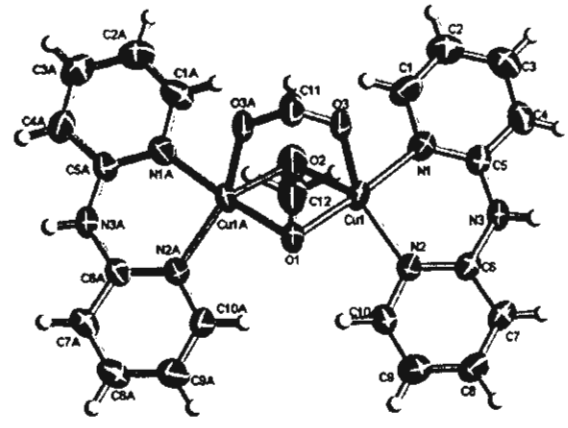

Fig. 2. ORTEP 50% probability plot of the cation in $[Cu_2(dpyam)_2(\mu\text{-}O_2CH)(\mu\text{-}OH)(\mu\text{-}OMe)](ClO_4)$ (2) Atoms with an "A" are generated by a mirror plane.

ligand (Cu–O(1) distance 1.918(4) Å). This is typical for the trigonal-bipyramidal geometry [25]. The formate anion bridges two copper atoms in a *syn–syn* arrangement [26,27]. The Cu–Cu distance is 3.023(1) Å. The bridging Cu(1)–O(1)–Cu(1A) and Cu(1)–O(2)–Cu(1A) angles are 104.0(3)° and 88.3(2)°, respectively. The dpyam ligands are essentially planar, with only a dihedral angle of 6.9° between the individual pyridine rings. The bite angles of the dpyam ligands (N–Cu–N, 91.4(2)°) are only slightly greater than 90°. The lattice is further stabilized by hydrogen bonding between the amine N and the oxygen atom of bridging formato group with a N···O contact of 2.869 Å. Details of the hydrogen bonding are also listed in Table 3.

3.3. Description of $[Cu_2(dpyam)_2(\mu\text{-}O_2CH)(\mu\text{-}OH)(\mu\text{-}Cl)](ClO_4)\cdot 0.5H_2O$ (3)

The structure of compound **3** consists of symmetric dinuclear $[Cu_2(dpyam)_2(\mu\text{-}O_2CH)(\mu\text{-}OH)(\mu\text{-}Cl)]^+$

Table 3
Selected bond lengths (Å) and angles (°) with e.s.d.s. in parentheses of $[Cu_2(dpyam)_2(\mu\text{-}O_2CH)(\mu\text{-}OH)(\mu\text{-}OMe)](ClO_4)$ (2)

Cu(1)–N(1)		1.961(4)	Cu(1)–O(2)	2.169(5)
Cu(1)–N(2)		2.010(4)	Cu(1)–O(3)	2.175(3)
Cu(1)–O(1)		1.918(4)	Cu(1)–Cu(1A)	3.023(1)
O(1)–Cu(1)–O(2)		81.9(2)	N(1)–Cu(1)–Cu(1A)	138.2(1)
O(1)–Cu(1)–O(3)		88.5(2)	N(1)–Cu(1)–N(2)	91.1(2)
O(1)–Cu(1)–N(1)		174.8(2)	N(2)–Cu(1)–O(2)	133.0(3)
O(1)–Cu(1)–N(2)		93.7(2)	N(2)–Cu(1)–O(3)	135.7(2)
O(1)–Cu(1)–Cu(1A)		38.0(1)	N(2)–Cu(1)–Cu(1A)	125.3(1)
O(2)–Cu(1)–O(3)		91.1(2)	Cu(1)–O(1)–Cu(1A)	104.0(3)
O(2)–Cu(1)–Cu(1A)		45.8(1)	Cu(1)–O(2)–Cu(1A)	88.3(2)
O(3)–Cu(1)–Cu(1A)		79.7(1)	C(11)–O(3)–Cu(1)	126.5(3)
N(1)–Cu(1)–O(2)		95.6(2)	O(3)–C(11)–O(3A)	126.6(6)
N(1)–Cu(1)–O(3)		86.9(2)		
Hydrogen bonds	D–H	H···A	D···A	D–H···A
N(3)–H(5)···O(3)B	0.86	2.12	2.869	146

A, $[-x, y, z]$; B, $[1/2 - x, 1/2 + y, z]$.

cation, a ClO_4^- counter anion and half a molecule of lattice water. This unit is depicted in Fig. 3 together with the used numbering scheme, with selected distances and angles listed in Table 4. In the dinuclear unit, the copper(II) ions are triply bridged through three different ligands, i.e., formate, chloride and hydroxide anions. Each copper(II) center is coordinated by two oxygen atoms and an chloride atom of the triple bridges and two nitrogen atoms of a dpyam ligand, leading to the five-coordinated, distorted trigonal-bipyramidal geometry with CuN_2O_2Cl chromophore ($\tau = 0.67$). The trigonal plane consists of a nitrogen atom of the dpyam ligand (Cu–N(2) distance 2.027(2) Å), a bridging chloro ligand (Cu–Cl(1) distance 2.478(2) Å) and an oxygen atom of the bridging formato ligand (Cu–O(2) distance 2.158(1) Å). The apical coordination sites are occupied by another nitrogen atom of the dpyam ligand (Cu–N(1) distance 1.975(1) Å) and an oxygen atom of the bridging hydroxo group (Cu–O(1) distance 1.916(1) Å). The Cu–Cu distance is 3.036(1) Å. The bridging Cu(1)–O(1)–Cu(1A) and Cu(1)–Cl(1)–Cu(1A) angles are 104.8(1)° and 75.6(1)°, respectively. The dpyam ligands are planar, the dihedral angle between the individual pyridine rings is as low as 6.6°.

The lattice is further stabilized by hydrogen bonding between the amine N and the oxygen atom of bridging formato group with a N···O distance of 2.864 Å; between the oxygen atom of bridging hydroxo group and

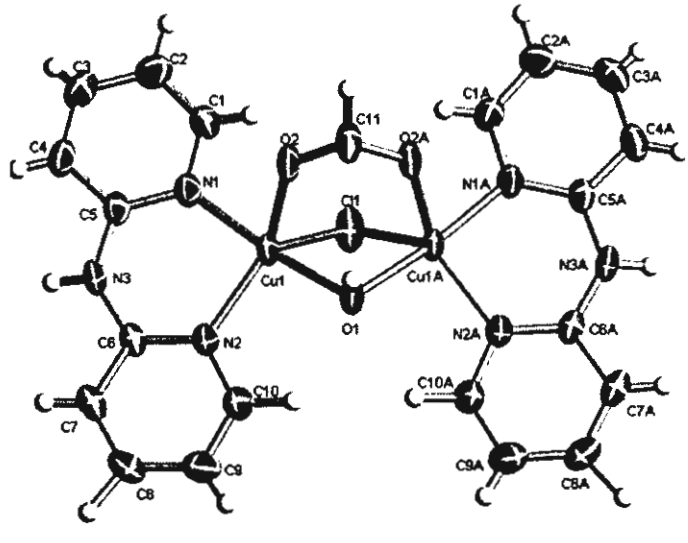

Fig. 3. ORTEP 50% probability plot of the cation in $[Cu_2(dpyam)_2(\mu\text{-}O_2CH)(\mu\text{-}OH)(\mu\text{-}Cl)](ClO_4) \cdot 0.5H_2O$ (3) Atoms with an "A" are generated by a mirror plane.

Table 4
Selected bond lengths (Å) and angles (°) with e.s.d.s. in parentheses of $[Cu_2(dpyam)_2(\mu\text{-}O_2CH)(\mu\text{-}OH)(\mu\text{-}Cl)](ClO_4)\cdot 0.5H_2O$ (3)

Cu(1)–N(1)		1.975(1)	Cu(1)–O(1)	1.916(2)
Cu(1)–N(2)		2.027(2)	Cu(1)–O(2)	2.158(1)
Cu(1)–Cl(1)		2.478(2)	Cu(1)–Cu(1A)	3.036(1)
O(1)–Cu(1)–N(1)		173.8(1)	N(1)–Cu(1)–Cl(1)	96.4(1)
O(1)–Cu(1)–N(2)		94.1(1)	N(1)–Cu(1)–Cu(1A)	138.0(1)
O(1)–Cu(1)–O(2)		88.1(1)	N(2)–Cu(1)–O(2)	133.6(1)
O(1)–Cu(1)–Cl(1)		82.5(1)	N(2)–Cu(1)–Cl(1)	119.1(1)
O(1)–Cu(1)–Cu(1A)		37.6(1)	N(2)–Cu(1)–Cu(1A)	126.3(1)
O(2)–Cu(1)–Cl(1)		107.2(1)	Cu(1)–O(1)–Cu(1A)	104. 8(1)
O(2)–Cu(1)–Cu(1A)		79.4(1)	Cu(1)–Cl(1)–Cu(1A)	75.6(1)
N(1)–Cu(1)–N(2)		91.7(1)	C(11)–O(2)–Cu(1)	126.8(1)
N(1)–Cu(1)–O(2)		86.4(1)	O(2)–C(11)–O(2A)	127.1(3)
Hydrogen bonds	D–H	H···A	D···A	D–H···A
N(3)–H(5)···O(2)B	0.83	2.06	2.864	164
O(1)–H(12)···O(4)C	0.66	2.33	2.922	151

A, $[-x+2, y, z]$; B, $[1/2-x, 1/2+y, z]$; C, $[-x, 1-y, 1/2+z]$.

the oxygen atom of perchlorate molecule with an O···O contact of 2.922 Å. Details of the hydrogen bondings are also listed in Table 4.

3.4. Structure comparison

Compound **1** involves a tetrahedrally distorted square-planar species with CuN_2O_2 chromophore. The Cu_2O_2 network is exactly planar (dihedral angle between CuO_2 and CuO_2, 180.0°), however, the marked tetrahedral twist in the CuN_2O_2 chromophore (dihedral angle between CuN_2 and CuO_2, 21.9°) is less common. Both dihedral angles are compared to those of the other dihydroxo compounds in the literature, as summarized in Table 5. The non-planarity of the CuN_2O_2 group reduces the antiferromagnetic character that causes the J value in this compound to be smaller.

The cationic unit of the compounds **2** and **3** consist of a triply bridged pair of five-coordinated copper(II) ions. Each copper(II) ion is in a distorted trigonal-bipyramidal geometry. The copper(II) orbital ground state for this geometry is based on the orbital d_{z^2} with the z-axis aligned along the axial direction. The d_{z^2} orbitals, one on each copper(II) center, are more favorably positioned to overlap directly in a σ fashion with the hydroxo bridging. So an exchange interaction becomes possible between the unpaired electron via the σ orbital of the hydroxo bridge. The comparable exchange parameters, J, are shown in Table 5.

3.5. IR and electronic spectra

The infrared spectra of compounds **1**, **2** and **3** show a broad band at 3460, 3467 and 3449 cm^{-1}, respectively, which can be assigned to the bridging OH vibrations of the hydroxo bridge and/or lattice water. For compounds **2** and **3**, the spectra also exhibit the broad and intense band at 1570 cm^{-1} correspond to the $\nu_{as}(COO^-)$ vibration and a medium broad band at 1435 and 1434 cm^{-1} correspond to the $\nu_s(COO^-)$ vibration of the didentate bridging coordination mode of the formate group within a dinuclear species. Moreover, the spectra of compounds **2** and **3** exhibit the broad and strong band about 1104–1082 cm^{-1} correspond to the characteristic vibration of non-coordinated ClO_4^- group [28].

The electronic diffuse reflectance spectrum of compound **1** shows a broad band centered at 16 750 cm^{-1}. The relatively low energy of the spectrum may be associated with the slight tetrahedral twist of the CuN_2O_2 chromophore. This observed single broad peak is consistent with the tetrahedrally distorted square planar stereochemistry and assigned to be the d_{z^2}, d_{xy}, d_{xz}, d_{yz}, $\rightarrow d_{x^2-y^2}$ transition. The reflectance spectra of compounds **2** and **3** display a broad band centered at 12 740 and 12 610 cm^{-1}, respectively. These spectra are typical for the distorted trigonal-bipyramidal geometry and the bands are assigned to be the $d_{x^2-y^2}$, d_{xy}, d_{xz}, $d_{yz} \rightarrow d_{z^2}$ transition. A regular trigonal-bipyramidal geometry is usually characterized by an asymmetric broad peak at ≈11 500 cm^{-1} with a possible high-energy shoulder at ≈14 500 cm^{-1}. The principal absorption may be assigned as a $d_{x^2-y^2} \rightarrow d_{z^2}$ transition, with the high-energy shoulder assigned as a $d_{xz} \approx d_{yz} \rightarrow d_{z^2}$ [29,30].

3.6. EPR and magnetic properties

For all three compounds, the X-band EPR spectra (measured on polycrystalline samples at r.t. and 77 K) in all cases are either very weak (some of them show a g_{par} at 2.07) or broad (g_{iso} at 2.11), and no hyperfine is resolved. Therefore, magnetic susceptibility studies were undertaken.

Table 5
Structural and magnetic data for planar dihydroxo-bridged dinuclear copper(II) compounds

Compound[a]	Coordination geometry[b]	Chromophore	CuN_2/CuO_2 (°)	CuO_2/CuO_2 (°)	Axial distance (Å)	Cu–O–Cu (°)	J (cm^{-1})	Reference
Planar dihydroxo-bridged								
$[Cu_2(dpyam)_2(OH)_2]I_2$ (1)	Sq.	CuN_2O_2	21.9	180.0	–	98.5, 98.5	−15.3	this work
$[Cu_2(dpyam)_2(OH)_2(NO_3)_2]$	Spy.	CuN_2O_2O'	16.7, 20.7	173.3	2.400, 2.500	98.9, 99.4	[c]	[35]
$[Cu_2(dpyam)_2(OH)_2Br_2](H_2O)_4$	Spy.	CuN_2O_2Br	21.8, 21.4	179.9	2.803, 2.804	98.1, 100.1	−48.6(5)[f]	[36]
$[Cu_2(dpyam)_2(OH)_2(BF_4)_2]$	Spy.	CuN_2O_2F	24.0	[c]	2.745, 2.745	99.3	[c]	[37]
$[Cu_2(dpyam)_2(OH)_2(ClO_4)_2]$	Oct.	$CuN_2O_2O'_2$	22.6	180.0	2.725,2.725	99.4, 99.4	−37.2/29.3[d]	[38]
$[Cu_2(dpyam)_2(OH)_2(CF_3SO_3)_2]$	Oct.	$CuN_2O_2O'_2$	10.2, 10.0	174.8	2.698, 2.894	100.7, 97.8	82.5(1)/84.7(2)[e]	[36]
$[Cu_2(C_6H_{11}NH_2)_4(OH)_2](ClO_4)_2$	Sq.	CuN_2O_2	[c]	147.5	–	96.6, 99.7	−256	[39]
$[Cu_2(ampym)_4(OH)_2(CF_3SO_3)_2](ampym)_2$	Spy.	CuN_2O_2O'	[c]	[c]	2.503, 2.503	97.96	−7.2	[40]
$[\{Cu(bipy)(PhNHpy)\}_2(OH)_2](PF_6)_2$	Spy.	CuO_2N_2N'	[c]	180.0	2.28, 2.28	98.7	−12.1	[41]
$[Cu_2(dmbipy)_2(OH)_2(CF_3SO_3)_2]$	Oct.	$CuN_2O_2O'_2$	[c]	[c]	2.578, 2.666	94.5	148	[42]
$[Cu_2L_4(OH)_2(ClO_4)_2]$	Oct.	$CuN_2O_2O'_2$	14.7	180.0	2.602, 2.673	99.30	−34.1	[43]

[a] *Abbreviations*: dpyam, di-2-pyridylamine; $C_6H_{11}NH_2$, cyclohexylamine; ampym, 2-aminopyrimidine; bipy, 2,2′-bipyridine; PhNHpy, *N*-phenyl-2-pyridinamine, dmbipy, 4,4′-dimethyl-2,2′-bipyridine; L, 2-amino-4-methylpyrimidine.

[b] Sq., square planar; Spy., square-pyramidal; Oct., octrahedral.

[c] Not reported.

[d] This compound has a crystallographic phase transition. The values correspond with the different temperature ranges.

[e] Depending on the fitting procedure.

[f] No accurate fitting could be performed, as the compound contained a mixture of two species, see [36].

The magnetic susceptibility of a powdered sample of compound **1** was measured from 5 to 280 K. The magnetic property of **1** is depicted in Fig. 4 in the form of μ_{eff} versus T for two Cu(II) ions. At 280 K, the μ_{eff} starts at a value of about $2.43\mu_B$ (this values is close to what is expected for two spin = 1/2 uncoupled centres). Upon cooling, the effective moment of **1** stays almost constant and at about 50 K is started to decrease to reach the value of $1.07\mu_B$ at 5 K. This behaviour is typical for a weak antiferromagnetic interaction.

The theoretical expression for the magnetic susceptibility for two interacting $S = 1/2$ centres, which is based on the general Hamiltonian [2], is: $H_{ex} = -JS_1S_2$, in which the exchange parameter J, is negative for antiferromagnetic and positive for ferromagnetic interaction. The magnetic data were fitted to the equation given in the literature for dinuclear copper compounds [2, p. 132]:

$$\chi_m = (2Ng^2\beta^2)[kT - (2zJ'/(3 + \exp(-J/kT)))]^{-1}$$
$$[3 + \exp(-J/kT)]^{-1}(1 - p) + \chi_p p + \mathrm{TIP},$$

in which N, g, β, k and T have their usual meanings. The parameter p denotes the fraction of paramagnetic impurity in the sample and zJ' the interaction between neighbouring dinuclear identities. A temperature independent paramagnetism (TIP) was also considered and fixed at 60×10^{-6} per copper ion. The fit was accomplished by minimisation of $R = \sum(\chi_m \cdot T_{calc} - \chi_m \cdot T_{obs})^2/(\chi_m \cdot T_{obs})^2$ by least-squares procedure. The best fit was obtained for $J = -15.3$ cm^{-1}, $g = 1.98$, $zJ' = 0.56$ cm^{-1}, $p = 0.06$, with a final R of 4.2×10^{-2} (see Fig. 4). The antiferromagnetic behavior nicely corresponds to the structural data, i.e., with a Cu–O–Cu angle larger than 97.5°.

The magnetic properties of compounds **2** and **3** mutually show a very similar behaviour and are depicted in Figs. 5 and 6, respectively, also in the form of μ_{eff} versus T for two Cu(II) ions. At 280 K, μ_{eff} is $2.56\mu_B$ for compound **2** ($2.78\mu_B$ for compound **3**) which agrees well with the spin-only value of Cu(II) calculated for two uncoupled spin = 1/2 centres. Upon cooling, it raises gradually to reach $2.74\mu_B$ and 2.97 at 30 K, for compounds **2** and **3**, respectively. This is typical for a ferromagnetically coupled Cu(II) dinuclear compound. Below that temperature, μ_{eff} then diminishes till a value of $2.63\mu_B$ at 5 K for compound **2** (2.76 for compound **3**), which may originate from intermolecular antiferromagnetic interactions, or from zero-field splitting of the $S = 1$ state of the dinuclear species.

The best fit was obtained for compound **2** with the following values: $J = 62.5$ cm^{-1}, $g = 1.99$, $zJ' = -3.80$ cm^{-1}, $p = 0.06$, with a final R of 1.4×10^{-3} (see Fig. 5). For compound **3**, these values are $J = 79.1$ cm^{-1},

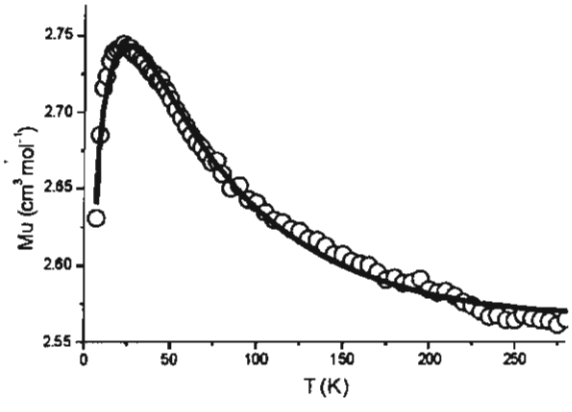

Fig. 5. A plot of the temperature dependence of μ_{eff} vs. T for compound (**2**). The solid line represents the calculated curve for the parameters $J = 62.5$ cm^{-1}, $g = 1.99$, $zJ' = -3.80$ cm^{-1} (see text).

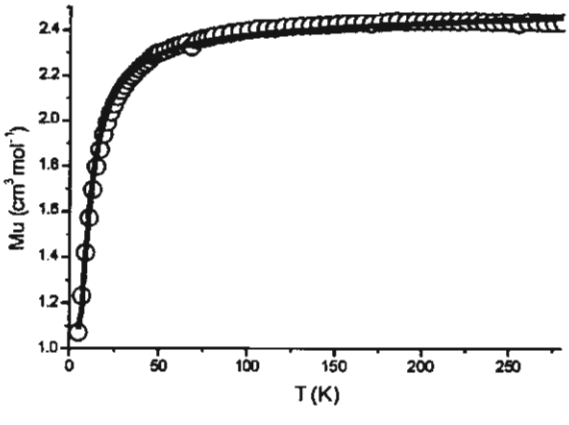

Fig. 4. A plot of the temperature dependence of μ_{eff} vs. T for compound (**1**). The solid line represents the calculated curve for the parameters $J = -15.3$ cm^{-1}, $g = 1.98$, $zJ' = 0.56$ cm^{-1} (see text).

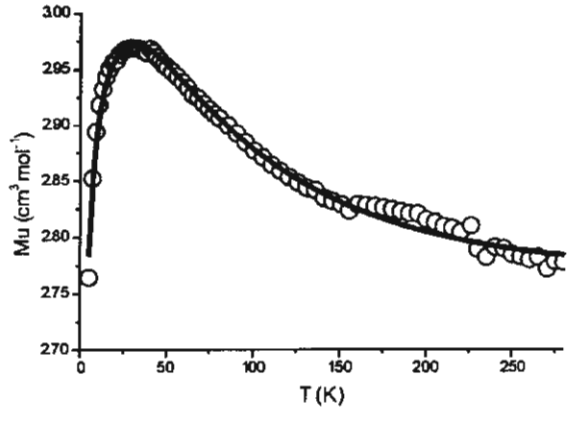

Fig. 6. A plot of the temperature dependence of μ_{eff} vs. T for compound (**3**). The solid line represents the calculated curve for the parameters $J = 79.1$ cm^{-1}, $g = 2.14$, $zJ' = -4.27$ cm^{-1} (see text).

Table 6
Structural and magnetic data for singly and triply bridged dinuclear copper(II) compounds

Compound[a]	Coordination geometry[b]	τ	Chromophore	μ-OH position[c]	Cu–OH–Cu (°)	J (cm^{-1})	Reference
Triply bridged							
$[Cu_2(dpyam)_2(O_2CH)(OH)(OMe)](ClO_4)$ (2)	Dist. TBP	0.65	CuN_2O_3	Axial/Axial	88.6, 104.5	62.5	this work
$[Cu_2(dpyam)_2(O_2CH)(OH)(Cl)](ClO_4)\cdot 0.5H_2O$ (3)	Dist. TBP	0.67	CuN_2O_2Cl	Axial/Axial	104.8	79.1	this work
$[Cu_2(bpy)_2(\mu\text{-}O_2CCH_3)_3](ClO_4)$	Dist. Spy., Intermediate	0.14[e], 0.47[e]	CuN_2O_3, CuN_2O_3	–	–	3.6	[34]
$[Cu_2(bpy)_2(OH)(H_2O)(O_2CCH_3)](ClO_4)_2$	Dist. Spy.	0.14, 0.25[e]	CuN_2O_3	Eq./Eq	78.7, 103.8	19.3	[34]
$[Cu_2(EtBITP)(OH)Cl_3]\cdot DMF$	Dist. TBP	0.58, 0.55[e]	CuN_2Cl_2O	Axial/Axial	104.7	−260	[44]
$[Cu_2(PTP)(OH)Cl_3]\cdot 2CH_3CN$	Intermediate	0.51	CuN_2Cl_2O	–	106.2	−296	[45]
$[Cu_2(PAP)(OH)(IO_3)_3]\cdot 4H_2O$	Dist. Spy.[d]	0.40[d]	CuN_2O_3	Axial/Axial	113.8	−283	[45–47]
$[Cu_2(PAP)(OH)Cl(SO_4)]\cdot 2H_2O$	Dist. Spy.	0.35, 0.37[e]	CuN_2O_3	Eq./Eq	115.5	−532	[48]
Singly bridged							
$[Cu_2(bpy)_2(OH)](ClO_4)_3$	Dist. TBP	0.32, 0.71[e]	CuN_4O	Eq./Eq.	141.6	−322	[31]
$[Cu_2(LL)(OH)](BF_4)_3$	Dist. Sq.	0.13[e]	CuS_2ON	Eq./Eq.	132.2	−820	[48,49]

[a] *Abbreviations*: dpyam, di-2-pyridylamine; bpy, 2,2′-bipyridine; EtBITP, 3,6-bis(2-benzimidazolylthio)pyridazine; PTP, 3,6-bis(2-pyridylthio)phthalazine; PAP, 1,4-bis-(2-pyrodyl amino)phthalazine); LL, 1,4-bis((1-oxa-4,10-dithia-7-azacyclododecan-7-yl)methyl)benzene).
[b] Dist. TBP, distorted trigonal-bipyramidal, Dist. Spy., distorted square-pyramidal.
[c] Eq., equatorial.
[d] Average trigonality (τ_{av}). According to the τ value of 0.40, the preferred geometry should be intermediate towards distorted square-pyramidal.
[e] Calculated from the known structural parameters.

$g = 2.14$, $zJ' = -4.27$ cm^{-1}, $p = 0.025$, with a final R of 1.6×10^{-3} (see Fig. 6).

These J values do not correspond to the values expected from the correlation of J and Cu–O–Cu angle for dihydroxo-bridged species. Two origins are to be held responsible for this. The copper(II) ions in both compounds have a five-coordinate trigonal-bipyramidal geometry with the d_{z^2} ground state, whereas the dihydroxo-bridged copper(II) complexes are square-pyramidal with $d_{x^2-y^2}$ ground state. A change in electron density of the magnetic orbital can have a pronounced effect on the sign and magnitude of a magnetic exchange interaction [31,32]. In this case, for both complexes, a single pathway via (Cu–OH–Cu) is possible for the electron delocalization via the d_{z^2} magnetic orbitals, corresponding to the weak, or intermediately strong, ferromagnetic interaction. Secondly, also the formato bridge plays a role in the magnetic interaction, a fact already described earlier in the literature as a so-called "countercomplementary effect" [2,34,50–52].

The obvious explanation for the single hydroxo-bridged and triply bridged dinuclear copper(II) complexes lies in the fact that the most complexes have an intermediate geometry between the square-pyramidal and trigonal-bipyramidal extremes [31–33,44–49]. It should be noted that when the copper(II) geometry is close to regular square-pyramidal, an often strong antiferromagnetic interaction will be predominant, but a reduction of an antiferromagnetic contribution will be observed when the geometry becomes closer to trigonal-bipyramidal (see Table 6).

It is somewhat surprising that compounds **2** and **3** exhibit a moderately strong ferromagnetic interaction which may originate from the triply bridged nature of both compounds. So far only a few closely related structures in the triply bridged copper(II) compounds have reported ferromagnetic properties, examples being $[Cu_2(bpy)_2(\mu\text{-}O_2CCH_3)_3](ClO_4)_2$ and $[Cu_2(bpy)_2(\mu\text{-}OH)(\text{-}OH_2)(\mu\text{-}O_2CCH_3)](ClO_4)_2$ with $J = 3.6$ and 19.3 cm^{-1}, respectively [34]. The comparison of the trigonality, the parameter τ, and exchange parameter, J, are summarized in Table 6.

4. Conclusions

The structure of the dihydroxo-bridged compound **1** displays a strictly planar Cu_2O_2 network of copper(II) dinuclear species. Each copper(II) ion is in a tetrahedrally distorted square planar geometry with the unpaired electron occupying the $d_{x^2-y^2}$ orbital. However, the value of singlet–triplet energy gap ($J = -15.3$ cm^{-1}) is noticeably smaller than the value calculated from the correlation of Hatfield and Hodgson for the hydroxo-bridged compounds for a bridging angle of 98.5(2)° ($J = -71$ cm^{-1}). Such a deviation is not uncommon (see Table 5) and the tetrahedral distortion is to be held responsible for this significant deviation of the magnetic behaviour.

Compounds **2** and **3** contain a triply bridged dinuclear copper(II) unit both with a hydroxo and a formato bridge. The coordination geometry around each cop-

per(II) ion is slightly distorted trigonal-bipyramidal. A strong magnetic interaction requires both good σ orientation of the magnetic orbitals and good superexchange properties of the bridging atom(s) [2,52]. The magnetic orbital is d_{z^2} for both copper(II) centers with lobes directed toward the bridging hydroxo ligand, but also the formato bridge cannot be excluded as a countercomplementary effect. Further it must be kept in mind that both compounds have a third bridging molecule, i.e., a methoxo group and chloride for compounds **2** and **3**, respectively. Therefore, the "overall" effect is in this case a moderate ferromagnetic exchange.

5. Supplementary material

Crystallographic data (excluding structure factors) for the structures in this paper have been deposited with the Cambridge Crystallographic Data Centre as supplementary publication no. CCDC-219202-04 for structures **1**, **2** and **3**, respectively. Copies of the data can be obtained free of charge on application to CCDC, 12 Union Road, Cambridge CB2 1EZ, UK [fax: (internat.) +44(1223)336-033, e-mail: deposit@ccdc.cam.ac.uk].

Acknowledgements

The authors thank The Thailand Research Fund and Khon Kaen University for research grant. Support of the Postgraduate Education and Research Program in Chemistry is also gratefully acknowledged. The work described in the present paper has been supported by the Leiden University Study group WFMO (Werkgroep Fundamenteel Materialen Onderzoek). Support of the NRSC Catalysis (a Research School Combination of HRSMC and NIOK) is kindly acknowledged.

References

[1] O. Kahn, Y. Pei, Y. Journaux, in: Q.W. Bruce, D.D. O'Hare (Eds.), Inorganic Materials, Wiley, Chichester, UK, 1992.
[2] O. Kahn, Molecular Magnetism, VCH Publishers, New York, 1993.
[3] V.H. Crawford, H.W. Richardson, J.R. Wasson, D.J. Hodgson, W.E. Hatfield, Inorg. Chem. 15 (1976) 2107.
[4] J.A. Barnes, D.J. Hodgson, W.E. Hatfield, Inorg. Chem. 11 (1972) 144.
[5] P.J. Hay, J.C. Thibeault, R. Hoffmann, J. Am. Chem. Soc. 97 (1975) 4884.
[6] A. Bencini, D. Gatteschi, Inorg. Chim. Acta 31 (1978) 11.
[7] L. Banci, A. Bencini, D. Gatteschi, J. Am. Chem. Soc. 105 (1983) 761.
[8] O. Kahn, M.F. Charlot, Inorg. Chem. 19 (1980) 1410.
[9] E. Ruiz, P. Alemany, S. Alvarez, J. Cano, Inorg. Chem. 36 (1997) 3683.
[10] E. Ruiz, P. Alemany, S. Alvarez, J. Cano, J. Am. Chem. Soc. 119 (1997) 1297.
[11] B. Graham, M.T.W. Hearn, P.C. Junk, C.M. Kepert, F.E. Mabbs, B. Moubaraki, K.S. Murray, L. Spiccia, Inorg. Chem. 40 (2001) 1536.
[12] A. Yatani, M. Fujii, Y. Nakao, S. Kashino, M. Kinoshita, W. Mori, S. Suzuki, Inorg. Chim. Acta 316 (2001) 127.
[13] T.M. Rajendiran, R. Kannappan, R. Venkatesan, P.S. Rao, M. Kandaswamy, Polyhedron 18 (1999) 3085.
[14] S.P. Perlepes, J.C. Huffman, G. Christou, Polyhedron 10 (1991) 2301.
[15] V. McKee, M. Zvagulis, C.A. Reed, Inorg. Chem. 24 (1985) 2914.
[16] W.B. Tolman, R.L. Rardin, S.J. Lippard, J. Am. Chem. Soc. 111 (1989) 4532.
[17] B. Żurowska, J. Mroziński, Inorg. Chim. Acta 342 (2003) 23.
[18] A. Neels, H. Stoeckli-Evans, A. Escuer, R. Vicente, Inorg. Chim. Acta 260 (1997) 189.
[19] M. Julve, M. Verdaguer, A. Gleizes, M. Philoche-Levisalles, O. Kahn, Inorg. Chem. 23 (1984) 3808.
[20] Siemens, SAINT, Version 4 Software Reference Manual, Siemens Analytical X-Ray Systems, Inc., Madison, WI, USA, 1996.
[21] G.M. Sheldrick, SADABS, Program for Empirical Absorption correction of Area Dectector Data, University of Göttingen, Göttingen, Germany, 1996.
[22] Bruker, XSHELL, Version 6.12, Reference Manual, Bruker AXS, Inc., Madison, WI, USA, 1999.
[23] A.W. Addison, T.N. Rao, J. Reedijk, J. van Rijn, G.C. Verschoor, J. Chem. Soc., Dalton Trans. (1984) 1349.
[24] M. Brophy, G. Murphy, C. O'Sullivan, B. Hathaway, B. Murphy, Polyhedron 18 (1999) 611.
[25] G. Murphy, P. Nagle, B. Murphy, B. Hathaway, J. Chem. Soc., Dalton Trans. (1997) 2645.
[26] D.K. Towle, S.K. Hoffmann, W.E. Hatfield, P. Singh, P. Chaudhuri, Inorg. Chem. 27 (1988) 394.
[27] W.A. Wojtczak, M.J. Hampden-Smith, E.N. Duesler, Inorg. Chem. 37 (1998) 1781.
[28] V.H. Crawford, H.W. Richardson, J.R. Wasson, D.J. Hodgson, W.E. Hatfield, Inorg. Chem. 15 (1976) 2107.
[29] G. Murphy, C. Murphy, B. Murphy, B. Hathaway, J. Chem. Soc., Dalton Trans. (1997) 2653.
[30] G. Murphy, C. O'Sullivan, B. Murphy, B. Hathaway, Inorg. Chem. 37 (1998) 240.
[31] M.S. Haddad, S.R. Wilson, D.J. Hodgson, D.N. Hendrickson, J. Am. Chem. Soc. 103 (1981) 384.
[32] M.S. Haddad, D.N. Hendrickson, Inorg. Chim. Acta 28 (1978) L121.
[33] T.R. Felthouse, E.J. Laskowski, D.N. Hendrickson, Inorg. Chem. 16 (1977) 1077.
[34] G. Christou, S.P. Perlepes, E. Libby, K. Folting, J.C. Huffman, R.J. Webb, D.N. Hendrickson, Inorg. Chem. 29 (1990) 3657.
[35] S. Youngme, W. Somjitsripunya, K. Chinnakali, S. Chantrapromma, H.K. Fun, Polyhedron 18 (1999) 857.
[36] S. Youngme, G.A. van Albada, O. Roubeau, C. Pakawatchai, N. Chaichit, J. Reedijk, Inorg. Chim. Acta 342 (2003) 48.
[37] L.-P. Wu, M.E. Keniry, B.J. Hathaway, Acta Crystallogr., Sect. C 48 (1992) 35.
[38] S. Youngme, G.A. van Albada, H. Kooijman, O. Roubeau, W. Somjitsripunya, A.L. Spek, C. Pakawatchai, J. Reedijk, Eur. J. Inorg. Chem. (2002) 2367.
[39] M.F. Charlot, S. Jeannin, Y. Jeannin, O. Kahn, J. Lucrece-Abaul, J. Martin-Frere, Inorg. Chem. 18 (1979) 1675.
[40] G.A. van Albada, I. Mutikainen, W.J.J. Smeets, A.L. Spek, U. Turpeinen, J. Reedijk, Inorg. Chim. Acta 327 (2002) 134.
[41] J.M. Seco, U. Amador, M.J. González Garmendia, Polyhedron 18 (1999) 3605.
[42] G.A. van Albada, I. Mutikainen, U. Turpeinen, J. Reedijk, Inorg. Chim. Acta 324 (2001) 273.
[43] S. Amani Komaei, G.A. van Albada, J.G. Haasnoot, H. Kooijman, A.L. Spek, J. Reedijk, Inorg. Chim. Acta 286 (1999) 24.

[44] L.K. Thompson, S.K. Mandal, L. Rosenberg, Inorg. Chim. Acta 133 (1987) 81.
[45] L. Chen, L.K. Thompson, J.N. Bridson, Inorg. Chim. Acta 244 (1996) 87.
[46] L.K. Thompson, F.L. Lee, E.J. Gabe, Inorg. Chem. 27 (1988) 39.
[47] L.K. Thompson, Can. J. Chem. 61 (1983) 579.
[48] L.K. Thompson, A.W. Hanson, B.S. Ramaswamy, Inorg. Chem. 23 (1984) 2459.
[49] P.L. Burk, J.A. Osborn, M.T. Youinou, J. Am. Chem. Soc. 103 (1981) 1273.
[50] Y. Nishida, S. Kida, J. Chem. Soc., Dalton Trans. (1986) 2633.
[51] V. McKee, M. Zvagulis, C.A. Reed, Inorg. Chem. 24 (1985) 2914.
[52] V. McKee, M. Zvagulis, J.V. Dagdigian, M.G. Patch, C.A. Reed, J. Am. Chem. Soc. 106 (1984) 4765.

Available online at www.sciencedirect.com
SCIENCE DIRECT®
Inorganica Chimica Acta 358 (2005) 1068–1078
Inorganica Chimica Acta
www.elsevier.com/locate/ica

Dinuclear triply-bridged copper(II) compounds containing carboxylato bridges and di-2-pyridylamine as a ligand: synthesis, crystal structure, spectroscopic and magnetic properties

Sujittra Youngme [a,*], Chatkaew Chailuecha [a], Gerard A. van Albada [b], Chaveng Pakawatchai [c], Narongsak Chaichit [d], Jan Reedijk [b]

[a] Department of Chemistry, Faculty of science, Khon Kaen University, Khon Kaen 40002, Thailand
[b] Gorlaeus Laboratories, Leiden Institute of Chemistry, Leiden University, P.O. Box 9502, 2300 RA Leiden, The Netherlands
[c] Department of Chemistry, Faculty of Science, Prince of Songkla University, Hatyai, Songkla 90112, Thailand
[d] Department of Physics, Faculty of Science and Technology, Thammasat University Rangsit, Pathumthani 12121, Thailand

Received 26 August 2004; accepted 10 November 2004
Available online 7 February 2005

Abstract

Three new triply-bridged dinuclear copper(II) compounds with carboxylato bridges, $[Cu_2(\mu\text{-}O_2CH)(\mu\text{-}OH)(\mu\text{-}Cl)(dpyam)_2](PF_6)$ **(1)**, $[Cu_2(\mu\text{-}O_2CH)_2(\mu\text{-}OH)(dpyam)_2](PF_6)$ **(2)** and $[Cu_2(\mu\text{-}O_2CCH_2CH_3)_2(\mu\text{-}OH)(dpyam)_2](ClO_4)$ **(3)** (dpyam = di-2-pyridylamine) have been synthesized and characterized crystallographically and spectroscopically. Compound **1** consists of a dinuclear unit in which both copper(II) ions are bridged by three different ligands, i.e., formate, chloride and hydroxide anions, providing a distorted trigonal bipyramidal geometry with a CuN_2O_2Cl chromophore. Compounds **2** and **3** have two bridging formato ligands and two bridging propionato ligands, respectively, together with a hydroxo bridge. The carboxylato ligands in both compounds **2** and **3** exhibit different coordination modes. One is in a syn, syn $\eta^1{:}\eta^1{:}\mu_2$ bridging mode and the other is in a monoatomic bridging mode. The structure of compound **2** involves a dinuclear unit, with a distorted trigonal bipyramidal geometry around each Cu(II) ion with a CuN_2O_3 chromophore. Compound **3** contains a non-centrosymmetric unit; the coordination environment around Cu(1) is a distorted square–pyramidal geometry and an intermediate geometry of sp and tbp around the Cu(II) ion. The Cu···Cu separations are 3.061, 3.113 and 3.006 Å for compounds **1**, **2** and **3**, respectively. The EPR spectra of all three compounds show a broad isotropic signal with a g value around 2.10.

The magnetic susceptibility measurements, measured from 5 to 280 K, revealed a moderate ferromagnetic interaction between the Cu(II) ions with a singlet–triplet energy gap (J) of 79.7, 47.8 and 24.1 cm^{-1}, for compounds **1**, **2** and **3**, respectively. Also a very weak intermolecular antiferromagnetic interaction was observed between the dinuclear units.

Keywords: Copper carboxylate complexes; Copper(II) complexes; Crystal structures; EPR spectra; Magnetic properties; Triply-bridged dinuclear copper(II) complexes; Carboxylato-bridged

1. Introduction

Triply-bridged dinuclear copper(II) compounds with one or more carboxylate moieties have recently received considerable attention [1–9], due to the various possible super-exchange pathways between coupled copper(II) centers. The magnetic exchange interactions are depending on the coordination geometry around the copper(II) centers. Structurally, the triply-bridged dinuclear copper(II) carboxylato compounds with didentate chelating ligands and a five coordination of the Cu(II) ion, show

* Corresponding author. Tel.: +664320222241; fax : +6643202373.
E-mail address: sujittra@kku.ac.th (S. Youngme).

0020-1693/$ - see front matter © 2004 Elsevier B.V. All rights reserved.
doi:10.1016/j.ica.2004.11.019

an extensive range of compounds with a distortion between regular trigonal bipyramidal and regular square-based pyramidal. This feature can be useful for understanding the relationships between structural features and the value of the intramolecular magnetic exchange interaction in the dinuclear unit.

With the ligand 2,2′-bipyridine (abbreviated as bpy) a number of carboxylated triply-bridged dinuclear copper(II) compounds, $[Cu_2(\mu\text{-}O_2CCH_3)_3(bpy)_2](ClO_4)$ [1]; $[Cu_2(\mu\text{-}O_2CCH_3)(\mu\text{-}OH)(\mu\text{-}OH_2)(bpy)_2](ClO_4)_2$ [1]; $[Cu_2(\mu\text{-}O_2CCH_3)(\mu\text{-}OH)(\mu\text{-}Cl)(bpy)_2](ClO_4)\cdot H_2O$ [2]; $[Cu_2(\mu\text{-}O_2CCH_3)_2(\mu\text{-}OEt)(bpy)_2](PF_6)$ [3] and $[Cu_2(\mu\text{-}O_2CCH_3)_2(\mu\text{-}OMe)(bpy)_2](PF_6)$ [3] have been reported in the literature [1–3]. These compounds exhibit many types of bridging conformations of the carboxylato molecule and various geometries of the Cu(II) ions. However, compounds with formate and propionate as bridging molecules, in contrary to acetate bridges, have rarely been reported for bpy and related ligands. To obtain more insight into the geometries displayed by the Cu(II) ion in connection with the magnetic properties we now use the ligand dpyam (dpyam = di-2-pyridylamine).

In this study three new triply-bridged dinuclear copper(II) compounds with hydroxo, formato and propionato bridges, $[Cu_2(\mu\text{-}O_2CH)(\mu\text{-}OH)(\mu\text{-}Cl)(dpyam)_2](PF_6)$ **(1)**, $[Cu_2(\mu\text{-}O_2CH)_2(\mu\text{-}OH)(dpyam)_2](PF_6)$ **(2)** and $[Cu_2(\mu\text{-}O_2CCH_2CH_3)_2(\mu\text{-}OH)(dpyam)_2](ClO_4)$ **(3)** have been synthesized and characterized by X-ray crystallography, IR, EPR and electronic spectra. Also the magnetic susceptibility has been investigated and will be discussed in comparison with other relevant compounds.

2. Experimental

2.1. General

The ligand di-2-pyridylamine and all reagents are commercial grade materials and were used without further purification. Elemental analyses (C, H, N) were determined on a Perkin-Elmer PE 2400 CHNS Analyzer by Microanalytical Service of Science and Technological Research Equipment Center, Chulalongkorn University.

IR spectra were recorded on a Perkin–Elmer Spectrum One FT-IR spectrophotometer as KBr disc in the 4000–450 cm^{-1} spectral range. Solid-state (diffuse reflectance) electronic spectra were measured as polycrystalline samples on a Perkin–Elmer Lambda2S spectrophotometer, within the range 8000–18000 cm^{-1}. The X-band powder EPR spectra were obtained on polycrystalline samples at room temperature and 77 K with a JEOL RE2X electron spin resonance spectrometer with DPPH ($g = 2.0036$) as a reference. Magnetic susceptibility measurements (5–280 K) were carried out using a Quantum design MPMS-5 5T SQUID magnetometer (measurements carried out at 1000 Gauss) performed at Leiden University. Data were corrected for magnetization of the sample holder and for diamagnetic contributions, which were estimated from the Pascal constants.

2.2. Syntheses of the compounds

2.2.1. $[Cu_2(\mu\text{-}O_2CH)(\mu\text{-}OH)(\mu\text{-}Cl)(dpyam)_2](PF_6)$ (1)

A hot DMF solution (10 ml) of dpyam (0.171 g, 1.0 mmol) was added to a hot DMF solution (10 ml) of $CuCl_2\cdot 2H_2O$ (0.171 g, 1.0 mmol). Then solid HCOONa (0.136 g, 2.0 mmol) was added to the mixture yielding a brown solution. Its color became green by addition of an aqueous solution (5 ml) of KPF_6 (0.184 g, 1.0 mmol). After a month, green polygon-shape crystals of compound **1** were obtained which were filtered off, washed with the mother liquid and air-dried. *Anal.* Calc. for $C_{21}H_{20}ClCu_2F_6N_6O_3P$: C, 35.4; H, 2.8; N, 11.8. Found: C, 35.5; H, 2.5; N, 11.6%.

2.2.2. $Cu_2(\mu\text{-}O_2CH)_2(\mu\text{-}OH)(dpyam)_2](PF_6)$ (2)

This compound was prepared by adding a hot DMSO solution (5 ml) of dpyam (0.171 g, 1.0 mmol), to a hot aqueous solution (10 ml) of $Cu(COOH)_2$ (0.154 g, 1.0 mmol), after which a hot methanol solution (10 ml) of KPF_6 (0.184 g, 1.0 mmol) was added. The resulting green solution was allowed to evaporate at room temperature. After two weeks, needle green crystals of compound **2** were obtained which were filtered off, washed with the mother liquid and air-dried. *Anal.* Calc. for $C_{22}H_{21}Cu_2F_6N_6O_5P$: C, 36.6; H, 2.9; N, 11.7. Found: C 36.1; H 2.6; N, 11.8%.

2.2.3. $[Cu_2(dpyam)_2(\mu\text{-}O_2CCH_2CH_3)_2(\mu\text{-}OH)](ClO_4)$ (3)

Compound **3** was prepared by adding an aqueous solution (10 ml) of $Cu(ClO_4)_2\cdot 6H_2O$ (0.370 g, 1.0 mmol) to a solution of dpyam (0.171 g, 1.0 mmol) in acetone (10 ml), then a solution of CH_3CH_2COONa (0.384 g, 4.0 mmol) in ethanol (10 ml) was added, yielding a bluish-green solution. The solution was allowed to evaporate at room temperature. After a week, bluish-green hexagon crystals of compound **3** were formed. They were filtered off, washed with mother liquid and air-dried. *Anal.* Calc. for $C_{26}H_{29}ClCu_2N_6O_9$: C, 42.7; H, 4.0; N, 11.5. Found: C, 42.4; H, 4.1; N, 11.3%.

2.3. Crystallography

The X-ray single-crystal data were collected at 293 K for compounds **1** and **2** and 100 K for compound **3** on a 4 K Bruker SMART APEX CCD area-detector

diffractometer (rotating anode, graphite-monochromated Mo Kα radiation, $\lambda = 0.71073$ Å) using SMART program [10]. Raw data frame integration was performed with SAINT [11], which also applied correction for Lorentz and polarization effects. An empirical absorption correction by using the SADABS [12] program was applied, which resulted in transmission coefficients ranging from 1.000 to 0.733 for **1**, 1.000 to 0.800 for **2**, 1.000 to 0.801 for **3**.

The structures were solved by direct methods and refined by full matrix least-squares method on $(F_{obs})^2$ with anisotropic thermal parameters for all non-hydrogen atoms except disordered F atoms of the PF_6^- groups in **1** using the SHELXTL-PC v 6.12 software package. For the structure determination of compound **1** and **2**, the two F atoms of each PF_6^- group showed disorder; the occupancies of the disordered positions were initially refined and later fixed at 0.49 and 0.51 for compound **1** and 0.47 and 0.53 for compound **2**. Furthermore, for compound **2**, one O atom of a formato group is also disordered and refined with site occupancies of 0.5. Three O atoms of the ClO_4^- anion in compound **3** found also to be disordered and were refined into two sets with occupancies of 0.49 and 0.51. All hydrogen atoms in **1**, **2** and **3** were located geometrically and refined isotropically, except for nine H atoms of the dpyam ligand in **2** which were fixed and allowed to ride on the attached atoms. The molecular structure pictures were created by using SHELXTL-PC package [13]. The crystal and refinement details for compounds **1**, **2** and **3** are listed in Table 1.

3. Results and discussion

3.1. Synthesis

Reaction of $CuCl_2 \cdot 2H_2O$ with one equivalent of dpyam in DMF/H_2O followed by addition of HCOONa and KPF_6 led to the very rare example of a triply-bridged dinuclear copper(II) complexes, $[Cu_2(O_2CH)(OH)Cl(dpyam)_2](PF_6)$ **(1)** containing three different anionic bridging ligands. Its formation can be summarized in Eq. (1).

$$2CuCl \cdot 2H_2O + 2dpyam + HCO_2^- + PF_6^- \xrightarrow{DMF/H_2O} [Cu_2(O_2CH)(OH)Cl(dpyam)_2](PF_6) + 3Cl^- + H^+ \quad (1)$$

Treatment of $Cu(O_2CH)_2$ in water with one equivalent of dpyam in DMSO followed by addition of KPF_6 in MeOH (Eq. (2)) gave a clear green solution, from which pure, highly crystalline $[Cu_2(O_2CH)_2(OH)(dpyam)_2](PF_6)$ **(2)** can be obtained.

$$2Cu(O_2CH)_2 + 2dpyam + PF_6^- \xrightarrow{DMSO/H_2O/MeOH} [Cu_2(O_2CH)_2(OH)(dpyam)_2](PF_6) + 2HCO_2^- + H^+ \quad (2)$$

In a similar fashion, treatment of $Cu(ClO_4)_2 \cdot 6H_2O$ in water with one equivalent of dpyam in acetone and CH_3CH_2COONa in EtOH led to the triply-bridged dinuclear complex $[Cu_2(O_2CCH_2CH_3)(OH)(dpyam)_2](ClO_4)$ **(3)**. The reaction stoichiometry is presented in Eq. (3).

Table 1
Crystal and refinement data for complexes **1**, **2** and **3**

Complex	1	2	3
Molecular formula	$[Cu_2(\mu\text{-}O_2CH)(\mu\text{-}OH)(\mu\text{-}Cl)(dpyam)_2](PF_6)$	$[Cu_2(\mu\text{-}O_2CH)_2(\mu\text{-}OH)(dpyam)_2](PF_6)$	$[Cu_2(\mu\text{-}O_2CCH_2CH_3)_2(\mu\text{-}OH)(dpyam)_2](ClO_4)$
Molecular weight	711.94	721.50	732.08
T (K)	293(2)	293(2)	100(2)
Crystal system	orthorhombic	orthorhombic	monoclinic
Space group	$Cmc2_1$	$Cmc2_1$	$P2_1/c$
a (Å)	16.8665(1)	17.011(4)	11.0890(7)
b (Å)	7.829	8.031(2)	16.7467(11)
c (Å)	19.4941(1)	19.258(5)	16.1864(10)
β (°)	90	90	107.7110(10)
V (Å^3)	2574.22(2)	2631.1(11)	2863.4(3)
Z	4	4	4
D_c (g cm^3)	1.837	1.821	1.698
μ (mm^{-1})	1.900	1.767	1.644
F(0 0 0)	1424	1448	1496
Crystal size (mm)	0.13 × 0.28 × 0.33	0.25 × 0.12 × 0.05	0.26 × 0.20 × 0.09
Number of reflection collected	9380	11 030	16 907
Number of unique reflections (R_{int})	3725 (0.0224)	3180 (0.0355)	6660 (0.0380)
Data/restraints/parameter	3725/1/234	3180/1/234	6660/0/541
Goodness-of-fit	1.033	1.022	1.039
Final R indices [$I > 2\sigma(I)$]	$R_1 = 0.0387$, $wR_2 = 0.1073$	$R_1 = 0.0515$, $wR_2 = 0.1194$	$R_1 = 0.0440$, $wR_2 = 0.0857$
R indices (all data)	$R_1 = 0.0441$, $wR_2 = 0.1115$	$R_1 = 0.0699$, $wR_2 = 0.1296$	$R_1 = 0.0618$, $wR_2 = 0.0916$
Largest differential peak and hole (e Å^3)	0.651 and −0.672	0.669 and −0.468	0.519 and −0.464

$$2Cu(ClO_4)_2\cdot 6H_2O + 2dpyam + 2CH_3CH_2CO_2^- \xrightarrow{EtOH/H_2O/acetone} [Cu_2(O_2CCH_2CH_3)_2(OH)(dpyam)_2](PF_6) + 3ClO_4^- + H^+ \quad (3)$$

3.2. Description of structures

3.2.1. Description of $[Cu_2(\mu\text{-}O_2CH)(\mu\text{-}OH)(\mu\text{-}Cl)(dpyam)_2](PF_6)$ (1)

The structure of compound **1** consists of a dinuclear $[Cu_2(\mu\text{-}O_2CH)(\mu\text{-}OH)(\mu\text{-}Cl)(dpyam)_2]^+$ cation and a disordered PF_6^- counteranion. This unit is depicted in Fig. 1 together with the numbering scheme. Selected distances and angles are listed in Table 2. Each copper(II) ion has a distorted trigonal bipyramidal geometry ($\tau = 0.72$, the structure index is defined as $\tau = (\beta - \alpha)/60$, where β and are the largest coordination angles, $\tau = 0$ for square pyramidal (SP) and $\tau = 1$ for trigonal bipyramidal (TBP) geometry) [14], of the CuN_2O_2Cl chromophore, with a nitrogen atom of the dpyam ligand (Cu(1)–N(1) 2.031(3) Å), an oxygen atom of the bridging formato ligand (Cu(1)–O(1) 2.183(2) Å) and a bridging chloro ligand (Cu(1)–Cl(1) 2.451(1) Å) forming the trigonal plane. The axial site of each copper(II) atom is occupied by another nitrogen atom of the dpyam ligand (Cu(1)–N(2) 1.983(2) Å) and an oxygen atom of the hydroxo ligand (Cu(1)–O(2) 1.918(2) Å), which are shorter than those of the equatorial plane corresponding to the typical environment of the trigonal bipyramidal geometry [15]. The symmetric syn,syn-coordinated formato ligand bridges the two equatorial planes, giving a Cu···Cu distance of 3.061(5) Å. The dihedral angle between the equatorial planes is 86.8°. The bridging angles (Cu(1)–O(2)–Cu(1)A and Cu(1)–Cl(1)–Cu(1)A are 105.9(1) and 77.2(1)°, respectively. The dpyam ligands are essentially planar, with only a dihedral angle of 4.4° between the individual pyridine rings.

The crystal lattice is stabilized by hydrogen bonding between the amine N and the oxygen atom of bridging formato group with a N···O distance 2.860(3) Å and between the oxygen atom of bridging hydroxo group and the fluoride atom of PF_6^- anion with O···F contact of 2.954(7) Å. Details of the hydrogen bonding are listed in Table 2.

3.2.2. Description of $[Cu_2(\mu\text{-}O_2CH)_2(\mu\text{-}OH)(dpyam)_2](PF_6)$ (2)

Compound **2** is made up of one-half $[Cu(\mu\text{-}O_2CH)_2(\mu\text{-}OH)(dpyam)]^+$ moiety, which the other half being symmetry related via a mirror plane and a disordered PF_6^- anion. This unit is depicted in Fig. 2 together with the numbering scheme. Selected distances and angles are listed in Table 3. The formato ligands, one of which is in a disordered position, in compound **2** exhibit a different coordination mode. Both copper(II) ions within the dinuclear unit are bridged by three ligands, i.e., a hydroxo group and two formato ligands, of which one formato ligand is in a didentate syn,syn $\eta^1{:}\eta^1{:}\mu_2$-bridging mode [16,17] and the other is in the disordered monoatomic bridging mode. A terminal dpyam ligand completes the five coordination at each copper atom, which has a distorted trigonal bipyramidal geometry ($\tau = 0.71$) of the CuN_2O_3 chromophore. An oxygen atom of the monoatomic bridged formato ligand (Cu(1)–O(2) 2.144(6) Å), an oxygen atom of the $\eta^1{:}\eta^1{:}\mu_2$-bridging formato ligand (Cu(1)–O(4) 2.200(3) Å) and a nitrogen atom of the dpyam ligand (Cu(1)–N(2) 2.029(4) Å) comprise the trigonal plane. These equatorial distances are considerably longer than the two axial bonds occupied by an oxygen atom of the

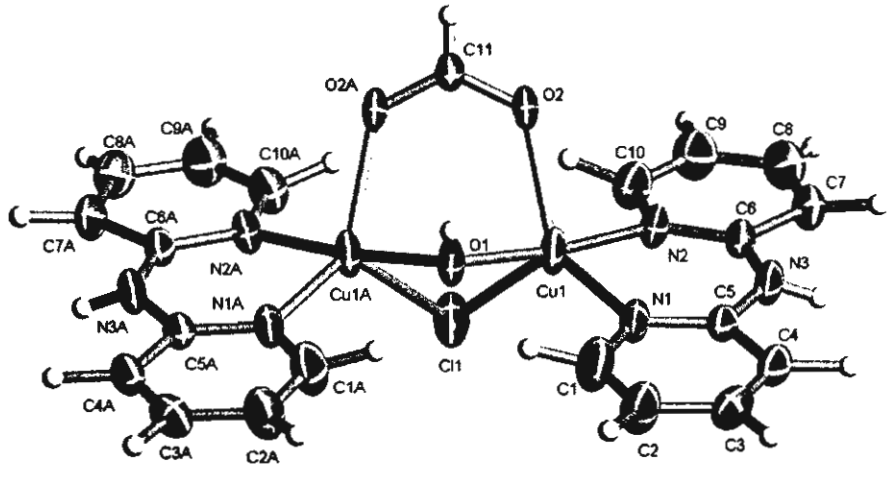

Fig. 1. Thermal ellipsoid (50% probability) plot of $[Cu_2(\mu\text{-}O_2CH)(\mu\text{-}OH)(\mu\text{-}Cl)(dpyam)_2](PF_6)$ (**1**). Atoms with an "A" are generated by a mirror plane. The uncoordinated PF_6 anion is omitted for clarity.

Table 2
Selected bond lengths (Å) and angles (°) of $[Cu_2(\mu\text{-}O_2CH)(\mu\text{-}OH)(\mu\text{-}Cl)(dpyam)_2](PF_6)$ **(1)**

Cu(1)–N(1)		2.031(3)	Cu(1)–O(1)	2.183(2)
Cu(1)–N(2)		1.983(2)	Cu(1)–O(2)	1.918(2)
Cu(1)–Cl(1)		2.451(1)	Cu(1)–Cu(1)A	3.061(5)
O(1)–Cu(1)–N(1)		130.6(1)	N(1)–Cu(1)–Cl(1)	124.1(1)
O(1)–Cu(1)–N(2)		86.7(1)	N(2)–Cu(1)–O(2)	173.8(1)
O(1)–Cu(1)–O(2)		87.3(1)	N(2)–Cu(1)–Cl(1)	97.7(1)
O(1)–Cu(1)–Cl(1)		104.8(1)	Cu(1)–O(2)–Cu(1)A	105.9(1)
O(2)–Cu(1)–Cl(1)		82.3(1)	Cu(1)–Cl(1)–Cu(1)A	77.2(1)
N(1)–Cu(1)–N(2)		91.8(1)	C(11)–O(1)–Cu(1)	127.5(2)
N(1)–Cu(1)–O(2)		93.2(1)	O(1)–C(11)–O(1)A	126.5(4)
Hydrogen bonds	D–H	H···A	D···A	D–H···A
N(3)–H(5)···O(1) [1/2 − x, 1/2 + y, z]	0.81(3)	2.08(3)	2.860(3)	162(3)
O(2)–H(12)···F(6) [−1/2 − x, −1/2 + y, z]	0.81(8)	2.18(7)	2.954(7)	159(7)

e.s.d.s. in parentheses.
A = [−x + 1, y, z].

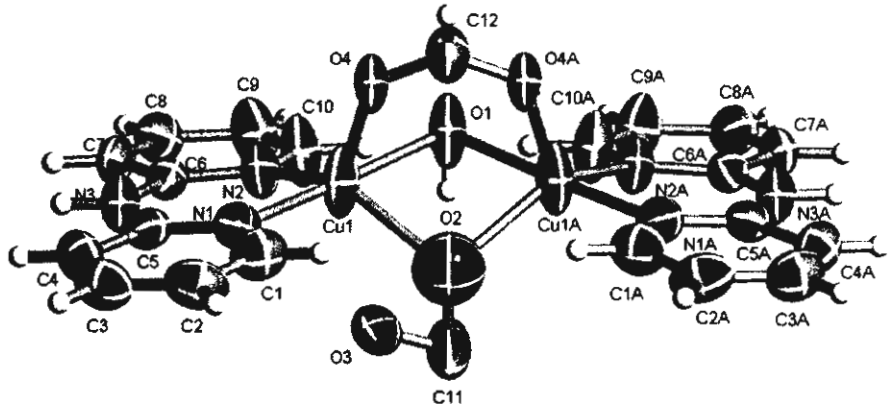

Fig. 2. Thermal ellipsoid (50% probability) plot of $[Cu_2(\mu\text{-}O_2CH)_2(\mu\text{-}OH)(dpyam)_2](PF_6)$ **(2)**. Atoms with an "A" are generated by a mirror plane. The uncoordinated PF_6 anion is omitted for clarity. Only one site occupancy of the disordered formato molecule is shown.

Table 3
Selected bond lengths (Å) and angles (°) of $[Cu_2(\mu\text{-}O_2CH)_2(\mu\text{-}OH)(dpyam)_2](PF_6)$ **(2)**

Cu(1)–N(1)	1.972(4)	Cu(1)–O(2)	2.144(6)	
Cu(1)–N(2)	2.029(4)	Cu(1)–O(4)	2.200(3)	
Cu(1)–O(1)	1.934(5)	Cu(1)–Cu(1)A	3.113(5)	
Cu(1)–O(3)	2.246(5)			
O(1)–Cu(1)–O(2)	78.2(2)	N(1)–Cu(1)–O(2)	100.5(2)	
O(1)–Cu(1)–O(4)	96.6(2)	N(1)–Cu(1)–O(4)	87.2(1)	
O(1)–Cu(1)–N(1)	173.6(2)	N(1)–Cu(1)–N(2)	91.7(1)	
O(1)–Cu(1)–N(2)	93.3(2)	N(2)–Cu(1)–O(2)	138.3(3)	
O(2)–Cu(1)–O(4)	89.7(3)	N(2)–Cu(1)–O(4)	130.9(1)	
C(12)–O(4)–Cu(1)	127.4(4)	O(4)–C(12)–O(4)A	127.5(7)	
Cu(1)–O(1)–Cu(1)A	107.2(4)	Cu(1)–O(2)–Cu(1)A	93.1(4)	
Hydrogen bonds	D–H	H···A	D···A	D–H···A
N(3)–H(5)···O(4) [3/2 − x, −1/2 + y, z]	0.86	2.15	2.917(5)	148

e.s.d.s. in parentheses.
A = [−x + 2, y, z].

bridging hydroxo ligand (Cu(1)–O(1) 1.934(5) Å) and another nitrogen atom of the dpyam ligand (Cu(1)–N(1) 1.972(4) Å) corresponding to the typical environment of the trigonal bipyramidal geometry [15]. The Cu···Cu separation is 3.113(5) Å. The bridging Cu(1)–O(1)–Cu(1)A, Cu(1)–O(2)–Cu(1)A angles are 107.2(4), 93.1(4)°, respectively. The dihedral angle between the two equatorial planes is 90.3°. The dpyam ligands are essentially planar, with only very small dihedral angles varies for individual pyridine rings.

The crystal lattice is stabilized by hydrogen bonding between the amine N and the oxygen atom of bridging formato group with a N···O contact of 2.917(5) Å. Details of the hydrogen bonding are listed in Table 3.

3.2.3. Description of $[Cu_2(\mu\text{-}O_2CCH_2CH_3)_2(\mu\text{-}OH)(dpyam)_2](ClO_4)$ (3)

The structure of **3** consists of a dinuclear $[Cu_2(\mu\text{-}O_2CCH_2CH_3)_2(\mu\text{-}OH)(dpyam)_2]^+$ cation and a disordered uncoordinated ClO_4^- anion. This unit is depicted in Fig. 3, together with the numbering scheme used. Selected distances and angles are listed in Table 4. The Cu(II) ions are triply bridged by two propionate ligands and a hydroxo group. One of the propionato ligands is in the didentate syn,syn $\eta^1:\eta^1:\mu_2$-bridging mode and the other is in the monoatomic bridging mode, similar to those of the formato ligands in compound **2**. The Cu···Cu separation is 3.006(2) Å. The coordination environment around Cu(1) can be best described as distorted square pyramidal, with a CuN_2O_2O chromophore and a τ value of 0.22. The four shorter bonds in the basal plane involve two nitrogen atoms of the dpyam ligand (Cu–N 1.985(2) and 2.018(2) Å), an oxygen atom of the bridging hydroxo ligand (Cu(1)–O(1) 1.931(2) Å) and an oxygen atom of the didentate bridging propionato ligand (Cu(1)–O(3) 1.959(2) Å). An oxygen atom of the monoatomic bridging propionato ligand completes the five-coordination of Cu(1) (Cu–O(4) 2.318(2) Å), consistent with a square–pyramidal geometry [18]. The four basal atoms are not coplanar, showing a significant tetrahedral distortion with a dihedral angle of 25.7° formed between CuO_2 and CuN_2 planes and the copper atom is displaced by 0.112 Å from the basal plane towards the O(4) atom.

The geometry around Cu(2) is an intermediate between a trigonal bipyramid and a square pyramid which is distorted via a Berry–Twist process [19], with a τ value of 0.43.The basal plane comprises of two nitrogen atoms of the dpyam ligand (Cu–N 1.986(2) and 2.010(2) Å), an oxygen atom of the bridging hydroxo ligand (Cu(2)–O(1) 1.942(2) Å) and an oxygen atom of the monoatomic bridging propionato ligand (Cu(2)–O(4) 2.065(2) Å). The fifth apical coordination site is occupied by an oxygen atom of the didentate-bridging

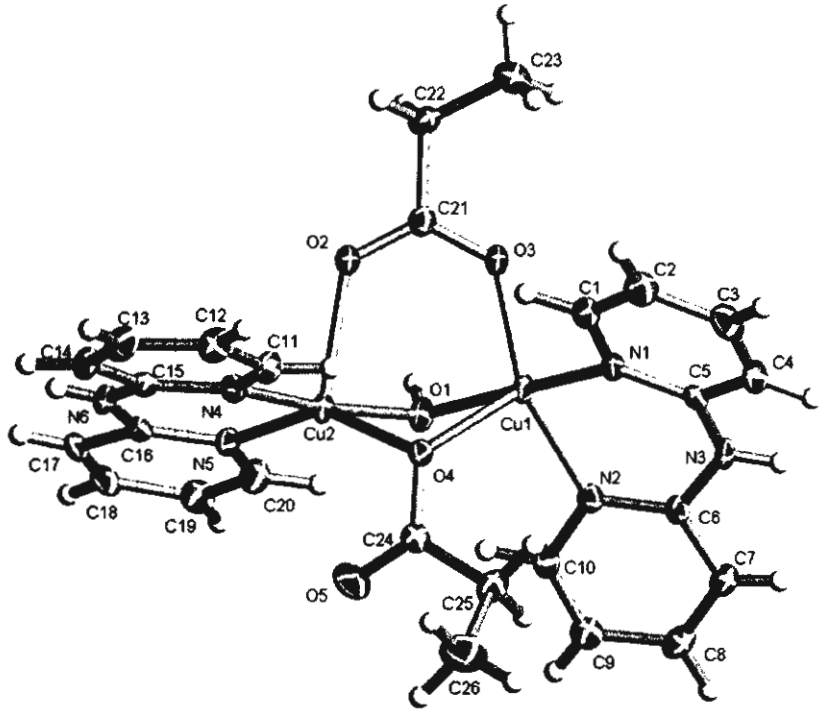

Fig. 3. Thermal ellipsoid (50% probability) plot of $[Cu_2(\mu\text{-}O_2CCH_2CH_3)_2(\mu\text{-}OH)(dpyam)_2](ClO_4)$ (**3**). The uncoordinated ClO_4 anion is omitted for clarity.

Table 4
Selected bond lengths (Å) and angles (°) of $[Cu_2(\mu\text{-}O_2CCH_2CH_3)_2(\mu\text{-}OH)(dpyam)_2](ClO_4)$ (3)

Cu(1)–N(1)		1.985(2)	Cu(2)–N(4)	1.986(2)
Cu(1)–N(2)		2.018(2)	Cu(2)–N(5)	2.010(2)
Cu(1)–O(1)		1.931(2)	Cu(2)–O(1)	1.942(2)
Cu(1)–O(3)		1.959(2)	Cu(2)–O(2)	2.236(2)
Cu(1)–O(4)		2.318(2)	Cu(2)–O(4)	2.065(1)
Cu(1)–Cu(1)A		3.006(5)		
O(1)–Cu(1)–O(3)		93.0(1)	O(1)–Cu(2)–O(2)	88.4(1)
O(1)–Cu(1)–O(4)		75.9(1)	O(1)–Cu(2)–O(4)	82.0(1)
O(1)–Cu(1)–N(1)		169.2(1)	O(1)–Cu(2)–N(4)	171.9(2)
O(1)–Cu(1)–N(2)		93.4(1)	O(1)–Cu(2)–N(5)	95.3(7)
O(3)–Cu(1)–O(4)		104.3(1)	O(2)–Cu(2)–O(4)	100.3(1)
N(1)–Cu(1)–O(3)		87.6(1)	N(4)–Cu(2)–O(2)	85.4(1)
N(1)–Cu(1)–O(4)		93.5(1)	N(4)–Cu(2)–O(4)	94.0(1)
N(1)–Cu(1)–N(2)		90.4(1)	N(4)–Cu(2)–N(5)	91.8(1)
N(2)–Cu(1)–O(3)		156.0(1)	N(5)–Cu(2)–O(2)	113.4(1)
N(2)–Cu(1)–O(4)		99.6(1)	N(5)–Cu(2)–O(4)	146.2(1)
C(21)–O(3)–Cu(1)		129.7(1)	Cu(1)–O(1)–Cu(2)	101.8(1)
C(21)–O(2)–Cu(2)		126.0(1)	Cu(1)–O(4)–Cu(2)	86.4(1)
O(2)–C(21)–O(3)		125.1(3)		
Hydrogen bonds	**D–H**	**H···A**	**D···A**	**D–H···A**
O(1)–H(21)···O(8)				
[x, 1/2 − y, −1/2 + z]	0.75(3)	2.23(3)	2.986(3)	176(3)
N(3)–H(5)···O(5)				
[x, 1/2 − y, −1/2 + z]	0.83(3)	1.95(3)	2.763(3)	165(3)
N(6)–H(15)···O(2)				
[1 − x, −y, 1 − z]	0.75(4)	2.10(4)	2.827(3)	165(5)

e.s.d.s. in parentheses.
A = [x, 1/2 − y, −1/2 + z].

propionato ligand with a Cu(2)–O(2) distance of 2.236(2) Å, providing a distorted square-pyramidal CuN_2O_2O' chromophore with a marked tetrahedral twist, 34.4° between CuN_2 and CuO_2 planes. The copper atom is displaced 0.246 Å from the basal plane toward O(2) atom. The bridging Cu(1)–O(1)–Cu(2) and Cu(1)–O(4)–Cu(2) angles are 101.8(1)° and 86.4(1)°, respectively.

The crystal lattice is stabilized by a hydrogen bonding between the amine N and an oxygen atom of bridging propionato group with N···O contacts of 2.763(3)–2.827(3) Å and between the oxygen atom of bridging hydroxo group and the oxygen atom of ClO_4^- anion with a distance of 2.986(3) Å. Details of the hydrogen bonding are listed in Table 4.

3.3. Structure comparison

The compounds together with a number of related dinuclear triply-bridged copper(II) compounds are listed in Table 5. The molecular structures and the copper(II) chromophores of $[Cu_2(\mu\text{-}O_2CCH_3)(\mu\text{-}OH)(\mu\text{-}Cl)(bpy)_2](ClO_4)\cdot H_2O$ **(8)** ($\tau = 0.40$) [2] and $[Cu_2(\mu\text{-}O_2CH)(\mu\text{-}OH)(\mu\text{-}Cl)(dpyam)_2](ClO_4)\cdot 0.5H_2O$ **(11)** ($\tau = 0.67$) [5] are comparable to that of compound **1** ($\tau = 0.72$) (see Table 5), in which two copper(II) atoms are bridged through three different bridging ligands: carboxylate, hydroxide and chloride anions. The carboxylate bridges in these three compounds display the same syn, syn $\eta^1{:}\eta^1{:}\mu_2$-bridging mode. However, the coordination geometry of compound **8** is slightly different in distortion towards the square pyramid geometry ($\tau = 0.40$), presumably due to the more flexibility of the dpyam ligand.

The structure of compound **2** ($\tau = 0.71$) shows some similarity to those of $[Cu_2(\mu\text{-}O_2CCH_3)_2(\mu\text{-}OCH_3)(bpy)_2](PF_6)$ **(9)** ($\tau = 0.66$ and 0.59) [3] and $[Cu_2(\mu\text{-}O_2CH)(\mu\text{-}OH)(\mu\text{-}OCH_3)(dpyam)_2](ClO_4)$ **(10)** ($\tau = 0.65$) [5], all of which involve a distorted trigonal bipyramidal geometry with a CuN_2O_3 chromophore (see Table 5). Compounds **10** and **2** have two monoatomic bridges, which one connects two apical sites of the trigonal bipyramidal copper(II) chromophores whereas, compound **9** has only one monoatomic bridge (a methoxo group), which connects two apical sites of the trigonal bipyramidal geometry.

The copper(II) environments of compound **3** ($\tau = 0.22$ and 0.43) are related to those of the known dinuclear structures, $[Cu_2(\mu\text{-}O_2CCH_3)_2(\mu\text{-}OEt)(bpy)_2](PF_6)$ **(4)** ($\tau = 0.23$ and 0.10) [3], $[Cu_2(\mu\text{-}OH)(\mu\text{-}O_2CH)_2(bpy)_2](BF_4)$ **(5)** ($\tau = 0.11$ and 0.43) [4], $[Cu_2(\mu\text{-}O_2CCH_3)_3(bpy)_2](ClO_4)$ **(6)** ($\tau = 0.14$ and 0.47) [1] and $[Cu_2(\mu\text{-}O_2CCH_3)(\mu\text{-}OH)(\mu\text{-}H_2O)(bpy)_2](ClO_4)_2$ **(7)** ($\tau = 0.14$ and 0.25) [1] (see Table 5). The apical distances in these compounds are typical Cu–O distances of 2.2–2.7 Å [20]. The molecular structure

Table 5
Structural and magnetic data for triply-bridged dinuclear copper(II) carboxylato compounds

Compound[a]	Coordination geometry[b]	τ	Chromophore	Cu···Cu	Cu–O		J (cm^{-1})	Cu–X–Cu (Å)	Reference
					Axial	Equatorial			
$[Cu_2(\mu\text{-}O_2CCH_3)_2(\mu\text{-}OEt)(bpy)_2](PF_6)$ **(4)**	Dist. Spy.	0.23, 0.10	CuN_2O_2O'	3.230	2.155–2.164	1.939–1.982		112.1(OEt)	[3]
$[Cu_2(\mu\text{-}OH)(\mu\text{-}O_2CH)_2(bpy)_2](BF_4)$ **(5)**	Dist. Spy., intermediate	0.11[c], 0.43[c]	CuN_2O_3, CuN_2O_3	3.171	2.140 2.190	1.927–2.029 1.928–2.012	99.0	110.7(OH)	[4]
$[Cu_2(\mu\text{-}O_2CCH_3)_3(bpy)_2](ClO_4)$ **(6)**	Dist. Spy., Intermediate[d]	0.14[c], 0.47[c]	CuN_2O_2O' CuN_2O_3	3.392	2.238 1.930	1.939–1.977 1.974–2.169	3.6	109.8(O_2CCH_3)	[1]
$[Cu_2(\mu\text{-}O_2CCH_3\mu\text{-}OH)(\mu\text{-}H_2O)(bpy)_2](ClO_4)_2$ **(7)**	Dist. Spy.	0.14[c], 0.25[c]	CuN_2O_2O'	3.035	2.379–2.405	2.006–2.010	19.3	103.8(OH) 78.7(H_2O)	[1]
$[Cu_2(\mu\text{-}O_2CCH_3\mu\text{-}OH)(\mu\text{-}Cl)(bpy)_2](ClO_4) \cdot H_2O$ **(8)**	Dist. Spy.	0.40	CuN_2O_2Cl	2.957		1.920–1.971		100.7(OH) 70.6(Cl)	[2]
$[Cu_2(\mu\text{-}O_2CCH_3)_2(\mu\text{-}OCH_3)(bpy)_2](PF_6)$ **(9)**	Dist. TBP.	0.66, 0.59	CuN_2O_3	3.093	1.922–1.931	1.933–2.099		106.8(OCH_3)	[3]
$[Cu_2(\mu\text{-}O_2CH)(\mu\text{-}OH)(\mu\text{-}OCH_3)(dpyam)_2](ClO_4)$ **(10)**	Dist. TBP.	0.65	CuN_2O_3	3.023	1.918	2.169–2.175	62.5	104.0(OH) 88.3(OCH_3)	[5]
$[Cu_2(\mu\text{-}O_2CH)(\mu\text{-}OH)(\mu\text{-}Cl)\ (dpyam)_2](ClO_4) \cdot 0.5H_2O$ **(11)**	Dist. TBP.	0.67	CuN_2O_2Cl	3.036	1.916	2.158	79.1	104.8(OH) 75.6(Cl)	[5]
$[Cu_2(\mu\text{-}O_2CH)(\mu\text{-}OH)(\mu\text{-}Cl)(dpyam)_2](PF_6)$ **(1)**	Dist. TBP.	0.72	CuN_2O_2Cl	3.061	1.918	2.183	79.7	105.8(OH) 77.3(Cl)	This work
$[Cu_2(\mu\text{-}O_2CH)_2(\mu\text{-}OH)(dpyam)_2](PF_6)$ **(2)**	Dist. TBP.	0.71	CuN_2O_3	3.113	1.934	2.144–2.200	47.8	107.2(OH) 93.1(O_2CH)	This work
$[Cu_2(\mu\text{-}O_2CCH_2CH_3)_2(\mu\text{-}OH)(dpyam)_2](ClO_4)$ **(3)**	Dist. Spy.,	0.22,	CuN_2O_2O'	3.006	2.236–2.318	1.931–1.959	24.1	101.8(OH)	This work
	Intermediate	0.43	CuN_2O_3					86.4($O_2CCH_2CH_3$)	

[a] Abbreviations: bpy = 2,2′-bipyridine; bppz = 2,5-bis(2-pyridyl)pyrazine; dpyam = di-2-pyridylamine.
[b] Dist. Spy. = distorted square pyramidal, Dist. TBP = distorted trigonal bipyramidal.
[c] Calculated from the known structural parameters.
[d] The original paper describes as Dist. TBP. for the calculated τ value of 0.47.

and the copper(II) chromophores of compound **3** are very comparable to that of compound **7**, both of them have two monoatomic bridges and a triatomic bridge.

3.4. Spectral characterization and EPR measurements

The IR spectra of compounds **1**, **2** and **3** show broad and intense bands of the ionic PF_6^- anion (843 cm^{-1} for **1** and 842 cm^{-1} for **2**) and ionic ClO_4^- anion (1086 cm^{-1} for **3**). The spectra also exhibit a broad band at 3563, 3580 and 3750 cm^{-1} for compounds **1**, **2** and **3**, respectively, which can be assigned to the bridging OH group. The broad and intense bands at 1571 and 1396 cm^{-1} in compound **1** correspond to the $\nu_{as}(COO^-)$ and $\nu_s(COO^-)$ vibration of the didentate bridging coordination mode of the carboxylate group within a dinuclear species [5]. Owing to the presence of two different coordination modes of carboxylate bridges in **2** and **3**, two $\nu_{as}(COO^-)$ and two $\nu_s(COO^-)$ bands are observed in its IR spectrum (1619 and 1385 cm^{-1} bands for compound **2** and 1600 and 1392 cm^{-1} for compound **3**). These bands are assigned to the stretching modes of the monoatomic carboxylate bridges [1,8]. The vibrations observed at 1603 and 1436 cm^{-1} for compound **2** and 1556 and 1435 cm^{-1} for compound **3** are consistent with the triatomic carboxylate bridge [1,8].

The electronic reflectance spectrum of compound **1** shows a broad asymmetric band at ≈11 800 cm^{-1} with a high-energy shoulder at ca. 14 600 cm^{-1} consistent with a distorted trigonal bipyramidal geometry [21,22]. Compound **2** has a very broad band centered at ca. 12 810 cm^{-1}. Compound **3** exhibits a broad asymmetric band centered at ca. 12 810 cm^{-1} with a high-energy shoulder at ca. 14 710 cm^{-1}, which would be consistent with two different metal geometries ($\tau = 0.22$ and 0.43) within the complex.

The X-band EPR measured on polycrystalline samples at RT and 77 K showed in all three compounds a broad isotropic signal with a g_{iso} at around 2.10 and no hyperfine is resolved. To have more insight into the magnetic behaviour magnetic susceptibility studies were undertaken of a powdered sample from 5 to 280 K (see below).

3.5. Magnetic properties

The magnetic properties of the compounds are depicted in Figs. 4–6, for compounds **1**, **2** and **3**, respectively, in the form of μ_{eff} versus T plots for two Cu(II) ions.

The magnetic properties of all three compounds show a very similar behaviour. At 280 K the μ_{eff} is 2.75 μ_B for compound **1** (2.40 $_B$ and 2.60 μ_B, for **2** and **3**) which agrees reasonable with the spin-only value calculated for two uncoupled spin = 1/2 Cu(II) centers. Upon cooling it raises gradually to reach 3.02, 2.68 and 2.78 μ_B, at

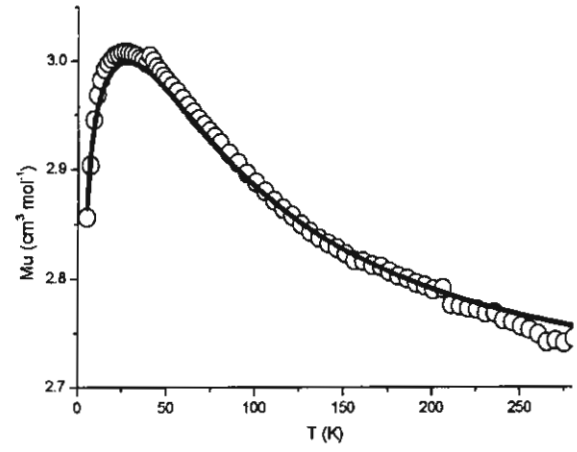

Fig. 4. A plot of the temperature dependence of μ_{eff} vs. T for compound **1**. The solid line represents the calculated curve (see text).

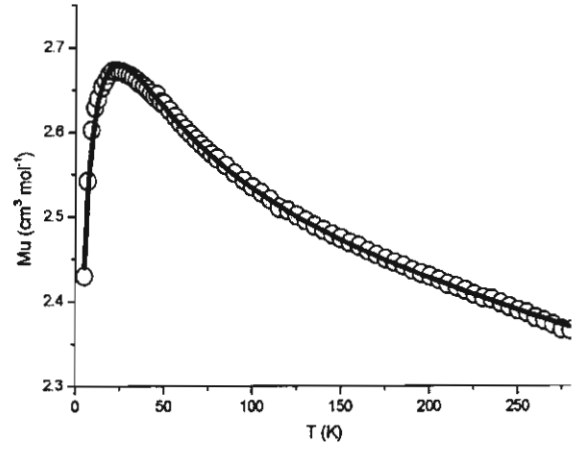

Fig. 5. A plot of the temperature dependence of μ_{eff} vs. T for compound **2**. The solid line represents the calculated curve (see text).

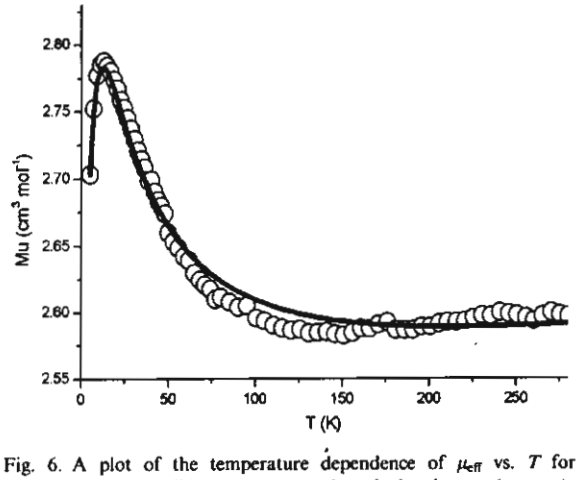

Fig. 6. A plot of the temperature dependence of μ_{eff} vs. T for compound **3**. The solid line represents the calculated curve (see text).

around 30 K, for compounds **1**, **2** and **3**, respectively. This behaviour is typical for a ferromagnetically coupled Cu(II) dinuclear compound. Below that temperature, μ_{eff} then diminishes till a value around 2.85–2.45 μ_B at 5 K for the three compounds, which may originate from intermolecular antiferromagnetic interactions, or from zero-field splitting of the $S = 1$ state of the dinuclear species. The theoretical expression for the magnetic susceptibility for two interacting $S = 1/2$ centers, which is based on the general Hamiltonian [23] is: $H_{ex} = -JS_1S_2$, in which the exchange parameter J, is negative for antiferromagnetic and positive for ferromagnetic interaction. The magnetic data were fitted to the equation given in the literature for dinuclear copper compounds [23, p. 132].

$\chi_m = (2Ng^2\beta^2)[kT - (2zJ'/(3 + \exp(-J/kT)))]^{-1}[3 + \exp(-J/kT)]^{-1}(1 - p) + \chi_p p + \text{TIP}$, in which N, g, β, k and T have their usual meanings. The parameter p denotes the fraction of paramagnetic impurity in the sample and zJ' the interaction between neighbouring dinuclear identities. A temperature independent paramagnetism (TIP) was also considered and fixed at 60×10^{-6} per copper ion. The fit was accomplished by minimization of $R = \sum(\chi_m \cdot T_{calc} - \chi_m \cdot T_{obs})^2/(\chi_m \cdot T_{obs})^2$ by least-squares procedure.

The best fit was obtained for compound **1** with the following values: $J = 79.7$ cm^{-1}, $g = 2.15$, $zJ' = -2.9$ cm^{-1}, $p = 0.0$, with a final R of 1.0×10^{-3} (see Fig. 4). For compound **2** these values are $J = 47.8$ cm^{-1}, $g = 1.99$, $zJ' = -7.6$ cm^{-1}, $p = 0.002$, with a final R of $1.6 \cdot 10^{-3}$ (see Fig. 5). For compound **3** these values are $J = 24.1$ cm^{-1}, $g = 2.05$, $zJ' = -3.4$ cm^{-1}, $p = 0.0$, with a final R of 1.2×10^{-3} (see Fig. 6).

This overall ferromagnetic behaviour has been observed earlier for many other triply-bridged dpyam compounds, also containing a hydroxo bridge [5], i.e., compounds **10** and **11** in Table 5. For dinuclear bis-hydroxo-bridged compounds a correlation is known between J and the Cu–O–Cu angle; an antiferromagnetic interaction was found when the Cu–O–Cu angle is larger than 97.5°, but when the Cu–O–Cu angle is smaller than 97.5° a ferromagnetic interaction would be expected [24]. In this study the angles vary between 101.8° and 107.2° and by neglecting the other bridges an antiferromagnetic exchange would have been expected. However, the difference between the compounds with only hydroxo bridges and the triply bridges is great. The copper(II) ions in compounds **1**–**3** (and also **10** and **11** in Table 5) have a five-coordinate (more or less distorted) trigonal bipyramidal geometry with the d_{z^2} ground state, whereas the dihydroxo-bridged copper(II) complexes are square pyramidal with $d_{x^2-y^2}$ ground states. Also it is known that a change in electron density of the magnetic orbital can have a pronounced effect on the sign and magnitude of a magnetic exchange interaction [25,26]. In this case, for compounds **1**–**3**, a single pathway via the unit (Cu–OH–Cu) is possible for the electron delocalization via the d_{z^2} magnetic orbitals, corresponding to the weak, or intermediate, ferromagnetic interaction. Secondly also the carboxylato bridge plays a role in the magnetic interaction, which was described in the literature as a so-called "countercomplementary effect" [23,27–29]. This effect cannot be quantitated, however.

From Table 5 it can anyway be noted that for almost all triply bridges Cu(II) dinuclear compounds, when the copper(II) geometry is (distorted) trigonal bipyramidal a moderate overall ferromagnetic interaction is observed (compounds **10**, **11**, **1** and **2**) and when the geometry becomes more distorted to square pyramidal (compounds **6**, **7** and **3**) the overall ferromagnetic interaction becomes, in general, weaker.

4. Conclusions

Three new triply-bridged compounds with dpyam are synthesized, characterized and their magnetic interaction studied. All three compounds contain a dinuclear copper(II) unit with a hydroxo and a formato/chloride bridge (compound **1**), two formato bridges (compound **2**) and two propionato bridges (compound **3**). The coordination geometry around each copper(II) ion is slightly distorted trigonal bipyramidal for **1** and **2** and an intermediate between SP and TBP for **3**. A strong magnetic interaction requires both good σ orientation of the magnetic orbitals and good superexchange properties of the bridging atom(s) [23,29]. The magnetic orbital is d_{z^2} for the copper(II) centers with lobes (more or less) directed toward the bridging hydroxo ligand, but also the formato/propionato/chloride bridge(s) cannot be excluded as a countercomplementary contribution. Therefore the "overall" effect is in this case a moderate ferromagnetic exchange, as can be seen for compounds **10**, **11**, **1** and **2** with the same type of geometry, while in compounds **3**, **6** and **7** the distortion is large, the overlap of the orbitals becomes weaker and also the ferromagnetic interaction becomes weaker. An exception appears to be compound **5**, but in this compound, both Cu(II) ions have differently distorted 5 coordinated geometries and a fairly large Cu–O–Cu angle.

5. Supplementary material

Crystallographic data (excluding structure factors) for the structures in this paper have been deposited with the Cambridge Crystallographic Data Centre as Supplementary Publication Nos. CCDC 243062–64 for structures **1**, **2** and **3**, respectively. Copies of the data can be obtained free of charge on application to CCDC, 12 Union Road, Cambridge CB2 1EZ, UK [fax: (internat.) +44(1223)336 033, e-mail: deposit@ccdc.ac.uk].

Acknowledgements

The authors thank The Thailand Research Fund and Khon Kaen University for research grant. Support of the Postgraduate Education and Research Program in Chemistry is also gratefully acknowledged. The work described in the present paper has been supported by the Leiden University Study group WFMO (Werkgroep Fundamenteel Materialen Onderzoek). Support of the NRSC Catalysis (a Research School Combination of HRSMC and NIOK) is kindly acknowledged.

References

[1] G. Christou, S.P. Perlepes, E. Libby, K. Folting, J.C. Huffman, R.J. Webb, D.N. Hendrickson, Inorg. Chem. 29 (1990) 3657.
[2] S.P. Perlepes, J.C. Huffman, G. Christou, Polyhedron 10 (1991) 2301.
[3] S.P. Perlepes, J.C. Huffman, G. Christou, S. Paschalidou, Polyhedron 14 (1995) 1073.
[4] T. Tokii, M. Nagamatsu, H. Hamada, M. Nakashima, Chem. Lett. (1992) 1091.
[5] (a) S. Youngme, C. Chailuecha, G.A. van Albada, C. Pakawatchai, N. Chaichit, J. Reedijk, Inorg. Chim. Acta 357 (2004) 2532; (b) W. Huang, D. Hu, S. Gou, H. Qian, H.-K. Fun, S.S.S. Raj, Q. Meng, J. Mol. Struct. 649 (2003) 269.
[6] B. Graham, M.T.W. Hearn, P.C. Junk, C.M. Kepert, F.E. Mabbs, B. Moubaraki, K.S. Murray, L. Spiccia, Inorg. Chem. 40 (2001) 1536.
[7] T.M. Rajendiran, R. Kannappan, R. Venkatesan, P.S. Rao, M. Kandaswamy, Polyhedron 18 (1999) 3085.
[8] I. Chadjistamatis, A. Terzis, C.P. Raptopoulou, S.P. Perlepes, Inorg. Chem. Commun. 6 (2003) 1365.
[9] M. Lubben, R. Hage, A. Meetsma, K. Byma, B.L. Feringa, Inorg. Chem. 34 (1995) 2217.
[10] Bruker, SMART (version 5.6), Bruker AXS Inc., Madison, Wisconsin, USA, 2000.
[11] Bruker, SAINT (version 5.6), Bruker AXS Inc., Madison, Wisconsin, USA, 2000.
[12] Bruker, SADABS (version 5.6), Bruker AXS Inc., Madison, Wisconsin, USA, 2000.
[13] Bruker, SHELXTL (version 6.12), Bruker AXS Inc., Madison, Wisconsin, USA, 2000.
[14] A.W. Addison, T.N. Rao, J. Reedijk, J. van Rijn, G.C. Verschoor, J. Chem. Soc., Dalton Trans. (1984) 1349.
[15] F. Huq, A.C. Shapski, J. Chem. Soc. A (1971) 1927.
[16] D.K. Towle, S.K. Hoffmann, W.E. Hatfield, P. Singh, P. Chaudhuri, Inorg. Chem. 27 (1988) 394.
[17] W.A. Wojtczak, M.J. Hampden-Smith, E.N. Duesler, Inorg. Chem. 37 (1998) 1781.
[18] S. Youngme, G.A. van Albada, O. Roubeau, C. Pakawatchai, N. Chaichit, J. Reedijk, Inorg. Chim. Acta 342 (2003) 48.
[19] S. Berry, J. Chem. Phys. 32 (1960) 933.
[20] S. Youngme, W. Somjitsripunya, K. Chinnakali, S. Chantrapromma, H.K. Fun, Polyhedron 18 (1999) 857.
[21] G. Murphy, C. Murphy, B. Murphy, B. Hathaway, J. Chem. Soc., Dalton Trans. (1997) 2653.
[22] G. Murphy, P. Nagle, B. Murphy, B. Hathaway, J. Chem. Soc., Dalton Trans. (1997) 2645.
[23] O. Kahn, Molecular Magnetism, VCH Publishers, New York, 1993.
[24] V.H. Crawford, H.W. Richardson, J.R. Wasson, D.J. Hodgson, W.E. Hatfield, Inorg. Chem. 15 (1976) 2107.
[25] M.S. Haddad, S.R. Wilson, D.J. Hodgson, D.N. Hendrickson, J. Am. Chem. Soc. 103 (1981) 384.
[26] M.S. Haddad, D.N. Hendrickson, Inorg. Chim. Acta 28 (1978) L121.
[27] Y. Nishida, S. Kida, J. Chem. Soc., Dalton Trans. (1986) 2633.
[28] V. McKee, M. Zvagulis, C.A. Reed, Inorg. Chem. 24 (1985) 2914.
[29] V. McKee, M. Zvagulis, J.V. Dagdigian, M.G. Patch, C.A. Reed, J. Am. Chem. Soc. 106 (1984) 4765.

Available online at www.sciencedirect.com
SCIENCE DIRECT®
Inorganica Chimica Acta 358 (2005) 3267–3271
Inorganica Chimica Acta
www.elsevier.com/locate/ica

Note

Synthesis, crystal structure and magnetic properties of a polynuclear Cu(II) complex: *catena*-poly-[aqua(di-2-pyridylamine)copper(II)(μ-formato-*O*,*O*′)nitrate]

Sujittra Youngme [a,*], Pongthipun Phuengphai [a], Narongsak Chaichit [b], Gerard A. van Albada [c], Stefania Tanase [c], Jan Reedijk [c]

[a] *Department of Chemistry, Faculty of Science, Khon Kaen University, Khon Kaen 40002, Thailand*
[b] *Department of Physics, Faculty of Science and Technology, Thammasat University Rangsit, Pathumthani 12121, Thailand*
[c] *Gorlaeus Laboratories, Leiden Institute of Chemistry, Leiden University, P.O. Box 9502, 2300 RA Leiden, The Netherlands*

Received 11 November 2004; accepted 28 December 2004
Available online 11 February 2005

Abstract

The synthesis, X-ray structure, spectroscopic and magnetic properties of a zig-zag formato-bridged chain complex with the formula $[Cu(dpyam)(\mu\text{-}O_2CH)(OH_2)]_n(NO_3)_n$ (1) (in which dpyam = di-2-pyridylamine) is described.

The geometry of the copper(II) ion is distorted square pyramidal with a basal plane consisting of two nitrogen atoms of the dpyam ligand (Cu–N distances 1.987(3) and 2.010(3) Å) and two oxygen atoms of two different formato ligands (Cu–O distances 1.974(2) and 1.975(2) Å). A coordinated water molecule occupies the axial position at a distance of 2.222(3) Å. The copper atoms are bridged unsymmetrically by a formato anion in a syn-anti arrangement, resulting in a polymeric zig-zag chain structure.

The magnetic susceptibility measurements (5–280 K) agree with a very weak ferromagnetic chain interaction between the Cu centres with a J value of 0.75 cm^{-1}.

Keywords: Copper(II) complex; Di-2-pyridylamine; Magnetic properties; Crystal structure

1. Introduction

Reported complexes of copper(II) and didentate mono(chelating) ligands with monovalent oxoanions may be grouped in several classes for each type of oxoanion, depending on coordinating nature. Complexes with monovalent oxoanions formulated as $Cu(LL)(anion1)_2 \cdot nH_2O$, or Cu(chelate)(anion1)(anion2) · nH_2O, (in which anion1 and/or anion2 = NO_2^-, NO_3^-, ClO_4^-, $CH_3CH_2COO^-$, CH_3COO^- or $HCOO^-$ and LL = didentate chelating ligand), were found to exhibit four types of local molecular structures: (A) mononuclear tetrahedrally-distorted elongated octahedral units with an extremely asymmetric didentate coordination of both oxoanions [1]; (B) polymeric elongated tetragonal (or rhombic) octahedral units with the nearly symmetric didentate coordination of a basal oxoanion and the bridging didentate coordination in the axial positions of the second one [2]; (C) polymeric tetrahedrally distorted square pyramid with non-bridging monodentate and bridging didentate oxoanions [3,4]; (D) dinuclear tetrahedrally distorted square pyramidal with non-bridging monodentate and bridging didentate oxoanions [5,6]. An example of each class is presented in Scheme 1.

X-ray studies of polynuclear formato-bridged Cu(II) compounds with N-donor ligands are relatively rare

* Corresponding author. Tel.: +66 43 202 222 41; fax: +66 43 202 373.
E-mail address: sujittra@kku.ac.th (S. Youngme).

0020-1693/$ - see front matter © 2005 Elsevier B.V. All rights reserved.
doi:10.1016/j.ica.2004.12.032

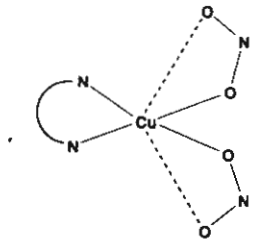

Class A: $[Cu(dpyam)(NO_2)_2]$[26]

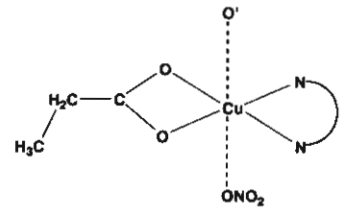

Class B: $[Cu(dpyam)(NO_3)(O_2CCH_2CH_3)]$ [2]

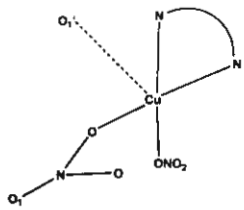

Class C: $[Cu(Prdpa)(NO_3)_2]$ [3,4]

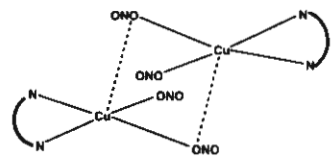

Class D: $[Cu_2(dpyam)_2(ONO)_2(\mu\text{-}ONO)_2]\cdot 2CH_3CN$ [5]

Scheme 1.

[7–12] and the number of magnetic studies undertaken with these compounds is even more scarce [7,8]. Also polynuclear Cu(II) compounds with the ligand used in this study, di-2-pyridylamine (abbreviated as dpyam) are relatively rare, as only a few are reported to date [1,3,22–25]. With the ligand dpyam and formato as a bridging ligand only one dinuclear compound, $[Cu_2(dpyam)_2(\mu\text{-}O_2CH)(O_2CH)_3(H_2O)](H_2O)$, has been reported [6].

In this study we describe the synthesis, spectroscopic properties, magnetic study and EPR of a chain-type formato-bridged Cu(II) compound, $[Cu(dpyam)(\mu\text{-}O_2CH)(H_2O)]_n(NO_3)_n$ (1).

2. Experimental

2.1. Synthesis of $[Cu(dpyam)(\mu\text{-}O_2CH)(H_2O)]_n(NO_3)_n$ (1)

Solid NaHCOO (0.136 g, 2.0 mmol) dissolved in water (10 ml) was added to a warm solution of di-2-pyridylamine (0.171 g, 1.0 mmol) in methanol (10 ml) yielding a pale-yellow solution. Its colour became greenish by slow addition of an aqueous solution (10 ml) of $Cu(NO_3)_2 \cdot 2.5H_2O$ (0.232 g, 1.0 mmol). The resulting green solution was allowed to evaporate at room temperature. After several days, blue-green crystals of 1 were deposited. Yield: ca. 60%. *Anal.* Calc. for $C_{11}H_{12}CuN_4O_6$: C, 36.7; H, 3.4; N, 15.6. Found: C, 36.3; H, 3.3; N, 15.4%. IR (KBr; cm^{-1}): ν_{as}(C–O) 1591(s), ν_{as}(N–O) 1384(s), ν_s(C–O) 1354(s), ν_s(N–O) 1340(s) and δ (O–C–O) 906(w).

2.2. Physical measurements

Elemental analyses (C, H, N) were determined on a Perkin–Elmer PE2400 CHNS/O Analyzer by the Microanalytical Service of Science and Technological Research Equipment Center, Chulalongkorn University, Thailand. IR spectrum was recorded on a Spectrum One Perkin–Elmer FT-IR spectrophotometer as KBr pellets in the 4000–450 cm^{-1} spectral range. Diffuse reflectance measurement from 9000 to 20 000 cm^{-1} was recorded as polycrystalline samples using a Perkin–Elmer Lambda 2S spectrophotometer equipped with an integrating sphere attachment. Barium sulfate was used as the reflectance standard. X-band powder EPR spectrum was recorded on a JEOL RE2x electron spin resonance spectrometer using DPPH ($g = 2.0036$) as a standard. Magnetic susceptibility measurements (5–300 K) were carried out using a Quantum Design MPMS-5 5T SQUID magnetometer (measurements carried out at 1000 G) performed at Leiden University. Data were corrected for magnetisation of the sample holder and for diamagnetic contributions, which were estimated from Pascal constants.

2.3. Crystallography

Reflection data were collected at 293 K on a 1 K Bruker SMART CCD area-detector diffractometer using

graphite monochromated Mo Kα radiation (λ = 0.71073 Å) at a detector distance of 4.5 cm and swing angle of −35°. A hemisphere of the reciprocal space was covered by a combination of three sets of exposures; each set had a different ϕ angle (0°, 88°, 180°) and each exposure of 15 s for **1**, covered 0.3° in ω. Data reduction and cell refinements were performed using the program SAINT [13]. An empirical absorption correction by using the SADABS [14] program was applied, which resulted in transmission coefficients ranging from 0.7662 to 1.0000 for **1**. The structure was solved by direct methods and refined by full-matrix least-squares method on $(F_{obs})^2$ with anisotropic thermal parameters for all non-hydrogen atoms using the SHELXTL-PC V 6.1 [15] software package. All hydrogen atoms in **1** were located by difference synthesis and refined isotropically. The nitrate group is disordered with site occupancies of 0.50 for both conformers and the average bond length, 1.216(6) Å and bond angle, 119.8(3)° are within the typical values for the uncoordinated nitrate group [16]. The molecular graphics were created by using SHELXTL-PC. The crystal and refinement details are listed in Table 1.

3. Results and discussion

3.1. Description of the structure

A plot of the structure together with the used numbering system is shown in Fig. 1 with selected bond distances and angles given in Table 2. The structure of **1** consists of a polynuclear $[Cu(dpyam)(\mu\text{-}O_2CH)(H_2O)]^+$ cation, and an uncoordinated disordered NO_3^- anion.

Table 1
Crystal and refinement data of $[Cu(dpyam)(\mu\text{-}O_2CH)(OH_2)]_n(NO_3)_n$

Molecular formula	$C_{11}H_{12}CuN_4O_6$
Molecular weight	359.79
T (K)	293(2)
Crystal system	monoclinic
Space group	$P2_1/c$
a (Å)	9.7179(2)
b (Å)	19.06310(10)
c (Å)	7.5064(2)
β (Å)	94.8530(10)
V (Å^3)	1385.60(5)
Z	4
D_{calc} (Mg m^{-3})	1.725
μ (mm^{-1})	1.613
Crystal size (mm)	0.05 × 0.13 × 0.38
θ Range (°)	2.10–30.47
Number of reflections collected	10 187
Number of unique reflections	3941 (R_{int} = 0.0462)
Goodness-of-fit	1.042
Final R indices [$I > 2\sigma(I)$], wR_2 = 0.0752	R_1 = 0.0541; wR_2 = 0.0971
R indices (all data)	R_1 = 0.1057; wR_2 = 0.1147
Largest difference peak and hole (e Å^{-3})	0.538, −0.461

$R = \sum \|F_o| - |F_c\| / \sum |F_o|$, $R_w = [\sum w\{|F_o| - |F_c|\}^2 / w|F_o|^2]^{1/2}$.

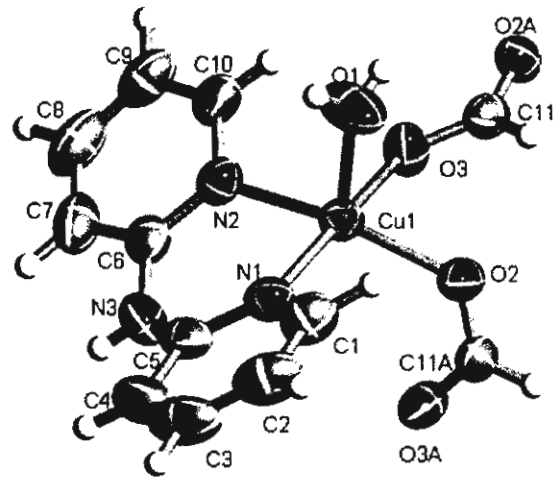

Fig. 1. Thermal ellipsoid plot (50% probability) of $[Cu(dpyam)(\mu\text{-}O_2CH)(H_2O)]_n(NO_3)_n$ (**1**). The uncoordinated nitrate anion has been omitted for clarity.

The copper atoms are bridged unsymmetrically by a formate group in a syn-anti arrangement [17], resulting in a polymeric zig-zag chain structure (Fig. 2). The Cu(II) atom is five-coordinated with a basal plane consisting of two nitrogen atoms of the dpyam ligand (Cu–N distances 1.987(3) and 2.010(3) Å) and two oxygen atoms of two different formato ligands (Cu–O distances 1.974(2) and 1.975(2) Å). The coordinated water molecule occupies the axial position at a distance of 2.222(3) Å. The CuN_2O_2 chromophore is non-planar with a tetrahedral twist of 14.4(1)°. The Cu atom lies above this plane, 0.202 Å toward O(1). The copper chromophore can be described as having a slightly distorted square pyramidal geometry. The distortion of square pyramidal can be best described by the structural parameter τ (τ = 0 for square pyramid and τ = 1 for trigonal bipyramidal [18]), which in this case is 0.11. The Cu···Cu distance is 4.881(3) Å.

The lattice structure is stabilised by a hydrogen-bonding network between the N–H atom of the ligand and oxygen atoms of the nitrate anion with N–H···O contacts of 2.839(8)–3.072(17) Å and between the hydrogen of water oxygen atom and the nitrate oxygen atoms with O–H···O contacts of 2.617(12)–3.096(16) Å. A plot of the hydrogen bond system is given in Fig. 3 and details are given in Table 2.

3.2. EPR and magnetic measurements

The polycrystalline EPR spectrum of **1**, at both room temperature and liquid nitrogen temperature (77 K) shows a rhombic spectrum with g_1 = 2.06, g_2 = 2.15 and g_3 = 2.21, consistent with the $d_{x^2-y^2}$ ground state for the square pyramidal geometry of the $CuN_2O_2(O)$ chromophore [19]. No hyperfine splitting is resolved.

Table 2
Selected bond lengths (Å) and angles (°) with e.s.d. in parentheses of compound **1**

Cu(1)–O(3)	1.975(2)	Cu(1)–O(2)	1.974(2)
Cu(1)–N(1)	1.987(3)	Cu(1)–N(2)	2.010(3)
Cu(1)–O(1)	2.222(3)	Cu(1)···Cu(1A)	4.881(3)
O(3)–Cu(1)–O(2)	90.8(1)	O(3)–Cu(1)–N(1)	173.3(1)
O(2)–Cu(1)–N(1)	91.4(1)	O(3)–Cu(1)–N(2)	87.3(1)
O(2)–Cu(1)–N(2)	166.8(1)	N(1)–Cu(1)–N(2)	89.0(1)
O(3)–Cu(1)–O(1)	95.1(1)	O(2)–Cu(1)–O(1)	94.9(1)
N(1)–Cu(1)–O(1)	90.8(1)	N(2)–Cu(1)–O(1)	98.1(1)

D-H···A (°)	D–H (Å)	H···A (Å)	D···A (Å)	D–H···A
Hydrogen-bonding parameters				
N(3)–H(5)···*O(4) [−1 + x,y,−1 + z]	0.75(4)	2.37(4)	3.072(17)	154(4)
N(3)–H(5)···*O(6A) [−1 + x,y,−1 + z]	0.75(4)	2.13(4)	2.839(8)	157(4)
O(1)–H(11)···*O(4) [1 − x,−y,1 − z]	0.82(6)	2.32(6)	3.050(16)	149(5)
O(1)–H(11)···*O(4A) [1 − x,−y,1 − z]	0.82(6)	1.98(6)	2.790(11)	168(5)
O(1)–H(11)···*O(5) [1 − x,−y,1 − z]	0.82(6)	2.33(6)	3.096(16)	156(5)
O(1)–H(12)···*O(5)	0.68(6)	2.00(6)	2.617(12)	153(6)
O(1)–H(12)···*O(5A)	0.68(6)	2.08(6)	2.749(8)	170(6)

Fig. 2. The polymeric zig-zag chain of $[Cu(dpyam)(\mu\text{-}O_2CH)(H_2O)]_n\cdot(NO_3)_n$. The uncoordinated nitrate anion has been omitted for clarity.

The EPR recorded in a frozen solution (DMF) at 77 K reveal a well-resolved axial spectrum with a $g_\perp$ of 2.05 a $g_\parallel$ of 2.28 and with an $A_\parallel$ of 16.5 mT, indicating that in solution the geometry around the Cu(II) ion has been changed. These solution EPR values have also observed for another formato-bridged Cu(II) compound with an $CuN_2O_2(O)$ chromophore [7] and indicate that

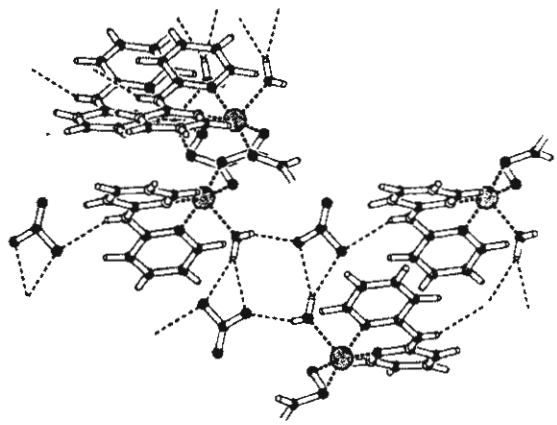

Fig. 3. A plot showing the H-bond system. Only one conformation of the disordered nitrate anion is showing here.

also the DMF molecule plays an important role in the coordination.

The magnetisation of a powdered sample of **1** was measured from 5 to 300 K in an applied field of 0.1 T. The resulting molar magnetic susceptibility, χ_M, and the product $\chi_M T$ are plotted in Fig. 4. At around 300 K, the compound exhibits a $\chi_M T$ value of 0.34 $cm^3\ mol^{-1}\ K$, which is close to the theoretical value expected for one non-coupled Cu(II) centre with $S = 1/2$ ($\chi_M T = 0.375\ cm^3\ mol^{-1}\ K$). On lowering the temperature, the $\chi_M T$ value stays almost constant till around 50 K when it start to increase until it reaches a value of about 0.68 $cm^3\ mol^{-1}\ K$ at 5 K, a behaviour indicative of a weak ferromagnetic coupling between Cu centres.

The temperature dependence of χ_m has been fitted using the equation [20] derived from the Heisenberg exchange Hamiltonian for an uniformly spaced chain of spins with $S = 1/2$: $H = -J\sum_{i=1}^{n-1} S_{Ai}\cdot S_{Ai+1}$ (in which A_i

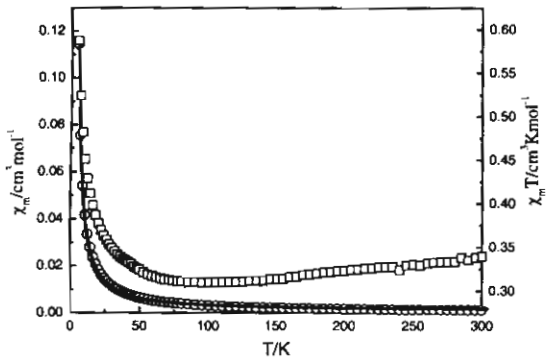

Fig. 4. A plot of temperature dependence of $X_M T$ vs. T (□) and X_M vs. T (○) for compound **1**. The solid line for X_M vs. T represents the calculated curve for the parameters $J = 0.75\ cm^{-1}$, $g = 2.00$ (see text).

are the nearest neighbour Cu(II) ions and the exchange parameter J is positive for ferromagnetic and negative for an antiferromagnetic interaction). A Temperature Independent Paramagnetism (TIP) of $60 \times 10^{-6}\ cm^3\ mol^{-1}$ per Cu(II) ion has been used. The best fit of the experimental magnetic susceptibility data for a chain (solid line in Fig. 3) was obtained using the magnetic parameters $g = 2.00$, $J = 0.75\ cm^{-1}$, with $R = 1.09 \times 10^{-6}$. As the Cu···Cu distance is fairly large (4.881(3) Å) this very weak ferromagnetic interaction most likely occurs via the Cu–O–C–O–Cu pathway. Similar cases have been observed in the literature [8], although in one example even no interaction was found at all for such a bridge [7]. Such a weak ferromagnetic interaction has also been observed for a number of polynuclear malonate-bridged Cu(II) compounds [21].

4. Supplementary material

Crystallographic data for the structure in this paper have been deposited with the Cambridge Crystallographic Data Centre as Supplementary Publication CCDC No. 240813 for structure **1**. Copies of the data can be obtained free of charge from The Director, CCDC, 12 Union Road, Cambridge CB2 1EZ, UK (fax: +44 1223 336033; e-mail: deposit@ccdc.cam.ac.uk, http://www.ccdc.cam.ac.uk).

Acknowledgements

The authors thank The Thailand Research Fund and Khon Kaen University for a research grant. Support of the Postgraduate Education and Research Program in Chemistry (Thailand) is also gratefully acknowledged.

The work described in the present paper has been supported by the Leiden University Study group WFMO (Werkgroep Fundamenteel MaterialenOnderzoek).

References

[1] S. Youngme, N. Chaichit, K. Damnatara, Polyhedron 21 (2002) 943 (references cited therein).
[2] S. Youngme, C. Pakawatchai, H.K. Fun, Acta Crystallogr. Sect. C 54 (1998) 451.
[3] T.D. Coombs, B.J. Brisdon, C.P. Curtis, M.F. Mahon, S.A. Brewer, C.R. Willis, Polyhedron 20 (2001) 2935.
[4] S. Youngme, P. Phuengphai, N. Chaichit, C. Pakawatchai, G.A. van Albada, O. Roubeau, J. Reedijk, Inorg. Chim. Acta 357 (2004) 3603.
[5] A. Camus, N. Marsich, A.M.M. Lanfredi, F. Ugozzoli, C. Massera, Inorg. Chim. Acta 309 (2000) 1.
[6] S. Youngme, W. Somjitsripunya, K. Chinnakali, S. Chantrapromma, H.K. Fun, Polyhedron 18 (1999) 857.
[7] G.A. van Albada, S. Amani Komaei, H. Kooijman, A.L. Spek, J. Reedijk, Inorg. Chim. Acta 287 (1999) 226.
[8] J.L. Manson, J.G. Lecher, J. Gu, U. Geiser, J.A. Schlueter, R. Henning, X. Wang, A.J. Schultz, H.-J. Koo, M.-H. Whangbo, J. Chem. Soc., Dalton Trans. (2003) 2905.
[9] G. Davey, F.S. Stephens, J. Chem. Soc. A (1971) 103.
[10] B.A. Cartwright, L. Couchman, A.C. Skapski, Acta Crystallogr., Sect. B 35 (1979) 824.
[11] M.A. Bernard, M.M. Borel, F. Busnot, A. Leclaire, Rev. Chim. Miner. 16 (1979) 124.
[12] M. Bukowska-Strzyzewska, A. Tosik, Acta Crystallogr., Sect. C 39 (1983) 203.
[13] Siemens. SAINT 1996, Version 4 Software Reference Manual, Siemens Analytical X-Ray Systems, Inc., Madison, WI, USA, 1996.
[14] G.M. Sheldrick, SADABS, Program for Empirical Absorption Correction of Area Dectector Data, University of Göttingen, Göttingen, Germany, 1996.
[15] Siemens. SHELXTL 1996, Version 5 Reference Manual, Siemens Analytical X-Ray Systems, Inc., Madison, WI, USA, 1996.
[16] C.C. Addison, N. Logan, S.C. Wallwork, C.D. Garner, Q. Rev. Chem. Soc. 25 (1971) 289.
[17] G. Davey, F.S. Stephens, J. Chem. Soc. A (1971) 103.
[18] A.W. Addison, T.N. Rao, J. Reedijk, J. van Rijn, G.C. Verschoor, J. Chem. Soc., Dalton Trans. (1984) 1349.
[19] B.J. Hathaway, in: G. Wilkinson, R.D. Gill, J.A. McCleverty (Eds.), Comprehensive Coordination Chemistry, vol. 5, Pergamon Press, Oxford, 1987.
[20] O. Kahn, Molecular Magnetism, VCH Publication, New York, 1993, p. 253.
[21] J. Pasán, F.S. Delgado, Y. Rodríguez-Martín, M. Hernández-Molina, C. Ruiz-Pérez, J. Sanchiz, F. Lloret, M. Julve, Polyhedron 22 (2003) 2143.
[22] S. Youngme, N. Chaichit, C. Pakawatchai, S. Booncoon, Polyhedron 21 (2002) 1279.
[23] S. Youngme, C. Pakawatchai, H.K. Fun, K. Chinnakali, Acta Crystallogr., Sect. C 54 (1998) 1586.
[24] N. Ray, S. Tyagi, B.J. Hathaway, Acta Crystallogr., Sect. B 38 (1982) 1574.
[25] J. Sletten, Acta Chem. Scand., Sect. A 38 (1984) 491.
[26] S. Youngme, S. Tonpho, K. Chinnakali, S. Chantrapromma, H.-K. Fun, Polyhedron 18 (1999) 851.